ZooKeys 1189: 1–32 (2023)
DOI: 10.3897/zookeys.1189.109734

Research Article

New records of *Provanna* (Gastropoda, Provannidae) from the Costa Rica Margin and an identification key for the genus

Melissa J. Betters[1], Erik E. Cordes[1]

1 *Department of Biology, Temple University, Philadelphia, PA, USA*
Corresponding author: Melissa J. Betters (melissajbetters@gmail.com)

Abstract

Consistent species identification is foundational to biological research and requires coordination among a diversity of researchers and institutions. However, such consistency may be hindered for rare organisms where specimens, identification resources, and taxonomic experts are few. This is often the case for deep-sea taxonomic groups. For example, the deep-sea gastropod genus *Provanna* Dall, 1918 is common at chemosynthetic sites throughout the world's oceans, yet no formal guide to these species has yet been produced. Recent exploration has recovered new specimens of *Provanna* from hydrocarbon seeps off the Pacific Costa Rica Margin. The current work assesses the species identity of these specimens using shell morphology, radular morphology, and genetic barcoding (mitochondrial CO1 and nuclear H3). Records of occurrence for *P. laevis* Warén & Ponder, 1991, *P. ios* Warén & Bouchet, 1986, and *P. pacifica* Warén & Bouchet, 1986 are herein presented from the Costa Rica Margin. A critical taxonomic review of the 29 extant species within this genus was conducted and their genetic, morphological, and biogeographical distinction assessed. In this review, genetic and morphological support was found for nearly all current species delineations except for *P. glabra* Okutani et al., 1992, **syn. nov.** and *P. laevis*, **syn. nov.**, which are herein synonymized to *P. laevis*, and for *P. ios*, **syn. nov.** and *P. goniata* Warén & Bouchet, 1986, **syn. nov.**, which are synonymized to *P. ios*. Finally, the first species identification key for the extant species in this genus is presented. This work clarifies the taxonomy and systematics of this deep-sea gastropod genus and contributes a novel polytomous key for use in future research.

Key words: Gastropoda, identification, species delimitation, systematics, taxonomy

Academic editor: Eike Neubert
Received: 18 July 2023
Accepted: 20 November 2023
Published: 12 January 2024

ZooBank: https://zoobank.org/C2269924-E29A-4D66-8FA9-6A21E34330D4

Citation: Betters MJ, Cordes EE (2023) New records of *Provanna* (Gastropoda, Provannidae) from the Costa Rica Margin and an identification key for the genus. ZooKeys 1189: 1–32. https://doi.org/10.3897/zookeys.1189.109734

Introduction

Consistent species identification is foundational to biological research. Studies of populations, communities, and ecosystems all rely on authors from a wide range of backgrounds and locations coordinating species definitions. This is particularly salient for the global endeavor of deep-sea research, where many species are recent discoveries. As many regions of the ocean remain unexplored, taxonomic characterization of marine invertebrates are hindered by a lack of collections, occurrence records, identification resources, and taxonomic experts (Sigwart et al. 2019; Engel et al. 2021).

Throughout the world's oceans, ecosystems reliant on chemosynthetic activity, such as hydrothermal vents and hydrocarbon seeps, are hotspots for productivity on the ocean floor, hosting an anomalously high biomass community consisting of numerous endemic species (Sibuet and Olu 1998). These ecosystems often host abundant gastropod populations which act as the primary grazers at these sites, feeding on the biofilms and bacterial mats that coat the hard surfaces of these environments (Sasaki et al. 2010). To identify such gastropods to the species level, researchers commonly rely on data sources such as shell morphology, genetic barcoding (e.g., mitochondrial cytochrome oxidase I gene (CO1)), and radular imaging (e.g., Nekhaev 2023). However, not all known species have been genetically barcoded, precluding the utility of these data in every case. With few taxonomic resources available for these ecosystems, researchers must rely on formal descriptions to identify species which assume a thorough, prior knowledge of taxon-specific language. Furthermore, comparisons across dozens of species may be necessary to come to a confident identification which can be arduous and time-consuming, particularly when species identification is just one part of a broader study. A solution to this problem is a key, which synthesizes a set of informative criteria and guides researchers to a workable species hypothesis. Keys are typically more easily implemented by researchers across expertise levels than formal descriptions, thus presenting an effective method with which to streamline and standardize species identifications.

The current work centers on aa genus of Abyssochrysoid snails *Provanna* (Dall, 1918), presenting new records, a taxonomic review, and a new identification key for its species. *Provanna* occur worldwide and are endemic to chemosynthetic environments (Johnson et al. 2010; Amano and Little 2012; Linse et al. 2019). In total, 29 extant species of *Provanna* are currently recognized on the World Register of Marine Species (WoRMs), six of which have recently been designated as Endangered or Critically Endangered on the IUCN Red List (Molloy et al. 2020a, b, c; Thomas and Sigwart 2020; Molloy and Thomas 2021a, b; IUCN 2022). Despite their cosmopolitan distribution and their threatened status, however, identification resources for this group are lacking, increasing the likelihood that some of the recognized species are synonymous and that other species are cryptic and have gone unrecognized within this genus. An understanding of the conservation status of species must begin with a confident identification of the species.

Species of *Provanna*, like other deep-sea gastropods, may be distinguished by their shell and radular morphology, making a morphology-based identification key useful. All *Provanna* share certain characteristics that distinguish the genus. Specimens have small, turbinate, dextral shells, a thin periostracum, no umbilicus, and usually no more than 2–3 shell whorls intact, regardless of size. They are never wider than they are tall and their apertures have a distinct shape; They are rarely circular or ovate. Rather, the columellar lip typically curves inwards near the bottom of the shell, such that it forms a near-right angle with the lower lip (see Fig. 2A for an example). They are also small, with one of the largest specimens recorded just 2 cm in length (Chen et al. 2018). They may be distinguished from their sister genus *Desbruyeresia* in that *Desbruyeresia* typically have tall, intact spires of > 3–4 whorls and more slender, turriform shells (Warén and Bouchet 1993). They also have distinct radular characteristics, with

Desbruyeresia having multiple denticles on the cusps of their central teeth while *Provanna* have none (Warén and Bouchet 1993). Protoconchs (larval shells) are also useful in distinguishing these genera; However, protoconchs are almost unanimously missing in *Provanna* specimens (Warén and Ponder 1991; Warén and Bouchet 1993). Finally, genetic characterization of this group is still ongoing, with gene sequences currently unavailable for *P. abyssalis* (Okutani & Fujikura, 2002), *P. admetoides* (Warén & Ponder, 1991), *P. chevalieri* (Warén & Bouchet, 2009), *P. goniata* (Warén & Bouchet, 1986), *P. muricata* (Warén & Bouchet, 1986), *P. nassariaeformis* (Okutani, 1990), nor *P. reticulata* (Warén & Bouchet, 2009). This lack of sequence data makes an identification key based on morphology particularly relevant, especially one that is created using an integrative taxonomy approach that includes genetic data.

In the present study, we present formal records of *Provanna* from hydrocarbon seeps at the Costa Rica Margin that were sampled from 700 to 2000 meters depth. These sites were sampled during three cruises from 2017–2019, representing one of the most intensive sampling efforts in this region to date. The hydrocarbon seepage in this region is driven by the subduction of the Cocos Plate beneath the Caribbean plate (Suess 2014) and fuels chemosynthetic primary productivity at these sites (Cavanaugh et al. 1981; Suess 2014). This investigation aims to identify these Costa Rican hydrocarbon seep *Provanna* down to the species level using both morphological and genetic data. While the ecology and depth partitioning of these *Provanna* specimens have been recently investigated (Betters et al. 2023), the present study details the rigorous taxonomic identification of these specimens. We incorporate these data into a holistic review of the genus with the aim of assessing the morphological and genetic distinction among its extant species. Finally, we synthesize these results into the first polytomous species identification key for all currently known, extant *Provanna* species.

Materials and methods

Specimen collection

Specimens of *Provanna* were obtained from one of six sites at the Pacific Costa Rica Margin (CRM) during research expeditions conducted from 2017 to 2019 (Fig. 1, Table 1). *Provanna* were sampled by the human-operated vehicle (HOV) ‘Alvin’ and the remotely operated vehicle (ROV) ‘Subastian’ using various sampling tools attached to the HOV or ROV such as the manipulator arm or suction hose. The locations of sampling events were recorded for all specimens collected. Upon arrival to the surface, specimens were kept cold before being promptly preserved in > 95% ethanol. Specimens were then stored long term in ethanol at room temperature (20–25 °C).

Morphological analysis

All morphological characters and measurements are defined in Fig. 2 and Table 2. To begin identifying our specimens and constructing the key, original taxonomic descriptions of all extant *Provanna* species were obtained. The following shell characters were annotated for each species: The number of axial

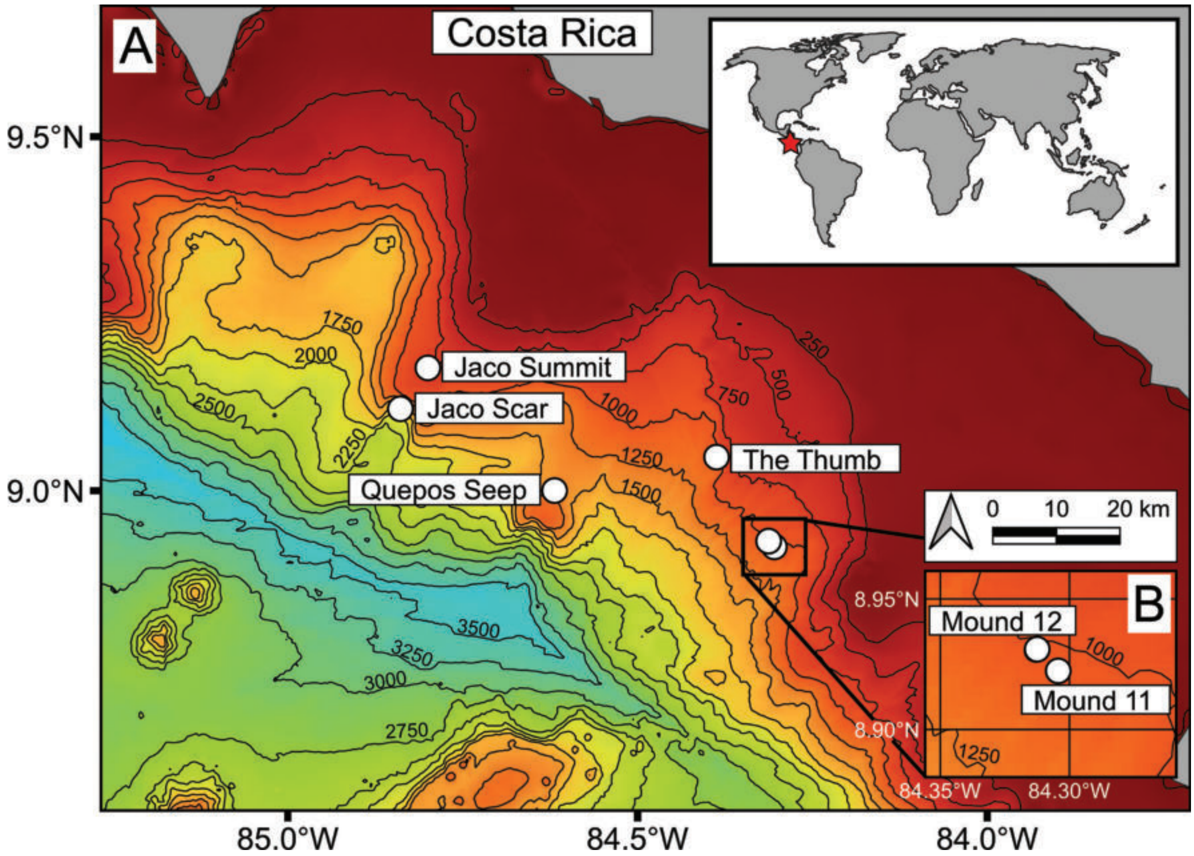

Figure 1. Map of the Costa Rica Margin **A** overview of the Costa Rica continental shelf with hydrocarbon seep sites labelled **B** close-up view of the sites Mound 12 and Mound 11, which appear overlapping in the larger map. Bottom bathymetry is demarcated by black lines every 250 m.

Table 1. Summary of hydrocarbon seep sites sampled at the Costa Rica Margin and their associated species yield. Abbreviations in cruise identities are defined as follows: FK = R/V 'Falkor' cruise number, AT = R/V 'Atlantis' cruise number. Abbreviations: SD = ROV 'Subastian' dive number, AD = HOV 'Alvin' dive number. *Previously identified as *P. goniata*.

Seep site	Number of specimens	Species composition	GPS coordinates	Depth (m)	Cruise ID	Dive ID
Jaco Summit	6	*P. laevis* (100%)	9.174°N, 84.800°W	740–760	FK19-0106 AT37-10 AT37-13	SD213 AD4874 AD4912 AD4913 AD4914
Jaco Scar	180	*P. ios* (100%)*	9.115°N, 84.836°W	1800–2000	AT42-03	AD4971 AD4973 AD4977 AD4989
					FK19-0106	SD214
Quepos Seep	6	*P. pacifica* (100%)	8.922°N, 84.305°W	1000–1100	AT37-13	AD4924
The Thumb	815	*P. laevis* (100%)	9.049°N, 84.354°W	1071–1075	FK19-0106	SD217
Mound 12	803	*P. laevis* (100%)	8.930°N, 84.313°W	900–1050	AT37-13	AD4907 AD4910 AD4917
					AT42-03	AD4974 AD4978 AD4984 AD4985 AD4987
Mound 11	5	*P. lomana* (40%), *P. pacifica* (60%)	9.031°N, 84.619°W	1300–1500	AT42-03	AD4988

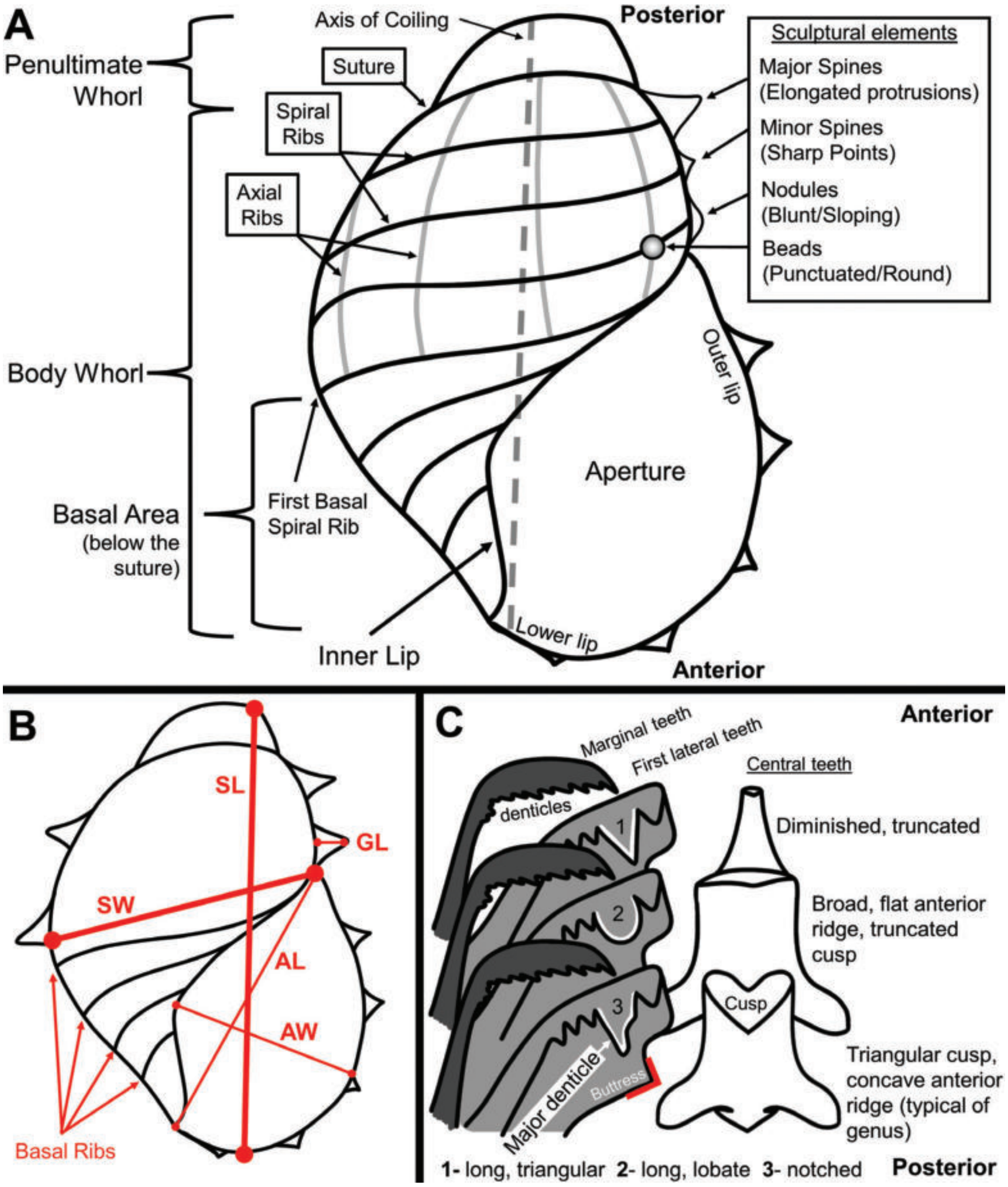

Figure 2. Visual definitions of morphological characters and measurements used in the study **A** shell morphological characters **B** informative measurements assessed for our own specimens **C** radular terminology and morphological characters. Abbreviations: SW: Shell Width, SL: Truncated Shell Length, GL: Maximum Granule Length, AL: Aperture Length, AW: Aperture Width.

and spiral ribs on the body whorl, the relative strength of the body whorl sculptures, sculptural elements formed, how far down the body whorl the axial ribs extend, the presence of basal ribs, the average roundness (width / length) of the original holotype and paratype shells, the depth of the shell suture, and the descriptive shape of the aperture (Table 3). The following radular characters were also annotated: The relative width of the central teeth, the descriptive shape of the central teeth cusps, the roundedness of the central teeth's anterior ridges, the number of denticles on the first lateral teeth, which denticle on the first lateral teeth is the most longest ("major" denticle), the descriptive shape of the first lateral major denticles, the angle of the first lateral posterior buttress, and the number of marginal tooth denticles (Table 3).

Table 2. Definitions for selected terminology used to describe morphological characters.

Aperture	The opening of the shell from which the gastropod body would protrude
Axis of coiling	The imaginary line that runs from the top of a shell's spire to the tip of its base around which the shell is coiled
Axial sculpture	The sculpturing of the shell running parallel to the axis of coiling
Growth lines	Fine transverse lines marking shell growth. They are distinguished from axial sculpturing in that they are not raised or grooved.
Sculpture	Three-dimensional, linear ornamentation on the outer surface of the shell. These rise away from the shell surface
Sculptural element	Knob-, bead-, or spike-like protrusions that occur at intersections of the axial and spiral sculptures and that are raised higher than either sculpture. **Note:** If a Provanna shell has structural elements, it will typically have both an axial and spiral sculpture.
Body whorl margin	The length between the posterior end of the aperture and the previous suture line
Spiral sculpture	The sculpturing of the shell running perpendicular to the axis of coiling
Suture	Where the whorls of the shell are fused, including where the aperture is fused with the body whorl
Whorl	One complete revolution of shell growth

To begin identifying the specimens from the CRM, they were first sorted into distinct morphotypes. Representatives from the full geographic, temporal, and size range of each morphotype were then selected for detailed morphological assessment. The following characters were measured for each specimen: Shell width (mm), truncated shell length (measured from the right, posterior tip of the penultimate whorl to the lowest point of the aperture (mm)), aperture length (mm), aperture width (mm), number of basal ribs (counted), relative shell texture (maximum granule length on the body whorl / truncated shell length), aperture roundness (width / length), and shell roundness (width / length). Truncated shell length was used as most *Provanna* lack any whorl past the penultimate whorl. Measurements of characters were taken from photographs captured by a mounted AmScope microscope adapter camera attached to a standard dissection microscope (Leica S6D, Leica Microsystems GmbH). A standardized 1-mm marker was present in every photo to allow for standardized measurements. Specimens were kept submerged in > 95% ethanol while images were taken. The line measurement tool within AmScope was used to measure morphological characters. To identify any potential collinearity among shell morphological characters, Pearson correlation coefficients (PCC) were calculated using the package Ggally (Schloerke et al. 2021) in R (v. 4.2.3; R Core Team 2022). One-way ANOVAs were then conducted in base R to identify significant differences in shell morphology among the morphotypes sampled from Costa Rica.

To characterize the radulae of each morphotype, we performed the following protocol. First, the body whorl of the shell was punctured using a sharp probe. The whole animal was then incubated in a 1.5 mL microcentrifuge tube containing a 10% solution of proteinase-k for 5–15 min at 56 °C. Incubation was monitored and terminated once tissue was visibly loose and degraded, but not fully digested. The microcentrifuge tube was removed from the heat source, pulse-vortexed three times, and then its contents were rinsed into a clean glass petri dish using deionized (DI) water. Under a dissection scope, the radular ribbon was identified, extricated from any remaining soft tissue, and moved to another clean glass petri dish containing DI water to further dilute the proteinase-k solution and prevent further breakdown of the radular ribbon.

Table 3. Summary of morphological characteristics for the type specimens of each *Provanna* species.

Species	Axial ribs on body whorl	Spiral ribs on body whorl	Relative strength of ribs on body whorl	Sculptural elements	Axial body sculpture extends to…
P. abyssalis Okutani & Fujikura, 2002	0	0	NA	Absent	NA
P. admetoides Warén & Ponder, 1991	35–45	2–3	Variable	Minor spines/Absent	Posterior end of aperture
P. annae Nekhaev, 2023	0	0	NA	Absent	NA
P. beebi Linse et al., 2019	>20	0–6	Spiral > Axial	Beaded/ Absent	Anterior end of shell
P. buccinoides Warén & Bouchet, 1993	10–20	3–4	Spiral < Axial	Nodules	Posterior end of aperture
P. chevalieri Warén & Bouchet, 2009	10–20	0–3	Spiral < Axial	Absent	Mid-body whorl
P. cingulata Chen et al., 2018	0	4–6	Spiral > Axial	Absent	NA
P. clathrata Sasaki et al., 2016	10–20	3–5	Variable	Nodules/ Minor Spines	Posterior end of aperture
P. cooki Linse et al., 2019	0	0–5	Spiral > Axial	Absent	NA
P. exquisita Chen & Watanabe, 2022	14–18	2–3	Spiral > Axial	Major Spines/Keel	Posterior end of aperture
P. fenestrata Chen et al., 2019	16–20	1–2	Variable	Nodules/ Absent	Posterior end of aperture
P. glabra Okutani et al., 1992	0	0	NA	Absent	NA
P. goniata Warén & Bouchet, 1986	15–20	2–3	Spiral > Axial	Major Spines	Posterior end of aperture
P. ios Warén & Bouchet, 1986	15	2	Spiral > Axial	Minor Spines	Posterior end of aperture
P. kuroshimensis Sasaki et al., 2016	0	0	NA	Absent	NA
P. laevis Warén & Ponder, 1991	0	0	NA	Absent	NA
P. lomana Warén & Bouchet, 1986	10–20	0	Spiral < Axial	Absent	Posterior end of aperture
P. lucida Sasaki et al., 2016	0	0–3	Spiral > Axial	Absent	NA
P. macleani Warén & Bouchet, 1989	10–20	4–5	Spiral > Axial	Absent	Posterior end of aperture
P. muricata Warén & Bouchet, 1986	14–16	1–2	Spiral < Axial	Nodules/ Minor Spines	Posterior end of aperture
P. nassariaeformis Okutani, 1990	20–25	3–5	Spiral = Axial	Beaded	Anterior end of shell
P. pacifica Warén & Bouchet, 1986	12–16	2–3	Spiral > Axial	Nodules/ Minor Spines	Posterior end of aperture
P. reticulata Warén & Bouchet, 2009	0–15	2–4	Spiral = Axial	Minor Spines	Posterior end of aperture
P. sculpta Warén & Ponder, 1991	15	3	Spiral < Axial	Beaded	Posterior end of aperture
P. segonzaci Warén & Ponder, 1991	10–20	2–3	Spiral < Axial	Nodules/ Minor Spines	Posterior end of aperture
P. shinkaiae Okutani & Fujikura, 2002	10–20	2–3	Spiral > Axial	Major Spines	Posterior end of aperture
P. stephanos Chen et al., 2019	10–20	2–3	Spiral > Axial	Major Spines/Keel	Posterior end of aperture
P. subglabra Sasaki et al., 2016	0	0	NA	Absent	NA
P. variabilis Warén & Bouchet, 1986	0–20	1–3	Spiral > Axial	Nodules/ Absent	Posterior end of aperture

Species	Basal spiral ribs	Width / Length	Depth of suture	Aperture shape description	Central tooth width	Central tooth cusp
P. abyssalis Okutani & Fujikura, 2002	Absent	0.5	Constricted	Globose	Typical	Long, triangular
P. admetoides Warén & Ponder, 1991	Present	0.61	Moderate	Fusiform	Very narrow	Very truncated
P. annae Nekhaev, 2023	Absent	0.6	Constricted	Globose	Typical	Long, triangular

Species	Basal spiral ribs	Width / Length	Depth of suture	Aperture shape description	Central tooth width	Central tooth cusp
P. beebi Linse et al., 2019	Present	0.59	Moderate	Fusiform/ Semicircle	Broad	Blunt, truncated
P. buccinoides Warén & Bouchet, 1993	Present	0.63	Moderate	Globose	Broad	Blunt, truncated
P. chevalieri Warén & Bouchet, 2009	Present	0.55	Constricted	Globose	Broad	Very short, triangular
P. cingulata Chen et al., 2018	Absent	0.61	Constricted	Globose	Broad	Short, triangular
P. clathrata Sasaki et al., 2016	Present	0.61	Constricted	Fusiform	Typical	Long, triangular
P. cooki Linse et al., 2019	Absent	0.57	Constricted	Fusiform	Broad	Triangular
P. exquisita Chen & Watanabe, 2022	Present	0.55	Constricted	Semicircular	Typical	Triangular
P. fenestrata Chen et al., 2019	Present	0.59	Moderate	Variable	Typical	Triangular
P. glabra Okutani et al., 1992	Absent	0.6	Flat	Globose	Typical	Triangular, blunt
P. goniata Warén & Bouchet, 1986	Present	0.59	Moderate	Globose/ Fusiform	Typical	Long, triangular
P. ios Warén & Bouchet, 1986	Variable	0.54	Constricted	Fusiform/ Semicircle	NA	Long, triangular
P. kuroshimensis Sasaki et al., 2016	Absent	0.58	Flat	Fusiform	Typical	Long, triangular
P. laevis Warén & Ponder, 1991	Absent	0.56	Flat	Variable	Typical	Short, triangular
P. lomana Warén & Bouchet, 1986	Present	0.55	Moderate	Globose	Typical	Long, triangular
P. lucida Sasaki et al., 2016	Absent	0.59	Constricted	Globose	Typical	Short, triangular
P. macleani Warén & Bouchet, 1989	Present	0.61	Moderate	Fusiform	Very narrow	Very truncated
P. muricata Warén & Bouchet, 1986	Present	0.56	Constricted	Globose	Typical	Triangular
P. nassariaeformis Okutani, 1990	Present	0.7	Flat	Fusiform	Broad	Triangular, blunt, truncated
P. pacifica Warén & Bouchet, 1986	Present	0.61	Moderate	Fusiform	Very narrow	Very truncated
P. reticulata Warén & Bouchet, 2009	Present	0.57	Moderate	Fusiform	Broad	Blunt, truncated
P. sculpta Warén & Ponder, 1991	Present	0.55	Moderate	Fusiform	Typical	Long, triangular
P. segonzaci Warén & Ponder, 1991	Present	0.59	Constricted	Fusiform	Typical	Triangular
P. shinkaiae Okutani & Fujikura, 2002	Present	0.51	Moderate	Semicircle	Typical	Long, triangular
P. stephanos Chen et al., 2019	Present	0.61	Flat	Globose	Typical	Short, triangular
P. subglabra Sasaki et al., 2016	Absent	0.61	Flat	Fusiform	Typical	Long, triangular
P. variabilis Warén & Bouchet, 1986	Variable	0.55	Moderate	Globose	Typical	Long, triangular

Species	Central tooth anterior ridge	First lateral tooth cusps	First lateral major cusp	First lateral major cusp shape	First lateral buttress angle	Marginal tooth cusps
P. abyssalis Okutani & Fujikura, 2002	Concave	6–7	2nd	Triangular, fused with first	Right	9–10
P. admetoides Warén & Ponder, 1991	Rounded	3–4	2nd	Spatulate	Obtuse	Alternating 7 or 14+
P. annae Nekhaev, 2023	Concave	3–4	2nd	Long, lobate	Right	7–9
P. beebi Linse et al., 2019	Flat	4–5	2nd	Truncated, lobate	Absent	13–17
P. buccinoides Warén & Bouchet, 1993	Rounded/Flat	7	Fourth	Very truncated, lobate	Absent	~30
P. chevalieri Warén & Bouchet, 2009	Variable	4–5	2nd	Very truncated, lobate	Sloping/ Absent	13–18
P. cingulata Chen et al., 2018	Round/Flat	4–5	3rd or 4th	Rhomboid	Absent	15–18
P. clathrata Sasaki et al., 2016	Concave	4–5	2nd	Long, triangular	Right/ Acute	9–10
P. cooki Linse et al., 2019	Concave	5–6	2nd	Long, lobate	Obtuse	11–14

Species	Central tooth anterior ridge	First lateral tooth cusps	First lateral major cusp	First lateral major cusp shape	First lateral buttress angle	Marginal tooth cusps
P. exquisita Chen & Watanabe, 2022	Concave	4–5	2nd	Truncated, lobate	Right/ Obtuse	20–24
P. fenestrata Chen et al., 2019	Concave	4–5	2nd	Long, triangular	Right	9–10
P. glabra Okutani et al., 1992	Concave	4–5	2nd	Long, lobate	Right/ Acute	8–12
P. goniata Warén & Bouchet, 1986	Concave	5–6	2nd	Long, triangular	Right/ Acute	15–25
P. ios Waren & Bouchet, 1986	Concave	4–5	2nd	Long, triangular	Right/ Acute	15–25
P. kuroshimensis Sasaki et al., 2016	Concave	4–5	2nd	Long, lobate	Right	10–13
P. laevis Warén & Ponder, 1991	Concave	4–5	2nd	Truncated, lobate	Acute	15–20
P. lomana Waren & Bouchet, 1986	Concave	4–5	2nd	Long, triangular	Acute	Alternating 7 or 14+
P. lucida Sasaki et al., 2016	Concave	4–5	2nd	Long, triangular	Right/ Acute	13–15
P. macleani Warén & Bouchet, 1989	Rounded	3–4	2nd	Spatulate	Sloping/ Absent	15–20
P. muricata Warén & Bouchet, 1986	Concave	4–5	2nd	Lobate	Sloping/ Obtuse	15–20
P. nassariaeformis Okutani, 1990	Concave/Flat	4–5	2nd	Truncated, lobate	Absent	15–20
P. pacifica Warén & Bouchet, 1986	Rounded	3	2nd	Lobate/ Spatulate	Sloping/ Obtuse	5–7
P. reticulata Warén & Bouchet, 2009	Concave	2–3	2nd	Truncated, lobate	Absent	15–20
P. sculpta Warén & Ponder, 1991	Concave	3–5	2nd	Long, triangular	Acute	15–20
P. segonzaci Warén & Ponder, 1991	Concave	5–7	2nd	Multilobate	Right/ Obtuse	15–20
P. shinkaiae Okutani & Fujikura, 2002	Concave	2–5	2nd	Long, lobate	Acute	10–14
P. stephanos Chen et al., 2019	Concave	4–5	2nd or 3rd	Long, triangular, blunt	Obtuse	12–14
P. subglabra Sasaki et al., 2016	Concave	4–5	2nd	Long, triangular	Right/ Obtuse	15–20
P. variabilis Warén & Bouchet, 1986	Concave	4–5	2nd	Long, triangular	Acute	Alternating 7 or 14+

Silicon wafer chips cut into ~ 1 cm^3 squares were used as mounting substrate for scanning electron microscopy. To mount the radula, a very small droplet of DI water was placed onto a chip. The radula was then placed into this water droplet and manipulated under a light microscope into a flat, teeth-up position using forceps or a sharp probe. Manipulation was most successful when the radula was wet but not submerged. The radula's position was monitored and adjusted under a light microscope while the water was allowed to evaporate. Once dry, radulae naturally adhered to the chip's surface and were then stored dry until imaging. Scanning electron microscopy was undertaken using a QuantaTM 450 FEG scanning electron microscope (FEI 2012) in its low-vacuum setting at Temple University College of Engineering's Nano Instrumentation Center. High-quality images were obtained without sputter coating. Tentative morphological identities were then ascribed to our specimens.

Genetic analysis

To confirm the morphological identifications, the cytochrome oxidase 1 (CO1) mitochondrial gene and the histone 3 (H3) nuclear gene were sequenced. Tissue was obtained by pulling aside the operculum and pinching off a small sample of tissue from the foot (approximately 1 mm^3). This tissue was then digested and its DNA extracted using a Qiagen Blood and Tissue DNA Extraction kit (QIAGEN, Valencia, CA). Extracted DNA was quantitated using a Nanodrop 2000 spectrophotometer. DNA was kept frozen at -20 °C following extraction. A 710 base pair (bp) section of the CO1 gene was targeted for sequencing using the primers LCO1490/HCO2198 and polymerase chain reaction protocol put forth by Folmer et al. (1994). A 274 bp section of the H3 gene was targeted for sequencing using the H3F/H3R primers put forth by Colgan et al. (2000) and the following PCR protocol: 94 °C for 1 min, 40 cycles of 95 °C for 30 seconds, 55 °C for 30 seconds, and 72 °C for 30 seconds, followed by a final extension period of 72 °C for 7 min. Forward and reverse reads were obtained through GeneWiz (Azenta Life Sciences, South Plainfield, NJ). Each sequence was quality-assured, trimmed, and reverse reads were reverse-complemented using the BioEdit desktop software (v. 7.2.5; Hall 1999). Forward and reverse reads were then used to create one consensus sequence per individual.

For all phylogenetic analyses, sequences were input and aligned using ClustalW embedded within the MEGA-X environment (v. 10.0.1; Kumar et al. 2018). The Model Finder embedded within MEGA-X was used to find the best-fit substitution model based on the lowest Bayesian Information Criterion. All base positions with less than 95% site coverage were excluded from analyses. Bootstrap confidences of branch points were assessed using 10,000 bootstrap replicates within MEGA-X. Bayesian topologies and Bayesian posterior probabilities (BPP) of branch points were computed using the joint programs BEAUti (v. 1.10.4) and BEAST (v. 1.10.4) (Suchard et al. 2018). The maximum clade credibility tree was then selected from the BEAST output using TreeAnnotator (v. 1.10.4). The resulting figures were cleaned and finalized using FigTree (v. 1.4.4) (Rambaut 2018) and Adobe Illustrator (v. 27.3.1). All published gene sequences were downloaded from the National Center for Biotechnology Information (NCBI) nucleotide database. All alignments are freely available on Github (Repository: melissajbetters/CRM_Provanna).

To verify inclusion within the genus *Provanna*, we assessed our novel sequences in relation to other Abyssochrysoids including species in the genera *Abyssochrysos* (Tomlin, 1927), *Cordesia* (Warén & Bouchet, 2009), *Rubyspira* (Johnson et al., 2010), *Desbruyeresia* (Warén & Bouchet, 1993), *Alviniconcha* (Okutani & Ohta, 1988), and *Ifremeria* (Bouchet & Warén, 1991). The Vetigastropods *Caymanabyssia solis* (Kano et al., 2016) and *Notocrater pustulosus* (Thiele, 1925) were used as the outgroup for investigations of CO1. The Vetigastropods *Lepetodrilus pustulosus* (McLean, 1988) and *Pyropelta* sp. (McLean & Haszprunar, 1987) were used as outgroup for investigations of H3. To verify the specific identity of our specimens, we assessed our novel CO1 sequences in relation to all other *Provanna* species available on NCBI. While CO1 sequences exist for *P. annae* (Nekhaev, 2023), these were amplified using a primer set that targeted a different region of the CO1 gene from our novel sequences, thus precluding comparison. To account for intraspecific variation, a maximum of three sequences per species (chosen at random) were included in the tree. Additionally, gene sequences with tentative or unknown identities were also included in case our novel sequences matched these. *Desbruyeresia melanioides* (Warén & Bouchet, 1993) was used as the outgroup.

To assess the robustness of current species delimitations within the genus, we calculated the average pairwise sequence divergence (APD) across CO1 sequences for *Provanna*. All sequences with verified species identities were included; Sequences with tentative or unknown species identities were excluded. Our novel sequences were assigned to their hypothesized species identities. All sequences were aligned using ClustalW embedded within MEGA-X and assessed using a Tamura 3-parameter substitution model (Tamura 1992), the pairwise deletion option (threshold = 95%), and 5,000 bootstrap replicates within MEGA-X. We then tested the number of species partitions supported within this dataset using the hierarchical clustering program ASAP (Assemble Species by Automatic Partitioning) (Puillandre et al. 2021).

Key construction

Using the conclusions drawn from the preceding sections, a taxonomic key for all genetically supported, extant species of *Provanna* was constructed.

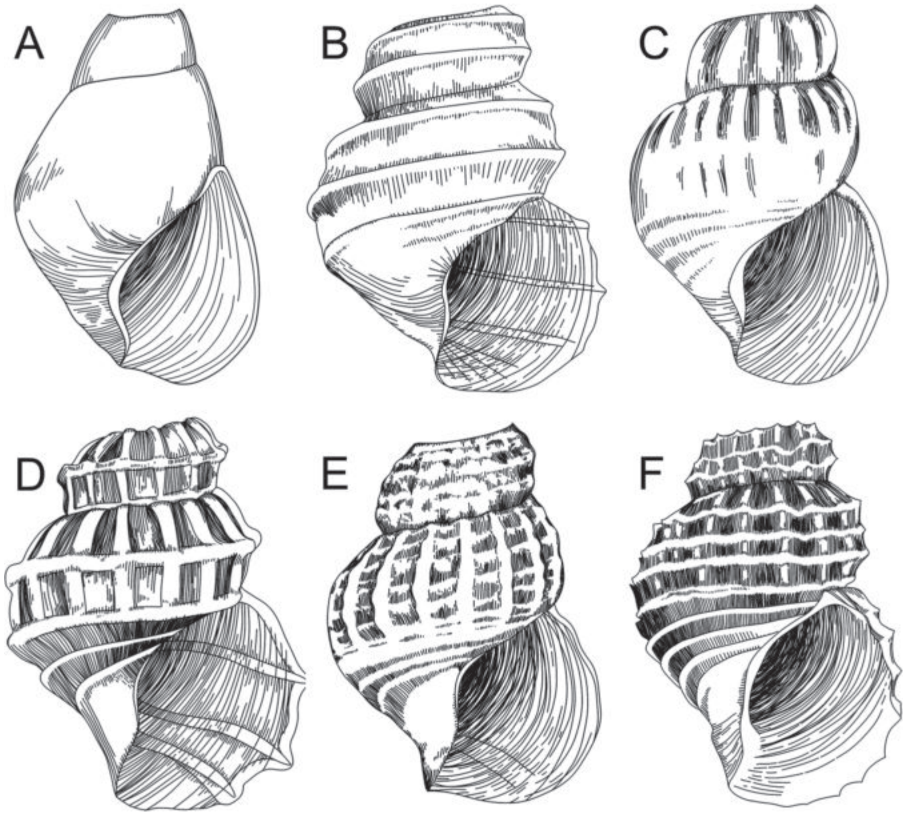

Figure 3. Examples of *Provanna* shell morphological variety **A** *P. kuroshimensis*, no sculpturing, growth lines present, flattened suture **B–F** constricted suture: **B** *P. cooki*, spiral sculpture only, no sculptural elements **C** *P. chevalieri*, axial sculpture only, no sculptural elements **D–F** both axial and spiral sculpturing: **D** *P. fenestrata*, sculptures about equal in strength, no sculptural elements **E** *P. clathrata*, axial sculpture stronger than spiral, blunt, sloping nodules **F** *P. reticulata*, spiral sculpture stronger than axial, minor spines.

A polytomous key was chosen as the format to capture the natural variation found in *Provanna* shells (Fig. 3). Of the morphological characters annotated, we prioritized sorting shells based on aspects of shell sculpturing, as these characters are easily recognized and do not require additional processing to observe. Radular characteristics were only utilized within the key when no other shell character could discern between species. Several morphological characters were excluded from the key either because we determined that they would introduce too much subjectivity in responses (precluding consistent utility), overlapped among species, overlapped with other characters, or varied too much within species. Incorporating our own morphological results, the presence and number of basal ribs and penultimate whorl morphological characters were excluded. It is noted in the key where there is uncertainty in a species hypothesis which is then addressed in the Discussion.

Results

New occurrence records

Superfamily Abyssochrysoidea
Family Provannidae
Genus *Provanna* (Dall, 1918)

Provanna laevis Warén & Ponder, 1991

New records. Costa Rica • 25 specimens; Costa Rica Margin, Mound 12; 8.930°N, 84.313°W; 999 m; 22 May 2017; Lisa Levin, Charlotte Seid leg.; ALVIN Dive 4907, from wood; Scripps Benthic Invertebrate Collection (SBIC) M16112. 11 specimens; Costa Rica Margin, Mound 12; 8.930°N, 84.313°W; 1004 m; 25 May 2017; Greg Rouse, Todd Litke leg.; ALVIN Dive 4910, from rock; SBIC M16104 and M16106. 16 specimens; Costa Rica Margin, Mound 12; 8.929°N, 84.315°W; 964 m; 1 June 2017; Greg Rouse, Ben Moran leg.; ALVIN Dive 4917, from mussel shells; SBIC M16176. 89 specimens; Costa Rica Margin, Mound 12; 8.930°N, 84.313°W; 1003 m; 20 October 2018; Lisa Levin, Kyle Metcalfe leg.; ALVIN Dive 4974, from mussel shells; SBIC M16765. 78 specimens; Costa Rica Margin, Mound 12; 8.931°N, 84.313°W; 1004 m; 24 October 2018; Erik Cordes, Melissa Betters leg.; ALVIN Dive 4978, from mussel shells. 104 specimens; Costa Rica Margin, Mound 12; 8.931°N, 84.313°W; 1002–1004 m; 30 October 2018; Erik Cordes, Melissa Betters leg.; ALVIN Dive 4984, from mussel shells. 5 specimens; Costa Rica Margin, Mound 12; 8.930°N, 84.313°W; 1001 m; 31 October 2018; Erik Cordes, Melissa Betters leg.; ALVIN Dive 4985, from mussel shells. 475 specimens; Costa Rica Margin, Mound 12; 8.930°N, 84.312–84.313°W; 1002–1007 m; 2 November 2018; Erik Cordes, Melissa Betters leg.; ALVIN Dive 4987, from tubeworms. 6 specimens; Costa Rica Margin, Jaco Summit; 9.174°N, 84.800°W; 742 m; 6 January 2019; Greg Rouse, Allison Miller leg.; SUBASTIAN Dive 213, from wood; SBIC M17030. 793 specimens; Costa Rica Margin, The Thumb; 9.049°N, 84.354–84.394°W; 1071–1075 m; 10 January 2019; Erik Cordes, Melissa Betters leg.; SUBASTIAN Dive 217, from mussel shells. 22 specimens; Costa Rica Margin, The Thumb; 9.049°N, 84.354–

84.394°W; 1071–1075 m; 10 January 2019; Erik Cordes, Melissa Betters leg.; SUBASTIAN Dive 217, from tubeworms.

Remarks. The range of *P. laevis* is here expanded to three hydrocarbon seep locations at the CRM: Mound 12, Jaco Summit, and The Thumb. Their known distribution in the Eastern Pacific Ocean ranges from the Juan de Fuca Ridge to the Costa Rica Margin. Their known depth distribution in the Eastern Pacific Ocean is between 700–2000 m (Table 4).

Provanna ios Warén & Bouchet, 1986

New records. Costa Rica • 42 specimens; Costa Rica Margin, Jaco Scar; 9.118°N, 84.839°W; 1757 m; 20 March 2017; Elena Perez, Geoff Cook leg.; ALVIN Dive 4874, from tubeworms; SBIC M12301. 3 specimens; Costa Rica Margin, Jaco Scar; 9.115°N, 84.836°W; 1834 m; 27 March 2017; Victoria Orphan, Kat Dawson leg.; ALVIN Dive 4912, from mussels; SBIC M16110 and M16127. 1 specimen; Costa Rica Margin, Jaco Scar; 9.116°N, 84.840°W; 1898 m; 28 March 2017; Greg Rouse, Jorge Cortes leg.; ALVIN Dive 4913, from tubeworms; SBIC M16144. 10 specimens; Costa Rica Margin, Jaco Scar; 9.117°N, 84.840°W; 1802 m; 29 March 2017; Chris Roman, Alanna Durkin leg.; ALVIN Dive 4914, from tubeworms; SBIC M16153, M16164, and M16166. 7 specimens; Costa Rica Margin, Jaco Scar; 9.117°N, 84.840°W; 1806 m; 17 October 2018; Erik Cordes, Rebecca Rutstein leg.; ALVIN Dive 4971, from rocks; SBIC M16730 and M16754. 1 specimen; Costa Rica Margin, Jaco Scar; 9.118°N, 84.840°W; 1803 m; 19 October 2018; Victoria Orphan, Natalya Gallo leg.; ALVIN Dive 4973, from mussels; SBIC M16724. 1 specimen; Costa Rica Margin, Jaco Scar; 9.118°N, 84.840°W; 1803 m; 19 October 2018; Victoria Orphan, Natalya Gallo leg.; ALVIN Dive 4973, from rock; SBIC M16741. 38 specimens; Costa Rica Margin, Jaco Scar; 9.118°N, 84.840°W; 1803 m; 23 October 2018; Erik Cordes, Joanna Klein leg.; ALVIN Dive 4977, from mussels; SBIC M16807. 37 specimens; Costa Rica Margin, Jaco Scar; 9.118°N, 84.841°W; 1780 m; 4 November 2018; Erik Cordes, Melissa Betters leg.; ALVIN Dive 4989, from tubeworms. 40 specimens; Costa Rica Margin, Jaco Scar; 9.117°N, 84.840°W; 1802–1812 m; 7 January 2019; Erik Cordes, Melissa Betters leg.; SUBASTIAN Dive 214, from mussels.

Remarks. Detailed in full below, the specimens of *P. ios* presented here were previously referred to as *P. goniata* (Betters et al. 2023). The range of *P. ios* (inclusive of *P. goniata*), is here expanded to one seep locality at the CRM (Jaco Scar). Their range now includes the sites 17S, 13N, and 21N at the East Pacific Rise, the Guaymas Basin, the Galapagos Rift Zone, and the Costa Rica Margin between 2000–2616 m depth (Table 4).

Provanna pacifica Warén & Bouchet, 1986

New records. Costa Rica • 3 specimens; Costa Rica Margin, Quepos Seep; 9.031°N, 84.619°W; 1413 m; 7 June 2017; Lisa Levin, Kris Krasnosky leg.; ALVIN Dive 4924, from mussels; SBIC M16204. 6 specimens; Costa Rica Margin,

Table 4. Summary of biogeographic information for each known species of *Provanna*. S = Seep, V = Vent, F = Organic Fall. Note that *P. glabra* is herein synonymized with *P. laevis* and *P. goniata* is herein synonymized with *P. ios*.

Species	Region(s)	Localities	Depth (m)	Habitat	Citations
P. abyssalis Okutani & Fujikura, 2002	W Pacific	Japan Trench	5379	S	Okutani and Fujikura 2002
P. admetoides Warén & Ponder, 1991	Gulf of Mexico	Off St. Petersburg, Gulf of Mexico	624–631	S	Waren and Ponder 1991
P. annae Nekhaev, 2023	N Pacific	Piip Volcano, Bering Sea	387–472		Nekhaev 2023; Rybakova et al. 2023
P. beebi Linse et al., 2019	Caribbean Sea	Beebe Vent Field, Mid-Cayman Spreading Center	4956–4972	V	Linse et al. 2019
P. buccinoides Warén & Bouchet, 1993	W Pacific	Hine Hina, Lau Basin; North Fiji Basin	1900–2765	V	Waren and Bouchet 1993
P. chevalieri Warén & Bouchet, 2009	E Atlantic	Regab, off West Africa	3150	S	Waren and Bouchet 2009
P. cingulata Chen et al., 2018	W Pacific	Shinkai Seep Field, Mariana Forearc	5687	S	Chen et al. 2018
P. clathrata Sasaki et al., 2016	W Pacific	Irabu Knoll, Hatoma Knoll, Yaeyama Knoll, Okinawa Trough; Haima seep, South China Sea; Manus Basin	1385–2190	V,S	Sasaki et al. 2016; Miyazaki et al. 2017; Poitrimol et al. 2022; He et al. 2023
P. cooki Linse et al., 2019	Southern	East Scotia Ridge, Southern Ocean	2396–2639	V	Linse et al. 2019
P. exquisita Chen & Watanabe, 2022	W Pacific	Eifuku Volcano, Mariana Arc	1606	V	Chen and Watanabe 2022
P. fenestrata Chen et al., 2019	W Pacific	Crane, Tarama Hill, Okinawa Trough; Sakai vent field; Haima seep, South China Sea	1385–1973	V,S	Chen et al. 2019; He et al. 2023
P. ios Warén & Bouchet, 1986 (Synonymous with: *P. goniata* Warén & Bouchet, 1986)	E Pacific	17 S, 13 N, 21 N, EPR; Guaymas Basin, Gulf of California; Galapagos Rift Zone; Costa Rica Margin	2000–2616	V,S	Waren and Bouchet 1986; Waren and Ponder 1991; Waren and Bouchet 2001; **This study**
P. kuroshimensis Sasaki et al., 2016	W Pacific	Kuroshima Knoll, off Okinawa	644	S	Sasaki et al. 2016
P. laevis Warén & Ponder, 1991 (Synonymous with: *P. glabra* Okutani et al., 1992)	W & E Pacific	Guaymas Basin, Gulf of California; Juan de Fuca; Oregon Margin; Off Hatsushima, Sagami Bay; Minami-Ensei Knoll, Iheya Ridge, Okinawa Trough; Costa Rica Margin	500–2004	V,S	Okutani et al. 1992; Waren and Ponder 1991; Okutani and Fujiwara 2000; Waren and Bouchet 2001; Fujikura et al. 2002; **This study**
P. lomana Warén & Bouchet, 1986	E Pacific	Off San Diego, off Point Dume, California; Oregon Margin; Off San Nicolas	450–1200	V,F	Waren and Bouchet 1986; Waren and Bouchet 2001; Smith and Baco 2003
P. lucida Sasaki et al., 2016	W Pacific	Minami-Ensei Knoll, Okinawa Trough	701	V	Sasaki et al. 2016
P. macleani Warén & Bouchet, 1989	E Pacific	Oregon Margin	2750	F	Waren and Ponder 2001
P. muricata Warén & Bouchet, 1986	E Pacific	21 N, East Pacific Rise; Galapagos Rift	2450–2615	V	Waren and Bouchet 1986; Waren and Ponder 1991
P. nassariaeformis Okutani, 1990	W Pacific	Snail Pit, Mariana Back-Arc Basin; Manus Basin	1912–3680	V	Okutani 1990; Wang et al. 2018
P. pacifica Warén & Bouchet, 1986	E Pacific	Gulf of Panama; Oregon Margin; Costa Rica Margin	1017–2750	F	Waren and Bouchet 1986; Waren and Bouchet 2001; **This study**
P. reticulata Warén & Bouchet, 2009	E Atlantic	Regab, off West Africa	3150	S	Waren and Bouchet 2009
P. sculpta Warén & Ponder, 1991	Gulf of Mexico	Off Louisiana, Gulf of Mexico	576	S	Waren and Ponder 1991; Waren and Bouchet 2001
P. segonzaci Warén & Ponder, 1991	W Pacific	Fiji Back-Arc; Hine Hina, Lau Basin	1750–1900	V	Waren and Ponder 1991; Waren and Bouchet 1993
P. shinkaiae Okutani & Fujikura, 2002	W Pacific	Japan Trench	5343	S	Okutani and Fujikura 2002
P. stephanos Chen et al., 2019	W Pacific	Off Hatsushima, Sagami Bay	860–908	S	Chen et al. 2019; Chen and Nomaki 2021
P. subglabra Sasaki et al., 2016	W Pacific	Hatoma Knoll, Izena Hole, Irabu Knoll, Minami-Ensei Knoll, Yaeyama Knoll, Okinawa Trough; Haima Seep, South China Sea	710–2190	V,S	Sasaki et al. 2016; Miyazaki et al. 2017; Xu et al. 2016; He et al. 2023
P. variabilis Warén & Bouchet, 1986	E Pacific	Endeavor Segment, Axial Seamount, Explorers Ridge, Juan de Fuca Ridge; Oregon Margin	1500–2927	V	Waren and Bouchet 1986; Waren and Bouchet 1993; Waren and Bouchet 2001

Mound 11; 8.922°N, 84.305°W; 1017 m; 3 November 2018; Victoria Orphan, Hang Yu leg.; ALVIN Dive 4988, on wood; SBIC 16955.

Remarks. The range of *P. pacifica* is here expanded to one hydrocarbon seep (Quepos Seep) and one organic fall at the CRM (Mound 11). Their occurrence here on Bathymodiolin mussels represents the first time they have been observed as, potentially, permanent denizens of a hydrocarbon seep environment. Their distribution now includes the Oregon Margin, the Costa Rica Margin, and the Gulf of Panama between 1017–2750 m depth (Table 4).

Morphological analysis

In total, 1,817 *Provanna* specimens were sampled from six sites at the CRM (see Table 1 for details). All specimens were sorted into one of four distinct morphotypes and subsequently assigned the following species identities: *Provanna laevis* (*n* = 1624) sampled from Jaco Summit, The Thumb, and Mound 12, *Provanna ios* (*n* = 180) sampled from Jaco Scar, *Provanna pacifica* (*n* = 9) sampled from Quepos Seep and Mound 11, and *Provanna* cf. *lomana* (*n* = 2) sampled from Mound 11 (Fig. 4). Provanna *laevis* was identified as it is the only smooth-shelled species from the Eastern Pacific. Our specimens of *P. ios* fit most closely the morphological description of *P. goniata* and were originally designated as such (Warén and Bouchet 1986; Betters et al. 2023) However, given our genetic results (detailed in the Results section Genetic Analysis), we amend this original identification to *P. ios* and address the validity of *P. goniata* as a distinct species in the Discussion. Specimens of *P. pacifica* were identified based on their sculpturing, their relatively small size, and the fact that this species was originally described from a soft-bottom, low-productivity seep in the Gulf of Panama very similar to its habitat at Costa Rica (Warén and Bouchet 1986). *Provanna* cf. *lomana* was tentatively identified by its unique feature of having only axial sculpturing on its body whorl. Of these specimens, a total of 158 representative *Provanna* covering the full geographic, temporal, and size range of each morphotype were measured (*P. laevis*, *n* = 96; *P. ios*, *n* = 52; *P. pacifica*, *n* = 8; and *P.* cf. *lomana*, *n* = 2). Representative radulae were successfully extracted and imaged for all species except *P.* cf. *lomana* (Fig. 5).

Across all Costa Rican specimens, measurements of shell length, shell width, aperture length, and aperture width showed significant collinearity (PCC > +0.95, all pairs). Because the whorls past the body whorl showed variable levels of degradation, shell size was represented in analyses by aperture length alone, as we had more confidence in this measurement. All species sampled were comparable in size, with *Provanna ios* being the largest and *P. pacifica* being the smallest (Fig. 6B). The number of basal ribs, despite being commonly used to describe *Provanna* species, showed variation across all morphotypes (Fig. 6C). The difference in relative texture between *P. ios* and *P. pacifica* was significant ($p < 0.001$), supporting the utility of their sculptural elements in delineating species (Fig. 6D). In general, shells with granules longer than 3% of the shell length (major spines) were reliably *P. ios*. *Provanna ios* had the most oblique shell shape overall (Fig. 6E) and *P. laevis* had the most oblique aperture shape overall (Fig. 6F).

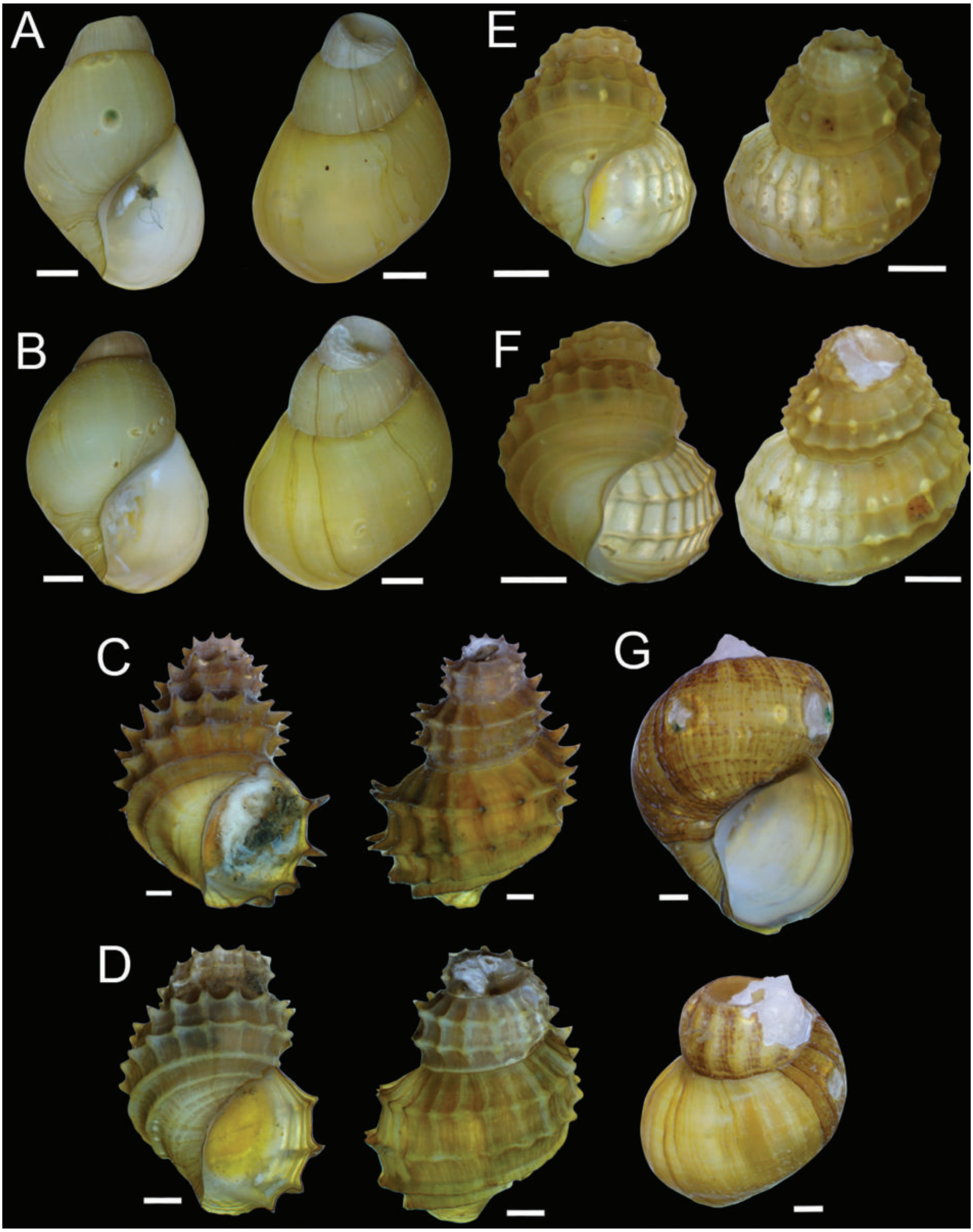

Figure 4. *Provanna* morphotypes sampled from the CRM **A, B** *P. laevis* from mussel shells, Mound 12, AD4917, 965 m **C, D** *P. ios* from unknown substrate, Jaco Scar, SD214, 1803 m **E** Specimens of *P. pacifica* from sunken wood, Mound 11, AD4988, 1017 m **F** Specimen of *P.* cf. *lomana* from mussel shells, Quepos Seep, AD4924, 1413 m. Both the dorsal and ventral view of each shell is shown. Scale bars: 1 mm.

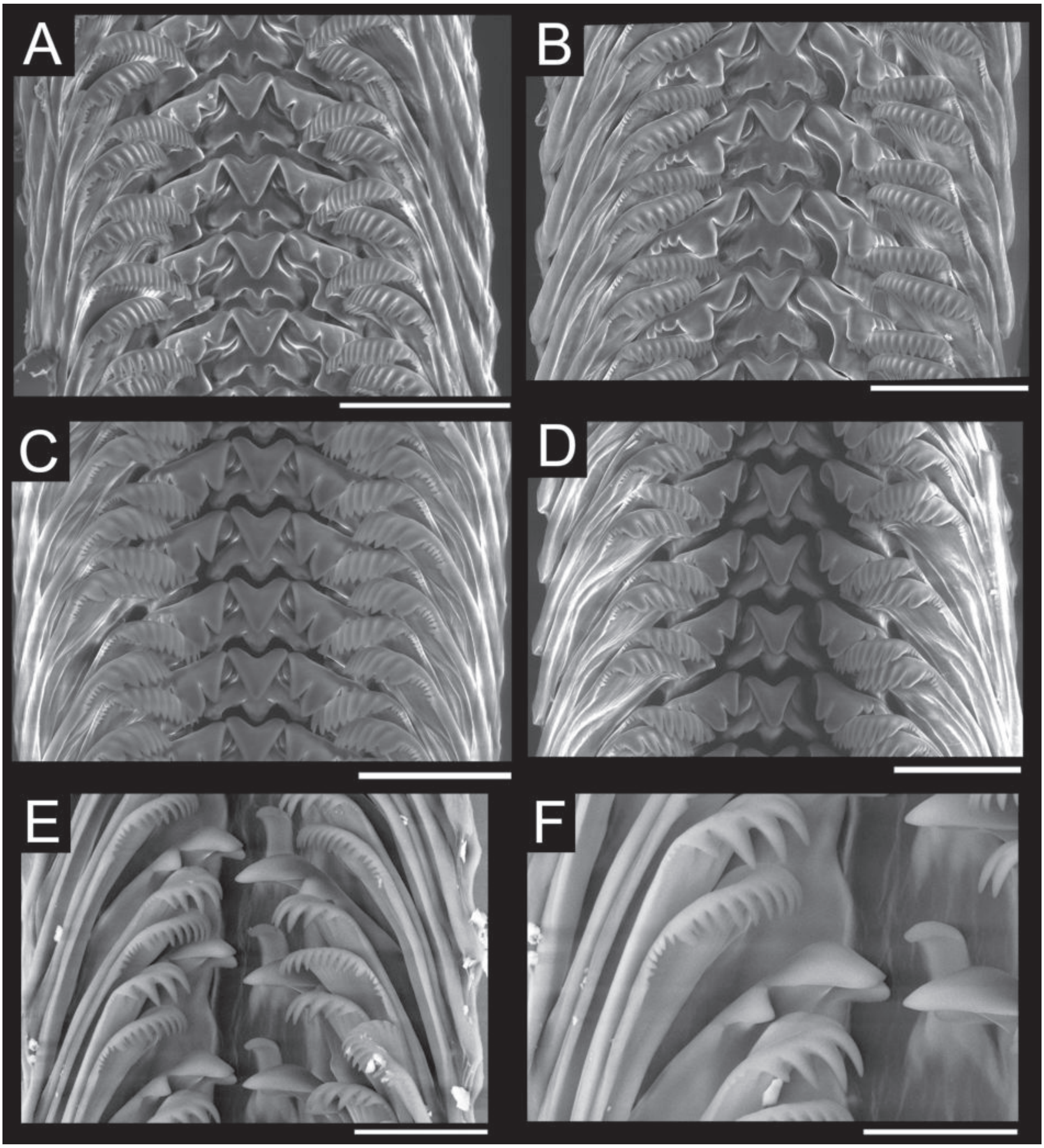

Figure 5. Representative radulae of Costa Rican *Provanna* species **A** *P. laevis* from mussel shells **B** *P. laevis* from unknown substrate **C** *P. ios* from mussel shells **D** *P. ios* from unknown substrate **E, F** *P. pacifica* from wood. Scale bars: 20 µm (**F**); 30 µm (**E**); 40 µm (**C**); 50 µm (**A, B, D**).

Genetic analysis

CO1 sequences were obtained from our specimens of *P. laevis* (*n* = 4), *P. ios* (*n* = 2), and *P. pacifica* (*n* = 2). All efforts to amplify CO1 for specimens of *P.* cf. *lomana* were unsuccessful. CO1 sequences generated were uploaded to GenBank and assigned accession numbers (OM914402–OM914408 & OP577954). H3

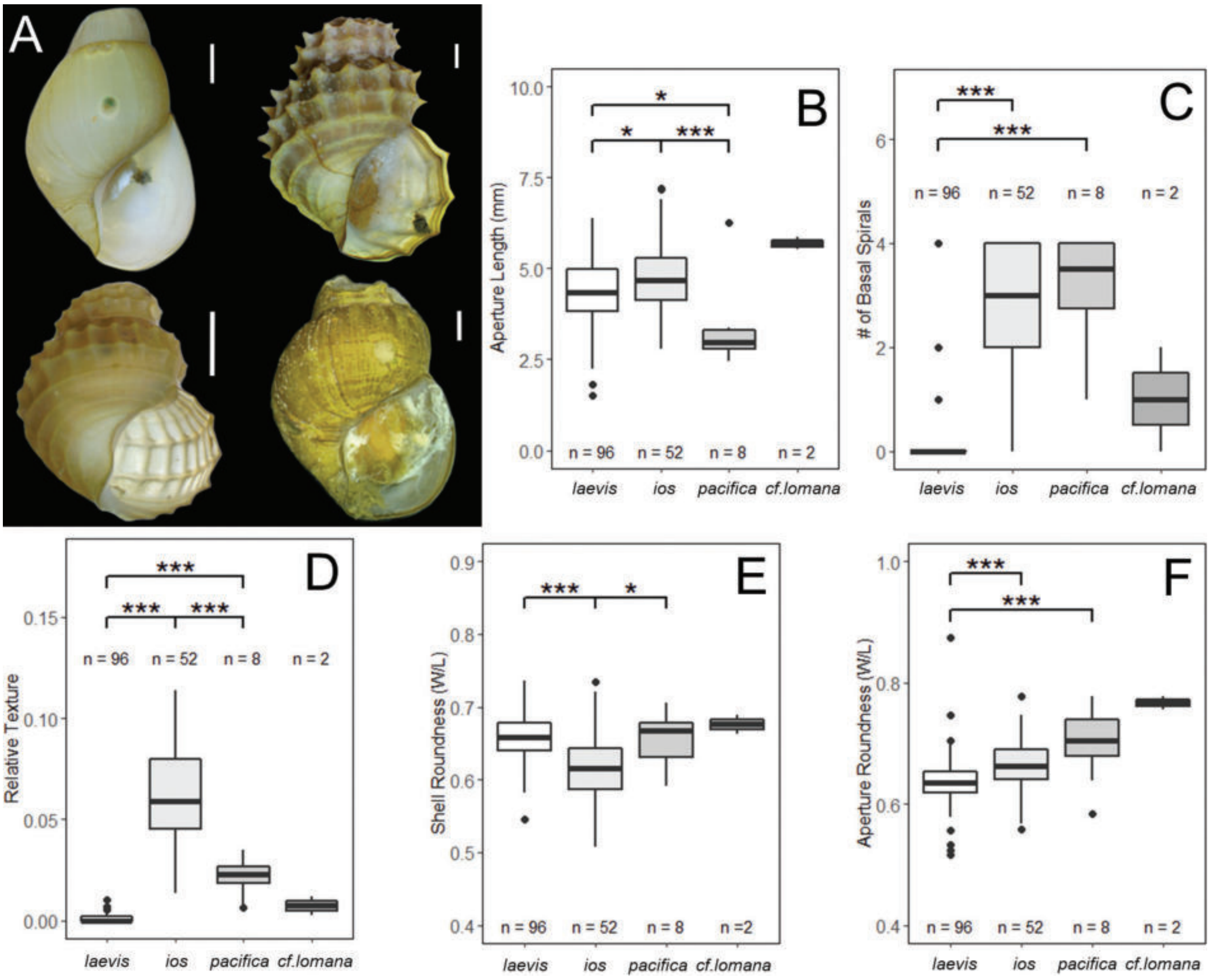

Figure 6. A the four morphotypes sampled **B–F** comparison of morphological traits among each morphotype. The number of individuals represented on the graph and included in one-way ANOVAs are denoted by "*n* =" above or below each bar. Resultant p-values from one-way ANOVAs are denoted above each graph (p-value: 0 < *** < 0.001 < ** < 0.01 < * 0.05). *Provanna* cf. *lomana* was excluded from all ANOVAs due to the small number of individuals, but is included here for graphical comparison. Note that the graphs of Shell Roundness **E** and Aperture Roundness **F** have y-axes that do not start at zero. Scale bars: 1 mm.

sequences were obtained from our specimens of *P. laevis* (*n* = 1), *P. ios* (*n* = 2), *P. pacifica* (*n* = 2), and *P.* cf. *lomana* (*n* = 1). H3 sequences generated were uploaded to GenBank and assigned accession numbers (OR687645–OR687650).

Phylogenetic analyses support the inclusion of our specimens in the genus *Provanna* with high confidence for CO1 (Bayesian Posterior Probability (BPP) = 100, ML = 90) (Fig. 7A) and H3 (BPP = 100, ML = 93) (Fig. 7B). Species-level investigations showed that sequences from the same *Provanna* species nested together and away from others on the tree (Fig. 8). Our specimens of *P. laevis* nested among *P. laevis* and *P. glabra* with high confidence and little to no distinction (BPP = 100, Bootstrap = 92). Despite our samples matching the physical description of *P. goniata*, these grouped together with sequences of *P. ios* and *P.* aff. *ios* with moderate confidence (BPP = 85). These were, however, all delineated as the sister group to *P. variabilis* (BPP = 100, Bootstrap = 80). Our specimens of *P. pacifica* grouped together and away from all

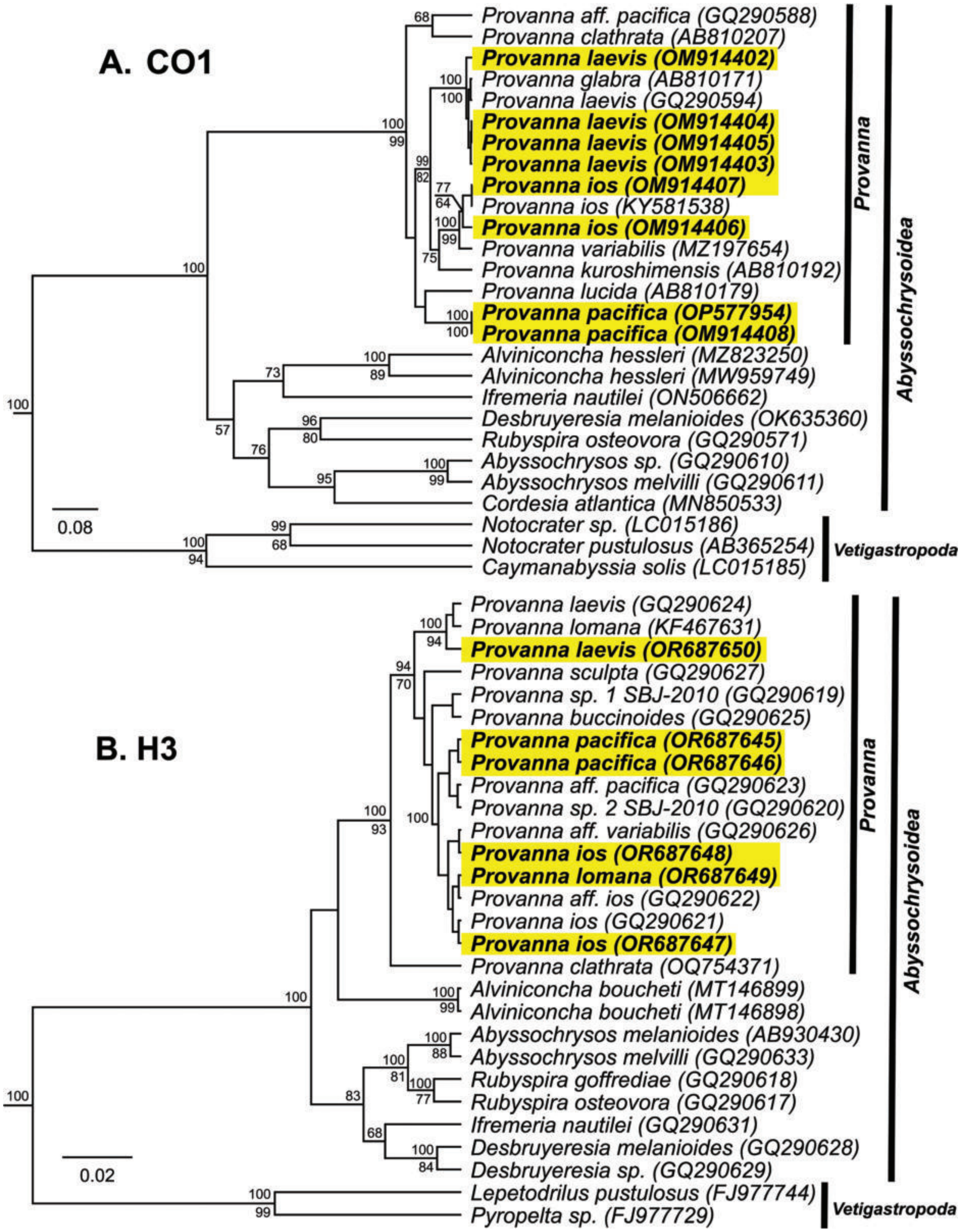

Figure 7. Bayesian topology of Abyssochrysoid gastropod mollusks **A** topology based on a 449 bp region of the mitochondrial CO1 gene. Topology was inferred using the HKY+G+I substitution model **B** topology based on a 266 bp region of the nuclear H3 gene. Novel sequences are bolded and highlighted in yellow. Numbers above branch nodes represent Bayesian posterior probabilities. Numbers below branch nodes represent the proportion of replicate trees in which the associated taxa clustered together in the bootstrap test (10,000 replicates). Only values above 50% are shown. The tree is drawn to scale, with branch lengths representing the number of base substitutions accumulated over time.

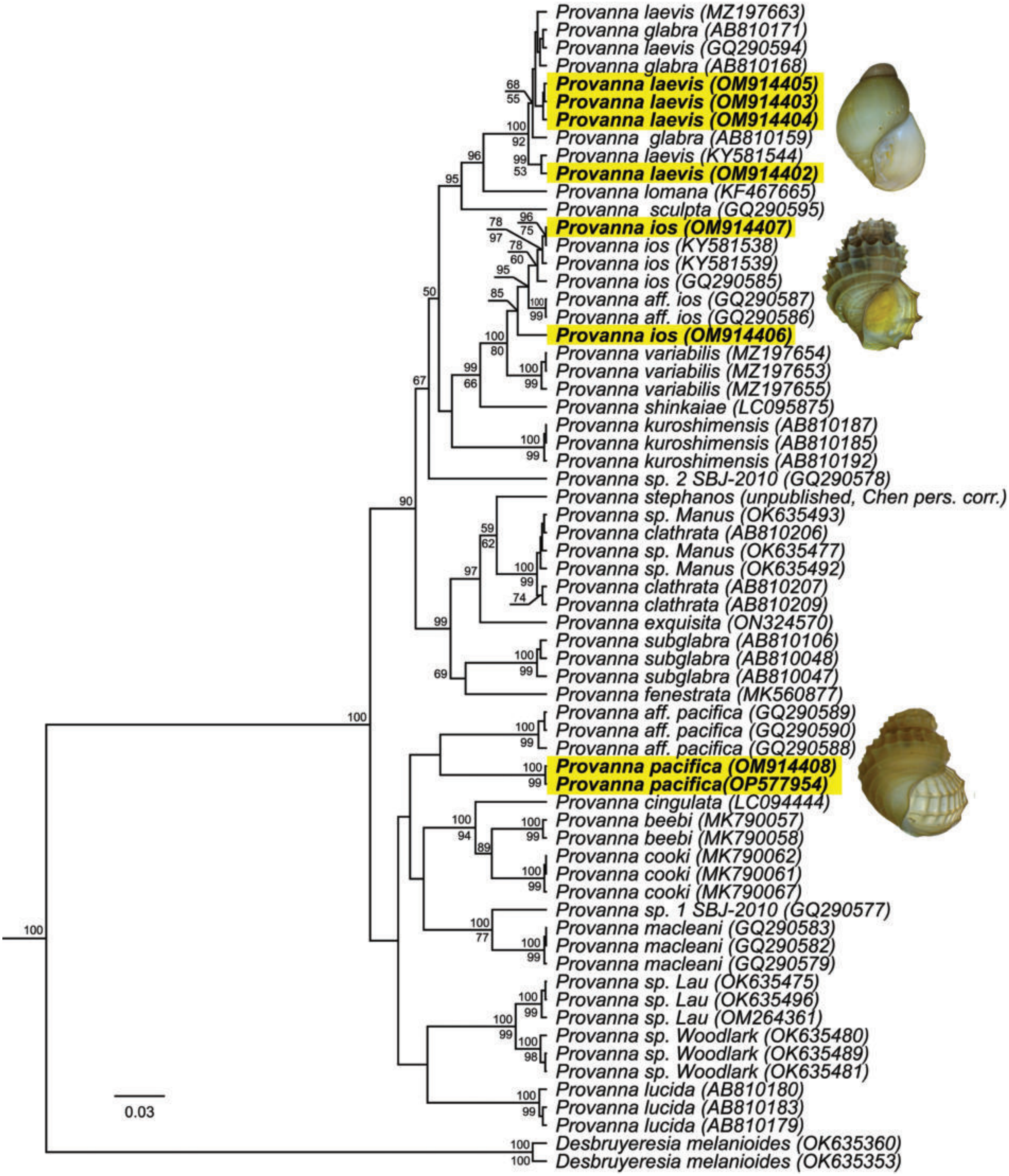

Figure 8. Bayesian phylogenetic tree of *Provanna* based on a 452 bp region of the mitochondrial CO1 gene. Novel sequences are bolded and highlighted in yellow. Topology was inferred using the HKY+G+I substitution model. Numbers above branch nodes represent Bayesian posterior probabilities. Numbers below branch nodes represent the proportion of replicate trees in which the associated taxa clustered together in the bootstrap test (10,000 replicates). Only values above 50 are shown. The tree is drawn to scale, with branch lengths representing the number of base substitutions accumulated over time.

other species on the tree (BPP = 100, Bootstrap = 99), though they were most closely related to *P.* aff. *pacifica*. However, given that *P. pacifica* has never been barcoded before, and that our specimens closely match the physical description and geographic distribution of the species proper, we assert that our specimens are indeed *P. pacifica*.

Sequences of unknown identity (*Provanna* sp. 1 (GQ290577) and *Provanna* sp. 2 (GQ290578)) did not group together with any known species on the tree. Sequences from the Manus Basin that were previously identified as *P. clathrata* (Poitrimol et al. 2022) nested with high confidence among sequences of *P. clathrata* from the Okinawa Trough (Sasaki et al. 2016) (BPP = 100, Bootstrap = 99), confirming this identification and the range expansion for this species (see Table 4). As previously found, sequences from the Woodlark and Lau Basins group apart from all other known species on tree, as well as each other (Poitrimol et al. 2022) (BPP = 100, Bootstrap = 99). However, more detailed morphological investigations are needed to address whether these represent *P. buccinoides*, *P. segonzaci*, or one or more new species.

Average pairwise sequence divergences (APD) were computed across CO1 sequences (*n* = 236) (Table 5). APD calculations confirmed *Provanna* species as being more closely related to each other than to the outgroup (ingroup < 0.2 < outgroup). Almost all APD calculations fell between 0.05–0.13, confirming robust species distinctions overall within this genus (Hebert et al. 2003; Johnson et al. 2008). One exception to this was *P. glabra* and *P. laevis*, which showed very low sequence divergence (APD = 0.01, SE = 0.00).

Table 5. Genetic distance estimates among and within known *Provanna* species. Distances were calculated using the Tamura 3-parameter model and 5,000 bootstrap replicates. Numbers below central margin represent the number of base substitutions per site, averaging over all sequence pairs. Numbers above central margin represents standard errors. The central margin represents within-group genetic distances. Calculations were conducted using 236 total nucleotide sequences. Outgroup = *Desbruyeresia melanioides*.

Provanna	**1**	**2**	**3**	**4**	**5**	**6**	**7**	**8**	**9**	**10**	**11**	**12**	**13**	**14**	**15**	**16**	**17**	**18**	**19**	**20**
1. beebi	0.00	*0.01*	*0.02*	*0.01*	*0.02*	*0.02*	*0.02*	*0.02*	*0.02*	*0.02*	*0.02*	*0.02*	*0.02*	*0.01*	*0.02*	*0.02*	*0.01*	*0.02*	*0.02*	*0.03*
2. cingulata	0.06	NA	*0.02*	*0.01*	*0.03*	*0.02*	*0.02*	*0.02*	*0.02*	*0.02*	*0.02*	*0.02*	*0.02*	*0.02*	*0.02*	*0.02*	*0.02*	*0.02*	*0.02*	*0.03*
3. clathrata	0.11	0.12	0.01	*0.02*	*0.02*	*0.01*	*0.02*	*0.02*	*0.02*	*0.02*	*0.02*	*0.02*	*0.02*	*0.02*	*0.02*	*0.02*	*0.01*	*0.01*	*0.02*	*0.03*
4. cooki	0.06	0.06	0.11	NA	*0.02*	*0.02*	*0.02*	*0.02*	*0.02*	*0.02*	*0.02*	*0.02*	*0.02*	*0.02*	*0.02*	*0.02*	*0.02*	*0.02*	*0.02*	*0.03*
5. exquisita	0.09	0.11	0.08	0.09	NA	*0.02*	*0.02*	*0.02*	*0.02*	*0.02*	*0.02*	*0.03*	*0.03*	*0.02*	*0.02*	*0.03*	*0.02*	*0.02*	*0.02*	*0.05*
6. fenestrata	0.11	0.11	0.08	0.10	0.08	NA	*0.02*	*0.02*	*0.01*	*0.02*	*0.01*	*0.02*	*0.02*	*0.02*	*0.02*	*0.02*	*0.01*	*0.02*	*0.02*	*0.03*
7. glabra	0.09	0.12	0.11	0.10	0.08	0.09	0.01	*0.01*	*0.02*	*0.00*	*0.01*	*0.02*	*0.02*	*0.02*	*0.02*	*0.02*	*0.02*	*0.02*	*0.01*	*0.04*
8. ios	0.10	0.11	0.10	0.11	0.08	0.10	0.08	0.02	*0.01*	*0.01*	*0.01*	*0.02*	*0.02*	*0.02*	*0.01*	*0.01*	*0.02*	*0.02*	*0.01*	*0.04*
9. kuroshimensis	0.10	0.11	0.11	0.09	0.10	0.08	0.08	0.08	0.01	*0.02*	*0.01*	*0.02*	*0.02*	*0.01*	*0.02*	*0.02*	*0.02*	*0.02*	*0.01*	*0.03*
10. laevis	0.09	0.11	0.10	0.10	0.08	0.09	0.01	0.07	0.08	0.01	*0.01*	*0.02*	*0.02*	*0.02*	*0.01*	*0.02*	*0.02*	*0.02*	*0.01*	*0.04*
11. lomana	0.10	0.10	0.10	0.08	0.07	0.08	0.06	0.08	0.07	0.07	NA	*0.02*	*0.02*	*0.02*	*0.01*	*0.02*	*0.02*	*0.02*	*0.01*	*0.03*
12. lucida	0.13	0.12	0.11	0.11	0.12	0.12	0.14	0.13	0.11	0.14	0.12	0.00	*0.02*	*0.02*	*0.02*	*0.02*	*0.02*	*0.02*	*0.02*	*0.03*
13. macleani	0.09	0.10	0.11	0.09	0.10	0.10	0.09	0.11	0.09	0.09	0.11	0.12	0.00	*0.02*	*0.02*	*0.02*	*0.02*	*0.02*	*0.02*	*0.03*
14. pacifica	0.08	0.09	0.08	0.09	0.08	0.08	0.09	0.09	0.08	0.09	0.08	0.10	0.09	0.00	*0.01*	*0.02*	*0.01*	*0.02*	*0.02*	*0.03*
15. sculpta	0.09	0.10	0.08	0.09	0.06	0.08	0.08	0.08	0.08	0.08	0.06	0.13	0.11	0.08	NA	*0.02*	*0.01*	*0.02*	*0.01*	*0.03*
16. shinkaiae	0.09	0.11	0.10	0.11	0.10	0.11	0.09	0.06	0.09	0.09	0.09	0.11	0.11	0.10	0.09	NA	*0.02*	*0.02*	*0.01*	*0.04*
17. stephanos	0.09	0.10	0.04	0.10	0.05	0.07	0.10	0.08	0.09	0.09	0.08	0.10	0.10	0.07	0.07	0.10	NA	*0.01*	*0.01*	*0.03*
18. subglabra	0.10	0.10	0.07	0.11	0.08	0.09	0.10	0.10	0.12	0.10	0.09	0.14	0.11	0.12	0.09	0.11	0.08	0.01	*0.02*	*0.03*
19. variabilis	0.11	0.11	0.11	0.11	0.08	0.10	0.08	0.04	0.08	0.08	0.08	0.13	0.11	0.10	0.08	0.07	0.09	0.11	0.03	*0.03*
20. Outgroup	0.23	0.24	0.22	0.25	0.24	0.24	0.26	0.27	0.24	0.26	0.25	0.24	0.22	0.25	0.25	0.28	0.24	0.24	0.26	0.01

Provanna variabilis also appeared closely related to *P. ios* (APD = 0.04, SE = 0.01), supporting the topology from Fig. 8 designating them as sister clades. Comparisons within species were limited to those with more than one representative CO1 sequence, thus excluding *P. cingulata*, *P. cooki*, *P. exquisita*, *P. fenestrata*, *P. lomana*, *P. sculpta*, *P. shinkaiae*, and *P. stephanos*. Of the remaining species, average within-species APD's fell below 0.03, confirming that intraspecific divergence was lower than interspecific divergence across *Provanna* species.

Hierarchical clustering performed by ASAP yielded 14 discreet subsets from an input of 19 hypothesized species (*n* = 236 sequences, $p < 0.0001$): (1) *P. glabra*-*P. laevis*, (2) *P. variabilis*-*P. ios*, (3) *P. pacifica*, (4) *P. fenestrata*, (5) *P. cooki*, (6), *P. beebi*, (7), *P. cingulata*, (8) *P. exquisita*-*P. stephanos*-*P. clathrata*, (9) *P. sculpta*, (10) *P. lomana*, (11) *P. macleani*, (12) *P. subglabra*, (13) *P. kuroshimensis*, (14) *P. lucida*. The threshold distance (Dt) used to partition the samples into species was 0.0496 ($p < 0.0001$) and the most common genetic distance between sequence pairs fell between 0.09–0.1.

Polytomous key for species identification

1 Only axial sculpturing **2**
– Only spiral sculpturing **3**
– Both axial and spiral sculpturing **4**
– No sculpturing present **5**
2 Axial sculpture extends to the posterior end of the aperture, but not into the basal area .... ***P. lomana***
– Axial sculpture does not extend to the posterior end of the aperture, instead stopping midway down the body whorl .... ***P. chevalieri***
3 Shell is thin and translucent; One can easily see through the shell **6**
– Shell is not noticeably translucent; One cannot easily see through the shell **7**
4 Sculptural elements absent **9**
– Sculptural elements present **10**
5 Sculptural elements present .... ***P. beebi***
– Sculptural elements absent **26**
6 1–3 spiral ribs on the body whorl above the posterior end of the aperture .... ***P. lucida***
– 4 or more spiral ribs on the body whorl above the posterior end of the aperture .... ***P. cingulata***
7 Central radular teeth highly diminished, being very narrow with a very truncated, cusp (see Fig. 2C for definitions) .... ***P. macleani***
– Central radular teeth broad with a truncated cusp and a flat or rounded anterior ridge .... ***P. beebi***
– Central radular teeth broad with a very short cusp and concave anterior ridge .... ***P. reticulata***
– Central teeth are typical of genus with a triangular cusp **8**
8 First lateral teeth have long, lobate major denticles and an obtuse buttress angle (see Fig. 2C for definitions) .... ***P. cooki* (see Discussion)**
– First lateral teeth have long, triangular major denticles and an acute buttress angle .... ***P. variabilis* (see Discussion)**

9 Axial and spiral sculptures are strong, raised, and equally spaced, creating a regular lattice-like sculpture (see Fig. 3D for example **11**
– Regular, lattice-like sculpture is not formed **12**
10 Sculptural elements are major spines (see Fig. 2A for definitions) **13**
– Sculptural elements are minor spines **14**
– Sculptural elements are punctuated, rounded beads **15**
– Sculptural elements are blunt and sloping nodules **16**
11 There are more than 30 axial ribs on the body whorl and 2–3 spiral ribs .... ***P. admetoides***
– There are 15–20 spiral ribs on the body whorl and 1–2 spiral ribs .... ***P. fenestrata***
12 Central radular teeth highly diminished and narrow with a very truncated, cusp (see Fig. 2C for definitions) .... ***P. macleani***
– Central radular teeth broad with a short cusp and a flattened anterior ridge .... ***P. chevalieri***
13 Major spines on the second or third spiral rib on the body whorl connect at times to form a flattened shelf or keel **17**
– Major spines do not obviously connect nor do they form a flattened keel **18**
14 There are more than 30 axial ribs on the body whorl, forming a regular, lattice-like sculpture .... ***P. admetoides***
– There are fewer than 30 axial ribs on the body whorl **19**
15 Shell globose; Shell roundness (Shell Width / Truncated Length) (see Fig. 2B) > 0.65 .... ***P. nassariaeformis***
– Shell not globose; Shell roundness < 0.65 .... **22**
16 Axial and spiral sculptures are strong, evenly raised, and equally spaced, creating a regular lattice-like sculpture (see Fig. 3D for example) .... ***P. fenestrata***
– Axial and spiral sculptures vary in strength across the body whorl; Regular, lattice-like sculpture is not formed **23**
17 Axial ribs form clear cords that are present along the entire body whorl, rectangular lattice-like sculpturing formed (see Fig. 3D for example) .... ***P. exquisita***
– Axial ribs vary in strength along the body whorl, sometimes disappearing entirely, no clear lattice-like sculpturing formed .... ***P. stephanos***
18 Shell is very slender; Shell roundness (Shell Width / Truncated Length) (see Fig. 2B) < 0.55 .... ***P. shinkaiae* (see Discussion)**
– Shell roundness > 0.55 .... ***P. ios* (previously *P. goniata*) (see Discussion)**
19 Central radular teeth highly diminished and narrow with a very truncated, cusp (see Fig. 2C for definitions) .... ***P. pacifica***
– Central radular teeth broad with a very short, blunt cusp .... ***P. reticulata***
– Central radular teeth are typical of genus with a triangular cusp **20**
20 Anterior end of aperture has a round, globose shape .... ***P. muricata***
– Anterior end of aperture has elongated, tapering shape **21**
21 First lateral teeth have major denticles that are notched on the internal edge and rounded (see Fig. 2C for definitions) .... ***P. segonzaci***
– First lateral teeth have major denticles that are not notched **22**
22 Shell is globose; Shell roundness (Shell Width / Truncated Length) (see Fig. 2B) ≥ 0.6 .... ***P. clathrata* (see Discussion)**
– Shell is slender; Shell roundness ≤ 0.55 .... ***P. ios* (previously *goniata*) (see Discussion)**

23 Sculptural elements appear as small pockmarks and extend to the anterior end of the shell...***P. beebi***

– Sculptural elements appear as flat lines of beads arranged longitudinally, stopping abruptly at the first basal rib ....***P. sculpta***

24 Axial sculpture varies in strength across the body whorl, sometimes disappearing entirely or extending only part of the way down the body whorl..... ....***P. variabilis***

– Axial sculpture is strong and even along the body whorl **25**

25 Central radular teeth are highly diminished and narrow with a very truncated, cusp (see Fig. 2C for definitions) ....***P. pacifica***

– Central radular teeth are broad with blunt cusps and rounded or flat anterior ridges...***P. buccinoides***

– Central radular teeth are typical of genus with triangular cusps..............**26**

26 First lateral teeth have major denticles that are notched interiorly and lobate (see Fig. 2C for definitions)... ***P. segonzaci***

– Marginal teeth alternate in form between having 15–20 denticles .... ***P. muricata***

– Marginal teeth all have between 9–10 denticles .... ***P. clathrata***

27 Shell is thin and translucent, one can easily see the body through the shell..**28**

– Shell is not noticeably translucent **29**

28 Central radular teeth have a long, triangular cusp; first lateral teeth have major denticles that are long and lobate (see Fig. 2C for definitions)......... ....***P. annae*** **(see Discussion)**

– Central radular teeth have a short, triangular cusp; first lateral teeth have major denticles that are long and triangular.......***P. lucida*** **(see Discussion)**

29 Shell suture is highly constricted, giving the whorls an inflated, rounded appearance **30**

– Shell suture is not highly constricted...**31**

30 Shell roundness (Shell Width / Truncated Length) (see Fig. 2B) ~ 0.5........ ....***P. abyssalis***

– Shell roundness ~ 0.6 ....***P. cooki***

31 First lateral teeth have very truncated, short denticles................... ***P. laevis***

– First lateral teeth have long major denticles **32**

32 Central teeth have short, blunt cusps; lateral teeth have major denticles that are long, lobate (see Fig. 2C for definitions)..... ***P. laevis*** **(previously *P. glabra*)**

– Central teeth have long, sharp, triangular cusps; lateral teeth have major denticles that are long, lobate .... ***P. kuroshimensis*** **(see Discussion)**

– Central teeth have long, sharp, triangular cusps; lateral teeth have major denticles that are long, sharp .... ***P. subglabra*** **(see Discussion)**

Discussion

This study presents new records and gene sequences for *P. laevis*, *P. ios*, *P. pacifica*, and *P.* cf. *lomana* from the Costa Rica Margin. Integrating these novel morphological and genetic data, we review the distinction among species and present the first polytomous identification key for the genus *Provanna*. In both our morphological and genetic investigations, similarities among species were revealed and are discussed below.

Cryptic species

Several *Provanna* species show little to no morphological distinction. For example, certain shell morphotypes of *P. clathrata* and *P. ios* have no discernable differences from one another besides the number of denticles on their outer marginal teeth (*P. clathrata* have about ten while *P. ios* have about 20) (Table 3). Certain shell morphotypes of *P. ios* and *P. shinkaiae* may also resemble one another. Yet, the lobate major denticles of *P. shinkaiae*'s first lateral teeth distinguish it from *P. ios*. Depending on morphotype, *P. cooki* and *P. variabilis* may also display criticism. Both may have no axial ribs, three spiral ribs on the body whorl, and no sculptural elements. However, they may be distinguished by the shape of the major denticles of their first lateral teeth (Table 3). Finally, *P. annae* and *P. lucida* both have unsculptured, translucent shells with constricted sutures. Their distinguishing feature is the shape of the major denticles of their first lateral teeth (*P. annae* are lobate, *P. lucida* are triangular). Regardless of the reliability of these radular characteristics, each of these species pairs may also be readily distinguished through CO1 barcoding (Table 5) (Nekhaev 2023).

The smooth-shelled species *P. laevis*, *P. glabra*, *P. kuroshimensis*, and *P. subglabra* are also morphologically indistinguishable based on shell characters (Table 3). All species have no sculpturing, slender shells, and a flattened suture. Provanna *subglabra* may be distinguished from the other three by having long, sharp major denticles on its first lateral teeth. Similarly, *P. laevis* should be distinguishable by having truncated, lobate denticles on its first lateral teeth and its location in the Eastern Pacific. Contrary to expectations, the radulae of our specimens from the CRM closely resembled that of *P. glabra* or *P. kuroshimensis* with long, lobate major denticles (Fig. 5A, B). Genetic characterization could not distinguish *P. laevis* from *P. glabra*, but could readily distinguish *P. kuroshimensis* (Fig. 8, Table 5).

Specimens collected from the Costa Rica Margin revealed that not all shell characters are useful in delineating species. Despite its widespread use in taxonomic descriptions, the number of basal ribs showed notable variation within species. Furthermore, as basal ribs are often very weak and difficult to count consistently, these were not used as a taxonomically informative characters in the key, nor do we recommend their use in distinguishing species in the future.

Species delimitation

Our genetic investigations supported most current taxonomic delimitations, finding robust genetic distances among the 19 species from which CO1 sequences exist. Nonetheless, automatic partitioning based on CO1 supported the consolidation of several species. *Provanna variabilis* and *P. ios*, for example, were not partitioned. However, as these species are distinguished in both our phylogenetic analyses as well as by their morphological characteristics, more data are needed to verify this genetic similarity before taxonomic revision is undertaken. Similarly, the species *P. exquisita*, *P. stephanos*, and *P. clathrata* were also not partitioned. However, as these are also distinguished in our phylogenetic analyses and by their shell and radular characteristics, we believe more data are needed to warrant collapse.

Provanna laevis from the Eastern Pacific and *P. glabra* from the Western Pacific exhibited significant genetic overlap in our species-level phylogeny (Fig. 8), our distance matrix (Table 5) and were not distinguished during automatic partitioning. This similarity has been noted by previous studies (Sasaki et al. 2016; Linse et al. 2019). Given that CO1 seems informative for the rest of this genus, this similarity is noteworthy. Both *P. laevis* and *P. glabra* inhabit similar depth ranges, a variety of chemosynthesis-based environments, and are morphologically indistinct in all but radular morphology (Warén and Bouchet 1986; Okutani et al. 1992), which may not be sufficient to indicate complete lineage sorting. They have typically been distinguished by their distributions. Nevertheless, there may be numerous, undiscovered chemosynthetic sites, including large biomass falls (e.g., whale falls) that could provide the stepping stones necessary for connectivity across the Pacific. Furthermore, Pacific northern equatorial and subsurface counter currents may transport upper and lower layers of water, respectively, from west to east along the 7°N latitude (Kessler 2006), coinciding neatly with the region of study in Costa Rica (~ 8–9°N). Conversely, water upwelled at the Costa Rica Dome may flow east across the Pacific via the Northern Equatorial Current (Kessler 2006) and into the North Pacific Gyre, where it may realistically encounter the Eastern shores of Japan and even the Western shores of North America. Recent work supports the highly adaptable nature of *P. laevis*, which may explain a very broad distribution (Betters et al. 2023). Given these morphological, genetic, and biogeographic data, collected over several independent studies (Sasaki et al. 2016; Linse et al. 2019; Betters et al. 2023) and supported once again here, it is thus recommended that *P. glabra* and *P. laevis* be considered one species. As *P. glabra* is the younger name, we here synonymize it with *P. laevis*, as per the International Code of Zoological Nomenclature Article 23.1. These species are thus treated as synonymous hereafter.

Specimens of *P. ios* from the CRM were originally identified as *P. goniata*, given that their shells are decorated with major spines rather than minor spines (Fig. 4C, D) and that they are found at hydrocarbon seeps, rather than that at hydrothermal vents (Betters et al. 2023). We first reconsidered this identification when genetic barcoding of both CO1 and H3 could not reliably distinguish these specimens from *P. ios* (Figs 7, 8, Table 5). Furthermore, recent work has found that when specimens at the CRM were sampled from higher concentrations of hydrocarbons and sulfides, they tended to have more slender, thinner, and larger shells (Betters et al. 2023). This means that as they inhabit more vent-like conditions, they resemble more closely the vent species *P. ios* (Table 3). Thus, it is highly likely that these two species are actually ecotypes of a single molecular taxonomic unit, where *P. ios* is the vent ecotype and *P. goniata* is the seep ecotype. Additionally, both species are found at similar depths in the Eastern Tropical Pacific. Given that this study presents one of the most extensive collections of the morphospecies *P. goniata* known to date and is the first to genetically characterize them, we suggest that *P. goniata* and *P. ios* are one species. As *P. goniata* is the younger name, we here synonymize it with *P. ios*, as per the International Code of Zoological Nomenclature Article 23.1. These species are thus treated as synonymous hereafter.

Biogeography

Provanna are currently found in nearly every oceanic basin (Table 4). While many original descriptions distinguish species based on oceanic basin, the effect of geographic distance on population divergence of these gastropods from chemosynthetic habitats remains unclear (Distel et al. 2000; Vrijenhoek 2010; Breusing et al. 2023). For instance, while *P. laevis* (inclusive of *P. glabra*) spans the entire perimeter of the Northern Pacific Gyre with little genetic distinction, *P. laevis*, *P. kuroshimensis*, *P. lucida*, and *P. subglabra* all have overlapping biogeographic ranges at the Okinawa Trough yet display marked genetic divergence. *Provanna* are also notably adaptable across habitats, with six species currently known from more than one chemosynthesis-based ecosystem. These results indicate that more work is still needed to understand the drivers of genetic variation and isolation within this genus across a variety of contexts.

Finally, this study amends the biogeographic distribution of *P. muricata*. This species is listed as present in the North Fiji and Lau Basins in several secondary sources (Sasaki et al. 2016; Linse et al. 2019) based on Desbruyeres et al. (2006). This resource, however, does not present new records of occurrence, and instead summarizes known occurrence records. However, no primary literature nor museum specimens exist that place this species there. Therefore, until specimens are collected from the Western Pacific Basins and positively identified as *P. muricata*, this study proposes an amendment to their published biogeographic range, limiting it to the Eastern Pacific vents from which they were first found and described (Table 4).

Conclusions

This study expands the ranges of *P. laevis*, *P. ios*, and *P. pacifica* to hydrocarbon seeps at the Pacific Costa Rica Margin. We also present a thorough review of the genus *Provanna*, consolidating the geographic distributions, genetics, and morphology for each extant species. We find that shell and radular morphological characters may be used to identify *Provanna* species and present the first identification key for this group. We also find that current species delineations within the genus *Provanna* are, for the most part, well-supported by genetic data. For those that are not, we herein synonymize *P. glabra* with *P. laevis* and *P. goniata* with *P. ios*. Future work will no doubt reveal new morphological varieties, species, and occurrences of *Provanna* snails. This key is designed to be a starting point from which researchers may begin this vital work.

Acknowledgements

We thank the crews of the R/V Falkor during FK19-0106, the R/V Atlantis during AT37-10, AT37-13, and AT42-03, as well as the operating teams of HOV ALVIN, ROV SUBASTIAN, and AUV Sentry from 2017–2019. We thank Ellen Strong, Greg Rouse, Charlotte Seid, Daniel Geiger, and Shannon Johnson for providing material that benefitted this project. We thank Dmitriy Dikin for his assistance in capturing scanning electron microscope images as well as Chloe Berger and Liv Nguyen for their molecular laboratory assistance. We also thank the science team aboard the R/V Thompson cruise TN401 for volunteering to test an early draft of this key. We thank Chong Chen, Eike Neubert, and one anonymous reviewer for their valuable feedback which improved this manuscript. Finally, we thank the people and nation of Costa Rica for allowing us to conduct this scientific research in their national waters.

Additional information

Conflict of interest

The authors have declared that no competing interests exist.

Ethical statement

No ethical statement was reported.

Funding

This research was supported by the National Science Foundation (OCE 1635219), Temple Uni-versity, and the American Malacological Society.

Author contributions

Conceptualization: EEC, MJB. Data curation: MJB. Formal analysis: MJB. Funding acquisition: EEC. Investigation: MJB. Methodology: MJB. Supervision: EEC. Validation: EEC. Visualization: MJB. Writing – original draft: MJB. Writing – review and editing: EEC.

Author ORCIDs

Melissa J. Betters https://orcid.org/0000-0002-8975-257X
Erik E. Cordes https://orcid.org/0000-0002-6989-2348

Data availability

Gene sequences generated in this study are accessible on GenBank under the accession numbers OM914402–OM914408, OP577954, and OR687645–OR687650. Morphological and genetic data from novel specimens are available on Github (Repository: melissajbetters/CRM_Provanna) or through correspondence with the lead author. The data underpinning the analysis reported in this paper are deposited at GBIF, the Global Biodiversity Information Facility, and are available at [https://doi.org/10.15468/4w9oc7] and [https://ipt.pensoft.net/resource?r=crm_provanna].

References

Amano K, Little CT (2012) Miocene abyssochrysoid gastropod *Provanna* from Japanese seep and whale-fall sites. Acta Palaeontologica Polonica 59(1): 163–172. https://doi.org/10.4202/app.2012.0002

Betters M, Stabbins A, Keller A, Cordes E (2023) Biogeography and depth partitioning in deep-sea gastropods at the Pacific Costa Rica Margin. Journal of Biogeography 50(12): 2109–2121. https://doi.org/10.1111/jbi.14722

Bouchet P, Warén A (1991) *Ifremeria nautilei*, nouveau gastéropode d'évents hydrothermaux, probablement associé à des bactéries symbiotiques. Comptes Rendus de l'Académie des Sciences, Paris 312(3): 495–501.

Breusing C, Johnson SB, Mitarai S, Beinart RA, Tunnicliffe V (2023) Differential patterns of connectivity in Western Pacific hydrothermal vent metapopulations: A comparison of biophysical and genetic models. Evolutionary Applications 16(1): 22–35. https://doi.org/10.1111/eva.13326

Cavanaugh CM, Gardiner SL, Jones ML, Jannasch HW, Waterbury JB (1981) Prokaryotic cells in the hydrothermal vent tube worm *Riftia pachyptila* Jones: Possible chemoautotrophic symbionts. Science 213(4505): 340–342. https://doi.org/10.1126/science.213.4505.340

Chen C, Nomaki H (2021) Noteworthy observations and records of rare bathyal gastropods from unusual habitats in Sagami Bay, Japan. Marine Biodiversity 51(4): e66. https://doi.org/10.1007/s12526-021-01212-w

Chen C, Watanabe HK, Ohara Y (2018) A very deep *Provanna* (Gastropoda: Abyssochrysoidea) discovered from the Shinkai seep field, southern Mariana Forearc. Journal of the Marine Biological Association of the United Kingdom 98(3): 439–447. https://doi.org/10.1017/S0025315416001648

Chen C, Watanabe HK, Sasaki T (2019) Four new deep-sea provannid snails (Gastropoda: Abyssochrysoidea) discovered from hydrocarbon seep and hydrothermal vents in Japan. Royal Society Open Science 6(7): e190393. https://doi.org/10.1098/rsos.190393

Chen C, Watanabe HK (2022) A new provannid snail (Gastropoda, Abyssochrysoidea) discovered from Northwest Eifuku Volcano, Mariana Arc. ZooKeys 1112: 123–137. https://doi.org/10.3897/zookeys.1112.85950

Colgan DJ, Ponder WF, Eggler PE (2000) Gastropod evolutionary rates and phylogenetic relationships assessed using partial 28S rDNA and histone H3 sequences. Zoologica Scripta 29(1): 29–63. https://doi.org/10.1046/j.1463-6409.2000.00021.x

Dall WH (1918) Notes on the nomenclature of the mollusks of the family Turritidae. Proceedings of the United States National Museum 54(2238): 313–333. https://doi.org/10.5479/si.00963801.54-2238.313

Desbruyeres D, Segonzac M, Bright M (2006) Handbook of deep-sea hydrothermal vent fauna. Denisia 18: e132.

Distel DL, Baco AR, Chuang E, Morrill W, Cavanaugh C, Smith CR (2000) Do mussels take wooden steps to deep-sea vents? Nature 403(6771): 725–726. https://doi.org/10.1038/35001667

Engel MS, Ceríaco LM, Daniel GM, Dellapé PM, Löbl I, Marinov M, Reis RE, Young MT, Dubois A, Agarwal I, Lehmann AP (2021) The taxonomic impediment: A shortage of taxonomists, not the lack of technical approaches. Zoological Journal of the Linnean Society 193(2): 381–387. https://doi.org/10.1093/zoolinnean/zlab072

Folmer O, Black M, Hoeh W, Lutz R, Vrijenhoek R (1994) DNA primers for amplification of mitochondrial cytochrome c oxidase subunit I from diverse metazoan invertebrates. Molecular Marine Biology and Biotechnology 3(5): 294–299. https://europepmc.org/article/med/7881515

Fujikura K, Hashimoto J, Okutani T (2002) Estimated population densities of megafauna in two chemosynthesis based communities: A cold seep in Sagami Bay and a hydrothermal vent in the Okinawa Trough. Benthos Research 57(1): 21–30. https://doi.org/10.5179/benthos1996.57.1_21

Hall TA (1999) BioEdit: A user-friendly biological sequence alignment editor and analysis program for Windows 95/98/NT. Nucleic Acids Symposium Series 41: 95–98.

He X, Xu T, Chen C, Liu X, Li YX, Zhong Z, Gu X, Lin YT, Lan Y, Yan G, Sun Y, Qiu J-W, Qian P-Y, Sun J (2023) Same (sea) bed different dreams: Biological community structure of the Haima seep reveals distinct biogeographic affinities. The Innovation Geoscience 1(2): e100019. https://doi.org/10.59717/j.xinn-geo.2023.100019

Hebert PD, Cywinska A, Ball SL, DeWaard JR (2003) Biological identifications through DNA barcodes. Proceedings of the Royal Society of London, Series B, Biological Sciences 270(1512): 313–321. https://doi.org/10.1098/rspb.2002.2218

IUCN (2022) The IUCN Red List of Threatened Species. Version 2022-2. https://www.iucnredlist.org [Accessed 1 July 2023]

Johnson SB, Warén A, Lee RW, Kano Y, Kaim A, Davis A, Strong EE, Vrijenhoek RC (2010) *Rubyspira*, new genus and two new species of bone-eating deep-sea snails with ancient habits. The Biological Bulletin 219(2): 166–177. https://doi.org/10.1086/BBLv219n2p166

Johnson SB, Warén A, Vrijenhoek RC (2008) DNA barcoding of *Lepetodrilus* limpets reveals cryptic species. Journal of Shellfish Research 27(1): 43–51. https://doi.org/10.2983/0730-8000(2008)27[43:DBOLLR]2.0.CO;2

Kano Y, Takano T, Schwabe E, Warén A (2016) Phylogenetic position and systematics of the wood-associate limpet genus *Caymanabyssia* and implications for ecological radiation into deep-sea organic substrates by lepetelloid gastropods. Marine Ecology 37(5): 1116–1130. https://doi.org/10.1111/maec.12376

Kessler WS (2006) The circulation of the eastern tropical Pacific: A review. Progress in Oceanography 69(2–4): 181–217. https://doi.org/10.1016/j.pocean.2006.03.009

Kumar S, Stecher G, Li M, Knyaz C, Tamura K (2018) MEGA X: Molecular evolutionary genetics analysis across computing platforms. Molecular Biology and Evolution 35(6): 1547–1549. https://doi.org/10.1093/molbev/msy096

Linse K, Nye V, Copley JT, Chen C (2019) On the systematics and ecology of two new species of *Provanna* (Gastropoda: Provannidae) from deep-sea hydrothermal vents in the Caribbean Sea and Southern Ocean. The Journal of Molluscan Studies 85(4): 425–438. https://doi.org/10.1093/mollus/eyz024

Miyazaki J, Kawagucci S, Makabe A, Takahashi A, Kitada K, Torimoto J, Matsui Y, Tasumi E, Shibuya T, Nakamura K, Horai S, Sato S, Ishibashi J, Kanzaki H, Nakagawa S, Hirai M, Takaki Y, Okino K, Watanabe HK, Kumagai H, Chen C (2017) Deepest and hottest hydrothermal activity in the Okinawa Trough: The Yokosuka site at Yaeyama Knoll. Royal Society Open Science 4(12): e171570. https://doi.org/10.1098/rsos.171570

McLean JH (1988) New archaeogastropod limpets from hydrothermal vents; superfamily Lepetodrilacea I. Systematic descriptions. Philosophical Transactions of the Royal Society of London, Series B, Biological Sciences 319(1192): 1–32. https://doi.org/10.1098/rstb.1988.0031

McLean JH, Haszprunar G (1987) Pyropeltidae, a new family of cocculiniform limpets from hydrothermal vents. The Veliger 30(2): 196–205. http://pascal-francis.inist.fr/vibad/index.php?action=getRecordDetail&idt=7375627

Molloy A, Thomas EA, Chen C, Sigwart J (2020a) *Provanna clathrata*. The IUCN Red List of Threatened Species T157783956A157787119. https://doi.org/10.2305/IUCN.UK.2020-3.RLTS.T157778795A157787094.en

Molloy A, Thomas EA, Chen C, Sigwart J (2020b) *Provanna lucida*. The IUCN Red List of Threatened Species T157781173A157787104. https://doi.org/10.2305/IUCN.UK.2020-3.RLTS.T157781173A157787104.en

Molloy A, Thomas EA, Chen C, Sigwart J (2020c) *Provanna subglabra*. The IUCN Red List of Threatened Species T157783956A157787119. https://doi.org/10.2305/IUCN.UK.2020-3.RLTS.T157783956A157787119.en

Molloy A, Thomas, EA (2021a) *Provanna buccinoides*. The IUCN Red List of Threatened Species T157777615A157787089. https://doi.org/10.2305/IUCN.UK.2021-2.RLTS.T157777615A157787089.en

Molloy A, Thomas EA (2021b) *Provanna segonzaci*. The IUCN Red List of Threatened Species T157783266A157787114. https://doi.org/10.2305/IUCN.UK.2021-2.RLTS.T157783266A157787114.en

Nekhaev IO (2023) Who lives in the hot heart of the cold sea? A new species of *Provanna* (Caenogastropoda: Provannidae) from the Hydrothermal zone of Piip Volcano, Northwestern Pacific. Diversity 15(4): e581. https://doi.org/10.3390/d15040581

Okutani T (1990) Two new species of *Provanna* (Gastropoda: Cerithiacea) from “snail pit” in the hydrothermal vent site at the Mariana Back-Arc Basin. Venus 49(1): 19–24. https://doi.org/10.18941/venusjjm.49.1_19 [Japanese Journal of Malacology]

Okutani T, Fujikura K (2002) Abyssal gastropods and bivalves collected by Shinkai 6500 on slope of the Japan Trench. Venus 60(4): 211–224. https://doi.org/10.18941/venus.60.4_211 [Journal of the Malacological Society of Japan]

Okutani T, Ohta S (1988) A new gastropod mollusk associated with hydrothermal vents in the Mariana Back-Arc Basin, western Pacific. Venus 47(1): 1–9. https://doi.org/10.18941/venusjjm.47.1_1

Okutani T, Tsuchida E, Fujikura K (1992) Five bathyal gastropods living within or near the *Calyptogena*-community of the Hatsushima Islet, Sagami Bay. Venus 51(3): 137–148. https://doi.org/10.18941/venusjjm.51.3_137

Poitrimol C, Thiébaut É, Daguin-Thiébaut C, Le Port AS, Ballenghien M, Tran Lu YA, Jollivet D, Hourdez S, Matabos M (2022) Contrasted phylogeographic patterns of hydrothermal vent gastropods along South West Pacific: Woodlark Basin, a possible contact zone and/or stepping-stone. PLOS ONE 17(10): e0275638. https://doi.org/10.1371/journal.pone.0275638

Puillandre N, Brouillet S, Achaz G (2021) ASAP: Assemble species by automatic partitioning. Molecular Ecology Resources 21(2): 609–620. https://doi.org/10.1111/1755-0998.13281

R Core Team (2022) R: A language and environment for statistical computing. R Foundation for Statistical Computing, Vienna. https://www.R-project.org/ [Accessed 1 December 2023]

Rambaut A (2018) Figtree Software (v. 1.4. 4). http://tree.bio.ed.ac.uk/software/figtree/ [Accessed 1 December 2023]

Rybakova E, Krylova E, Mordukhovich V, Galkin S, Alalykina I, Sanamyan N, Nekhaev I, Vinogradov G, Shilov V, Pakhnevich A, Gebruk A, Adrianov A (2023) Mega-and macrofauna of the hydrothermally active submarine Piip Volcano (the southwestern Bering Sea). Deep-sea Research, Part II, Topical Studies in Oceanography 208: e105268. https://doi.org/10.1016/j.dsr2.2023.105268

Sasaki T, Ogura T, Watanabe HK, Fujikura K (2016) Four new species of *Provanna* (Gastropoda: Provannidae) from vents and a seep off Nansei-shoto area, southwestern Japan. Venus 74: 1–7. https://doi.org/10.18941/venus.74.1-2_1

Sasaki T, Warén A, Kano Y, Okutani T, Fujikura K (2010) Gastropods from recent hot vents and cold seeps: systematics, diversity and life strategies. In: Kiel S (Ed.) The Vent and Seep Biota: Aspects from Microbes to Ecosystems. Springer Science & Business Media, Dordrecht, 169–254. https://doi.org/10.1007/978-90-481-9572-5_7

Schloerke B, Cook D, Larmarange J, Briatte F, Marbach M, Thoen E, Elberg A, Crowley J (2021) GGally: Extension to ‘ggplot2’_. R package (v. 2.1.2). https://CRAN.R-project.org/package=GGally [Accessed 1 December 2023]

Sibuet M, Olu K (1998) Biogeography, biodiversity and fluid dependence of deep-sea cold-seep communities at active and passive margins. Deep-sea Research, Part II, Topical Studies in Oceanography 45(1–3): 517–567. https://doi.org/10.1016/S0967-0645(97)00074-X

Sigwart JD, Chen C, Thomas EA, Allcock AL, Böhm M, Seddon M (2019) Red Listing can protect deep-sea biodiversity. Nature Ecology & Evolution 3(8): e1134. https://doi.org/10.1038/s41559-019-0930-2

Smith CR, Baco AR (2003) Ecology of whale falls at the deep-sea floor. Oceanography and Marine Biology – an Annual Review 41: 311–354. https://www.funeralnatural.net/sites/default/files/articulo/archivo/smith_baco_2003.pdf

Suchard MA, Lemey P, Baele G, Ayres DL, Drummond AJ, Rambaut A (2018) Bayesian phylogenetic and phylodynamic data integration using BEAST 1.10. Virus Evolution 4(1): vey016. https://doi.org/10.1093/ve/vey016

Suess E (2014) Marine cold seeps and their manifestations: Geological control, biogeochemical criteria and environmental conditions. International Journal of Earth Sciences 103(7): 1889–1916. https://doi.org/10.1007/s00531-014-1010-0

Tamura K (1992) Estimation of the number of nucleotide substitutions when there are strong transition-transversion and G+ C-content biases. Molecular Biology and Evolution 9(4): 678–687. https://doi.org/10.1093/oxfordjournals.molbev.a040752

Thomas EA, Sigwart J (2020) *Provanna fenestrata*. The IUCN Red List of Threatened Species T158153228A158153282. https://doi.org/10.2305/IUCN.UK.2020-2.RLTS.T158153228A158153282.en

Vrijenhoek RC (2010) Genetic diversity and connectivity of deep-sea hydrothermal vent metapopulations. Molecular Ecology 19(20): 4391–4411. https://doi.org/10.1111/j.1365-294X.2010.04789.x

Thiele J (1925) Gastropoden der Deutschen Tiefsee-Expedition. II Teil. Wissenschaftliche Ergebnisse der Deutschen Tiefsee-Expedition auf dem Dampfer "Valdivia" 1898–1899. 17(2): 35–382.

Tomlin JRB (1927) Reports on the Marine Mollusca in the Collections of the South African Museum. II. Families Abyssochrysidae, Oocorythidae, Haliotidae, Tonnidae. Annals of the South African Museum 25(1): 77–83.

Wang X, Li C, Wang M, Zheng P (2018) Stable isotope signatures and nutritional sources of some dominant species from the PACManus hydrothermal area and the Desmos caldera. PLoS ONE 13(12): e0208887. https://doi.org/10.1371/journal.pone.0208887

Warén A, Bouchet P (1986) Four new species of *Provanna* Dall (Prosobranchia, Cerithiacea?) from East Pacific hydrothermal sites. Zoologica Scripta 15(2): 157–164. https://doi.org/10.1111/j.1463-6409.1986.tb00218.x

Warén A, Bouchet P (1989) New gastropods from East Pacific hydrothermal vents. Zoologica Scripta 18(1): 67–102. https://doi.org/10.1111/j.1463-6409.1989.tb00124.x

Warén A, Bouchet P (1993) New records, species, genera, and a new family of gastropods from hydrothermal vents and hydrocarbon seeps. Zoologica Scripta 22(1): 1–90. https://doi.org/10.1111/j.1463-6409.1993.tb00342.x

Warén A, Bouchet P (2009) New gastropods from deep-sea hydrocarbon seeps off West Africa. Deep-sea Research, Part II, Topical Studies in Oceanography 56(23): 2326–2349. https://doi.org/10.1016/j.dsr2.2009.04.013

Warén A, Ponder WF (1991) New species, anatomy, and systematic position of the hydrothermal vent and hydrocarbon seep gastropod family Provannidae fam. n. (Caenogastropoda). Zoologica Scripta 20(1): 27–56. https://doi.org/10.1111/j.1463-6409.1991.tb00273.x

Xu T, Sun J, Chen C, Qian PY, Qiu JW (2016) The mitochondrial genome of the deep-sea snail *Provanna* sp. (Gastropoda: Provannidae). Mitochondrial DNA, Part A, DNA Mapping, Sequencing, and Analysis 27(6): 4026–4027. https://doi.org/10.3109/19401736.2014.1003827

ZooKeys 1189: 33–54 (2024)
DOI: 10.3897/zookeys.1189.115621

Research Article

A new species of *Amolops* (Amphibia, Anura, Ranidae) from Guizhou Province, China

Shi-Ze Li[1,2], Jing Liu[1], Xiao-Cong Ke[3], Gang Cheng[4], Bin Wang[2]

1 *Department of Food Science and Engineering, Moutai Institute, Renhuai 564500, China*
2 *Chengdu Institute of Biology, Chinese Academy of Sciences, Chengdu 610041, China*
3 *Guizhou Yahua Forestry Engineering Design Consulting Co., Ltd., Guiyang, 550002, China*
4 *College of Materials Science and Engineering, Guiyang College, Guiyang, 550002, China*
Corresponding authors: Bin Wang (wangbin@cib.ac.cn); Gang Cheng (25965716@qq.com)

Abstract

The Torrent frogs of the genus *Amolops* are widely distributed in Nepal and northern India eastwards to southern China and southwards to Malaysia. The genus currently contains 84 species. Previous studies indicated underestimated species diversity in the genus. In the context, a new species occurring from the mountains in the northwestern Guizhou Province, China is found and described based on morphological comparisons and molecular phylogenetic analyses, *Amolops dafangensis* **sp. nov.** Phylogenetic analyses based on DNA sequences of the mitochondrial 16S rRNA and COI genes supported the new species as an independent lineage. The uncorrected genetic distances between the 16S rRNA and COI genes in the new species and its closest congener were 0.7% and 2.6%, respectively, which are higher than or at the same level as those among many pairs of congeners. Morphologically, the new species can be distinguished from its congeners by a combination of the following characters: body size moderate (SVL 43.2–46.8 mm in males); head length larger than head width slightly; tympanum distinct, oval; vocal sacs absent; vomerine teeth present; dorsolateral folds weak formed by series of glands; nuptial pads present on the base of finger I; heels overlapping when thighs are positioned at right angles to the body; tibiotarsal articulation reaching the level far beyond the tip of the snout when leg stretched forward.

Key words: Mitochondrial gene, taxonomy

Academic editor: Anthony Herrel
Received: 11 November 2023
Accepted: 13 December 2023
Published: 12 January 2024

ZooBank: https://zoobank.org/7351F342-928A-44C1-8EA4-55A706758838

Citation: Li S-Z, Liu J, Ke X-C, Cheng G, Wang B (2024) A new species of *Amolops* (Amphibia, Anura, Ranidae) from Guizhou Province, China. ZooKeys 1189: 33–54. https://doi.org/10.3897/zookeys.1189.115621

Introduction

The Torrent frogs of the genus *Amolops* Cope, 1865 are widespread in Asia, from the southern and eastern Himalayas eastward to the southeastern mainland China and southwards to the Peninsular Malaysia (Wu et al. 2020; Zeng et al. 2020; Frost 2023). The frogs live in the fast-flowing water and occupy specialized features that help them cling to rocks and navigate the turbulent currents (Fei et al. 2009; Fei et al. 2012). The genus currently contains 84 species, of which 51 species have been recorded in China (Fei et al. 2012; Amphibia China 2023; Frost 2023). Recently, according to the phylogenetic framework of the genus, the 84 *Amolops* species were divided into ten species groups, namely the *A. monticola* group, *A. chayuensis* group, *A. hainanensis* group, *A. ricketti* group, *A. spinapectoralis* group, *A. marmoratus* group, *A. larutensis* group, *A. daiyunensis* group, *A. viridimaculatus* group, and the *A. mantzorum* group (Lyu et al. 2019b; Wu et al. 2020; Zeng et al. 2020, 2021; Jiang et al. 2021; Patel et al. 2021; Mahony et al. 2022; Saikia et al. 2022a, 2022b, 2023; Wang et al. 2022; Pham et al. 2023; Qian et al. 2023; Tang et al. 2023; Sheridan et al. 2023). Among them, the *A. mantzorum* group, to which *Amolops dafangensis* sp. nov. belongs, was proposed by Fei et al. (1999) and is mainly distributed along the eastern margin of the Qinghai-Tibet Plateau (Fei et al. 2009; Lu et al. 2014; Zeng et al. 2020) and currently comprises eleven species (Jiang et al. 2021; Qian et al. 2023; Tang et al. 2023): *Amolops ailao* Tang, Sun, Liu, Luo, Yu & Du, 2023, *A. mantzorum* (David, 1872), *A. granulosus* (Liu & Hu, 1961), *A. loloensis* (Liu, 1950), *A. lifanensis* (Liu, 1945), *A. jinjiangensis* Su, Yang & Li, 1986, *A. tuberodepressus* Liu & Yang, 2000, *A. sangzhiensis* Qian, Xiang, Jiang, Yang & Gui, 2023, A. *shuichengnicus* Lyu & Wang, 2019, *A. ottorum* Pham, Sung, Pham, Le, Zieger & Nguyen, 2019, and *A. minutus* Orlov & Ho, 2007. In this species group, *A. ottorum* and *A. minutus* are only known from northwestern Vietnam, and the other species are known from southwestern China (Frost 2023). However, within the group, the phylogenetic relationships between species remain controversial (Lu et al. 2014; Lyu et al. 2019b; Zeng et al. 2020; Wu et al. 2020), and the species diversity of it is also expected to be underestimated (Jiang et al. 2021; Qian et al. 2023; Tang et al. 2023).

Guizhou Province is one of the richest areas for amphibians in China and three *Amolops* species (*A. chaochin*, *A. chunganensis*, and *A. sinensis*) were have been recorded (Amphibia China 2023). During fieldwork in Dafang County, Guizhou Province, some *Amolops* specimens were collected. By our comparisons, these specimens were different from *A. chaochin*, *A. chunganensis*, and *A. sinensis* by the dorsolateral folds being weak, formed by series of glands, and the presence of a circum-marginal groove on the disc of the first finger. Molecular phylogenetic analyses based on mitochondrial DNA and comprehensive morphological comparisons all indicated that the specimens from Dafang County were an undescribed species, herein described as a new species, *Amolops dafangensis* sp. nov.

Materials and methods

Sampling

Five specimens of *Amolops dafangensis* sp. nov. including three adult males and two juveniles, were collected from Dafang County, Guizhou Province, China (Fig. 1). All specimens were fixed in 10% buffered formalin for one day, and then transferred to 70% ethanol. Tissue samples were preserved separately in 95% prior to fixation. Specimens collected in this work were all deposited in Maotai Institute (**MT**), Renhuai City, Guizhou Province, China.

Collection of molecular data

DNA was extracted from tissue using a standard phenol-chloroform extraction protocol (Sambrook et al. 1989). Two mitochondrial genes, partial 16S ribosomal RNA gene (16S) and cytochrome oxidase subunit I (COI), were amplified.

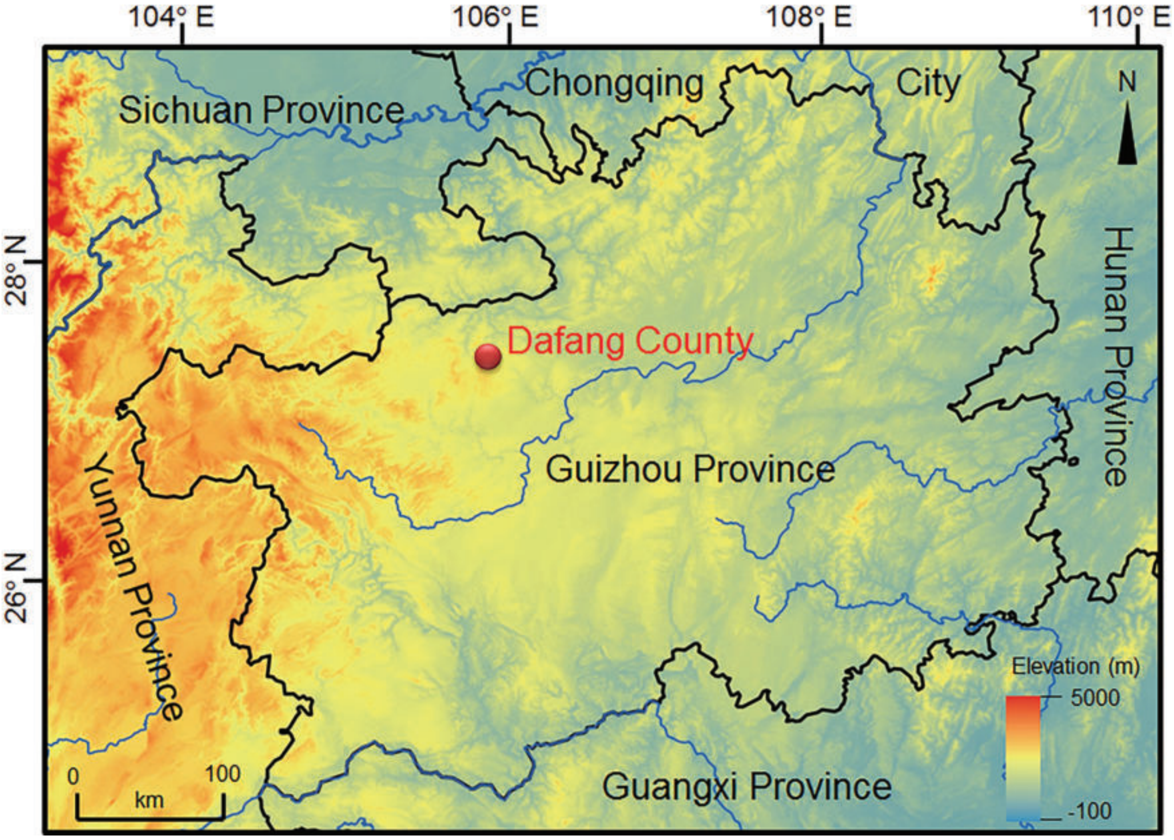

Figure 1. Geographical location of the type locality of *Amolops dafangensis* sp. nov. in Dafang County, Guizhou Province, China.

The primers used for 16S were P7 (5'- CGCCTGTTTACCAAAAACAT -3') and P8 (5'-CCGGTCTGAACTCAGATCACGT') following Simon et al. (1994), and that for COI were Chmf4 (5'-TYTCWACWAAYCAYAAAGAYATCGG-3') and Chmr4 (5'-ACYTCRGGRTGRCCRAARAATCA-3') following Che et al. (2012). PCR amplification reactions were performed in a 30 μl reaction with the following cycling conditions: an initial denaturing step at 95 °C for 4 min; 35 cycles of denaturing at 95 °C for 40 s, annealing at 48 °C/46 °C (16S/COI) for 40 s and extending at 72 °C for 70 s, and a final extending step of 72 °C for 10 min. PCR products were purified with spin columns and then were sequenced with both forward and reverse primers same as PCR. Sequencing was conducted using an ABI Prism 3730 automated DNA sequencer in Chengdu TSING KE Biological Technology Co. Ltd. (Chengdu, China). All sequences were deposited in GenBank (for GenBank Accession numbers refer to Table 1). For phylogenetic analyses, we downloaded corresponding sequences for all related species from GenBank according to previous studies (Qian et al. 2023; Tang et al. 2023; for GenBank accession numbers see Table 1).

Phylogenetic analyses and genetic distance

Sequences were assembled and aligned using the Clustalw module in BioEdit 7.0.9.0 (Hall 1999) with default settings. The datasets were checked by eye and revised manually if necessary. Based on the 16S + COI concatenated dataset, phylogenetic analyses were conducted using maximum likelihood (ML) and

Table 1. Information for samples used in molecular phylogenetic analyses in this study.

ID	Species	Locality	Voucher number	GenBank accession number	
				16S	**COI**
1	*Amolops dafangensis* sp. nov.	Dafang, Guizhou, China	MT DF20230601002	OR936315	OR924345
2	*Amolops dafangensis* sp. nov.	Dafang, Guizhou, China	MT DF20230601001	OR936314	OR924344
3	*Amolops dafangensis* sp. nov.	Dafang, Guizhou, China	MT DF20230601003	OR936316	OR924346
4	*Amolops dafangensis* sp. nov.	Dafang, Guizhou, China	MT DF20230601004	OR936317	OR924347
5	*Amolops dafangensis* sp. nov.	Dafang, Guizhou, China	MT DF20230601005	OR936318	OR924348
6	*A. mantzorum*	Wolong, Sichuan, China	SCUM 045817HX	MN953706	MN961408
7	*A. mantzorum*	Fengtongzhai, Sichuan, China	SYS a005365	MK573808	MK568323
8	*A. mantzorum*	Dayi, Sichuan, China	SCUM 045825HX	MN953707	MN961409
9	*A. mantzorum*	Mt. Wawu, Sichuan, China	SYS a005337	MK604853	MK605611
10	*A. mantzorum*	Kangding, Sichuan, China	KIZ 041127	MN953764	MN961465
11	*A. mantzorum*	Kangding, Sichuan, China	KIZ 041129	MN953765	MN961466
12	*A. mantzorum*	Fengtongzhai, Sichuan, China	SYS a005366	MK604862	MK605620
13	*A. mantzorum*	Kangding, Sichuan, China	SYS a005356	MK604858	MK605616
14	*A. mantzorum*	Kangding, Sichuan, China	SYS a005357	MK604859	MK605617
15	*A. mantzorum*	Mt. Wawu, Sichuan, China	SYS a005336	MK573804	MK568319
16	*A. ailao*	Mt. Ailao, Xinping, Yunnan, China	GXNU YU000001	MN650752	MN650738
17	*A. ailao*	Mt. Ailao, Xinping, Yunnan, China	GXNU YU000002	MN650753	MN650739
18	*A. tuberodepressus*	Jingdong, Yunnan, China	SCUM 050433CHX	MN953729	MN961432
19	*A. tuberodepressus*	Mt. Wuliang, Yunnan, China	SYS a003931	MK573799	MG991933
20	*A. tuberodepressus*	Jingdong, Yunnan, China	SCUM 050430CHX	MN953730	MN961433
21	*A. tuberodepressus*	Mt. Wuliang, Yunnan, China	SYS a003932	MK573800	MG991934
22	*A. tuberodepressus*	Mt. Ailao, Yunnan, China	SYS a003900	MK573797	MK568314
23	*A. tuberodepressus*	Mt. Ailao, Yunnan, China	SYS a003901	MK573798	MK568315
24	*A. granulosus*	Mt. Guangwu, Sichuan, China	SYS a005399	MK573811	MK568326
25	*A. granulosus*	Mt. Guangwu, Sichuan, China	SYS a005400	MK573812	MK568327
26	*A. granulosus*	Mt. Wawu, Sichuan, China	SYS a005315	MK604850	MK605608
27	*A. granulosus*	Mt. Wawu, Sichuan, China	SYS a005316	MK604851	MK605609
28	*A. granulosus*	China: Dayi, Sichuan	SCUM 045823HX	MN953680	JN700804
29	*A. granulosus*	China: Anxian, Sichuan	SCUM 060911HX	MN953681	MN961381
30	*A. shuichengicus*	Shuicheng, Guizhou, China	SYS a004956	MK604845	MK605603
31	*A. shuichengicus*	Shuicheng, Guizhou, China	SYS a004957	MK604846	MK605604
32	*A. jinjiangensis*	Mt. Gaoligong, Yunnan, China	SYS a004571	MK573801	MK568316
33	*A. jinjiangensis*	Deqing, Yunnan, China	SCUM 050434CHX	MN953700	MN961402
34	*A. jinjiangensis*	Deqing, Yunnan, China	SCUM 050435CHX	EF453741	MN961403
35	*A. jinjiangensis*	Chuxiong, Yunnan, China	KIZ 047905	MN953701	MN961404
36	*A. loloensis*	Zhaojue, Sichuan, China	SYS a005346	MK604854	MK605612
37	*A. loloensis*	Zhaojue, Sichuan, China	SYS a005347	MK604855	MK605613
38	*A. loloensis*	Xichang, Sichuan, China	SCUM 045806HX	MN953704	MN961407
39	*A. loloensis*	Xichang, Sichuan, China	SCUM 045807HX	EF453743	MN961456
40	*A. sangzhiensis*	Mt. Doupeng, Sangzhi, Hunan, China	CSUFT 901	OQ079538	OQ078903
41	*A. sangzhiensis*	Mt. Doupeng, Sangzhi, Hunan, China	CSUFT 907	OQ079540	OQ078905
42	*A. sangzhiensis*	Mt. Doupeng, Sangzhi, Hunan, China	CSUFT 912	OQ079541	OQ078906

ID	Species	Locality	Voucher number	GenBank accession number	
				16S	COI
43	*A. sangzhiensis*	Mt. Doupeng, Sangzhi, Hunan, China	CSUFT 916	OQ079542	OQ078907
44	*A. sangzhiensis*	Mt. Doupeng, Sangzhi, Hunan, China	CSUFT 927	OQ079543	OQ078908
45	*A. sangzhiensis*	Mt. Doupeng, Sangzhi, Hunan, China	CSUFT 930	OQ079544	OQ078909
46	*A. sangzhiensis*	Mt. Doupeng, Sangzhi, Hunan, China	CSUFT 933	OQ079545	OQ078910
47	*A. lifanensis*	Lixian, Sichuan, China	SYS a005374	MK573809	MK568324
48	*A. lifanensis*	Lixian, Sichuan, China	SYS a005375	MK573810	MK568325
49	*A. lifanensis*	Maoxian, Sichuan, China	SCUM 045801HX	MN953702	MN961405
50	*A. lifanensis*	Maoxian, Sichuan, China	SCUM 045803HX	MN953703	MN961406
51	*A. chunganensis*	Mt. Jinggang, Jiangxi, China	SYS a004212	MK263263	MG991914
52	*A. ricketti*	Mt. Wuyi, Fujian, China	SYS a004141	MK263259	MG991927

Bayesian Inference (BI) methods, implemented in PhyML 3.0 (Guindon et al. 2010) and MrBayes 3.12 (Ronquist and Huelsenbeck 2003), respectively. The best-fit model was obtained by the Bayesian inference criteria (BIC) computed with PartitionFinder 2 (Lanfear et al. 2012). In this analysis, 16S gene and each codon position of COI gene were defined, and Bayesian Inference Criteria was used. As a result, the analysis suggested that the best partition scheme is16S gene/each codon position of COI gene, and selected GTR + G + I model as the best model for each partition. For ML analysis, the bootstrap consensus tree inferred from 1000 replicates was used to estimate nodal supports of inferred relationships on phylogenetic trees. For Bayesian analyses, four Markov chains were run for 50 million generations with sampling every 1000 generations. The first 25% of the trees were discarded, representing the burn-in phase of the analyses, and the remaining trees were used to calculate the Bayesian posterior probabilities. Genetic distance between species of *A. mantzorum* group were estimated on 16S and COI genes, respectively, based on uncorrected *p*-distance model using MEGA 6.06 (Tamura et al. 2013).

Morphological comparisons

Morphological measurements were made with dial calipers to nearest 0.1 mm by S-ZL following Fei et al. (2009). In total, twenty morphological characteristics were measured for the adult specimens:

ED	eye diameter (distance from the anterior corner to the posterior corner of the eye);
FL	foot length (distance from tarsus to the tip of fourth toe);
HDL	head length (distance from the tip of the snout to the articulation of jaw);
HDW	maximum head width (greatest width between the left and right articulations of jaw);
HLL	hindlimb length (maximum length from the vent to the distal tip of the Toe IV);
IND	internasal distance (minimum distance between the inner margins of the external nares);
IOD	interorbital distance (minimum distance between the inner edges of the upper eyelids);

LAL	length of lower arm and hand (distance from the elbow to the distal end of the Finger IV);
ML	manus length (distance from tip of third digit to proximal edge of inner palmar tubercle);
NED	nasal to eye distance (distance between the nasal and the anterior corner of the eye);
NSD	nasal to snout distance (distance between the nasal the posterior edge of the vent);
LW	lower arm width (maximum width of the lower arm);
SVL	snout-vent length (distance from the tip of the snout to the posterior edge of the vent);
SL	snout length (distance from the tip of the snout to the anterior corner of the eye);
TFL	length of foot and tarsus (distance from the tibiotarsal articulation to the distal end of the Toe IV);
THL	thigh length (distance from vent to knee);
TL	tibia length (distance from knee to tarsus);
TW	maximal tibia width;
TYD	maximal tympanum diameter;
UEW	upper eyelid width (greatest width of the upper eyelid margins measured perpendicular to the anterior-posterior axis).

We also compared the morphological characters of the new taxon with other species of *Amolops*. Comparative data were obtained from the literature for all species of *Amolops* (Table 2).

Results

Phylogenetic analyses

The ML and BI phylogenetic trees were constructed based on concatenated DNA sequences of the mitochondrial 16S (425 bp) and COI (606 bp) genes. ML and BI analyses resulted in essentially identical topologies though some basal relationships between clades were not resolved (Fig. 2). The new taxon was indicated as an independent clade. Furthermore, the smallest uncorrected *p*-distance between *Amolops dafangensis* sp. nov. and its most closely-related congeners is 0.7% (vs *A. sangzhiensis*) on 16S gene (Suppl. material 1), and 2.6% (vs *A. loloensis*) on COI gene (Suppl. material 2), which was higher or at the same level with those among many pairs of congeners, for example, 0.3% between *A. sangzhiensis* and *A. jinjiangensis* on the 16S gene, and 3.2% between *A. jinjiangensis* and *A. loloensis* on the COI gene.

Morphological comparisons

Morphological measurements are given in Table 3. The new taxon could be identified from its congeners by a series of differences in morphological characters.

Table 2. References for morphological characters for congeners of the genus *Amolops*.

Species	Literature
A. adicola Patel, Garg, Das, Stuart & Biju, 2021	Patel et al. 2021
A. afghanus (Günther, 1858)	Günther 1858
A. ailao Tang, Sun, Liu, Luo, Yu & Du, 2023	Tang et al. 2023
A. akhaorum Stuart, Bain, Phimmachak & Spence, 2010	Stuart et al. 2010
A. albispinus Sung, Wang & Wang, 2016	Sung et al. 2016
A. aniqiaoensis Dong, Rao & Lü, 2005	Zhao et al. 2005
A. archotaphus (Inger & Chan-ard, 1997)	Inger and Chan-ard 1997
A. attiguus Sheridan, Phimmachak, Sivongxay & Stuart, 2023	Sheridan et al. 2023
A. assamensis Sengupta, Hussain, Choudhury, Gogoi, Ahmed & Choudhury, 2008	Sengupta et al. 2008
A. australis Chan, Abraham, Grismer & Grismer, 2018	Chan et al. 2018
A. beibengensis Jiang, Li, Zou, Yan & Che, 2020	Che et al. 2020
A. bellulus Liu, Yang, Ferraris & Matsui, 2000	Liu et al. 2000
*A. binchachaensi*s Rao, Hui, Ma & Zhu, 2022“2020”	Zhu and Rao 2022
A. chakrataensis Ray, 1992	Ray 1992
A. chanakya Saikia, Laskar, Dinesh, Shabnam & Sinha, 2022	Saikia et al. 2022a
A. chaochin Jiang, Ren, Lyu & Li, 2021	Jiang et al. 2021
A. chayuensis Sun, Luo, Sun & Zhang, 2013	Sun et al. 2013
A. chunganensis (Pope, 1929)	Pope 1929
A. compotrix (Bain, Stuart & Orlov, 2006)	Bain et al. 2006
A. cremnobatus Inger and Kottelat, 1998	Inger and Kottelat 1998
A. cucae (Bain, Stuart & Orlov, 2006)	Bain et al. 2006
A. daiyunensis (Liu & Hu, 1975)	Liu and Hu 1975
A. daorum (Bain, Lathrop, Murphy, Orlov & Ho, 2003)	Bain et al. 2003
A. deng Jiang, Wang & Che, 2020	Che et al. 2020
A. formosus (Günther, 1876)	Günther 1876 “1875”
A. gerbillus (Annandale, 1912)	Annandale 1912
A. gerutu Chan, Abraham, Grismer & Grismer, 2018	Chan et al. 2018
A. granulosus (Liu & Hu, 1961)	Liu and Hu 1961
A. hainanensis (Boulenger, 1900)	Boulenger 1900 “1899”
A. himalayanus (Boulenger, 1888)	Boulenger 1888
A. hongkongensis (Pope & Romer, 1951)	Pope and Romer 1951
A. indoburmanensis Dever, Fuiten, Konu & Wilkinson, 2012	Dever et al. 2012
A. iriodes (Bain & Nguyen, 2004)	Bain and Nguyen 2004
A. jaunsari Ray, 1992	Ray 1992
A. jinjiangensis Su, Yang & Li, 1986	Su et al. 1986
A. kaulbacki (Smith, 1940)	Smith 1940
A. kohimaensis Biju, Mahony & Kamei, 2010	Biju et al. 2010
A. kottelati Sheridan, Phimmachak, Sivongxay & Stuart, 2023	Sheridan et al. 2023
A. larutensis (Boulenger, 1899)	Boulenger 1899a
A. latopalmatus (Boulenger, 1882)	Boulenger 1882
A. lifanensis (Liu, 1945)	Liu 1945
A. loloensis (Liu, 1950)	Liu 1950
A. longimanus (Andersson, 1939)	Andersson 1939 “1938”
A. mahabharatensis Khatiwada, Shu, Wang, Zhao, Xie & Jiang, 2020	Khatiwada et al. 2020
A. mantzorum (David, 1872)	David 1872 “1871”
A. marmoratus (Blyth, 1855)	Blyth 1855
A. medogensis Li & Rao, 2005	Zhao et al. 2005

Species	Literature
A. mengdingensis Yu, Wu & Yang, 2019	Yu et al. 2019
A. mengyangensis Wu & Tian, 1995	Wu and Tian 1995
A. minutus Orlov & Ho, 2007	Orlov and Ho 2007
A. monticola (Anderson, 1871)	Anderson 1871
A. nepalicus Yang, 1991	Yang 1991
A. nidorbellus Biju, Mahony & Kamei, 2010	Biju et al. 2010
A. nyingchiensis Jiang, Wang, Xie, Jiang & Che, 2016	Jiang et al. 2016
A. ottorum Pham, Sung, Pham, Le, Ziegler & Nguyen, 2019	Pham et al. 2019
A. pallasitatus Qi, Zhou, Lyu, Lu & Li, 2019	Qi et al. 2019
A. panhai Matsui & Nabhitabhata, 2006	Matsui and Nabhitabhata 2006
A. putaoensis Gan, Qin, Lwin, Li, Quan, Liu & Yu, 2020	Gan et al. 2020b
A. ricketti (Boulenger, 1899)	Boulenger 1899b
A. sangzhiensis Qian, Xiang, Jiang, Yang & Gui, 2023	Qian et al. 2023
A. senchalensis Chanda, 1987	Chanda 1987
A. sengae Sheridan, Phimmachak, Sivongxay & Stuart, 2023	Sheridan et al. 2023
A. shihaitaoi Wang, Li, Du, Hou & Yu, 2022	Wang et al. 2022
A. shuichengicus Lyu & Wang, 2019	Lyu et al. 2019a
A. siju Saikia, Sinha, Shabnam & Dinesh, 2023	Saikia et al. 2023
A. sinensis Lyu, Wang & Wang, 2019	Lyu et al. 2019b
A. spinapectoralis Inger, Orlov & Darevsky, 1999	Inger et al. 1999
A. tanfuilianae Sheridan, Phimmachak, Sivongxay & Stuart, 2023	Sheridan et al. 2023
A. tawang Saikia, Laskar, Dinesh, Shabnam & Sinha, 2022	Saikia et al. 2022a
A. teochew Zeng, Wang, Lyu & Wang, 2021	Zeng et al. 2021
A. terraorchis Saikia, Sinha, Laskar, Shabnam & Dinesh, 2022	Saikia et al. 2022b
A. tonkinensis (Ahl, 1927 “1926”)	Ahl 1927 “1926”
A. torrentis (Smith, 1923)	Smith 1923
A. truongi Pham, Pham, Ngo, Sung, Ziegler & Le, 2023	Pham et al. 2023
A. tuanjieensis Gan, Yu & Wu, 2020	Gan et al. 2020a
A. tuberodepressus Liu & Yang, 2000	Liu and Yang 2000
A. viridimaculatus (Jiang, 1983)	Jiang 1983
A. vitreus (Bain, Stuart & Orlov, 2006)	Bain et al. 2006
A. wangyali Mahony, Nidup, Streicher, Teeling & Kamei, 2022	Mahony et al. 2022
A. wangyufani Jiang, 2020	Che et al. 2020
A. wenshanensis Yuan, Jin, Li, Stuart & Wu, 2018	Yuan et al. 2018
A. wuyiensis (Liu & Hu, 1975)	Liu and Hu 1975
A. yatseni Lyu, Wang & Wang, 2019	Lyu et al. 2019
A. yunkaiensis Lyu, Wang, Liu, Zeng & Wang, 2018	Lyu et al. 2018

Taxonomic account

Amolops dafangensis **sp. nov.**

https://zoobank.org/22D19386-8779-4FBC-8BF9-71FB7070403B
Figs 3–5

Material examined. *Holotype*. MT DF20230601002, adult male, collected by Shize Li on 1 June 2023 in Dafang County (27.40078312°N, 105.92804027°E; elevation 1300 m a.s.l.), Guizhou Province, China. ***Paratypes*.** One male MT DF20230601003 collected by Jing Liu on 1 June 2023, one male MT DF20230601001 and two juveniles MT DF20230601004 and MT DF20230601005 were collected by Xiaocong Ke on 1 June 2023 from the same place as holotype.

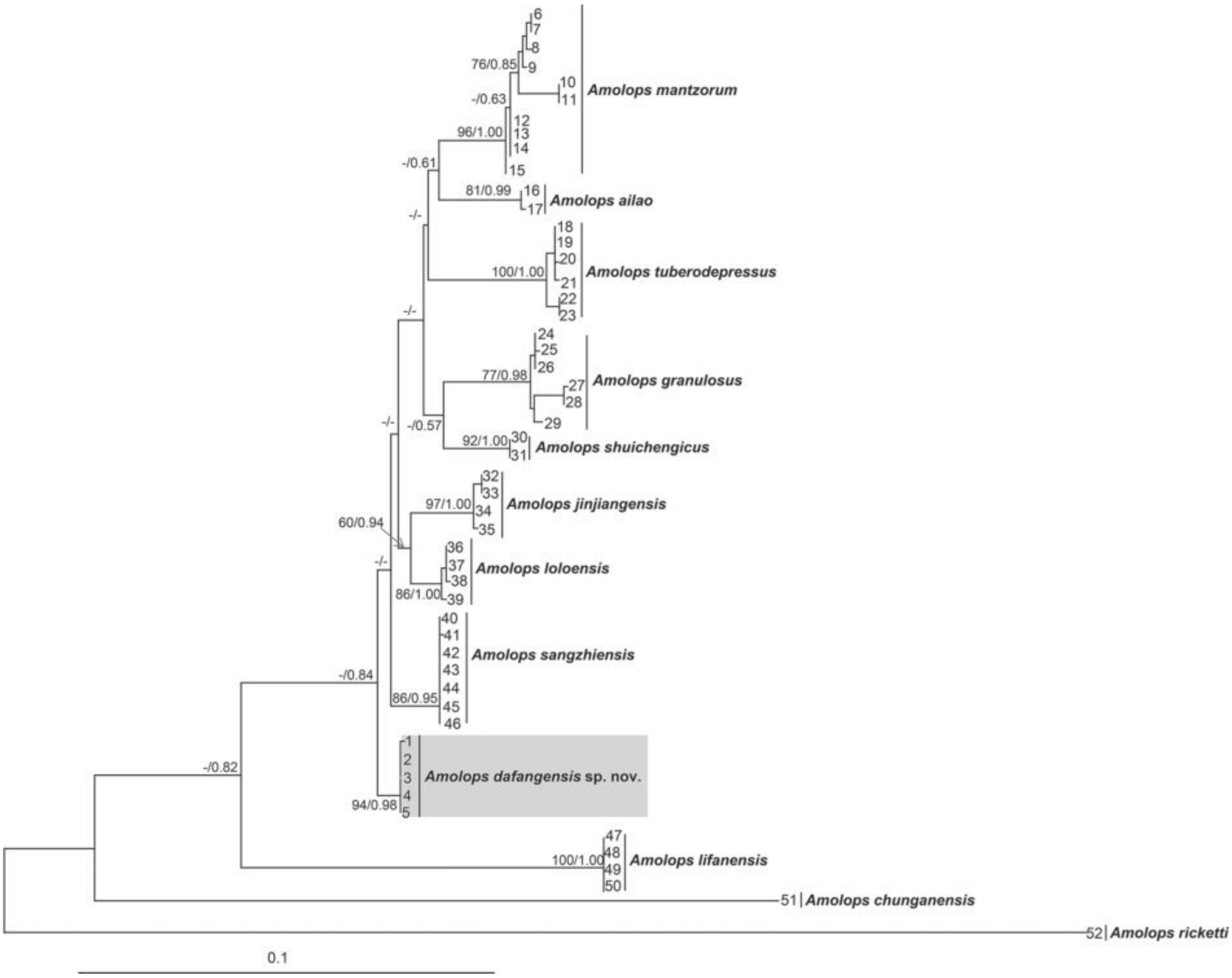

Figure 2. Maximum likelihood (ML) tree of *Amolops mantzorum* group based on the 16S and CO1 genes. ML bootstrap supports (BS) /Bayesian posterior probability (BPP) were denoted beside each node, and "-" denotes BS < 50% or BPP < 0.60. Samples 1–52 refer to Table 1.

Diagnosis. *Amolops dafangensis* sp. nov. resembles members of the *A. mantzorum* group in the absence of true dorsolateral folds and the presence of a circum-marginal groove on the disc of the first finger. The tarsal fold and tarsal glands are absent, and a nuptial pad is present on the first finger in males (Jiang et al. 2021).

Amolops dafangensis sp. nov. can be distinguished from other congeners by the following characters: (1) body size moderate (SVL 43.2 – 46.8 mm in males); (2) head length larger than head width slightly; (3) tympanum distinct, oval; (4) vocal sacs absent; (5) vomerine teeth present; (6) dorsolateral folds weak formed by series of glands; (7) nuptial pads present on base of finger I; (8) heels overlapping when thighs are positioned at right angles to the body; tibiotarsal articulation reaching the level far beyond the tip of the snout when leg stretched forward.

Description of holotype. Adult male (Figs 3, 4), body size moderate, SVL 44.7 mm. head length larger than head width slightly (HDL: HDW = 1.02); snout short, rounded in dorsal view, projecting beyond lower jaw; eye large and convex, eye diameter 0.74× of snout length; nostril rounded, between to tip of snout and eyes; internasal distance larger than interorbital distance; tympanum circular,

Table 3. Measurements of the adult specimens of *Amolops dafangensis* sp. nov. Units are given in mm. See abbreviations for the morphological characters in Materials and methods section.

Voucher	MT DF20230601001	MT DF20230601002	MT DF20230601003	Range	Mean ± SD
Sex	male	male	male		
SVL	43.2	44.7	46.8	43.2–46.8	44.9 ± 1.8
HDL	14.5	15.0	15.6	14.5–15.6	14.9 ± 0.6
HDW	14.3	14.7	15.1	14.3–15.1	14.8 ± 0.4
SL	6.1	6.1	6.6	6.1–6.6	6.3 ± 0.3
ED	3.9	4.5	4.3	3.9–4.5	4.3 ± 0.3
UEW	3.5	3.9	3.8	3.5–3.9	3.7 ± 0.2
IOD	4.4	4.1	4.7	4.1–4.7	4.4 ± 0.3
IND	5.2	5.4	5.7	5.2–5.7	5.4 ± 0.3
NED	2.7	2.4	3.0	2.4–3.0	2.7 ± 0.3
NSD	3.2	2.4	3.0	2.4–3.2	2.9 ± 0.4
TYD	1.9	2.4	1.7	1.7–2.4	2.0 ± 0.4
LAL	22.5	24.0	23.5	22.5–24.0	23.3 ± 0.8
LW	3.2	3.8	3.8	3.2–3.8	3.6 ± 0.3
ML	13.8	14.4	14.6	13.8–14.6	14.3 ± 0.4
HLL	80.4	83.4	87.3	80.4–87.3	83.7 ± 3.4
THL	22.3	24.0	24.9	22.3–24.9	23.7 ± 1.3
TL	25.8	26.2	27.9	25.8–27.9	26.6 ± 1.1
TW	5.0	5.4	5.8	5.0–5.8	5.4 ± 0.4
TFL	36.3	38.1	39.5	36.3–39.5	38.0 ± 1.6
FL	22.3	22.8	24.6	22.3–24.6	23.2 ± 1.2

distinct, 0.56× of eye diameter; loreal region slightly concave; nares oval; pineal ocellus visible; supratympanic fold extends from back of eye to above shoulder; vomerine teeth present; tongue deeply notched posteriorly; vocal sac absent.

Forelimbs robust (LW/SVL=0.08); lower arm and hand beyond one-second of body length (LAL/SVL=0.51); fingers slender, relative finger lengths I < II < IV < III; finger tips on II–IV dilated to wide cordiform disks with circum-marginal grooves, tip of first finger with small disk but without circum-marginal groove; all fingers without webbing and lateral fringes; subarticular tubercle prominent; supernumerary tubercle indistinct; inner metacarpal tubercle oval, elongate; outer metacarpal tubercles small round; velvety nuptial pad on finger I.

Hindlimbs long, nearly 2× SVL (HLL/SVL = 1.87); tibiotarsal articulation reaching the level far beyond the tip of the snout when leg stretched forward; tibias longer than thigh length, heels overlapped; toes slender, relative lengths I < II < III < V < IV; toes entirely webbed; tips of toes expanded into disc with circum-marginal grooves; outer metatarsal tubercle absent; inner metatarsal tubercle small but well developed.

Skin on dorsum and dorsal surfaces of limbs smooth; dorsolateral folds weak, formed by series of glands been an incomplete line, extending from above shoulder to vent; weak dorsolateral glandular lines; ventral surface of bell and limbs smooth except a few small tubercles on posterior surface of thigh and around vent.

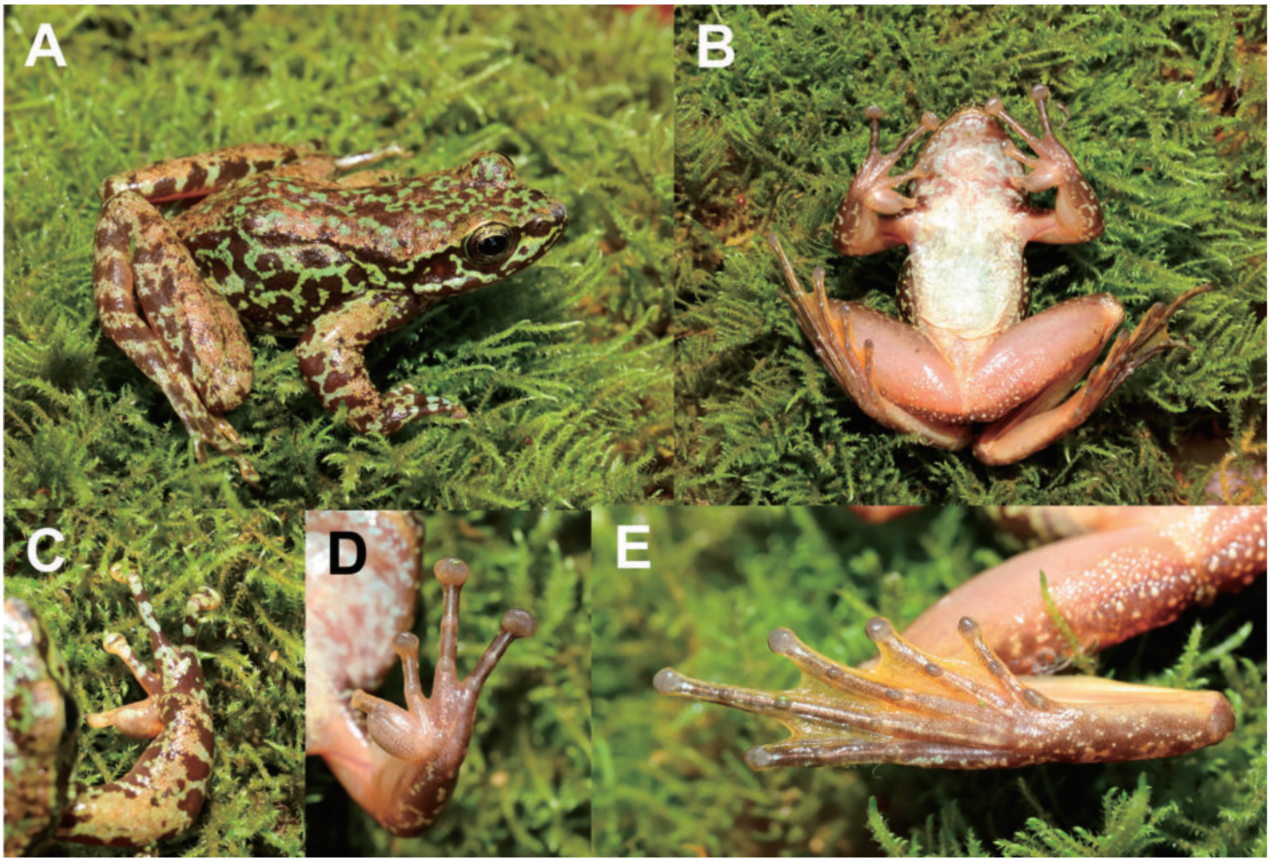

Figure 3. Photographs of the holotype MT DF20230601002 of *Amolops dafangensis* sp. nov. in life **A** dorsal view **B** ventral view **C** dorsal view of hand **D** ventral view of hand **E** ventral view of foot.

Coloration in life. In life, iris pale brown with dark wash; top of head and dorsum golden brown with large rounded black brown and green spots; sides of head with a pale green stripe extending from loreal region to region behind and below eye along upper lip; a black brown band from the tip of the snout through the nostril to an anterior border of the eye, continuing behind the eye to the shoulder; temporal region black brown with green blotches; the flank green with some back brown spots; limbs dorsally golden brown with black brown bands; chest and venter white, throat white with pale brown; ventral surface of anterior forelimbs brown with green spots; finger I and II fresh-colored, finger III and IV brown; ventral surface of hindlimbs fresh-colored (Fig. 3).

Color in preservative. Dorsal surface fade to pale brown with beige brown and black spots on head, flank and on limbs; ventral surface fade to creamy white, marbled with brown on throat and chest (Fig. 4).

Variation. Measurements of all specimens are listed in Table 3. All specimens were very similar in morphology, but in MT DF20230601001 the dorsum was golden brown with few green spots (Fig. 5A); in MT DF20230601003 the dorsum and dorsal surfaces of limbs were green with brown spots (Fig. 5B); in the juvenile specimen MT DF20230601004 the flank was mainly green with black spots and the ventral surface of the throat and chest were white with pale brown spots (Fig. 5C, D).

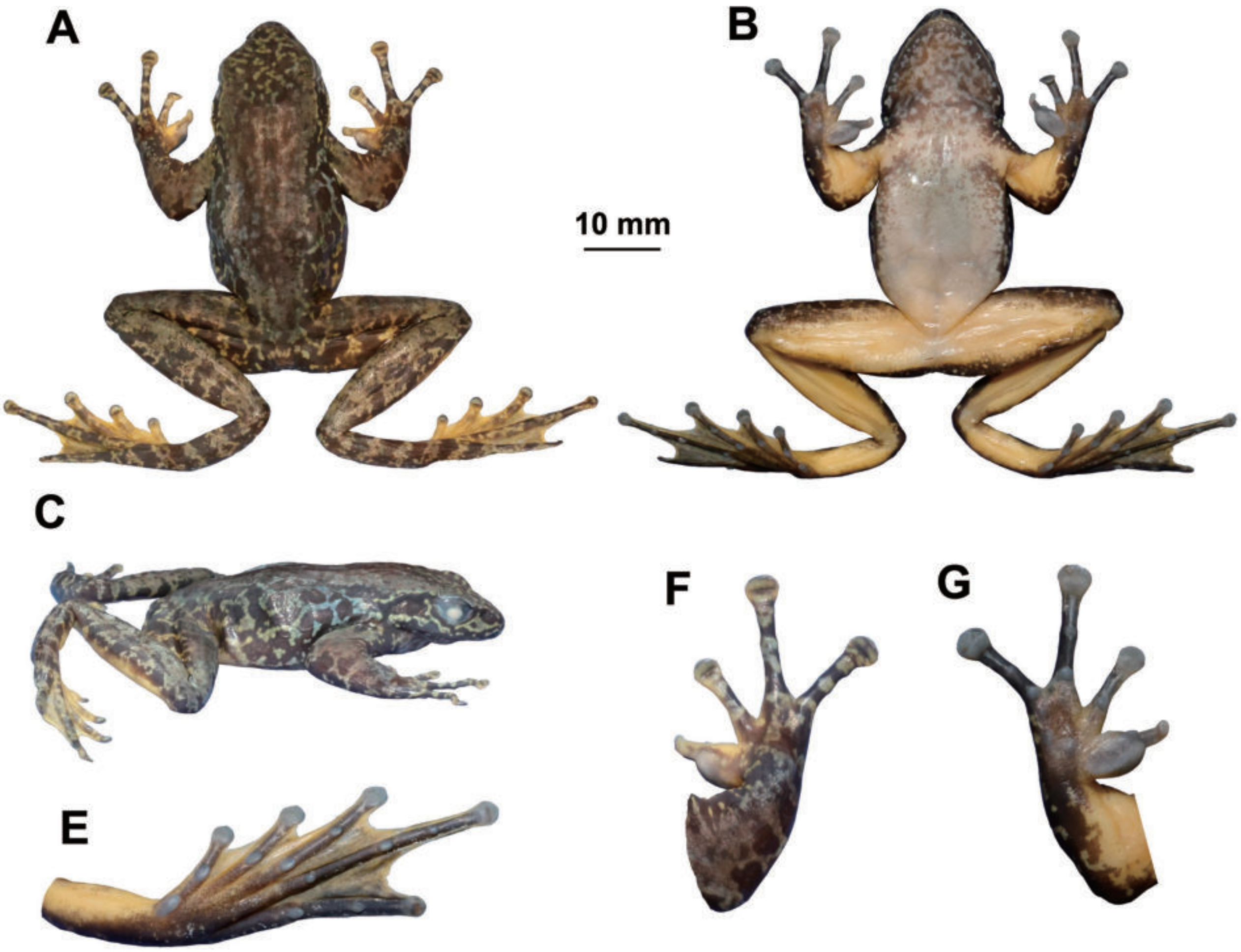

Figure 4. The holotype specimen MT DF20230601002 of *Amolops dafangensis* sp. nov. **A** dorsal view **B** ventral view **C** lateral view **D** dorsal view of hand **E** ventral view of hand **F** ventral view of foot.

Secondary sexual characteristics. Adult males lack vocal sacs. In breeding, pale yellow glandular nuptial pads are present on finger I in males.

Morphological comparisons. The molecular phylogenetic results placed the new species as an independent clade into *A. marmoratus* group. Within the *A. mantzorum* group, the new species can be distinguished from *A. ailao* by having a larger body size (adult males SVL 43.2–46.8 mm vs 33.0–35.1 mm); by vomerine teeth present (vs absent), and by tibiotarsal articulation reaching the level far beyond the tip of the snout when leg stretched forward (vs reaching beyond anterior corner of eye); differs from *A. granulosus* by having a smooth dorsum skin (vs rough with spinules in males) and the absence of vocal sacs in males (vs present); differs from *A. lifanensis* by having a smaller body size (adult males SVL 43.2–46.8 mm vs 52.0–56.0) and having distinct tympanum (vs indistinct); differs from *A. mantzorum* by having a smaller body size (adult males SVL 43.2 – 46.8 mm vs 49.0–57.0 mm), head length about equal to or larger than head width (vs head length smaller than head width); differs from *A. minutus* by having a larger body size (adult males SVL 43.2–46.8 mm vs 29.70–36.42 mm), and the absence of vocal sacs and gular pouches in males (vs well developed); differs from *A. ottorum* by the presence of vomerine teeth (vs absent); differs from *A. shuichengicus* by having a larger body size in males (adult males SVL 43.2–46.8 mm vs 34.6–39.6 mm), and having

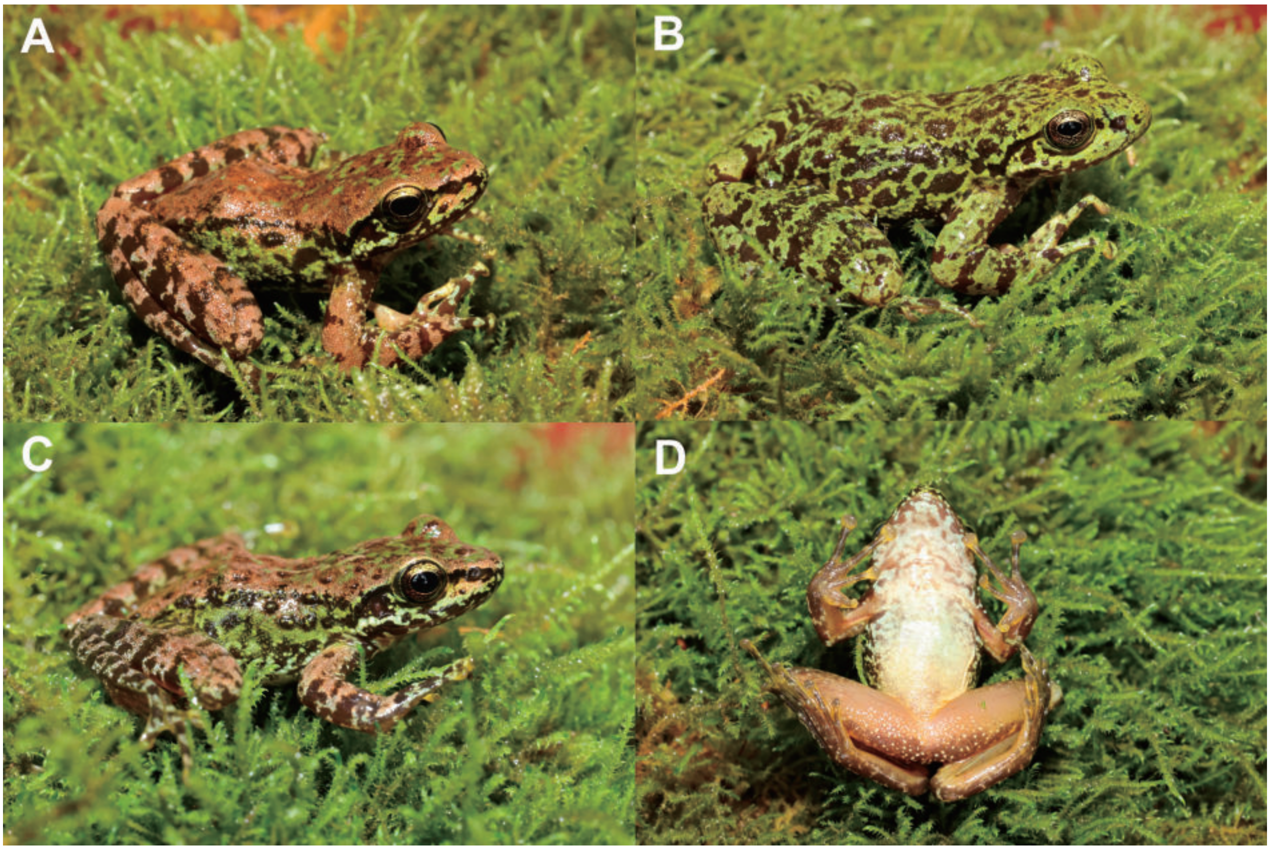

Figure 5. Color variation in *Amolops dafangensis* sp. nov. **A** dorsolateral view of the male specimen MT DF20230601001 **B** dorsolateral view of the male specimen MT DF20230601003 **C** dorsolateral view of the juvenile specimen MT DF20230601004 **D** ventral view of the male specimen juvenile specimen MT DF20230601004

weak dorsolateral glandular lines (vs strong dorsolateral folds); differs from *A. tuberodepressus* by having a smaller body size (adult males SVL 43.2–46.8 mm vs 48–56mm), and by having weak dorsolateral glandular lines (vs absent); differs from *A. jinjiangensis* by having distinct tympanum (vs indistinct).

Amolops dafangensis sp. nov. is phylogenetically most closed to *A. loloensis* and *A. sangzhiensis*, and the new species could be distinguished from *A. loloensis* by having a smaller body size in males (adult males SVL 43.2–46.8 mm vs 55–62 mm), having distinct tympanum (vs indistinct), tibiotarsal articulation reaching the level far beyond the tip of the snout when leg stretched forward (vs just reaching eye or nostrils), spots on head and dorsum irregular (vs spots on head and dorsum round or oval); differs from *A. sangzhiensis* by having a larger body size in males (adult males SVL 43.2–46.8 mm vs 40.3–40.9 mm), having distinct tympanum (vs indistinct),tibiotarsal articulation reaching the level far beyond the tip of the snout when leg stretched forward (vs just reaching nostrils), mouth corner smooth (vs with dense spiny tubercles around the mouth corner).

Amolops dafangensis sp. nov. differs from the species of the *A. monticola* group namely *A. adicola*, *A. akhaorum*, *A. aniqiaoensis*, *A. archotaphus*, *A. bellulus*, *A. binchachaensis*, *chakrataensis*, *A. chaochin*, *A. chunganensis*, *A. compotrix*, *A. cucae*, *A. daorum*, *A. deng*, *A. iri*, *A. kohimaensis*, *A. mengdingensis*, *A. mengyangensis*, *A. monticola*, *A. nyingchiensis*, *A. putaoensis*, *A. truongi*, *A. tuanjieensis*, *A. vitreus*, and *A. wenshanensis* by dorsolateral folds weak formed by series of glands (vs truth dorsolateral folds present), further distinguished from *A. adicola*, *A. akhaorum*, *A. aniqiaoensis*, *A. archotaphus*, *A. chaochin*, *A. chunganensis*, *A. compotrix*, *A. cucae*, *A. daorum*, *A. iriodes*, *A. kohimaensis*, *A. mengdingensis*, *A. mengyangensi*s, *A. monticola*, *A. putaoensis*, *A. truongi*, *A. tuanjieensis*, *A. vitreus*, and *A. wenshanensis* by vocal sac absent (vs present).

Amolops dafangensis sp. nov. differs from *A. chayuensis*, the sole member of the *A. chayuensis group*, by dorsolateral folds weak formed by series of glands (vs truth dorsolateral folds present), and vocal sacs absent (vs present).

Amolops dafangensis sp. nov. differs from the *A. viridimaculatus* group contains 14 species, namely *A. beibengensis*, *A. chanakya*, *A. formosus*, *A. himalayanus*, *A. kaulbacki*, *A. longimanus*, *A. medogensis*, *A. nidorbellus*, *A. pallasitatus*, *A. senchalensis*, *A. tawang*, *A. wangyali*, *A. wangyufani*, and *A. viridimaculatus* by dorsolateral folds weak formed by series of glands (vs dorsolateral folds absent) and smaller body size (vs male SVL 75.8 mm in *A. beibengensis*, male SVL 76.4 mm in *A. chanakya*, males SVL 61.3–63.1 mm in *A. formosus*, male SVL 80 mm in *A. himalayanus*, males SVL 70–72 mm in *A. kaulbacki*, male SVL 95 mm in *A. medogensis*, males SVL 76.4–82.3 mm in *A. nidorbellus*, male SVL 46.2 mm in *A. senchalensis*, male SVL 82.5 mm in *A. tawang*, males SVL 71.4–76.7 mm in *A. wangyali*, males SVL 68.3–69.0 mm in *A. wangyufani*, and males SVL 72.7–82.3 mm in *A. viridimaculatus*).

Amolops dafangensis sp. nov. differs from the *A. marmoratus* group of 13 species (*A. afghanus*, *A. assamensis*, *A. gerbillus*, *A. indoburmanensis*, *A. jaunsari*, *A. latopalmatus*, *A. mahabharatensis*, *A. marmoratus*, *A. nepalicus*, *A. panhai*, *A. siju*, and *A. terraorchis*) by circum-marginal groove on disc of finger I absent (vs present), and vocal sac absent (vs present with the exception of *A. siju*).

Amolops dafangensis sp. nov. differs from *A. spinapectoralis*, the sole member of the *A. spinapectoralis* group, by circum-marginal groove on disc of finger I absent (vs present), and vocal sac absent (vs present).

Amolops dafangensis sp. nov. differs from the *A. larutensis* group with eight species, namely *A. attiguus*, *A. australis*, *A. cremnobatus*, *A. gerutu*, *A. kottelati*, *A. larutensis*, *A. sengae*, and *A. tanfuilianae* by circum-marginal groove on disc of finger I absent (vs present), and vocal sac absent (vs present).

Amolops dafangensis sp. nov. differs from the *A. ricketti* group that contains eight species (*A. shihaitaoi*, *A. sinensis*, *A. ricketti*, *A. wuyiensis*, *A. yunkaiensis*, *A. albispinus*, *A. yatseni*, and *A. tonkinensis*) by circum-marginal groove on disc of finger I absent (vs present), dorsolateral glandular folds present (vs absent), and nuptial pad without conical or papillate nuptial spines (vs present).

Amolops dafangensis sp. nov. differs from the *A. daiyunensis* group of three species, namely *A. daiyunensis*, *A. teochewiensis* and *A. teochew*, by circum-marginal groove on disc of finger I absent (vs present), vomerine teeth present (vs absent) and and vocal sac absent (vs present).

Amolops dafangensis sp. nov. differs from the *A. hainanensis* group (*A. hainanensis* and *A. torrentis*) by vomerine teeth present (vs absent) and further differs from *A. hainanensis* by having a smaller body size (adult males SVL 43.2–46.8 mm vs 71–93 mm) and circum-marginal groove on disc of finger I absent (vs present); further differs from *A. torrentis* by having a larger body size (adult males SVL 43.2–46.8 mm vs 28–33 mm) and vocal sac absent (vs present).

Distribution and ecology. At present, *Amolops dafangensis* sp. nov. was only found on vegetation in a mountain stream in Dafang County, Guizhou Province, China at approximately 1600 m elevation. The rocks of this stream are covered with moss, and low vegetation grows out of the cracks (Fig. 6). We did not find eggs, nor *Amolops dafangensis* sp. nov. tadpoles or females, and advertisement calls were not recorded, but we observed distinct nuptial pad in the males. Based on our surveys, we speculate that the breeding season is probably in early June. *Boulenophrys jiangi* (Liu, Li, Wei, Xu, Cheng, Wang & Wu, 2020), *Boulenophrys qianbeiensis* (Su, Shi, Wu, Li, Yao, Wang & Li, 2020), and *Leptobrachella jinshaensis* Cheng, Shi, Li, Liu, Li & Wang, 2021were also found in the type locality.

Etymology. The specific epithet *dafangensis* refers to the distribution of this species, Dafang County, Guizhou Province, China. We propose the common English name “Dafang cascade frogs” for this species and Chinese name as “Da Fang Tuan Wa (大方湍蛙)”.

Figure 6. Habitat of *Amolops dafangensis* sp. nov. in the type locality, Dafang County, Guizhou Province, China.

Discussion

In this study, we describe a new species based on morphological comparisons and molecular phylogenetic analyses; although the genetic distance between the new species and its most closely-related congeners is 0.7% for the 16S gene, the morphological characters differ from those of other species of the genus *Amolops*. This small genetic difference is likely due to the limited phylogenetic information content in this particular gene fragment (Chan et al. 2022). Speciation usually begins with spatial isolation or adaptation to unique environments without strict isolation (Schilthuizen 2000). Significant spatial isolation and subsequent formation of unique lineages may be due to isolation or long-range dispersal across barriers such as mountains, rivers, or other intervening unsuitable habitats (Mayr 1963; Avise 2000; Rundle and Nosil 2005; Schluter 2009). The geographical distances between *Amolops dafangensis* sp. nov. and its closely-related congeners *A. sangzhiensis* and *A. loloensis* are more than 800 km and 370 km, respectively, and the type locality of the three species are in different mountains: the new species is distributed in Dalou Mountains, *A. sangzhiensis* in easternmost Wuling Mountains, and *A. loloensis* in the Daliangshan Mountains, with significantly different biota. Therefore, we speculate that isolation is likely to have promoted speciation between the lineages and led to the evolution of different morphologies between the new species, *A. sangzhiensis*, and *A. loloensis*.

In the last five years, 25 new frog species have been described in Guizhou Province, China (Frost 2023). Dafang County is in the northwest of Guizhou Province, China, and there have been few surveys of amphibians in the area over the years. From 2020 to 2023 we conducted five surveys in this region. Only in June 2023 was the new species discovered, and only three adult males and two juveniles were found in a range of ~ 100 meters below the source of the stream. Therefore, we infer that the population of the new species is small. We recommend the new species be assigned as vulnerable (VU) according to the evaluation criteria of the IUCN Red List of threatened Species (IUCN 2012). Future research should focus on determining the distribution and elevational range of the species.

Additional information

Conflict of interest

The authors have declared that no competing interests exist.

Ethical statement

No ethical statement was reported.

Funding

This work was supported by the Projects from the West Light Foundation of The Chinese Academy of Sciences (Grant No. 2021XBZG_XBQNXZ_A_006), the National Natural Science Foundation of China (Nos. 32270498, 31960099, 32260136, and 32070426), Guizhou Provincial Science and Technology Projects (Nos. ZK[2022]540 and [2023] 099), Forestry Science and Technology Research Project of Guizhou Forestry Department (No. [2020]13, [2020]04); Guizhou Provincial Department of Education Youth Science and Technology Talents Growth Project (Nos. KY[2020]234 and KY[2020]237), and High-level personnel research start-up funding projects of Moutai Institute (Nos. mygccrc[2022]055, mygccrc[2022]067, mygccrc[2022]083).

Author contributions

Funding acquisition: GC. Investigation: JL, XCK. Writing - original draft: SZL. Writing - review and editing: BW.

Author ORCIDs

Bin Wang https://orcid.org/0000-0001-6036-5579

Data availability

All of the data that support the findings of this study are available in the main text or Supplementary Information.

References

Ahl E (1927) [1925] Ueber neue oder seltene Froschlurche aus dem Zoologischen Museum Berlin Sitzungsberichte der Gesellschaft Naturforschender Freunde zu Berlin, 111–117.

Amphibia China (2023) The database of Chinese amphibians. Electronic Database. Kunming Institute of Zoology (CAS), Kunming, Yunnan, China. http://www.amphibiachina.org/

Anderson J (1871) A list of the reptilian accession to the Indian Museum, Calcutta from 1865 to 1870, with a description of some new species. Journal of the Asiatic Society of Bengal 40: 12–39.

Andersson LG (1939) [1938] Batrachians from Burma collected by Dr. R. Malaise, and from Bolivia and Ecuador collected by Dr. C. Hammarlund. Arkiv för Zoologi 30(23): 1–24.

Annandale (1912) Zoological results of the Abor Expedition, 1911–1912. I. Amphibia. Records of the Indian Museum 8: 7–36. https://doi.org/10.5962/bhl.part.1186

Avise JC (2000) Phylogeography: the history and formation of species. Harvard University Press, London, 447 pp. https://doi.org/10.2307/j.ctv1nzfgj7

Bain RH, Nguyen TQ (2004) Herpetofauna diversity of Ha Giang Province in northeastern Vietnam, with descriptions of two new species. American Museum Novitates 3453: 1–42. https://doi.org/10.1206/0003-0082(2004)453<0001:HDOHGP>2.0.CO;2

Bain RH, Lathrop A, Murphy RW, Orlov NL, Ho C (2003) Cryptic species of a cascade frog from Southeast Asia: Taxonomic revisions and descriptions of six new species. American Museum Novitates 3417: 1–60. https://doi.org/10.1206/0003-0082(2003)417<0001:CSOACF>2.0.CO;2

Bain RH, Stuart BL, Orlov NL (2006) Three new Indochinese species of cascade frogs (Amphibia: Ranidae) allied to *Rana archotaphus*. Copeia 2006(1): 43–50. https://doi.org/10.1643/0045-8511(2006)006[0043:TNISOC]2.0.CO;2

Biju SD, Mahony S, Kamei RG (2010) Description of two new species of torrent frog, *Amolops* Cope (Anura: Ranidae) from a degrading forest in the northeast Indian state of Nagaland. Zootaxa 2408(1): 31–46. https://doi.org/10.11646/zootaxa.2408.1.2

Blyth E (1855) Report of the Curator; Zoological Department, for March meeting. Journal of the Asiatic Society of Bengal 24: 187–188.

Boulenger G (1882) Catalogue of the Batrachia Salientias. Ecaudata in the Collection of the British Museum (2nd edn.) Taylor and Francis, Oxford, 503 pp. https://doi.org/10.5962/bhl.title.8307

Boulenger G (1888) Descriptions of two new Indian species of *Rana*. Annals and Magazine of Natural History Series 6 2(12): 506–508. https://doi.org/10.1080/00222938809487521

Boulenger G (1899a) Descriptions of new batrachians in the collection of the British Museum (Natural History). Annals and Magazine of Natural History Series 7 3(16): 273–277. https://doi.org/10.1080/00222939908678122

Boulenger G (1899b) On a collection of reptiles and batrachians made by Mr. J. D. Latouche in N.W. Fokien, China. Proceedings of the Zoological Society of London 1899: 159–172. https://doi.org/10.1111/j.1469-7998.1899.tb06855.x

Boulenger G (1900) [1899] On the reptiles, batrachians, and fishes collected by the late Mr. John Whitehead in the interior of Hainan. Proceedings of the Zoological Society of London 1899: 956–962.

Chan KO, Abraham RK, Grismer LL (2018) Elevational size variation and two new species of torrent frogs from Peninsular Malaysia (Anura: Ranidae: *Amolops* Cope). Zootaxa 4434: 250–264. https://doi.org/10.11646/zootaxa.4434.2.2

Chan KO, Hertwig ST, Neokleous DN, Flury JM, Brown RM (2022) Widely used, short 16S rRNA mitochondrial gene fragments yield poor and erratic results in phylogenetic estimation and species delimitation of amphibians. BMC Evolutionary Biology 22(1): 37. https://doi.org/10.1186/s12862-022-01994-y

Chanda SK (1987) [1986] On a collection of anuran amphibians from Darjeeling and Sikkim Himalayas, with description of a new species of *Rana* (Ranidae). Journal of the Bengal Natural History Society. New Series 5: 140–151.

Che J, Chen HM, Yang JX, Jin JQ, Jiang K, Yuan ZY, Murphy RW, Zhang YP (2012) Universal COI primers for DNA barcoding amphibians. Molecular Ecology Resources 12(2): 247–258. https://doi.org/10.1111/j.1755-0998.2011.03090.x

Che J, Jiang K, Yan F, Zhang YP (2020) Amphibians and Reptiles in Tibet–Diversity and Evolution. Science Press, Beijing, 836 pp.

David A (1872) [1871] Rapport adressé a MM. les Professeurs-Administráteurs du Museum d'histoire naturelle. Nouvelles Archives du Muséum d'Histoire Naturelle Paris 7: 75–100.

Dever JA, Fuiten AM, Konu Ö, Wilkinson JA (2012) Cryptic Torrent frogs of Myanmar: An examination of the *Amolops marmoratus* species complex with the resurrection of *Amolops afghanus* and the identification of a new species. Copeia 2012(1): 57–76. https://doi.org/10.1643/CH-10-180

Fei L, Ye CY, Huang YZ, Liu MY (1999) Atlas of Amphibians of China. Henan Science and Technology Press, Zhengzhou, 432 pp.

Fei L, Hu SQ, Ye CY, Huang YZ (2009) Fauna Sinica. Amphibia Vol. 2 Anura. Science Press, Beijing, 957 pp.

Fei L, Ye CY, Jiang JP (2012) Colored atlas of Chinese amphibians and their distributions. Sichuan Publishing House of Science & Technology, Chengdu, 619 pp.

Frost DR (2023) Amphibian Species of the World: an Online Reference. Version 6.1. Electronic Database. American Museum of Natural History, New York, USA. http://research.amnh.org/herpetology/amphibia/index.html [Accessed 28 August 2023]

Gan YL, Yu GH, Wu ZJ (2020a) A new species of the genus *Amolops* (Anura: Ranidae) from Yunnan, China. Zoological Research 41: 1–6. https://doi.org/10.24272/j.issn.2095-8137.2020.125

Gan YL, Qin T, Lwin YH, Li GG, Quan RC, Liu S, Yu GH (2020b) A new species of *Amolops* (Anura: Ranidae) from northern Myanmar. Zoological Research 41(6): 733–739. https://doi.org/10.24272/j.issn.2095-8137.2020.125

Guindon S, Dufayard JF, Lefort V, Anisimova M, Hordijk W, Gascuel O (2010) New algorithms and methods to estimate maximum-likelihood phylogenies: Assessing the performance of PhyML 3.0. Systematic Biology 59(3): 307–321. https://doi.org/10.1093/sysbio/syq010

Günther ACLG (1858) Neue Batrachier in der Sammlung des britischen Museums. Archiv für Naturgeschichte 24: 319–328. https://doi.org/10.5962/bhl.part.5288

Günther ACLG (1876) [1875] Third report on collections of Indian reptiles obtained by the British Museum. Proceedings of the Zoological Society of London 1875: 567–577.

Hall TA (1999) BIOEDIT: A user-friendly biological sequence alignment editor and analysis program for Windows 95/98/NT. Nucleic Acids Symposium Series 41(41): 95–98.

Inger RF, Chan-ard T (1997) A new species of ranid frog from Thailand, with comments on *Rana livida* (Blyth). The Natural History Bulletin of the Siam Society 45: 65–70.

Inger RF, Kottelat M (1998) A new species of ranid frog from Laos. The Raffles Bulletin of Zoology 46: 29–34.

Inger RF, Orlov N L, Darevsky IS (1999) Frogs of Vietnam: A report on new collections. Fieldiana Zoology New Series 92: 1–46.

IUCN (2012) IUCN Red List Categories and Criteria: Version 3.1, 2nd edn. Cambridge, Gland, 16 pp.

Jiang YM (1983) A new species of the genus *Staurois* (Ranidae), *Staurois viridimaculatus*. Acta Herpetologica Sinica. New Series. Chengdu 2(3): 71.

Jiang K, Wang K, Xie J, Zou DH, Liu WL, Jiang JP, Li C, Che J (2016) A new species of the genus *Amolops* (Amphibia: Ranidae) from southeastern Tibet, China. Zoological Research 37: 31–40.

Jiang K, Ren JL, Lyu ZT, Wang D, Wang Z, Lv K, Wu JW, Li JT (2021) Taxonomic revision of *Amolops chunganensis* (Pope, 1929) (Amphibia: Anura) and description of a new species from southwestern China, with discussion on *Amolops monticola* group and assignment of species groups of the genus *Amolops*. Zoological Research 42(5): 574–591. https://doi.org/10.24272/j.issn.2095-8137.2021.107

Khatiwada JR, Shu GC, Wang B, Zhao T, Xie F, Jiang JP (2020) Description of a new species of *Amolops* Cope, 1865 (Amphibia: Ranidae) from Nepal and nomenclatural validation of *Amolops nepalicus* Yang, 1991. Asian Herpetological Research 11: 71–95. https://doi.org/10.16373/j.cnki.ahr.190052

Lanfear R, Calcott B, Ho SYW, Guindon S (2012) PartitionFinder: Combined selection of partitioning schemes and substitution models for phylogenetic analyses. Molecular Biology and Evolution 29(6): 1695–1701. https://doi.org/10.1093/molbev/mss020

Liu CC (1945) New frogs from West China. Journal of the West China Border Research Society, Series B 15: 28–44.

Liu CC (1950) Amphibians of western China. Fieldiana. Zoology Memoirs 2: 353–356. https://doi.org/10.5962/bhl.part.4737

Liu CC, Hu SQ (1961) Tailless Amphibians of China. Science Press, Beijing, 233–235.

Liu CC, Hu SQ (1975) Report on three new species of Amphibia from Fujian Province. Dong Wu Xue Bao 21: 265–271.

Liu WZ, Yang DT (2000) A new species of *Amolops* (Anura: Ranidae) from Yunnan, China, with a discussion of karyological diversity in *Amolops*. Herpetologica 56: 231–238. https://doi.org/10.1643/0045-8511(2000)000[0536:ABANSO]2.0.CO;2

Liu WZ, Yang DT, Ferraris C, Matsui M (2000) *Amolops bellulus*: a new species of stream-breeding frog from western Yunnan, China (Anura: Ranidae). Copeia 2000(2): 536–541. https://doi.org/10.1643/0045-8511(2000)000[0536:ABANSO]2.0.CO;2

Lu B, Bi K, Fu JZ (2014) A phylogeographic evaluation of the *Amolops mantzorum* species group: Cryptic species and plateau uplift. Molecular Phylogenetics and Evolution 73: 40–52. https://doi.org/10.1016/j.ympev.2014.01.008

Lyu ZT, Wu J, Wang J, Sung Y-H, Liu Z-Y, Zeng Z-C, Wang X, Li Y-Y, Wang Y-Y (2018) A new species of *Amolops* (Anura: Ranidae) from southwestern Guangdong, China. Zootaxa 4418(6): 562–576. https://doi.org/10.11646/zootaxa.4418.6.4

Lyu ZT, Huang LS, Wang J, Li YQ, Chen HH, Qi S, Wang YY (2019a) Description of two cryptic species of the *Amolops ricketti* group (Anura, Ranidae) from southeastern China. ZooKeys 812: 133–156. https://doi.org/10.3897/zookeys.812.29956

Lyu ZT, Zeng ZC, Wan H, Yang JH, Li YL, Pang H, Wang YY (2019b) A new species of *Amolops* (Anura: Ranidae) from China, with taxonomic comments on *A. liangshanensis* and Chinese populations of *A. marmoratus*. Zootaxa 4609(2): 247–268. https://doi.org/10.11646/zootaxa.4609.2.3

Mahony S, Nidup T, Streicher JW, Teeling EC, Kamei RG (2022) A review of torrent frogs (*Amolops*: Ranidae) from Bhutan, the description of a new species, and reassessment of the taxonomic validity of some *A. viridimaculatus* group species aided by archival DNA sequences of century-old type specimens. The Herpetological Journal 32(3): 142–175. https://doi.org/10.33256/32.3.142175

Matsui M, Nabhitabhata J (2006) A new species of *Amolops* from Thailand (Amphibia, Anura, Ranidae). Zoological Science 23(8): 727–732. https://doi.org/10.2108/zsj.23.727

Mayr E (1963) Animal species and evolution. Belknap Press of Harvard University Press, London, 797 pp. https://doi.org/10.4159/harvard.9780674865327

Orlov NL, Ho CT (2007) Two new species of cascade ranids of *Amolops* genus (Amphibia: Anura: Ranidae) from Lai Chau Province (Northwest Vietnam). Russian Journal of Herpetology 14: 211–229.

Patel NG, Garg S, Das A, Stuart BL, Biju SD (2021) Phylogenetic position of the poorly known montane cascade frog *Amolops monticola* (Ranidae) and description of a new closely related species from Northeast India. Journal of Natural History 55(21–22): 1403–1440. https://doi.org/10.1080/00222933.2021.1946185

Pham AV, Sung NB, Pham CT, Le MD, Ziegler T, Nguyen TQ (2019) A new species of *Amolop*s (Anura: Ranidae) from Vietnam. The Raffles Bulletin of Zoology 67: 363–377.

Pham AV, Pham CT, Ngo HT, Sung NB, Ziegler T, Le MD (2023) A new species of *Amolops* (Anura: Ranidae) from Son La Province, northwestern Vietnam. The Raffles Bulletin of Zoology 71: 59–69. https://doi.org/10.26107/RBZ-2023-0004

Pope CH (1929) Four new frogs from Fukien Province, China. American Museum Novitates 352: 1–5.

Pope CH, Romer JD (1951) A new ranid frog (*Staurois*) from the Colony of Hongkong. Fieldiana. Zoology 31: 609–612.

Qi S, Zhou ZY, Lyu ZT, Lu YY, Wan H, Hou M, Guo K, Li PP (2019) Description of a New Species of *Amolops* (Anura: Ranidae) from Tibet, China. Asian Herpetological Research 10: 219–229. https://doi.org/10.16373/j.cnki.ahr.190016

Qian TY, Xiang JJ, Jiang JP, Yang DD, Gui J (2023) A new species of the *Amolops mantzorum* group (Anura: Ranidae: *Amolops*) from northwestern Hunan Province, China. Asian Herpetological Research 14: 54–64.

Ray P (1992) Two new hill-stream frogs of the genus *Amolops* Cope (Amphibia: Anura: Ranidae) from Uttar Pradesh (India). Indian Journal of Forestry 15: 346–350.

Ronquist FR, Huelsenbeck JP (2003) MrBayes3: Bayesian phylogenetic inference under mixedmodels. Bioinformatics 19(12): 1572–1574. https://doi.org/10.1093/bioinformatics/btg180

Rundle HD, Nosil P (2005) Ecological speciation. Ecology Letters 8(3): 336–352. https://doi.org/10.1111/j.1461-0248.2004.00715.x

Saikia B, Laskar MA, Dinesh KP, Shabnam A, Sinha B (2022a) Description of two new species of *Amolops* (Anura: Ranidae) from Arunachal Pradesh, Northeast India under the morphological '*Viridimaculatus* species group'. Records of the Zoological Survey of India 122: 247–266.

Saikia B, Sinha B, Laskar MA, Shabnam A, Dinesh KP (2022b) A new species of *Amolops* (Anura: Ranidae) representing the morphological '*Marmoratus* species group' from Sessa Orchid Sanctuary, Arunachal Pradesh, Northeast India. Records of the Zoological Survey of India 122: 303–322.

Saikia B, Sinha B, Shabnam A, Dinesh KP (2023) Description of a new species of *Amolops* Cope (Anura: Ranidae) from a cave ecosystem in Meghalaya, Northeast India. Journal of Animal Diversity 5(1): 36–54. https://doi.org/10.61186/JAD.5.1.36

Sambrook J, Fritsch EF, Maniatis T (1989) Molecular Cloning: A Laboratory Manual. Cold Spring Harbor Laboratory Press, New York, 125 pp.

Schilthuizen M (2000) Dualism and conflicts in understanding speciation. BioEssays 22(12): 1134–1141. https://doi.org/10.1002/1521-1878(200012)22:12<1134::AID-BIES11>3.0.CO;2-5

Schluter D (2009) Evidence for ecological speciation and its alternative. Science 80(323): 737–741. https://doi.org/10.1126/science.1160006

Sengupta S, Hussain B, Choudhury PK, Gogoi J, Ahmed MF, Choudhury NK (2008) A new species of *Amolops* (Anura: Ranidae) from Assam, north-eastern India. Hamadryad Madras 32: 5–12.

Sheridan JA, Phimmachak S, Sivongxay N, Stuart BL (2023) Systematics of the Lao torrent frog, *Amolops cremnobatus* Inger & Kottelat, 1998 (Anura: Ranidae), with descriptions of four new species. Vertebrate Zoology 73: 931–956. https://doi.org/10.3897/vz.73.e102475

Simon CF, Frari F, Beckenbach A, Crespi B, Liu H, Flook P (1994) Evolution, weighting and Phylogenetic utility of mitochondrial gene sequences and a compilation of conserved Polymerase chain reaction Primers. Annals of the Entomological Society of America 87(6): 651–701. https://doi.org/10.1093/aesa/87.6.651

Smith MA (1923) On a collection of reptiles and batrachians from the Island of Hainan. The Journal of the Natural History Society of Siam 6: 195–212.

Smith MA (1940) The amphibians and reptiles obtained by Mr. Ronald Kaulback in Upper Burma. Records of the Indian Museum 42: 465–486. https://doi.org/10.26515/rzsi/v42/i3/1940/162431

Stuart BL, Bain RH, Phimmachak S, Spence K (2010) Phylogenetic systematics of the *Amolops monticola* group (Amphibia: Ranidae), with description of a new species from northwestern Laos. Herpetologica 66(1): 52–66. https://doi.org/10.1655/08-073.1

Su CY, Yang DT, Li SM (1986) A new species of *Amolops* from the Hengduan Shan Mountains. Acta Herpetologica Sinica 5(3): 204–206.

Sun GZ, Luo WX, Sun HY, Zhang GY (2013) A new species of Cascade Frog from Tibet: China. Forestry Construction 20: 14–16.

Sung YH, Hu P, Wang J, Liu HJ, Wang YY (2016) A new species of *Amolops* (Anura: Ranidae) from southern China. Zootaxa 4170(3): 525–538. https://doi.org/10.11646/zootaxa.4170.3.6

Tamura K, Stecher G, Peterson D, Fiipski A, Kumar S (2013) MEGA6: Molecular evolutionary genetics analysis, version 6.0. Molecular Biology and Evolution 30(12): 2725–2729. https://doi.org/10.1093/molbev/mst197

Tang SJ, Sun T, Liu S, Luo SD, Yu GH, Du LN (2023) A new species of cascade frog (Anura: Ranidae: *Amolops*) from central Yunnan, China. Zoological Letters 9(15): 1–19. https://doi.org/10.1186/s40851-023-00214-9

Wang J, Li J, Du L, Hou M, Yu GH (2022) A cryptic species of the *Amolops ricketti* species group (Anura, Ranidae) from China-Vietnam border regions. ZooKeys 1112: 139–159. https://doi.org/10.3897/zookeys.1112.82551

Wu GF, Tian WS (1995) A new *Amolops* species from southern Yunnan. In: Zhao EM (Ed.) Amphibian Zoogeographic Division of China. A Symposium Issued to Celebrate the Second Asian Herpetological Meeting Held at Ashgabat, Turkmenistan, 6 to 10 September 1995. Sichuan Journal of Zoology, Supplement, 51–52.

Wu YH, Yan F, Stuart BL, Prendini E, Suwannapoom C, Dahn HA, Zhang BL, Cai HX, Xu YB, Jiang K, Chen HM, Lemmon EM, Raxworthy CJ, Orlov NL, Murphy RW, Che J (2020) A combined approach of mitochondrial DNA and anchored nuclear phylogenomics sheds light on unrecognized diversity, phylogeny, and historical biogeography of the torrent frogs, genus Amolops (Anura: Ranidae. Molecular Phylogenetics and Evolution 144(106701): 1–13. https://doi.org/10.1016/j.ympev.2020.106789

Yu GH, Wu ZJ, Yang JX (2019) A new species of the *Amolops monticola* group (Anura: Ranidae) from southwestern Yunnan, China. Zootaxa 4577(3): 548–560. https://doi.org/10.11646/zootaxa.4577.3.8

Yuan ZY, Jin JQ, Li J, Stuart BL, Wu J (2018) A new species of cascade frog (Amphibia: Ranidae) in the *Amolops monticola* group from China. Zootaxa 4415(3): 498–512. https://doi.org/10.11646/zootaxa.4415.3.5

Zeng Z, Liang D, Li JX, Lyu ZT, Wang YY, Zhang P (2020) Phylogenetic relationships of the Chinese torrent frogs (Ranidae: *Amolops*) revealed by phylogenomic analyses of AFLP-Capture data. Molecular Phylogenetics and Evolution 146: 106753. https://doi.org/10.1016/j.ympev.2020.106753

Zeng ZC, Wang J, Lyu ZT, Wang YY (2021) A new species of Torrent frog (Anura, Ranidae, *Amolops*) from the Coastal Hills of Southeastern China. Zootaxa 5004(1): 151–166. https://doi.org/10.11646/zootaxa.5004.1.6

Zhao WG, Rao DQ, Lü SQ, Dong BJ (2005) Herpetological surveys of Xizang autonomous region 2. Medog. Sichuan Journal of Zoology 24: 250–253.

Zhu JG, Rao D (2022) Atlas of Wildlife in Southwest China: Amphibian. Beijing Publishing Group, Beijing, 295 pp.

Supplementary material 1

Uncorrected p-distances between species in the *Amolops mantzorum* group based on the 16S gene sequences

Authors: Shi-Ze Li, Jing Liu, Xiao-Cong Ke, Gang Cheng, Bin Wang

Data type: xlsx

Link: https://doi.org/10.3897/zookeys.1189.115621.suppl1

Supplementary material 2

Uncorrected p-distances between species in the *Amolops mantzorum* group based on the COI gene sequences

Authors: Shi-Ze Li, Jing Liu, Xiao-Cong Ke, Gang Cheng, Bin Wang

Data type: xlsx

Link: https://doi.org/10.3897/zookeys.1189.115621.suppl2

ZooKeys 1189: 55–81 (2024)
DOI: 10.3897/zookeys.1189.111064

Research Article

Three new species and five new records within the genus *Lilioceris* (Coleoptera, Chrysomelidae, Criocerinae) from China

Yuan Xu[1,2], Hongbin Liang[1]

1 *Key Laboratory of Zoological Systematics and Evolution, Institute of Zoology, Chinese Academy of Sciences, Beijing 100101, China*
2 *College of Life Science, University of Chinese Academy of Sciences, Beijing 100049, China*
Corresponding author: Hongbin Liang (lianghb@ioz.ac.cn)

Abstract

The Chinese species of *Lilioceris* are revised, and three new species are described from Tibet, China: *Lilioceris zhentangensis* Xu & Liang, **sp. nov.**, *Lilioceris medogensis* Xu & Liang, **sp. nov.** and *Lilioceris zayuensis* Xu & Liang, **sp. nov.** Five species of *Lilioceris* are reported for China as new records: *L. dromedarius* (Baly, 1861), *L. pulchella* (Baly, 1859), *L. semicostata* (Jacoby, 1908), *L. unicolor* (Hope, 1831) and *L. nepalensis* Takizawa, 1989. *Lilioceris seminigra* (Jacoby, 1889) is proposed as a junior synonym of *L. unicolor* Hope, 1831. Redescriptions, habitus photographs, geographic distributions, host plants (if available) and habitats are provided for these species.

Key words: Habitat, host plant, map, new synonym, Shining leaf beetle, taxonomy, Tibet

Academic editor: A. Konstantinov
Received: 12 August 2023
Accepted: 11 December 2023
Published: 12 January 2024

ZooBank: https://zoobank.org/A337B9F1-F9E7-47DC-9422-D8B68316A66B

Citation: Xu Y, Liang H (2024) Three new species and five new records within the genus *Lilioceris* (Coleoptera, Chrysomelidae, Criocerinae) from China. ZooKeys 1189: 55–81. https://doi.org/10.3897/zookeys.1189.111064

Introduction

Lilioceris Reitter, 1913 is the second largest genus of Criocerinae, containing approximately 160 species in the world and 60 species in China. Most of the species of *Lilioceris* are distributed in the Oriental region (Clavareau 1913; Monrós 1960) and the Chinese species are mainly distributed in the southern part of China (Bezděk and Schmitt 2017).

Tibet is the second largest autonomous region in China, with various climatic zones from the tropics to frigid mountains. However, *Lilioceris* in Tibet has been poorly investigated in the past: only four species have been recorded (Yang 2004). *Lilioceris subpolita* (Motschulsky) was obviously misidentified from Tibet and is excluded from its fauna (Bezděk and Schmitt 2017; Xu et al. 2021). In recent years seven expeditions were made in Tibet and Yunnan. These expeditions resulted in more than two thousand specimens of Criocerinae. Among *Lilioceris* collected in Dinggyê, Mêdog and Zayü were species new to science. We also identified five species, collected in Tibet and Yunnan that were originally recorded in India, Nepal or Cambodia.

The purpose of this paper is three-fold: to describe three new species from Tibet, to report five new distribution records from Tibet, Yunnan and Hainan, and to synonymize a species of *Lilioceris*.

Material and methods

Specimens from several museums and collections were examined. The collections cited in this article are indicated by the following abbreviations: **IZCAS** = National Zoological Museum, Institute of Zoology, Chinese Academy of Sciences, Beijing, China; **MNHN** = Museum national d'Histoire naturelle, Paris, France; **NHML** = Natural History Museum, London, UK; **SEHU** = Systematic Entomology, Graduate School of Agriculture, Hokkaido University, Japan.

Dry specimens were soaked in hot water for 1–2 hours. Then the abdomen was opened at its latero-apical margin and genitalia removed using forceps, soaked in warm 10% KOH for 1 h, and dyed in Chlorazol Black E. The basal orifice of the aedeagus was injected with 100% ethanol with a micro-injector until the internal sac was fully everted. The aedeagus with its everted internal sac was photographed using a large depth-of-field 3D digital microscope (Keyence VHX–1000C) and edited in Adobe Photoshop (CC). For storage, a microvial with genitalia was pinned to the specimen from which the genitalia were removed.

Body length (**BL**) was measured from the anterior margin of the labrum to the apex of the elytra; body width (**BW**) was measured along the greatest elytral width.

Other methods of specimen observation and preparation follow previous publications (Tishechkin et al. 2011; Li et al. 2013). Morphological terminology follows Chou et al. (1993) and Matsumura et al. (2013). Redescriptions are provided for newly recorded species because of their insufficient original information.

Taxonomic account

Lilioceris zhentangensis **Xu & Liang, sp. nov.**
https://zoobank.org/1AAF4F83-3597-4A54-BE59-5BA316F1D980
Figs 1, 2, 19A–D, 22A–D, 28A–C, 36, 42–45

Material examined. Total 47 specimens. ***Holotype*****:** 1♂, Tibet, Dinggyê, Zhêntang, Nadang village / 2021.6.25 / 27.85317°N, 87.44903°E, 2491 m / Hongbin Liang, Yuan Xu and Neng Zhang coll. (IZCAS); ***Paratypes*****:** 7♀9♂, Tibet, Dinggyê, Zhêntang, Nadang village / 2021.6.25 / 27.85317°N, 87.44903°E, 2491 m / Hongbin Liang, Yuan Xu and Neng Zhang coll. (IZCAS); 3♀1♂, Tibet, Dinggyê, Zhêntang, Jiuyan Hot Spring / 2021.6.24 / 27.9068°N, 87.3777°E, 2704 m / Hongbin Liang, Yuan Xu and Neng Zhang coll. (IZCAS); 1♀2♂, Tibet, Dinggyê, Zhêntang, Qizi Tang / 2021.6.23 / 27.91232°N, 87.38273°E, 2619 m / Hongbin Liang, Yuan Xu and Neng Zhang coll. (IZCAS); 3♀6♂, Tibet, Nyingchi, Lunang road, Dongjiu village / 2022.7.23 / 29.913910°N, 94.798072°E, 2643 m / Hongbin Liang, Yuan Xu and Neng Zhang coll. (IZCAS); 3♀5♂, Tibet, Nyingchi, Lunang, Baimu village / 2022.7.24 / 29.988540°N, 94.746077°E, 2622 m / Hongbin Liang, Yuan Xu and Neng Zhang coll. (IZCAS); 2♀2♂, Tibet, Nyingchi, Lunang, Baga village / 2022.7.24 / 29.998361°N, 94.695714°E, 2771 m / Hongbin Liang, Yuan Xu and Neng Zhang coll. (IZCAS); 2♀, Tibet, Bomi, Yi'ong, Bayu village / 2022.7.25 / 30.334625°N, 94.804114°E, 2296 m / Hongbin Liang, Yuan Xu and Neng Zhang coll. (IZCAS).

Diagnosis. Antennae nearly half as long as body length, antennomeres V–X quadrate. Pronotum with distinct anterior and posterior transverse impressions, pronotal disc with two rows of fine and irregular punctures in middle.

Elytral punctures sparse on basal 2/3 and absent on apical 1/3. Lateroposterior corner of metasternum densely pubescent.

Description. BL = 7.0–9.0 mm, BW = 3.3–4.2 mm. Head, legs, scutellum, mesosternum, lateral metasternum, and metepisternum black; pronotum, elytra, middle metasternum, and abdomen brownish red.

Head (Fig. 1). Vertex with shallow groove in middle, punctate and pubescent, almost smooth; frontoclypeal area triangular, lateral side of disc with sparse punctures and pubescence; labrum transverse, with sparse long pubescence; antennae nearly half as long as body, antennomeres I–IV nearly globular, antennomeres V–X 1.2 times as long as wide, III–XI densely pubescent and punctate.

Pronotum (Figs 1, 19A). Anterior angle protruding, posterior angle not protruding; sides distinctly constricted in middle; anterior and posterior transverse impression distinct; middle of disc with two rows of fine and irregular punctures; basal transverse groove indistinct. Scutellum triangular and densely pubescent.

Elytra (Fig. 1). Humeri protruding, humeral groove shallow, basal impression distinct; striae with large punctures at base, punctures diminished posteriorly and absent on apical 1/3, intervals without punctures; epipleura raised, with row of fine punctures.

Mesosternum pubescent; apical portion of mesosternal process narrow and flat, obliquely pointed, not horizontally connected with metasternum. Metasternal disc very sparsely pubescent, lateroposterior corner with short strip of pubescence. Metepisternum densely pubescent (Fig. 19B).

Abdominal sternites (Fig. 19C). Lateral transverse impressions distinct on sternites I–IV, area of transverse impressions and middle of sternites I–IV smooth, other areas with dense pubescence and punctures.

Legs (Fig. 2). Femora with dense pubescence on dorsal surface, with sparse pubescence on ventral surface, middle area widened.

Male genitalia (Fig. 22A–D). Apical foramen occupying 1/5 length of median lobe (Fig. 22A); apex hooked (Fig. 22B); tegmen Y-shaped, basal piece of tegmen oval and broad, lateral lobes slightly sclerotized and combined with second connecting membrane; internal sac with distinct dorsal and ventral sclerites, posterior part of dorsal sclerite in dorsal view parallel, ventral sclerite extended and tubular, median sclerite very small (Fig. 22C, D).

Female reproductive organs (Fig. 28A–C). Tergites VIII and IX, and sternites VIII and IX of female sclerotized, posterior areas of tergite VIII and sternite VIII with pubescence and apodemes, spiculum gastrale Y-shaped and long; ovipositor with dense pubescence, distal part of ovipositor cylindrical, short, with protuberance; spermatheca simple and curved.

Distribution (Fig. 36). China (Tibet).

Etymology. The specific name *zhentangensis* refers to its type locality Zhêntang, Dinggyê County, Tibet.

Host plant and habitat (Figs 42–45). The host plant is *Smilax menispermoidea* A. DC., (Smilacaceae) according to our observations in Zhêntang town. Zhêntang is located in a deep valley at the southern part of the Himalayas. Warm and humid air currents from the Indian Ocean enter the valley frequently. Abundant rainfall and rugged topography in the valley make the biodiversity of Zhêntang very rich. This species occurs at the altitude of 2200 to 2800 m. The habitat is open, composed of tall trees, woody vines and weeds.

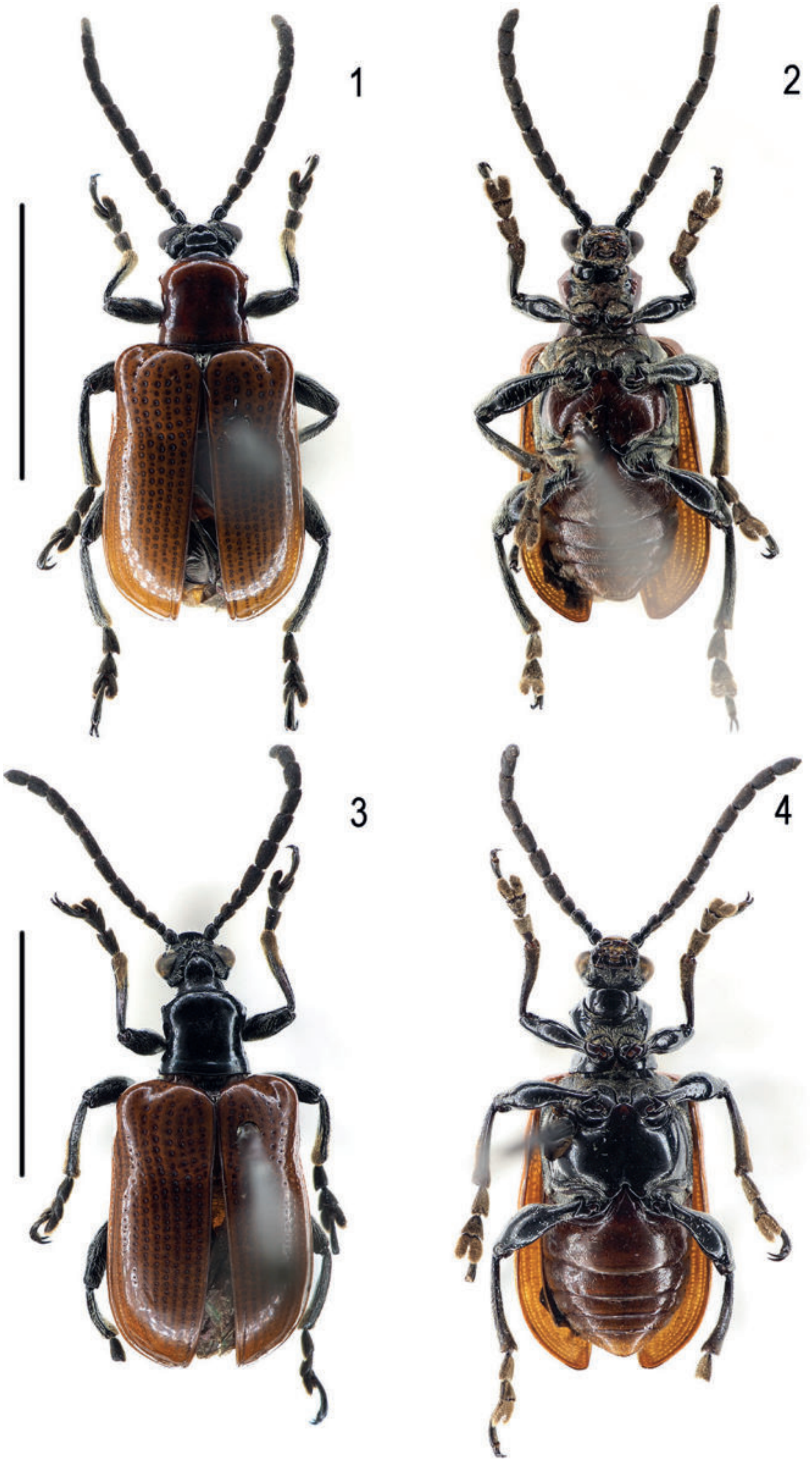

Figures 1–4. Habitus of new *Lilioceris* species (holotypes) **1, 2** *L. zhentangensis*, holotype, China (Tibet) **3, 4** *L. medogensis*, holotype, China (Tibet). Scale bars: 5.0 mm.

Remarks. This species looks similar to *L. cyanicollis* (Pic, 1916) (our concept is based on a specimen determined by J. L. Gressitt, NHML), but is differentiated by its pronotum with distinct anterior and posterior transverse impressions; head, antennae, and legs without blue metallic luster. In *L. cyanicollis*, the pronotum only with a weak posterior transverse impression; head, antennae, and legs with a blue metallic luster. It is also similar to *L. latissima* (Pic, 1932) (based on a syntype studied, MNHN), but differs by the metasternum with a short strip of pubescence. In *L. latissima*, the metasternum is glabrous.

Lilioceris medogensis **Xu & Liang, sp. nov.**

https://zoobank.org/88E1CB44-7DD5-47FF-9373-D6A0679F670A
Figs 3, 4, 20A–D, 23A–D, 29A–C, 36, 38–41

Material examined. Total 51 specimens. ***Holotype*****:** 1♂, Tibet, Mêdog, Renqingbung temple / 2020.9.3 / 29.30564°N, 95.35326°E, 1982 m / Hongbin Liang and Neng Zhang coll. (IZCAS); ***Paratypes*****:** 7♀7♂, Tibet, Mêdog, Renqingbung temple / 2020.9.3 / 29.30564°N, 95.35326°E, 1982 m / Hongbin Liang and Neng Zhang coll. (IZCAS); 4♀5♂, Tibet, Mêdog, Renqingbung temple / 2020.9.12 / 29.30564°N, 95.35326°E, 1982 m / Hongbin Liang and Neng Zhang coll. (IZCAS); 2♀4♂, Tibet, Mêdog, Renqingbung temple / 2021.6.9 / 29.30564°N, 95.35326°E, 1982 m / Hongbin Liang, Yuan Xu and Neng Zhang coll. (IZCAS); 3♀8♂, Tibet, Mêdog, Renqingbung temple / 2022.7.18 / 29.30564°N, 95.35326°E, 1982 m / Hongbin Liang, Yuan Xu and Neng Zhang coll. (IZCAS); 5♀5♂, Tibet, Mêdog, Renqingbung temple / 2023.7.13 / 29.30564°N, 95.35326°E, 1982 m / Neng Zhang coll. (IZCAS); 1♂, Tibet, Mêdog, Baibung, Dergong village / 2019.8.12, 29.19711°N, 95.14767°E, 1529 m / Hongbin Liang and Yuan Xu coll. (IZCAS); 1♂, Tibet, Mêdog, Baibung, Dergong village / 2022.7.17, 29.180592°N, 95.143494°E, 1656 m / Yuan Xu coll. (IZCAS); 1♂, Tibet, Mêdog, Baibung, Gelin village / 2019.8.12 29.22012°N, 95.17479°E, 1652 m / Hongbin Liang and Yuan Xu coll. (IZCAS); 4♀4♂, Tibet, Mêdog, Baibung, 11 km on Gelin road / 2021.6.11–15, 29.23370°N, 95.17707°E, 1408 m / Hongbin Liang, Yuan Xu and Neng Zhang coll. (IZCAS); 1♂, Tibet, Mêdog, Baibung Tea farm / 2020.9.7, 29.26310°N, 95.20983°E, 1047 m / Hongbin Liang coll. (IZCAS); 1♂, Tibet, Mêdog, Baibung, Ani bridge / 2023.7.15 / 29.315211°N, 95.175172°E, 923 m / Neng Zhang coll. (IZCAS).

Diagnosis. Elytra and abdomen brownish red, rest of body black. Antennae nearly half as long as body length, antennomeres V–X quadrate. Pronotal disc with two rows of fine punctures in middle. Elytral punctures sparse and absent on apical 1/3.

Description. BL = 8.0–10.0 mm, BW = 3.5–4.5 mm. Body black except elytra and abdomen brownish red.

Head (Fig. 3). Vertex with shallow groove in middle, punctate and pubescent sparsely; frontoclypeal area triangular, lateral side of disc with sparse punctures and pubescence; labrum transverse, with sparse long pubescence; antennae nearly half as long as body, antennomeres I–IV nearly globular, antennomere II shortest, antennomeres V–X 1.2 times as long as wide, V–XI densely pubescent and punctate.

Pronotum (Figs 3, 20B). Anterior angle protruding, posterior angle not protruding; sides distinctly constricted in middle; middle of disc with two rows of fine punctures; anterior and posterior transverse impression shallow, basal transverse groove indistinct. Scutellum triangular and densely pubescent.

Elytra (Fig. 3). Humeri protruding, humeral groove and basal impression distinct; striae with large punctures at base, punctures diminished posteriorly and absent on apical 1/3, intervals without punctures; epipleura raised, with row of fine punctures.

Mesosternum pubescent; apical portion of mesosternal process narrow and flat, obliquely pointed, not horizontally connected with metasternum. Metasternal disc almost glabrous, posterior margin with sparse pubescence (Fig. 20B). Metepisternum densely pubescent.

Abdominal sternites (Fig. 20C). Lateral transverse impressions distinct on sternites I–IV. Lateral side of sternite I–IV and pygidium densely pubescent, other areas with sparse pubescence and punctures.

Legs (Fig. 4). Femora with dense pubescence on dorsal surface, sparse pubescence on ventral surface, middle area widened.

Male genitalia (Fig. 23A–D). Apical foramen occupying 1/5 length of median lobe (Fig. 23A); apex hooked (Fig. 23B); tegmen Y-shaped, basal piece of tegmen oval and broad, lateral lobes slightly sclerotized and combined with second connecting membrane; internal sac with distinct dorsal and ventral sclerites, posterior part of dorsal sclerite in dorsal view widened, ventral sclerite extended and tubular, median sclerite very small (Fig. 23C, D).

Female reproductive organs (Fig. 29A–C). Tergites VIII and IX, and sternites VIII and IX sclerotized, posterior areas of tergite VIII and sternite VIII with pubescence and apodemes, spiculum gastrale Y-shaped and short; ovipositor with dense pubescence, distal part of ovipositor cylindrical, short and with protuberance; spermatheca simple and curved.

Distribution (Fig. 36). China (Tibet).

Etymology. The specific name *medogensis* refers to its type locality Mêdog, Tibet, China.

Host plant and habitat (Figs 38–41). Beetles were found to feed on *Smilax ferox* Wall. Ex Kunth (Smilacaceae) in Mêdog in the northernmost edge of the tropics (China, Tibet, Mêdog), with altitudes of ~ 1000 to 2000 m. The type locality Renqingbung temple is located on a mountain in Mêdog County, with high temperatures, high humidity and plentiful precipitation. Vegetation type is subtropical evergreen broadleaved forest.

Remarks. *Lilioceris medogensis* sp. nov. and *L. zhentangensis* sp. nov. are similar in their pronotia having anterior and posterior transverse depressions, which are easily distinguished from those of the other members of *Lilioceris*. However, *L. medogensis* sp. nov. is different from *L. zhentangensis* sp. nov. by the brownish red pronotum (Fig. 20A) and metasternum (Fig. 20B), only the lateral side of the metasternum is black; the lateroposterior corner of the metasternum is glabrous; and the posterior part of the dorsal sclerite of the male genitalia in dorsal view is widened (Fig. 23C). In *L. zhentangensis*, the pronotum and metasternum are black (Fig. 19A); the lateroposterior corner of the metasternum has a strip of pubescence (Fig. 19B); and the posterior part of the dorsal sclerite in dorsal view is parallel (Fig. 22C). In addition, their host plants and habitats are also different: *L. medogensis* lives on *Smilax ferox* in warmer and lower altitudes, while *L. zhentangensis* inhabits *Smilax menispermoidea* in colder, higher altitudes.

Lilioceris zayuensis Xu & Liang, sp. nov.

https://zoobank.org/8D02C295-41CB-4A11-8A6A-88C5F4861D67
Figs 5, 6, 21A–D, 24A–D, 30A–C, 36, 46, 47

Material examined. Total 8 specimens. ***Holotype*:** 1♂, Tibet, Zayü, Zhowagoin, Xiongjiu village / 2022.7.13 / 28.60668°N, 97.28165°E, 1901 m / Hongbin Liang, Yuan Xu and Neng Zhang coll. (IZCAS); ***Paratypes*:** 4♀1♂, Tibet, Zayü, Zhowagoin, Xiongjiu village / 2022.7.13 / 28.60668°N, 97.28165°E, 1901 m / Hongbin Liang, Yuan Xu and Neng Zhang coll. (IZCAS); 2♀, Tibet, Zayü, Zhowagoin, Xiongjiu village / 2021.7.1 / 28.60668°N, 97.28165°E, 1901 m / Hongbin Liang, Yuan Xu and Neng Zhang coll. (IZCAS).

Diagnosis. Antennae nearly half as long as body length, antennomeres V–IX quadrate. Pronotum without distinct anterior and posterior transverse impression, pronotal disc with four or five fine punctures in middle. Elytral punctures sparse and absent on apical 1/3. Metasternal disc almost glabrous, posterior margin with sparse pubescence.

Description. BL = 8.5–10.0 mm, BW = 3.8–4.5 mm. Head, most of legs, scutellum black, pronotum, elytra, femora of legs and underside brownish red.

Head (Fig. 5). Vertex flat and without groove in middle, lateral side with sparse punctures and pubescence; clypeofrontal area triangular, lateral side of disc with sparse punctures and pubescence; labrum transverse, with sparse long pubescence; antennae nearly half as long as body, antennomeres I–IV nearly globular, antennomeres V–X 1.5 times as long as wide, III–XI densely pubescent and punctate.

Pronotum (Figs 6, 21A). Anterior angle protruding, posterior angle not protruding; sides distinctly constricted in middle; without anterior and posterior transverse impression of disc; disc almost smooth and with four or five fine punctures in middle; basal transverse groove indistinct. Scutellum triangular and densely pubescent.

Elytra (Fig. 5). Humeri protruding, humeral groove shallow, basal impression indistinct; striae with large punctures at base, punctures diminished posteriorly and absent on apical 1/3, intervals without punctures; epipleura raised, with row of fine punctures.

Mesosternum pubescent, apical portion of mesosternal process strongly widened and convex, horizontally connected with metasternum (Fig. 21B); Metasternal disc almost glabrous, posterior margin with sparse pubescence. Metepisternum densely pubescent.

***Abdominal sternites*.** Lateral transverse impressions distinct on sternites I–IV, area of transverse impressions smooth, middle of sternite I with dense pubescence, other areas of sternites I–IV with sparse pubescence and punctures (Fig. 21C).

Legs (Fig. 6). Femora with dense pubescence on dorsal surface, sparse pubescence on ventral surface, middle area widened.

Male genitalia (Fig. 24A–D). Apical foramen occupying 1/5 length of median lobe (Fig. 24A); apex rounded (Fig. 24B); tegmen Y-shaped, basal piece of tegmen triangle and broad, lateral lobes slightly sclerotized and combined with second connecting membrane; internal sac with distinct dorsal, median, and ventral sclerites, posterior part of dorsal sclerite in dorsal view widened and rounded, ventral sclerite short and flat, median sclerite small (Fig. 24C, D).

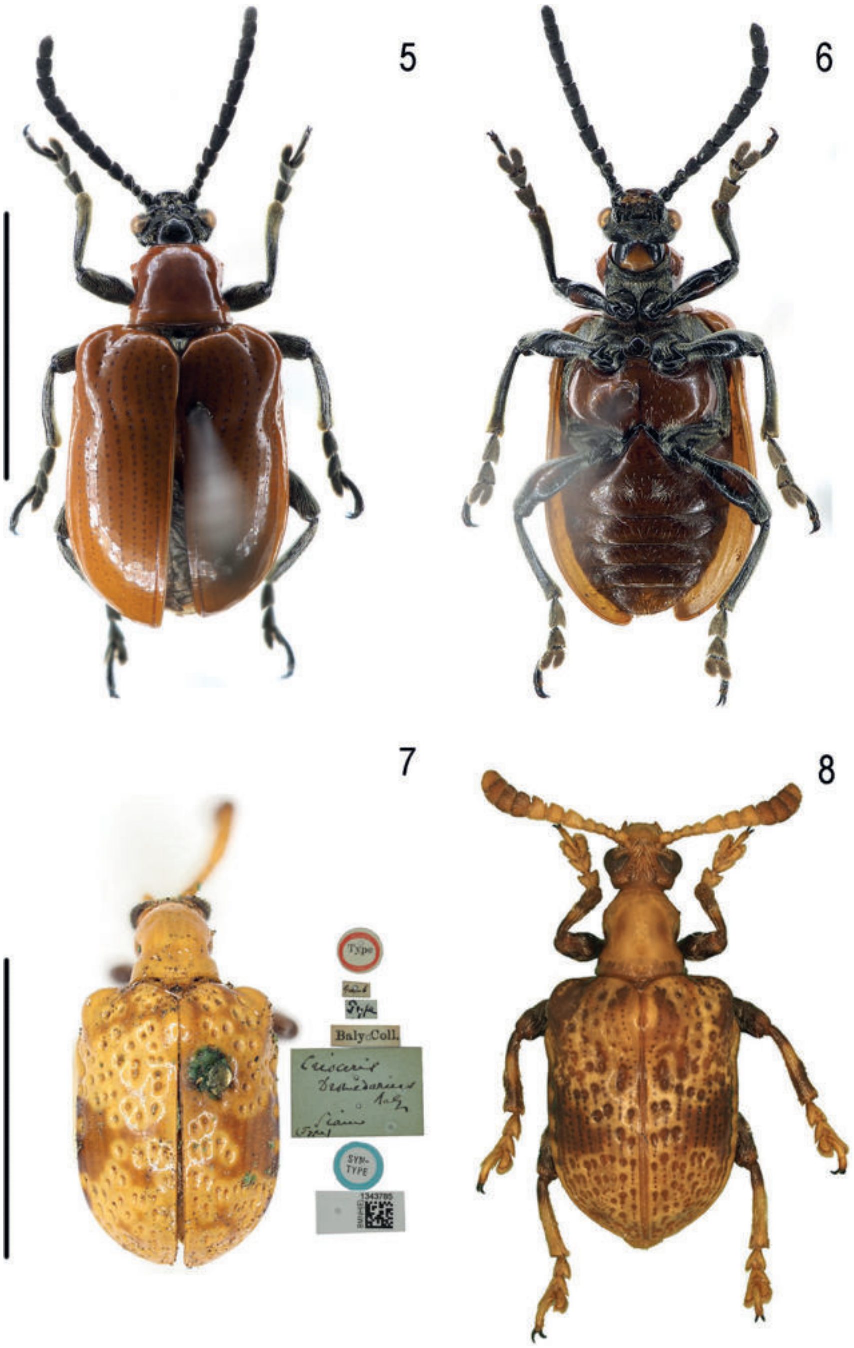

Figures 5–8. Habitus of *Lilioceris* spp. **5, 6** *L. zayuensis*, holotype, Tibet **7** *L. dromedarius*, syntype, Thailand **8** *L. dromedarius*, specimen from Hainan. Scale bars: 5.0 mm.

Female reproductive organs (Fig. 30A–C). Tergites VIII and IX, sternites VIII and IX sclerotized, posterior areas of tergite VIII and sternite VIII with pubescence and apodemes, spiculum gastrale Y-shaped and long; ovipositor with dense pubescence, distal part of ovipositor cylindrical, long and with protuberance; spermatheca greatly convoluted.

Distribution (Fig. 36). China (Tibet).

Etymology. The specific name *zayuensis* refers to its type locality Zayü County, Tibet, China.

Host plant and habitat (Figs 46, 47). Beetles were collected feeding on *Smilax longebracteolata* J. D. Hooker (Smilacaceae) in Zayü. This species is confined to subtropical areas, at an elevation of ~ 1900 m. Xiongjiu village, Zayü has a mild climate and abundant rainfall. The habitat is secondary forest along a roadside, composed of tall trees, woody vines and many weeds.

Remarks. This new species is a member of the *neptis* species group, and can be keyed out in couplet 4 with *L. cantonensis* (Heinze, 1943) and *L. neptis* (Weise, 1922) in the key by Xu et al. (2021: 301). It is different from *L. cantonensis* by its middle femora being completely black; elytral strial punctures dense and large at the base, diminished posteriorly, and absent on the apical 1/3 or 1/4; apical portion of the dorsal sclerite of the male genitalia is rounded. In *L. cantonensis*, the middle femora are bicolored, black with the middle brownish red on their ventral surfaces, and the elytral strial punctures sparse and large in basal impression, but absent on the apical 1/2 or 1/3; apical portion of the dorsal sclerite of the male genitalia truncated. It is also different from *L. neptis* by the black middle femora; metasternum almost glabrous, with only the posterior margin with sparse pubescence. In *L. neptis*, the middle femora are brownish red, and the metasternum has a long strip of setae extending from the anterior to the posterior margin.

This species is only found at the type locality. It seems that the local population was very low. We explored this place three times, but only collected eight specimens. We also tried several other places in Zayü County, but no specimens of this species were found.

New record for China

Lilioceris dromedarius **(Baly, 1861)**

Figs 7, 8, 31A–C, 37

Crioceris dromedarius Baly, 1861: 279 (Cambodia, syntype).
Lilioceris dromedarius: Monrós 1960: 175.
Crioceris rouyeri Pic, 1916: 18 (Java). Synonymized by Monrós 1960: 175.
Crioceris foveolata Pic, 1921: 33 (Cochinchina). Synonymized by Kimoto and Gressitt 1979: 221.

Type material examined. 1 ***syntype*** of *Lilioceris dromedarius* (NHML, photo), Type / Baly Coll. / *Crioceris dromedarius* Baly, Siam (Type) / SYNTYPE / BMNH(E)1345164.

Other material examined. 1 specimen. **Hainan**: 1♀, Wuzhi Shan, Shuiman township, Hudiegu (butterfly valley), 18.87482°N, 109.66819°E / 664 m, 2009.11.27, Meiying Lin coll. (IZCAS).

Diagnosis. Antennae nearly half as long as body length, antennomeres VIII–X widened, twice as wide as long. Pronotal disc with two rows of fine punctures in middle. Elytra raised near suture at base, elytral punctures sparse and coarse, but absent at apex.

Redescription. BL = 8.8 mm, BW = 4.5 mm. Antennomeres VIII–IX, head, femora and tibiae brownish, claws black, antennomeres I–VII, pronotum, elytra and abdomen brownish yellow, each elytron with big brownish marking in middle of lateral area, abdominal sternites except pygidium with three black markings in lateral side and middle.

Head (Figs 7, 8). Vertex with groove in middle, punctate and pubescent densely; frontoclypeal area triangular, lateral side of disc with sparse punctures and pubescence; labrum transverse, with sparse long pubescence; antennae nearly 1/2 as long as body, antennomeres I–IV nearly globular, antennomere II shortest, antennomere V longest, antennomeres VI and VII length as long as width, antennomeres VIII–X widest, wide 2 times as long as length, antennomeres V–XI densely pubescent and punctate.

Pronotum (Figs 7, 8). Anterior angle protruding, posterior angle not protruding; sides slight constricted in middle; middle of disc with two rows of fine punctures; anterior and posterior transverse impression indistinct, basal transverse groove very weak. Scutellum triangular and densely pubescent.

Elytra (Figs 7, 8). Suture at base with raised hump; humeri protruding, humeral groove and basal impression distinct; striae with very sparse and coarse punctures, puncture absent at elytral brownish black marking area, intervals smooth; epipleura slightly raised, with row of fine punctures.

Mesosternum pubescent; apical portion of mesosternal process narrow and flat, obliquely pointed, not horizontally connected with metasternum. Metasternal disc and metepisternum densely pubescent.

Abdominal sternites**.** Lateral transverse impressions distinct on sternites I–IV, area of transverse impressions smooth, other areas with dense pubescence and punctures.

Legs**.** Femora with dense pubescence on dorsal surface, with sparse pubescence on ventral surface, middle area widened.

Male genitalia**.** Unknown.

Female reproductive organs (Fig. 31A–C). Tergites VIII and IX, sternites VIII and IX sclerotized, posterior areas of tergite VIII and sternite VIII with pubescence and apodemes, spiculum gastrale Y-shaped and distinctly widen in distal part; ovipositor with dense pubescence, distal part of ovipositor cylindrical, long and with protuberance; spermatheca greatly convoluted.

Host plant and habitat. A host plant is unknown. A single specimen in IZCAS was collected by Meiying Lin when beating vegetation. The collecting site, Hudiegu, is located in a tropical area in Wuzhi Shan of Hainan Province, with high temperatures, high humidity, and plentiful precipitation. Vegetation type is tropical evergreen broadleaved forest.

Distribution (Fig. 37). China (Hainan); Vietnam; Thailand; Cambodia; Indonesia.

Remarks. This species is very similar to *Lilioceris gibba* (Baly, 1861) (based on a syntype studied, NHML) but differs from the latter by antennomeres V–X being twice as wide as long (in *L. gibba*, antennomeres V–X as wide as long). In addition, the pronotum and elytra are yellow in *L. dromedarius* (dark brown in *L. gibba*).

New records

Lilioceris pulchella **(Baly, 1859)**

Figs 9, 10, 32A–C, 37

Crioceris pulchella Baly, 1859: 152 (India, syntype).
Lilioceris pulchella: Monrós 1960: 171.

Type material examined. 1 ***syntype*** of *Lilioceris pulchella* (NHML, photo), Type / Baly Coll. / *Crioceris pulchella* Baly, India (Type) / BMNH(E) 1343669.

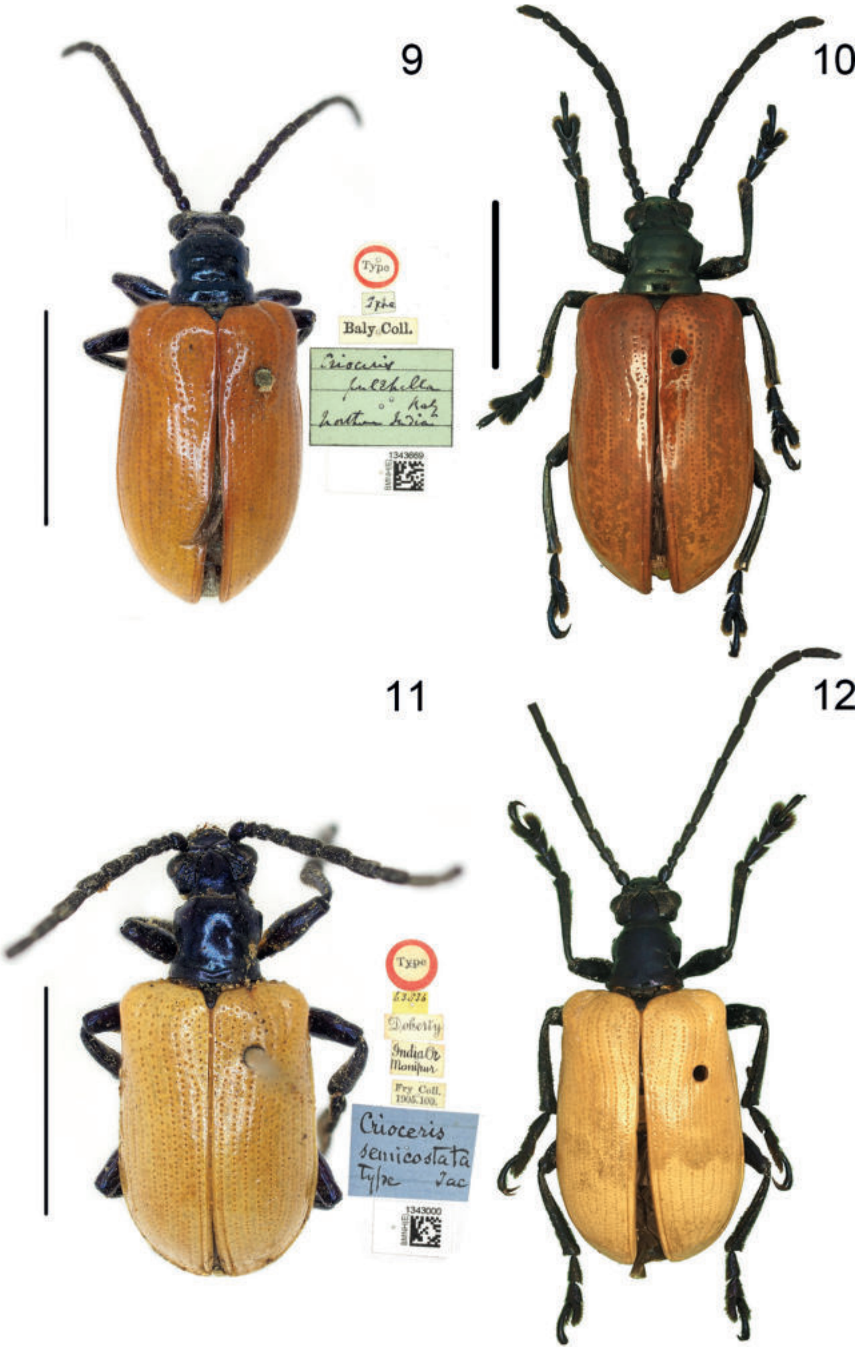

Figures 9–12. Habitus of *Lilioceris* spp. photographed by HBL **9, 10** *L. pulchella*, type, India **11, 12** *L. semicostata*, type, India (Manipur). Scale bars: 5.0 mm.

Other material examined. 1 specimen. **Tibet:** 1♀, Hanmi–Lage, 2005.08.28, Dakang Zhou coll. (IZCAS).

Diagnosis. Antennae ~ 1/3 as long as body, antennomeres V–X cylindrical. Pronotum with distinct posterior transverse impression, pronotal disc with two rows of fine punctures in middle, scutellum pubescent. Elytral punctures fine, diminishing posteriorly, but not absent. Lateral side of metasternite with long narrow strip of pubescence.

Redescription. BL = 11.0 mm, BW = 5.0 mm. Antennae, head, pronotum, scutellum, prosternum, mesosternum, legs, and half of first abdominal sternite black, with blue metallic luster, elytra and remainder of abdominal sternite brownish red.

Head (Figs 9, 10). Vertex with deep groove in middle, sparsely punctate and pubescent in lateral area; frontoclypeal area triangular, lateral side of disc with sparse punctures and pubescence; labrum transverse, middle of anterior margin concave, disc with sparse punctures and pubescence; antennae nearly 3/5 length of body, antennomeres I–IV nearly globular, antennomere II shortest, antennomeres V–XI cylindrical, 3 times as long as wide.

Pronotum (Figs 9, 10). Anterior angle protruding, posterior angle not protruding; sides constricted in middle; anterior and posterior transverse impression distinct; disc with irregular fine punctures in middle; scutellum triangular and densely pubescent.

Elytra (Figs 9, 10). Humeri protruding, humeral groove distinct, basal impression indistinct; striae with fine punctures, diminishing posteriorly and absent at end, intervals smooth; epipleura raised, with row of fine punctures.

Mesosternum pubescent; apical portion of mesosternal process narrow and flat, obliquely pointed, not horizontally connected with metasternum. Lateral side of metasternite with a long narrow strip of pubescence extending from the lateroposterior corner to anterior margin. Metepisternum densely pubescent.

***Abdominal sternites*.** Lateral transverse impressions indistinct on sternites I–IV. Lateral side of sternite I–IV with densely pubescent, other areas with sparse pubescence and punctures.

***Legs*.** Femora with dense pubescence in dorsal surface, with sparse pubescence on ventral surface, middle area widened. Claws distinctly asymmetrical, outer one is longer than inner one.

***Male genitalia*.** Unknown.

Female reproductive organs (Fig. 32A–C). Tergites VIII and IX, sternites VIII and IX sclerotized, posterior areas of tergite VIII and sternite VIII with pubescence and apodemes, spiculum gastrale X-shaped and short; ovipositor with dense pubescence, distal part of ovipositor cylindrical, short, and with protuberance; spermatheca simple and folded.

Distribution (Fig. 37). China (Tibet); India.

Host plant and habitat. A host plant is unknown. This species was collected in an environment between Hanmi and Lage according to the collector. Hanmi and Lage are two small courier stations on an old trail from Doxong La pass to Baibung town in Mêdog County, at altitudes of 2000–3000 m. They are located in a subtropical area, with a primary forest composed of large trees, woody vines and many shrubs.

Remarks. A single specimen found in IZCAS was collected by Mr Dakang Zhou with a sweeping net in 2005. In recent years, we have surveyed Hanmi, Mêdog several times, but no more specimens have been found.

Lilioceris semicostata **(Jacoby, 1908)**

Figs 11, 12, 25A–D, 33A–C, 37

Crioceris semicostata Jacoby, 1908: 77 (India: Manipur, syntype).
Lilioceris semicostata: Monrós 1960: 179.

Type material examined. 1 ***syntype*** of *Lilioceris semicostata* (NHML, photo), Type /63836 /Doherty / India Or. Manipuria / Frey Coll., 1905.100. / *Crioceris semicostata*, Type, Jac / BMNH(E)1343000.

Other material examined. 2 specimens. **Tibet:** 1♀, Mêdog, Baibung Town, Hanmi / 29.36739°N, 95.12728°E, 2123 m, 2011.07.24 / Ye Liu coll. (IZCAS); 1♂, China, Tibet, Mêdog, Baibung, Hanmi / host unknown / 29.3664°N, 95.1277°E, 2120 m, 2011.07.26 / Xiaodong Yang coll. (IZCAS).

Diagnosis. Antennae nearly as long as body, antennomeres V–X cylindrical. Pronotum with distinct posterior transverse impression, pronotal disc almost smooth, scutellum pubescent. Elytral punctures diminishing posteriorly, but not absent. Metasternite with scattered and sparse pubescence.

Redescription. BL = 12.0–15.0 mm, BW = 4.0–6.0 mm. Elytra yellow, rest of body black and with blue metallic luster.

Head (Figs 11, 12). Vertex raised, with deep groove in middle, sparsely punctate and pubescent in lateral area; frontoclypeal area triangular, lateral side of disc with sparse punctures and pubescence; labrum transverse, middle of anterior margin concave, disc with sparse punctures and long pubescence; antennae nearly as long as body length, antennomeres I–III nearly globular, antennomere II shortest, antennomeres IV–XI cylindrical, 3 times as long as wide.

Pronotum (Figs 11, 12). Anterior angle protruding, posterior angle not protruding; sides slightly constricted in middle; posterior transverse impression distinct, disc almost smooth; scutellum triangular and smooth.

Elytra (Figs 11, 12). Humeri protruding, humeral groove distinct, basal impression indistinct; striae with fine punctures, punctures diminishing posteriorly but not absent, intervals smooth; epipleura raised, with row of fine punctures.

Mesosternum pubescent; apical portion of mesosternal process narrow and flat, obliquely pointed, not horizontally connected with metasternum. Metasternite with scattered and sparse pubescence. Metepisternum sparsely pubescent.

Abdominal sternites**.** Lateral transverse impressions indistinct on sternites I–IV. Lateral sides of sternites I–IV with denser pubescence, other areas with sparse or scattered pubescence.

Legs**.** Femora with dense pubescence on dorsal surface, with sparse pubescence on ventral surface, middle area widened. Claws distinctly asymmetrical, outer one longer than inner one.

Male genitalia (Fig. 25A–D). Apical foramen occupying 1/5 length of median lobe (Fig. 25A); apex truncated (Fig. 25B); tegmen Y-shaped, basal piece of tegmen triangular and broad, lateral lobes slightly sclerotized and combined with second connecting membrane; internal sac with distinct dorsal, median and ventral sclerites, posterior part of dorsal sclerite in dorsal view widen, ventral sclerite short and flat, median sclerite distinct (Fig. 25C, D).

Female reproductive organs (Fig. 33A–C). Tergites VIII and IX, sternites VIII and IX sclerotized, posterior areas of tergite VIII and sternite VIII with pubescence and apodemes, spiculum gastrale X-shaped and long; ovipositor with dense pubescence, distal part of ovipositor cylindrical, short and with protuberance; spermatheca simple and curved.

Distribution (Fig. 37). China (Tibet); India.

Host plant and habitat. Host plant is unknown. Specimens of this species in IZCAS were collected in Hanmi by Ye Liu and Xiaodong Yang when sweeping the vegetation canopy. Hami is located in the subtropical area of Mêdog, with primary forest composed of large trees, woody vines and many shrubs.

Remarks. This species is very similar to *Lilioceris flavipennis* (Baly, 1859) (based on a syntype studied, NHML), but differs from the latter by the pronotum being slightly constricted in middle, anterior and posterior angles not protruding; elytral striae regular. In *L. flavipennis*, pronotum is strongly constricted in middle, anterior and posterior angles are strongly protruding; elytral striae are irregular.

Lilioceris unicolor **(Hope, 1831)**

Figs 13–16, 26A–D, 35A–C, 37

Crioceris unicolor Hope, 1831: 28 (Nepal, lectotype).
Lilioceris unicolor: Monrós 1960: 172.
Crioceris badia Lacordaire, 1845: 560 (Siam. Type not found). Synonymized by Clavareau 1913: 51.
Crioceris seminigra Jacoby, 1889: 153 (Birma: Tenasserim, syntype). syn. nov.
Lilioceris seminigra: Monrós 1960: 171.

Type material examined. 1♂ ***lectotype*** of *Lilioceris unicolor* (NHML, photo, antennae, sternites middle and hind legs missing), Type / Nepal / Hardwicke, Bequest / unicolor Hope / Lectotype, *Lilioceris unicolor* (Hope) des. A. Konstantinov & A. Tishechkin 2010 / Loan BMNH August 2010 # 2010-471/ BMNH(E)1343990; 1 ***syntype*** of *Lilioceris seminigra* (NHML, photo), Rangoon, Brimania, Fea. VI. 1886/ in copula / Jacoby Coll., 1909–28a. / BMNH(E), 1343036.

Other material examined. 5 specimens. **Thailand:** 1 specimen of *Lilioceris unicolor* (NHML, photo): Siam/ Baly coll./ *Crioceris badia* Lac. Siam "illegible"/ *Lilioceris unicolor* Hope, det. A. Konstantinov and Tishechkin 2010/ Loan BMNH August 2010 # 2010-471 A. Konstantinov/ BMNH (E)1344002; 1♀, locality is illegible / *Crioceris seminigra* Jac. var. (handwriting seems Jacoby's), (IZCAS); **Yunnan:** 1♀, Longchuan / 1150 m, 1979.VII.16 / *Lilioceris seminigra* Jacoby, det. Peiyu Yu, (IZCAS); 1♀, Yunnan, Yingjiang, Nongzhang, Jiemao, Xianrendong, 24.52567°N, 97.79818°E / 837 m, 2020.5.27, Hongbin Liang and Yuan Xu coll. (IZCAS); 1♂, Longchuan, Jinghan, Longbazhai, S223 road/ 24.27601°N, 97.85190°E, 902 m, 2020.5.26, Hongbin Liang and Yuan Xu coll. (IZCAS).

Diagnosis. Antennae ~ 1/3 as long as body, antennomeres V–XI quadrate. Pronotum without anterior and posterior transverse impression, pronotal disc with one or two rows of punctures in middle. Elytral punctures large, not diminishing posteriorly, intervals slightly convex on apical 1/4; epipleura raised, with row of fine punctures.

Redescription. BL = 8.0 mm, BW = 3.8 mm. Body brownish red.

Head (Figs 13–16). Vertex with shallow groove in middle, sparsely punctate and pubescent in lateral area; frontoclypeal area triangular, disc with sparse punctures and pubescence; labrum transverse, disc with sparse long pubescence; antennae nearly 1/3 length of body, antennomeres I–IV nearly globular, antennomere II shortest, antennomeres V–X strongly widened, 2 times as wide as long.

Pronotum (Figs 13–16). Anterior angle protruding, posterior angle not protruding; sides constricted in middle; anterior and posterior transverse impression absent; middle of disc with one or two rows of fine punctures. Scutellum triangular and pubescent.

Elytra (Figs 13–16). Humeri protruding, humeral groove distinct, basal impression indistinct; striae with large punctures, punctures not diminishing posteriorly, intervals slightly convex on apical 1/4; epipleura raised, with row of fine punctures.

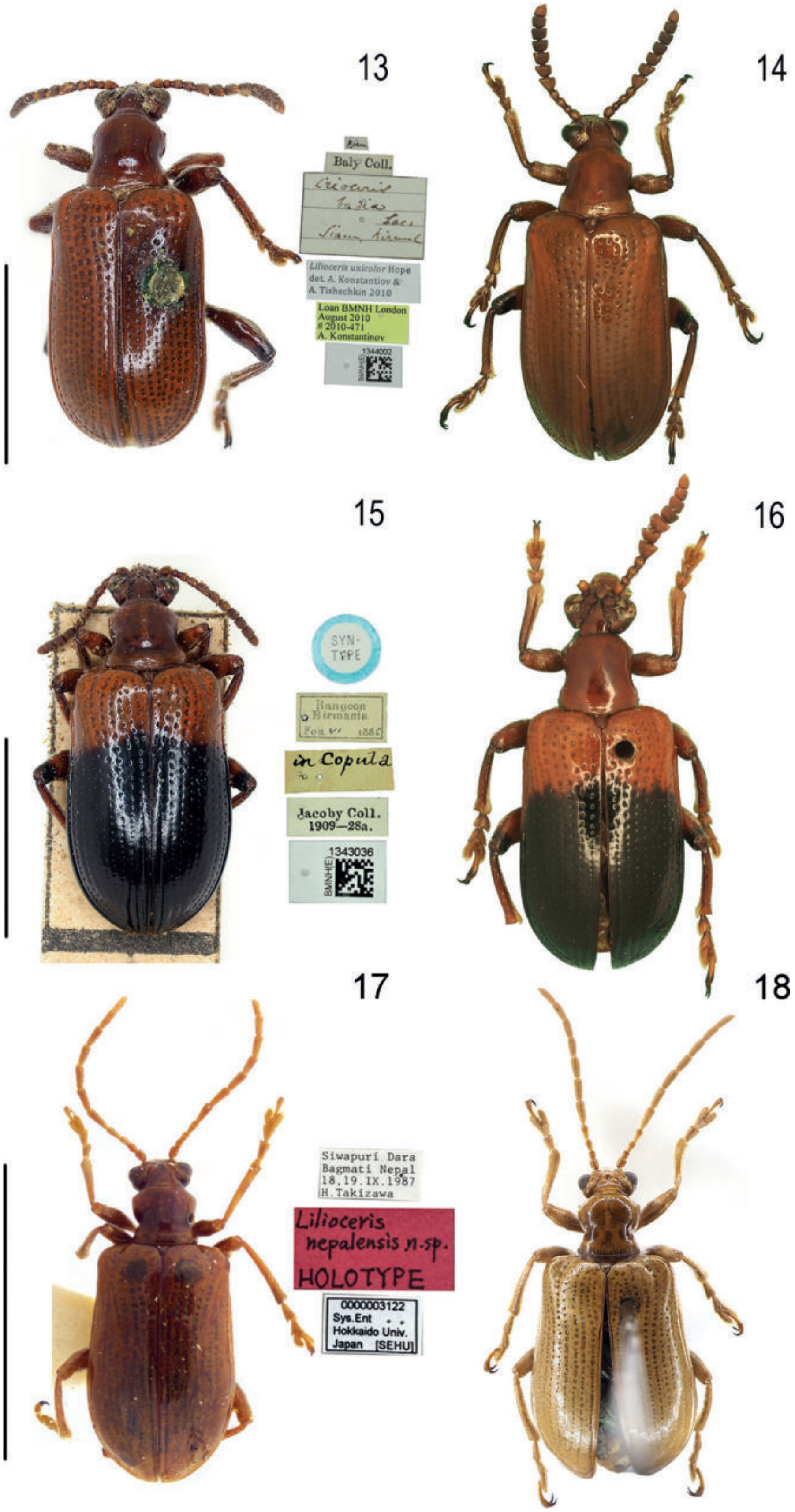

Figures 13–18. Habitus of *Lilioceris* spp. **13** *L. unicolor*, specimen from Thailand **14** *L. unicolor*, specimen from China (Yunnan) **15** *L. seminigra*, syntype, Myanmar **16** *L. seminigra*, specimen from Yunnan **17** *L. nepalensis*, holotype, Nepal (Bagmati), photographed by Takuya Takemoto **18** *L. nepalensis*, specimen from China (Dinggyê) Scale bars: 5.0 mm.

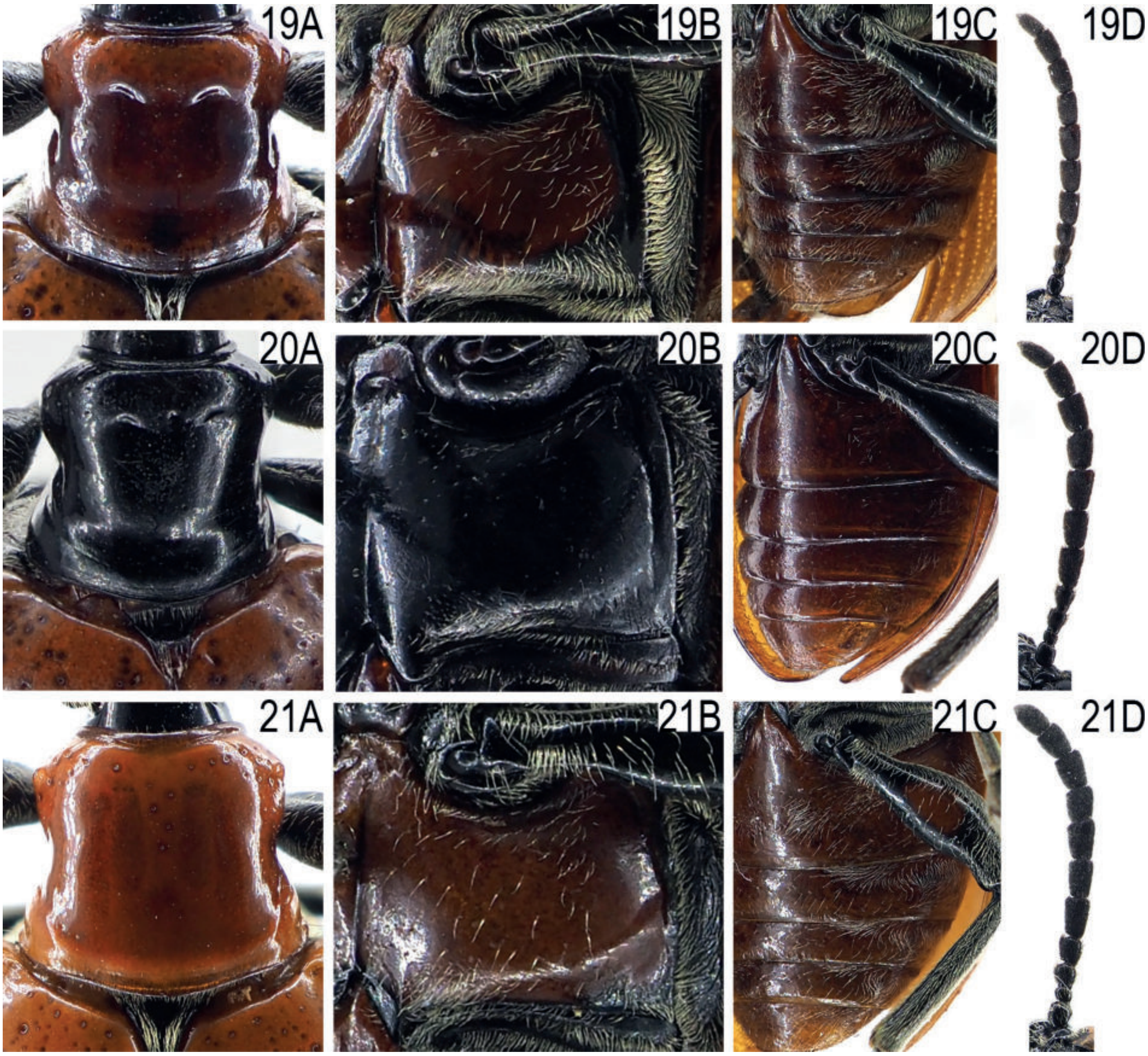

Figures 19–21. Pronotum, mesosternal disc, abdominal sternites and antennae of *Lilioceris* spp. **19** *L. zhentangensis*, ♂, China (Tibet: Zhêntang) **20** *L. medogensis*, ♂, China (Tibet: Mêdog) **21** *L. zayuensis*, ♂, China (Tibet: Zayü) **A** pronotum **B** mesosternal disc **C** abdominal sternite **D** antennae.

Mesosternum pubescent; apical portion of mesosternal process widened and flat, obliquely pointed, not horizontally connected with metasternum. Metasternum with long strip of pubescence along outer side, extending from anterior to posterior margin. Metepisternum densely pubescent.

***Abdominal sternites*.** Lateral transverse impressions indistinct on sternites I–V, lateral sides of sternites I–V with dense pubescence, only with sparse pubescence in middle.

***Legs*.** Femora with dense pubescence on dorsal surface, with sparse pubescence on ventral surface, middle area widened.

Male genitalia (Fig. 26A–D). Apical foramen occupying 1/5 length of median lobe (Fig. 26A); apex hooked (Fig. 26B); tegmen Y-shaped, basal piece of tegmen triangle and broad, lateral lobes slightly sclerotized and combined with second connecting membrane; internal sac with distinct dorsal, median

Figures 22–24. Male genitalia of three new *Lilioceris* species (holotypes) **22** *L. zhentangensis*, China (Tibet: Dinggyê) **23** *L. medogensis*, China (Tibet: Mêdog) **24** *L. zayuensis*, China (Tibet: Zayü) **A** aedeagus, lateral view **B** aedeagus, dorsal view **C** dorsal sclerite, dorsal view **D** sclerites in internal sac, lateral view. Scale bars: 0.5 mm (**A, B**); 0.2 mm (**C, D**).

and ventral sclerites, posterior part of dorsal sclerite in dorsal view widen and anterior part of dorsal sclerite distinctly extended, ventral sclerite short and flat, median sclerite distinct (Fig. 26C, D).

Female reproductive organs (Fig. 35A–C). Tergites VIII and IX, sternites VIII and IX sclerotized, posterior areas of tergite VIII and sternite VIII with pubescence and apodemes, spiculum gastrale Y-shaped and long; ovipositor with dense pubescence, distal part of ovipositor cylindrical, short and with protuberance; spermatheca convoluted.

Distribution (Fig. 37). China (Yunnan); Nepal, Myanmar.

Host plant and habitat. We collected two adults of *L. unicolor* on *Dioscorea* sp. (Dioscoreaceae) in the villages of Jiemao and Longbazhai of Yunnan Province, but feeding was not observed, so their host plant needs confirmation. Jiemao and Longbazhai are located in a subtropical area, at elevations of 800–900 m. These two places have a mild climate and abundant rainfall. The habitat in Jiemao is a large secondary forest, composed of tall trees, woody vines, shrubs and weeds. The habitat in Longbazhai is a very small secondary forest of several thousand square meters, surrounded by crop fields.

Remarks. We examined the lectotype and a non-type specimen of *L. unicolor* present at NHML. The specimens in IZCAS from Yunnan are not significantly different from the lectotype. The punctures on pronotum are variable: the lectotype has two rows of punctures in the middle of the pronotum, the non-type specimen in NHML and the specimen in IZCAS have only one row of punctures in the middle of the pronotum. The male genitalia of our specimen from Yunnan (Fig. 26C, D) are identical to those of the lectotype in NHML (Tishechkin et al. 2011: 80, fig. 30).

We also examined a syntype of *L. seminigra* in NHML, and no significant morphological difference was found from the lectotype of *L. unicolor*, except for the bi-coloration on the elytra of *L. seminigra*. When Jacoby (1889: 153) described *L. seminigra*, he noticed a variant: “Var. Elytra entirely fulvous”. In four Chinese specimens in IZCAS, the elytrae are all brownish-red in two specimens of *L. unicolor*; but the apical 2/3 of each elytron is black, 1/3 of base is brownish-red in one specimen of *L. seminigra*, and completely brownish-red in another specimen. The female reproductive organs of these two species were dissected and compared, and no significant differences were found. Therefore, we conclude that *L. unicolor* and *L. seminigra* are conspecific, and elytral bi-coloration in *L. seminigra* is simply a variation. In addition, antennomeres V–X in this species are flat, strongly transverse, and the outer distal angle of antennomeres V–VII is protruding. These characteristics are unique among *Lilioceris* species.

Lilioceris nepalensis **Takizawa, 1989**

Figs 17, 18, 27A–D, 34A–C, 37, 48–51

Lilioceris nepalensis Takizawa, 1989: 327 (Nepal: Bagmati, holotype).

Type material examined. *Holotype* of *Lilioceris nepalensis* (SEHU, photo), *Lilioceris nepalensis* n.sp., Holotype / Siwapuri Dara Bagmati Nepal 18, 19.IX.1987, H. Takizawa / 0000003122, Sys. Ent Hokkaido Univ. Japan [SEHU].

Figures 25–27. Male genitalia of new records of *Lilioceris* species in China **25** *L. semicostata*, China (Tibet: Mêdog) **26** *L. unicolor*, China (Yunnan: Longchuan) **27** *L. nepalensis*, China (Tibet: Dinggyê) **A** aedeagus, lateral view **B** aedeagus, dorsal view **C** dorsal sclerite, dorsal view **D** sclerites in internal sac, lateral view. Scale bars: 0.5 mm (**A, B**); 0.2 mm (**C, D**).

Figures 28–30. Female reproductive organs of three new *Lilioceris* species (paratypes) **28** *L. zhentangensis*, China (Tibet: Dinggyê) **29** *L. medogensis*, China (Tibet: Mêdog) **30** *L. zayuensis*, China (Tibet: Zayü) **A** dorsal view **B** ventral view **C** spermatheca. Scale bars: 0.5 mm.

Other material examined. 32 specimens. **TIBET:** 9♀12♂, Dinggyê, Zhêntang, Nadang village, 27.85317°N, 87.44903°E / 2491 m, 2021.6.25, Hongbin Liang, Yuan Xu and Neng Zhang coll. (IZCAS); 4♀2♂, Jilong, near to Zhaoti Bilei,

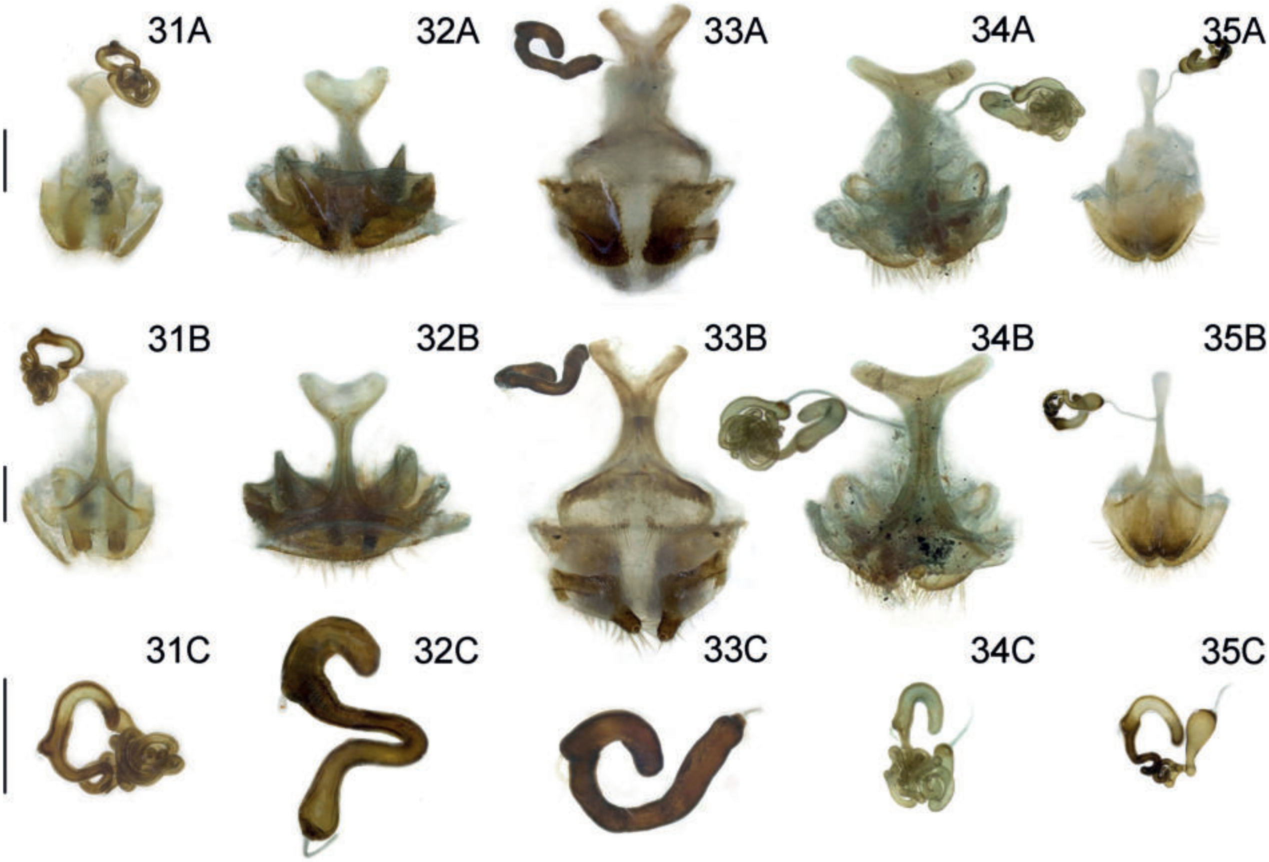

Figures 31–35. Female reproductive organs of five new records of *Lilioceris* species in China **31** *L. dromedarius*, China (Hainan: Wuzhi Shan) **32** *L. pulchella*, China (Tibet: Mêdog) **33** *L. semicostata*, China (Tibet: Mêdog) **34** *L. nepalensis*, China (Tibet: Dinggyê) **35** *L. unicolor*, China (Yunnan: Yingjiang) **A** dorsal view **B** ventral view **C** spermatheca. Scale bars: 0.5 mm (**A–C**).

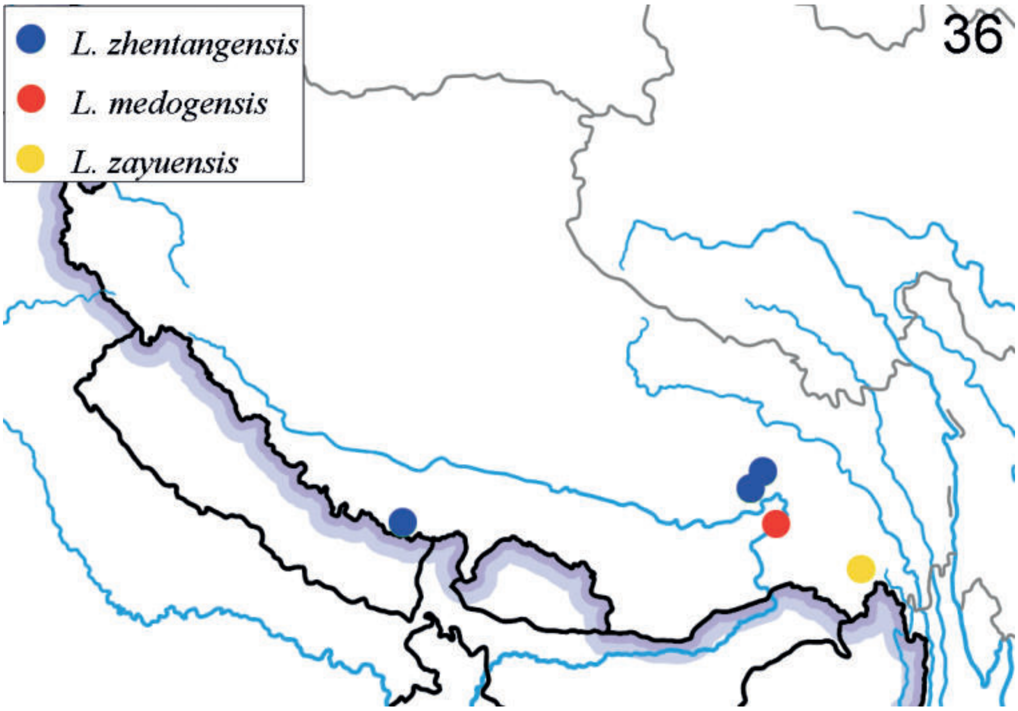

Figure 36. Collecting sites of three new *Lilioceris* species.

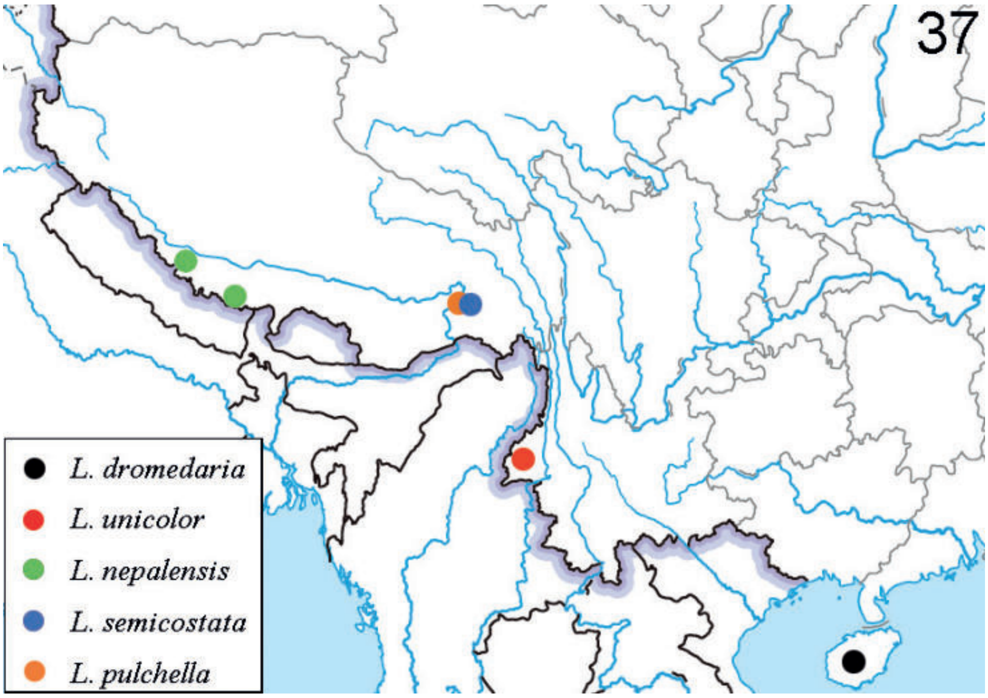

Figure 37. Collecting sites of five new records of *Lilioceris* species in China (distributions outside China are not marked here because of the lack of precise locality data).

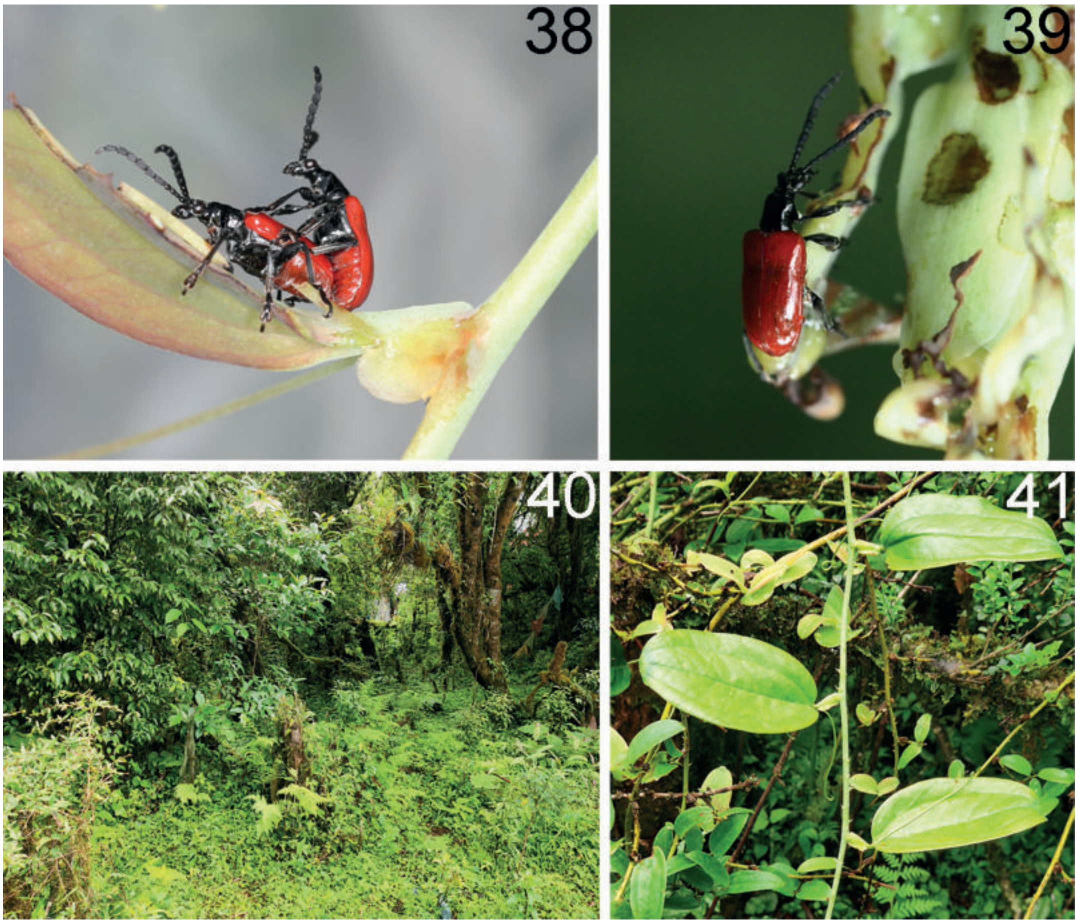

Figures 38–41. *Lilioceris medogensis* in Tibet (Mêdog), 2021.VI.9 **38, 39** adult **40** habitat **41** host plant: *Smilax ferox* **38** photographed by HBL **39–41** photographed by YX.

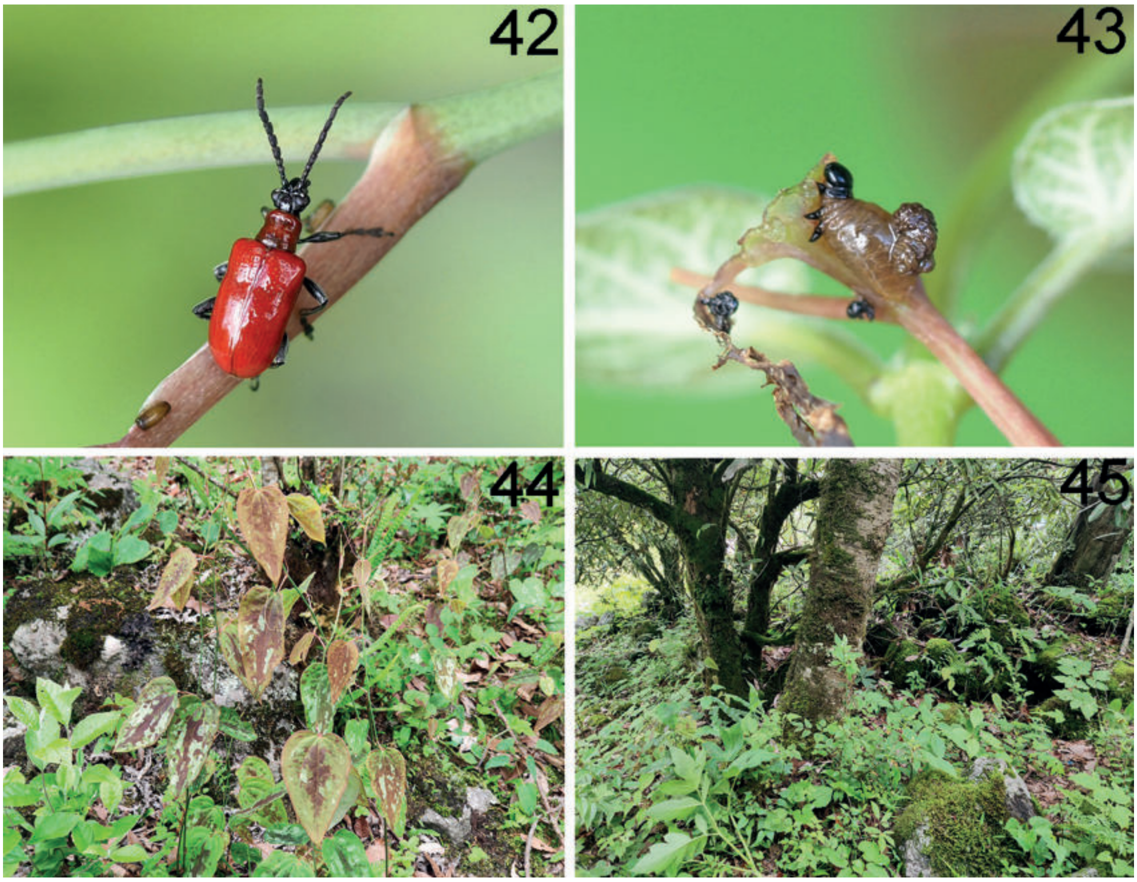

Figures 42–45. *Lilioceris zhentangensis* in Tibet (Dinggyê), 2021.VI.24, photographed by YX **42** adult **43** larva **44** host plant: *Smilax menispermoidea* **45** habitat.

Figures 46, 47. *Lilioceris zayuensis* in Tibet (Zayü), 2022.VII.13, photographed by YX **46** adult **47** host plant: *Smilax longebracteolata*.

28.49216°N, 85.22383°E / 3219 m, 2023.7.16, Yuyao Qin and Yong Wang coll. (IZCAS); 2♀3♂, Cona, 1 km north of Mama township, 27.89875°N, 91.80188°E / 2939 m, 2023.9.2–3, Hongbin Liang coll. (IZCAS).

Diagnosis. Antennae ~ 2/3 as long as body, antennomeres V–X cylindrical. Pronotum with distinct posterior transverse impression, pronotal disc smooth. Elytral punctures sparse on basal half but absent on apical half. Metasternite smooth.

Redescription. BL = 4.8.0–6.5 mm, BW = 3.0–4.0 mm. Body almost brownish red, only sternum and abdominal sternites I and II black.

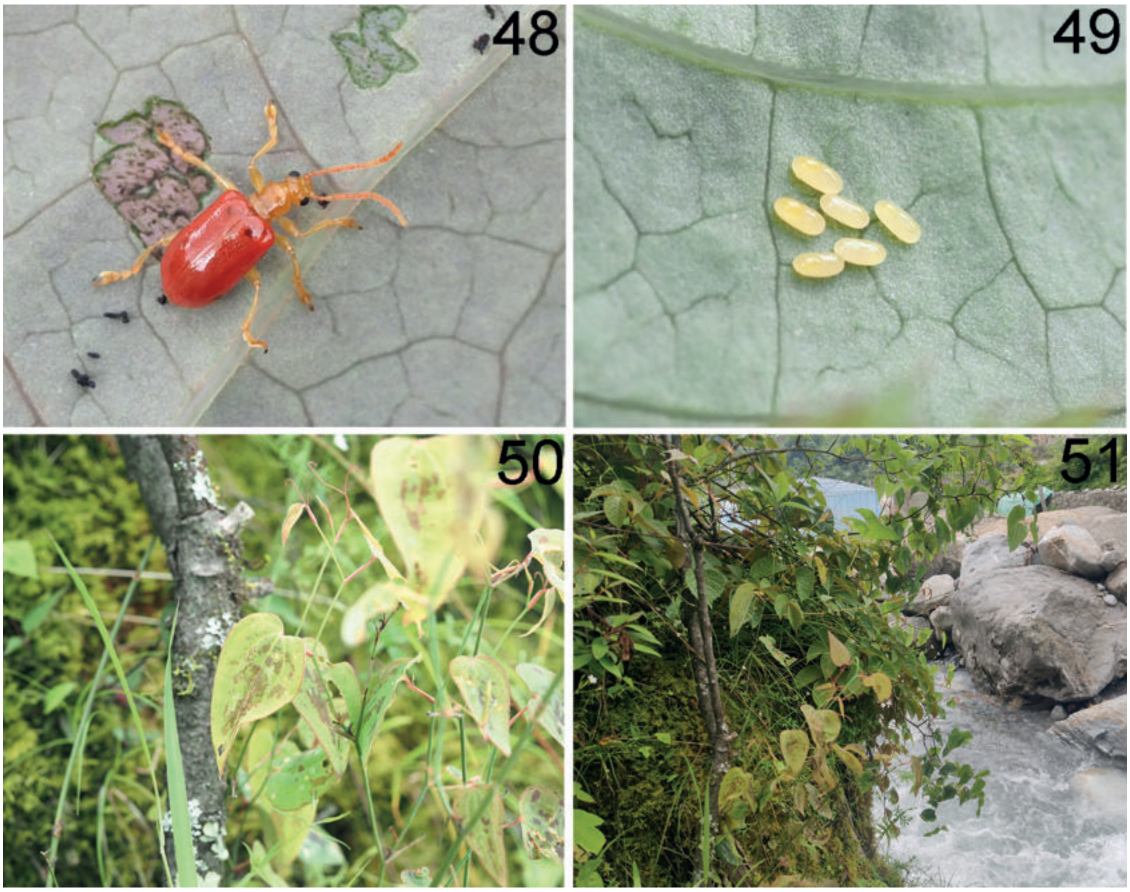

Figures 48–51. *Lilioceris nepalensis* in Tibet (Zhêntang), 2021.VI.24, photographed by YX **48** adult **49** egg **50** host plant: *Smilax menispermoidea* **51** habitat.

Head (Figs 17, 18). Vertex flat, with shallow groove in middle, punctate and pubescent in lateral area; frontoclypeal area triangular, disc with fine punctures and sparse pubescence; labrum transverse, with sparse pubescence; antennae 2/3 length of body, antennomeres I–III nearly globular, antennomeres IV–XI cylindrical, antennomeres V–XI 3 times as long as wide.

Pronotum (Figs 17, 18). Anterior angle protruding; posterior angle not protruding; sides distinctly constricted in middle; posterior transverse impression distinct, disc almost smooth; scutellum triangular and smooth.

Elytra (Figs 17, 18). Humeri protruding, humeral groove distinct, basal transverse impression indistinct; strial punctures large at base, diminishing posteriorly and absent on apical 1/2, intervals smooth; epipleura raised, with row of fine punctures.

Mesosternum pubescent; apical portion of mesosternal process narrow and flat, obliquely pointed, not horizontally connected with metasternum. Metasternum and metepisternum smooth.

Abdominal sternites. Lateral transverse impressions absent on sternites I–IV. Sternites I–IV smooth.

Legs. Femora with dense pubescence on dorsal surface, with sparse pubescence on ventral surface. Claws distinctly asymmetrical, outer one longer than inner one.

Male genitalia (Fig. 27A–D). Apical foramen occupying 1/5 length of median lobe (Fig. 27A); apex rounded (Fig. 27B); tegmen Y-shaped, basal piece of tegmen triangle and broad, lateral lobes slightly sclerotized and combined with second connecting membrane; internal sac with distinct dorsal, median and ventral sclerites, posterior part of dorsal sclerite in dorsal view slightly widen, ventral sclerite short and flat, median sclerite distinct (Fig. 27C, D).

Female reproductive organs (Fig. 34A–C). Tergites VIII and IV, sternites VIII and IV sclerotized, posterior areas of tergite VIII and sternite VIII with pubescence and apodemes, spiculum gastrale X-shaped and short; ovipositor with dense pubescence, distal part of ovipositor cylindrical, short and with protuberance; spermatheca greatly convoluted.

Distribution (Fig. 37). China (Tibet); Nepal; India.

Host plant and habitat (Figs 48–51). The host plant of this species is *Smilax menispermoidea* A. DC. (Smilacaceae) according to our observations in Dinggyê. *Lilioceris nepalensis* was found on its host plant near rivers at altitudes of 2400 to 3200 m, sharing the same habitat with *L. zhentangensis* in Nadang village of Zhêntang, Dinggyê.

Remarks. This species is only ~ 5.0 mm long. It shares the following characteristics with *L. pulchella*, *L. semicostata*, *L. flavipennis* and *L. adonis* (Baly, 1859) (based on a syntype studied, NHML): antennae length > 1/2 of body length, antennomeres IV–X cylindrical, 3 times as long as wide; claws distinctly asymmetrical, outer one longer than inner one.

The black spots on the elytra are actually black spots on the exoskeleton covering the flight muscles under the elytra. These black muscles can be seen clearly when this insect is alive (Fig. 48), but when it is dead, they may be visible as spots (Fig. 17) or not (Fig. 18).

Acknowledgements

We thank Dr Beulah Garner (NHML) and Dr Michael Geiser (NHML) for hosting the second author (LHB) at NHML, Dr Takuya Takemoto (Hokkaido University, Japan) for providing type specimen photos; Mr Neng Zhang (Yunnan, Kunming) for collecting specimens; Dr Pan Li (Zhejiang University, Zhejiang, Hangzhou) for identifying host plants; Mr Pingzhou Zhu (China Agricultural University, Beijing) for his advice and suggestions on this paper.

Additional information

Conflict of interest

The authors have declared that no competing interests exist.

Ethical statement

No ethical statement was reported.

Funding

This work was supported by National Natural Science Foundation of China (31970400), Chinese Academy of Sciences strategic biological resources planning capacity building project (Grant No. KFJ–BRP–017–081), and the survey of wildlife resources in key areas of Tibet (ZL202203601).

Author contributions

All authors have contributed equally.

Data availability

All of the data that support the findings of this study are available in the main text.

References

Baly Esq JS (1859) Descriptions of new species of phytophagous insects. Transactions of Entomological Society of London 5: 146–161. https://doi.org/10.1111/j.1365-2311.1859.tb01840.x

Baly Esq JS (1861) Descriptions of new genera and species of phytophaga. Journal of Entomology, London 1: 275–302.

Bezděk J, Schmitt M (2017) Subfamily Criocerinae. In: Löbl I, Smetana A (Eds) Catalogue of Palaearctic Coleoptera (Vol. 6), Corrigenda et Addenda. Entomologische Blätter und Coleoptera 113(2): 113–135.

Chou I, Liu SK, Xie WP (1993) Taxonomist's Glossary of Genitalia in Insects. Tianze Eldonejo, Hong Kong, 194 pp.

Clavareau H (1913) Pars 51: Chrysomelidae: 1. Sagrinae, 2. Donaciinae, 3. Orsodacninae, 4. Criocerinae. In: Schenbkling S (Ed.) Coleopterorum Catalogus. W. Junk, Berlin, 103 pp.

Heinze E (1943) Über bekannte und neue Criocerinen. Stettiner entomologische Zeitung 104: 101–109.

Hope F (1831) Synopsis of the new species of Nepal insects in the collection of Major General Hardwicke. In: Gray JE (Ed.) The Zoological Miscellany1. Treuttel, Wurtz and Co., London, 21–31. [40 pp. 4 pls.]

Jacoby M (1889) List of the Phytophagous Coleoptera obtained by Signor L. Fea at Burmah and Tenasserim, with descriptions of the new species. Annali del Museo Civico Storia Naturale Genova, ser. 2 7: 147–237.

Jacoby M (1908) The Fauna of British India, Including Ceylon and Burma. Coleoptera Chrysomelidae (Vol. 1). Taylor & Francis, London, 534 pp. [2 pls.]

Kimoto S, Gressitt J (1979) Chrysomelidae (Coleoptera) of Thailand, Cambodia, Laos and Vietnam. I. Sagrinae, Donaciinae, Zeugophorinae, Megalopodinae and Criocerinae. Pacific Insects, Honolulu 20(2/3): 191–256.

Lacordaire J (1845) Monographie des coléoptères subpentamères de la famille des phytophages. Tome premier. Mémoires de la Société Royale des Sciences de Liège 3(1): LIII+740. https://doi.org/10.5962/bhl.title.48433

Li K, Liang Z, Liang H (2013) Two new species of the genus *Temnaspis* Lacordaire, 1845, (Coleoptera: Chrysomeloidea: Megalopodidae) from China and Myanmar, with notes on the biology of the genus. Zootaxa 3737(4): 379–398. https://doi.org/10.11646/zootaxa.3737.4.3

Matsumura Y, Machida R, Wipfler B, Beutel R, Yoshizawa K (2013) Parallel evolution of novelties: Extremely long intromittent organs in the leaf beetle subfamily Criocerinae. Evolution & Development 15(4): 305–315. https://doi.org/10.1111/ede.12036

Monrós F (1960) Los géneros de Chrysomelidae (Chrysomelidae). Opera Lilloana (Tucumán) 3: 1–337. [3 pls.]

Pic M (1916) Descriptions abrégées diverses. Mélanges Exotico-Entomologiques 21: 2–20.

Pic M (1932) Nouveautés diverses. Mélanges Exotico-Entomologiques 59: 10–36.

Reitter E (1913) Fauna Germanica. Die Käfer des Deutschen Reiches. Band IV. K. G. Lutz' Verlag, Stuttgart, 236 pp. [+ 22 pls.]

Takizawa H (1989) Chrysomelid beetles of Nepal, northeastern India and western Sikkim collected by the Himalaya Expeditions of the National Science Museum, Tokyo. Part 1. Japanese Journal of Entomology 57: 319–332.

Tishechkin A, Konstantinov A, Bista S, Pemberton R, Center T (2011) Review of the continental Oriental species of *Lilioceris* Reitter (Coleoptera, Chrysomelidae, Criocerinae) closely related to *Lilioceris impressa* (F.). ZooKeys 103: 63–83. https://doi.org/10.3897/zookeys.103.983

Weise J (1922) Chrysomeliden der Indo-Malayischen Region. Tijdschrift voor Entomologie 65: 39–130.

Xu Y, Xiong Y, Liang H (2021) A review of the neptis species group of the genus *Lilioceris* (Coleoptera: Chrysomelidae: Criocerinae). Zoological Systematics 46(4): 300–316.

Yang X (2004) Insects of the Great Yarlung Zangbo Canyon of Xizang, China. China Science and Technology Press 339: 1–7.

ZooKeys 1189: 83–184 (2024)
DOI: 10.3897/zookeys.1189.107506

Monograph

Systematic revision of the ant subfamily Leptanillinae (Hymenoptera, Formicidae)

Zachary Griebenow[1,2]

1 *Department of Entomology & Nematology, University of California, Davis, CA USA*
2 *Department of Agricultural Biology, Colorado State University, Fort Collins, CO USA*
Corresponding author: Zachary Griebenow (zachary.griebenow@colostate.edu)

Abstract

The genus-level taxonomy of the ant subfamily Leptanillinae (Hymenoptera: Formicidae) is here revised, with the aim of delimiting genus-level taxa that are reciprocally monophyletic and readily diagnosable based upon all adult forms. This new classification reflects molecular phylogenetics and is informed by joint consideration of both male and worker morphology. Three valid genera are recognized in the Leptanillinae: *Opamyrma*, *Leptanilla* (= *Scyphodon* **syn. nov.**, *Phaulomyrma*, *Leptomesites*, *Noonilla* **syn. nov.**, *Yavnella* **syn. nov.**), and *Protanilla* (= *Anomalomyrma* **syn. nov.**, *Furcotanilla*). *Leptanilla* and *Protanilla* are further divided into informal, monophyletic species groups. Synoptic diagnoses are provided for all genera and informal supraspecific groupings. In addition, worker-based keys to all described species within the Leptanillinae for which the worker caste is known are provided; and male-based keys to all species for which males are known, plus undescribed male morphospecies for which molecular data are published. The following species are described as new: *Protanilla wallacei* **sp. nov.**, *Leptanilla acherontia* **sp. nov.**, *Leptanilla belantan* **sp. nov.**, *Leptanilla bethyloides* **sp. nov.**, and *Leptanilla najaphalla* **sp. nov.**

Key words: Morphology, phylogenetics, subterranean biology, taxonomy

Academic editor: Jeffrey Sosa-Calvo
Received: 6 June 2023
Accepted: 6 September 2023
Published: 16 January 2024

ZooBank: https://zoobank.org/FF5E2B39-43DB-497E-B546-587BD91F794B

Citation: Griebenow Z (2024) Systematic revision of the ant subfamily Leptanillinae (Hymenoptera, Formicidae). ZooKeys 1189: 83–184. https://doi.org/10.3897/zookeys.1189.107506

Table of contents

Introduction

The subfamily Leptanillinae (Hymenoptera: Formicidae), sometimes called legionary vampire ants (Ward and Boudinot 2021), consists of cryptic, hypogaeic ants largely restricted to tropical and warm temperate regions of the Old World, although *Protanilla beijingensis* Man, Ran, Chen & Xu, 2017 and *Leptanilla taiwanensis* Ogata, Terayama & Masuko, 1995 have been collected in a cold temperate climate. Most of their diversity is concentrated in the Indo-Malayan region. While the affinities of the Leptanillinae to other ants have historically been controversial, phylogenetic inference from molecular data that corrects for compositional heterogeneity in nucleotides supports the monotypic Neotropical genus *Martialis* Rabeling & Verhaagh as the sister group of the Leptanillinae, with this clade collectively being sister to all other extant Formicidae (Borowiec et al. 2019; Romiguier et al. 2022).

The internal taxonomy of the Leptanillinae has been afflicted with probable parallelism, since males are collected more often than workers or gynes: both genus- and species group names were established based solely upon male specimens. The sexes are only directly associated in *L. japonica* Baroni Urbani, 1977 (Ogata et al. 1995) and *Opamyrma hungvuong* Yamane, Bui & Eguchi, 2008 (Yamada et al. 2020), while Griebenow (2020) associated the sexes of *Protanilla lini* Terayama, 2009 with phylogenomic inference. The genera *Scyphodon* Brues, *Noonilla* Petersen, and *Yavnella* Kugler were all described solely from male material, with the worker of *Yavnella* being identified ex post facto by phylogenomic inference (Griebenow et al. 2022). Total-evidence Bayesian inference recovered the male-based genus *Phaulomyrma* Wheeler & Wheeler within *Leptanilla* s. str. (Griebenow 2021), resulting in its synonymy under *Leptanilla*, with Griebenow (2020, 2021) delimiting *Leptanilla* s. l. to also include *Noonilla* and *Scyphodon*, with two major clades of *Leptanilla* s. l. known only from undescribed male morphospecies. The boundaries of *Leptanilla* relative to the three male-based genera must therefore be formally revised. Generic boundaries in the former Anomalomyrmini require revision as well, with phylogenetic inference consistently recovering *Protanilla* as paraphyletic relative to *Anomalomyrma* irrespective of dataset or statistical framework (e.g., Borowiec et al. 2019; pers. obs.).

Colonies of *Protanilla jongi* Hsu, Hsu, Hsiao & Lin, 2017 and *Leptanilla belantan* sp. nov. were collected in decaying wood (Hsu et al. 2017; this study), and foraging workers of *Protanilla lini* Terayama, 2009 in Sea, Land and Air Malaise (SLAM) traps (Griebenow 2020), but leptanilline workers are otherwise exclusively subterranean. Based on limited observations of live colonies, it appears that leptanilline ants are specialized predators of geophilomorph centipedes or forcepstails (Diplura: Japygidae) (Masuko 1990; Hsu et al. 2017; Ito et al. 2022), with *P. lini* feeding on other prey (e.g., lithobiomorph centipedes, cockroaches) in captivity (Katayama and Tsuji 2011; Yamamuro 2018). *Leptanilla* display aspects of the "army ant syndrome" commonly associated with *Dorylus*, *Eciton*, and related lineages in the subfamily Dorylinae: *Leptanilla japonica* Baroni Urbani, 1977 and *Leptanilla clypeata* Yamane & Ito, 2001 engage in synchronized brood production (Masuko 1990; Ito and Yamane 2020) and regular colony migration, with the physogastry reported in *Leptanilla charonea* Barandica, López, Martínez & Ortuño, 1994 and *Leptanilla zaballosi* Barandica, López, Martínez & Ortuño, 1994, indicating synchronized brood production in at least those species as well (López et al. 1994). Gynes of *Leptanilla* are always wingless and blind. It is unclear whether *Protanilla* (the only other leptanilline genus for which any bionomic data are available) display legionary behavior, but the alate condition of *Protanilla* gynes (except for *Protanilla wallacei* sp. nov.; see Billen et al. 2013; Ito et al. 2022) contradict this assumption. Intracolonial uniformity of larval instar in *Protanilla gengma* Xu, 2012 (pers. obs.) indicates synchronized brood production in at least that species. Gynes of *L. japonica* and *L. clypeata*, and the worker of *L. clypeata*, engage in larval hemolymph feeding (LHF) via a specialized "larval hemolymph tap" (Masuko 1989) that acts as an exudatorium (Wheeler 1918), facilitating non-traumatic LHF (Masuko 1989; Ito and Yamane 2020); such an exudatorium is otherwise known in ants only in *Proceratium itoi* (Forel, 1918) (Proceratiinae) (Masuko 2019). Larvae of *Leptanilla* bear a prothoracic process (Wheeler 1918; Kugler 1987; Wheeler and Wheeler 1988; Barandica et al. 1994) that is used as a grip by workers during colony migration (Masuko 1990). The larvae of *P. jongi* examined in this study lack this process.

With the internal phylogeny of the tribe Leptanillini confidently resolved by a combination of total-evidence and phylogenomic approaches (pers. obs.), including the identification of workers of *Yavnella* and *Scyphodon* s. l., worker and male morphology can be contextualized on this robust phylogeny. Therefore, the time is ripe for revision of the Leptanillinae at the genus level. What follows is a systematic revision of the subfamily to establish reciprocally monophyletic and consistently diagnosable genera and species groups. *Protanilla wallacei* sp. nov., *Leptanilla acherontia* sp. nov., and *Leptanilla belantan* sp. nov. are described based upon worker specimens. To provide a formal name for the Bornean morphospecies group of *Leptanilla* s. l. (Griebenow 2020, 2021), known only from bizarre males, *Leptanilla najaphalla* sp. nov. is described based solely upon male specimens. Likewise, to establish a formal name for the Indochinese morphospecies group (Griebenow et al. in press), *Leptanilla bethyloides* sp. nov. is described based on male specimens. The first global worker-based keys to all species of the Leptanillinae are also provided, with male-based species-level keys.

Materials and methods

Specimens were imaged using the same equipment as reported in Griebenow (2020, 2021) and Griebenow et al. (2022), with the addition of a VHX-970F digital microscope (Keyence, Osaka, Japan). Accession numbers and a subset of collection data for all specimens consulted in this study not previously included in Griebenow (2020, 2021) or Griebenow et al. (2022) are provided in Suppl. material 1:

BPBM	Bernice P. Bishop Museum, Honolulu, USA;

CAS	California Academy of Sciences, San Francisco, USA;
CSCA	California State Collection of Arthropods, Sacramento, USA;
HKUBM	Biodiversity Museum, University of Hong Kong, China;
JAZM	Jalal Afshar Zoological Museum, Department of Plant Protection, College of Agriculture and Natural Resources, University of Tehran, Karaj, Iran;
LACM	Los Angeles County Museum of Natural History, Los Angeles, USA;
MCZC	Museum of Comparative Zoology, Cambridge, USA;
MHNG	Muséum d'Histoire Naturelle, Geneva, Switzerland;
MZLS	Museé Zoologique, Lausanne, Switzerland;
MZLU	Lund University, Lund, Sweden;
NCUE	National Changhua University of Education, Changhua, Taiwan;
OIST	Okinawa Institute of Science and Technology, Onna-son, Japan;
ROME	Royal Ontario Museum, Toronto, Canada;
UCDC	R. M. Bohart Museum of Entomology, University of California, Davis, USA;
ZMHB	Museum für Naturkunde der Humboldt-Universität, Berlin, Germany;
TAU	Tel Aviv University, Tel Aviv, Israel;
ZMUI	Zoological Museum, University of Isfahan, Isfahan, Iran.

I also consulted the personal collections of José María Gómez-Durán, John T. Longino, and Philip Ward. Discrepancy in provisional morphospecies identifiers with those used in previous studies is resolved by Table 1.

Table 1. Concordance of morphospecies identifiers used in this study that conflict with Griebenow (2020, 2021), Griebenow et al. (2022), and Griebenow et al. (in press).

Current identifier	Previous identifier
Leptanilla MM01	*Yavnella* MM01
Leptanilla TH02	*Yavnella* TH02
Leptanilla TH03	*Yavnella* TH03
Leptanilla TH04	*Yavnella* TH04
Leptanilla TH06	*Yavnella* TH06
Leptanilla TH07	*Leptanilla* TH07
Leptanilla TH08	*Yavnella* TH08
Leptanilla zhg-bt03	*Yavnella* zhg-bt01
Leptanilla zhg-mm14	*Yavnella* indet.
Leptanilla najaphalla	*Leptanilla* zhg-my02
Leptanilla zhg-my10	*Noonilla* zhg-my01
Leptanilla zhg-my11	*Noonilla* zhg-my02
Leptanilla zhg-my14	*Noonilla* zhg-my06
Leptanilla zhg-my16	*Yavnella* zhg-my02
Leptanilla zhg-th02	*Yavnella* zhg-th01
Leptanilla zhg-th04	*Yavnella* zhg-th03
Leptanilla zhg-th05	*Yavnella* zhg-th04
Protanilla gengma	*Protanilla* VN01
Protanilla id01	*Anomalomyrma* indet.

Measurements

Definitions pertain to all adult forms unless otherwise noted.

HW	Head Width, maximum width of cranium in full-face view, including compound eyes if present;
HL	Head Length, maximum length of head in full-face view from anterior margin of head capsule to cranial vertex;
EW	Eye Width, maximum breadth of compound eye measured perpendicular to anteroposterior axis of head (male);
EL	Eye Length, maximum length of compound eye measured parallel to anteroposterior axis of head (male);
SL	Scape Length, maximum length of scape in medial view, excluding bulbus;
LF2	Third Antennomere Length, length of the basal flagellomere;
ML	Mandible Length, maximum length of mandible from view orthogonal to lateral mandibular margin, measured from ventral mandibular articulation to mandibular apex;
MaL	Mandalar Length, maximum length of mandalus, measured along proximodistal axis of mandible;
WL	Weber's Length, maximum diagonal distance measured from most anterior extent of pronotum excluding (female) or including (male) cervical shield to most posteroventral extremity of the mesosoma, including propodeal lobes if present;
PrW	Pronotal width, maximum width of pronotum, measured in dorsal view;
MW	Mesonotal width, maximum width of mesonotum in dorsal view, measured immediately anterior to mesocoxal foramina;
MSW	Mesoscutal width, maximum width of mesoscutum in dorsal view (male);
MSL	Mesoscutal length, maximum length of mesoscutum in dorsal view (male);
PTL	Petiolar length, maximum length of petiole in dorsal view, not including presclerites;
PTH	Petiolar height, maximum height of petiole in profile view, including sternal process and dorsal node, if distinct;
PTW	Petiolar width, maximum width of petiole in dorsal view orthogonal anteroposterior axis;
PPL	Postpetiolar length, maximum length of postpetiole in dorsal view, not including presclerites;
PPW	Postpetiolar width, maximum width of postpetiole in dorsal view;
PPH	Postpetiolar height, maximum height of postpetiole in profile view, including sternal process and dorsal node, if distinct;
TW4	Width of abdominal tergite IV, maximum width of abdominal tergite IV measured in dorsal view.

Indices

CI	(HW / HL) × 100;
SI	(SL / HW) × 100;
MI	(ML / HW) × 100;

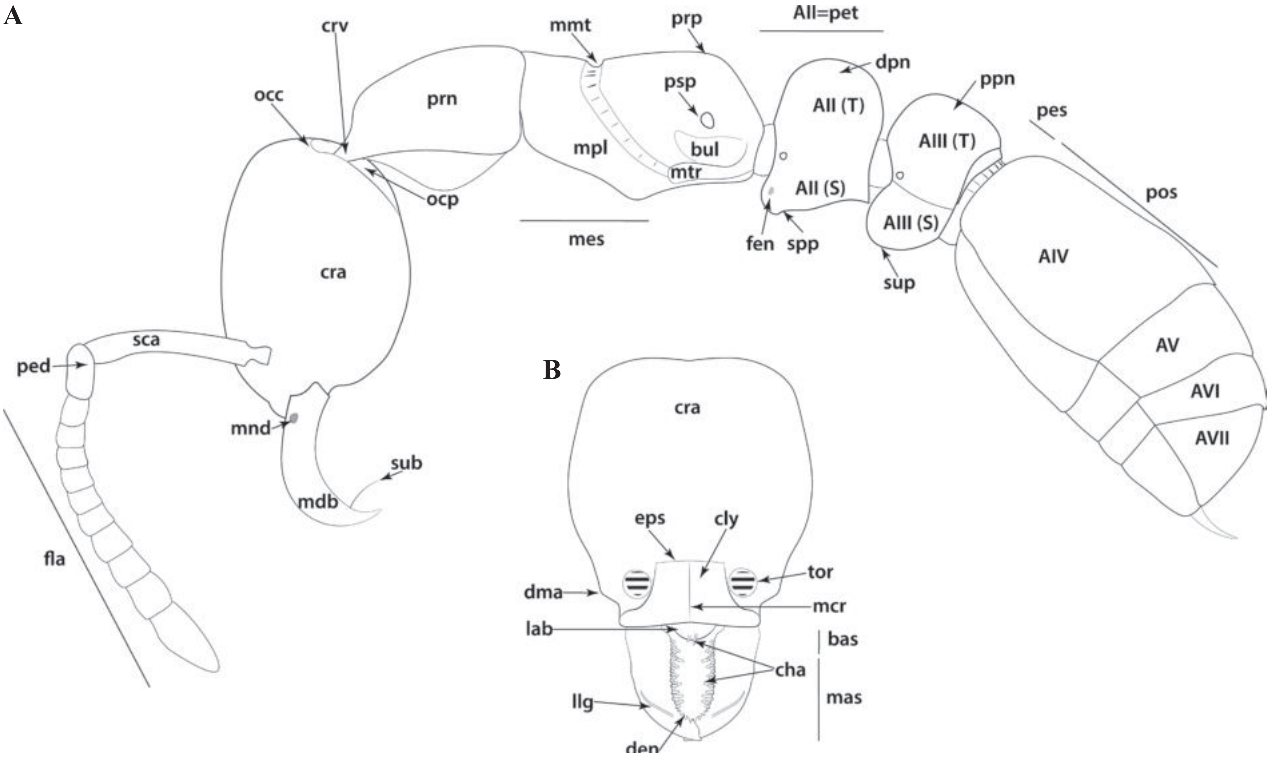

Figure 1. Glossary of morphological terms used to describe the worker soma in the Leptanillinae, with *Protanilla beijingensis* as template **A** profile habitus **B** full-face view. Abbreviations: A = abdominal segment; bas = basal mandibular margin; bul = bulla; cha = chaetae; cly = clypeus; cra = cranium; crv = cervical shield; den = denticle; dma = dorsal mandibular articulation; dpn = petiolar node; eps = epistomal sulcus; fen = fenestra; fla = flagellum; lab = labrum; llg = laterodorsal longitudinal groove; mas = masticatory mandibular margin; mcr = median clypeal ridge; mdb = mandible; mes = mesothorax; mmt = meso-metapleural suture; mnd = mandalus; mpl = mesopleuron; mtr = metapleural trench; occ = occipital carina; ocp = occiput; ped = pedicel; pes = presternite; pos = poststernite; ppn = postpetiolar node; prn = pronotum; prp = propodeum; psp = propodeal spiracle; S = sternite; sca = scape; spp = subpetiolar process; sub = subapical mandibular seta; sup = sub-post-petiolar process; T = tergite; tor = torulus.

OI	(EW / EL) × 100;
MSI	(MSW / MSL) × 100;
PI	(PTW / PTL) × 100;
PPI	(PPW / PPL) × 100;
TI1	(PPW / TW4) × 100.

Nomenclature

Nomenclature for sculpture and setation combines Harris (1979), Wilson (1955), and Boudinot et al. (2020). Notational conventions for palp and tibial spur formulae follow Bolton (2003). Cephalic nomenclature follows Richter et al. (2021) and Boudinot et al. (2021). Mesosomal nomenclature follows Liu et al. (2019); metasomal, Lieberman et al. (2022). Male genital nomenclature follows Boudinot (2018). Descriptive terms for larval morphology follow Wheeler and Wheeler (1986, 1976). Wing venation is described using Brown and Nutting (1949) and Ogata (1991), with interpretation of homologies in male wing venation following Boudinot (2015) in some ambiguous cases observed in *Leptanilla*. Any morphological terms unaddressed in these publications follow the Hymenoptera Anatomy Ontology (Yoder et al. 2010). Glossaries of exter-

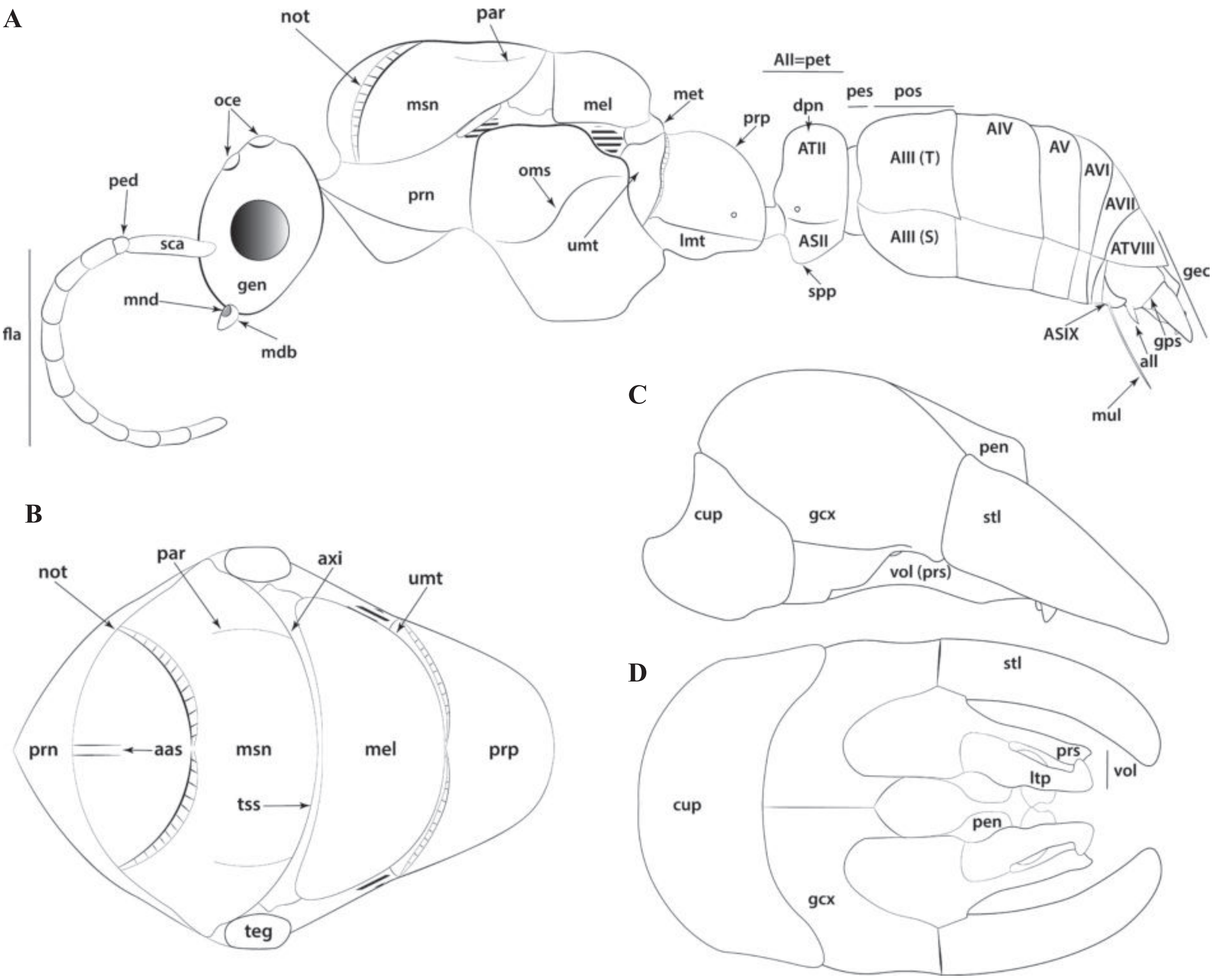

Figure 2. Glossary of morphological terms used to describe male morphology in the Leptanillinae. Figure A, B is chimeric, but *Protanilla* zhg-vn01 is the template for Fig. 2C, D **A** profile habitus **B** mesosomal dorsum **C** genitalia, profile view **D** genitalia, ventral view. Abbreviations: A = abdominal segment; aas = antero-admedian signum; all = apicolateral gonocoxital lamina; axi = axilla; cup = cupula; dpn = petiolar node; fla = flagellum; gcx = gonocoxites; gec = genital capsule; gen = gena; gps = gonopodital suture; ltp = lateropenite (=digitus); mdb = mandible; mel = mesoscutellum; met = metascutellum; mnd = mandalus; msn = mesonotum; mul = mulceators; not = notauli; oce = ocelli; oms = oblique mesopleural sulcus; par = parapsidal signa; ped = pedicel; pen = penial sclerites; pes = presternite; pet = petiole; prn = pronotum; prp = propodeum; prs = parossiculus (= cuspis *partim*); S = sternite; sca = scape; spp = subpetiolar process; stl = gonostylus; T = tergite; teg = tegula; tss = transscutal line; umt = upper metapleuron; vol = volsella.

nal morphological terms for worker and male Leptanillinae are summarized in Figs 1–3. In instances where the homology of the terminal abdominal sternite is ambiguous, this sternite is termed a hypopygium.

Species concept

I here follow Barraclough (2019) in treating a species as an evolutionarily independent population of organisms that is genetically and phenotypically distinct from other such populations (Simpson 1961). In sexually reproducing organisms, such as the Leptanillinae (so far as is known), reproductive isolation sufficient to maintain interspecific distinctiveness—in other words, the absence of genotypic and phenotypic intermediates—is an expected property of species. Mechanically incompatible genitalia are an expected corollary of reproductive isolation, and thus would indicate interspecific differentiation, but may only be asserted to be so for sibling populations that occur in sympatry and exhibit consistent phenotypic differentiation. The degree of differentiation between such species serves as a "yardstick" by which to assess whether allopatric populations diverge sufficiently in phenotype to be considered heterospecific (Tobias et al. 2010; Ward and Branstetter 2022). Scenarios that allow this calibration of phenotypic difference are fulfilled thrice among the leptanilline morphospecies for which UCEs have been successfully enriched: one instance being *Leptanilla najaphalla* sp. nov. and *Leptanilla* zhg-my05 (Sabah, Malaysia); another, *Leptanilla charonea* and *Leptanilla* cf. *zaballosi* (Madrid, Spain); and the last, *Leptanilla* zhg-bt01 and -02 (Bhutan). In all cases the two putative sympatric species are recovered as closely related terminals by phylogenomic inference (Griebenow 2020, 2021; Griebenow et al. 2022), and males of each species pair exhibit a phenotype uniformly distinguishable across all available specimens by the proportions of the genitalia. Variation among the syntopic specimen series assigned to these morphotypes is bimodal, with the exceptions to this bimodality not constituting intermediates. Thus, there is no indication that any differentiation in genital shape among these sympatric species can be considered intraspecific.

Results

Protanilla wallacei sp. nov.

https://zoobank.org/6AC428A6-E31D-412A-93E4-9E0BCF7B716E
Fig. 4A–C

Type material. ***Holotype*.** MALAYSIA – Sarawak • 1 worker; Gunung Mulu National Park, 4th division; 4.09°N, 114.89°E (estimated from Google Earth to nearest minute); May–Aug. 1978, P. M. Hammond and J. E. Marshall leg.; CASENT0902782; BM1978–49, BMNH(E) 1015826. BMNH. ***Paratype*.** MALAYSIA – Sabah • 1 worker; Gunung Silam, Lahad Datu; 4.96°N, 118.17°E (estimated from Google Earth to nearest minute); 630m a.s.l.; 1983; R. Leakey leg; CASENT0842699; UCDC.

Other material examined. MALAYSIA – Sabah • 1 worker; 8km S Sapulut, 4.62844°N, 116.47175°E; 325m a.s.l.; 31.vii.2014; P. S. Ward leg.; sifted litter (leaf mold, rotten wood), rainforest; CASENT0842640; PSW17199–01. UCDC.

Measurements (mm) and indices. *Holotype*: N/A ***Paratype*:** HL = 0.42; HW = 0.33; SL = 0.22; PW = 0.27; WL = 0.68; PTL = 0.2; PTW = 0.19; PPTL = 0.19; PPTW = 0.2; CI = 79; SI = 106; PI = 98; PPI = 113. **Other material examined** (*n* = 2): HL = 0.43–0.46; HW = 0.35–0.36; SL = 0.33–0.39; ML = 0.21–0.24; PW = 0.26–0.29; WL = 0.64–0.72; PTL = 0.19–0.21; PTW = 0.2; PPTL = 0.19–0.21; PPTW = 0.2–0.23; CI = 78–80; SI = 97–102; PI = 93–101; PPI = 105–108

Description. Lateral cranial margins converging anteriorly; cranium not bulging towards vertex. Genal angle laterad antennal toruli obtuse. Outline of clypeus campaniform in full-face view, laterally elevated above cranium, posteriorly not elevated above frons; clypeal surface planar; anterior clypeal margin slightly emarginate, posteromedian clypeal margin emarginate; median clypeal

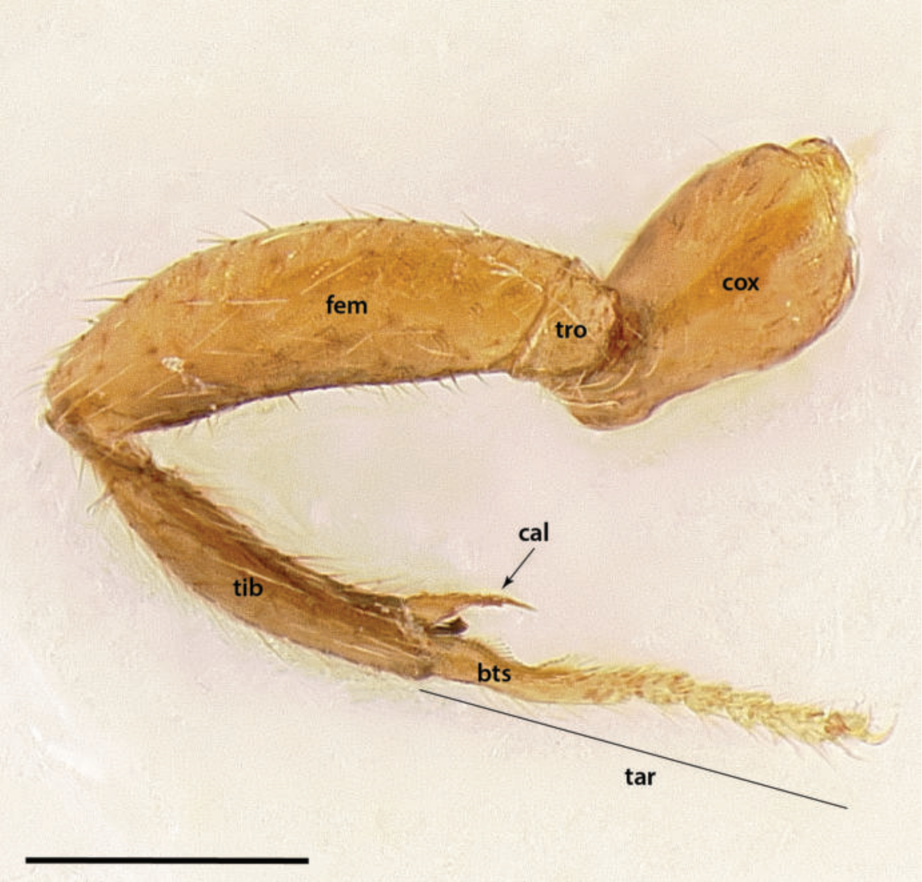

Figure 3. Glossary of leg nomenclature used for the Formicidae, with the male foreleg of *Leptanilla* zhg-my11 (CASENT0842593) as template. Abbreviations: bts = basitarsus; cal = calcar; cox = coxa; fem = femur; tar = tarsus; tib = tibia; tro = trochanter. Scale bar: 0.2 mm.

ridge present on mesal surface of clypeus, externally visible. Labrum visible in full-face view; anterodorsal apex of labrum armed with three or four dentiform, peg-like chaetae; venter with vestiture of suberect lanose setae. Mandibles elongate relative to head (CI = 79–80), linear, apex curved downward distally; vertical dorsal lamella absent; laterodorsal longitudinal groove present; dorsomedial margin of mandible with single row of ~ 12 dentiform, peg-like chaetae; lateral mandibular face glabrous. Labial palp 1-merous. Anterior tentorial pits faint, situated anterad the toruli, not visible in full-face view. Postgenal ridge complete. Scape long (SL 0.34–0.39 mm), reaching slightly beyond occipital margin when antennae retracted. Flagellum submoniliform; apical flagellomere 3× longer than broad. Pronotum broader than mesonotum in dorsal view, with lateral margins convex. Mesonotum narrow, with lateral margins parallel in dorsal view. Meso-metapleural suture narrow laterally, broader along dorsal surface; scrobiculate, with transverse ridges larger and more widely spaced along dorsal surface of meso-metapleural suture; posteriorly distinct from metapleural trench. Maximum breadth of metapectal-propodeal complex greater than that of mesonotum in dorsal view, slightly narrowed anteriorly, posterior outline convex in profile view. Bulla large, extending anterior to propodeal spiracle. Propodeum rounded in profile view. Tarsomeres longer than broad. Meso- and

Figure 4. *Protanilla wallacei*, holotype (CASENT0902782; Ziv Lieberman), worker **A** profile view **B** dorsal view **C** full-face view. Scale bars: 0.2 mm (**A, B**); 0.1 mm (**C**).

metatibial spur formula 0,1p. Petiole sessile. Abdominal segments II and III without tergotergal and sternosternal fusion. Abdominal segment II slightly longer than wide in dorsal view (PI 94–99), with distinct dorsal node, in profile view anterior and posterior faces subequal in height; anterior face of petiolar node linear in profile view. Subpetiolar process present, abdominal sternite II with concavity posterior to subpetiolar process so that margin of abdominal sternite II is sinuate in profile view; fenestra present, elliptical, anteroposteriorly compressed. Lengths of abdominal segments II–III subequal. Abdominal sternite II projecting no further than abdominal sternite III towards venter. Abdominal segment III slightly broader than long in dorsal view (PPI = 105–113), with distinct dorsal node; in profile view, anterior face of dorsal node abruptly vertical and bulging, posterior face gently sloping. Post-petiole with distinct tergosternal suture. Abdominal segments III–IV separated by pronounced constriction, with presclerites of abdominal segment IV distinct; pretergite IV planar in profile view, shorter than presternite IV; presternite IV slightly convex in profile view; cinctus of abdominal segment IV scrobiculate. Anterior margin of abdominal post-tergite IV shallowly emarginate in dorsal view. Outline of postpetiolar node trapezoidal in dorsal view, corners rounded, slightly narrowed anteriorly. Soma concolorous, color castaneous. Vestiture of suberect to erect setae present; length of setae variable.

Etymology. Named for Alfred Russel Wallace, commonly thought to be the progenitor of the discipline of biogeography and still well-regarded for his study of the biota of the Malay Archipelago, where this ant is native. The specific epithet is masculine, in genitive case.

Remarks. The worker caste of *P. wallacei* is extremely close to that of *P. lini* but differs in overall smaller size and the shallowness of the postpetiolar node, with the posterior declivity of the postpetiolar node being gradual (Fig. 5B) rather than abrupt (Fig. 5A). PPI tends to be greater in *P. wallacei* ($\underline{x}$ = 109) than in *P. lini* ($\underline{x}$ = 100) but cannot be consistently used to discriminate the two. Interestingly, all known gynes of *P. wallacei* are ergatoid (Billen et al. 2013; Ito et al. 2022), whereas those of *P. lini* are alate (Hsu et al. 2017).

Protanilla wallacei appeared as a nomen nudum in Hölldobler and Wilson (1990), with the name purportedly being under description by Robert W. Taylor based upon material from Sabah. Such a description has not appeared. CASENT0842699 was identified as *P. wallacei* by Barry Bolton with reference to “type” material under description by Taylor, which, based on a paratype label assigned by Taylor, included CASENT0902782. Billen et al. (2013) described the glandular complement of specimens from peninsular Malaysia that was attributed to this nomen nudum by Taylor, while Ito et al. (2022) reported on the behavioral observations of specimens from that same series, referring to this species as *Protanilla* sp. *Protanilla wallacei* is here made an available name, described based upon worker specimens from Sabah. Judging from Billen et al. (2013: fig. 5E), the series referred to in that study and in Ito et al. (2022) conforms to the diagnosis of *P. wallacei* here given. The unidentified *Protanilla* that was the sole representative of the Leptanillinae in the phylogenomic analyses of Branstetter et al. (2017) (CASENT0634862) is here identified as *P. wallacei*. *Protanilla wallacei* shows intraspecific variation in labral chaeta count, which is also observed in putatively conspecific allopatric specimens of *P. gengma* (Aswaj et al. 2020; pers. obs.) and *P. beijingensis* (this study).

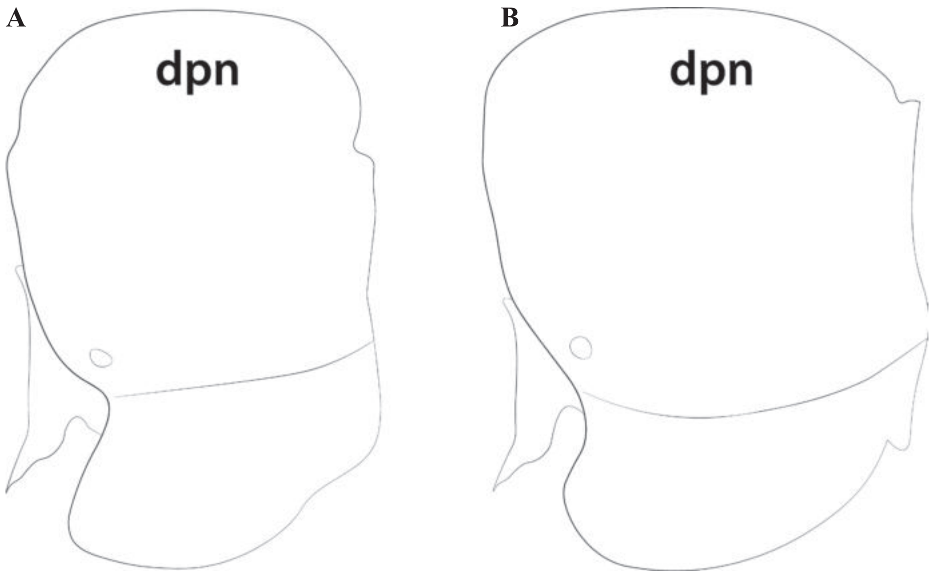

Figure 5. Worker petiole of *Protanilla lini* (**a**) and *Protanilla wallacei* sp. nov. (**b**), profile view. Abbreviation: dpn = petiolar node.

Protanilla wallacei and *P. lini* are recovered as sister taxa in phylogenomic inference sampling from across the geographical range of the latter species (pers. obs.). *Protanilla lini* ranges across Taiwan and the Ryukyu Islands, while the *P. wallacei* specimens examined in this study originate in the Sundan region. This allows for the possibility that these putative species are populations from extreme ends of a contiguous swath of metapopulations extending throughout southeast Asia. Further sampling in mainland southeast Asia may reciprocally efface the morphometric distinction between these species, and with the other members of the *Protanilla lini* species complex.

Leptanilla belantan **sp. nov.**
https://zoobank.org/3EB67585-11A5-418D-B30D-38A9440C92B3
Figs 6A–C, 7, 8A–C

Type material. ***Holotype*****.** Malaysia – Selangor • 1 worker; Genting Highlands, below Sri Layan; 1.iv.1981; W. L. Brown leg.; hill forest, red-rotten wood; MCZ:Ent:00728278. MCZC ***Paratypes*****.** Malaysia – Selangor • 1 gyne; same data as for holotype; MCZ:Ent:00728275; MCZC • 3 worker, same data as for holotype; MCZ:Ent:00728276, MCZ:Ent:00728277, MCZ:Ent:00793731; MCZC • 2 worker, same data as for holotype; MCZ:Ent:00793729, MCZ:Ent:00793730; UCDC.

Measurements (mm) and indices, worker. ***Holotype*****:** HW = 0.34; HL = 0.44; SL = 0.28; LF2 = 0.05; ML = 0.2; WL = 0.56; PrW = 0.22; MW = 0.148; PTL = 0.14; PTH = 0.13; PTW = 0.08; PPL = 0.11; PPW = 0.10; PPH = 0.16; TW4 = 0.29; CI = 77; SI = 82.38; MI = 58; PI = 59; PPI = 91; TI1 = 33. ***Paratypes*** (*n* = 5): HW = 0.33–0.35; HL = 0.42–0.45; SL = 0.24–0.28; ML = 0.18–0.21; WL = 0.54–0.57; PrW = 0.224 –0.23; MW = 0.15–0.16; PTL = 0.14–0.16; PTH = 0.11–0.13; PTW = 0.08–0.09; PPL = 0.10–0.11; PPW = 0.09–0.10; PPH = 0.15–0.16; TW4 = 0.29–0.31; CI = 75–77; SI = 74–82; MI = 52–60; PI = 55–59; PPI = 89–98; TI1 = 32–35

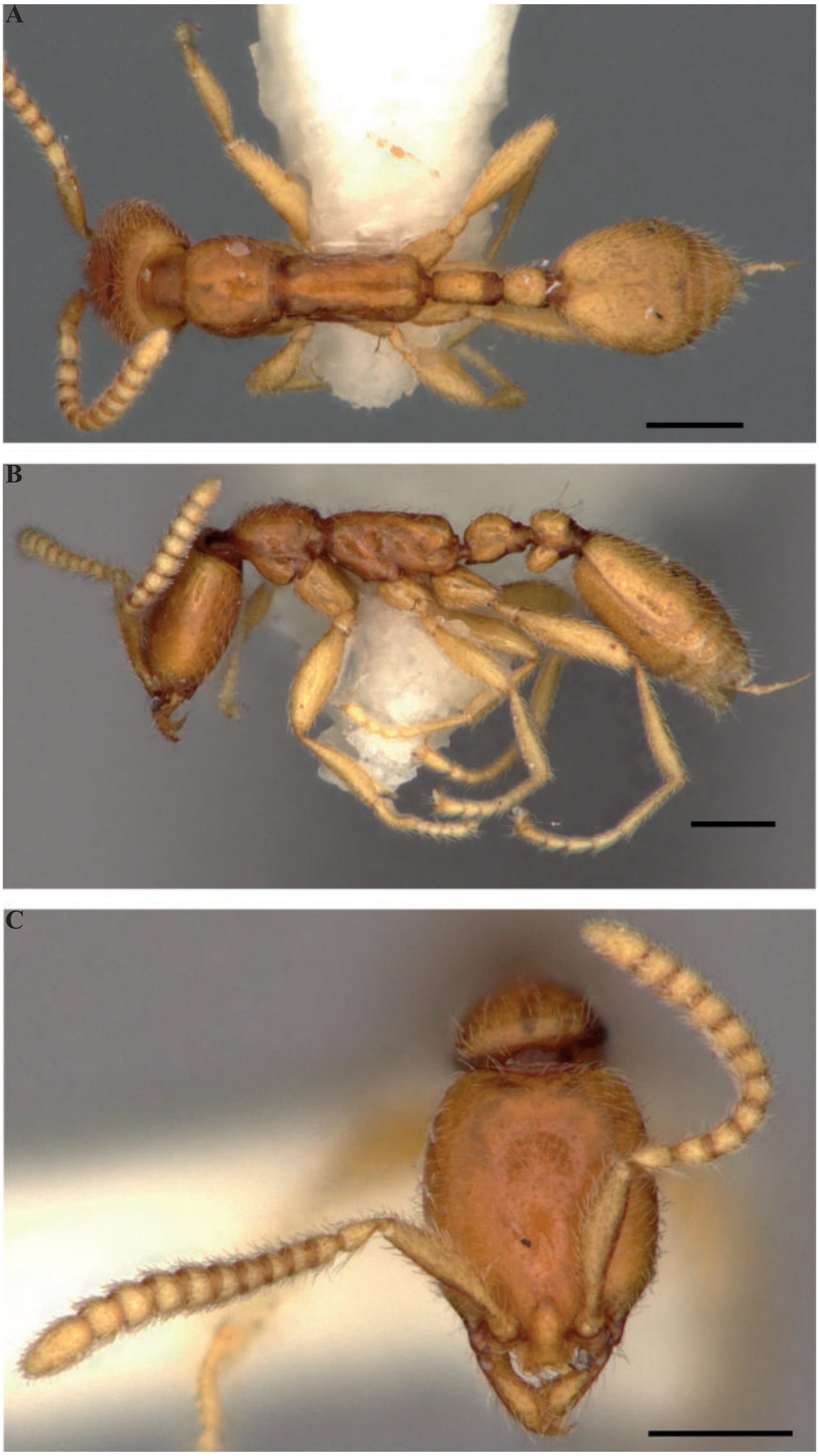

Figure 6. *Leptanilla belantan*, holotype (MCZ:Ent:00728278), worker **A** profile view **B** dorsal view **C** full-face view. Scale bars: 0.2 mm.

Measurements (mm) and indices, gyne. HW = 0.47; HL = 0.56; SL = 0.29; LF2 = 0.06; ML = 0.20; PrW = 0.30; MW = 0.31; PTL = 0.30; PTH = 0.21; PTW = 0.22; CI = 84; SI = 61; MI = 43; PI = 72

Worker. Lateral margins of cranium slightly convex. Occipital carina distinct. Frontoclypeal process present, delimited from cranium by lateral carinae, with posteromedian delimitation from cranium, projecting well anterior of labrum in full-face view; apex robust, broad in outline, emarginate, bordered by laminae. Mandible short relative to head. Four teeth present on mandible; two teeth proximad apical tooth acute, subequal in size, with two denticles interposed; most proximal tooth large, distally recurved, blunt, enlarged apically (Fig. 7). Large, tapering basal seta absent from mandible; subapical tapering seta present (Fig. 7). Maxillary palp 2-merous. Scape short, not reaching cranial vertex at rest, somewhat expanded towards apex. Pedicel length subequal to that of basal flagellomere. Flagellum submoniliform; antennomere 3 subequal in length to distal antennomeres; apical flagellomere 2× longer than subapical flagellomere. In dorsal view, pronotal margins strongly convex, pronotal width distinctly greater than mesonotal width. Pronotal dorsum moderately convex, slightly elevated above dorsal mesonotal vertex. Lateral margins of mesonotum and metapectal-propodeal complex subparallel in dorsal view; mesonotum not constricted anteriorly. Meso-metapleural suture entirely absent; fusion of mesonotum with propodeum marked by shallow excavation. Propodeum angular in profile view; propodeal declivity slanted; posterolateral corners rounded. Tarsomeres longer than broad. Meso- and metatibial spur formula 2b,2(1s,1p). Anterior margin of petiole linear in dorsal view. Abdominal segment II longer than wide, with distinct dorsal node; margins parallel in dorsal view; margin of abdominal sternite II linear in profile view, angled ventrally anteriorly; subpetiolar process present, not lamellate, anterior face concave in profile view. Length of abdominal segment II distinctly greater than that of III. Abdominal segment III longer than wide in dorsal view. Breadth of abdominal segment III less than half the breadth of abdominal segment IV in dorsal view (TI1 = 30–33). Anteroposterior length of abdominal tergite IV greater than that of V–VIII combined. Respective anteroposterior lengths of abdominal segments V–VII subequal. Coloration brown.

Gyne. As for genus. Mandible with distinct basal and masticatory margins, edentate, not demarcated by a distinct subapical incisor; masticatory margin longer than basal margin. In dorsal view, breadth of mesonotum less than that of pronotum or metanotal-propodeal complex. Petiole longer than broad in dorsal view (PI = 0.719), constricted anteriorly along both transverse and dorsoventral axes; subpetiolar process absent. Dorsal node situated towards posterior of petiole. Abdominal segment III axial relative to posterad abdominal segments. Postsclerites of abdominal segments III–VII subequal in length. Vestiture consisting of short subdecumbent to suberect setae, longer and more abundant on gaster than on remainder of soma.

Etymology. “Belantan” is Malay for a club-like weapon, in reference to the shape of the proximal tooth of the worker mandible, the apical expansion of which is unique in mandibular teeth observed in *Leptanilla*. The specific epithet is a noun in apposition and therefore invariant.

Remarks. The worker of *Leptanilla belantan* is closest to that of *Leptanilla judaica* Kugler, 1987 and *Leptanilla ujjalai* Saroj, Mandi & Dubey, 2022 in appearance. Like *L. ujjalai*, *L. belantan* possesses an enlarged, truncate proximal tooth on the mandible, which in the latter species is bent distally; *L. belantan*

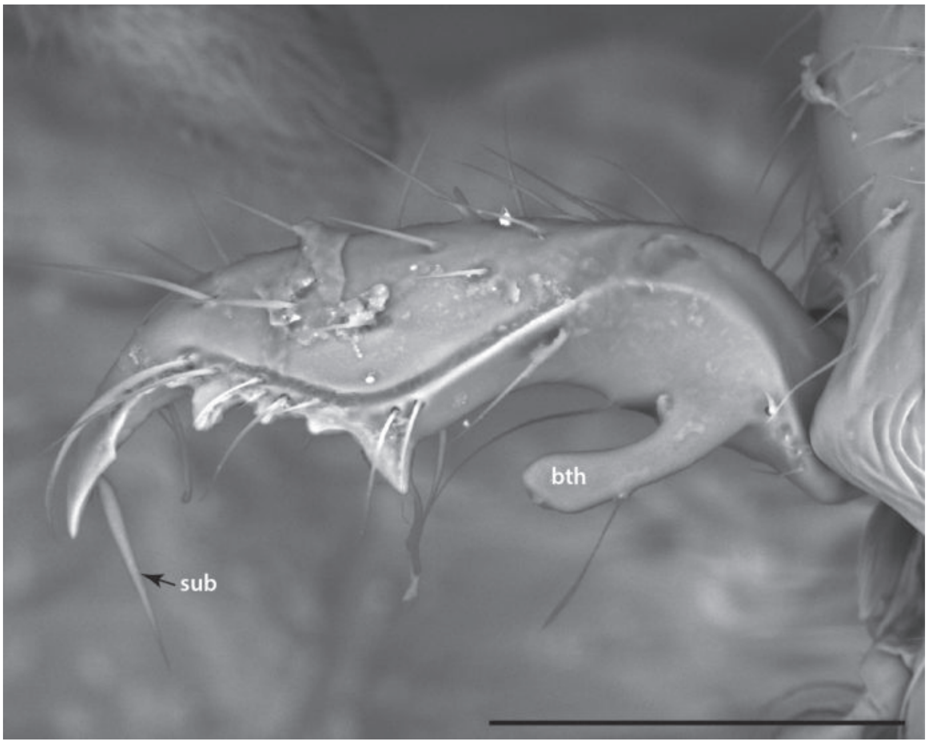

Figure 7. Mandible of *Leptanilla belantan* (MCZ:Ent:00728277), dorsal view, worker. Abbreviations: sub = subapical mandibular seta; bth = most proximal tooth. Scale bar: 0.1 mm.

differs from *L. ujjalai* in not having a serrated subpetiolar process and in the apex of the frontoclypeal process being emarginate, rather than entire. Castaneous coloration and lack of a meso-metapleural furrow set *L. belantan* apart from *L. judaica*. The gyne habitus of *L. belantan* is nearest to *Leptanilla escheri* (Kutter, 1948), differing in the elongation of the masticatory margin and the complete absence of ommatidia.

It is quite possible that the specimens identified as *L. escheri* and mentioned by Hölldobler et al. (1989) in fact belong to this species, since these also originated in peninsular Malaysia, although this speculation is unprovable because the repository of those specimens was not reported. It is also possible but unconfirmable that the undescribed *Leptanilla* species portrayed in Bolton (1990b: figs 8–11) corresponds to *L. belantan*. As with *L. escheri*, the placement of *L. belantan* in the *Leptanilla thai* species group must be regarded with some caution until this hypothesis can be tested with phylogenomic inference. It is conceivable that *L. belantan* instead belongs to the *Leptanilla havilandi* species group, since the worker caste of the two clades are at times distinguishable only by phenetic minutiae such as sculpturation. Unlike its putative close relatives within the *Leptanilla thai* species group, *L. belantan* exists in parapatry with the *Leptanilla havilandi* species group, allowing for the possibility that this species belongs to the latter clade.

The mandible of the gyne of *L. belantan* differs from the falcate facies observed in all other *Leptanilla* gynes, with the masticatory margin being longer than the basal margin. The gyne mandible in *L. belantan* therefore converges with the synapomorphic condition of the Poneroformicines (Richter et al. 2022).

Figure 8. Gyne of *Leptanilla belantan* (MCZ:Ent:00728275) **A** profile view **B** dorsal view **C** full-face view. Scale bars: 0.5 mm (**A, B**); 0.2 mm (**C**).

Leptanilla acherontia **sp. nov.**
https://zoobank.org/497DDEFF-A7AA-4AFE-9C29-E7F29D2F43F2
Figs 9A–C, 10

Type material. ***Holotype*****.** Kenya – Kakamega • 1 worker; Kakamega Forest, Isecheno; 00.24°N, 34.85°E; 6 Nov. 2002; 1550m a.s.l.; W. Okeka leg.; equatorial rainforest, sifted litter in soil under *Morus mesozygia*; CASENT0842720; UCDC ***Paratype*****.** Kenya – Kakamega • 1 worker; same data as for holotype; CASENT0178284; LACM.

Other material examined. Kenya – Kakamega • 1 worker; same data as for holotype; CASENT0842721; UCDC.

Measurements (mm) and indices. ***Holotype*:** HW = 0.22; HL = 0.29; ML = 0.11; SL = 0.13; WL = N/A; PrW = 0.139; MW = 0.12; PTL = 0.11; PTH = N/A; PTW = 0.10; PPW = 0.11; TW4 = 0.21; CI = 75; SI = 62; MI = 52; PPI = 128.09; TI1 = 54.81. ***Other material examined*:** HW = 0.21; HL = 0.28; ML = 0.11; SL = 0.12; WL = 0.37; PrW = 0.13; MW = 0.11; PTL = 0.10; PTW = 0.09; PPL = 0.09; PPW = 0.10; TW4 = 0.20; CI = 75; SI = 58; MI = 55; PPI = 113; TI1 = 47.

Description. Lateral margins of cranium subparallel. Occipital carina indistinct. Frontoclypeal process absent; frontoclypeal margin with median portion slightly raised, entire. Mandibles short relative to head. Three teeth present on mandible; apical and subapical teeth entire, intermediate tooth shallowly bifid (Fig. 10); irregular denticles interposed between all three teeth. Large, tapering basal seta absent from mandible; subapical tapering seta present. Scape short, not reaching cranial vertex at rest, somewhat expanded towards apex. Pedicel length distinctly greater than that of basal flagellomere. Flagellum submoniliform; length of basal flagellomere distinctly less than that of distal antennomeres; apical flagellomere 2× longer than subapical flagellomere. In dorsal view, pronotal margins moderately convex, pronotal width only slightly greater than mesonotal width. Pronotal dorsum planar, not elevated above dorsal mesonotal vertex. Lateral margins of mesonotum and metapectal-propodeal complex subparallel in dorsal view; mesonotum not constricted anteriorly. Meso-metapleural suture absent dorsally; pleural portion visible as sinuate signum in oblique anterior view. Propodeum convex in profile view; propodeal declivity vertical and linear; posterolateral corners of propodeum rounded. Tarsomeres broader than long. Meso- and metatibial spur formula 1b,2(1b,1p). Anterior margin of petiole linear in dorsal view. Length and breadth of abdominal segment II subequal, distinct dorsal node present; margins parallel in dorsal view; subpetiolar process absent. Lengths of abdominal segments II–III subequal. Abdominal segment III slightly broader than long in dorsal view. Breadth of abdominal segment III approximately half that of abdominal segment IV in dorsal view (TI1 = 47–54). Abdominal tergites IV–VII visible in posterodorsal view. Anteroposterior length of abdominal tergite IV twice anteroposterior length of abdominal tergite V in dorsal view. Anteroposterior lengths of abdominal tergites V–VI subequal; anteroposterior length of abdominal tergite VII much less than that of abdominal tergite VI. Sculpture largely absent. Vestiture consisting of short subdecumbent setae, longer and more abundant on gaster than on remainder of soma. Coloration yellowish.

Etymology. The specific epithet refers to Acheron, a subterranean river in Greek mythology, continuing a theme established by the specific epithets of the related Iberian species *Leptanilla charonea* and *Leptanilla plutonia* López, Martínez & Barandica, 1994. The gender is feminine.

Remarks. *Leptanilla acherontia* sp. nov. most closely resembles *Leptanilla revelierii* Emery, 1870, *Leptanilla kubotai* Baroni Urbani, 1977, and *Leptanilla okinawensis* Terayama, 2013, with three mandibular teeth and a linear clypeal margin. Abdominal tergite V is proportionally longer in dorsal view in *L. acherontia* than *L. revelierii*, while *L. acherontia* differs from *L. kubotai* and *L. okinawensis* in pedicel shape and larger body size, respectively. Based on consultation of AntWeb images (https://www.antweb.org), *Leptanilla* UG01, known only from equatorial rainforest in Kibale National Park, Uganda, is almost certainly conspecific with *L. acherontia*.

Figure 9. *Leptanilla acherontia*, holotype (CASENT0842720), worker **A** profile view **B** dorsal view **C** full-face view. Scale bars: 0.5 mm.

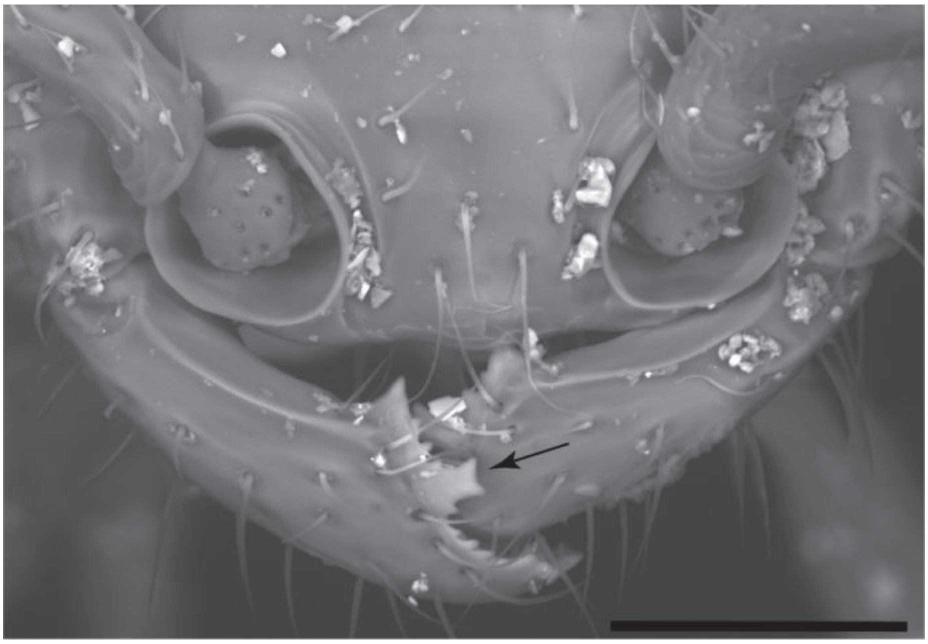

Figure 10. Mandibles of *Leptanilla acherontia* (CASENT0842721), dorsal view, worker. Bifid tooth marked with arrow. Scale bar: 0.05 mm.

With *Leptanilla boltoni* Baroni Urbani, *L. acherontia* is one of only two described Afrotropical *Leptanilla* species for which the worker caste is known. Phylogenomic inference indicates that *Leptanilla* zhg-ke02 may represent the male of *L. acherontia* (pers. obs.), but further sampling of sympatric *Leptanilla* would be required for this association to be decisive. The type locality of *L. acherontia* is situated in perhumid equatorial rainforest, contrasting with the semi-arid provenance of *Leptanilla* zhg-ke01 and other Afrotropical and Western Palaearctic *Leptanilla*. It is unclear to what degree climatic conditions dictate the distributions of *Leptanilla* species.

Leptanilla bethyloides **sp. nov.**

https://zoobank.org/5955A34E-6467-442B-8A30-4FD9F24FCB8D
Figs 11A–C, 12

Type material. ***Holotype*****.** China – Hong Kong • 1 male; Tai Po Kau; 22.44°N, 114.18°E (estimated from Google Earth to nearest minute), 15 Jun. 1964; W. J. Voss and W. M. Hui leg.; CASENT0842864. BPBM. ***Paratype*****.** China – Hong Kong • 1 male; same locality as for preceding; 2–6 Jul. 1964; L. K. and H. W. Ming leg.; light trap; CASENT0842865. BPBM.

Measurements (mm) and indices, male. ***Holotype*****:** HW = 0.27; HL = 0.32; SL = 0.10; LF2 = 0.04; EL = 0.11; EW = 0.12; WL = 0.59; MSL = 0.35; MSW = 0.23; PTW = 0.25; PTL = 0.10; PTH = 0.13; REL = 34; SI = 36; CI = 244; OI = 113; MSI = 152.38; PI = 247.52. ***Paratype*****:** HW = 0.25; HL = 0.30; SL = 0.08; LF2 = 0.04; EL = 0.11; EW = 0.12; WL = 0.53; MSL = 0.31; MSW = 0.22; PTH = 0.12; REL = 35; SI = 32; CI = 219; OI = 110; MSI = 139

Description. Cranial outline quadrate. Occiput emarginate in full-face view. Frons not produced into anterior shelf. Mandible articulated to gena; broader than long. Mandalus large, covering entire anterodorsal mandibular surface. Maxillary palp 1-merous. Clypeus anteroposteriorly reduced, not discernible in full-face view. Anterior tentorial pits not discernible. Compound eyes wider than long in profile view (OI = 110–112), posterior margin slightly emarginate, all other margins convex. Anteromedian ocellus and compound eyes not intersecting line drawn perpendicular to anteroposterior axis of cranium. Scape anteroposteriorly compressed, longer than wide (SL = 0.081–0.095 mm), shorter than anteroposterior length of compound eye; pedicel short, subcylindrical, lateral margins parallel, length 0.5× that of scape; antennomere 3 short (LF2 = 0.037–0.039 mm), subcylindrical, length subequal to that of pedicel; flagellum submoniliform, not extending posterior to mesoscutum if folded flat over mesosoma. Pronotum and mesoscutum posteriorly prolonged. In profile view anterodorsal pronotal face diagonal to craniocaudal axis at ~45° angle, but profile of pronotum otherwise obscured by vestiture. Mesoscutal dorsum slightly convex; mesoscutum longer than broad (MSI = 139–152). Antero-admedian signum absent. Notauli absent. Parapsidal signa present, impressed. Mesoscutellum longer than tall, dorsum not lower than that of mesoscutum, posterodorsal mesoscutellar face convex, posteriorly produced, not recurved. Oblique mesopleural sulcus present, not intersecting metapectal-propodeal complex. Metapleuron distinct, transected by transverse sulcus. Metapleural gland absent. Propodeum convex in profile view, without distinct dorsal and posterior faces. Pro- and metacoxa subequal in length, metacoxa somewhat more massive; mesocoxa shorter than pro- and metacoxa. Protrochanters sphenoid in outline, distally truncate. Profemur not markedly constricted at base, anteroposteriorly compressed, incrassate; acute distal flange on posterior surface absent; arcuate medial carina absent. Protibial and profemoral length subequal; protibia not dorsoventrally compressed, without ventromedian carina; protibial comb absent; probasitarsal seta not hypertrophied. Meso- and metatibial spur formula 2b,2(1b,1p). C and Sc+R+Rs fused, tubular; *2s-rs*+R+4-6 and M+Cu tubular; all other venation absent. Costal infuscation absent. Abdominal segment II anteroposteriorly compressed, broader than long in dorsal view excluding presclerites; dorsal node present, well-developed; with median dorsal excavation. Abdominal sternite II without process, planar in profile view. Presclerites of abdominal segments IV–VIII inconspicuous. Abdominal segments III–VII without tergosternal fusion. Tergosternal fusion of abdominal segment VIII–IX unknown. Abdominal tergites III–VIII not anteroposteriorly compressed, lateral margins subparallel; breadth of abdominal tergite VIII subequal to that of abdominal tergite VII in posterodorsal view. Abdominal sternite VIII anteroposteriorly compressed, visible without dissection, posterior margin entire. Abdominal sternite IX not visible without dissection. Mulceators absent. Gonopodites articulate. Gonocoxites without complete dorsomedian and ventromedian fusion; ventromedial margin of gonocoxite with lamina; apicoventral laminae absent. Gonostylus present, outline lanceolate, apex entire. Volsellae absent. Penial sclerites dorsoventrally compressed, not basally recurved, ventromedian carina extending along most of length, without lateral laminate margins. Phallotreme dorsal, concealed by gonostyli in available specimens. Somal sclerites with thick vestiture of decumbent to suberect setae, sparsest on meso- and metapleuron; setae appressed to decumbent on antennae and legs; gonostyli with similar vestiture to abdominal

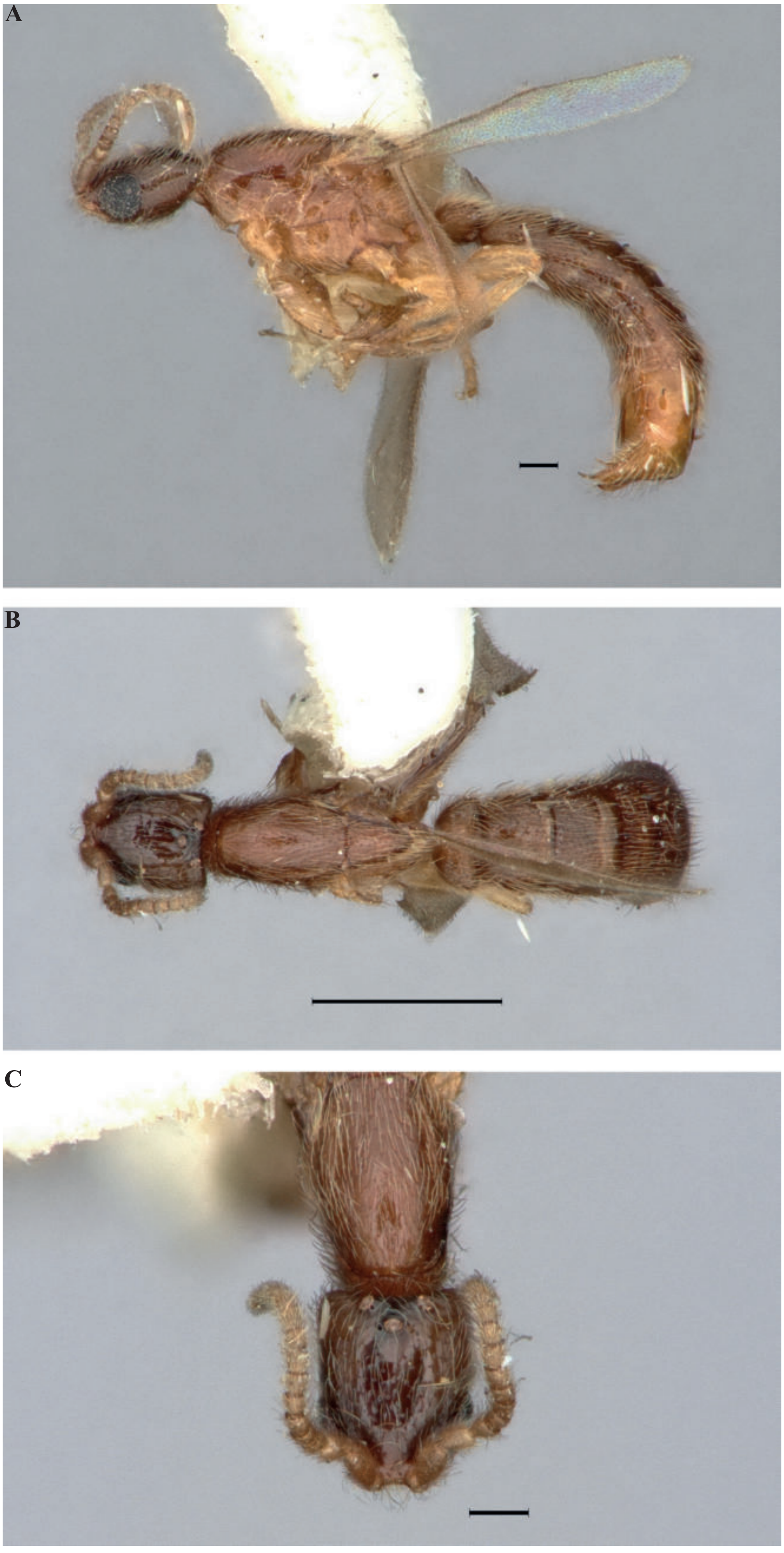

Figure 11. *Leptanilla bethyloides*, holotype (CASENT0842864), male **A** profile view **B** dorsal view **C** full-face view. Scale bars: 0.1 mm (**A, C**); 0.5 mm (**B**).

Figure 12. Wings of *Leptanilla bethyloides* (CASENT0842865), male. Scale bar: 0.2 mm.

postsclerites, genitalia otherwise glabrous. Base of forewing costa bearing row of exceptionally long, suberect setae. Cuticle bearing piligerous punctae; sculpture otherwise absent.

Etymology. The specific epithet refers to the gestalt of this ant, which resembles that of the flat wasps (Chrysidoidea: Bethylidae). While superficial, this resemblance was pronounced enough that the holotype and paratype of *L. bethyloides* were initially mis-sorted to Bethylidae incertae sedis at the Bishop Museum. The specific epithet is neuter.

Remarks. Among the *Leptanilla bethyloides* species group, of which this is the only described species, *L. bethyloides* most closely resembles multiple undescribed morphospecies from southern Burma, differing in larger size (WL = 0.532–0.594 mm) and the proportions of the metasomal segments. Describing a new species of *Leptanilla* based solely upon male specimens, as here done for *L. bethyloides*, was eloquently argued against by Bolton (1990b), since it exacerbates the probable redundancy that plagues the taxonomy of *Leptanilla*. This description of *L. bethyloides* is justified only to give a formal species group name (i.e., the *Leptanilla bethyloides* species group) to a major clade of *Leptanilla* known only from male specimens.

The volsellae are known to be wholly lacking in *Leptanilla* zhg-mm03 (Griebenow et al. in press), which shows very close morphological affinity to *L. bethyloides*; therefore, I infer the absence of the volsellae in this species. The condition of the volsellae cannot be assessed in any other representatives of the *Leptanilla bethyloides* species group besides *Leptanilla* zhg-mm03. Given the relative lack of phylogenetic signal in the worker phenotype of *Leptanilla* and the scarcity of species in which the worker caste and phylogenetic position are both known, it is difficult to predict the morphology of the unknown worker of *L. bethyloides* or other members of the *Leptanilla bethyloides* species group, beyond a probable 1,1 palpal formula. It is conceivable that *Leptanilla macauensis* Leong, Yamane & Guénard, 2018 represents this worker, although unlikely, given the conformity of *L. macauensis* to the worker diagnosis for the *Leptanilla revelierii* species group, where it is placed in this study.

***Leptanilla najaphalla* sp. nov.**

https://zoobank.org/C6B1D1A1-5138-4E52-9A50-FD7054D31187
Figs 13A–C, 14A–D, 15, 16

Type material. *Holotype*. Malaysia – Sabah • 1 male; Sipitang Dist., Mendolong; 4.917°N, 115.767°E (estimated from Google Earth to nearest minute); 27 Apr. 1988; S. Adebratt leg.; A1L; CASENT0106427 (MZLU00174197); MZLU. ***Paratypes*.** 5 male; same locality as for preceding; 16 Apr. 1988; S. Adebratt leg.; A1L; CASENT0106416 (MZLU00174186), CASENT0106417 (MZLU00174187), CASENT0106438 (MZLU00174208), CASENT0106444 (MZLU00174214), CASENT0106457 (MZLU00174227); MZLU • 5 male; same locality as for preceding; 19 Apr. 1988; S. Adebratt leg.; W5L; CASENT0106421, CASENT0106432, CASENT0106433, CASENT0106449, CASENT0106450; UCDC • 2 male; same locality as for preceding; 7 Apr. 1988; S. Adebratt leg.; A1L; CASENT0106435 (MZLU00174205), CASENT0106437 (MZLU00174207); MZLU • 1 male; same locality as for preceding; 4 May 1988; S. Adebratt leg.; T4/R; CASENT0106412; MCZC • 2 male; same locality as for preceding; 5 May 1988; S. Adebratt leg.; A1L; CASENT0106418, CASENT0106453; MCZC • 3 male; MALAYSIA, Sabah: same locality as for preceding; 13 May 1988; T4/R; CASENT0106414, CASENT0106415, CASENT0106429; CAS.

Measurements (mm) and indices, male. *Holotype*: HW = 0.29; HL = 0.35; SL = 0.14; LF2 = 0.05; LF2 = 0.05; EL = 0.16; EW = 0.16; WL = 0.80; MSW = 0.26; MSL = 0.48; PTW = N/A; PTL = N/A; PTH = 0.24; REL = 46; SI = 48; CI = 82; OI = 98; MSI = 54. ***Paratypes*** (*n* = 18): HW = 0.27–0.31; HL = 0.27–0.40; SL = 0.12–0.16; LF2 = 0.05–0.06; EL = 0.14–0.17; EW = 0.14–0.16; WL = 0.69–0.83; MSW = 0.22–0.27; MSL = 0.42–0.53; PTW = 0.15–0.18; PTL = 0.12–0.15; PTH = 0.23–0.28; REL = 40–57; SI = 45–55; CI = 74–103; OI = 82–103; MSI = 48–54; PI = 105–140.

Description. Cranial outline quadrate. Occiput emarginate in full-face view. Frons produced into anterior shelf. Mandible articulated to gena; distinctly longer than broad. Mandalus large, covering most of anterodorsal mandibular surface. Maxillary palp 1-merous. Clypeus anteroposteriorly reduced, concealed by frontal shelf in full-face view. Anterior tentorial pits not discernible. Compound eyes somewhat longer than wide in profile view, or EW and EL subequal (OI = 82–102), posterior margin slightly emarginate, all other margins convex. Anteromedian ocellus and compound eyes not intersecting line drawn perpendicular to anteroposterior axis of cranium. Scape anteroposteriorly compressed, longer than wide (SL = 0.124–0.154), shorter than anteroposterior length of compound eye; pedicel short, subcylindrical, lateral margins parallel, length 0.5 that of scape; antennomere 3 short, subcylindrical, length less than that of pedicel or scape; flagellum submoniliform, not extending posterior to mesoscutellum if folded flat over mesosoma. Pronotum and mesoscutum posteriorly prolonged. In profile view anterodorsal pronotal face slightly convex, diagonal to craniocaudal axis at ~ 45° angle. Mesoscutal dorsum planar; mesoscutum longer than broad (MSI = 48–53). Antero-admedian signum absent. Notauli absent. Parapsidal signa present, not impressed. Mesoscutellum longer than tall, dorsum not lower than that of mesoscutum, posterodorsal mesoscutellar face convex, not posteriorly produced. Oblique mesopleural sulcus present, not intersecting metapectal-propodeal complex. Metapleuron indistinct.

Figure 13. *Leptanilla najaphalla*, holotype (CASENT0106427), male **A** profile view **B** dorsal view **C** full-face view. Scale bars: 0.5 mm (**A, B**); 0.2 mm (**C**).

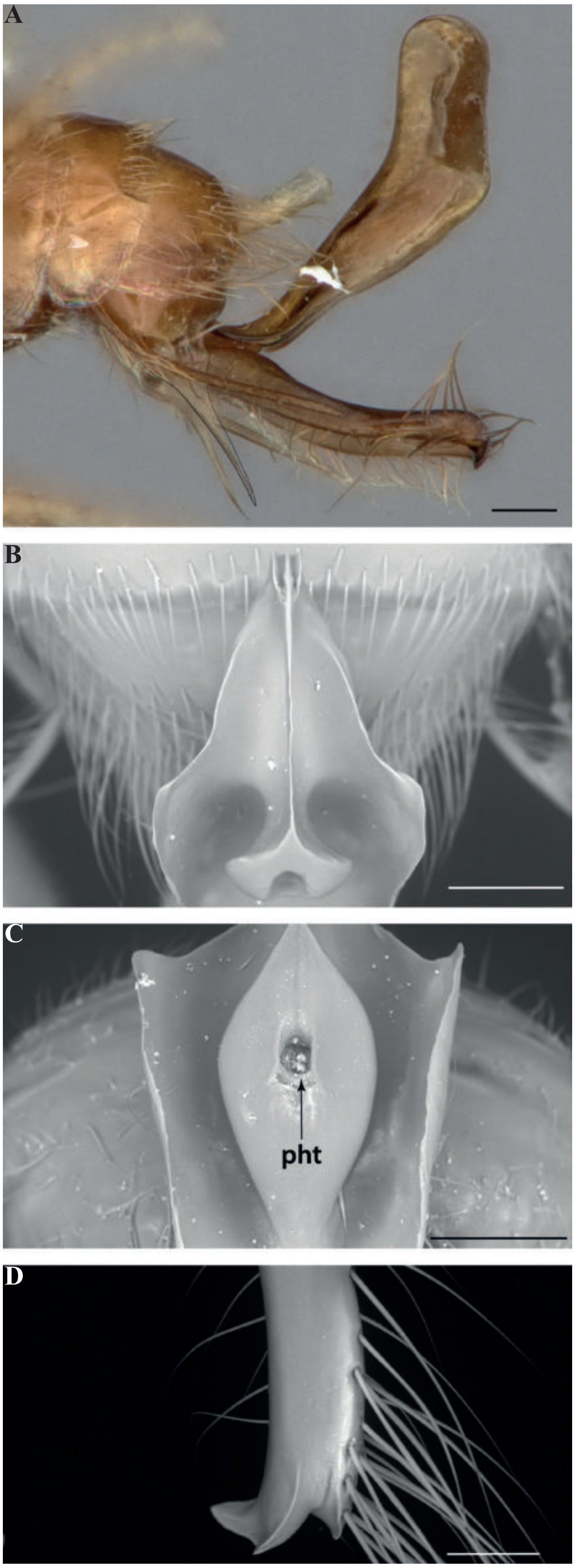

Figure 14. Male genitalia of *Leptanilla najaphalla* **A** profile view, apicolateral gonocoxital lamina outlined (CASENT0106424) **B** penial apex, posteroventral view (CASENT0106421) **C** penial sclerites and phallotreme, ventral view (CASENT0106433) **D** volsellar apex, dorsal view (CASENT0106421). Abbreviation: pht = phallotreme. Scale bars: 0.1 mm (**A, C, D**); 0.2 mm (**B**).

Metapleural gland absent. Propodeum convex in profile view, with distinct dorsal and posterior faces; areas of these faces subequal. Procoxa longer than meso- and metacoxa; procoxa without distal transverse carina. Protrochanters sphenoid in outline, distally truncate. Profemur markedly constricted at base, anteroposteriorly compressed, incrassate; acute distal flange on posterior surface present; arcuate medial carina absent. Protibia > 0.5× length of profemur, not dorsoventrally compressed, without ventromedian carina; protibial comb present, length of processes decreasing distally; probasitarsal seta not hypertrophied. Meso- and metatibial spur formula 2b,2b. C, Sc+R+Rs, *2s-rs*+R+4-6, Rf, Mf1, *cu-a*, and Cuf+1A tubular; M+Cu and 1A nebulous; all other venation absent. Cuf+1A spectral apically, not reaching anal margin. Costal infuscation present proximal to *2s-rs*+R+4-6; C extending well beyond infuscation. Abdominal segment II anteroposteriorly compressed, slightly broader than long in dorsal view (PI = 105–133); dorsal node present, well-developed, without median excavation. Abdominal sternite II with process along posterior half of length, outline cuneiform in profile view, apex rounded. Presclerites of abdominal segments IV–VIII inconspicuous. Abdominal segments III–IX without tergosternal fusion (Griebenow et al. in press). Abdominal tergites IV–VII each broader than preceding tergite in dorsal view, lateral margins diverging posteriorly; breadth of abdominal tergite VIII less than that of abdominal tergite VII in posterodorsal view. Abdominal sternite VIII anteroposteriorly compressed, not visible without dissection, posterior margin entire (Griebenow et al. in press). Abdominal sternite IX with posteromedian fusion to gonocoxites (Griebenow et al. in press); anteroposteriorly compressed along median axis, laterally expanded and lobate. Mulceators present, subcircular in cross-section, longer than anteroposterior length of gonocoxites. Gonocoxites bulbous, with complete dorsomedian and ventromedian fusion; apicoventral laminae present, subulate in outline. Gonostyli absent. Volsellae present, with complete proximomedian fusion, subcircular in cross-section; sclerotized medial carina present at volsellar apex, produced into pair of denticles, dorsal denticle shorter than ventral one. Penial sclerites not dorsoventrally compressed, basally recurved, proximal ¼ subcircular in cross-section, apical 1/3 with ventromedian carina; rounded platform proximad this median carina with outline elliptical; phallotreme subapical and ventral, recessed, not surrounded by vestiture of setae; lateral laminate flanges present. Most sclerites with vestiture of subdecumbent to appressed setae; elongated on posterior margins of abdominal tergites III–VIII, increasing in length posteriorly; anterior faces of mulceators with elongate suberect setae; ectal faces of volsellae with suberect to erect setae, genitalia otherwise bare. Cuticle bearing piligerous punctae; sculpture fatiscent distad and proximad phallotreme (Fig. 16).

Etymology. The specific epithet derives from *Naja* (Squamata: Elapidae), the cobra, and *-phalla*, meaning penis. This refers to the florid facies of the penial sclerites, which recalls the threat display of these snakes: the dorsal curvature of the penial sclerites resembles the rearing posture, while the lateral laminae resemble the extended "hood" of the cobra. The specific epithet is feminine.

Remarks. The males of *L. najaphalla* uniformly differ from the sympatric undescribed morphospecies *Leptanilla* zhg-my05, to which *L. najaphalla* is sister, in the outline of the apicolateral gonocoxital lamina and the proportions of the penial sclerites and volsellae to the gonocoxites.

Figure 15. Forewing of *Leptanilla najaphalla* (CASENT0106419), male. Scale bar: 0.5 mm.

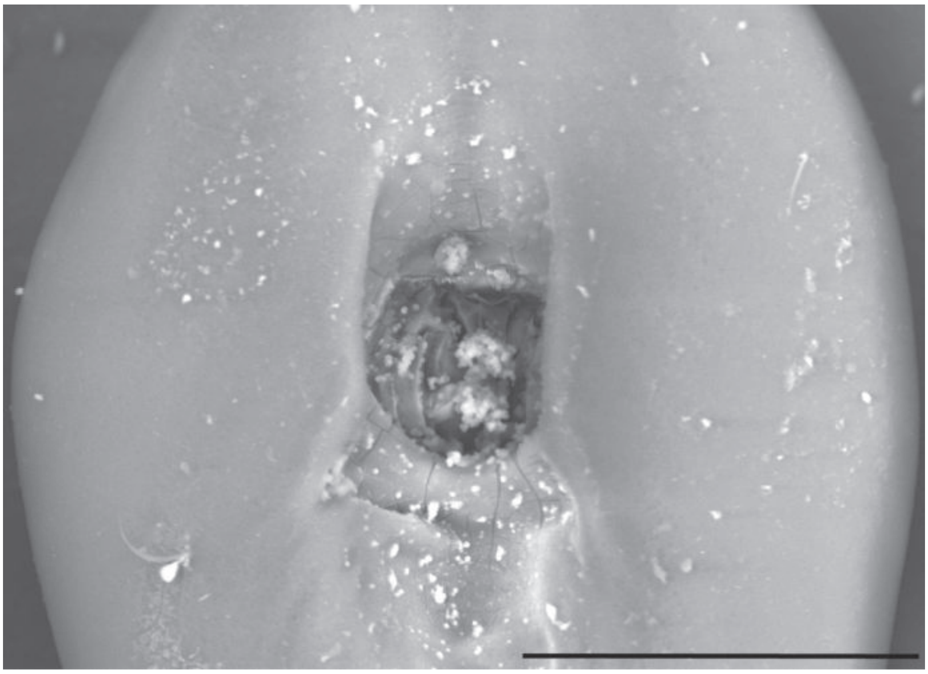

Figure 16. Phallotreme of *Leptanilla najaphalla* (CASENT0106433). Scale bar: 0.5 mm.

The description of *L. najaphalla* only from male specimens is justified for the same reasons as provided for the description of *L. bethyloides*, also only from male specimens (see "Remarks" concerning *L. bethyloides* above): the clade to which this species belongs, heretofore referred to as the "Bornean morphospecies group", is known only from male specimens. *Leptanilla najaphalla* was included in the phylogenetic analyses of Griebenow (2020, 2021) under the provisional identifier *Leptanilla* zhg-my02, with the genitalia being the subject of detailed morphological study using micro-computed tomography (Griebenow et al. in press) under that same provisional identifier.

Revised diagnosis and generic classification of Leptanillinae

Based upon total-evidence and phylogenomic inference (in preparation by the author) corroborated by previous studies (Griebenow 2020, 2021), I here enact a revised classification of the Leptanillinae, reducing the number of genera to three. Summaries of character states that in combination differentiate major clades of the Leptanillinae from their relatives are provided below. These summary diagnoses are based upon all adult castes and larvae, when available. Apomorphies relative to the parent taxon are italicized; characters of uncertain polarity are marked with an asterisk.

Leptanillinae Emery, 1910

Type genus. *Leptanilla* Emery, 1870: 196.

Worker diagnosis (modified from Bolton 2003):

1. Mandibles without differentiated basal and masticatory margins.
2. At least one preapical tooth or lobe present on mandible.
3. Frontal lobes absent.
4. Antennal sockets dorsal, fully exposed.
5. Compound eyes absent, if present (*Protanilla izanagi* Terayama, 2013) then reduced to two ommatidia (Fig. 17A).
6. Ocelli absent.
7. Antenna 12-merous.
8. Promesonotal suture fully articulated.
9. Propodeal lobes weakly present (Opamyrmini) or absent (Leptanillini).
10. Propodeal spiracle situated low on propodeum.
11. Metacoxal foramen small, fully closed (Fig. 18).
12. Suture absent from annulus surrounding metacoxal foramen.
13. Metapleural gland present.
14. Orifice of metapleural gland covered by dorsal cuticular flange.
15. Helcial sternite reduced and partly covered by corresponding tergite.
16. Spiracle of abdominal segment III large and placed far forward.
17. Spiracles of abdominal segments IV–VII concealed by posterior margins of preceding tergites.
18. Petiole sessile, rarely subsessile (*Protanilla taylori* species group).
19. Abdominal postsclerites II with (Leptanillini) or without (Opamyrmini) complete tergosternal fusion.
20. Abdominal postsclerites III with (Leptanillini) or without (Opamyrmini) tergosternal fusion.
21. Abdominal segment III petiolate (Leptanillini) or not (Opamyrmini).
22. Abdominal segment IV without tergosternal fusion.
23. Stridulitrum absent from abdominal segment IV.
24. Abdominal tergite VII large, with simple posterior margin.
25. Sting present.
26. Pretarsal claws edentate.

Gyne diagnosis. As above, but alate or dichthadiiform (rarely ergatoid). If alate then with ocelli and pterostigma; hindwing with R + Rs and 1A tubular, not intersecting distal wing margin. If dichthadiiform then compound eyes reduced to one or two ommatidia, or absent; ocelli absent; mandibles sometimes edentate.

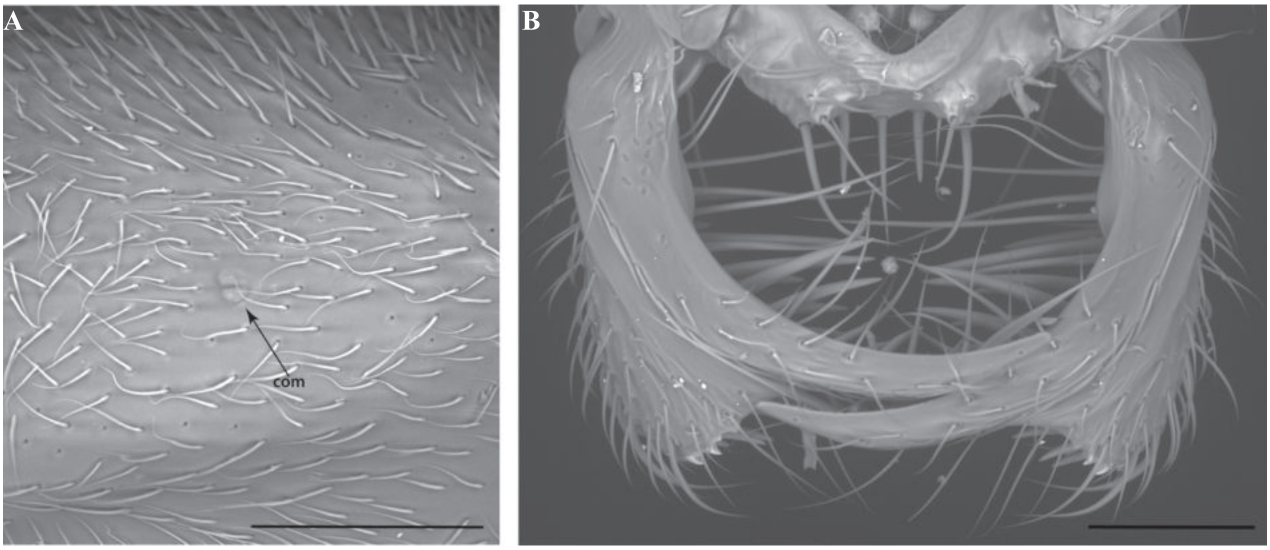

Figure 17. Aspects of *Protanilla izanagi*, worker **A** profile view of posterior half of cranium **B** ventral view of the mandibles. Abbreviation: com = compound eye. Scale bars: 0.1 mm (**A**); 0.2 mm (**B**).

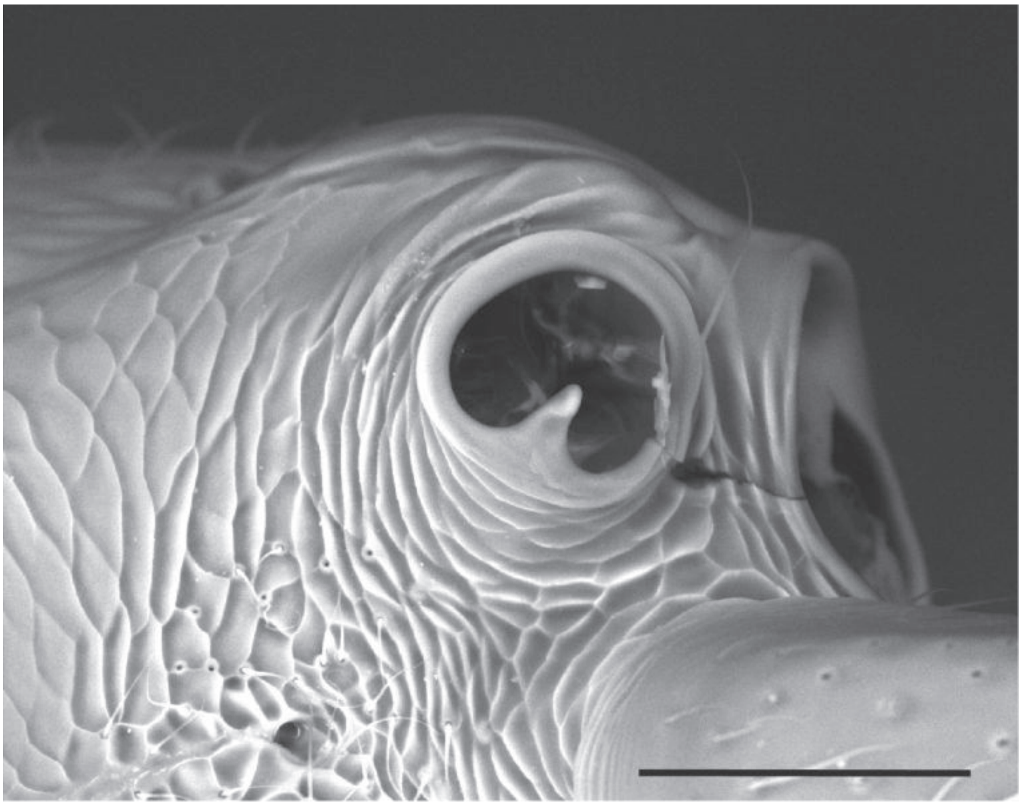

Figure 18. Metacoxal foramen of *Leptanilla havilandi* (CASENT0010809), ventral view, worker. Scale bar: 0.05 mm.

Male diagnosis (modified from Boudinot 2015):

1. Mandible edentate, nub-like or spatulate (*Leptanilla anomala* (Brues, 1925), comb. nov.).
2. Frontal carinae absent.
3. Cuticular pegs absent from anterior clypeal margin.
4. Antenna 13-merous.
5. Funiculus filiform to submoniliform.
6. Oblique mesopleural sulcus present or absent.
7. Metapleural spiracular plate absent.
8. Propodeal lobes inconspicuous or absent.
9. Metacoxal foramen small, fully closed.
10. Mesotibia with one or two spurs or none.
11. Metatibia with one or two spurs.
12. Metatarsus lacking posterolateral line of dense differentiated setae.
13. Pretarsal claws edentate.
14. Pterostigma present or absent.
15. Rs+M absent (Leptanillini) or present, nebulous (Opamyrmini).
16. *1m-cu* absent (Leptanillini) or present, nebulous (Opamyrmini).
17. Jugal lobe absent.
18. Hindwing venation reduced, at most R+Rs and 1A tubular.
19. Metapleural gland absent (Fig. 19A) or rarely present (Fig. 19B) (e.g., *Leptanilla* zhg-th02).
20. Petiole present or reduced to absent (*Leptanilla thai* species group, *Leptanilla havilandi* species group).
21. Helcium axial or infra-axial.
22. Abdominal segment III not petiolate, or rarely petiolate (*Protanilla bicolor* species group).

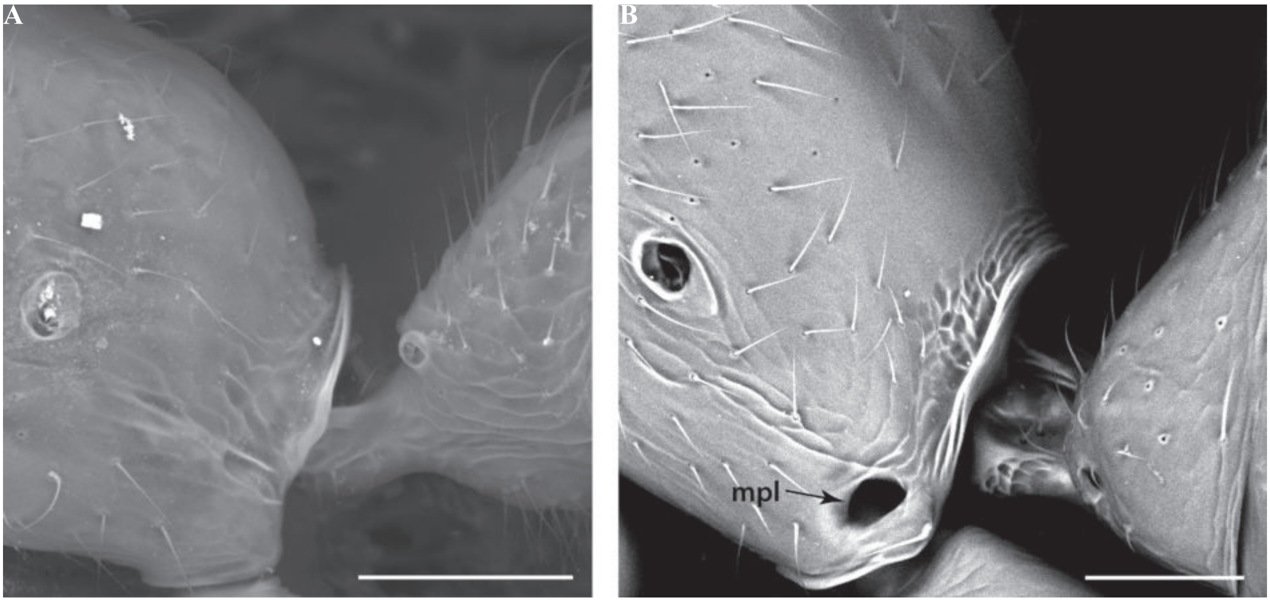

Figure 19. Metapleuron in male Leptanillinae **A** *Leptanilla* nr. *indica* (CASENT0106381) **B** *Leptanilla* zhg-th02 (CASENT0842615). Abbreviation: mpl = metapleural gland orifice. Scale bars: 0.05 mm.

23. Abdominal segment IV not vaulted, as long as, or distinctly longer than posterad abdominal segments.
24. Abdominal spiracles IV–VIII obscured by preceding tergites.
25. Posterior margin of abdominal sternite IX with posteromedian process, or entire, or emarginate, or with mulceators.
26. Cerci absent.

Larval diagnosis. Stenocephalous, with post-cranial soma moderately (i.e., habitus pogonomyrmecoid) to extremely (i.e., habitus leptanilloid) elongate. Mandibles typhlomyrmecoid or leptanilloid.

Opamyrmini Boudinot & Griebenow, tribe nov.

https://zoobank.org/B3CFA4FF-FECD-42E8-B7CB-814A16C23659

Opamyrma Yamane, Bui & Eguchi, 2008 (Fig. 20).

Worker diagnosis.

1. Medial mandibular surface with single peg-like chaeta.
2. Mandible with one tooth and several preapical lobes.
3. Labrum with multiple ranks of peg-like chaetae (Yamada et al. 2020: fig. 2F).
4. Maxillary palp 4-merous.
5. Labial palp 2-merous.
6. Clypeus extending posteriorly between antennal toruli.
7. Posteromedian epistomal sulcus not clearly discernible.
8. Occiput visible in full-face view.
9. Meso-metapleural suture absent.
10. Propodeal lobe weakly present.
11. Subpetiolar process absent.
12. Abdominal postsclerites II without tergosternal fusion.
13. Abdominal segment III not petiolate or narrower than posterad abdominal segments.
14. Abdominal postsclerites IV subequal in length to abdominal postsclerites V and VI.
15. Abdominal tergite VII hypertrophied, dome-like.

Gyne diagnosis. As above, but alate, with compound eyes and three ocelli; occipital carina with short medioventral interruption. M + Cu complete, tubular; *cu-a* present; Rs + M, Cuf2 and -3, and *1m-cu* present and spectral; *2r-rs* + Rsf4 adjoined by Rsf3.

Male diagnosis. As for the Leptanillinae, but Rs+M and *1m-cu* present, and abdominal segment II without tergosternal fusion. Cupula non-annular. Lateropenite present, fully articulated to parossiculus, and malleate.

Larval diagnosis. Habitus pogonomyrmecoid. Cranium subelliptical in full-face view. Mandibles typhlomyrmecoid, without teeth, lateral surfaces smooth. Setae short, suberect. Ventral prothoracic process and hemolymph tap on abdominal segment IV absent.

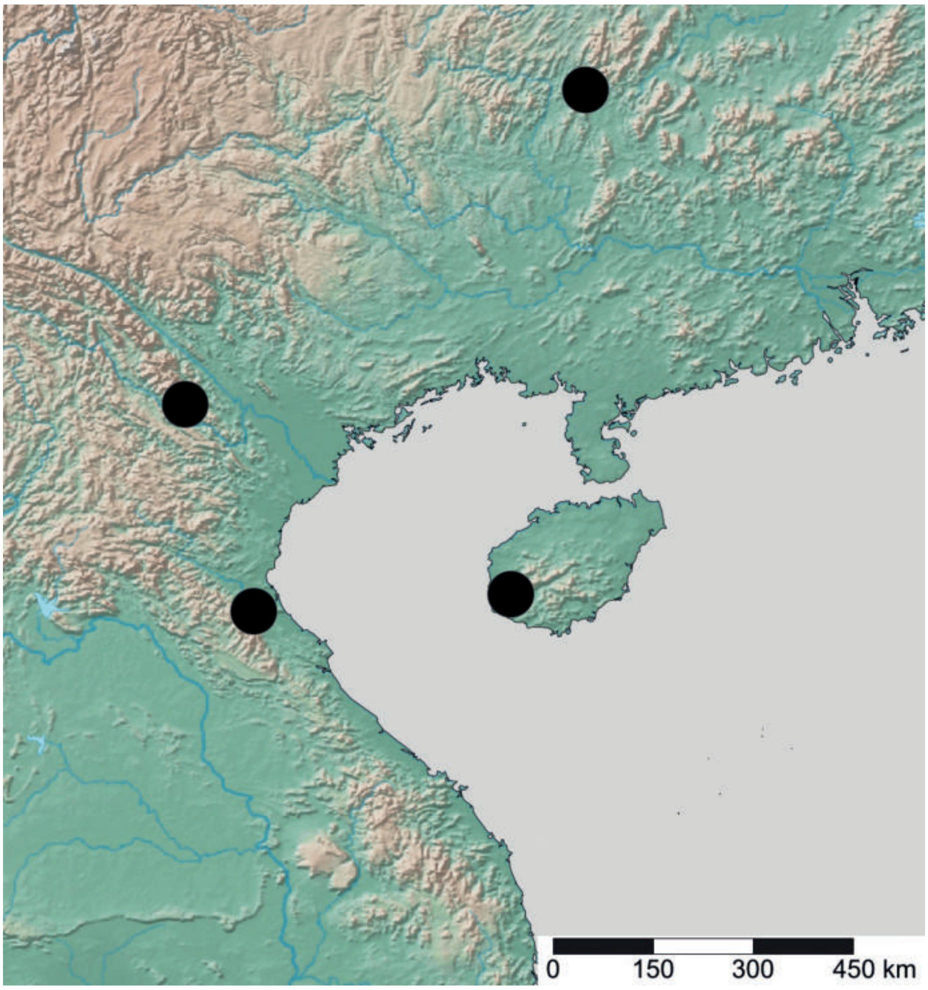

Figure 20. Geographical range of *Opamyrma*. Locality information derived from AntWeb and available literature, visualized with SimpleMappr.

Opamyrma Yamane, Bui & Eguchi, 2008

Opamyrma Yamane, Bui & Eguchi, 2008: 56. Type species: *Opamyrma hungvuong* Yamane et al., by monotypy.
Opamyrma hungvuong Yamane, Bui & Eguchi, 2008.

Diagnosis. As for tribe.

Remarks. *Opamyrma* was described in the Amblyoponinae, based solely upon worker morphology (Yamane et al. 2008), and was subsequently found by Ward and Fisher (2016) to belong to the Leptanillinae based upon phylogenetic inference from 11 nuclear loci. All subsequent phylogenetic inference consistently recovers *Opamyrma* as sister to the remaining Leptanillinae (Borowiec et al. 2019; Griebenow 2020, pers. obs.). All adult forms lack complete tergosternal fusion in abdominal segment II, a plesiomorphy unique among the Leptanillinae. The presence of weak propodeal lobes (Yamada et al. 2020: 34) is plesiomorphic relative to the Leptanillini, in which the propodeal lobes are absent in the worker caste. The lack of petiolation of abdominal segment III in the worker caste of *Opamyrma* is also unique among the Leptanillinae but this character state may not be plesiomorphic for the subfamily. The polarity of the proportions of abdominal postsclerites IV relative to V–VI within the Leptanillinae is also unclear.

Leptanillini Emery, 1910

Leptanilla Emery, 1870.
Protanilla Taylor in Bolton, 1990b.

Worker diagnosis.

1. Medial mandibular surface with or without peg-like chaetae.
2. Mandible with 0–4 teeth along medial margin.
3. Labrum with (Fig. 21A, B) or without multiple ranks of peg- or pencil-like chaetae.
4. Maxillary palp 4-, 2-, or 1-merous.
5. Labial palp 2- or 1-merous.
6. Clypeus extending posteriorly between antennal toruli (Fig. 22A) or not (Fig. 22B).
7. Posteromedian epistomal sulcus clearly discernible (Fig. 22A) or not (Fig. 22B).
8. Occiput not visible in full-face view.
9. Meso-metapleural suture present or absent.
10. Propodeal lobes absent.
11. Subpetiolar process present or absent.
12. Abdominal postsclerites II–III with tergosternal fusion.
13. Abdominal segment III petiolate, narrower than posterad abdominal segments.
14. Abdominal postsclerites IV subequal in length to, or greater in length than, abdominal postsclerites V–VI.
15. Abdominal tergite VII enlarged, not dome-like.

Gyne diagnosis. See respective gyne-based diagnoses for *Protanilla* and *Leptanilla* below.

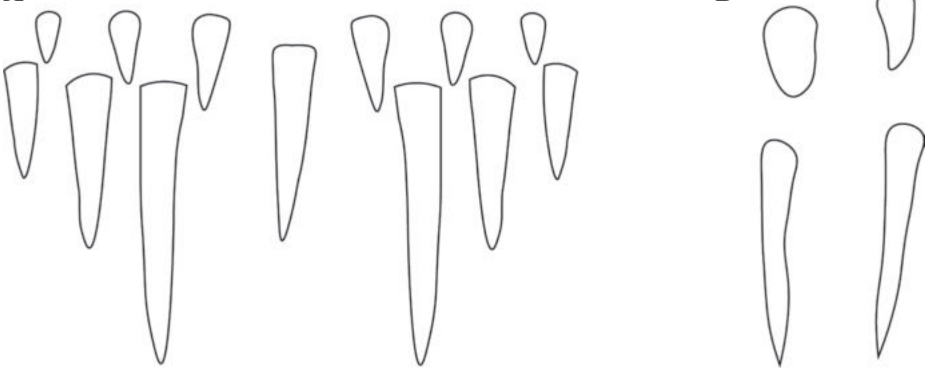

Figure 21. Labral chaetae in *Protanilla*, diagrammatic anterior view **A** *Protanilla* id01, gyne **B** *Protanilla wallacei* (CASENT0842699), worker.

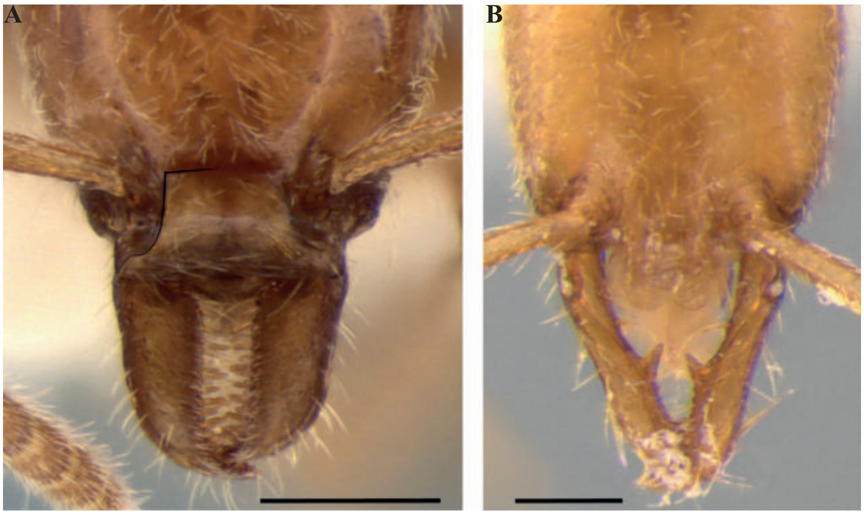

Figure 22. Condition of the worker frontoclypeal margin in *Protanilla* (**A**) and *Leptanilla* (**B**) **A** *Protanilla beijingensis* (CASENT0842639) **B** *Leptanilla laventa* (CASENT0842746). Scale bars: 0.5 mm (**A**); 0.1 mm (**B**).

Male diagnosis. As for the Leptanillinae, but Rs+M and *1m-cu* absent. Abdominal segment II with complete tergosternal fusion. Lateropenite present or absent; if present, then not articulated to parossiculus and never malleate.

Larval diagnosis. See respective larval diagnoses for *Protanilla* and *Leptanilla* below.

Protanilla **Taylor in Bolton, 1990b**

Fig. 23

Protanilla Taylor in Bolton, 1990b: 279. Type species: *Protanilla rafflesi* Taylor in Bolton, 1990b, by monotypy.

Anomalomyrma Taylor in Bolton, 1990b: 278. Type species: *Protanilla taylori* (Taylor in Bolton, 1990b), comb. nov., by monotypy. Syn. nov.

Furcotanilla Xu, 2012: 481. Type species: *Protanilla furcomandibula* Xu & Zhang, 2002, by original designation. Synonymy by Hsu et al. (2017). Holotype of *P. furcomandibula* not examined.

Protanilla rafflesi species group

Protanilla beijingensis Man, Ran, Chen & Xu, 2017.
Protanilla concolor Xu, 2002.
Protanilla eguchii Satria, Putri & Ahda, 2023.
Protanilla flamma Baidya & Bagchi, 2020.
Protanilla furcomandibula Xu & Zhang, 2002.
Protanilla jongi Hsu et al., 2017.
Protanilla lini Terayama, 2009.
Protanilla rafflesi Taylor in Bolton, 1990b.
Protanila schoedli Baroni Urbani & de Andrade, 2006.
Protanilla tibeta Xu, 2012.
Protanilla wardi Bharti & Akbar, 2015.

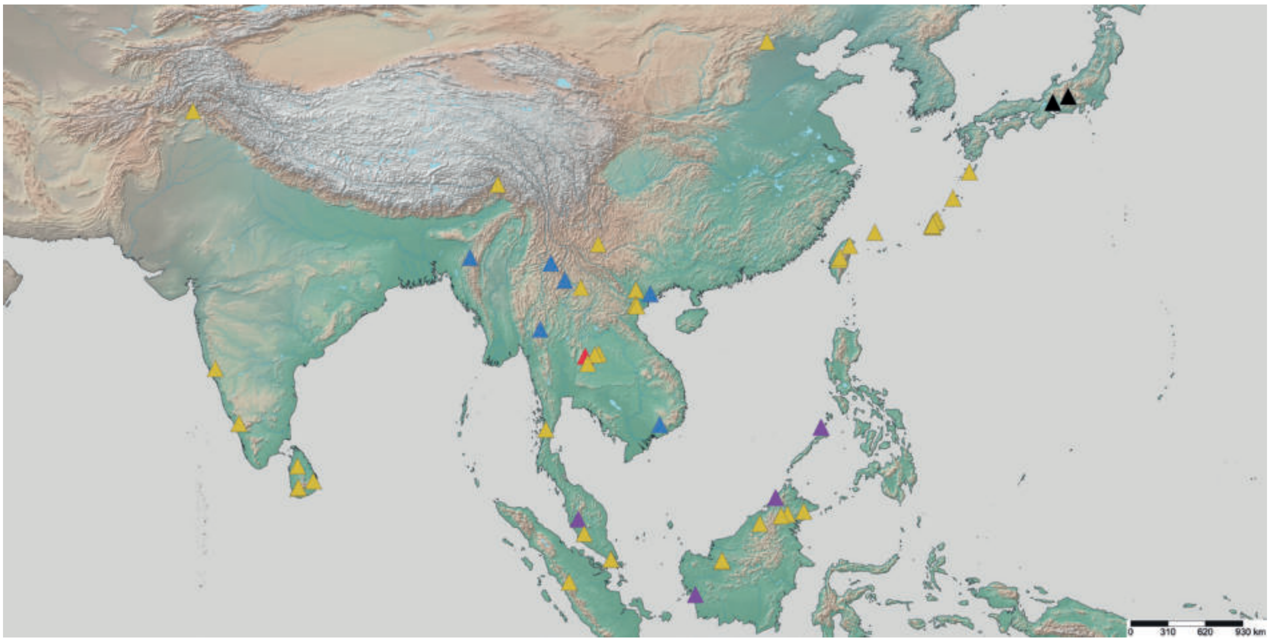

Figure 23. Geographical range of *Protanilla*. Locality information derived from AntWeb and available literature, visualized with SimpleMappr. Yellow = *Protanilla rafflesi* species group; blue = *Protanilla bicolor* species group; purple = *Protanilla taylori* species group; red = *Protanilla* zhg-th02; black = *Protanilla izanagi*.

Protanilla bicolor species group

Protanilla bicolor Xu, 2002.
Protanilla gengma Xu, 2012.

Protanilla taylori species group

Protanilla boltoni (Borowiec, Schultz, Alpert & Baňař, 2011), comb. nov.
Protanilla helenae (Borowiec, Schultz, Alpert & Baňař, 2011), comb. nov.
Protanilla taylori (Taylor in Bolton, 1990b), comb. nov.

Incertae sedis

Protanilla izanagi Terayama, 2013.

Worker diagnosis.

1. Medial mandibular surface with or without (*Protanilla taylori* species group) multiple rows of peg-like chaetae.
2. Medial mandibular margin with regularly spaced denticles.
3. Medial mandibular margin without teeth.
4. Ventromedial mandibular margin with or without subapical teeth.
5. Labrum with peg- or pencil-like chaetae (Fig. 21A, B).
6. Maxillary palp 4-merous.
7. Labial palp 2- or 1-merous.
8. Clypeus distinct, with epistomal sulcus present (Fig. 22A).

9. Dorsal mandibular articulation apparent in full-face view (Fig. 24B) or rarely not so (Fig. 24A) (*Protanilla concolor*).
10. Medial chaetae on second protarsomere (Fig. 25A).
11. Meso-metapleural suture present, strongly impressed, scrobiculate.
12. Subpetiolar process present.
13. Abdominal segment III narrowly or broadly conjoined to abdominal segment IV.
14. Length of abdominal postsclerites IV greater than that of abdominal postsclerites V–VI.
15. Somal sculpture largely absent, if present then irregularly reticulate to rugose (*Protanilla boltoni* (Borowiec et al., 2011), comb. nov.).

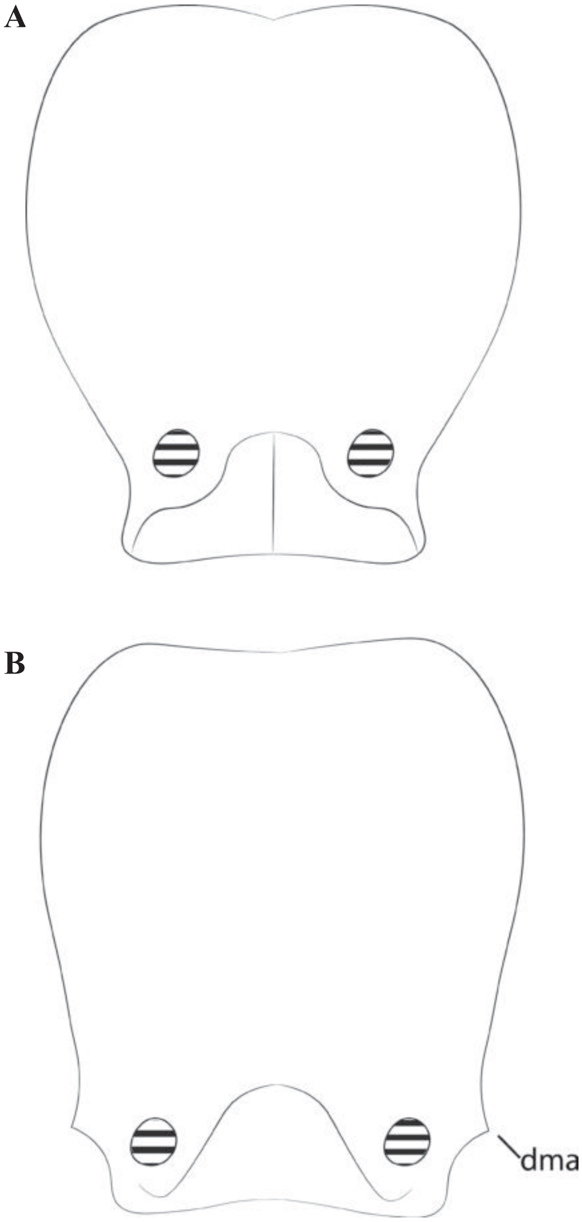

Figure 24. Worker cranium of *Protanilla concolor* (**A**) and *Protanilla bicolor* (**B**), diagrammatic full-face view, redrawn from Xu (2002: figs 18, 21). Abbreviation: dma = dorsal mandibular articulation.

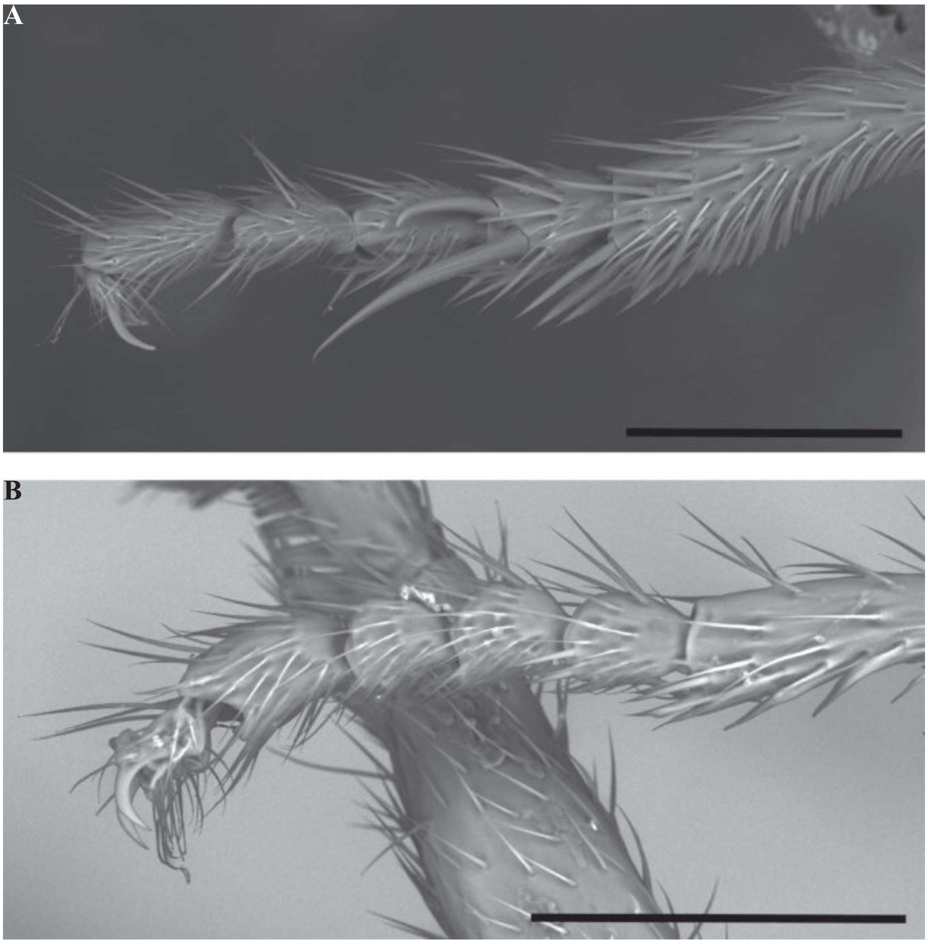

Figure 25. Condition of worker protarsus in *Protanilla* (**A**) and *Leptanilla* (**B**), profile view **A** *Protanilla lini* (CASENT0842702) **B** *Leptanilla belantan* sp. nov. (MCZENT00793731). Scale bars: 0.1 mm.

Gyne diagnosis. As in worker, but alate or rarely ergatoid; with compound eyes and 3 ocelli. If alate then venation Ogata Type IVb. M + Cu and Rsf3 absent; Rs + M, Cuf2-3, and *1m-cu* spectral or absent.

Male diagnosis.

1. Maxillary palp 4-merous.
2. Labial palp 2- to 1-merous.
3. Clypeus distinct.
4. Ocelli present, not set on tubercle.
5. Pronotum not anteroposteriorly prolonged.
6. Mesoscutum not anteroposteriorly prolonged.
7. Notauli present or absent.
8. Pterostigma present.
9. 1A in hindwing present or absent.
10. Upper metapleuron distinct from metapectal-propodeal complex.
11. Lower metapleuron indistinct from metapectal-propodeal complex.
12. Abdominal segment II petiolate.
13. Abdominal segment III petiolate or not.
14. Cupula present.

15. Volsellae present, parossiculus and lateropenite distinct.
16. Penial sclerites medially articulated.

Larval diagnosis. Habitus pogonomyrmecoid. Cranium subelliptical in full-face view. Mandibles typhlomyrmecoid, without teeth, lateral surfaces smooth. Setae short, suberect. Ventral prothoracic process absent; larval hemolymph tap apparently absent.

Remarks. The tribe Anomalomyrmini was erected by Taylor in Bolton (1990b) to include *Anomalomyrma* and *Protanilla*, which were both monotypic when established. Boudinot et al. (2022) merged the tribe into Leptanillini, although the Anomalomyrmini and Leptanillini sensu Bolton (1990b) are indubitably reciprocally monophyletic. All molecular phylogenetic inference (e.g., Borowiec et al. 2019; Griebenow 2020, pers. obs.) indicates the paraphyly of *Protanilla* relative to *Anomalomyrma*, with statistical support of varying strength. *Anomalomyrma* is therefore here synonymized with *Protanilla* (see "*Protanilla taylori* species group" for explanation of nomenclatural priority). The phylogeny of *Protanilla* remains debatable (pers. obs.), with morphological diagnoses formulated below for the major lineages revealed by these analyses, here treated as informal monophyletic species groups. These lineages are recovered on deeply separated internal nodes (pers. obs.). *Protanilla izanagi* Terayama is left unplaced to species group due to an absence of molecular data for this species and bizarrely modified mandibles which exclude it from the species groups as diagnosed here. The position of *Protanilla* zhg-th02, known only from a single male specimen, is unstable across different phylogenomic analyses (pers. obs.), but is always situated on a long branch. This morphospecies does not conform to the male-based diagnoses of any of the species groups here delimited for which male morphology is known and does not represent the as-yet unknown male of the *Protanilla taylori* species group. Based on this evidence, *Protanilla* zhg-th02 represents a major subclade of *Protanilla* for which workers remain to be discovered.

The *Protanilla rafflesi* species group is further divided into three species complexes, with two distinctive species left unplaced to species complex. Species boundaries in *Protanilla* require further inquiry, with it being possible that the clade is over-split; each species complex may respectively represent a widespread, geographically variable species. Both sexes are notably conservative in terms of morphology. Robust species delimitation, reciprocally illuminated by morphometric and molecular data, is impossible with material as scanty as is available for *Protanilla*, so no revisions to species-level taxonomy within this clade are made here.

Protanilla rafflesi species group

Worker diagnosis.

1. Medial mandibular surface armed with peg-like chaetae.
2. Mandible straight, not bowed along anteroposterior axis of cranium.
3. Vertical dorsal lamella absent from mandible (Fig. 26A).
4. Laterodorsal longitudinal groove present.
5. Clypeal surface flattened.
6. Median clypeal ridge externally visible.

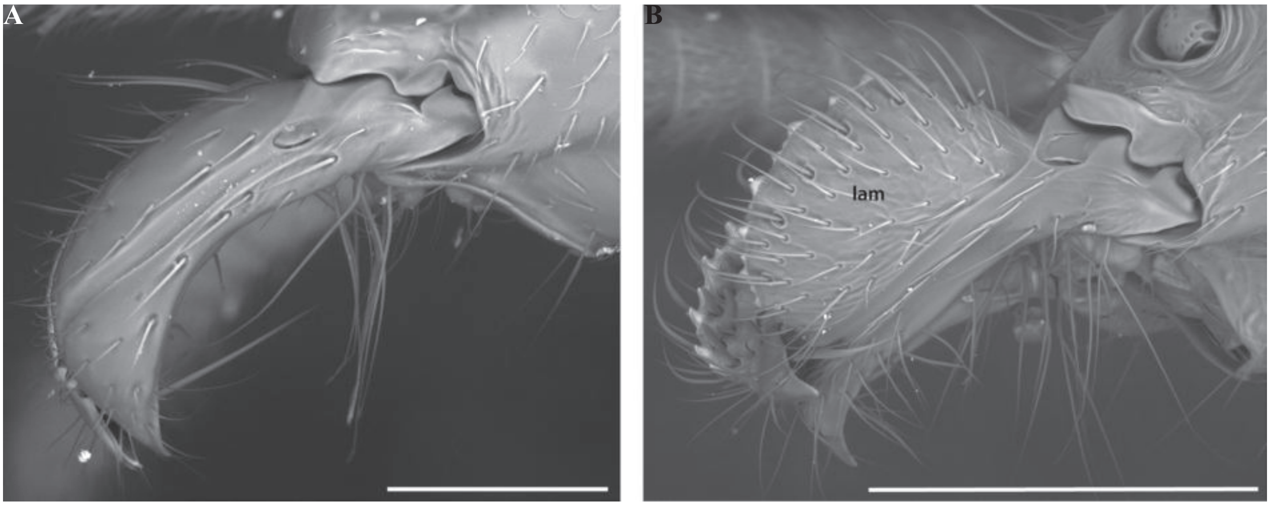

Figure 26. Worker mandibles in *Protanilla*, profile view **A** *Protanilla wallacei* (CASENT0842699) **B** *Protanilla izanagi* (CASENT0842850). Abbreviation: lam = vertical dorsal lamella. Scale bars: 0.1 mm (**A**); 0.2 mm (**B**).

7. Outline of clypeus in full-face view campaniform to oblate-trapezoidal.
8. Pronotal breadth subequal to propodeal breadth in dorsal view.
9. Mesotibia without spurs.
10. Petiole sessile.
11. Subpetiolar process with fenestra.
12. Abdominal sternite III convex, linear, or concave in profile view.
13. Abdominal segments II–III without tergotergal or sternosternal fusion.
14. Abdominal segments III–IV narrowly or broadly conjoined.
15. Anterior margin of abdominal post-tergite IV linear to strongly emarginate in dorsal view.
16. Soma concolorous.

Gyne diagnosis. As for genus, alate or ergatoid; if ergatoid than alar sclerites present.

Male diagnosis.

1. Distal 3 maxillary palpomeres of unequal lengths (Griebenow 2020: fig. 10A).
2. Labial palp 2- or 1-merous.
3. Antennomere 3 shorter than scape.
4. Antero-admedian signum present or absent; if present, then unsculptured.
5. Notauli present or absent; if present, then unsculptured.
6. Parapsidal lines present or absent.
7. 1A present in hindwing.
8. Abdominal segment III not petiolate.
9. Length of abdominal segment IV subequal to, or less than, respective lengths of abdominal segments V–VII.
10. Cupula non-annular.

Larval diagnosis. As for genus.

Remarks. This clade shows striking morphological conservatism in the worker caste and males, with their possibly being many cryptic species.

Protanilla jongi deviates from most of the clade in having broadly conjoined abdominal segments III–IV, and a ventral subapical mandibular tooth but is robustly confirmed to be nested well within the *P. rafflesi* species group by phylogenomic inference (pers. obs.). I therefore also place *P. furcomandibula* Xu & Zhang, 2002 in the *P. rafflesi* species group, as this species appears to be a close relative of *P. jongi* (Hsu et al. 2017), with the ventral subapical mandibular tooth being hypertrophied, and abdominal sternite II concave in profile view rather than linear to convex. The concavity of abdominal sternite II in profile view is homoplasious with the *Protanilla taylori* species group, as is the broad connection of abdominal segments III–IV.

A 4,2 palpal formula was confirmed for the worker of *Protanilla lini* by examination with micro-CT (Richter et al. 2021), while the palpal formula of the conspecific male was tentatively interpreted as 4,1 by Griebenow (2020). The palpal formula of the worker in the *Protanilla rafflesi* species group, and indeed *Protanilla* as a whole, has largely gone unreported, with this study being the first to confirm the palpal formula of any representative of the *Protanilla taylori* species group. Palpal formula across the Formicidae shows sexual monomorphism, with few exceptions (Bolton 2003; see sections on the *Protanilla bicolor* species group and *Leptanilla thai* species group below), meaning that the interpretation by Griebenow (2020) of the male labial palp in *P. lini* as 1-merous was in error.

Three species complexes are hereby recognized in the *Protanilla rafflesi* species group: the *rafflesi* complex (*Protanilla rafflesi* Taylor in Bolton, 1990b, *P. schoedli*, and *Protanilla wardi* Bharti & Akbar, 2015); the *concolor* (*Protanilla concolor* Xu, 2002; *Protanilla tibeta* Xu, 2012; and *Protanilla eguchii* Satria, Putri & Ahda, 2023); and the *lini* complex (*P. lini*, *P. beijingensis*, *P. flamma*, and *P. wallacei*). Each of these complexes consist of species that are extremely similar, but for which material is too scarce to query interspecific boundaries. *Protanilla furcomandibula* and *P. jongi* are presumably close relatives, but are readily distinguishable based on known specimens, and so are not consigned to a species complex. Without phylogenomic inference, it is unclear if these species complexes are reciprocally monophyletic. *Protanilla wallacei* sp. nov. based upon worker specimens is recovered as sister to *P. lini* (pers. obs.), as would be predicted based on observed worker phenotype.

A single specimen (CASENT0842639) of *Protanilla beijingensis* is herein reported from Khyber Pakhtunkhwa, Pakistan, in a remarkable range extension for a species heretofore known only from Beijing, China (Man et al. 2017). CASENT0842639 qualitatively differs from the type series in possessing a pair of peg-like chaetae on the labrum rather than a single median chaeta, but it is unknown whether this constitutes intra- or interspecific variation in *Protanilla*. This specimen is part of a series figured by Bolton (1990b: figs 1–6), for which coordinates are unavailable. Despite this, it appears that the collection was made at an elevation of 2400–2700 meters, in a cold temperate climate resembling that of the type locality.

Dias et al. (2019: 164) described the worker of *Protanilla schoedli* from ten specimens collected across Sri Lanka, based on “overall similarity in … general appearance” to the holotype gyne (CASENT0911228) and the implicit assumption that multiple *Protanilla* spp. cannot occur in sympatry. However, the putative worker *P. schoedli* display no more affinity to CASENT0911228 than to other members of the *Protanilla rafflesi* species group, with the anterior margin of the petiolar node being straight (Dias et al. 2019: 164) rather than concave in profile view, as in CASENT0911228 (Baroni Urbani and de Andrade 2006: 46). The morphology of the petiolar node is not dimorphic between worker and gyne in *Protanilla*. This lack of concavity excludes these worker specimens from the *Protanilla rafflesi* species complex to which *P. schoedli* belongs. The putative workers of *P. schoedli* (Dias et al. 2019) more closely resemble *Protanilla flamma* Baidya & Bagchi, 2020, but the difference in reported ranges of CI, SI, and PI between these two series supports their heterospecificity, if these morphometric differences reflect species boundaries. In this study, the putative *P. schoedli* (Dias et al., 2019) are regarded as an undescribed species belonging to the *Protanilla lini* species complex. While neither *P. schoedli* nor *P. flamma* have been sequenced, other members of their respective species complexes have (*P. wardi* vs. *P. lini* and *P. wallacei*), with phylogenomic inference therefrom supporting their heterospecificity (pers. obs.).

The *Protanilla rafflesi* species group contains some of the only *Protanilla* spp. for which bionomic data are available, with micro-computed tomographic studies of cephalic skeletomusculature in *P. lini* demonstrating the existence of “trap-jaw” capabilities in that species (Richter et al. 2021). The existence of putative trigger hairs across *Protanilla* (Griebenow et al. 2022: table 4) suggests that trap-jaw biology is a synapomorphy of the genus and paralleled in the Leptanillinae only by *Leptanilla laventa* (Griebenow, Moradmand, & Isaia in Griebenow, Isaia, & Moradmand, 2022), comb. nov.

Protanilla bicolor species group

Worker diagnosis.

1. Medial mandibular margin armed with peg-like chaetae.
2. Mandible straight, not bowed along anteroposterior axis of cranium.
3. Vertical dorsal lamella absent from mandible.
4. Laterodorsal longitudinal groove absent.
5. Clypeal surface concave.
6. Median clypeal ridge not externally visible.
7. Outline of clypeus in full-face view campaniform.
8. Breadth of pronotum subequal to propodeum in dorsal view.
9. Mesotibia with 1 spur.
10. Petiole sessile.
11. Subpetiolar process with fenestra.
12. Abdominal sternite III convex in profile view.
13. Abdominal segments II–III without tergotergal and sternosternal fusion.
14. Abdominal segments III and IV narrowly joined.
15. Anterior margin of abdominal post-tergite IV linear to slightly emarginate in dorsal view.
16. Soma bicolored, rarely concolorous.

Gyne diagnosis. As for genus, ergatoid, without alar sclerites (pers. obs.).

Male diagnosis.

1. Distal 3 maxillary palpomeres subequal in length (Griebenow 2020: fig. 10B).
2. Labial palp 2-merous.
3. Antennomere 3 longer than scape.
4. Antero-admedian signum absent.
5. Notauli present, scrobiculate.
6. Parapsidal lines absent.
7. 1A absent from hindwing.
8. Abdominal segment III petiolate.
9. Length of abdominal segment IV subequal to, or exceeding, combined length of abdominal segments V–VIII.
10. Cupula annular (Griebenow et al. in press).

Larval diagnosis. Larva unknown.

Remarks. Phenotypic differentiation between the *Protanilla bicolor* and *Protanilla rafflesi* species groups in the worker caste is comparatively slight, but the two clades are discretely distinguishable by tibial spur formula. The strong concavity of the anterior clypeal margin referred to in previous descriptive literature more correctly refers to the face of the clypeus: the anterior margin itself is in fact no more emarginate in this clade than in the *Protanilla rafflesi* species group. The morphology of *Protanilla* TH03, a male singleton attributable to this clade by molecular data (e.g., Borowiec et al. 2019), and that of male *P. gengma* (Griebenow et al. in press) differs from all other known males of *Protanilla* in multiple respects, most conspicuously in petiolation of abdominal segment III: this condition is unique among male Leptanillinae.

Workers of the *Protanilla bicolor* species group are unique among examined *Protanilla* workers in exhibiting a mesotibial spur, an apparent symplesiomorphy of this clade. Palpal formula could not be assessed in the worker caste due to a lack of fresh specimens, but given sexual monomorphism of palpal formula across the Formicidae save for the Ponerini, *Typhlomyrmex* (Bolton 2003), and probably the *Leptanilla thai* species group as well (this study), it is sound to predict a 4,2 formula.

Species boundaries in the *Protanilla bicolor* species group remain unclear. Specimens identified as *P. gengma* are known to vary in labral chaeta count according to geographical origin (Aswaj et al. 2020), but the relevance of this trait to species delimitation is unknown. *Protanilla* VN03 appears transitional in morphometric terms between *Protanilla bicolor* Xu, 2002 and *P. gengma*, but PTL in *Protanilla* VN03 falls outside the range observed in either of these species.

Protanilla taylori species group

Worker diagnosis.

1. Medial mandibular surface without peg-like chaetae.
2. Mandible straight, not bowed along anteroposterior axis of cranium.
3. Vertical dorsal lamella absent or present (*Protanilla taylori* (Taylor in Bolton, 1990b)) on mandible.
4. Laterodorsal longitudinal groove present.

5. Clypeal surface concave.
6. Median clypeal ridge not externally visible.
7. Outline of clypeus in full-face view an oblate trapezoid.
8. Pronotal breadth greater than propodeal breadth in dorsal view.
9. Mesotibia without spurs.
10. Petiole subsessile.
11. Subpetiolar process with fenestra present or absent.
12. Abdominal sternite II convex in profile view.
13. Abdominal segments II-III without tergotergal and sternosternal fusion.
14. Abdominal segment III broadly joined to abdominal segment IV.
15. Anterior margin of abdominal tergite IV entire in dorsal view.
16. Soma concolorous.

Gyne diagnosis. As for worker, but, alate. Pencil-like chaetae present on mandible; two or three rows of cuticular denticles along masticatory margin.

Male diagnosis. Male unknown.

Larval diagnosis. Larva unknown.

Remarks. *Anomalomyrma* was established for *Protanilla taylori* comb. nov. by Taylor in Bolton (1990b) on account of derived mandibular morphology and the tergotergal and sternosternal fusion of abdominal segments II–III, a character state unique among the Formicidae (Bolton 1990b, Borowiec et al. 2011). While *P. taylori* is known only from the gyne, Borowiec et al. (2011) described *Protanilla boltoni* (Borowiec, Schultz, Alpert & Baňař, 2011), comb. nov. and *Protanilla helenae* (Borowiec, Schultz, Alpert & Baňař, 2011), comb. nov. based on worker material, and refined the diagnosis of *Anomalomyrma*, demonstrating that the presence of a vertical mandibular lamella was of no diagnostic utility in the Anomalomyrmini at the genus level, and predicting that the resemblance between the mandibles of *Anomalomyrma* and the then-undescribed *Protanilla izanagi* (see below) was homoplasious. This hypothesis has not yet been tested with phylogenomic inference.

Given the paraphyly of *Protanilla* relative to *Anomalomyrma* under phylogenomic inference from several differently curated datasets (pers. obs.), the latter genus is synonymized under *Protanilla*. These names were established in the same publication (Bolton 1990b), and the latter is here given precedence as permitted in Article 24.2 of the International Code of Zoological Nomenclature. The *Protanilla taylori* species group is equivalent to the former genus *Anomalomyrma*.

The vertical dorsal lamella in *Protanilla taylori* and *P. izanagi* has few parallels within the Formicoidea, being comparable to the morphology observed in both female and male beast ants (Camelomeciidae: *Camelosphecia*), which are known only from Cretaceous burmite (Boudinot et al. 2020). Among extant formicoids, the mandible of these two *Protanilla* spp. is most reminiscent of that observed in armadillo ants (Agroecomyrmecinae: Agroecomyrmecini: *Tatuidris tatusia* Brown & Kempf, 1968), which is likewise bowed, but with the masticatory margin armed with a brush of robust feathery setae (Brown and Kempf 1968: fig. 3) rather than peg-like chaetae, cuticular denticles, or both.

The feeding ecology of *P. taylori* and *P. izanagi* may therefore resemble that of the armadillo ants. Brown and Kempf (1968: 189) hypothesized that armadillo ants feed on “slippery or active arthropod prey”, with William Brown speculating that these ants were specialist predators of oligochaetes (P. S. Ward, pers. comm. 2021). Given that known ant specialists on oligochaete prey, such as *Psalidomyrmex procerus* Emery (Formicidae: Ponerinae: Ponerini) (Lévieux 1983; Déjean et al. 1999), have mandibles quite unlike those of armadillo ants, this seems improbable. Food court experiments to determine the diet of these ants were unsuccessful, but isotopic analysis of armadillo ant tissue suggests that the unknown prey is itself predatory (Jacquemin et al. 2014: 5).

Protanilla taylori and *Protanilla* id01 differ notably from the species known only from workers in the presence of two and three ranks, respectively, of produced denticles on the mandible (Bolton 1990b; this study), as opposed to the condition observed in most *Protanilla*; with the presence of pencil-like chaetae on the mandible, which are absent in the worker-based species. The worker and gyne caste remain unassociated in all three described species of the *Protanilla taylori* species group, plus *Protanilla* id01. Until the female castes respectively unknown from these species are discovered, we cannot determine whether observed mandibular differences are to be credited to allospecificity, or to caste dimorphism.

Incertae sedis

Protanilla izanagi Terayama.

Worker diagnosis.

1. Medial mandibular surface with peg-like chaetae.
2. Mandible bowed along anteroposterior axis of cranium (Fig. 17B).
3. Vertical dorsal lamella present on mandible (Fig. 26B).
4. Laterodorsal longitudinal groove present on mandible.
5. Clypeal surface flattened.
6. Median clypeal ridge not externally visible.
7. Outline of clypeus in full-face view an oblate trapezoid.
8. Pronotal breadth greater than propodeal breadth in dorsal view.
9. Mesotibia without spurs.
10. Petiole sessile.
11. Subpetiolar process with fenestra present.
12. Abdominal sternite II convex in profile view.
13. Abdominal segments II–III without tergotergal and sternosternal fusion.
14. Abdominal segment III narrowly joined to abdominal segment IV.
15. Anterior margin of abdominal tergite IV entire in dorsal view.
16. Soma concolorous.

Gyne diagnosis. As for genus, alate.

Male diagnosis. Male unknown.

Larval diagnosis. Larva unknown.

Remarks. Prior to formal description, this peculiar species from southern Honshu was cited by Hölldobler and Wilson (1990) and Imai et al. (2003) as *Anomalomyrma* (the former authors referring to it under the *nomen nudum Anomalomyrma kubotai*), due to the presence of an erect mandibular lamella. Borowiec et al. (2011) concluded that this character state alone was insufficient to place the morphospecies in *Anomalomyrma*, with its habitus being otherwise consistent with that of *Protanilla*. Terayama (2013) accordingly described

Protanilla izanagi in that genus. The presence of distinct posterior faces on the dorsal petiolar and post-petiolar nodes, with abdominal segments III and IV not being broadly conjoined, shows an affinity to the *Protanilla rafflesi* and *Protanilla bicolor* species groups, but these character states are plesiomorphic for *Protanilla* (pers. obs.). It is likely that the similar mandibular morphology of *P. izanagi* and the *Protanilla taylori* species group reflects similar diet (see "Remarks" for the *Protanilla taylori* species group above) and is therefore homoplasious (Borowiec et al. 2011). Terayama (2013) describes the compound eye as being absent in the worker, but the specimens that I examined are remarkable in the retention of two ommatidia (Fig. 17A). The presence of any trace of the compound eye in the worker is unique among the Leptanillinae. No molecular data are available for *P. izanagi*, and so in the absence of compelling morphological evidence, this species must be left unplaced to species group within *Protanilla*. I predict, however, that molecular data will demonstrate that *Protanilla izanagi* belongs within the *Protanilla rafflesi* species group.

Leptanilla **Emery, 1870**

Leptanilla Emery, 1870: 196. Type species: *Leptanilla revelierii* Emery, 1870, by monotypy.

Scyphodon Brues, 1925: 93. Type species: *Leptanilla anomala* (Brues, 1925), comb. nov., by monotypy. Holotype of *L. anomala* examined; deposited at MHNG. Syn. nov.

Phaulomyrma Wheeler & Wheeler, 1930: 193. Type species: *Leptanilla javana* (Wheeler & Wheeler, 1930), by original designation. Holotype of *L. javana* examined; deposited at MCZC. Synonymy by Griebenow (2021).

Leptomesites Kutter, 1948: 286. Type species: *Leptanilla escheri* (Kutter, 1948), by monotypy. Holotype of *L. escheri* examined; deposited at MZLS. Synonymy by Baroni Urbani (1977).

Noonilla Petersen, 1968: 582. Type species: *Leptanilla copiosa* (Petersen, 1968), by monotypy. Holotype of *L. copiosa* not examined; deposited at NHMD. Syn. nov.

Yavnella Kugler, 1987 ("1986"): 52. Type species: *Leptanilla argamani* (Kugler, 1987 ("1986")), by original designation. Holotype of *L. argamani* not examined; deposited at TAU. Syn. nov.

Leptanilla thai **species group**

Leptanilla argamani (Kugler, 1987 ("1986")), comb. nov.
Leptanilla belantan sp. nov.
Leptanilla escheri (Kutter, 1948).
Leptanilla indica (Kugler, 1987 ("1986")), comb. nov.
Leptanilla judaica Kugler, 1987 ("1986").
Leptanilla kunmingensis Xu & Zhang, 2002.
Leptanilla lamellata Bharti & Kumar, 2012.
Leptanilla laventa (Griebenow, Moradmand, & Isaia in Griebenow, Isaia, & Moradmand, 2022), comb. nov.
Leptanilla thai Baroni Urbani, 1977.
Leptanilla ujjalai Saroj, Mandi & Dubey, 2022.

Leptanilla havilandi species group

Leptanilla anomala (Brues, 1925), comb. nov.
Leptanilla copiosa (Petersen, 1968), comb. nov.
Leptanilla havilandi Forel, 1901.

Leptanilla bethyloides species group

Leptanilla bethyloides sp. nov.

Leptanilla najaphalla species group

Leptanilla najaphalla sp. nov.

Leptanilla revelierii species group

Leptanilla acherontia sp. nov.
Leptanilla africana Baroni Urbani, 1977.
Leptanilla alexandri Dlussky, 1969.
Leptanilla astylina Petersen, 1968.
Leptanilla australis Baroni Urbani, 1977.
Leptanilla besucheti Baroni Urbani, 1977.
Leptanilla bifurcata Kugler, 1987 ("1986").
Leptanilla boltoni Baroni Urbani, 1977.
Leptanilla buddhista Baroni Urbani, 1977.
Leptanilla charonea Barandica, López, Martínez & Ortuño, 1994.
Leptanilla doderoi Emery, 1915.
Leptanilla exigua Santschi, 1908.
Leptanilla hunanensis Tang, Li & Chen, 1992.
Leptanilla islamica Baroni Urbani, 1977.
Leptanilla israelis Kugler, 1987 ("1986").
Leptanilla japonica Baroni Urbani, 1977.
Leptanilla javana (Wheeler & Wheeler, 1930).
Leptanilla kubotai Baroni Urbani, 1977.
Leptanilla macauensis Leong, Yamane, & Guénard, 2018.
Leptanilla minuscula Santschi, 1907.
Leptanilla morimotoi Yasumatsu, 1960.
Leptanilla nana Santschi, 1915.
Leptanilla oceanica Baroni Urbani, 1977.
Leptanilla okinawensis Terayama, 2013.
Leptanilla ortunoi López, Martínez, & Barandica, 1994.
Leptanilla plutonia López, Martínez, & Barandica, 1994.
Leptanilla poggii Mei, 1995.
Leptanilla revelierii Emery, 1870.
Leptanilla swani Wheeler, 1932.
Leptanilla taiwanensis Ogata, Terayama & Masuko, 1995.
Leptanilla tanakai Baroni Urbani, 1977.
Leptanilla tanit Santschi, 1907.
Leptanilla tenuis Santschi, 1907.

Leptanilla theryi Forel, 1903.
Leptanilla vaucheri Emery, 1899.
Leptanilla yunnanensis Xu, 2002.
Leptanilla zaballosi Barandica, López, Martínez & Ortuño, 1994.

Incertae sedis

Leptanilla butteli Forel, 1913.
Leptanilla clypeata Yamane & Ito, 2001.
Leptanilla hypodracos Wong & Guénard, 2016.
Leptanilla kebunraya Yamane & Ito, 2001.
Leptanilla palauensis (Smith, 1953).

Unplaced to species group

Leptanilla santschii Wheeler & Wheeler, 1930.

Worker diagnosis.

1. Medial mandibular margin without peg-like chaetae.
2. Medial mandibular margin with or without denticles, if present then irregularly spaced.
3. Medial mandibular margin with at least one subapical tooth.
4. Ventromedial mandibular margin without subapical teeth.
5. Labrum without peg-like chaetae.
6. Maxillary palp 1- to 2-merous.
7. Labial palp 1-merous.
8. Clypeus indistinct.
9. Dorsal mandibular articulation not visible in full-face view.
10. Medial chaetae absent from second protarsomere (Fig. 25B).
11. Meso-metapleural suture usually vestigial to absent, rarely present; if present then unsculptured.
12. Subpetiolar process present or absent.
13. Abdominal segment III narrowly joined to abdominal segment IV.
14. Length of abdominal postsclerites IV longer than or subequal to that of abdominal postsclerites V–VI.
15. Somal sculpture present and widespread, never punctate.

Gyne diagnosis. Dichthadiiform, and therefore lacking wings and axillary sclerites. Mandibles edentate or with three teeth (*Leptanilla kubotai*) (Terayama and Kinomura 2015). Compound eyes repressed or present; if present then consisting of one or two ommatidia. Abdominal segment III never petiolate.

Male diagnosis.

1. Maxillary palp 1- to 2-merous.
2. Labial palp 1-merous.
3. Clypeus distinct or indistinct.
4. Ocelli present or absent (*Leptanilla* TH03, *Leptanilla* zhg-bt03); if present then set on tubercle or rarely not (e.g., *Leptanilla najaphalla* sp. nov.).

5. Pronotum anteroposteriorly prolonged.
6. Mesoscutum anteroposteriorly prolonged.
7. Notauli absent.
8. Pterostigma absent.
9. 1A absent from hindwing.
10. Upper metapleuron distinct from metapectal-propodeal complex (*Leptanilla thai* species group, *Leptanilla bethyloides* sp. nov., *Leptanilla* zhg-th01) or indistinct.
11. Lower metapleuron indistinct or distinct from metapectal-propodeal complex (*Leptanilla havilandi* species group, *Leptanilla bethyloides* sp. nov., *Leptanilla* zhg-th01).
12. Abdominal segment II petiolate or not (e.g., *Leptanilla* TH02).
13. Abdominal segment III not petiolate.
14. Cupula present or absent; if present, then annular.
15. Volsellae present or absent (*Leptanilla havilandi* species group, *Leptanilla bethyloides* species group), if present then parossiculus and lateropenite indistinct (Griebenow et al. in press).
16. Penial sclerites medially fused or articulated (*Leptanilla astylina* Petersen, 1968), rarely partly articulated (*Leptanilla* TH03).

Larval diagnosis. Habitus leptanilloid. Cranium subpyriform in full-face view. Mandibles leptanilloid, with teeth, lateral surface shagreened with spinules. Setae short and suberect or flexuous, elongated, and subdecumbent to erect. Ventral prothoracic process and hemolymph taps present.

Remarks. The four genera known solely from males at the time of Bolton (1990b) were provisionally retained in the Leptanillini by that author, with the knowledge that at least some would prove to be satellite genera of *Leptanilla*. The phylogeny of the Leptanillini is now robustly resolved with phylogenomic and total-evidence approaches: *Leptanilla* s. l. (Griebenow 2020, 2021) includes *Scyphodon* and *Noonilla* (= *Scyphodon* s. l.; Griebenow et al. in press), with *Leptanilla* s. str., with which *Phaulomyrma* was synonymized (Griebenow 2021); and is sister to a well-supported clade first recovered by Borowiec et al. (2019) and identified as *Yavnella* by Griebenow (2020, 2021).

The question of the formal rank of major subclades in the Leptanillini depends upon practical utility. For generic ranking of subclades to be useful, these clades must be distinguishable based upon the morphology of both the male sex and available female castes. *Yavnella* and *Leptanilla* s. l. are readily diagnosed based upon males, as are the subclades of *Leptanilla* s. l. (pers. obs.). The taxonomic problem then lies in whether these groups can be distinguished based upon worker morphology.

Using phylogenomic inference, Griebenow et al. (2022) identified the worker of *Yavnella*, while *Leptanilla havilandi* Forel is sister to *Scyphodon* s. l. (in those analyses represented only by *Noonilla* spp.) and *Leptanilla thai* is robustly recovered within *Yavnella* as well (pers. obs.). The morphological similarities between *Leptanilla laventa* (Griebenow et al. 2022), comb. nov. and *L. thai* to the exclusion of *Leptanilla* s. str., such as the emarginate frontoclypeal process, cannot be interpreted as synapomorphic. *L. havilandi* and *thai* are extremely close morphologically, as noted by Baroni Urbani (1977). In this study, I find that these two species are discriminated by areolate sculpturation of the torulus in

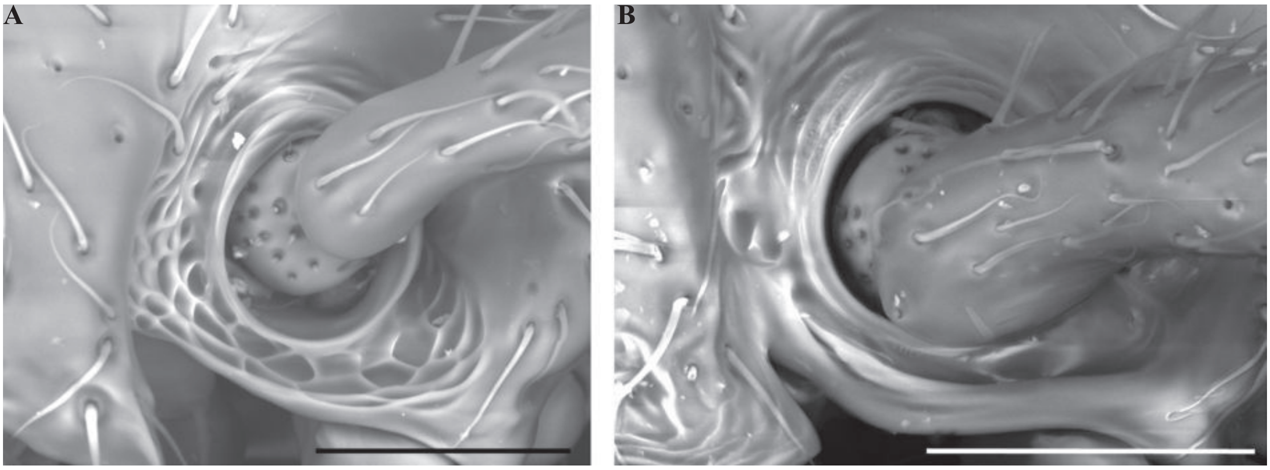

Figure 27. Antennal torulus in *Leptanilla thai* (**A**) and *Leptanilla havilandi* (**B**), worker. Scale bars: 0.04 mm (**A**); 0.05 mm (**B**).

L. thai (no such sculpture is observed in *L. havilandi*; Fig. 27), different mandibular dentition, and a more elevated frontoclypeal process in *L. havilandi*. Sculpturation requires scanning electron microscopy to be assessed, while elevation of the frontoclypeal process and mandibular dentition are difficult to accurately assess with light microscopy (as evidenced by the incorrect accounting of mandibular teeth in the description of *L. thai* (Baroni Urbani, 1977)), making these characters impractical for identification of leptanilline workers to genus. This impracticality, and lack of consistent morphological distinction between the worker castes across all *Yavnella* and *Leptanilla*, argues against maintaining the two as separate genera.

Therefore, the most conservative course of nomenclatural action is to synonymize *Scyphodon*, *Noonilla*, and *Yavnella* under *Leptanilla*. The diversity of *Leptanilla* is here organized in informal species groups, for which diagnoses based upon all known castes are provided below. Wherever sampling of molecular data across *Leptanilla* is sufficient for phylogeny of these species groups to be known, these are delimited to be monophyletic. Several aberrant species for which molecular data are unavailable are left unplaced to species group.

Leptanilla thai species group

Worker diagnosis.

1. Mandible with 3–4 teeth.
2. Maxillary palp 1- to 2-merous.
3. Frontoclypeal process present, apex emarginate.
4. Lateral clypeal teeth absent.
5. Meso-metapleural groove absent or present (*Leptanilla kunmingensis* Xu & Zhang, 2002).
6. Mesotibia with two spurs.
7. Metatibia with 1–2 spurs.
8. Length of abdominal segment II subequal to width in dorsal view, or length much greater than width (*Leptanilla laventa*).
9. Anterior of abdominal tergite IV lateromedially constricted in dorsal view (*Leptanilla laventa*) or not lateromedially constricted.

10. Length of abdominal tergite IV greater than combined length of posterior abdominal tergites in dorsal view.

Gyne diagnosis. As for genus, but petiole longer than broad in dorsal view, outline rectangular (*Leptanilla escheri*) to subpyriform (*Leptanilla belantan*). Placement of these two species in the *Leptanilla thai* species group is provisional (see Remarks).

Male diagnosis.

1. Mandalus ≥ 0.5× length of that of the mandible.
2. Mandible fused to cranium, rarely articulated.
3. Anteromedian ocellus orthogonally dorsal to compound eye in profile view.
4. LF2 > SL, rarely LF2 ≈ SL.
5. Distal transverse carina absent from procoxa.
6. Protrochanter not elongated.
7. Profemur not enlarged, sometimes proximally kurtotic.
8. Arcuate medial carina absent from profemur.
9. Apicoventral hook absent from profemur.
10. Ventromedian carina absent from protibia.
11. Protibial comb absent.
12. Antero-admedian signum present or absent.
13. Pronotum and mesoscutum not anteroposteriorly prolonged.
14. Mesoscutellum without recurved posteroventral process.
15. Adventitious spectral M+Cu absent from forewing.
16. Upper metapleuron distinct from metapectal-propodeal complex or indistinct.
17. Lower metapleuron indistinct from metapectal-propodeal complex.
18. Propodeal declivity concave in profile view.
19. Petiole without distinct dorsal node.
20. Abdominal sternite II without ventral process.
21. Abdominal tergite VIII broader than long in posterodorsal view.
22. Abdominal sternite IX posteriorly separate from gonocoxites.
23. Mulceators absent.
24. Cupula present.
25. Gonopodites inarticulate.
26. Gonocoxites with partial ventromedian fusion.
27. Gonocoxites without or rarely with dorsomedian fusion (*Leptanilla* TH03).
28. Gonocoxites partly fused to penial sclerites or unfused.
29. Gonostyli present or rarely absent (*Leptanilla* TH03).
30. Volsellae present.
31. Volsellae medially separate.
32. Volsella furcated, sometimes entire (*Leptanilla* TH03, *Leptanilla* zhg-bt03).
33. Penial sclerites usually with complete median fusion, rarely with partial median fusion.
34. Penial sclerites dorsoventrally compressed or not (*Leptanilla* TH03).
35. Phallotreme apical.
36. Phallotreme dorsal.
37. Dense phallotremal vestiture of setae absent.

Larval diagnosis. As for genus. Larva is known only in *Leptanilla escheri* and *Leptanilla judaica*, the placement of which in this species group has not been confirmed by molecular phylogenetic inference.

Remarks. *Leptanilla escheri*, *L. judaica*, *Leptanilla kunmingensis* Xu & Zhang, 2002, *Leptanilla lamellata* Bharti & Kumar, 2015, *L. ujjalai*, and *L. belantan* sp. nov. are placed in this species group with some caution, given a lack of molecular data for these species. These four species bear some resemblance to *Leptanilla laventa* comb. nov. (e.g., in the palpal formula being 2,1), which differs from them only in the elongation of the appendicular sclerites. Since worker morphology in *Leptanilla* is often indecisive when inferring phylogeny, or downright misleading (pers. obs.), these species may belong elsewhere within *Leptanilla*. With only species included in phylogenomic analysis under consideration, the *Leptanilla thai* and *Leptanilla havilandi* species groups are mutually indistinguishable based upon worker morphology without examination of cranial microsculpture. However, male specimens of the *Leptanilla havilandi* species group are known only from the Sundan region, and so extralimital worker specimens that conform to the worker-based morphological diagnosis of that species group presented here are instead referred to the *Leptanilla thai* species group. These two clades are only definitively known in sympatry from peninsular Malaysia (Fig. 28). Since phylogenomic inference confirms the position of *L. thai* within the former genus *Yavnella*, and this is the oldest species name assigned to that clade for which that hypothesized placement can be confirmed with molecular data, this clade is informally exemplified by that species.

As noted in Griebenow et al. (2022), the anatomical identity of the frontoclypeal process observed in the *Leptanilla thai* species group, the *Leptanilla havilandi* species group, *Leptanilla clypeata* and *Leptanilla hypodracos* Wong & Guénard, 2016 is unclear. Prior authors assumed a clypeal origin, which may be in part correct, but this hypothesis cannot be tested with external examination due to the absence in worker *Leptanilla* of apparent anterior tentorial pits or an unequivocal epistomal sulcus. Elision of the boundaries between the frons and clypeus also occurs in *Discothyrea* (Proceratiinae) and *Aulacopone relicta* Arnol'di, 1930 (Ectatomminae: Heteroponerini), likewise involved in an anteromedian projection from the cranium in full-face view (Taylor 1979). Detailed micro-CT study of the shelf-like frontoclypeal process in the *Discothyrea oculata* and *Discothyrea traegordhi* species complexes was able to confirm the identity of this process as a mosaic of the frons and clypeus (Hita-Garcia et al. 2019), and only similar data can possibly be used to clarify the anatomy of the frontoclypeal process in *Leptanilla*.

The palpal formula in the worker caste of *L. thai* and *L. laventa* is 2,1 (Griebenow et al. 2022), which, among those species that have been confirmed to belong to the *Leptanilla thai* species group by phylogenomic inference, are the only ones for which the worker caste is known. All known males of the *Leptanilla thai* species group examined in this study possess a 1-merous palp (cf. Kugler 1987), meaning that it is probable that the *Leptanilla thai* species group shows sexual dimorphism in palpal formula. This would be only confirmed by definitive association of conspecific worker and male specimens belonging to this clade. If confirmed, the *Leptanilla thai* species group would constitute only the third independent origin in the Formicidae of decoupled palpal formula between the sexes (Bolton 2003). Curiously, this would run opposite to the

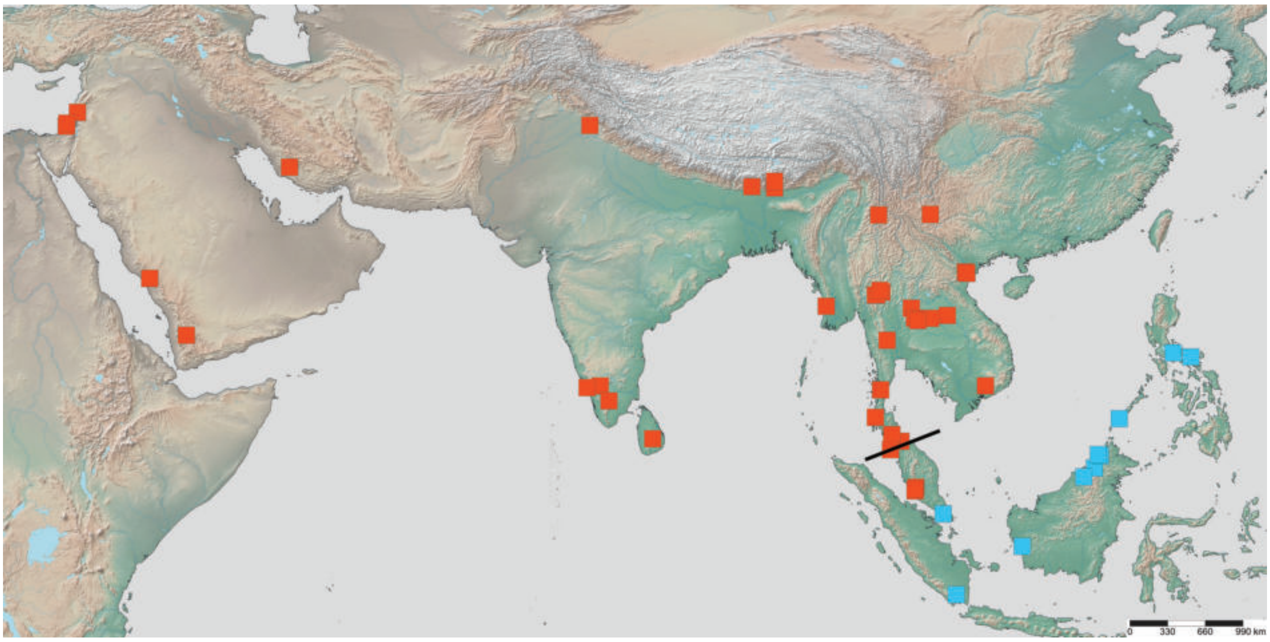

Figure 28. Geographical range of the *Leptanilla thai* species group (orange) and the *Leptanilla havilandi* species group (blue). The Pattani-Kangar Line is indicated in black. Locality information derived from AntWeb and available literature, visualized with SimpleMappr.

tendency in other cases of decoupling within the Formicidae, in which the palpomere counts of the worker are reduced relative to those in the male.

The *Leptanilla thai* species group is broadly distributed across southern Asia (Griebenow et al. 2022: fig. 20), with males being more diverse and abundant than any other leptanilline clade in Malaise trap residues from mainland Southeast Asia. An undescribed male morphospecies is recorded from Sana'a, Yemen (Collingwood and Agosti 1996), meaning that the *Leptanilla thai* species group extends at least to the extreme northeastern corner of the Afrotropics, but within that ecozone is perhaps restricted to the southern Arabian Peninsula. No specimens are yet known from the Eastern Palaearctic, with the nearest examples being *L. kunmingensis* and an undescribed worker specimen (CASENT0064302), both from Yunnan Province, China. This absence from the Eastern Palaearctic is notable given the thorough myrmecological sampling of Japan and to a lesser extent Taiwan. Better sampling of the Sundan region is needed, but members of the *Leptanilla thai* species group are conspicuously rare in collections from this area compared to mainland Southeast Asia, with only two male morphospecies being known from a single locality south of the Pattani-Kangar Line (Whitmore 1988), with *Leptanilla belantan*, which may represent the worker of either of these. It may be surmised from the distribution of the *Leptanilla thai* species group that this clade originated in subtropical seasonal forests of mainland Southeast Asia or the Indian subcontinent, explosively radiating in the former region and arid habitats of the Western Palaearctic and (marginally) the Afrotropics. The *Leptanilla thai* species group appears to have been mostly unsuccessful in penetrating perhumid equatorial rainforests. I propose that preoccupation of ecological niche space in the Sundan region by the *Leptanilla havilandi* species group is perhaps responsible, given the close functional similarities between the worker phenotypes in these two clades to the exclusion of confirmed worker morphology in the *Leptanilla revelierii* species group.

Leptanilla havilandi species group

Worker diagnosis.

1. Mandible with three teeth.
2. Maxillary palpomere 2-merous.
3. Frontoclypeal process present, apex emarginate.
4. Lateral clypeal teeth absent.
5. Meso-metapleural suture absent.
6. Mesotibia with two spurs.
7. Metatibia with two spurs.
8. Length of abdominal segment II subequal to width in dorsal view.
9. Anterior of abdominal tergite IV not lateromedially constricted in dorsal view.
10. Length of abdominal tergite IV greater than combined length of posterior abdominal tergites in dorsal view.

Gyne diagnosis. Gyne unknown.

Male diagnosis.

1. Mandalus ≥ 0.5× length of the mandible or < 0.5× length of mandible.
2. Mandible never fused to cranium, fully articulated.
3. Anteromedian ocellus orthogonally dorsal to compound eye in profile view or posterior to compound eye.
4. LF2 < SL, rarely LF2 ≈ SL (*Leptanilla copiosa* (Petersen, 1968)).
5. Distal transverse carina present on procoxa (Fig. 29A).
6. Protrochanter not elongated.
7. Profemur not enlarged, or moderately enlarged, sometimes proximally kurtotic.
8. Arcuate medial carina absent from profemur.
9. Apicoventral hook absent from profemur.
10. Ventromedian carina present on protibia.
11. Protibial comb absent.
12. Antero-admedian signum present or absent.
13. Pronotum and mesoscutum anteroposteriorly prolonged.
14. Mesoscutellum without recurved posteroventral process.
15. Adventitious spectral M+Cu absent from forewing.
16. Upper metapleuron indistinct from metapectal-propodeal complex.
17. Lower metapleuron usually distinct from metapectal-propodeal complex, rarely (*L. anomala* (Brues, 1925)) indistinct.
18. Propodeal declivity convex in profile view.
19. Petiole reduced, without distinct dorsal node.
20. Abdominal sternite II without ventral process.
21. Abdominal tergite VIII distinctly longer than broad in posterodorsal view.
22. Abdominal sternite IX completely fused to gonocoxites.
23. Mulceators absent.
24. Cupula absent.
25. Gonopodites articulate.
26. Gonocoxites with complete ventromedian fusion.
27. Gonocoxites with complete dorsomedian fusion.

28. Gonocoxites completely fused to penial sclerites.
29. Gonostyli present.
30. Volsellae absent.
31. ***Inapplicable*.**
32. ***Inapplicable*.**
33. Penial sclerites with complete median fusion.
34. Penial sclerites not dorsoventrally compressed.
35. Phallotreme preapical.
36. Phallotreme dorsal.
37. Dense phallotremal vestiture of setae present or absent.

Larval diagnosis. Larva unknown.

Remarks. This clade is restricted to the Sundan region and the Philippines (Fig. 28). Most known specimens are Bornean in origin. The bizarre males of the *Leptanilla havilandi* species group were first described as the genera *Scyphodon* and *Noonilla*, with *Leptanilla anomala* (Brues, 1925) being regarded as Hymenoptera incertae sedis (Brues 1925). Male morphospecies attributable to *Noonilla* in addition to the type species (*L. copiosa*) were identified and sequenced by Griebenow (2020, 2021). Griebenow et al. (in press) treats this clade as *Scyphodon* s. l., despite not yet having subjected the position of *Scyphodon* relative to *Noonilla* to phylogenetic analysis. Nonetheless, Bayesian total-evidence inference confirms the monophyly of *Scyphodon* s. l. inclusive of *L. havilandi* (pers. obs.), here formally synonymized with *Leptanilla*.

The worker of *L. havilandi* bears a striking resemblance to *L. thai*, including in the presence of an emarginate frontoclypeal process, but is distantly related, demonstrating the morphological conservatism of the worker caste in *Leptanilla*. *Leptanilla clypeata* and *L. hypodracos* are sympatric with the *Leptanilla havilandi* species group, and morphologically like *L. havilandi*, introducing the possibility that these are members of this clade. Given the lack of phylogenetic signal in leptanilline worker morphology, however, this hypothesis must be tested with molecular data.

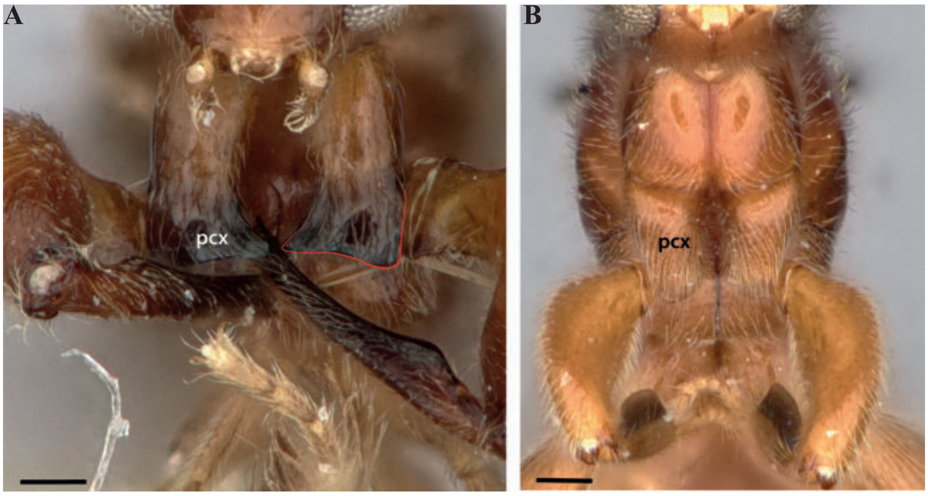

Figure 29. Condition of the male procoxa in *Leptanilla*, anterior view. Distal procoxal carina outlined in red **A** *Leptanilla* cf. *copiosa* (CASENT0842844) **B** *Leptanilla* zhg-my04 (CASENT0842567). Abbreviation: pcx = procoxa. Scale bars: 0.1 mm.

The close affinity of *L. anomala* and *L. copiosa*, to the exclusion of other described Leptanillinae, was not suggested by previous authors who argued for the placement of *L. anomala* within the Leptanillinae (Petersen 1968; Boudinot 2015). This is in part due to the preservation in balsam of the type series of *L. anomala*, a status that conceals autapomorphies of the *Leptanilla havilandi* species group, namely phallotremal setae and the distal transverse carina on the procoxa: examination of CASENT0106168 revealed these character states. In addition, the discovery of additional undescribed male morphospecies within the *Leptanilla havilandi* species group (Griebenow 2020, 2021; Griebenow et al. 2022) revealed intermediates in morphospace, juxtaposing the dorsoventrally compressed head and mesosoma of *L. anomala* with the nub-like, non-spatulate mandibles of *L. copiosa*.

Leptanilla bethyloides species group

Worker diagnosis. Worker unknown.

Gyne diagnosis. Gyne unknown.

Male diagnosis.

1. Mandalus ≥ 0.5× length of the mandible.
2. Mandible never fused to cranium, fully articulated.
3. Anteromedian ocellus posterior to compound eye.
4. LF2 < SL.
5. Distal transverse carina absent from procoxa.
6. Protrochanter not elongated.
7. Profemur not enlarged.
8. Arcuate medial carina absent from profemur.
9. Apicoventral hook absent from profemur.
10. Ventromedian carina absent from protibia.
11. Protibial comb absent.
12. Antero-admedian signum absent.
13. Pronotum and mesoscutum anteroposteriorly prolonged.
14. Mesoscutellum with or without recurved process.
15. Adventitious spectral M+Cu absent from forewing, or present (*Leptanilla* TH01).
16. Upper metapleuron distinct from metapectal-propodeal complex or indistinct.
17. Lower metapleuron distinct from metapectal-propodeal complex or indistinct.
18. Propodeal declivity convex in profile view.
19. Petiole well-developed, with or rarely without distinct dorsal node (*Leptanilla* TH07).
20. Abdominal sternite II with or without ventral process.
21. Abdominal tergite VIII broader than long in posterodorsal view.
22. Abdominal sternite IX posteriorly separate from gonocoxites.
23. Mulceators absent.
24. Cupula present (Griebenow et al. in press).
25. Gonopodites articulate.
26. Gonocoxites without ventromedian fusion.

27. Gonocoxites without complete dorsomedian fusion.
28. Gonocoxites unfused to penial sclerites.
29. Gonostyli present.
30. Volsellae absent.
31. ***Inapplicable*.**
32. ***Inapplicable*.**
33. Penial sclerites with complete median fusion.
34. Penial sclerites dorsoventrally compressed.
35. Phallotreme apical.
36. Dense phallotremal vestiture of setae absent.

Larval diagnosis. Larva unknown.

Remarks. This species group is restricted to mainland Southeast Asia north of the Pattani-Kangar Line (Fig. 30), with the type locality of *L. bethyloides* being their northernmost known extent. Like the *Leptanilla najaphalla* species group, the *Leptanilla bethyloides* species group is known only from male specimens. These are never abundant in known collections, with it therefore appearing that this species group exhibits genuine rather than artifactual rarity; no exemplars

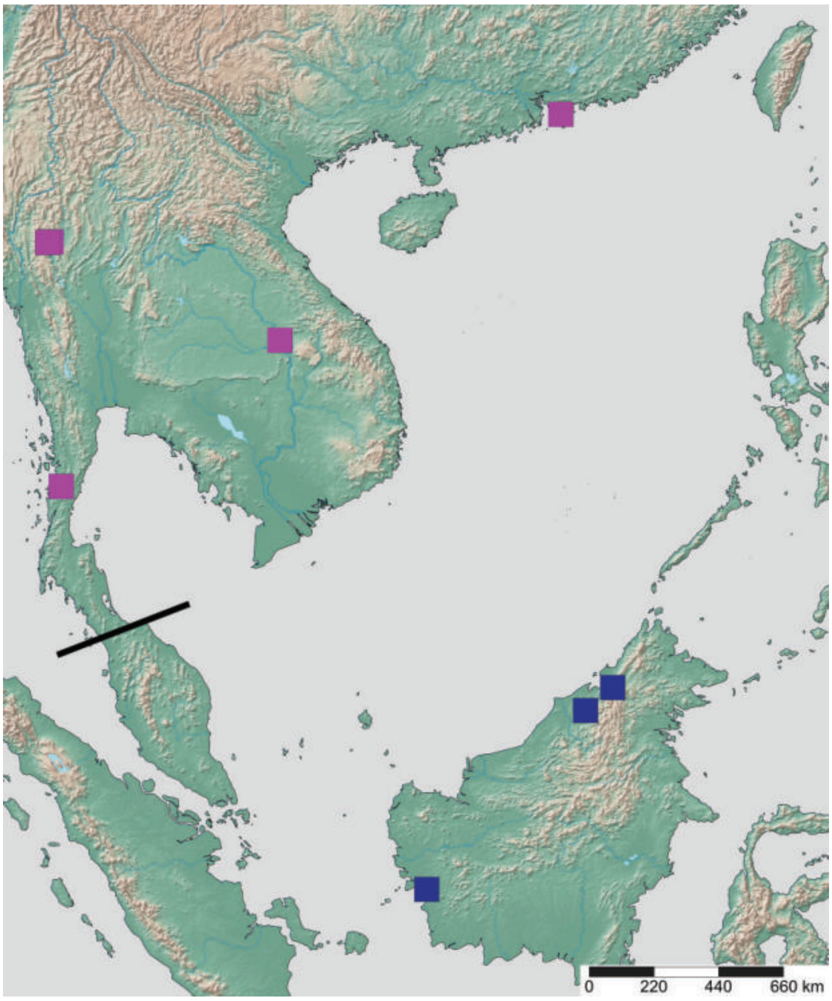

Figure 30. Geographical range of the *Leptanilla bethyloides* species group (pink) and the *Leptanilla najaphalla* species group (blue). Pattani-Kangar Line indicated in black. Locality information derived from AntWeb and visualized with SimpleMappr.

of this clade were described in detail by Griebenow et al. (in press), meaning that the male genital skeletomusculature of the *Leptanilla bethyloides* species group is more poorly understood than that of any other major leptanilline clade.

Volsellae are completely absent in *Leptanilla* zhg-mm03 (CASENT0842829), in a homoplasy with the *Leptanilla havilandi* species group (Griebenow et al. in press). The total absence, as opposed to extreme reduction, of the volsellae cannot yet be definitively confirmed for any other representatives of the *Leptanilla bethyloides* species group due to a lack of specimens for study.

The *Leptanilla bethyloides* species group qualitatively possesses male morphological diversity disproportionate to the depauperation of known lineages: the condition of the metapleuron varies from completely indiscernible (*Leptanilla* TH07) to both the upper and lower metapleuron being completely visible (e.g., *L. bethyloides*). However, the lower metapleuron is never distinct from the metapectal-propodeal complex in the absence of the same distinction for the upper metapleuron, as in most of the *Leptanilla havilandi* species group. Other conditions unusual among *Leptanilla* that are sporadically observed in the *Leptanilla bethyloides* species group include elongated antennomeres, a posteriorly recurved mesoscutellum (both only observed in *Leptanilla* zhg-th01), and a dorsomedian penial carina (*Leptanilla* TH01).

Leptanilla najaphalla species group

Worker diagnosis. Worker unknown.

Gyne diagnosis. Gyne unknown.

Male diagnosis.

1. Mandalus ≥ 0.5× length of the mandible.
2. Mandible never fused to cranium, fully articulated.
3. Anteromedian ocellus posterior to compound eye.
4. LF2 < SL.
5. Distal transverse carina absent from procoxa.
6. Protrochanter not elongated.
7. Profemur enlarged, sometimes markedly constricted proximally.
8. Arcuate medial carina absent from profemur.
9. Apicoventral hook present or absent from profemur.
10. Ventromedian carina absent from protibia.
11. Protibial comb present.
12. Antero-admedian signum absent.
13. Pronotum and mesoscutum anteroposteriorly prolonged.
14. Mesoscutellum without recurved posterodorsal process.
15. Adventitious spectral M+Cu present in forewing.
16. Upper metapleuron indistinct from metapectal-propodeal complex.
17. Lower metapleuron indistinct from metapectal-propodeal complex.
18. Propodeal declivity convex in profile view, with distinct dorsal and posterior faces, dorsal face parallel to craniocaudal axis.
19. Petiole well-developed, with distinct dorsal node.
20. Abdominal sternite II with or without ventral process.
21. Abdominal tergite VIII broader than long in posterodorsal view.
22. Abdominal sternite IX with narrow posteromedian fusion to gonocoxites.

23. Mulceators present.
24. Cupula absent or present (*Leptanilla* zhg-id01), if present then fused anteriorly to abdominal sternite IX and posteriorly to gonocoxites (Griebenow et al. in press).
25. Gonopodites inarticulate.
26. Gonocoxites with complete dorsomedian fusion.
27. Gonocoxites with complete ventromedian fusion.
28. Gonocoxites fused to penial sclerites or unfused.
29. Gonostyli present or absent.
30. Volsellae present.
31. Volsellae medially fused.
32. Volsella never furcated, although paired, recurved cuticular processes may be present at apex.
33. Penial sclerites with complete median fusion.
34. Penial sclerites lateromedially compressed or subcircular in cross-section.
35. Phallotreme apical or subapical.
36. Phallotreme dorsal or ventral.
37. Dense phallotremal vestiture of setae absent.

Larval diagnosis. Larva unknown.

Remarks. This clade remains known only from males, necessitating the regrettable description of a species based solely upon male material (*L. najaphalla*) to provide the "Bornean morphospecies group" (Griebenow 2020, 2021) with an informal species group name. The males of the *Leptanilla najaphalla* species group are flagrantly bizarre, defined by such autapomorphies as a protibial comb composed of parallel-sided cuticular processes (previously misidentified as setae; Griebenow 2020, 2021), the complete median fusion of the volsellae at the base, and the presence of mulceators. It appears that the protibial comb is serially homologous with the probasitarsal comb, a structure synapomorphic for the Hymenoptera (Basibuyuk and Quicke 1995). While the protibial comb and mulceators are unparalleled in the Hymenoptera, the medial fusion of the volsellae is also observed in *Sceliphron caementarium* (Drury, 1773) (Sphecidae: Sceliphrini) (Schulmeister 2003: fig. 11C).

Micro-CT scans reveal that all 7 morphospecies sampled in Griebenow et al. (in press) (including *L. najaphalla*, as *Leptanilla* zhg-my02) show posteromedian fusion of abdominal sternite IX to the gonocoxites, an apomorphy apparently derived independently from the anatomical condition observed in the *Leptanilla havilandi* species group (Griebenow et al. in press). This species group is robustly supported as sister to the *Leptanilla havilandi* species group (Griebenow 2020, 2021; Griebenow et al. 2022), which likewise is restricted to the Sundan region. Despite this phylogenetic position, no unequivocal male morphological synapomorphies are known for the two clades, with the fusion of S9 to the gonocoxites, and medial fusion of the gonocoxites, being perhaps homoplasious between the two according, given a lack of the Remanean homology criterion of "special quality" (Griebenow et al. in press). Further Winkler and pitfall sampling in the Sundan region, particularly Borneo, will be required to collect the unknown female castes of the *Leptanilla najaphalla* species group. It is also possible that *Leptanilla butteli* Forel, 1913 and *Leptanilla kebunraya* Yamane &

Ito, 2001, the worker morphology of which is aberrant among *Leptanilla*, are representatives of this clade.

Leptanilla revelierii species group

Worker diagnosis.

1. Mandible with 3–4 teeth.
2. Maxillary palpomere 1-merous.
3. Frontoclypeal process absent or present, never emarginate.
4. Lateral clypeal teeth absent.
5. Meso-metapleural suture absent or present (*Leptanilla hunanensis*).
6. Mesotibia with 0–1 spur.
7. Metatibia with two spurs.
8. Length of abdominal segment II subequal to width in dorsal view.
9. Anterior of abdominal tergite IV not lateromedially constricted in dorsal view.
10. Length of abdominal tergite IV equal or less than combined length of posterior abdominal tergites in dorsal view.

Gyne diagnosis. As for the genus, but petiole quadrate to distinctly broader than long in dorsal view.

Male diagnosis.

1. Mandalus ≥ 0.5× length of the mandible.
2. Mandible never fused to cranium, fully articulated.
3. Anteromedian ocellus posterior to compound eye.
4. LF2 < SL.
5. Distal transverse carina absent from procoxa.
6. Protrochanter rarely elongated (*Leptanilla* ci01) (Fig. 31) or not elongated.
7. Profemur enlarged or not enlarged.
8. Arcuate medial carina present on profemur (*Leptanilla* ci01) (Fig. 31) or absent from profemur.
9. Apicoventral hook absent from profemur.
10. Ventromedian carina absent from protibia.
11. Protibial comb absent.
12. Antero-admedian signum absent.
13. Pronotum and mesoscutum anteroposteriorly prolonged.
14. Mesoscutellum without recurved posterodorsal process.
15. Adventitious spectral M+Cu absent from forewing.
16. Upper metapleuron indistinct from metapectal-propodeal complex.
17. Lower metapleuron indistinct from metapectal-propodeal complex.
18. Propodeal declivity convex in profile view.
19. Petiole well-developed, with or without distinct dorsal node.
20. Abdominal sternite II with or without ventral process.
21. Abdominal tergite VIII broader than long in posterodorsal view or rarely longer than broad in posterodorsal view (*Leptanilla* ci01).
22. Abdominal sternite IX posteriorly separate from gonocoxites.
23. Mulceators absent.

24. Cupula absent or present (*L. astylina*).
25. Gonopodites articulate, rarely inarticulate (*Leptanilla exigua* Santschi, 1908).
26. Gonocoxites with ventromedian fusion partial to complete (*L. astylina*).
27. Gonocoxites without complete dorsomedian fusion.
28. Gonocoxites unfused to penial sclerites.
29. Gonostyli present.
30. Volsellae present.
31. Volsellae medially separate.
32. Volsella entire.
33. Penial sclerites with complete median fusion.
34. Penial sclerites dorsoventrally compressed, rarely lateromedially compressed (*L. astylina*, *Leptanilla* zhg-na01).
35. Phallotreme apical or subapical.
36. Phallotreme dorsal.
37. Dense phallotremal vestiture of setae absent.

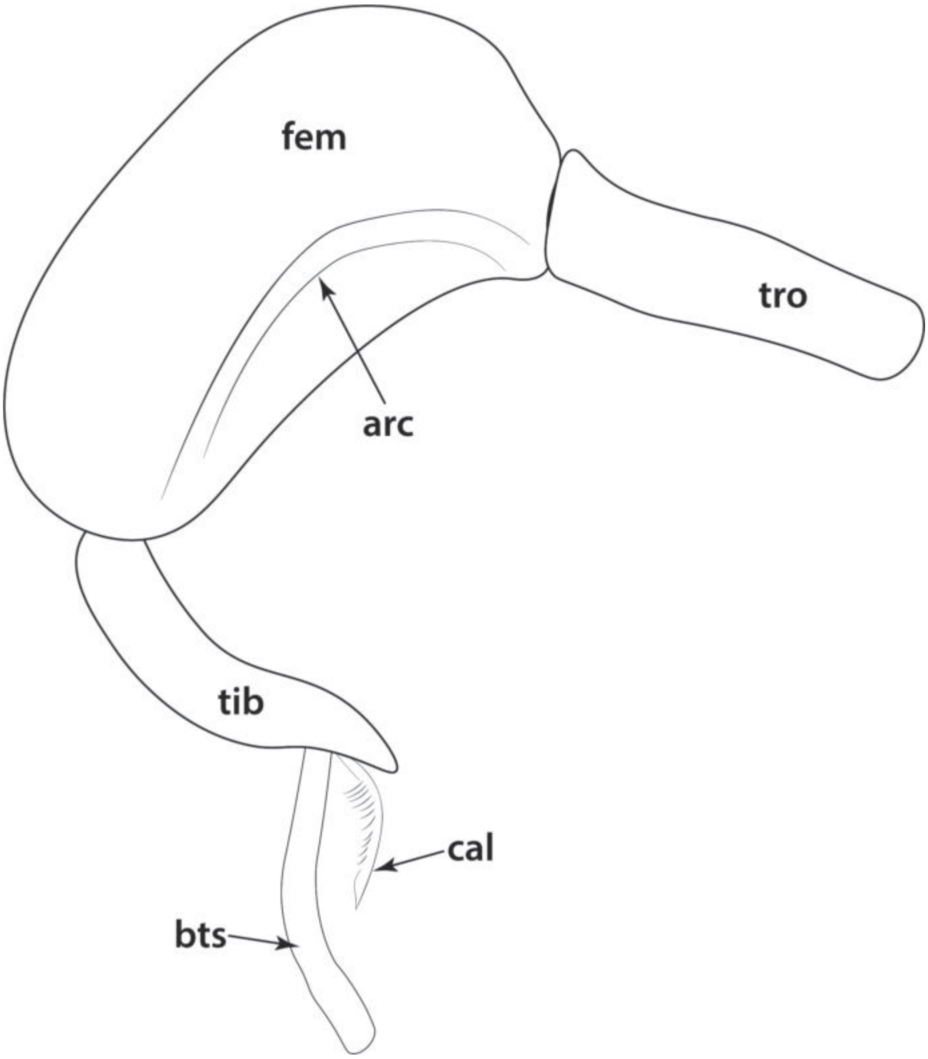

Figure 31. Foreleg of *Leptanilla* ci01, medial view, diagrammatic. Abbreviations: arc = arcuate medial carina; bts = probasitarsus; cal = calcar; fem = profemur; tib = protibia; tro = protrochanter.

Larval diagnosis. As for genus.

Remarks. The *Leptanilla revelierii* species group is by far the most geographically widespread clade within the Leptanillinae and correspondingly is the most speciose. *Leptanilla revelierii* Emery was the first species within the Leptanillinae to be scientifically described, while *Leptanilla japonica* Baroni Urbani is the leptanilline species that has been subjected to the most bionomic study. This is the only leptanilline clade to have expanded its range west of the Arabian subcontinent, radiating extensively throughout the Afrotropics and the Mediterranean Basin (Fig. 32). It does not appear that this species group extends into temperate latitudes of the Western Palaearctic, but *Leptanilla alexandri* Dlussky, 1969 is reported from Uzbekistan (Dlussky 1969). The *Leptanilla revelierii* species group, with the *Protanilla rafflesi* species group, are the sole leptanilline clades confirmed to range into the Eastern Palaearctic and occupy fully temperate climates (Fig. 33). In addition, the *Leptanilla revelierii* species group is so far the only clade within the Leptanillinae known to have traversed Wallace's Line. The apparent ease with which this clade has radiated across the Old World is striking when compared to its sister, which remains restricted to only a portion of the Indo-Malayan ecoregion.

Leptanilla swani Wheeler is the sole species of *Leptanilla* to be described from Australia, although the undescribed species-level diversity of *Leptanilla* from that continent is conspicuous, with richness highest in Queensland. Male specimens are known from as far south as the Australian Capital Territory.

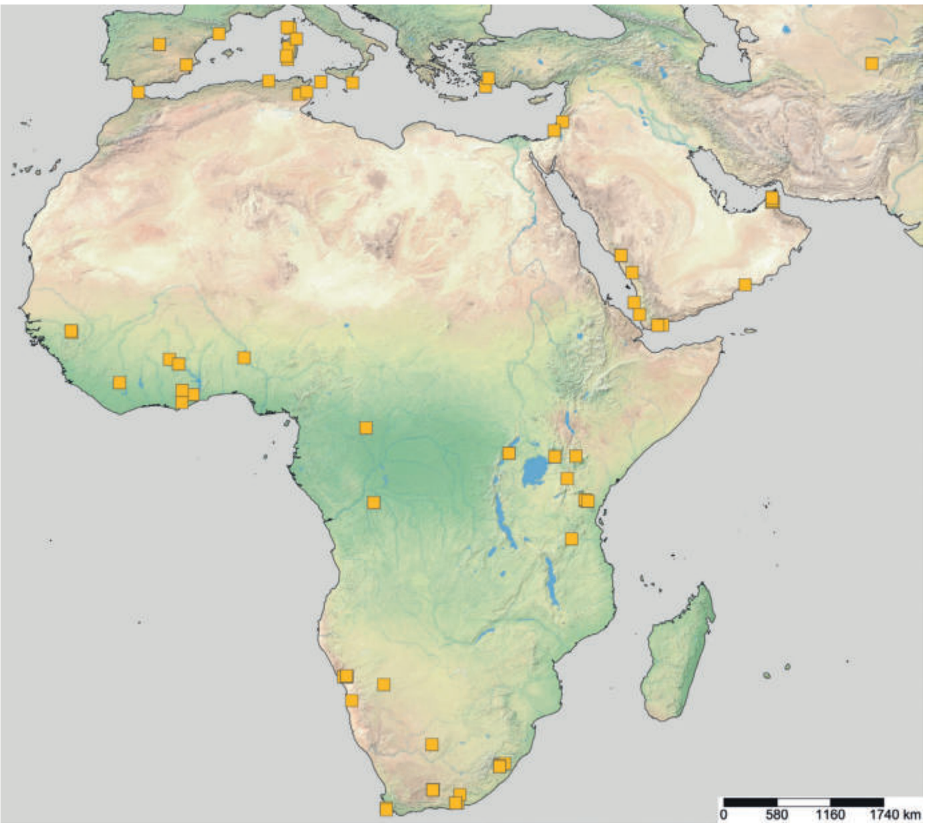

Figure 32. Geographical range of the *Leptanilla revelierii* species group in the Western Palaearctic and Afrotropics. Locality information derived from AntWeb and available literature, visualized with SimpleMappr.

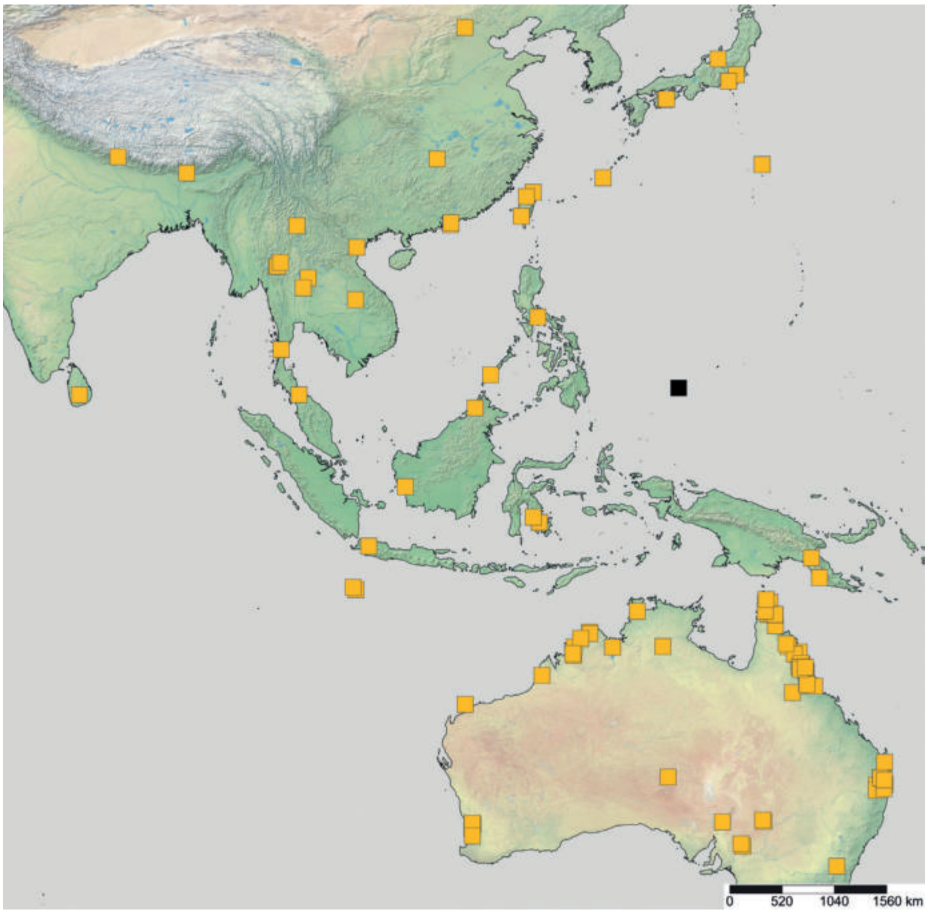

Figure 33. Geographical range of the *Leptanilla revelierii* species group (yellow) and *Leptanilla palauensis* (black) in the Eastern Palaearctic, Indo-Malaya, and Australasia. Locality information derived from AntWeb and available literature, visualized with SimpleMappr.

Leptanilla zhg-au06 is known from a single male specimen collected on Christmas Island, in what may be a human-mediated introduction. Contrary to the suggestion of Wheeler (1932) that *Leptanilla* are relict elements of the Australian ant fauna, the *Leptanilla revelierii* species group can be assumed to be recent arrivals to Australasia from the Indo-Malayan ecoregion. There is also a great undescribed diversity of the *Leptanilla revelierii* species group in the Afrotropics, with no fewer than nine male morphospecies purportedly being collected at the Brandberg Massif in Namibia (Robertson 2000). Malaise trapping in conjunction with syntopic soil sampling in the Afrotropics and Australasia will surely yield a large trove of new species belonging to the *Leptanilla revelierii* species group. Collections of the *Leptanilla revelierii* species group in the Indo-Malayan ecoregion remain scanty compared to sympatric members of other species groups of *Leptanilla*.

Leptanilla ci01 is here provisionally considered to belong to the *Leptanilla revelierii* species group, despite its extreme deviation from the male morphology observed in the rest of that clade, since (1) Bayesian total-evidence inference excludes this aberrant morphospecies from all other major *Leptanilla* clades with posterior probability greater than 0.95 (pers. obs.) and (2) no other clade of *Leptanilla* is known to exist in sub-Saharan Africa. Bayesian total-evidence inference likewise excludes *L. astylina* from all clades within the Leptanillinae besides the *Leptanilla revelierii* species group, with high posterior probability (pers. obs.). What were interpreted as “medially fused volsellar plates” by Petersen (1968: 581) appear in fact to be the gonocoxites, with the “large, valve-like” sclerites interpreted as the gonocoxites (Petersen 1968: 581) therefore corresponding to the gonostyli—the putative absence of gonostyli referred to by the specific epithet of *L. astylina* is therefore false. Even with this reinterpretation, the male genitalia in *L. astylina* deviate from what is observed in the rest of the *Leptanilla revelierii* species group, conspicuously in the presence of a cupula (Ogata et al. 1995), complete ventromedian fusion of the gonocoxites and the medial separation of the penial sclerites shown in Petersen (1968: figs 3, 4), which could not be confirmed by examination of the holotype. The medial concavity and ellipsoid outline of the gonostylus (Petersen 1968: fig. 3) is also aberrant among the *Leptanilla revelierii* species group, as is the lateral concealment of the gonocoxite by the gonostylus (Petersen 1968: fig. 5) and the exposure of the volsellae. *Leptanilla astylina* may be sister to the remainder of the *Leptanilla revelierii* species group.

Despite the variety and vast geographical range of the *Leptanilla revelierii* species group, male morphology within the clade is quite homogeneous relative to the other major subclades of *Leptanilla* for which males are known, particularly when compared to the species-poor *Leptanilla havilandi* and *Leptanilla najaphalla* species groups. The dramatic innovation observed across the male phenotype of *Leptanilla* ci01 is striking when considered in this context.

Incertae sedis

Molecular data are unavailable for these species of *Leptanilla*; even with the contextualization of leptanilline morphology onto a well-resolved phylogeny inferred from molecular data or jointly from those data and discretized male morphology (Griebenow 2021), these species cannot be confidently placed to the species groups delimited here, due to morphological evidence that is equivocal in phylogenetic signal or too aberrant to be of comparative use. *Leptanilla clypeata* Yamane & Ito, 2001 is known from both the worker and gyne; *Leptanilla palauensis* (M.R. Smith, 1953) from the male alone; and the remaining species only from the worker caste. Most of these morphospecies are known only from the Indo-Malayan ecoregion.

Leptanilla clypeata and *L. hypodracos* are very similar to one another, and closely conform to the worker-based diagnosis of the sympatric *Leptanilla havilandi* species group and the parapatric *Leptanilla thai* species group. The palpal formulae of these species would provide further evidence as to their phylogenetic position, but have not been described, and I was not able to obtain specimens for study. These species differ from the *Leptanilla havilandi* and *thai* species groups only in the emargination of the anterior petiolar margin in dorsal view. Worker morphology is quite invariable across *Leptanilla*, and so the phylogenetic significance of this character state cannot be extrapolated; given the relative morphological conformity of the worker caste between the phylogenetically distant *L. havilandi* and *L. thai*, even the phylogenetic affinity of *L. clypeata* and *L. hypodracos* with one another cannot be assumed without corroboration.

Leptanilla butteli resembles the *Leptanilla revelierii* species group overall but differs from the members of that clade in having two mandibular teeth rather than three or four, and abdominal sternite II projecting distinctly below the level of abdominal sternite III along the dorsoventral axis (Baroni Urbani 1977: fig. 25). *Leptanilla kebunraya* joins *L. butteli* in being one of the only two *Leptanilla* species in which the worker mandible has two teeth, but otherwise bears little apparent resemblance to *L. butteli* to the exclusion of other *Leptanilla*. *L. kebunraya* is unique among known *Leptanilla* in having anterolateral frontoclypeal projections, which invite comparison with the lateral clypeal teeth of *Feroponera ferox* Bolton & Fisher, 2008 (Ponerinae: Ponerini). This is of no help in inferring the function of these structures in *L. kebunraya* since the biology of *F. ferox* is largely unknown (Bolton and Fisher 2008).

Leptanilla palauensis was described as the first known male of *Probolomyrmex* Mayr (Proceratiinae: Probolomyrmecini), without associated workers or gynes (Smith 1953), and is still known only from the holotype. Taylor (1965) tentatively transferred the species to *Leptanilla*, with Petersen (1968) following this classification with some reservation, noting that William Brown and Edward O. Wilson doubted it was even an ant. Griebenow (2021) briefly mentioned *L. palauensis*, noting that examination of the holotype confirmed its placement within *Leptanilla* s. l. (Griebenow 2021: 628). This phylogenetic position is confirmed by Bayesian total-evidence inference (pers. obs.); however, the exact phylogenetic position of this morphospecies within *Leptanilla* remains poorly resolved, and the combination of character states observed in in *L. palauensis* excludes the species from all species groups of *Leptanilla* here delimited. The lateromedial compression of the penial sclerites, in conjunction with well-developed volsellae, perhaps implies a phylogenetic relation with the *Leptanilla najaphalla* species group, or with *Leptanilla* zhg-my08 (for which molecular data are unavailable), also incertae sedis; both these lineages are known only from Borneo. *L. palauensis* is a striking biogeographical outlier among the Leptanillinae, being known only from the volcanic island of Babeldaob in Palau, and therefore the only known leptanilline from Oceania (Fig. 33). All known *Leptanilla* gynes are flightless, limiting their dispersal capabilities, but the remote location of *L. palauensis* is paralleled by the presence of *Leptanilla oceanica* Baroni Urbani in the Ogasawara Islands (Baroni Urbani 1977).

Almost nothing is known of the biology of *Leptanilla butteli*, *L. kebunraya*, and *L. hypodracos*. Among *Leptanilla*, our biological knowledge of *L. clypeata* is second in comprehensiveness only to that available for *L. japonica*, with Ito and Yamane (2020) providing observations of live colonies, including feeding and egg-laying behavior. Billen et al. (2022) and Billen and Ito (2022) thoroughly described the exocrine glands of worker *L. clypeata*, with the dorsoproximal intramandibular gland discovered in this species being novel for the Formicidae.

Unplaced to species group

Molecular data are unavailable for *Leptanilla santschii* Wheeler & Wheeler, 1930, which is known only from the male holotype. The club-like volsellae and absent gonostyli of *Leptanilla santschii* (Wheeler and Wheeler 1930: fig. 2D; Petersen 1968) would exclude this species from the *Leptanilla revelierii* species group, if the description of Wheeler and Wheeler (1930) is accurate, but with the holotype missing (Stefan Cover, pers. comm. 2020), morphological data are too limited to permit Bayesian total-evidence inference to test this hypothesis.

Worker-based keys to the Leptanillinae

Most subclades of the Leptanillinae show strong morphological conservatism in the worker caste. It is consequently difficult to assess the scope of intraspecific phenotypic variation in workers, and the sparseness of collected specimens prevents algorithmic species delimitation using molecular data. Therefore, morphospecies known only from a single specimen are excluded from the following keys, even if phylogenomic data are available therefrom and no new species are described in this study based upon worker singletons. Any such species hypothesis would be weak due to lack of comparative context, and be falsifiable simply by the discovery of additional specimens (Bond et al. 2022).

1 Abdominal segment III not petiolate (Fig. 34A); occiput visible in full-face view (Opamyrmini) .... ***Opamyrma hungvuong*** **Yamane et al., 2008 (VIETNAM: Ha Tinh, Son La; CHINA: Hainan, Guangxi)**

– Abdominal segment III petiolate (Fig. 34B, C); occiput not visible in full-face view (Leptanillini)... **2**

2 Clypeus extending posteriorly between antennal toruli (Fig. 22A); epistomal sulcus present medially (*Protanilla*) **3**

– Clypeus not extending posteriorly between antennal toruli (Fig. 22B); epistomal sulcus indistinct medially (*Leptanilla*) **6**

3 Abdominal tergite II without distinct posterior face (Fig. 34C); clypeus oblate-trapezoidal in full-face view; peg-like chaetae absent from mandible .... ***Protanilla taylori* species group (p. 150)**

– Abdominal tergite II with distinct posterior face (Fig. 34B); clypeus campaniform in full-face view; peg-like chaetae present on mandible **4**

4 Clypeus oblate-trapezoidal in outline, elevated above frons posteriorly (Fig. 35A); mandible bowed along anteroposterior axis of cranium............. .... ***Protanilla izanagi* Terayama, 2013 (JAPAN: Honshu)**

– Clypeus campaniform in outline (Fig. 1B), not elevated above frons posteriorly (Fig. 35B); mandible straight **5**

5 Mesotibia with one spur; mandible without laterodorsal longitudinal groove; anterior margin of clypeus concave .... ***Protanilla bicolor* species group (p. 150)**

– Mesotibia without spurs; mandible with laterodorsal longitudinal groove; anterior margin of clypeus planar ....***Protanilla rafflesi* species group (p. 150)**

6 Anterior margin of cranium with median process.. **7**

– Anterior margin of cranium without median process **10**

7 Frontoclypeal process entire; length of abdominal tergite IV usually less than combined length of abdominal tergites V–VII in dorsal view, sometimes subequal ....***Leptanilla revelierii* species group (in part) (p. 152)**

– Frontoclypeal process emarginate; length of abdominal tergite IV usually greater than combined length of abdominal tergites V–VII in dorsal view, sometimes subequal.. **8**

8 Anterior margin of petiolar node entire in dorsal view (Leong et al. 2018: fig. 13A, D) .... ***Leptanilla thai* species group, *Leptanilla havilandi* species group (p. 152)**

– Anterior margin of petiolar node emarginate in dorsal view (Leong et al. 2018: fig. 13E, F).. **9**

9 In full-face view, mandible with most proximal tooth long and well-defined; petiolar node almost twice as long as wide in dorsal view; postpetiolar node longer than wide in dorsal view .... ***Leptanilla hypodracos*** **Wong & Guénard, 2016 (SINGAPORE)**

– In full-face view, mandible without most proximal tooth long and well-defined; length and width of petiolar node subequal in dorsal view; postpetiolar node distinctly wider than long in dorsal view ....***Leptanilla clypeata*** **Yamane & Ito, 2001 (INDONESIA: Java)**

10 Mandible with 3–4 teeth ....***Leptanilla revelierii*** **species group (in part) (p. 152)**

– Mandible with 2 teeth...**11**

11 Anterior margin of cranium with anterolateral frontoclypeal projections; abdominal sternites II-III projecting a subequal distance ventrad craniocaudal axis ....***Leptanilla kebunraya*** **Yamane & Ito, 2001 (INDONESIA: Java)**

– Anterior margin of cranium entire; abdominal sternite II projecting distinctly lower than abdominal sternite III.. ....***Leptanilla butteli*** **Forel, 1913 (MALAYSIA: Selangor)**

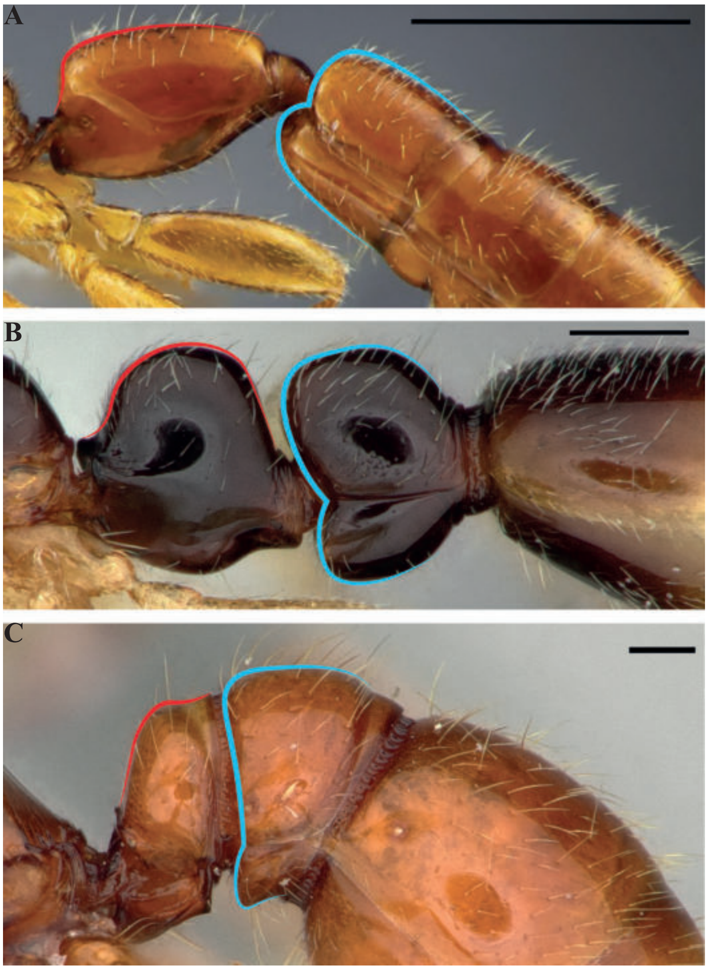

Figure 34. Abdominal segments II–III of female Leptanillinae, profile view. Abdominal tergite II outlined in red; anterior of abdominal segment III outlined in blue **A** *Opamyrma hungvuong* (AKY05vii17-06) (Yamada et al. 2020: fig. 1C), worker **B** *Protanilla gengma* (CASENT0179564), worker **C** *Protanilla* id01 (MCZENT00728282), gyne. Scale bars: 0.5 mm (**A**); 0.2 mm (**B, C**).

Figure 35. Anterior of the worker head in *Protanilla*, full-face view **A** *Protanilla izanagi* (CASENT0842850) **B** *Protanilla jongi* (CASENT0842693). Scale bars: 0.1 mm.

Worker-based key to the *Protanilla taylori* species group

Protanilla taylori comb. nov. and the undescribed *Protanilla* id01 are known only from the gyne, and thus excluded from this key. It does not appear that either *P. taylori* or *Protanilla* id01, which are known only from Borneo, represent the gyne of *P. boltoni* or *P. helenae* (Borowiec et al. 2011).

1 Cranium, pronotum and mesopleuron puncticulate to roughly sculptured; subpetiolar process lacking fenestra in profile view ....***Protanilla boltoni*** **(Borowiec et al., 2011), comb. nov. (MALAYSIA: Perak)**

– Cranium, pronotum and mesopleuron glabrous; subpetiolar process with fenestra in profile view ....***Protanilla helenae*** **(Borowiec et al., 2011), comb. nov. (PHILIPPINES: Palawan)**

Worker-based key to the *Protanilla bicolor* species group

1 Cranium black-brown; anterior face of petiolar node sloping in profile view .... ***Protanilla gengma*** **Xu, 2012 (CHINA: Yunnan; INDIA: Mizoram; VIETNAM: Dong Nai, Bac Giang, Ninh Binh)**

– Cranium yellowish; anterior face of petiolar node subvertical in profile view .... ***Protanilla bicolor*** **Xu, 2002 (CHINA: Yunnan)**

Worker-based key to the *Protanilla rafflesi* species group

Protanilla schoedli Baroni Urbani & de Andrade, 2006 is known only from the gyne (Baroni Urbani and de Andrade 2006) and is excluded from the key. Dias et al. (2019) described the putative worker; however, given known morphological variation in the worker caste among described species of *Protanilla*, I here consider this as representing an undescribed species, related to *Protanilla flamma* Baidya & Bagchi, 2020.

1 Abdominal sternite III linear to slightly concave in profile view; abdominal segments III–IV broadly conjoined, with abdominal tergite III lacking a distinct posterior face **2**

– Abdominal sternite III convex in profile view; abdominal segments III–IV not broadly conjoined, with abdominal tergite III having a distinct posterior face **3**

2 Anterior margin of abdominal tergite IV emarginate in dorsal view; two ventrolateral teeth present on mandible .... ***Protanilla furcomandibula* Xu & Zhang, 2002 (CHINA: Yunnan)**

– Anterior margin of abdominal tergite IV entire in dorsal view; one ventrolateral tooth present on mandible .... ***Protanilla jongi* Hsu et al., 2017 (TAIWAN)**

3 Anterior face of petiolar node concave in profile view **4**

– Anterior face of petiolar node linear in profile view **5**

4 In profile view anterodorsal corner of petiolar node projecting anteriorly; larger species (WL > 0.8 mm) .... ***Protanilla rafflesi* Taylor in Bolton, 1990 (SINGAPORE; MALAYSIA: Sabah, Sarawak)**

– In profile view anterodorsal corner of petiolar node not projecting anteriorly; smaller species (WL 0.70–0.80 mm) ($n = 2$) .... ***Protanilla wardi* Bharti & Akbar, 2015 (INDIA: Kerala)**

5 In dorsal view petiolar node breadth and length subequal; postpetiolar node not inclined anteriorly in profile view **6**

– In dorsal view petiolar node distinctly broader than long; postpetiolar node inclined anteriorly in profile view **9**

6 Coloration castaneous (Fig. 22A); larger species (HL = 0.63–0.70 mm; WL = 0.99 mm) ($n = 1$) .... ***Protanilla beijingensis* Man et al., 2017 (CHINA: Beijing; PAKISTAN: Khyber Pakhtunkhwa)**

– Coloration coppery or yellowish; smaller species (HL = 0.42–0.59 mm; WL = 0.64–0.94 mm) ($n = 16$) **7**

7 Scape not extending beyond occipital vertex of cranium in full-face view (SI ≤ 90); coloration coppery .... ***Protanilla flamma* Baidya & Bagchi, 2020 (INDIA: Goa)**

– Scape extending beyond occipital vertex of cranium in full-face view (SI > 90); coloration yellowish (Fig. 4A–C) **8**

8 Larger species (WL ≥ 0.75 mm) ($n = 2$); postpetiolar node prominent in profile view, with anterior and posterior declivities equally rounded (Fig. 6A) .... ***Protanilla lini* Terayama, 2009 (TAIWAN; JAPAN: Okinawa, Ryukyu Islands; Senkaku Islands)**

– Smaller species (WL < 0.75 mm) ($n = 14$); postpetiolar node shallow in profile view, with posterior declivity more gradual than anterior declivity (Fig. 5B) .... ***Protanilla wallacei* sp. nov. (MALAYSIA: Sabah, Selangor)**

9 Lateral margin of head with acute dorsal mandibular articulation in full-face view; anteroventral corner of sub-post-petiolar process obliquely truncated .... ***Protanilla tibeta* Xu, 2012 (CHINA: Xizang)**

– Lateral margin of head without dorsal mandibular articulation apparent in full-face view (Fig. 24A); anteroventral corner of sub-post-petiolar process rounded **10**

10 Meso-metapleural furrow deeply excavated in profile view; very large species (HW = 0.82–0.84 mm) (*n* = 3) (Satria et al. 2023) .... ***Protanilla eguchii* Satria et al., 2023 (INDONESIA: Sumatra)**

– Meso-metapleural furrow shallowly excavated in profile view; smaller species (HW = 0.48 mm) (*n* = 1).......... ***Protanilla concolor* Xu, 2002 (CHINA: Yunnan)**

Worker-based key to the *Leptanilla thai* species group and *Leptanilla havilandi* species group

1 SI > 100; length of petiole > 3× greater than maximum breadth in dorsal view (Griebenow et al. 2022: fig. 6B).. ***Leptanilla laventa* (Griebenow et al., 2022), comb. nov. (IRAN: Fārs)**

– SI ≤ 100; length of petiole ≤ 3× greater than maximum breadth in dorsal view (Fig. 6A) **2**

2 Length of metasomal setae bimodal **3**

– Length of metasomal setae unimodal **5**

3 Mandible with four teeth, with most proximal tooth truncate (Saroj et al. 2022: fig. 1E); ventromedian lamella of abdominal sternite II denticulate........................***Leptanilla ujjalai* Saroj et al., 2022 (INDIA: West Bengal)**

– Mandible with three teeth, with most proximal tooth not truncate; ventromedian lamella of abdominal sternite II not denticulate....................................**4**

4 Lateral pronotal margins weakly convex in dorsal view; PPTI = 73.68–76.47 (*n* = 11).... ***Leptanilla lamellata* Bharti & Kumar, 2012 (INDIA: Himachal Pradesh)**

– Lateral pronotal margins strongly convex in dorsal view; PPTI = 84.62–85.71 (*n* = 6).............. ***Leptanilla escheri* (Kutter, 1948) (INDIA: Tamil Nadu)**

5 Petiolar length ≥ 2× width **6**

– Petiolar length ≤ 1.5× width **8**

6 Meso-metapleural furrow absent; mandible with four teeth, most proximal tooth distally recurved, apex expanded .... ***Leptanilla belantan* sp. nov. / (MALAYSIA: Selangor)**

– Meso-metapleural furrow present; mandible with three teeth, most proximal tooth acute..**7**

7 Abdominal sternite III no more anteroposteriorly compressed than abdominal tergite III............ ***Leptanilla kunmingensis* Xu & Zhang, 2002 (CHINA: Yunnan)**

– Abdominal sternite III more anteroposteriorly compressed than abdominal tergite III .... ***Leptanilla judaica* Kugler, 1987 (WEST BANK)**

8 Subpetiolar process present, angular; torulus without areolate sculpture (Fig. 27B) ....***Leptanilla havilandi* Forel, 1901 (SINGAPORE; MALAYSIA: Sabah)**

– Subpetiolar process absent; torulus with medial and anterior areolate sculpture (Fig. 27A) ....***Leptanilla thai* Baroni Urbani, 1977 (THAILAND: Khao Chong)**

Worker-based key to the *Leptanilla revelierii* species group

1 Anterior margin of cranium with median process.......................................**2**

– Anterior margin of cranium without median process **4**

2 Mandible with four teeth......***Leptanilla boltoni* Baroni Urbani, 1977 (GHANA)**

– Mandible with three teeth **3**

3 Posteriorly recurved subpetiolar process present; PPI = 122–138 (*n* = 5) .... ***Leptanilla macauensis*** **Leong et al., 2018 (CHINA: Macau)**

– Posteriorly recurved subpetiolar process absent; PPI = 80–86 (*n* = 2) .... ***Leptanilla buddhista*** **Baroni Urbani, 1977 (NEPAL)**

4 Meso-metapleural groove present, impressed on dorsum of mesosoma ... ...***Leptanilla hunanensis*** **Tang et al., 1992 (CHINA: Hubei, Hunan, Yunnan)**

– Meso-metapleural groove absent from dorsum of mesosoma, sometimes faintly impressed on sides **5**

5 Anterior margin of cranium with median emargination..............................**6**

– Anterior margin of cranium entire, linear to convex **9**

6 Four mandibular teeth; greatest width of petiolar node in dorsal view distinctly posterior to midlength .... ***Leptanilla vaucheri*** **Emery, 1899 (MOROCCO)**

– Three mandibular teeth; greatest width of petiolar node in dorsal view not distinctly posterior to midlength **7**

7 Length of abdominal segment II subequal to that of abdominal segment III in dorsal view; abdominal tergite IV narrowed anteriorly in dorsal view (Fig. 36A) .... ***Leptanilla taiwanensis*** **Ogata et al., 1995 (TAIWAN; CHINA: Beijing)**

– Abdominal segment II longer than abdominal segment III in dorsal view; abdominal tergite IV not narrowed anteriorly in dorsal view (Fig. 36B).....**8**

8 Outline of abdominal segment III campaniform in dorsal view; frontoclypeal margin convex ....***Leptanilla oceanica*** **Baroni Urbani, 1977 (JAPAN: Ogasawara Islands)**

– Outline of abdominal segment III subrectangular in dorsal view; frontoclypeal margin linear .... ***Leptanilla swani*** **Wheeler, 1932 (AUSTRALIA: Western Australia)**

9 Mandible with four teeth (subapical tooth sometimes difficult to distinguish) **10**

– Mandible with three teeth **18**

10 Propodeum angular in profile view, with distinct posterior and dorsal faces.........................***Leptanilla ortunoi*** **López et al., 1994 (SPAIN: Ceuta)**

– Propodeum rounded in profile view, without distinct posterior and dorsal faces...**11**

11 Abdominal sternite II emarginate in profile view, with narrow trough-like indentation (Fig. 37A).......***Leptanilla poggii*** **Mei, 1995 (ITALY: Pantellaria)**

– Abdominal sternite II linear in profile view (Fig. 37B) **12**

12 Frontal margin of cranium convex in full-face view; scape strongly constricted at base.........................***Leptanilla nana*** **Santschi, 1915 (TUNISIA)**

– Frontal margin of cranium linear in full-face view; scape moderately constricted at base...**13**

13 Abdominal sternite II with planar face in profile view **14**

– Abdominal sternite II with rounded face in profile view............................**15**

14 Most proximal mandibular tooth large and distinct; abdominal tergite IV distinctly narrowed anteriorly in dorsal view .... ***Leptanilla tanakai*** **Baroni Urbani, 1977 (JAPAN: Yakushima)**

– Most proximal mandibular tooth small and indistinct; abdominal tergite IV not distinctly narrowed anteriorly in dorsal view.......................... ***Leptanilla japonica*** **Baroni Urbani, 1977 (JAPAN: Honshu, CHINA: Hong Kong)**

15 Height of metafemur in anterior view 0.5× metafemoral length in anterior view; coloration beige .... ***Leptanilla charonea*** **Barandica et al., 1994 (SPAIN)**

– Height of metafemur in anterior view < 0.5× of metafemoral length in anterior view; coloration yellowish **16**

16 Larger species (HL = 0.32–0.36 mm) **17**

– Smaller species (HL = 0.22–0.28 mm) (López et al. 1994).........................
.... ***Leptanilla zaballosi*** **Barandica et al., 1994 (SPAIN)**

17 PI = 66–77 (Pérez-González et al. 2020) ....
.... ***Leptanilla plutonia*** **López et al., 1994 (SPAIN)**

– PI = 84.6–100 (Pérez-González et al. 2020)...
...........................***Leptanilla theryi*** **Forel, 1903 (ALGERIA; TUNISIA; SPAIN)**

18 Abdominal sternite II sinuate in profile view...
....***Leptanilla doderoi*** **Emery, 1915 (ITALY: Sardinia)**

– Abdominal sternite II linear to convex in profile view, never sinuate **19**

19 Petiole distinctly wider than long ....
.... ***Leptanilla yunnanensis*** **Xu, 2002 (CHINA: Yunnan)**

– Petiole not distinctly wider than long...**20**

20 Frontal margin convex in full-face view **21**

– Frontal margin linear in full-face view **22**

21 Mesothorax anteriorly constricted in dorsal view ....
...............................***Leptanilla besucheti*** **Baroni Urbani, 1977 (SRI LANKA)**

– Mesothorax not anteriorly constricted in dorsal view..................................
.... ***Leptanilla morimotoi*** **Yasumatsu, 1960 (JAPAN: Kyushu)**

22 Length of abdominal tergite V > 0.5× length of abdominal tergite IV ....
....***Leptanilla revelierii*** **Emery, 1870 (FRANCE: Corsica; ITALY: Sardinia; SPAIN; PORTUGAL; MOROCCO)**

– Length of abdominal tergite V ≤ 0.5× length of abdominal tergite IV **23**

23 Pedicel distinctly longer than wide; abdominal sternite II linear in profile view ....***Leptanilla kubotai*** **Baroni Urbani, 1977 (JAPAN: Shikoku)**

– Pedicel length and width subequal; abdominal sternite II convex in profile view **24**

24 Smaller species (WL < 0.3 mm)...
.... ***Leptanilla okinawensis*** **Terayama, 2013 (JAPAN: Okinawa)**

– Larger species (WL ≥ 0.3 mm) ....
....***Leptanilla acherontia*** **sp. nov. (KENYA; UGANDA)**

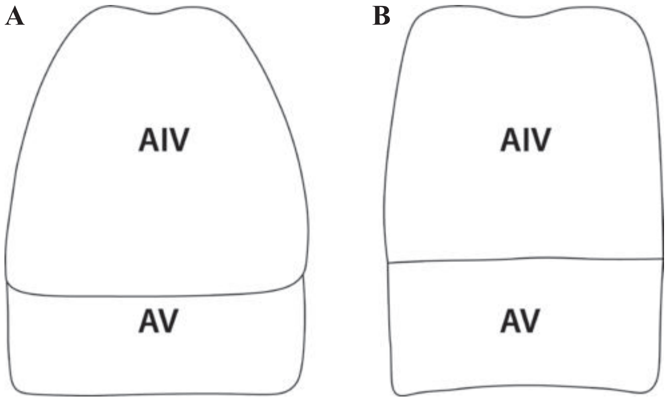

Figure 36. Worker abdominal segments IV-V in *Leptanilla taiwanensis* (**A**) and *Leptanilla oceanica* (**B**), diagrammatic dorsal view. Fig. 36B redrawn from Baroni Urbani (1977: fig. 19).

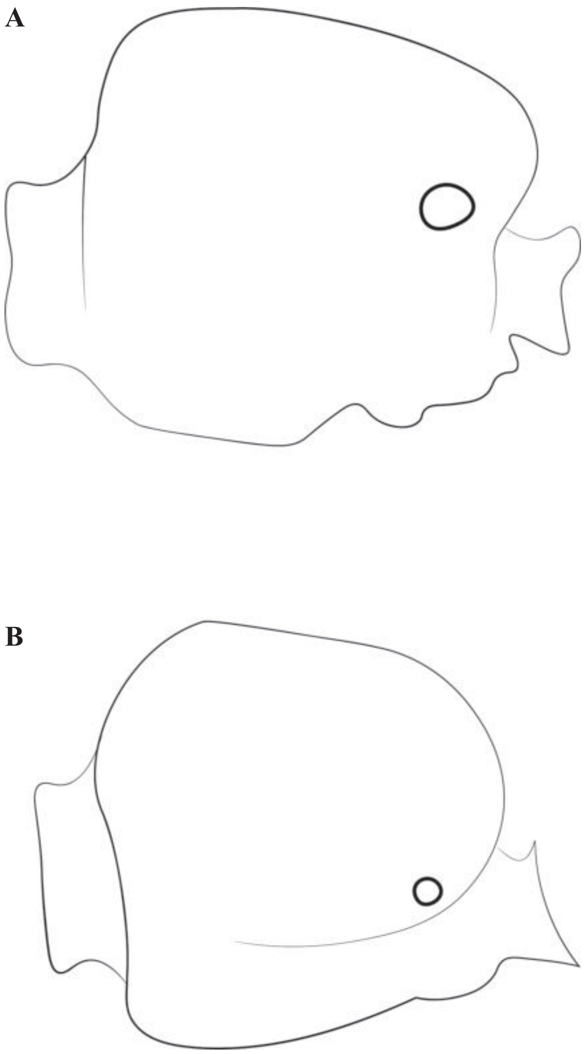

Figure 37. Profile condition of the petiole in the *Leptanilla revelierii* species group **A** *Leptanilla poggii* (after Mei 1995: fig. 4) **B** *Leptanilla theryi* (after Mei 1995: fig. 6).

Male-based key to the major subclades of the Leptanillinae

The following keys are corrected and extended from Griebenow (2020), with updated generic assignments for undescribed morphospecies; concordances of these morphospecies identifiers with previous publications are provided in Table 1. Respective male-based keys to each of the major subclades are subsequently provided.

These include all described species for which males are known, and all undescribed male morphospecies for which molecular data are or soon will be available, except for *Leptanilla* ZA01 (for which only genital morphology is known), *Leptanilla* TH07 and *Leptanilla* zhg-mm14 (for which genital morphology is unknown). Based on phylogenetic inference from both molecular and morphological data (Griebenow 2021; pers. obs.), these three morphospecies belong to the *Leptanilla revelierii* species group, the *Leptanilla bethyloides* species group, and the *Leptanilla thai* species group, respectively. *Leptanilla* zhg-au04 and zhg-au06, of the *Leptanilla revelierii* species group, are also excluded due to lacking observations of the gonopodital apex, making it impracticable to include these morphospecies in the male-based key to that clade.

1 Rs+M and *1m-cu* present (Fig. 38A); parossiculus (=cuspis in part) and lateropenite (=digitus) distinct, articulated (Opamyrmini) .... ***Opamyrma hungvuong*** **Yamane et al., 2008 (VIETNAM: Ha Tinh, Son La; CHINA: Hainan, Guangxi)**

– Rs+M and *1m-cu* absent (Fig. 38B–D); if volsella discernible, parossiculus and lateropenite distinct or indistinct, if distinct then inarticulate (Leptanillini) **2**

2 Pterostigma present (Fig. 39B); ocelli present, with ocellar tubercle absent (Fig. 40A); parossiculus and lateropenite distinct (*Protanilla*) **3**

– Pterostigma absent (Fig. 39A, C); ocelli present or absent, if present then set on ocellar tubercle (Fig. 40B, C), tubercle rarely absent (e.g., *Leptanilla najaphalla* sp. nov.); parossiculus and lateropenite not distinct (*Leptanilla*) **5**

3 MaL < 0.5× ML; apex of mandible acuminate .... ***Protanilla*** **zhg-th02 (THAILAND: Chaiyaphum)**

– ML ≥ 0.5× ML; apex of mandible rounded **4**

4 Abdominal segment III petiolate; abdominal segment IV equal in length to combined length of abdominal segments V–VIII (*Protanilla bicolor* species group) .... ***Protanilla*** **TH03 (THAILAND: Chiang Mai)**

– Abdominal segment III not petiolate; length of abdominal segment IV subequal to, or less than, respective lengths of abdominal segments V–VII ... . ***Protanilla rafflesi*** **species group (p. 161)**

5 Propodeum concave in profile view (Fig. 41A); anteromedian ocellus directly dorsal to compound eye in profile view; pronotum and mesoscutum not posteriorly prolonged................. ***Leptanilla thai*** **species group (p. 162)**

– Propodeum not concave in profile view (Fig. 41B, C); anteromedian ocellus posterad compound eye in profile view, rarely directly dorsal (*Leptanilla copiosa* (Petersen, 1968), comb. nov.); pronotum and mesoscutum posteriorly prolonged.. **6**

6 Propodeum with lateral longitudinal carinae on dorsum; penial sclerites lateromedially compressed .... ***Leptanilla palauensis*** **(M.R. Smith, 1953) (PALAU)**

– Propodeum without lateral longitudinal carinae on dorsum; penial sclerites sometimes lateromedially compressed, more often not..................... **7**

7 Dorsal propodeal face long, parallel to craniocaudal axis (Fig. 41B); mulceators present; protibial comb present (Fig. 42A) .... ***Leptanilla najaphalla*** **species group (p. 167)**

– Dorsal propodeal face short, with propodeal outline in profile view convex, if long and parallel to craniocaudal axis then upper metapleuron distinct from metapectal-propodeal complex; mulceators absent; protibial comb absent (Fig. 42B) **8**

8 Procoxa with distal transverse carina (Fig. 29A); phallotreme surrounded with decumbent setae, rarely bare (*Leptanilla* zhg-ph01); if lower metapleuron distinct from metapectal-propodeal complex then upper metapleuron not distinct .... ***Leptanilla havilandi*** **species group (p. 169)**

– Procoxa without distal transverse carina (Fig. 29B); phallotreme bare; lower metapleuron usually indistinct from metapectal-propodeal complex, if distinct then upper metapleuron distinct.. **9**

9 Metapleuron at least partly distinct; vestiture dense and pubescent; volsellae apparently absent ..... ***Leptanilla bethyloides* species group (p. 169)**

– Metapleuron never distinct; vestiture rarely dense, never pubescent; volsellae present **10**

10 Gonostylus absent; volsella distally expanded; Sc+R+Rs and Rf1 nebulous, *2s-rs*+Rsf4-6 absent .... ***Leptanilla santschii* Wheeler & Wheeler, 1930 (INDONESIA: Java)**

– Gonostylus present, articulated to gonocoxite, rarely inarticulate (*Leptanilla exigua* Santschi, 1908); volsella never distally expanded; Sc+R+Rs and Rf1 present or rarely absent, *2s-rs*+Rsf4-6 present or absent .... ***Leptanilla revelierii* species group (p. 169)**

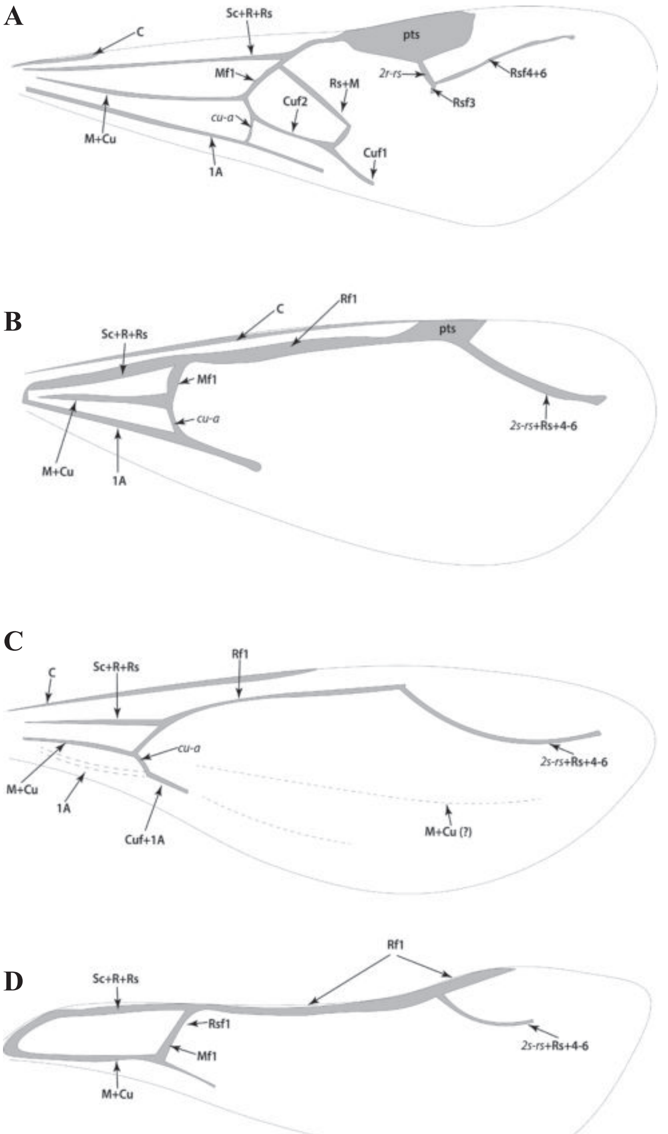

Figure 38. Exemplars of male wing venation across the Leptanillinae, diagrammatic **B, C** are typological generalizations of male wing venation in the clades that they represent **A** *Opamyrma hungvuong* **B** *Protanilla* **C** *Leptanilla najaphalla* species group **D** *Leptanilla javana*. Abbreviation: pts = pterostigma.

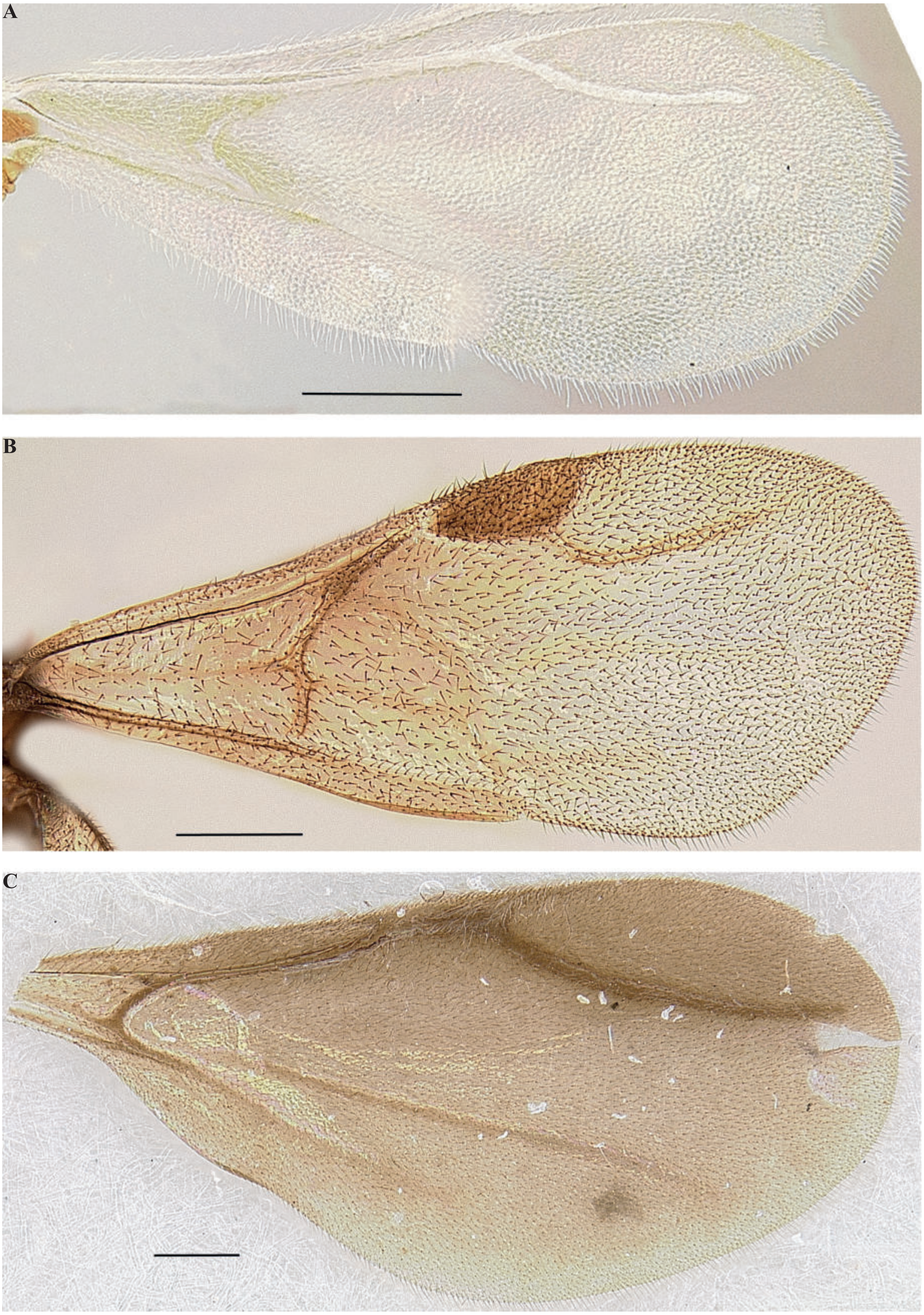

Figure 39. Condition of the pterostigma across the Leptanillini, mal **A** *Leptanilla indica* (CASENT0106380) **B** *Protanilla* zhg-vn01 (CASENT0842613) **C** *Leptanilla* zhg-my05 (CASENT0842571). Scale bars: 0.25 mm (**A, B**); 0.2 mm (**C**).

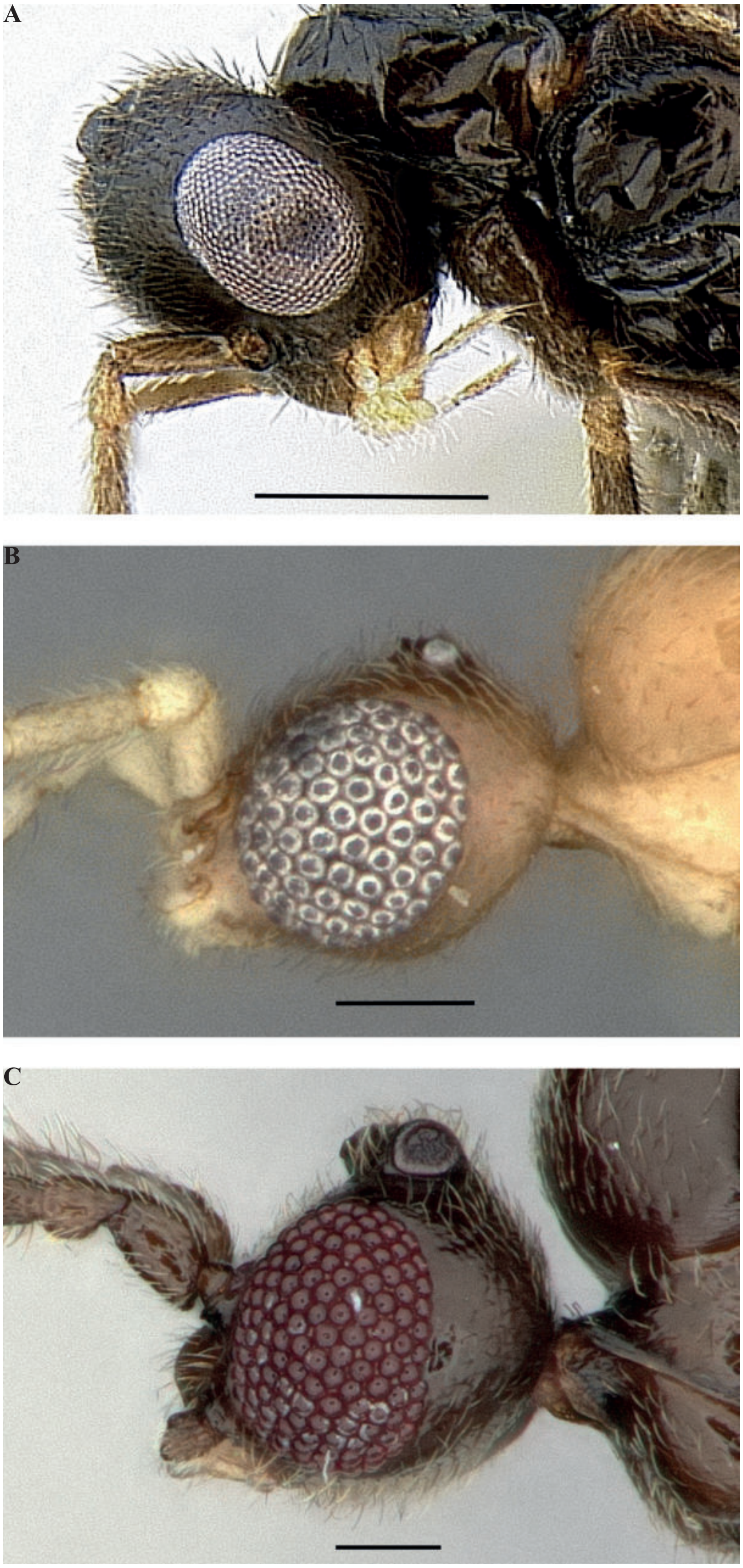

Figure 40. Condition of the male ocelli in the Leptanillini, profile view **A** *Protanilla lini* (OKENT0011097) **B** *Leptanilla indica* (CASENT0106366) **C** *Leptanilla argamani* (CASENT0235253). Scale bars: 0.25 mm (**A**); 0.1 mm (**B, C**).

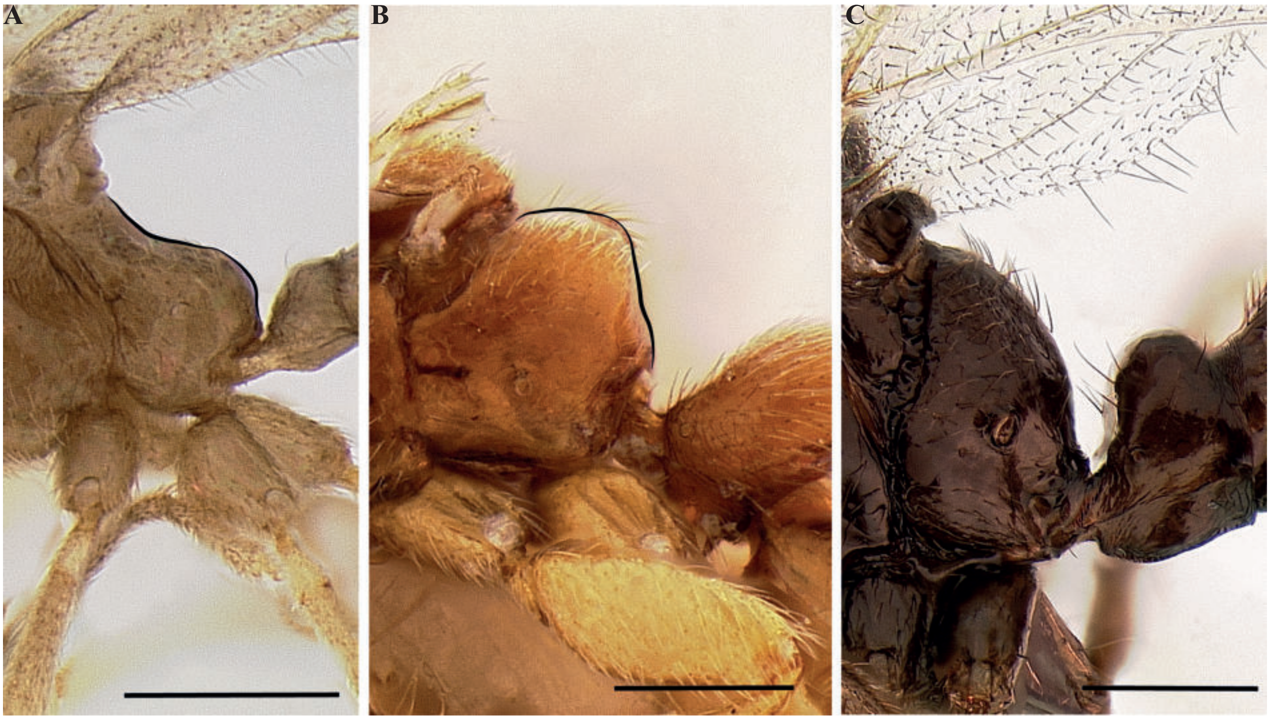

Figure 41. Propodeal outline in profile view across male Leptanillini, after Griebenow (2021: fig. 17). Propodeum outlined in black in Fig. 16A–C **A** *Leptanilla* zhg-bt03 (CASENT0106384) **B** *Leptanilla* zhg-my02 (CASENT0106456) **C** *Protanilla lini* (OKENT0011097). Scale bars: 0.15 mm (**A, C**); 0.2 mm (**B**).

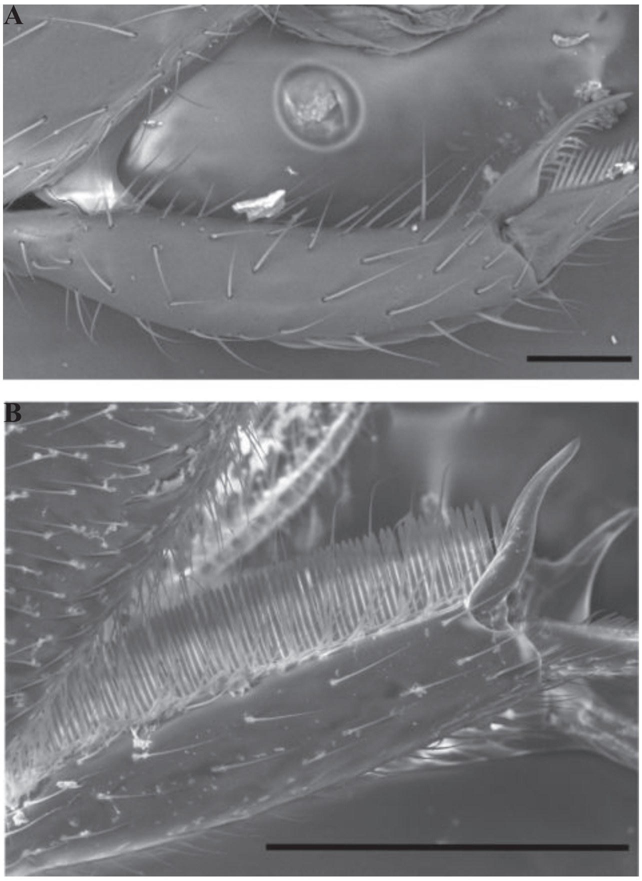

Figure 42. Protibia in male *Leptanilla*, posterior view **A** *Leptanilla* zhg-my11 (CASENT0842593) **B** *Leptanilla* zhg-my04 (CASENT0842555). Scale bars: 0.05 mm (**A**); 0.2 mm (**B**).

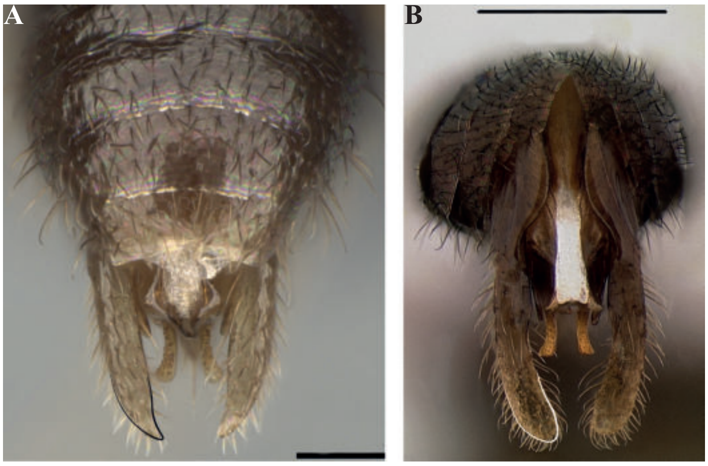

Figure 43. Gonostyli in *Protanilla*, posterodorsal view. After Griebenow (2020: fig. 9C) **A** *Protanilla* TH01 (CASENT0119776; Michele Esposito) **B** *Protanilla lini* (OKENT0011097). Scale bars: 0.1 mm (**A**); 0.5 mm (**B**).

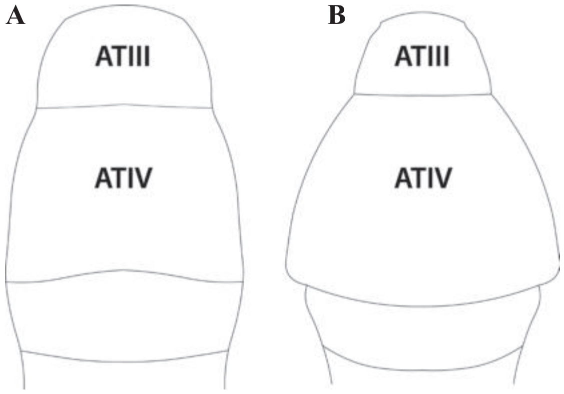

Figure 44. Proportions of male abdominal tergites III-IV in *Protanilla* zhg-vn01 (**A**) versus *Protanilla lini* (**B**), diagrammatic. Abbreviation: AT = abdominal tergite.

Male-based species-level key to the *Protanilla rafflesi* species group

1 Antero-admedian signum present .... ***Protanilla* TH02 (THAILAND: Chaiyaphum)**

– Antero-admedian signum absent **2**

2 Gonostylar apex pointed (Fig. 43A)... ***Protanilla* TH01 (THAILAND: Khon Kaen)**

– Gonostylar apex rounded (Fig. 43B)...**7**

3 Anterior face of subpetiolar process nearly perpendicular to craniocaudal axis in profile view; abdominal tergite III slightly narrower than IV in dorsal view (TI1 62–92) (*n* = 13) (Fig. 44A) .... ***Protanilla* zhg-vn01 (VIETNAM: Vinh Phuc)** ....***Protanilla* zhg-my01 (MALAYSIA: Sarawak)***

– Anterior face of subpetiolar process gently sloping relative to craniocaudal axis; abdominal tergite III much narrower than IV in dorsal view (TI1 50–55) (*n* = 4) (Fig. 44B) ....***Protanilla lini* Terayama, 2009 (TAIWAN; JAPAN: Ryukyu Islands, Senkaku Islands)**

---

* These morphospecies are recovered distantly within the *Protanilla rafflesi* species group by phylogenomic inference (pers. obs.), and so are presumed to be allospecific in the absence of further evidence.

Male-based species-level key to the *Leptanilla thai* species group

1 Gonocoxites entirely fused medially, without suture; hypopygium with posteromedian filiform process ....***Leptanilla* TH03 (THAILAND: Chiang Mai)**

– Gonocoxites partly to fully separate medially; hypopygium without posteromedian filiform process **2**

2 Ocelli absent (Fig. 45B); mandible articulated to gena (Fig. 46A)................. .... ***Leptanilla* zhg-bt03 (BHUTAN)**

– Ocelli present (Fig. 45A); mandible fused to gena (Fig. 46B), rarely articulate (*Leptanilla* TH04) **3**

3 Gonopodite shorter than (Fig. 47A), or subequal in length to, penial sclerites...**4**

– Gonopodite distinctly longer than penial sclerites (Fig. 47B).......................**6**

4 Internal margins of apical penial cleft distinctly separated; posteroventral gonocoxital margin entire (Fig. 48B).. ....***Leptanilla argamani* (Kugler, 1987), comb. nov. (ISRAEL, LEBANON)**

– Internal margins of apical cleft of penial sclerites subparallel; posteroventral gonocoxital margin sinuate (Fig. 48A)...**5**

5 Color castaneous; posterior margin of compound eye linear in profile view ....***Leptanilla indica* (Kugler, 1987), comb. nov. (INDIA: Kerala)**

– Color yellowish to pallid; posterior margin of compound eye convex in profile view ....***Leptanilla indica* (SRI LANKA)**

6 Dorsoventral margins of profemur not parallel (Fig. 49A) **7**

– Dorsoventral margins of profemur parallel (Fig. 49B).................................**10**

7 Volsella bifid, ventral process bifurcated (Fig. 50A)....................................... .... ***Leptanilla* zhg-th02 (THAILAND: Phetchabun)**

– Volsella usually bifid, rarely not (*Leptanilla* zhg-mm11), if bifid then ventral process entire (Fig. 50B)...**8**

8 Dorsal and ventral parossicular processes forming 90° angle; lengths of processes subequal ....***Leptanilla* TH02 (THAILAND: Khon Kaen)**

– Dorsal and ventral parossicular processes forming acute angle; ventral parossicular process 3× longer than length of dorsal process **9**

9 Diameter of compound eye > 4× span of ocellar tubercle; gonopodital apices not recurved towards medial axis ....***Leptanilla* zhg-th04 (THAILAND: Chaiyaphum)**

– Diameter of compound eye only slightly greater than span of ocellar tubercle; gonopodital apices sharply recurved towards medial axis..................... ....***Leptanilla* zhg-th05 (THAILAND: Chaiyaphum)**

10 Gonostylar apex subtriangular, entire..**11**

– Gonostylar apex tapering, entire or bifid (Fig. 47B)....................................**14**

11 Ventral margin of gonocoxites produced into two pairs of lobes (Fig. 51A); volsellae apparently not furcate (Fig. 52A)... .... ***Leptanilla* zhg-mm11 (BURMA: Taninthayi)**

– Ventral margin of gonocoxites not so produced (Fig. 51B); volsellae furcate (Fig. 52B)...**12**

12 Bifid processes of volsella oriented along lateromedial axis relative to genital capsule, lateral process shorter than medial process .... ***Leptanilla* MM01 (BURMA: Rakhine)**

– Bifid processes of volsella oriented along dorsoventral axis relative to genital capsule, lengths of processes subequal **13**

13 Larger species (WL > 0.5 mm); gonopodital suture absent........................... .... ***Leptanilla* zhg-mm13 (BURMA: Taninthayi)**

– Smaller species (WL ≤ 0.5 mm); gonopodital suture present, complete ....***Leptanilla* cf. zhg-mm10 (BURMA: Taninthayi)**

14 Head not broader than long in full-face view, including compound eyes; gonostylar apex bifurcated (Fig. 47B).. .... ***Leptanilla* TH08 (THAILAND: Surat Thani)**

– Head broader than long in full-face view, including compound eyes; gonostylar apex entire **15**

15 Penial sclerites distinctly longer than broad; volsella entire.......................**16**

– Penial sclerites not distinctly longer than broad; volsella bifid **17**

16 Gonocoxite with distodorsal carina; dorsal process of volsella recurved dorsally ....***Leptanilla* TH04 (THAILAND: Chiang Mai)**

– Gonocoxite without distodorsal carina; dorsal process of volsella recurved laterally..................................***Leptanilla* zhg-th05 (THAILAND: Chiang Mai)**

17 Gonostylar apex lobate in outline, covered with dense vestiture; coloration castaneous ....***Leptanilla* TH06 (THAILAND: Chiang Mai)**

– Gonostylar apex acuminate, glabrous; coloration beige................................ ....***Leptanilla* zhg-my16 (MALAYSIA: Selangor)**

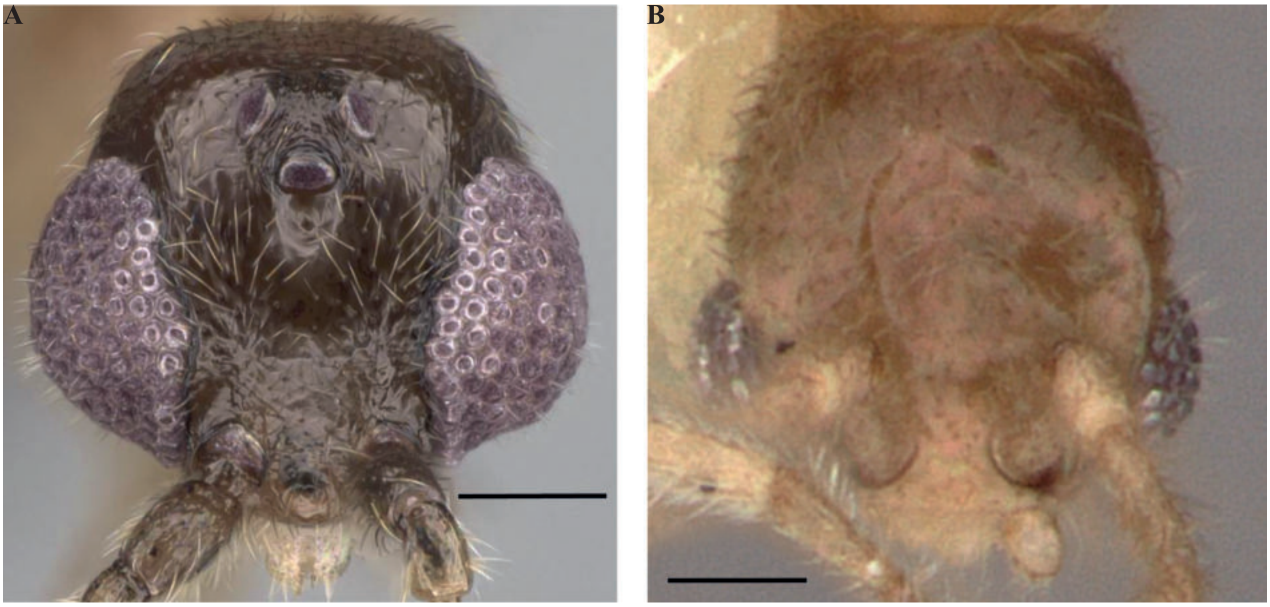

Figure 45. Condition of male ocelli in the Leptanillini, full-face view **A** *Leptanilla* TH02 (CASENT0119531; Shannon Hartman) **B** *Leptanilla* zhg-bt03 (CASENT0106384). Scale bars: 0.1 mm.

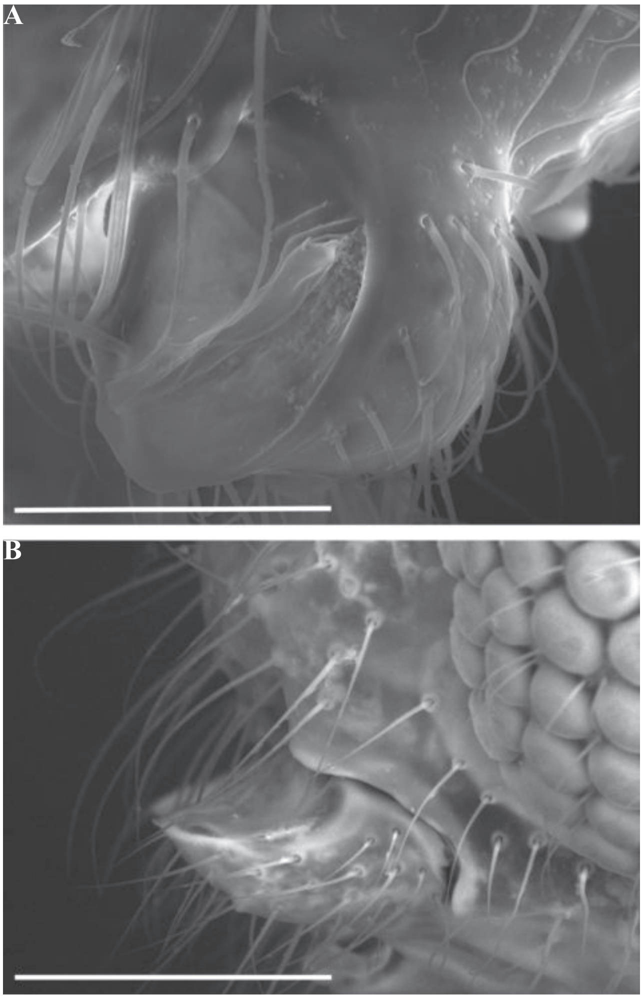

Figure 46. Articulation of the male mandible in the *Leptanilla thai* species group **A** *Leptanilla Indica* (CASENT0106377) **B** *Leptanilla* zhg-bt03 (CASENT0106384). Scale bars: 0.03 mm (**A**); 0.04 mm (**B**).

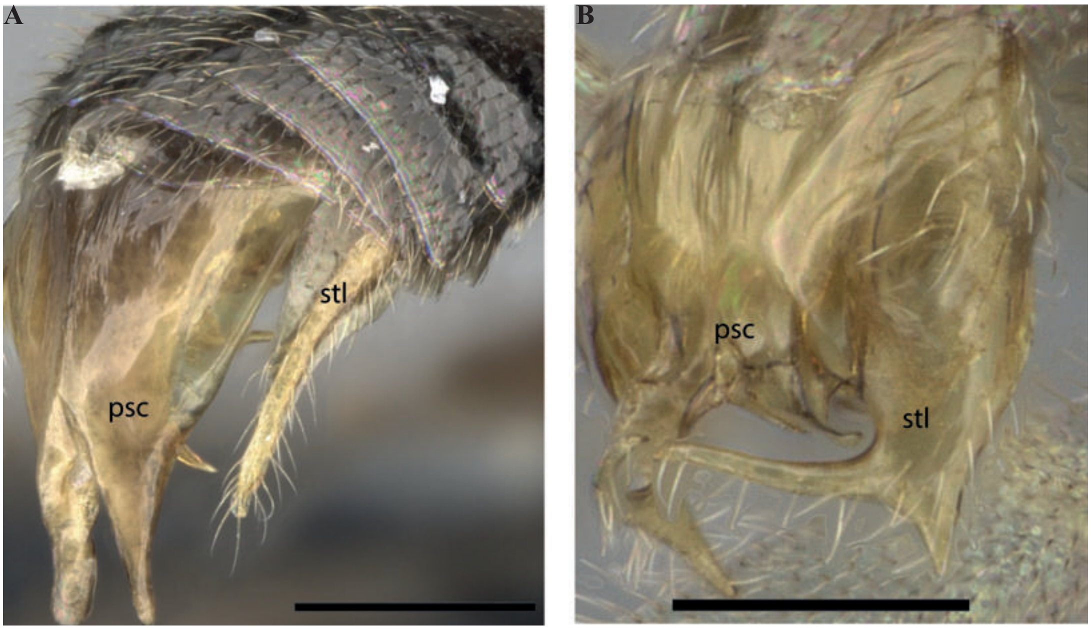

Figure 47. Proportions of the penial sclerites to the gonopodites in the *Leptanilla thai* species group **A** *Leptanilla argamani* **B** *Leptanilla* TH08. Abbreviations: stl = gonostyli; psc = penial sclerites. Scale bars: 0.2 mm (**A**); 0.1 mm (**B**).

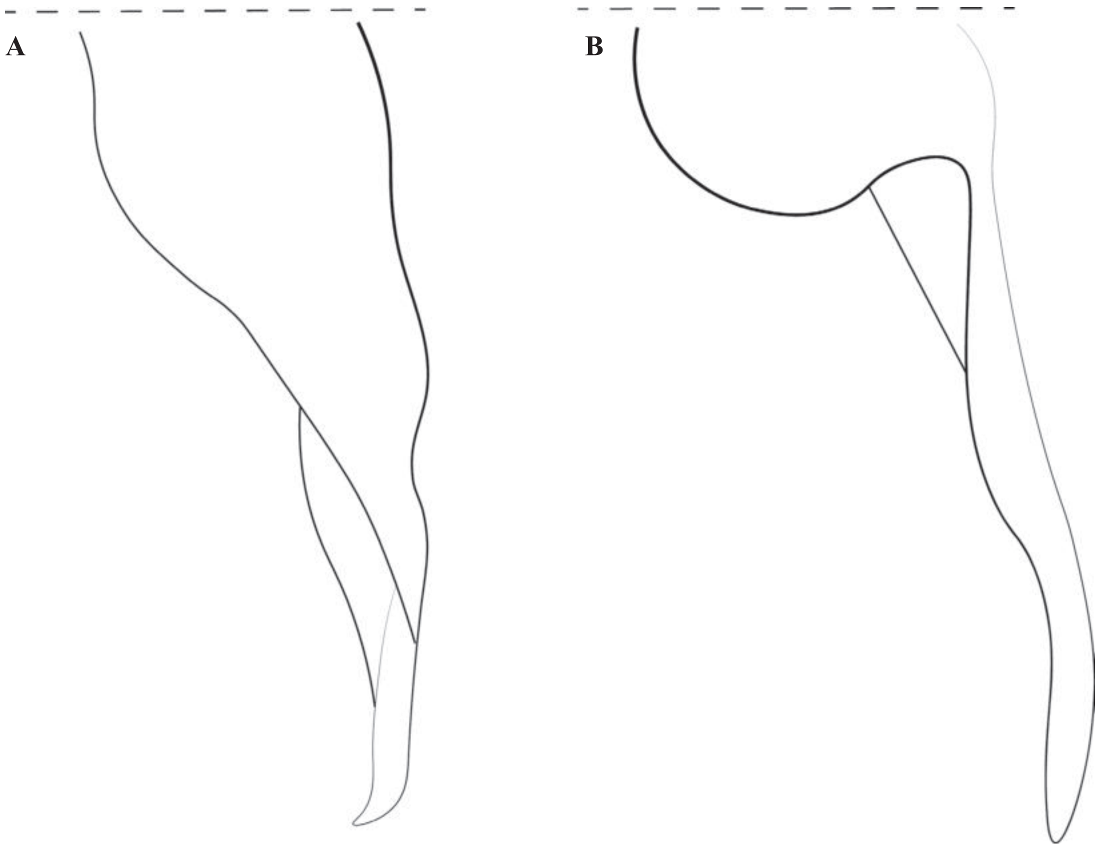

Figure 48. Outline of the gonopodites in *Leptanilla indica* (**A**) and *Leptanilla argamani* (**B**), ventral view, diagrammatic. Redrawn from Kugler (1987: figs 18, 22).

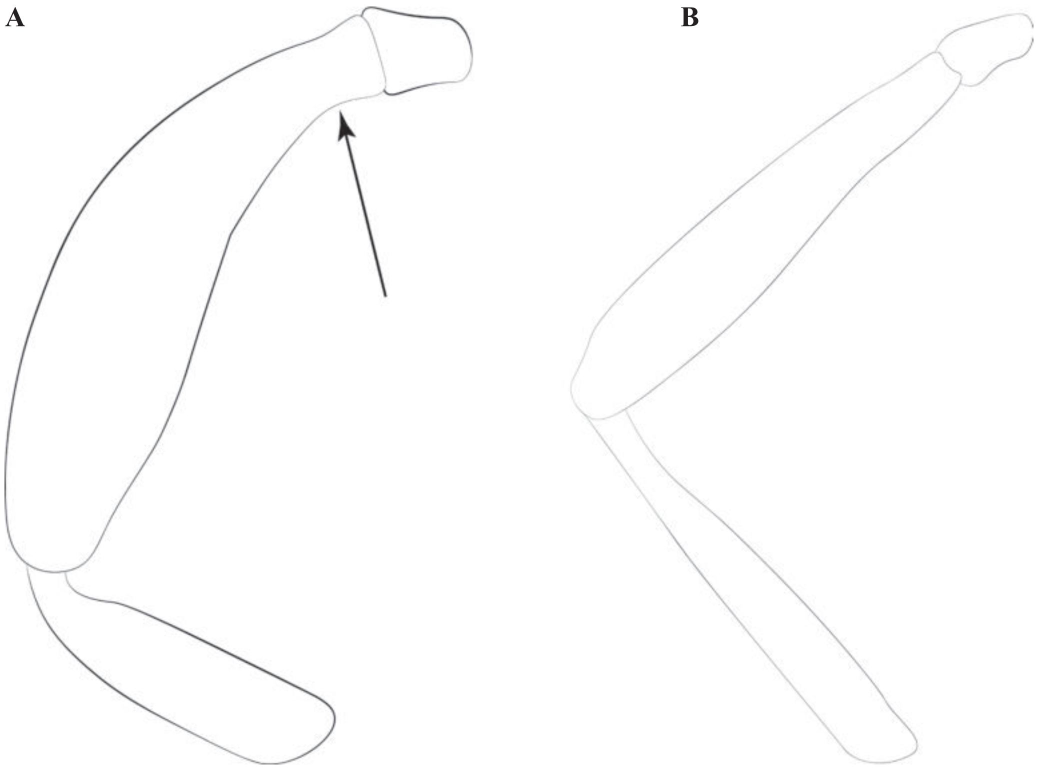

Figure 49. Male protrochanter, profemur, and protibia in the *Leptanilla thai* species group, diagrammatic. After Griebenow (2020: fig. 11B) **A** *Leptanilla* zhg-th02 **B** *Leptanilla* TH04.

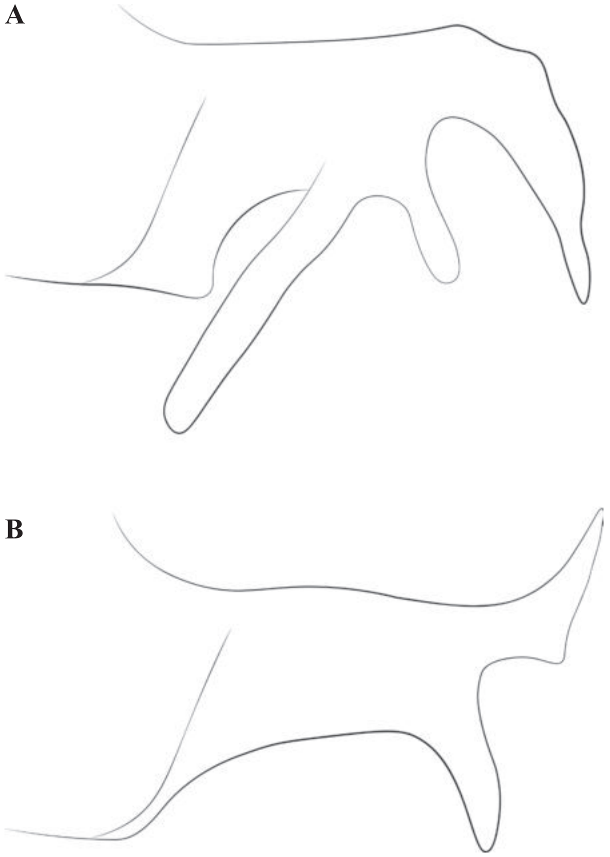

Figure 50. Volsella of the *Leptanilla thai* species group, medial view, diagrammatic, after Griebenow (2020: fig. 11C). Not to scale **A** *Leptanilla* zhg-th02 **B** *Leptanilla* TH02.

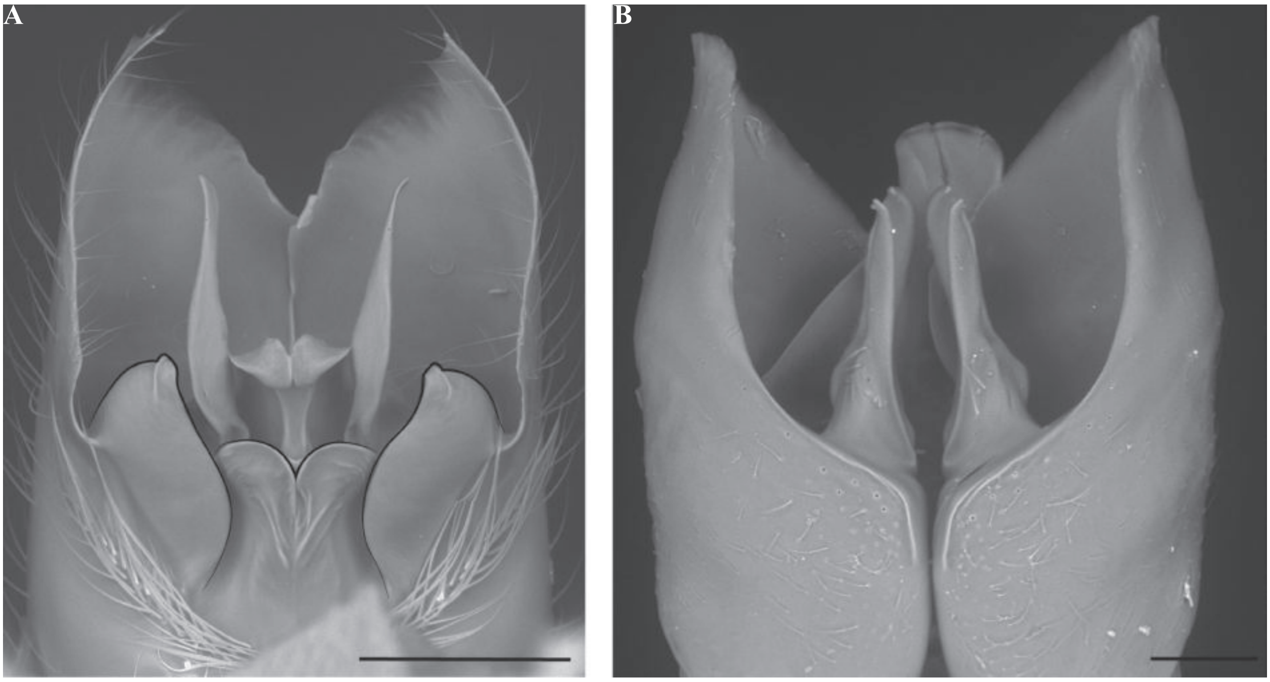

Figure 51. Gonopodital margins in the *Leptanilla thai* species group, ventral view. Gonocoxital lobes outlined in black **A** *Leptanilla* zhg-mm11 (CASENT0842848) **B** *Leptanilla* zhg-mm13 (CASENT0842670). Scale bars: 0.15 mm (**A**); 0.06 mm (**B**).

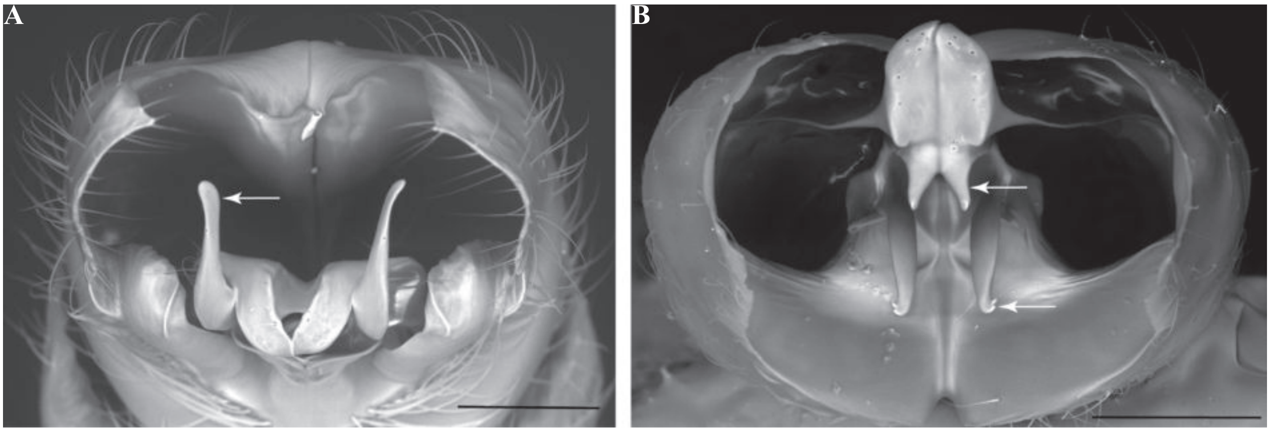

Figure 52. Volsellae in the *Leptanilla thai* species group, posterior view. Volsellar processes marked with arrows **A** *Leptanilla* zhg-mm11 (CASENT0842848) **B** *Leptanilla* zhg-mm13 (CASENT0842670). Scale bar: 0.1 mm.

Male-based species-level key to the *Leptanilla najaphalla* species group

1 Phallotreme at penial apex **2**

– Phallotreme proximad penial apex, anatomically ventral **3**

2 Penial sclerites dorsoventrally compressed at apex, without dorsomedian lamina (Fig. 53A) ....***Leptanilla* zhg-my03 (MALAYSIA: Sabah, Sarawak)**

– Penial sclerites lateromedially compressed at apex, with dorsomedian lamina (Fig. 53B)............................... ***Leptanilla* zhg-my04 (MALAYSIA: Sabah)**

3 Gonostylus present, articulated, tusk-like and lacking setae (Fig. 54); penial sclerites with recurved apical hook (Fig. 55A) ....***Leptanilla* zhg-id01 (INDONESIA: Kalimantan Barat)**

– Gonostylus absent; penial sclerites without recurved apical hook (Fig. 55B)..**4**

4 Apicolateral gonocoxital lamina subulate (Fig. 56A) .... ***Leptanilla najaphalla* sp. nov. (MALAYSIA: Sabah)**

– Apicolateral gonocoxital lamina lanceolate (Fig. 56B) .... ***Leptanilla* zhg-my05 (MALAYSIA: Sabah)**

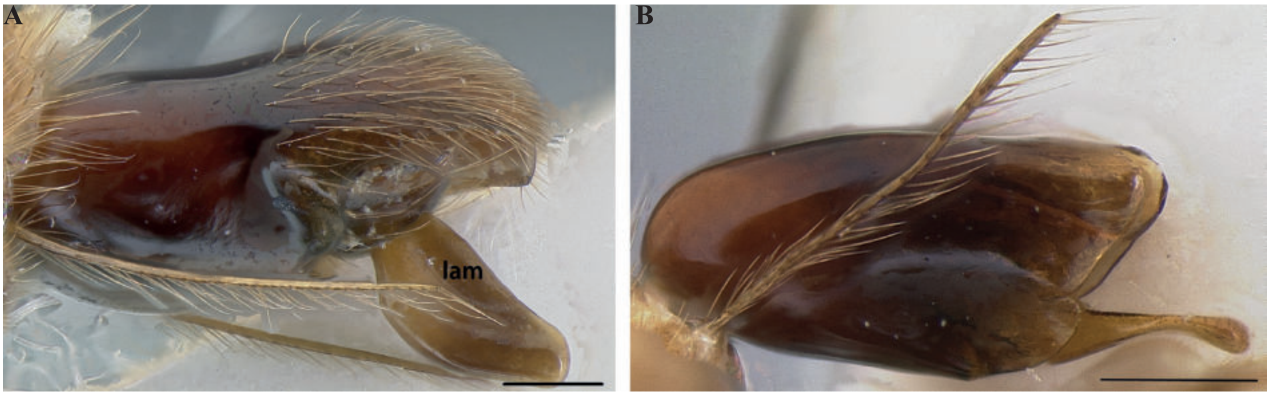

Figure 53. Male genitalia in the *Leptanilla najaphalla* species group, profile view. Abbreviation: lam = dorsomedian lamella of penial sclerites **A** *Leptanilla* zhg-my04 (CASENT0842558) **B** *Leptanilla* zhg-my03 (CASENT0842545). Scale bar: 0.2 mm.

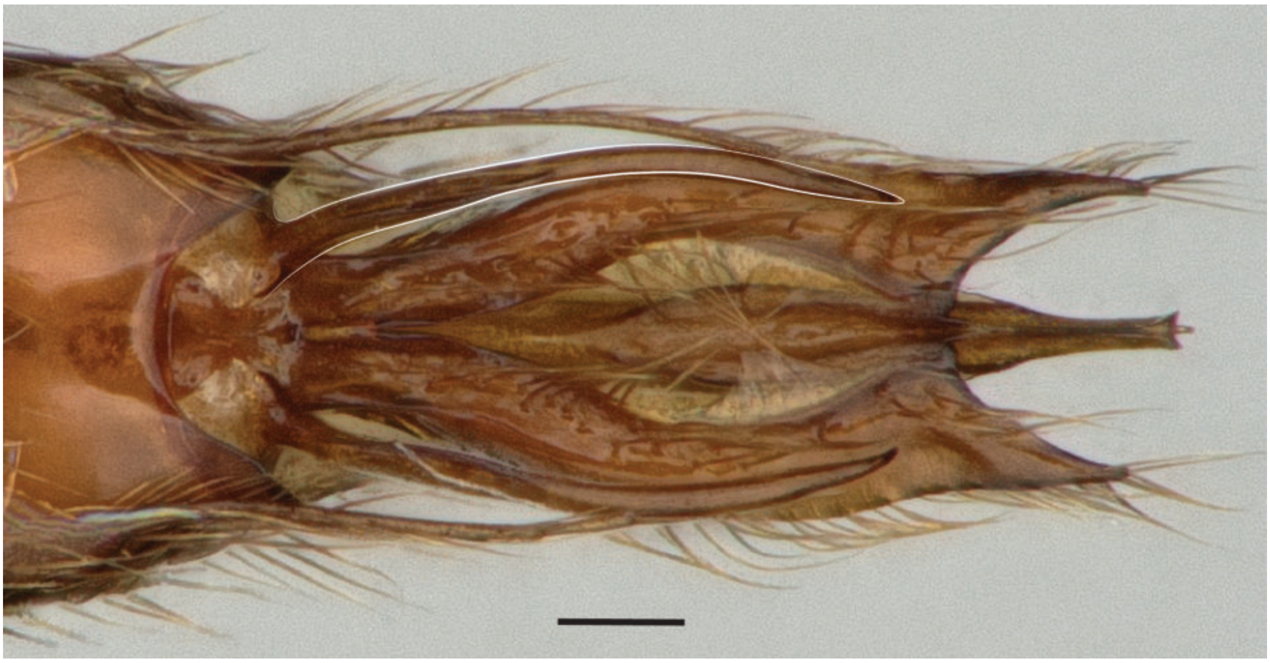

Figure 54. Male genitalia of *Leptanilla* zhg-id01 (CASENT0842625), ventral view. Gonostylus outlined in white. Scale bar: 0.1 mm.

Figure 55. Penial sclerites of the *Leptanilla najaphalla* species group, profile view, diagrammatic. Base (left) partly concealed by gonocoxites in situ **A** *Leptanilla* zhg-id01 **B** *Leptanilla* zhg-my05.

Figure 56. Apicolateral gonocoxital laminae in the *Leptanilla najaphalla* species group, profile view **A** *Leptanilla* zhg-my02 (CASENT0106427) **B** *Leptanilla* zhg-my05 (CASENT0842571). Scale bars: 0.3 mm (**A**); 0.5 mm (**B**).

Male-based species-level key to the *Leptanilla havilandi* species group

1 ML > SL, with mandible flattened and paddle-like; lower metapleuron indistinct...***Leptanilla anomala*** **(Brues, 1925), comb. nov. (INDONESIA: Sumatra, Kalimantan Barat)**

– ML ≤ SL, with mandible nub-like; lower metapleuron distinct **2**

2 Mandalus not extending to mandibular apex; anteromedian ocellus orthogonally dorsal to compound eye in profile view (Fig. 57A) ....***Leptanilla copiosa*** **(Petersen, 1968), comb. nov. (PHILIPPINES: Palawan)**

– Mandalus extending to mandibular apex; anteromedian ocellus positioned posterodorsal to compound eye in profile view (Fig. 57B) **3**

3 Gonostylus longer than gonocoxite (Fig. 58A) .... ***Leptanilla* zhg-my10 (MALAYSIA: Sabah)**

– Gonostylus shorter than, or subequal in length to gonocoxite (Fig. 58B) **4**

4 Penial apex produced into two ranks of aculeate processes; phallotremal rim glabrous........... ***Leptanilla* zhg-ph01 (PHILIPPINES: Camarines Sur; Quezon)**

– Penial apex produced into robust ventral carina, without process dorsad to carina; phallotremal rim with vestiture... **5**

5 Penial apex entire .... ***Leptanilla* zhg-my14 (MALAYSIA: Sabah)**

– Penial apex cleft .... ***Leptanilla* zhg-my11 (MALAYSIA: Sabah)**

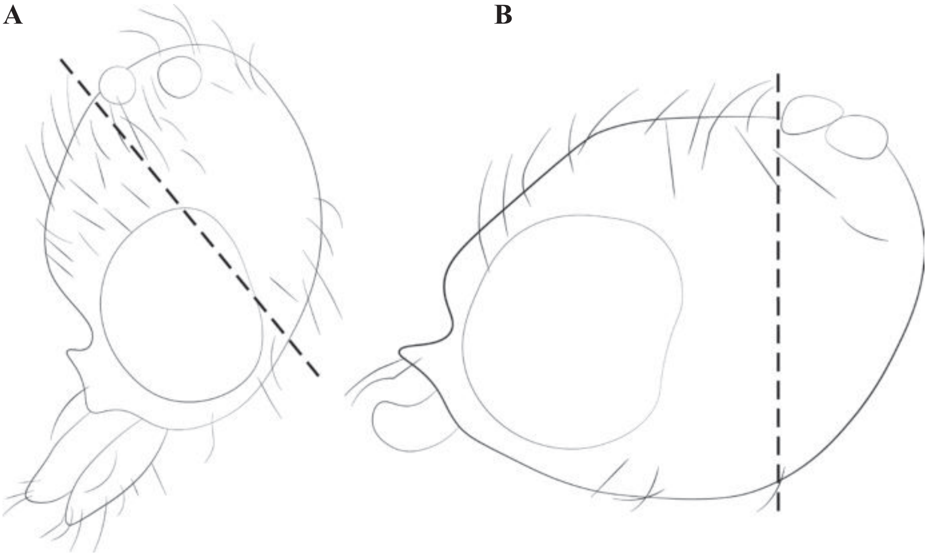

Figure 57. Position of the male anteromedian ocellus relative to the compound eye in *Leptanilla*, diagrammatic, after Griebenow (2020: fig. 12B) **A** *Leptanilla copiosa* **B** *Leptanilla* zhg-my10.

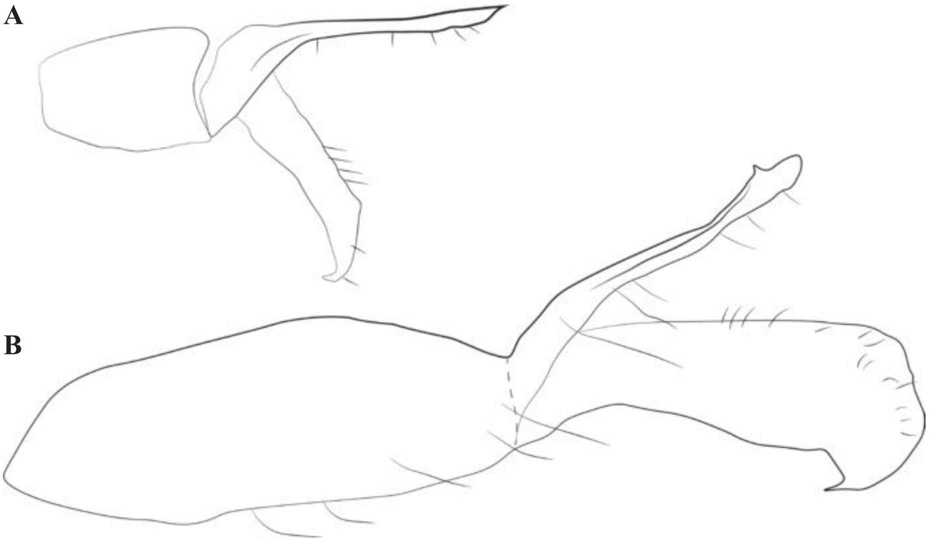

Figure 58. Male genitalia in the *Leptanilla havilandi* species group, profile view, diagrammatic, after Griebenow (2020: fig. 13A). Figures to scale **A** *Leptanilla* zhg-my10 **B** *Leptanilla* zhg-my11.

Male-based species-level key to the *Leptanilla bethyloides* species group

1 Mesoscutellum produced into recurved posterior process (Griebenow 2021: fig. 16B); LF2 > SL ....***Leptanilla* zhg-th01 (THAILAND: Chiang Mai)**
– Mesoscutellum not produced into recurved posterior process; LF2 ≤ SL...... **2**
2 Penial sclerites lateromedially compressed, with dorsomedian carina ....***Leptanilla* TH01 (THAILAND: Chiang Mai)**
– Penial sclerites dorsoventrally compressed, without dorsomedian carina; gonopodital apex bifid...**3**
3 Smaller species; abdominal postsclerites V–VII anteroposteriorly compressed relative to those of III–IV .... ***Leptanilla* zhg-mm05 (BURMA: Taninthayi)**
– Larger species; abdominal postsclerites V–VII with anteroposterior lengths subequal to those of III–IV ....***Leptanilla bethyloides* sp. nov. (CHINA: Hong Kong)**

Male-based species-level key to the *Leptanilla revelierii* species group

1 Gonostylus ellipsoid in outline (Griebenow 2020: fig. 11E); gonocoxites with complete ventromedian fusion.....***Leptanilla astylina* (PHILIPPINES: Palawan)**
– Gonostylus not ellipsoid; gonocoxites without ventromedian fusion **2**
2 Protibial length 0.5× profemoral length **3**
– Protibial length > 0.5× profemoral length...**4**
3 Length of probasitarsal seta less than that of calcar ....***Leptanilla africana* Baroni Urbani, 1977 (NIGERIA)**
– Length of probasitarsal seta subequal to that of calcar................................ ....***Leptanilla* TH09 (THAILAND: Phetchabun)**
4 Gonostylus bifurcated or emarginate...**5**
– Gonostylus entire, apex tapering or truncate...**14**
5 Abdominal segment II broadly joined to abdominal segment III (Santschi 1907: fig. 3) ....***Leptanilla minuscula* Santschi, 1907 (TUNISIA)**
– Abdominal segment III narrowly joined to abdominal segment III...............**6**
6 Ventromedial gonocoxital margin with sinuate process .... ***Leptanilla tanit* Santschi, 1907 (TUNISIA)**
– Ventromedial gonocoxital margin entire..**7**
7 Gonostylar apex with obtuse tooth subtending dorsal process.................... ....***Leptanilla* GR02 (GREECE: Rhodes)**
– Gonostylar apex lacking obtuse tooth subtending dorsal process..............**8**
8 Ventromedian margin of gonostylus excavated proximad apical furca .... ***Leptanilla* zhg-au02 (AUSTRALIA: New South Wales)**
– Ventromedian margin of gonostylus entire proximad apical furca..............**9**
9 Dorsal process of gonostylar apex acuminate..**10**
– Dorsal process of gonostylar apex rounded..**11**
10 Processes of gonostylar apex large, with apex appearing deeply bifurcated ....***Leptanilla tenuis* Santschi, 1907 (TUNISIA)**
– Processes of gonostylar apex small, with apex appearing nearly truncate...... ....***Leptanilla* zhg-mm02 (BURMA: Taninthayi)**
11 Penial apex entire **12**
– Penial apex emarginate..**13**

12 PTL ≈ PTH .... ***Leptanilla*** **GR01 (GREECE: Rhodes)**

– PTL > PTH .... ***Leptanilla*** **zhg-id02 (INDONESIA: Sulawesi Tenggara)**

13 Internal margins of apical penial cleft distinctly separated, ventral gonostylar process narrower than dorsal process .... ***Leptanilla bifurcata*** **Kugler, 1987 (ISRAEL)**

– Internal margins of apical penial cleft adjacent, gonostylar processes subequal in breadth .... ***Leptanilla israelis*** **Kugler, 1987 (ISRAEL)**

14 Gonostylar apex not tapering **15**

– Gonostylar apex tapering **17**

15 Gonostylus with expanded, rounded apex (Fig. 59A) .... ***Leptanilla islamica*** **Baroni Urbani, 1977 (YEMEN; OMAN)**

– Gonostylus with apex not expanded (Fig. 59B) **16**

16 Outline of penial sclerites attenuate in posterodorsal view (Fig. 60A) .... ***Leptanilla alexandri*** **Dlussky, 1969 (UZBEKISTAN)**

– Outline of penial sclerites elliptical in posterodorsal view (Fig. 60B) .... ***Leptanilla japonica*** **Baroni Urbani, 1977 (JAPAN: Honshu; CHINA: Hong Kong)**

17 Gonostylar apex acuminate **18**

– Gonostylar apex digitate **25**

18 Oblique mesopleural sulcus traversing posterior > 0.5× of mesopleuron **19**

– Oblique mesopleural sulcus traversing posterior ≤ 0.5× of mesopleuron **20**

19 Penial sclerites broad in posterodorsal view, apex entire; Rsf1+Mf1 present .... ***Leptanilla javana*** **(Wheeler & Wheeler, 1930) (INDONESIA: Java)**

– Penial sclerites narrow in posterodorsal view, apex emarginate; Rsf1+Mf1 absent .... ***Leptanilla*** **zhg-ke01 (KENYA: Laikipia)**

20 Abdominal sternite II without distinct subpetiolar process (Fig. 61A) .... ***Leptanilla*** **zhg-bt02 (BHUTAN)**

– Abdominal sternite II with distinct subpetiolar process (Fig. 61B) **21**

21 *2s-rs*+R+4-6 absent from forewing (Fig. 62A) **22**

– *2s-rs*+R+4-6 present in forewing (Fig. 62B) **24**

22 Posterior face of petiolar node shallower than anterior face; genital capsule subequal in overall dimensions to abdominal segment II .... ***Leptanilla*** **zhg-bt01 (BHUTAN)**

– Posterior face of petiolar node not shallower than anterior face; dimensions of genital capsule conspicuously greater than those of abdominal segment II ***23***

23 Oblique mesopleural sulcus adjoining metapectal-propodeal complex .... ***Leptanilla*** **zhg-au03 (AUSTRALIA: Queensland)**

– Oblique mesopleural sulcus not adjoining metapectal-propodeal complex .... ***Leptanilla*** **zhg-ke02 (KENYA: Kakamega)**

24 Apicolateral margins of penial sclerites emarginate; smaller species (WL = 0.37–0.44 mm) (*n* = 6) .... ***Leptanilla charonea*** **Barandica et al., 1994 (SPAIN)**

– Apicolateral margins of penial sclerites entire; larger species (WL = 0.46–0.50 mm) (*n* = 3) .... ***Leptanilla*** **cf. *zaballosi* López et al., 1994 (SPAIN)**

25 Penial sclerites broader than long (Fig. 63A) .... ***Leptanilla*** **GR03 (GREECE: Rhodes; TURKEY: Muğla)**
.... ***Leptanilla*** **zhg-tr01 (TURKEY: Muğla)**

– Penial sclerites longer than broad (Fig. 63B) **26**

26 Gonostylus not articulated to gonocoxite.. ....*Leptanilla exigua* **Santschi, 1908 (TUNISIA)**
– Gonostylus articulated to gonocoxite **27**
27 Abdominal sternite II produced ventrally, forming curve in profile view **28**
– Abdominal sternite II not produced ventrally, linear in profile view **29**
28 Gonocoxites with apicoventral laminae.. ....***Leptanilla*** **zhg-au05 (AUSTRALIA: Queensland)**
– Gonocoxites without apicoventral laminae ....***Leptanilla*** **zhg-au01 (AUSTRALIA: Queensland)**
29 Oblique mesopleural sulcus present; Sc+R+Rs tubular ....***Leptanilla*** **zhg-au07 (AUSTRALIA: Queensland)**
– Oblique mesopleural sulcus absent; Sc+R+Rs absent .... ***Leptanilla australis*** **Baroni Urbani, 1977 (SOUTH AFRICA: Cape Province)**

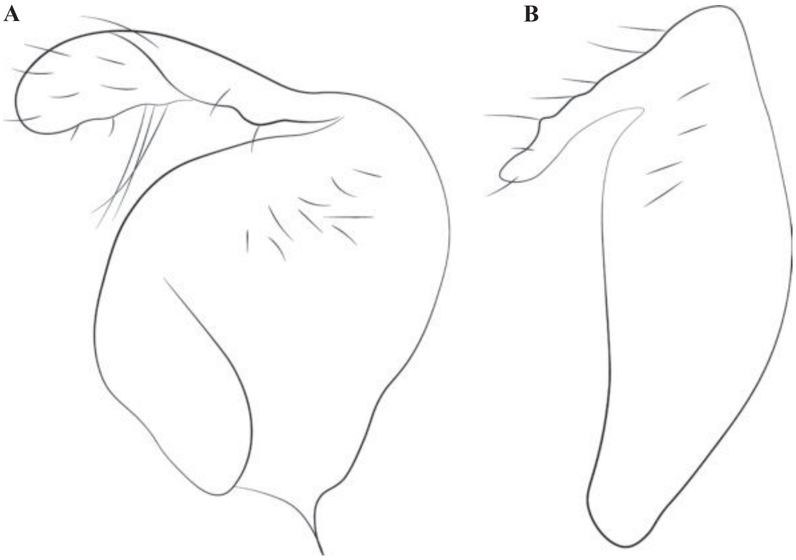

Figure 59. Gonostylar shape in the *Leptanilla revelierii* species group, after Griebenow (2020: fig. 13F) **A** *Leptanilla islamica* **B** *Leptanilla australis*.

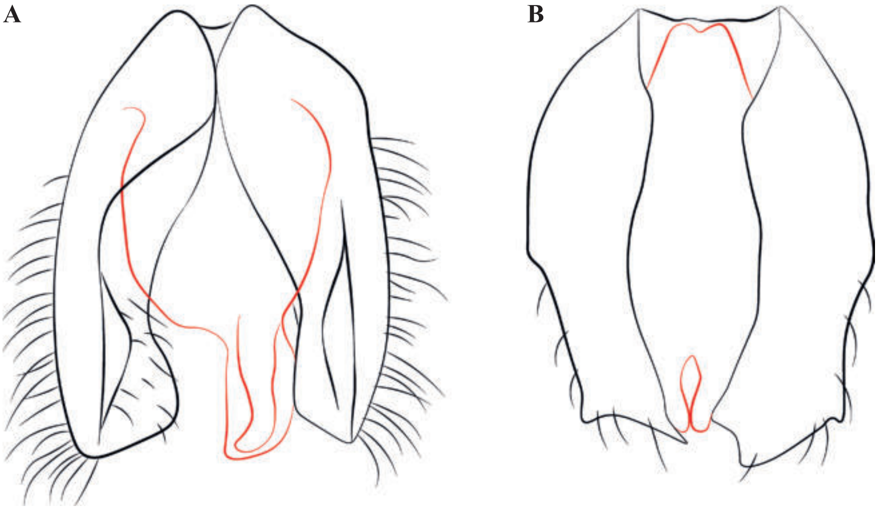

Figure 60. Dorsal outline of the penial sclerites (red) in the *Leptanilla revelierii* species group, diagrammatic, after Griebenow (2020: fig. 13G) **A** *Leptanilla alexandri* **B** *Leptanilla japonica*.

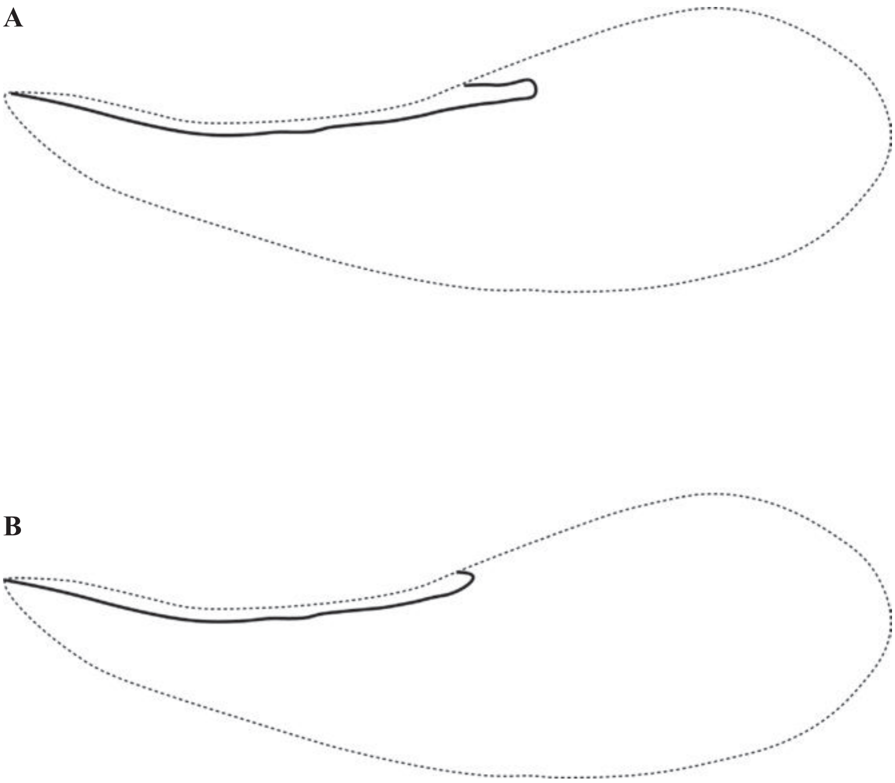

Figure 61. Presence (**A**) versus absence (**B**) of forewing *2s-rs*+R+4-6 in males of the *Leptanilla revelierii* species group, diagrammatic.

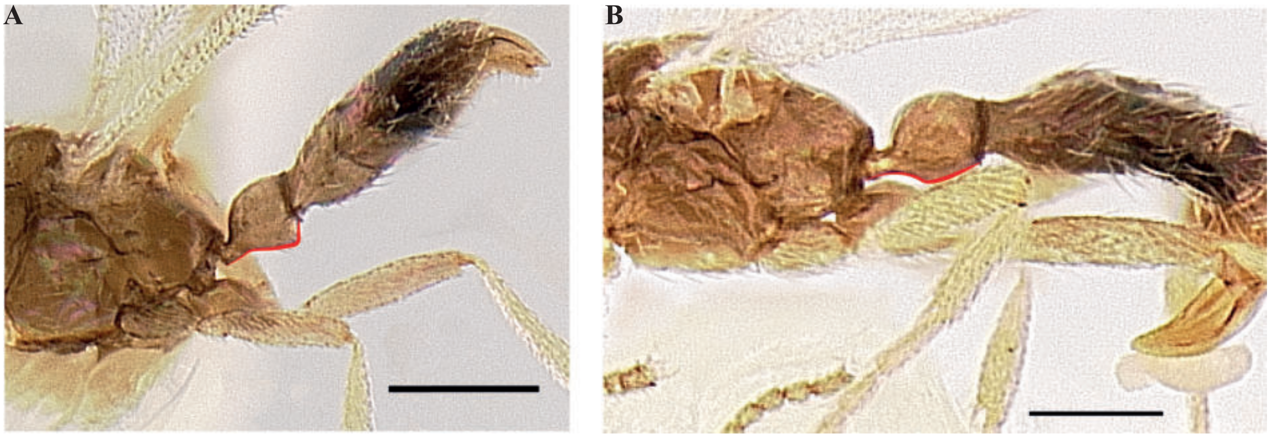

Figure 62. Abdominal segment II in males of the *Leptanilla revelierii* species group, profile view. Abdominal sternite II outlined in red **A** *Leptanilla* zhg-bt01 (CASENT0842617) **B** *Leptanilla* zhg-bt02 (CASENT0842612). Scale bars: 0.125 mm (**A**); 0.100 mm (**B**).

Discussion

Taxonomic history

Writing of the subfamily Leptanillinae, Brown (1954: 28) opined that " … it is doubtful that we shall ever be certain of its true affinities." Concomitantly, the classification of the Leptanillinae relative to other Formicidae has a convoluted history. Extreme morphological derivation (in males, larvae, and both female castes), varying markedly across the few lineages of the clade, is responsible for this.

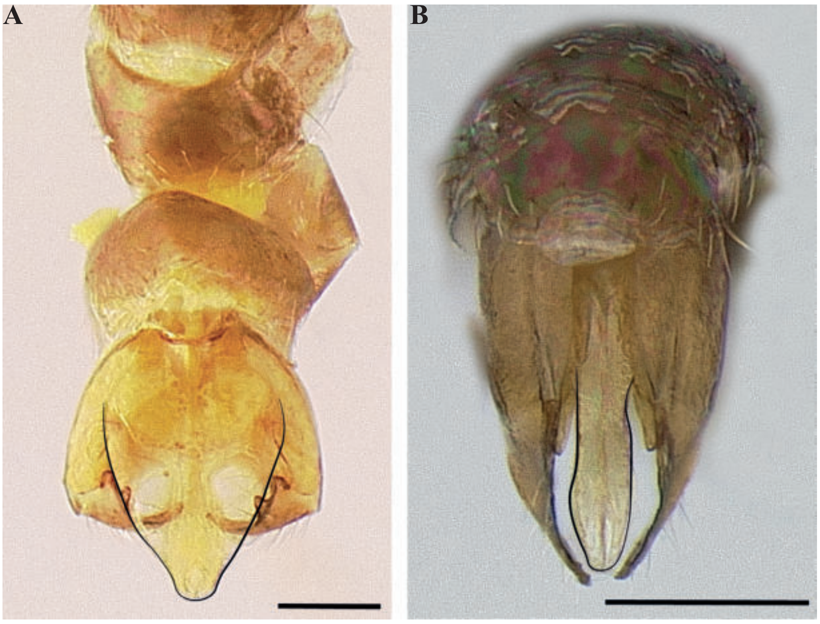

Figure 63. Penial sclerites in the *Leptanilla revelierii* species group, outlined in black, posterodorsal view **A** *Leptanilla* GR02 (CASENT0106068) **B** *Leptanilla* zhg-au01 (CASENT0758873). Scale bar: 0.1 mm.

For most of its taxonomic history, the subfamily Leptanillinae was subsumed within (Emery 1910), or affiliated with, the army ants (Dorylinae *sensu* Ashmead) (Baroni Urbani 1989; Hölldobler and Wilson 1990), with *Leptanilla* having been described within the Dorylinae (Emery 1870). Despite ill-interrogated placement in the Myrmicinae by many early authors (Emery and Forel 1879; Dalla Torre 1893; Ashmead 1905; Emery 1910), the description of dichthadiiform gynes in *Leptanilla* was interpreted as supporting its placement within the Dorylinae (Emery 1904), while Santschi (1907) asserted the similarity of putative male *Leptanilla* to male army ants. Wheeler (1923) was the first to elevate the then-monobasic Leptanillini to subfamily rank, an action also argued for by Wheeler (1928) and Wheeler and Wheeler (1965) due to the dissimilarity of the larval habitus between the Dorylinae and Leptanillinae. *Leptanilloides* (Dorylinae) was placed as Formicidae incertae sedis and likened to the Leptanillinae by Borgmeier (1955) due to that genus exhibiting "a mixture of characters of the Ecitonini (i.e., New World army ants) and Leptanillinae" (Borgmeier 1955: 652), but Brown (1975: 34) classified *Leptanilloides* within the "doryline section" (Bolton 1990a) due to its close resemblance to *Sphinctomyrmex sensu lato*, a classification followed by all subsequent authors and confirmed by phylogenetic inference from molecular data (e.g., Brady et al. 2014).

With the description of the tribe Anomalomyrmini within the Leptanillinae, Bolton (1990b: 267) "dispute(d) the indisputability" of leptanilline kinship with army ants, since *Protanilla* gynes are not dichthadiiform (Baroni Urbani and de Andrade 2006; Billen et al. 2013; Hsu et al. 2017), and dichthadiigynes are unequivocally homoplasious in their other occurrences across the Formicidae (Bolton 1990a). Bolton (1990b) transferred *Apomyrma* to the Leptanillinae from the Ponerinae *sensu* Bolton (1990b) and proposed that the resemblance of doryline to leptanilline gynes was homoplasious. Based on the theorized kinship of *Apomyrma* to the Leptanillinae (Apomyrminae and Leptanillinae constituting the "leptanillomorph subfamilies" *sensu* Bolton (2003)), these lineages were hypothesized to have affinity with the Amblyoponinae, or more generally the "poneroid" clade (Ward 2007).

The advent of molecular sequencing supported none of the above hypotheses: instead, Leptanillinae was consistently supported as an early-diverging lineage of the Formicidae not akin to *Apomyrma*, which was recovered as a poneroid, sister to the Amblyoponinae. In addition, Ward and Fisher (2016) robustly recovered the monotypic genus *Opamyrma*, which had been described within the Amblyoponinae on account of character states closely resembling those of *Apomyrma* (e.g., abdominal sternite II reduced), as sister to the remaining Leptanillinae (Ward and Fisher 2016). This inference is corroborated by male morphology.

The Leptanillinae have been afflicted by a dual taxonomy since the description of the first putative males by Santschi (1907, 1908). The first males of *Leptanilla* were described without association with workers, justified by purported similarity in head morphology, and "only with some doubt (n'est qu'avec doute)" (Santschi 1907: 312). The genus *Phaulomyrma* was erected for *Leptanilla javana* (Wheeler & Wheeler, 1930) and *Leptanilla tanit* Santschi, 1907, both known only from males (Wheeler and Wheeler 1930), whereas the bizarre monotypic genus *Scyphodon*, described by Brues (1925) as Hymenoptera incertae sedis, was found to represent a male leptanilline (Petersen 1968; Boudinot 2015), although Ogata et al. (1995) argued against the placement of *Scyphodon* in the Formicidae. The genera *Noonilla* and *Yavnella* were also described in the Leptanillinae based solely upon male specimens (Petersen 1968; Kugler 1987). Ogata et al. (1995) was the first to associate male and worker leptanilline specimens, describing the male of *Leptanilla japonica*, which was previously known from workers (Baroni Urbani 1977), and confirming the hypothesis of Santschi (1907). The two genera for which the tribe Anomalomyrmini was established were each initially known only from workers (*Protanilla*) or gynes (*Anomalomyrma*) (Bolton 1990b). Consideration of morphology illuminated by phylogenetic inference (Borowiec et al. 2019; Griebenow 2020, 2021; Griebenow et al. 2022) demonstrates a lack of reciprocal monophyly, and the two are here synonymized. Males were only subsequently associated with *Protanilla* (namely the *Protanilla rafflesi* species group) by means of phylogenomic inference (Griebenow 2020). The Opamyrmini have avoided comparable taxonomic problems, with the collection of the male of *O. hungvuong* in association with females (Yamada et al. 2020).

Biogeography and ecology

The Leptanillinae are, as per the 95% credibility interval inferred for the crown age of this clade by Borowiec et al. (2019), no older than the beginning of the Cenozoic Era (66 mya). The crown age of the Leptanillinae is no older than the estimated origins of several ant clades that have a circumtropical or cosmopolitan distribution, including *Odontomachus* (Ponerinae: Ponerini) (Schmidt 2013) and *Camponotus* (Formicinae: Camponotini) (Blaimer et al. 2015). Yet, curiously, the Leptanillinae are restricted to the Old World. The bulk of leptanilline diversity resides in the humid tropics, with the few temperate lineages (e.g., *Leptanilla taiwanensis*; Man et al. 2017) being close kin of tropical ones. This implies that the origin of the Leptanillinae occurred in tropical climates, conforming to the overall tendency observed in the Formicidae (Economo et al. 2018). In the absence of other data to explain the absence of this clade from the New World, I predict that leptanilline ants originated after the closure of the Thulean and Beringian land bridges to tropical biota, but this prediction remains to be tested.

The notable absence of the Leptanillinae from the Neotropics elicits inquiry into which ants occupy a similar ecological niche in this ecoregion. In terms of functional morphology and behavior, *Leptanilloides* differs from leptanilline ants in the presence of cincti on abdominal segments IV–VII and in being an obligate predator of ant brood, rather than hunting geophilomorph centipedes; despite their name, these minute dorylines are not a Neotropical analog to the Leptanillinae. Rather, it is probable that centipede predators such as *Prionopelta* and *Fulakora* (Amblyoponinae), which often display LHF (Ito and Billen 1998), are ecological counterparts to the Leptanillinae in the New World. This hypothesis is further supported by remarkable homoplasy between the Amblyoponinae and Leptanillinae, which resulted in the erroneous hypothesis that these clades were akin (Bolton 1990b, 2003).

Typhlomyrmex (Ectatomminae: Ectatommini), which are minute hypogaeic ants precinctive to the Neotropics, are also worth noting here on account of the leptanilloid gestalt of the worker. Coarse but pronounced resemblance in habitus implies functional parallels in *Typhlomyrmex* with the Leptanillinae, with the articulated meso-metapleural suture that is unique to *Typhlomyrmex* among the Ectatomminae (Bolton 2003) recalling that feature in *Protanilla* and certain *Leptanilla* species, while the tergosternal fusion of abdominal segment II constitutes convergence with the Leptanillini. Miniaturized and flexible relative to the robust, epigaeic members of their sister clade, *Gnamptogenys sensu stricto* (Camacho et al. 2022), *Typhlomyrmex* represent Ectatomminae that occupy a morphospace occupied outside the New World by the Leptanillinae.

Acknowledgements

I thank Jadranka Rota (MZLU), Debbie Jennings (ANIC), Masashi Yoshimura (OIST), Kevin Williams (CSCA), Jeremy Frank (BPBM), Crystal Maier (MCZC), Lars Vilhelmsen (NHMD), Suzanne Ryder (BMNH), Bonnie Blaimer (ZMHB), Brian Fisher (CASC), Chris Darling (ROME), Benoit Guénard (HKUBM), Po-Wei Hsu (NCUE), Majid Moradmand (ZMUI), Alberto Tinaut, Yu Hisasue, and José María Gómez-Durán for loaning or donating material used in this study.

Additional information

Conflict of interest

The authors have declared that no competing interests exist.

Ethical statement

No ethical statement was reported.

Funding

This project was supported in part by NSF grant DEB-1932405 to P. S. Ward, UC Davis Jastro-Shields, the UC-Davis Dept. of Entomology, the Helmsley Charitable Trust, SI Global Genome Initiative, and the staff of Flora & Fauna International (Burma).

Author contributions

The author solely contributed to this work.

Author ORCIDs

Zachary Griebenow https://orcid.org/0000-0003-3385-8479

Data availability

All of the data that support the findings of this study are available in the main text or Supplementary Information.

References

Ashmead WH (1905) A skeleton of a new arrangement of the families, subfamilies, tribes and genera of the ants, or the superfamily Formicoidea. Canadian Entomologist 37(11): 381–384. https://doi.org/10.4039/Ent37381-11

Aswaj P, Anoop K, Priyadarsanan DR (2020) First record of the rarely collected ant *Protanilla gengma* Xu, 2012 (Hymenoptera, Formicidae, Leptanillinae) from the Indian subcontinent. Check List 16(6): 1621–1625. https://doi.org/10.15560/16.6.1621

Barandica JM, López F, Martínez MD, Ortuño VM (1994) The larvae of *Leptanilla charonea* and *Leptanilla zaballosi* (Hymenoptera, Formicidae). Deutsche Entomologische Zeitschrift 41(1): 147–153. https://doi.org/10.1002/mmnd.19940410113

Baroni Urbani C (1977) Materiali per una revisione della sottofamiglia Leptanillinae Emery (Hymenoptera: Formicidae). Entomologica Basiliensia 2: 427–488.

Baroni Urbani C (1989) Phytogeny (sic!) and behavioural evolution in ants, with a discussion of the role of behaviour in evolutionary processes. Ethology Ecology and Evolution 1(2): 137–168.https://doi.org/10.1080/08927014.1989.9525520

Baroni Urbani C, de Andrade ML (2006) A new *Protanilla* Taylor, 1990 (Hymenoptera: Formicidae: Leptanillinae) from Sri Lanka. Myrmecologische Nachrichten 8: 45–47.

Barraclough TG (2019) The Evolutionary Biology of Species. Oxford University Press, Oxford, 284 pp. https://doi.org/10.1093/oso/9780198749745.001.0001

Basibuyuk HH, Quicke DLJ (1995) Morphology of the antenna cleaner in the Hymenoptera with particular reference to non-aculeate families (Insecta). Zoologica Scripta 24(2): 157–177. https://doi.org/10.1111/j.1463-6409.1995.tb00397.x

Billen J, Ito F (2022) The dorsoproximal intramandibular gland in *Leptanilla clypeata*, a novel exocrine gland in ants. Asian Myrmecology 15(e015002): 1–5. http://www.asian-myrmecology.org/publications/am15/billen-and-ito2022-am015002.pdf

Billen J, Bauweleers E, Hashim R, Ito F (2013) Survey of the exocrine system in *Protanilla wallacei* (Hymenoptera, Formicidae). Arthropod Structure & Development 42(3): 173–183. https://doi.org/10.1016/j.asd.2013.01.001

Blaimer BB, Brady SG, Schultz TR, Lloyd MW, Fisher BL, Ward PS (2015) Phylogenomic methods outperform traditional multi-locus approaches in resolving deep evolutionary history: A case study of formicine ants. BMC Evolutionary Biology 15(1): e271. https://doi.org/10.1186/s12862-015-0552-5

Bolton B (1990a) Army ants reassessed: The phylogeny and classification of the doryline section (Hymenoptera, Formicidae). Journal of Natural History 24(6): 1339–1364. https://doi.org/10.1080/00222939000770811

Bolton B (1990b) The higher classification of the ant subfamily Leptanillinae (Hymenoptera: Formicidae). Systematic Entomology 15(3): 267–282. https://doi.org/10.1111/j.1365-3113.1990.tb00063.x

Bolton B (2003) 71 Synopsis and Classification of the Formicidae. The American Entomological Institute, Gainesville, 370 pp.

Bolton B, Fisher BL (2008) Afrotropical ants of the ponerine genera *Centromyrmex* Mayr, *Promyopias* Santschi gen. rev. and *Feroponera* gen. n., with a revised key to genera of African Ponerinae (Hymenoptera: Formicidae). Zootaxa 1929(1): 1–37. https://doi.org/10.11646/zootaxa.1929.1.1

Bond JE, Godwin RL, Colby JD, Newton LG, Zahnle XJ, Agnarsson I, Hamilton CA, Kuntner M (2022) Improving Taxonomic Practices and Enhancing Its Extensibility—An Example from Araneology. Diversity 14(1): 1–5. https://doi.org/10.3390/d14010005

Borgmeier T (1955) Die Wanderameisen der neotropischen Region. Studia Entomologica 3: 1–720.

Borowiec ML, Schulz A, Alpert GD, Baňař P (2011) Discovery of the worker caste and descriptions of two new species of *Anomalomyrma* (Hymenoptera: Formicidae: Leptanillinae) with unique abdominal morphology. Zootaxa 2810(1): 1–14. https://doi.org/10.11646/zootaxa.2810.1.1

Borowiec ML, Rabeling C, Brady SG, Fisher BL, Schultz TR, Ward PS (2019) Compositional heterogeneity and outgroup choice influence the internal phylogeny of the ants. Molecular Phylogenetics and Evolution 134: 111–121. https://doi.org/10.1016/j.ympev.2019.01.024

Boudinot BE (2015) Contributions to the knowledge of Formicidae (Hymenoptera, Aculeata): A new diagnosis of the family, the first global male-based key to subfamilies, and a treatment of early branching lineages. European Journal of Taxonomy 120(120): 1–62. https://doi.org/10.5852/ejt.2015.120

Boudinot BE (2018) A general theory of genital homologies for the Hexapoda (Pancrustacea) derived from skeletomuscular correspondences, with emphasis on the Endopterygota. Arthropod Structure & Development 47: 563–613. https://doi.org/10.1016/j.asd.2018.11.001

Boudinot BE, Perrichot V, Chaul JCM (2020) †*Camelosphecia* gen. nov., lost ant-wasp intermediates from the mid-Cretaceous (Hymenoptera, Formicoidea). ZooKeys 1005: 21–55. https://doi.org/10.3897/zookeys.1005.57629

Boudinot BE, Moosdorf OTD, Beutel RG, Richter A (2021) Anatomy and evolution of the head of *Dorylus helvolus* (Formicidae: Dorylinae): Patterns of sex- and caste-limited traits in the sausagefly and the driver ant. Journal of Morphology 282: 1616–1658. https://doi.org/10.1002/jmor.21410

Boudinot BE, Khouri Z, Richter A, Griebenow ZH, van de Kamp T, Perrichot V, Barden P (2022) Evolution and systematics of the Aculeata and kin (Hymenoptera), with emphasis on the ants (Formicoidea: †@@@idae fam. nov., Formicidae). bioRxiv 2022.02.20.480183. https://doi.org/10.1101/2022.02.20.480183

Brady SG, Fisher BL, Schultz TR, Ward PS (2014) The rise of army ants and their relatives: Diversification of specialized predatory doryline ants. BMC Evolutionary Biology 14: 1–93. https://doi.org/10.1186/1471-2148-14-93

Branstetter MG, Longino JT, Ward PS, Faircloth BC (2017) Enriching the ant tree of life: Enhanced UCE bait set for genome-scale phylogenetics of ants and other Hymenoptera. Methods in Ecology and Evolution 8: 768–776. https://doi.org/10.1111/2041-210X.12742

Brown WL (1954) Remarks on the internal phylogeny and subfamily classification of the family Formicidae. Insectes Sociaux 1: 21–31. https://doi.org/10.1007/BF02223148

Brown WL (1975) Contributions toward a reclassification of the Formicidae. V. Ponerinae, tribes Platythyreini, Cerapachyini, Cylindromyrmecini, Acanthostichini, and Aenictogitini. Agriculture 5: 1–115.

Brown WL, Kempf WW (1968) *Tatuidris*, a remarkable new genus of Formicidae (Hymenoptera). Psyche 74(3): 183–190. https://doi.org/10.1155/1967/868759

Brown WL, Nutting WL (1949) Wing venation and the phylogeny of the Formicidae (Hymenoptera). Transactions of the American Entomological Society (1890-)75: 113–132. https://www.jstor.org/stable/25077603 [Accessed 2 April 2023]

Brues C (1925) *Scyphodon*, an anomalous genus of Hymenoptera of doubtful affinities. Treubia 6: 93–96.

Camacho GP, Franco W, Branstetter MG, Pie MR, Longino JT, Schultz TR, Feitosa RM (2022) Uce phylogenomics resolves major relationships among ectaheteromorph ants (Hymenoptera: Formicidae: Ectatomminae, Heteroponerinae): a new classification for the subfamilies and the description of a new genus. Insect Systematics and Diversity 6(1): 1–20. https://doi.org/10.1093/isd/ixab026

Collingwood CA, Agosti D (1996) Formicidae (Insecta: Hymenoptera) of Saudi Arabia (part 2). Fauna of Saudi Arabia 15: 300–385.

Dalla Torre KW (1893) Catalogus Hymenopterorum hucusque descriptorum systematicus et synonymicus (Vol. 7). Formicidae (Heterogyna). W. Engelmann, Leipzig, 289 pp. https://doi.org/10.5962/bhl.title.10348

Déjean A, Schatz B, Orivel J, Beugnon G (1999) Prey capture behavior of *Psalidomyrmex procerus* (Formicidae: Ponerinae), a specialist predator of earthworms (Annelida). Sociobiology 34: 545–554.

Dias RKS, Yamane S, Akbar SA, Peiris HAWS, Wachkoo AA (2019) Discovery of the worker caste of *Protanilla schoedli* Baroni Urbani & De Andrade (Formicidae: Leptanillinae) in Sri Lanka. Oriental Insects 53(2): 160–166. https://doi.org/10.1080/00305316.2018.1476273

Dlussky GM (1969) First finding of an ant from the subfamily Leptanillinae (Hymenoptera, Formicidae) in the USSR. Zoologichekiy jurnal [Зоологический журнал] 48: 1666–1671.

Economo EP, Narula N, Friedman NR, Weiser MD, Guénard B (2018) Macroecology and macroevolution of the latitudinal diversity gradient in ants. Nature Communications 9(1): e1778. https://doi.org/10.1038/s41467-018-04218-4

Emery C (1870) Studi mirmecologici. Bollettino della Società Entomologica Italiana 2: 193–201.

Emery C (1904) Le affinità del genere Leptanilla e i limiti delle Dorylinae. Archivio Zoologico Italiano 2: 107–116.

Emery C (1910) Hymenoptera. Fam. Formicidae. Subfam. Dorylinae. Genera Insectorum 102: 1–34.

Emery C, Forel A (1879) Catalogue des Formicides d'Europe. Mitteilungen der Schweizerische Entomologische Gesellschaft 5: 441–481.

Griebenow Z (2020) Delimitation of tribes in the subfamily Leptanillinae (Hymenoptera: Formicidae), with a description of the male of *Protanilla lini* Terayama, 2009. Myrmecological News 30. https://www.biotaxa.org/mn/article/view/65894 [Accessed 13 October 2021]

Griebenow ZH (2021) Synonymisation of the male-based ant genus *Phaulomyrma* (Hymenoptera: Formicidae) with Leptanilla based upon Bayesian total-evidence phylogenetic inference. Invertebrate Systematics 35(6): 603–636. https://doi.org/10.1071/IS20059

Griebenow ZH, Isaia M, Moradmand M (2022) A remarkable troglomorphic ant, *Yavnella laventa* sp. nov. (Hymenoptera: Formicidae: Leptanillinae), identified as the first known worker of *Yavnella* Kugler by phylogenomic inference. Invertebrate Systematics 36(12): 1118–1138. https://doi.org/10.1071/IS22035

Griebenow ZH, Richter AK, van de Kamp T, Economo EP, Lieberman ZE (in press) Comparative morphology of male genital skeletomusculature in the Leptanillinae (Hymenoptera: Formicidae), with a standardized muscular terminology for the male genitalia of Hymenoptera. Arthropod Systematics & Phylogeny.

Harris RA (1979) A glossary of surface sculpturing. Occasional Papers in Entomology 28: 1–31.

Hita-Garcia F, Lieberman Z, Audisio TL, Liu C, Economo EP (2019) Revision of the highly specialized ant genus *Discothyrea* (Hymenoptera: Formicidae) in the Afrotropics with X-ray microtomography and 3D cybertaxonomy. Insect Systematics and Diversity 3(6): 1–5. https://doi.org/10.1093/isd/ixz015

Hölldobler B, Wilson EO (1990) The Ants. Harvard University Press, Cambridge, 784 pp. https://doi.org/10.1007/978-3-662-10306-7

Hölldobler B, Palmer JM, Masuko K, Brown WL (1989) New exocrine glands in the legionary ants of the genus *Leptanilla* (Hymenoptera, Formicidae, Leptanillinae). Zoomorphology 108: 255–261. https://doi.org/10.1007/BF00312158

Hsu P-W, Hsu F-C, Hsiao Y, Lin C-C (2017) Taxonomic notes on the genus *Protanilla* (Hymenoptera: Formicidae: Leptanillinae) from Taiwan. Zootaxa 4268(1): 117–130. https://doi.org/10.11646/zootaxa.4268.1.7

Imai HT, Kihara A, Kondoh M, Kubota M, Kuribayashi S, Ogata K, Onoyama K, Taylor RW, Terayama M, Yoshimura M, Ugawa Y (2003) Ants of Japan. Gakken, Tokyo, 224 pp.

Ito F, Billen J (1998) Larval hemolymph feeding and oophagy: behavior of queen and workers in the primitive ponerine ant *Prionopelta kraepelini* (Hymenoptera, Formicidae). Belgian journal of zoology 128: 201–209.

Ito F, Yamane S (2020) Behavior of the queen of *Leptanilla clypeata* Yamane et Ito collected in the Bogor Botanical Gardens, West Java, Indonesia (Hymenoptera; Formicidae), with a note on colony composition and a description of the ergatoid queen. Asian Myrmecology 12: e012004. [1–7] https://doi.org/10.20362/AM.012004

Ito F, Hashim R, Mizuno R, Billen J (2022) Notes on the biology of *Protanilla* sp. (Hymenoptera, Formicidae) collected in Ulu Gombak, Peninsular Malaysia. Insectes Sociaux 69(1): 13–18. https://doi.org/10.1007/s00040-021-00839-z

Jacquemin J, Delsinne T, Maraun M, Leponce M (2014) Trophic ecology of the armadillo ant, Tatuidris tatusia, assessed by stable isotopes and behavioral observations. Journal of Insect Science 14: 1–12. https://doi.org/10.1093/jis/14.1.108

Katayama M, Tsuji K (2011) Notes on prey menu of *Protanilla lini* in Okinawa Island. ARI 31: 17–20.

Kugler J (1987) The Leptanillinae (Hymenoptera: Formicidae) of Israel and a description of a new species from India. Israel Journal of Entomology 20: 45–57.

Kutter H (1948) Beitrag zur Kenntnis der Leptanillinae (Hym. Formicidae). Eine neue Ameisengattung aus Süd-Indien. Mitteilungen der Schweizerische Entomologische Gesellschaft 21: 286–295.

Leong C-M, Yamane S, Guénard BS (2018) Lost in the city: discovery of the rare ant genus *Leptanilla* (Hymenoptera: Formicidae) in Macau with description of *Leptanilla macauensis* sp. nov. Asian Myrmecology 10: e010001. [1–16] https://doi.org/10.20362/AM.010001

Lévieux J (1983) A comparison of the ground dwelling ant populations between a Guinea savanna and an evergreen rain forest of the Ivory Coast. In: Breed MD, Michener CD, Evans HE (Eds) The Biology Of Social Insects. CRC Press, New York, 6 pp.

Lieberman ZE, Billen J, van de Kamp T, Boudinot BE (2022) The ant abdomen: the skeletomuscular and soft tissue anatomy of *Amblyopone australis* workers (Hymenoptera: Formicidae). Journal of Morphology 283(6): 693–770. https://doi.org/10.1002/jmor.21471

Liu S-P, Richter A, Stoessel A, Beutel RG (2019) The mesosomal anatomy of *Myrmecia nigrocincta* workers and evolutionary transformations in Formicidae (Hymenoptera). Arthropod Systematics & Phylogeny 77: 1–19.

López F, Martinez MD, Barandica JM (1994) Four new species of the genus *Leptanilla* (Hymenoptera: Formicidae) from Spain – relationships to other species and ecological issues 24: 179–212.

Man P, Ran H, Chen Z, Xu Z (2017) The northern-most record of Leptanillinae in China with description of *Protanilla beijingensis* sp. nov. (Hymenoptera: Formicidae). Asian Myrmecology 9: e009008. [1–12] https://doi.org/10.20362/AM.009008

Masuko K (1989) Larval hemolymph feeding in the ant *Leptanilla japonica* by use of a specialized duct organ, the "larval hemolymph tap" (Hymenoptera: Formicidae). Behavioral Ecology and Sociobiology 24(2): 127–132. https://doi.org/10.1007/BF00299644

Masuko K (1990) Behavior and ecology of the enigmatic ant *Leptanilla japonica* Baroni Urbani (Hymenoptera: Formicidae: Leptanillinae). Insectes Sociaux 37(1): 31–57. https://doi.org/10.1007/BF02223813

Masuko K (2019) Larval hemolymph feeding and hemolymph taps in the ant *Proceratium itoi* (Hymenoptera: Formicidae). Myrmecological News 29: 21–34. https://www.biotaxa.org/mn/article/view/45791 [January 18, 2023]

Mei M (1995) Hymenoptera Formicidae (con diagnosi di due nuove specie). Naturalista Siciliana 19: 753–772.

Ogata K (1991) A generic synopsis of the poneroid complex of the family Formicidae (Hymenoptera). Part II. Subfamily Myrmicinae. Bulletin of the Institute of Tropical Agriculture, Kyushu University 14: 61–149.

Ogata K, Terayama M, Masuko K (1995) The ant genus *Leptanilla*: discovery of the worker-associated male of L. japonica, and a description of a new species from Taiwan (Hymenoptera: Formicidae: Leptanillinae). Systematic Entomology 20(1): 27–34. https://doi.org/10.1111/j.1365-3113.1995.tb00081.x

Pérez-González S, Gómez-Durán JM, Martínez-Ibáñez MD (2020) Highlighting the elusive: New findings and a redescription of the rare ant *Leptanilla plutonia* López, Martínez et Barandica, 1994, presenting morphological novelties for the genus. Annales Zoologici 70(2): 289–304. https://doi.org/10.3161/00034541ANZ2020.70.2.009

Petersen B (1968) Some novelties in presumed males of the Leptanillinae (Hym., Formicidae). Entomologiske Meddelelser 36: 577–598.

Richter A, Garcia FH, Keller RA, Billen J, Katzke J, Boudinot BE, Economo EP, Beutel RG (2021) The head anatomy of *Protanilla lini* (Hymenoptera: Formicidae: Leptanillinae), with a hypothesis of their mandibular movement. Myrmecological News 31: 85–114. https://doi.org/10.25849/myrmecol.news_031:085

Richter A, Boudinot B, Yamamoto S, Katzke J, Beutel RG (2022) The first reconstruction of the head anatomy of a Cretaceous insect, †*Gerontoformica gracilis* (Hymenoptera: Formicidae), and the early evolution of ants. Insect Systematics and Diversity 6(5): 1–4. https://doi.org/10.1093/isd/ixac013

Robertson HG (2000) Formicidae (Hymenoptera: Vespoidea). Daures-biodiversity of the Brandberg Massif, Namibia. Cimbebasia Memoir 9: 371–382.

Romiguier J, Borowiec ML, Weyna A, Helleu Q, Loire E, La Mendola C, Rabeling C, Fisher BL, Ward PS, Keller L (2022) Ant phylogenomics reveals a natural selection hotspot preceding the origin of complex eusociality. Current Biology 32(13): 2942–2947.e4. https://doi.org/10.1016/j.cub.2022.05.001

Santschi F (1907) Fourmis de Tunisie capturées en 1906. Revue Suisse de Zoologie 15: 305–334. https://doi.org/10.5962/bhl.part.75189

Santschi F (1908) Nouvelles fourmis de l'Afrique du Nord (Égypte, Canaries, Tunisie). Annales de la Société Entomologique de France 77: 517–534.

Saroj S, Mandi A, Dubey AK (2022) A new species of the rare ant genus, *Leptanilla* Emery (Hymenoptera: Formicidae) from Eastern Himalaya, India. Asian Myrmecology 15: e015005. [1–9] https://doi.org/10.20362/AM.015005

Satria R, Putri DH, Ahda Y (2023) Genus *Protanilla* Taylor, 1990 (Hymenoptera: Formicidae: Leptanillinae) from Sumatra, with the description of a new species. Serangga 28: 69–78.

Schmidt C (2013) Molecular phylogenetics of ponerine ants (Hymenoptera: Formicidae: Ponerinae). Zootaxa 3647(2): 201–250. https://doi.org/10.11646/zootaxa.3647.2.1

Schulmeister S (2003) Genitalia and terminal abdominal segments of male basal Hymenoptera (Insecta): Morphology and evolution. Organisms, Diversity & Evolution 3(4): 253–279. https://doi.org/10.1078/1439-6092-00078

Simpson GG (1961) Principles of Animal Taxonomy. Columbia University Press, New York, 247 pp. https://doi.org/10.7312/simp92414

Smith MR (1953) A new species of *Probolomyrmex*, and the first description of a *Probolomyrmex* male (Hymenoptera, Formicidae). Journal of the New York Entomological Society 61: 127–129.

Taylor RW (1965) A monographic revision of the rare tropicopolitan ant genus *Probolomyrmex*. Transactions of the Royal Entomological Society of London 117(12): 345–365. https://doi.org/10.1111/j.1365-2311.1965.tb00044.x

Taylor RW (1979) Notes on the Russian endemic ant genus *Aulacopone* Arnoldi (Hymenoptera: Formicidae). Psyche 86(4): 353–361. https://doi.org/10.1155/1979/65643

Terayama M (2013) Additions to knowledge of the ant fauna of Japan (Hymenoptera; Formicidae). Memoirs of the Myrmecological Society of Japan 3: 1–24.

Terayama M, Kinomura K (2015) Rediscovery of *Leptanilla kubotai* Baroni Urbani (Hymenoptera: Formicidae) from Kochi Prefecture, Japan, with a description of queen. ARI 37: 17–22.

Tobias JA, Seddon N, Spottiswoode CN, Pilgrim JD, Fishpool LDC, Collar NJ (2010) Quantitative criteria for species delimitation. The Ibis 152(4): 724–746. https://doi.org/10.1111/j.1474-919X.2010.01051.x

Ward PS (2007) Phylogeny, classification, and species-level taxonomy of ants (Hymenoptera: Formicidae). Zootaxa 1668(1): 549–563. https://doi.org/10.11646/zootaxa.1668.1.26

Ward PS, Boudinot BE (2021) Grappling with homoplasy: taxonomic refinements and reassignments in the ant genera *Camponotus* and *Colobopsis* (Hymenoptera: Formicidae). Arthropod Systematics & Phylogeny 79: 37–56. https://doi.org/10.3897/asp.79.e66978

Ward PS, Branstetter MG (2022) Species paraphyly and social parasitism: phylogenomics, morphology, and geography clarify the evolution of the *Pseudomyrmex elongatulus* group (Hymenoptera: Formicidae), a Mesoamerican ant clade. Insect Systematics and Diversity 6(1): 1–4. https://doi.org/10.1093/isd/ixab025

Ward PS, Fisher BL (2016) Tales of dracula ants: the evolutionary history of the ant subfamily Amblyoponinae (Hymenoptera: Formicidae). Systematic Entomology 41(3): 683–693. https://doi.org/10.1111/syen.12186

Wheeler WM (1918) A study of some ant larvæ, with a consideration of the origin and meaning of the social habit among insects. Proceedings of the American Philosophical Society 57: 293–343. https://www.jstor.org/stable/983940 [Accessed 2 April 2023]

Wheeler WM (1923) Social life among the insects. Harcourt, Brace and Co., New York, 375 pp.

Wheeler GC (1928) The larva of *Leptanilla*. Psyche 38: 85–91. https://doi.org/10.1155/1928/34510

Wheeler WM (1932) An Australian *Leptanilla*. Psyche 39: 53–58. https://doi.org/10.1155/1932/81860

Wheeler GC, Wheeler J (1930) Two new ants from Java. Psyche 37(3): 193–201. https://doi.org/10.1155/1930/93593

Wheeler GC, Wheeler J (1965) The ant larvae of the subfamily Leptanillinae (Hymenoptera, Formicidae). Psyche 72: 24–34. https://doi.org/10.1155/1965/28458

Wheeler GC, Wheeler J (1976) Ant larvae: Review and synthesis. Proceedings of the Entomological Society of Washington 7: 1–108.

Wheeler GC, Wheeler J (1986) Ten-year supplement to "Ant larvae: Review and synthesis". Proceedings of the Entomological Society of Washington 88: 684–702.

Wheeler GC, Wheeler J (1988) The larva of *Leptanilla japonica*, with notes on the genus (Hymenoptera: Formicidae: Leptanillinae). Psyche: A Journal of Entomology 95: 185–189. https://doi.org/10.1155/1988/83074

Whitmore TC (1988) Tropical Rainforests of the Far East (2nd edn.). Clarendon Press, Oxford, 368 pp.

Wilson EO (1955) A monographic revision of the genus *Lasius*. Bulletin of the Museum of Comparative Zoology 113: 1–201.

Yamada A, Nguyen DD, Eguchi K (2020) Unveiling the morphology of the Oriental rare monotypic ant genus *Opamyrma* Yamane, Bui & Eguchi, 2008 (Hymenoptera: Formicidae: Leptanillinae) and its evolutionary implications, with first descriptions of the male, larva, tentorium, and sting apparatus. Myrmecological News 30: 111–124. https://www.biotaxa.org/mn/article/view/59255 [Accessed 12 October 2021]

Yamamuro K (2018) Biological notes of *Protanilla lini* (Formicidae, Leptanillinae) in captivity. Tsunekibachi 32: 19–24.

Yamane S, Bui TV, Eguchi K (2008) *Opamyrma hungvuong*, a new genus and species of ant related to *Apomyrma* (Hymenoptera: Formicidae: Amblyoponinae). Zootaxa 1767(1): 1–55. https://doi.org/10.11646/zootaxa.1767.1.3

Yoder MJ, Mikó I, Seltmann KC, Bertone MA, Deans AR (2010) A gross anatomy ontology for Hymenoptera. PLoS ONE 5(12): e15991. https://doi.org/10.1371/journal.pone.0015991

Supplementary material 1

Relevant collection data for specimens included in this study, if not previously reported in Griebenow (2020, 2021) or Griebenow et al. (2022)

Author: Zachary Griebenow

Data type: xlsx

Link: https://doi.org/10.3897/zookeys.1189.107506.suppl1

ZooKeys 1189: 185–202 (2024)
DOI: 10.3897/zookeys.1189.113635

Research Article

An overview of the Leucospidae (Hymenoptera, Chalcidoidea) of the Arabian Peninsula with description of a new species

Syed Kamran Ahmad[1], Syeda Uzma Usman[2], Farmanur Rahman Khan[3], Hossein Lotfalizadeh[4], Hassan A. Dawah[5], Parvez Qamar Rizvi[1], Prince Tarique Anwar[6]

1 *Department of Plant Protection, Faculty of Agricultural Sciences, Aligarh Muslim University, Aligarh – 202002, India*
2 *Department of Zoology, Mohammad Ali Jauhar University, Rampur – 244901, Uttar Pradesh, India*
3 *Department of Biology, Deanship of Educational Services, Qassim University, Buraidah – 51452, Al-Qassim, Saudi Arabia*
4 *Department of Plant Protection, East-Azarbaijan Agricultural and Natural Resources Research Center, Agricultural Research, Education and Extension Organization (AREEO), Tabriz, Iran*
5 *Centre for Environmental Research and Studies, Jazan University, P.O. Box 2095, Jazan, Saudi Arabia*
6 *Department of Zoology, School of Sciences, Aligarh College of Education, Chherat, Aligarh – 202122, India*
Corresponding authors: Syeda Uzma Usman (insect.11lab@gmail.com); Prince Tarique Anwar (ta.friday@gmail.com)

Abstract

An overview of the family Leucospidae (Hymenoptera, Chalcidoidea) is provided for the leucospid fauna of the Arabian Peninsula. Two genera containing four species are identified based on morphometrics and colour patterns. One species, *Leucospis ayezae* Usman, Anwar & Ahmad, **sp. nov.**, is described. *Leucospis elegans* Klug had been previously recorded from Arabia Felix (= Yemen) and is recorded here for the first time from Saudi Arabia. The status of *Leucospis* aff. *namibica* from Yemen has been clarified, and this species is placed here in the genus *Micrapion* Kriechbaumer as *M. clavaforme* Steffan. An updated key and a map showing the distribution of the family Leucospidae in the Arabian Peninsula is provided. The occurrence and color morphs of all leucospid species that have been recorded so far from the region are briefly discussed.

Key words: Biodiversity, ectoparasitoids, new species, taxonomy

Academic editor: Andreas Köhler
Received: 6 October 2023
Accepted: 10 December 2023
Published: 16 January 2024

ZooBank: https://zoobank.org/8D05BBE1-922C-4E76-8256-5B02AF30D857

Citation: Ahmad SK, Usman SU, Khan FR, Lotfalizadeh H, Dawah HA, Rizvi PQ, Anwar PT (2024) An overview of the Leucospidae (Hymenoptera, Chalcidoidea) of the Arabian Peninsula with description of a new species. ZooKeys 1189: 185–202. https://doi.org/10.3897/zookeys.1189.113635

Introduction

Members of the family Leucospidae (Hymenoptera, Chalcidoidea) are large chalcid wasps (6–15 mm) and develop as ectoparasitoids on aculeate wasps or bees (Lima and Dias 2018). They are mostly dark brown, red, or yellow, with a patterned, orange or white body, metafemur enlarged with teeth, and strongly curved metatibia. Females typically have a recurved ovipositor which lies along the dorsal side of the metasoma. Leucospids are cosmopolitan in their distribution but rarely encountered, and there are 144 described species worldwide which belong to four genera (Noyes 2019).

The family is mostly represented by the genus *Leucospis* Fabricius, which accounts for more than 86% of the total number of species. Bouček (1974) provided a comprehensive taxonomic revision of the Leucospidae and provided separate keys to American, African, and Asiatic-Australian *Leucospis* species. More recently, Ye et al. (2017) recognized and provided a key to 12 *Leucospis* species from China. In the Arabian Peninsula six valid leucospid species have been reported so far: *Leucospis elegans* Klug (Bouček 1974 from Saudi Arabia [= Arabia Felix i.e., Yemen]; Schmid-Egger 2010 from UAE), *L. insularis* Kirby (Kirby 1900 from Yemen), *L. vanharteni* Schmid-Egger (Schmid-Egger 2010 from UAE), *L. arabica* Gadallah & Soliman, *L. africana* Cameron, and *Micrapion clavaforme* Steffan (Gadallah et al. 2018 from Saudi Arabia).

Schmid-Egger (2010) tentatively identified two specimens of *Leucospis* as *L.* aff. *namibica*. On close examination of his figure (Schmid-Egger 2010: 321, pl. 3), there is no doubt that the specimens are not a *Leucospis* but *Micrapion clavaforme* Steffan instead. Some other important works on the Leucospidae from the Middle East were provided by Hesami et al. (2005), Lotfalizadeh and Fakhrzadeh (2012), Madl and Schwarz (2014), and Kareem et al. (2020). Schmid-Egger (2010) provided a key to four species of from the UAE and Yemen, and Gadallah et al. (2018) keyed five species of Leucospidae (one *Micrapion* Kriechbaumer species and four *Leucospis* species) from Saudi Arabia.

Here we describe a new species of *Leucospis* from Jazan, Saudi Arabia, and also report on some of the known *Leucospis* and *Micrapion* species. Diagnoses and illustrations of types are provided for two of them, *L. insularis* and *L. africana*. An extended and modified version of map (Fig. 1) and the key given by Schmid-Egger (2010) and Gadallah et al. (2018) is also provided to place our newly described species. All species treated herein are fully illustrated.

Methods

The study is based on the materials collected from three provinces of Saudi Arabia, Asir, Najran, and Jazan (Table 1). The specimens were collected mainly by one of two methods, either by sweep net (SN) or in a Malaise trap (MT). The collected specimens were primarily stored in 80% ethanol and were later mounted on rectangular cards. For each species, one pair of wings were removed and mounted on a slide. For the new species, *Leucospis ayzae*, the head and a hind leg was removed and mounted on the same card while one antenna was mounted on slide by following the methods described by Noyes (1982) with modifications as mentioned by Anwar et al. (2020). Photographs

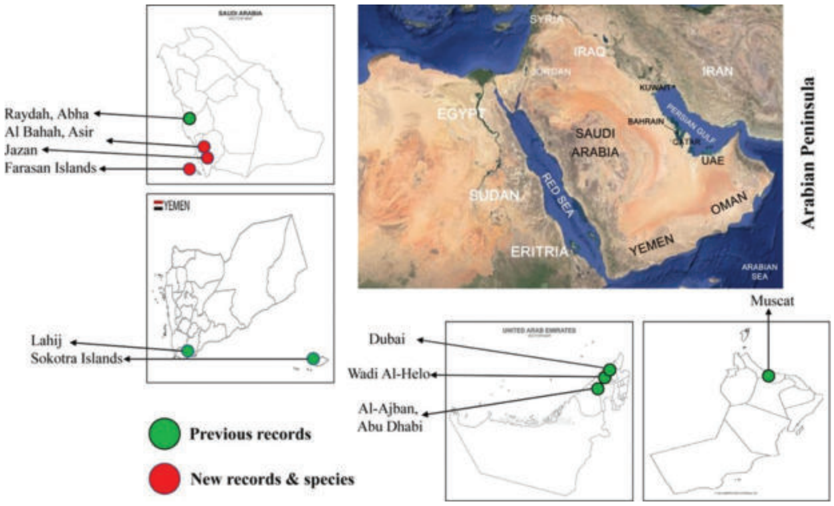

Figure 1. Distribution map of leucospid species in the Arabian Peninsula.

Table 1. List of sampling sites with coordinates, altitude, and sampling methods for Leucospidae collected from Southwest of Saudi Arabia.

Locality	Coordinates	Altitude (m)	Method
Abha, Hay Al-Menhel, vegetable farm	18°12'N, 42°29'E	2214	MT
Abha, Hay Al-Nusub (Abha Farm Centre) vegetable farm	18°13'N, 42°30'E	2226	MT, SN
Jazan, Farasan Island, Aziz Yousef Village	16°40'N, 42°50'E	3	MT, SN
Najran, Al-Shurfa	17°31'N, 44°15'E	1342	MT

of card-mounted specimens were taken using a Nikon SMZ 1000 stereozoom binocular microscope. Figs 3B, 5B, 8C, D were taken using a video camera and Synaptics Automontage software to produce a montage image of the species. Photographs of the slide-mounted parts were taken with a Leica DFC295 digital camera attached to a Leica DM 2500 compound microscope with automountage facility. The final figures were prepared using Adobe Photoshop v. 7.0.

Measurements were made with the use of an ocular micrometer attached to the eyepiece of the microscope and were later converted into micrometers (μm). All the determined and type materials were deposited at the Insect Collections Department of Zoology, Aligarh Muslim University, Aligarh, Uttar Pradesh, India.

The terms mentioned in the text follow Bouček (1974) and Lima and Dias (2018).

List of abbreviations used in the text: **AOL**, anterior-ocular length; **MOD**, midian ocellar diameter; **OCL,** ocular–occipit length; **OOL**, ocello–ocular line; **POL**, posterior ocellar line; **psa**, parascrobal area; **F**, antennal flagellomere; **PMV**, postmarginal vein of fore wing; **STV**, stigmal vein; **GT**, gastral or metasomal tergite; **MT**, Malaise trap; **SN**, Sweep net.

The following acronym is used for the depository:

BMNH	Natural History Museum [formerly British Museum (Natural History)], Department of Entomology, London, UK;
KSMA	King Saud University Museum of Arthropods, Plant Protection Department, College of Food and Agriculture Sciences, King Saud University, Riyadh, Saudi Arabia;
MNHN	Muséum National d'Histoire Naturelle, Paris, France;
NMWC	The National Museum of Wales, Cardiff, UK;
ZMHU	Zoological Museum, Humboldt University, Berlin, Germany;
ZDAMU	Department of Zoology, Aligarh Muslim University, Aligarh, India.

Results

Four species, including one new species, are among the materials examined. These belong to one of two genera, either *Leucospis* or *Micrapion*. The family Leucopsidae has seven species in total known from the Arabian Peninsula, and all seven species are keyed below.

An updated key to females of Leucospidae from the Arabian Peninsula

Modified from Schmid-Egger 2010 and Gadallah et al. 2018.

1 Clypeus curved convexly at posterior margin and without a median tooth; mandibles thin, setose, and notched at apex; gaster distinctly clavate,

basally narrow (Fig. 9A, C); GT4 with hind margin always produced backward and sharply angulate (Fig. 9A, C); GT6 fused to epipygium (gaster with coarse punctures; GT1 without band and with shiny interspaces; apical band of GT5 0.5× as broad as length of sheaths; metafemur relatively slender) .... ***Micrapion clavaforme*** **Steffan**

– Clypeus bilobed at posterior margin and often with a median tooth; mandibles robust, without setae; lower tooth stronger; gaster less clavate (Figs 3C, 4A, 5B, 7B, 8B); GT4 posteriorly straight; GT6 distinctly separated from epipygium .... **2 (genus *Leucospis* Fabricius)**

2 Pronotum with three distinct transverse carinae (Figs 3A, 5A, 7A, 8A) **3**

– Pronotum with at most two transverse, less-developed carinae (Fig. 4A)... **6**

3 Ovipositor short, not reaching anterior margin of GT5 (Fig. 7A) .... ***Leucospis africana*** **Cameron**

– Ovipositor long, reaching at least posterior margin of GT4 or beyond (Figs 3A, 4A, 5B, 8B) **4**

4 Discal carina on pronotum weak and straight (Fig. 8A); metafemur slender with nine ventral teeth, basal tooth angular and pointed (Fig. 8A); ovipositor distinctly reaching beyond (hind fifth) posterior margin of GT1 (Fig. 8B) .... ***Leucospis insularis*** **Kirby**

– Discal carina on pronotum strong and angulate; metafemur oval with eight or nine ventral teeth, basal tooth triangular and robust; ovipositor hardly reaching posterior margin of GT1 .... **5**

5 Metafemur with nine ventral teeth (Fig. 3B); ovipositor hardly reaching posterior margin of GT4 (Fig. 3C) .... ***Leucospis ayezae*** **Usman, Anwar & Ahmad sp. nov.**

– Metafemur with eight ventral teeth (Fig. 5A); ovipositor clearly reaching posterior margin of GT1 (Fig. 5B).......................... ***Leucospis elegans*** **Klug**

6 Pronotum red or orange, except black at base of mesopleuron; middle teeth of metafemur distinctly longer than basal triangular tooth .... ***Leucospis vanharteni*** **Schmid-Egger**

– Pronotum dark brown, except with a transverse yellow strip posteriorly between preapical and marginal carinae, continuing to lateral panel of pronotum as an oblique marking above ventral depression of panel (Fig. 4A); basal tooth of metafemur longer and more robust than any of the following teeth .... ***Leucospis arabica*** **Gadallah & Soliman**

Taxonomy

New species

Leucospis ayezae **Usman, Anwar & Ahmad, sp. nov.**
https://zoobank.org/02A1622A-412E-423C-B50C-028EE20D31EF
Figs 2, 3

Type material. ***Holotype*:** Saudi Arabia • ♀; Asir, Abha, Hay Al-Nusub; 18°13'N, 42°30'E; 2226 m alt.; 24.vii.2013; H.A. Dawah leg.; ZDAMU Reg. No. HYM.CH.873, body, dissected head with one antenna and one dissected hind leg on card; one pair of fore wing and antenna on slide under two coverslips, slide HYM.06.

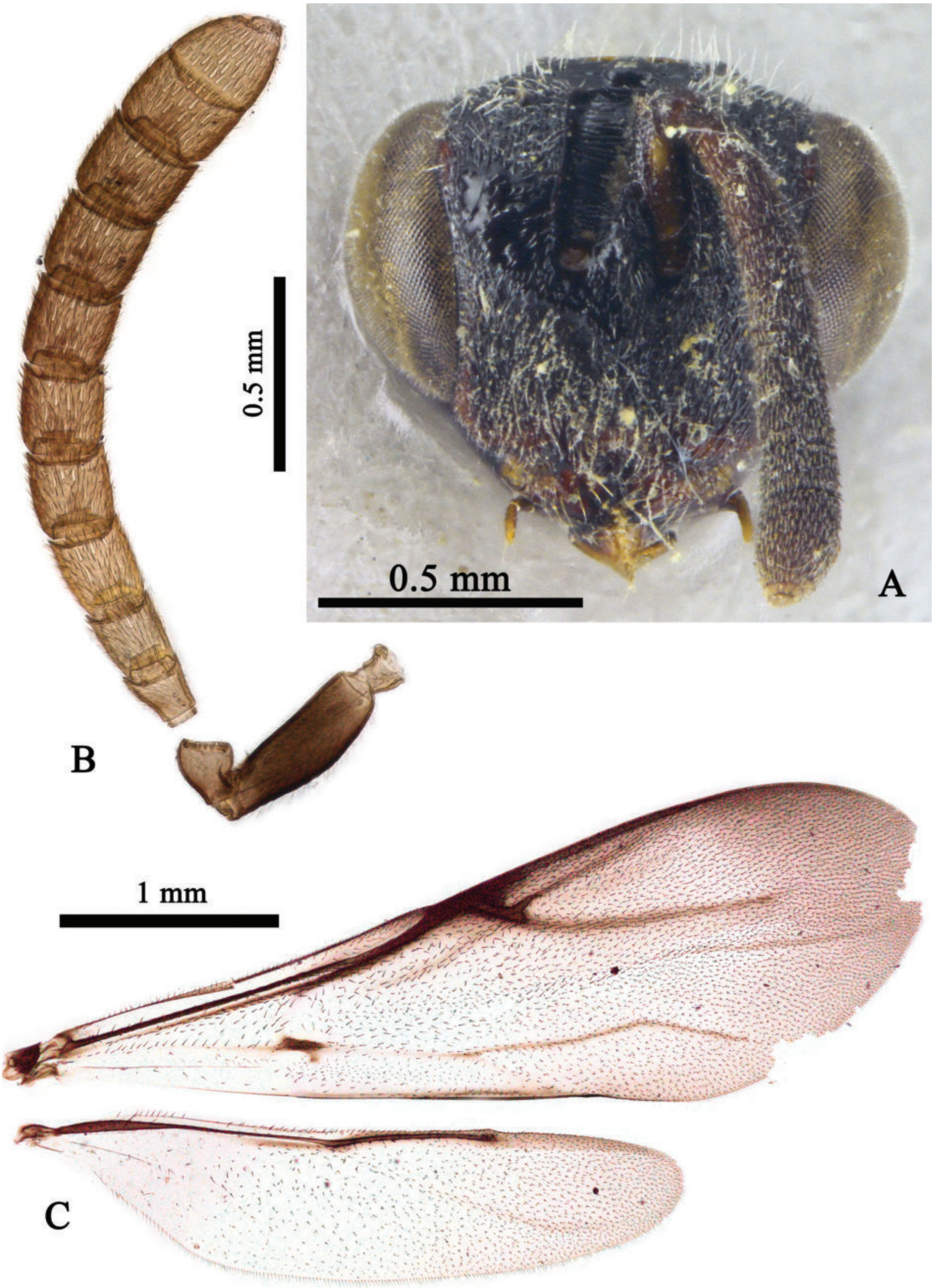

Figure 2. *Leucospis ayezae* Usman, Anwar & Ahmad sp. nov. holotype, female **A** head, frontal view **B** antenna **C** wings.

Figure 3. *Leucospis ayezae* Usman, Anwar & Ahmad sp. nov. holotype, female, habitus **A** lateral view **B** dorsal view.

Diagnosis. The new species is similar to *L. insularis* in having a yellow band on the pronotum and scutellum and distinct discal, preapical, and marginal carinae, but the new species differs from *L. insularis* as follows: discal carina on pronotum strong and angulate (discal carina on pronotum weak and straight in *L. insularis*); metafemora oval with eight ventral teeth, basal tooth triangular and robust (metafemora slender with nine ventral teeth, basal tooth angular and pointed in *L. insularis*); pubescence on sides of propodeum and metatibia relatively short and less dense (pubescence on sides of propodeum and metatibia long and more dense in *L. insularis*) ovipositor hardly reaching posterior margin of GT4 (ovipositor distinctly reaching beyond posterior margin of GT1 in *L. insularis*).

Description. ***Colour*** (Figs 2A, 3). Head dark brown; maxillary and labial palps yellowish brown; antenna dark brown except scape with posterior margin yellow. Mesosoma dark brown except a yellow transverse strip in front of discal carina, not continuing to sides of pronotum, and a narrow, transverse yellow strip on scutellum just above apex. Gaster largely reddish to dark brown, with transverse yellow strips medially on GT4 and apically on GT5. Basal two-thirds of ovipositor reddish brown; the rest dark brown. Pro- and mesofemur brown, with yellow tips where joining tibia; pro- and mesotibia reddish brown, with their margins yellow; hind legs dark brown except apex of coxa in ventral view and margins of femur yellow; all tarsi yellow. Fore wing below PMV and in apical half strongly infuscate, the rest hyaline.

Head (Fig. 2A). Head in frontal view 1.2× as broad as high and as wide as posterior margin of pronotum; less densely punctuate, medially at psa smooth, setae on face and eyes silvery, erect, and less dense; POL 2× OOL and 3× MOD; scrobe 1.5× as wide as parascrobal area, transversely carinate; occipital carina distinctly visible between and beyond posterior ocelli; malar space 0.35× eye height and as long as F7; flagellum with erect, black setae; F1 widened apically, as long as broad and shortest of all funicular segments individually; F3–F5 subequal in length; F7 longest; clava 1.7× as long as broad, distinctly longer than F7 and F8 combined (Fig. 2B); mandible tridentate.

Mesosoma (Fig. 3A, C). Mesosoma densely punctuate, punctures setigerous, with dense, long, pale setae; setae denser on propodeal callus; discal, preapical, and marginal carinae well developed, raised, and angulate; posterior margin of scutellum with punctures in a line with margins and with carina; propodeum medially with a complete carina. Hind leg with coxa punctuate, carinate and subserrate posterodorsally; metafemur oval, 1.9× as long as broad, punctuate, and setose, with eight ventral teeth; basal tooth robust, 3–5 longer than rest and subequal (Fig. 3B); metatibia with spine subequal to spur. Fore wing 3.2× as long as broad, with dense, black setation towards apical margin; STV with bifurcate uncus; uncus longer than apical process of stigmal vein (Fig. 2C). Hind wing 4.4× as long as broad (Fig. 2C).

Metasoma (Fig. 3A, C). Gaster moderately punctuate, with dense, pale setae; density of setae more at epipygium. GT1 wider than long, interiorly with triangular process attached to petiole and, medially with a raised carina, narrower than GT4 in dorsal view; GT4 with posterior margin entire; ovipositor sheaths long, nearly reaching anterior margin of GT3.

Measurements (holotype, mm): head width:length:height, 1.4:0.7:1.2; AOL, 0.14; MOD, 0.12; OCL, 0.03; OOL, 0.19; POL, 0.38; sh [scrobe height], 0.51; sw [scrobe weight], 0.4; psa, 0.33; ceh [compound eye height], 0.82; mls [malar space], 0.28; antennal segments length:width — radicle, 0.13:0.16; scape, 0.64:0.2; pedicel, 0.24:0.17; F1, 0.16:0.16; F2, 0.22:0.2; F3, 0.25:0.24; F4, 0.25:0.25; F5, 0.25:0.27; F6, 0.25:0.28; F7, 0.28:0.22; F8, 0.24:0.32; clava, 0.56:0.33; pronotum, 0.56; mesoscutum, 0.72; scutellum, 0.61; dorsellum, 0.16; propodeum, 0.24; fore wing length:width, 4.4:1.35; hind wing length:width, 3.1:7; metacoxa, 0.96:0.85; metafemur, 1.24:0.64; metatibia, 1.12; metatarsus, 1.12; petiole, 0.16:0.37; gaster, 2.8; GT1, 0.9; GT3, 0.1; GT4, 0.4; GT5, 0.7; GT6, 0.2; ovipositor, 1.4; hypopygeum, 0.8.

Male. Unknown.

Host. Unknown.

Distribution. Saudi Arabia: Asir.

Etymology. The species name after Ayeza Tarique, daughter of the authors SUU and PTA.

Other species

Leucospis arabica **Gadallah & Soliman, 2018**
Fig. 4

Leucospis arabica Gadallah & Soliman in Gadallah et al. 2018: 2079, female, male. Holotype, female (KSMA), Saudi Arabia (Jazan, Farasan Islands), not examined.

Materials examined. 8♀, 9♂. Saudi Arabia • Jazan, Farasan Island, Aziz Yousef Village; 16°40'N, 42°50'E; 3 m alt.; 6♀, 9♂ (each on cards; 2 females, 1 male with one pair of wings on slide under 1 coverslip, slide No. HYM.02, 03, 11), 15.v.2017; S.K. Ahmad leg.; 2♀ (on cards); 13.v.2017; H.A. Dawah leg.; ZDAMU.

Remarks. The examined specimens were collected from the type locality and differ from the holotype in size. The females were 5–15 mm long and males 2–10 mm long. In both sexes, the size of the yellow patch on the metafemur varies minute to broad.

Host. Unknown.

Distribution. Saudi Arabia: Jazan (Farasan Islands) and Egypt (Sinai Peninsula).

Leucospis elegans **Klug, 1834**
Figs 5, 6

Leucospis elegans Klug, 1834: 26. Holotype, female (ZMHU), Yemen, not examined.

Materials examined. 2♀, 1♂. Saudi Arabia • Jazan, Farasan Island, Aziz Yousef Village; 16°40'N, 42°50'E; 3 m alt.; 2♀ (on cards, one pair of fore wing of one female specimen on slide under 1 coverslip, slide No. HYM.04; one pair of fore wing and antenna of other female specimen on slide under 2 coverslips, slide No. HYM.05), 15.v.2017; S.K. Ahmad leg.; 1♂ (on card, one pair of fore wing and antenna on slide under 2 coverslips, slide No. HYM.10), 1.ii.2015; H.A. Dawah leg.; ZDAMU.

Figure 4. *Leucospis arabica* Gadallah & Soliman, habitus **A** female, lateral view **B** male, lateral view.

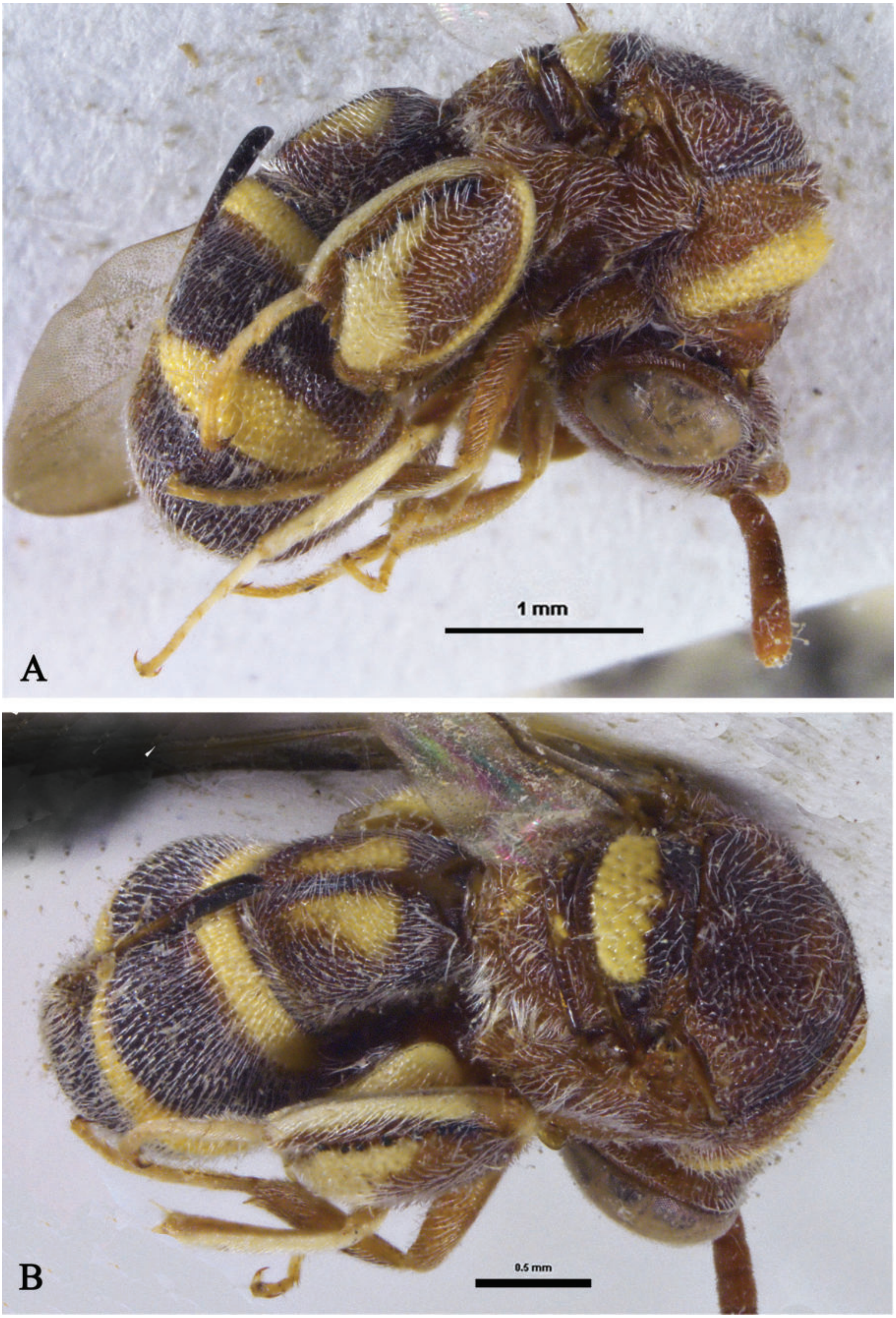

Figure 5. *Leucospis elegans* Klug, female, habitus **A** lateral view **B** dorsal view.

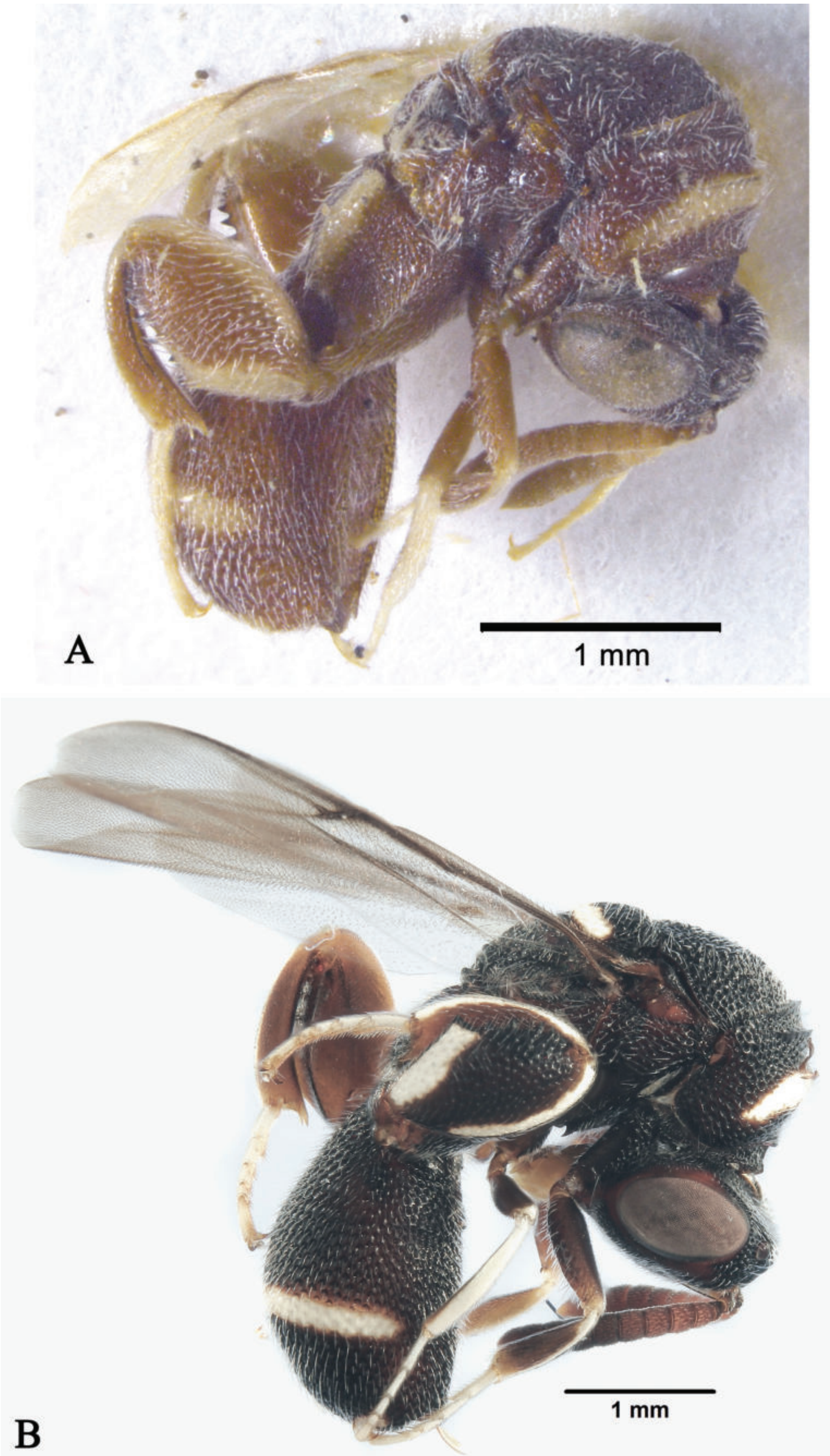

Figure 6. *Leucospis elegans* Klug, males, habitus, lateral view **A** reddish brown-yellow morph **B** dark brown-pale yellow morph.

Remarks. This is the first record of *L. elegans* from Saudi Arabia. However, Bouček (1974) included it in the fauna of Saudi Arabia but referred to Arabia Felix, which is a former name for Yemen. He briefly provided a diagnosis of *L. elegans* and described the male for the first time.

Host. Unknown.

Distribution. Afrotropical, Palaearctic, Oriental (Klug 1834; Bouček 1959, 1974; Narendran 1986; Schmid-Egger 2010; Madl and Schwarz 2014; Gadallah et al. 2018). Yemen (as Arabia Felix; Bouček 1974). Saudi Arabia (new record).

Leucospis africana **Cameron, 1907**

Fig. 7

Leucospis africana Cameron, 1907: 204. Lectotype, female (BMNH), designated by Bouček 1974: 104, South Africa (Cape Province), examined (illustrations only).

Remarks. Bouček (1974) recorded *L. africana* from several African countries and provided a brief diagnosis of females and described the males. He further recorded its host for the first time. Gadallah at al. (2018) recorded males from Saudi Arabia and provided a detailed diagnosis of males and a key identify it from other species of Saudi Arabia. Here, we figure the lectotype for the first time.

Host. *Serapista denticulata* (Smith) (Hymenoptera, Megachilidae) (Bouček 1974); *Megachile spinarum* Cockerell (Hymenoptera, Megachilidae) (Gess 1981).

Distribution. Afrotropical: Burundi, Central African Republic, Democratic Republic of Congo, Eretria, Ethiopia, Ghana, Ivory Coast, Kenya, Lesotho, Malawi, Mozambique, Nigeria, Rhodesia, South Africa, Tanzania, Uganda, Zambia, Zimbabwe (Cameron 1907; Bouček 1974; Noyes 2019); Saudi Arabia (Gadallah at al. 2018).

Leucospis insularis **Kirby, 1900**

Fig. 8

Leucospis insularis Kirby, 1900: 13. Holotype, female (BMNH), Yemen (Socotra Island), examined (illustrations only).

Remarks. *Leucospis insularis* is only known from the type locality Socotra Islands (Yemen). Bouček (1974) included *L. insularis* in a key to African *Leucospis*. Schmid-Egger (2010) included it his key to Arabian species. Here, we figure the holotype for the first time.

Host. Unknown.

Distribution. Afrotropical: Socotra Islands (Yemen) (Kirby 1900).

Micrapion clavaforme **Steffan, 1948**

Fig. 9

Micrapion clavaforme Steffan, 1948: 85, female. Lectotype, female (MNHN), designated by Bouček 1974: 220, Gabon (Ogowe), not examined.

Material examined. 3♀, 2♂. Saudi Arabia • Asir, Abha, Hay Al-Menhel; 18°12'N, 42°29'E; 2214 m alt.; 2♀ (one on card; one on card with one pair of fore wing on slide under 1 coverslip, slide No. HYM.01), 20.xii.2014; H.A. Dawah leg.; Najran • Al-Shurfa, Saleh Maqbol Farm, 17°31'N, 44°15'E; 1342 m alt.; 1♀ (on card, one

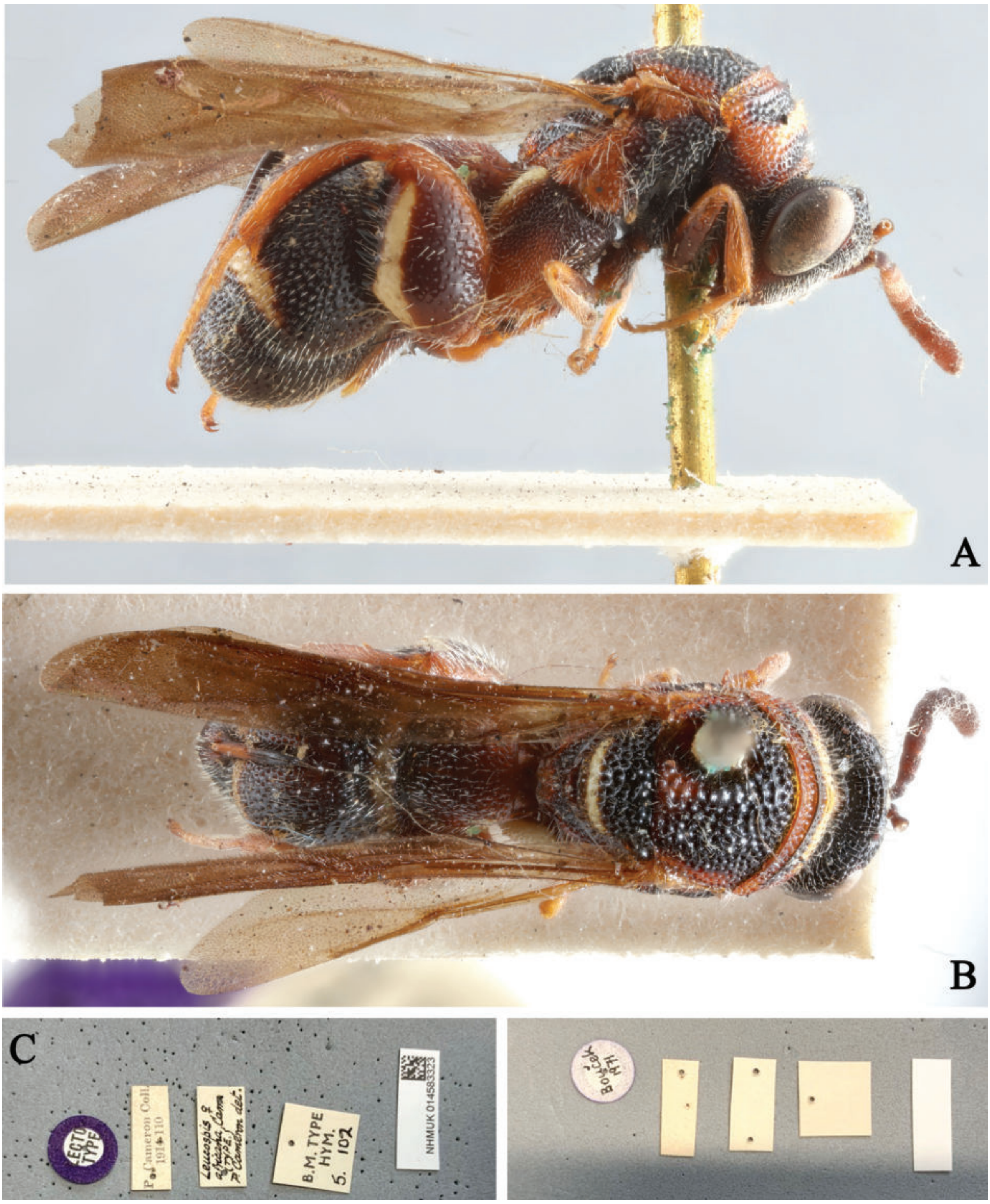

Figure 7. *Leucospis africana* Cameron, lectotype, female (photographs courtesy of Natalie Dale-Skey Papilloud, BMNH) **A** lateral view **B** dorsal view **C** labels.

Figure 8. *Leucospis insularis* Kirby, holotype, female (photographs courtesy of Natalie Dale-Skey Papilloud, BMNH) **A** lateral view **B** dorsal view **C** labels.

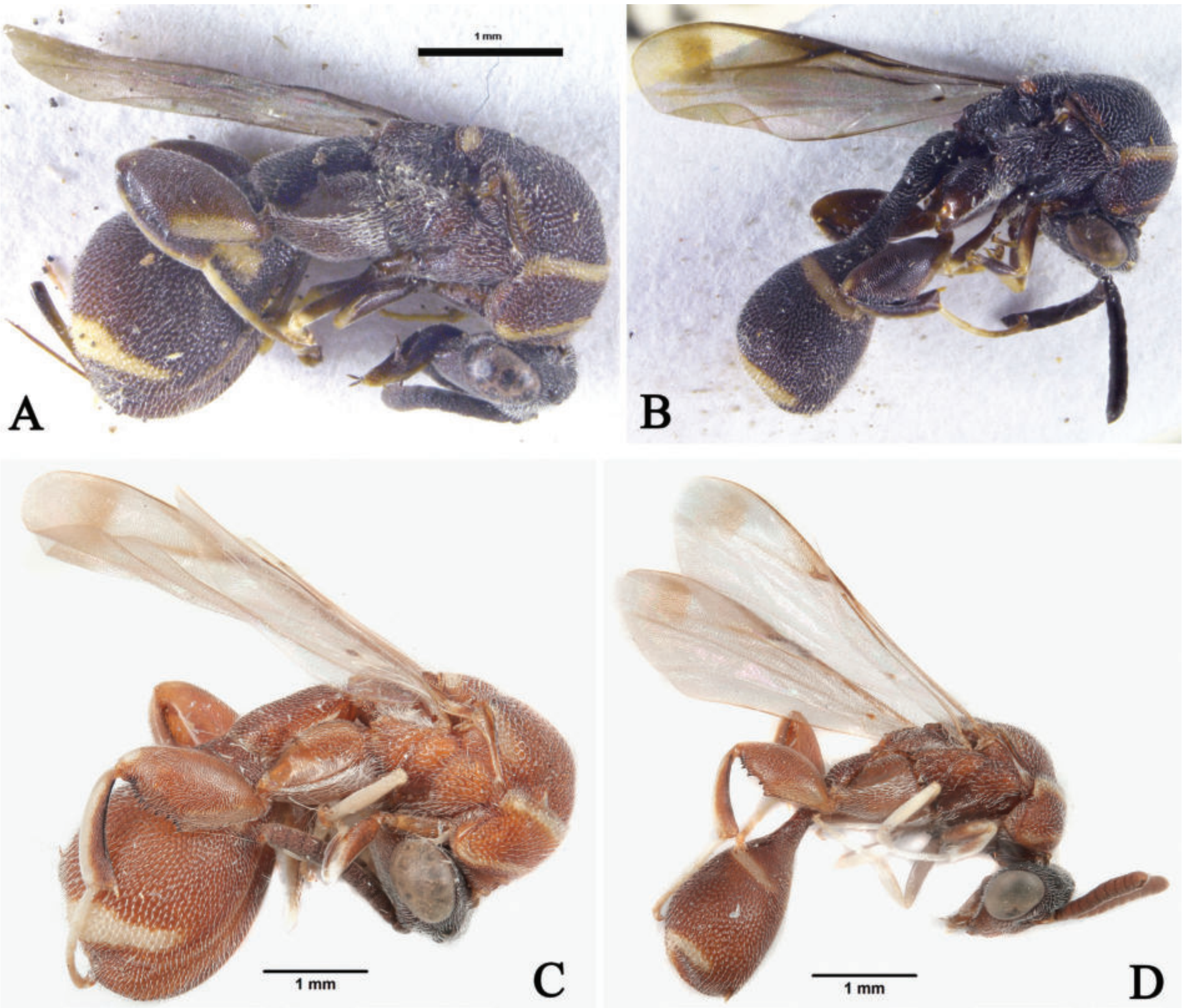

Figure 9. *Micrapion clavaforme* Steffan, habitus, lateral view **A, B** dark brown-pale yellow morph **A** female **B** male **C, D** reddish brown-yellow morph **C** female **D** male.

pair of fore wing on slide under 1 coverslip, slide No. HYM.09), 17.ix.2014; H.A. Dawah leg.; Asir, Abha, Hay Al-Nusub, 18°13'N, 42°30'E; 2226 m alt.; 2♂ (one on card; one on card with one pair of fore wing on slide under 1 coverslip, slide No. HYM.07), 3.vi.2015; H.A. Dawah leg.; ZDAMU.

Remarks. Females and males were collected in the present study from two sites in Saudi Arabia. They agree fairly well with the original description of *M. clavaforme* and the diagnoses by Bouček (1974) and Gadallah et al. (2018). In both sexes there are two colour morphs, one brown with ivory stripes and another reddish brown with yellow stripes. All specimens, however, exhibit almost no variation in stripe patterns and wing infuscation.

Schmid-Egger (2010) tentatively identified two *Leucospis* specimens from Yemen as *L.* aff. *namibica*. On close examination of his figure (Schmid-Egger 2010: 321, pl. 3) there is no doubt that these specimens are not a *Leucospis* species but *Micrapion* Kriechbaumer instead. Here, these specimens are re-identified as *M. clavaforme*.

Host. Solitary bees: *Ceratina* Latreille (Bouček 1974).

Distribution. Afrotropical: (Steffan 1948; Bouček 1974). Saudi Arabia (Al Bahah, Asir, Najran) (Gadallah et al. 2018); Yemen (Schmid-Egger 2010 as *Leucospis* aff. *namibica*).

Acknowledgements

We thank Dr Mohammad Hayat and Dr Shahid Bin Zeya (ZDAMU) for encouragement and for providing space to carry out our research. Natalie Dale-Skey Papilloud (BMNH), kindly provided photographs of type materials of *Leucospis africana* and *L. insularis*. The National Museum Wales is gratefully acknowledged for their painstaking efforts in imaging Figs 3B, 5B, and 8C, D. Farmanur R. Khan thanks the Deanship of Scientific Research, Qassim University, for funding the publication of this study.

Additional information

Conflict of interest

The authors have declared that no competing interests exist.

Ethical statement

No ethical statement was reported.

Funding

This study was supported by Qassim University.

Author contributions

SK Ahmad and HA Dawah carried out sampling identified the family Leucospidae, conceived the idea of the research and, helped in preparing the map work. SU Usman and PT Anwar identified the genus and species and, prepared the manuscript. H Lotfalizadeh provided various information and literature on the Leucospidae and, critically revised the MS. FR Khan helped in preparation of the manuscript and provided several information about the Arabian fauna of chalcid wasps. The entire work was carried out under the mentorship of PQ Rizvi.

Author ORCIDs

Syed Kamran Ahmad https://orcid.org/0000-0002-6211-2345
Syeda Uzma Usman https://orcid.org/0000-0003-2578-2515
Farmanur Rahman Khan https://orcid.org/0000-0001-8906-709X
Hossein Lotfalizadeh https://orcid.org/0000-0002-7927-819X
Hassan A. Dawah https://orcid.org/0000-0001-5642-7247
Parvez Qamar Rizvi https://orcid.org/0000-0002-2965-1806
Prince Tarique Anwar https://orcid.org/0000-0002-1682-0033

Data availability

All of the data that support the findings of this study are available in the main text.

References

Anwar PT, Zeya SB, Veenakumari K (2020) Fairyfly genus *Camptoptera* Foerster (Hymenoptera: Chalcidoidea: Mymaridae) in India and Sri Lanka, with descriptions of eleven new species. In: Paulus HF (Ed.) Zoologica (Vol. 165). Schweizerbart Science Publishers, Frankfurt, 89 pp.

Bouček Z (1959) A revised key to the West-Palaearctic species of *Leucospis* (Hym., Chalc.), with some new synonymy. Acta Entomologica Musei Nationalis Pragae 33(562): 435–444.

Bouček Z (1974) A revision of the Leucospidae (Hymenoptera: Chalcidoidea) of the world. Bulletin of the British Museum (Natural History). Entomology 23: 1–241. https://doi.org/10.5962/p.140909

Cameron P (1907) Descriptions of species of parasitic Hymenoptera, chiefly in the collections of the South African Museum, Cape Town. (Second paper). Annals of the South African Museum 5: 203–225.

Gadallah NS, Soliman AM, Abu El-Ghiet UM, Elsheikh TY, Al Dhafer HM (2018) The family Leucospidae (Hymenoptera: Chalcidoidea) from the South of Saudi Arabia, with the first report of the genus *Micrapion* and description of *Leucospis arabica* sp. nov. Journal of Natural History 52(31–32): 2071–2096. https://doi.org/10.1080/00222933.2018.1510557

Gess FW (1981) Some aspects of an ethological study of the aculeate wasps and the bees of a karroid area in the vicinity of Grahamstown, South Africa. Annals of the Cape Provincial Museums. Natural History 14(1): 1–80.

Hesami S, Akrami MA, Baur H (2005) *Leucospis dorsigera* Fabricius (Hymenoptera, Leucospidae) as a hyperparasitoid of Cerambycidae (Coleoptera) through Xoridinae (Hymenoptera: Ichneumonidae) in Iran. Journal of Hymenoptera Research 14(1): 66–68.

Kareem AA, Lotfalizadeh H, Aljaafari RK (2020) First record of *Leucospis bifasciata* Klug (Hymenoptera: Leucospidae) in Iraq. Journal of Insect Biodiversity and Systematics 6(3): 223–228. https://doi.org/10.52547/jibs.6.3.223

Kirby WF (1900) [The expedition to Sokotra.] XII. Description of new Hymenoptera. Bulletin of the Liverpool Museums 3: 13–24.

Klug FF (1834) Symbolae physicae, seu icons et descriptions insectorum, quae in itinere per Africam borealem et Asiam occidentalem Frederici Guilelmi Hemprich et Christiani Godofredi Ehrenberg, Studio, novae aut illustratae redierunt. Pars Zoologica. Insecta, 4 Berlin: G. Reimer, 31–40.

Lima AR, Dias PG (2018) The New World species of *Leucospis* Fabricius, 1775 (Hymenoptera, Chalcidoidea, Leucospidae): an update of Bouček's revision with description of two new species from Brazil. Zootaxa 4441(1): 001–045. https://doi.org/10.11646/zootaxa.4441.1.1

Lotfalizadeh H, Fakhrzadeh N (2012) A short review of the family Leucospidae (Hym.: Chalcidoidea) in Iran. Biharean Biologist 6(1): 51–54.

Madl M, Schwarz M (2014) Notes on Palaearctic species of the family Leucospidae (Hymenoptera, Chalcidoidea), with new records from North Africa and Middle East. Linzer Biologische Beitrage 46(2): 1569–1580.

Narendran TC (1986) Family Leucospidae. In: Subba Rao BR, Hayat M (Eds) The Chalcidoidea (Insecta; Hymenoptera) of India and the adjacent countries. Oriental Insects 20: 43–45. https://doi.org/10.1080/00305316.1986.10433717

Noyes JS (1982) Collecting and preserving chalcid wasps (Hymenoptera: Chalcidoidea). Journal of Natural History 16(3): 315–334. https://doi.org/10.1080/00222938200770261

Noyes JS (2019) Universal Chalcidoidea Database. https://www.nhm.ac.uk/our-science/data/chalcidoids

Schmid-Egger C (2010) Order Hymenoptera, family Leucospidae. Arthropod Fauna of the UAE 3: 319–324.

Steffan JR (1948) Le genre Micrapion Kriechb. (Hym. Chalcididae). Description de trois espèces nouvelles. Bulletin de la Société Entomologique de France 53(5): 81–88. https://doi.org/10.3406/bsef.1948.16036

Ye X-H, Achterberg CV, Yue Q, Xu Z-F (2017) Review of the Chinese Leucospidae (Hymenoptera: Chalcidoidea). ZooKeys 651: 107–157. https://doi.org/10.3897/zookeys.651.11235

ZooKeys 1189: 203–229 (2024)
DOI: 10.3897/zookeys.1189.115850

Research Article

Seven new species of the segmented spider genus *Liphistius* (Mesothelae, Liphistiidae) in Thailand and Myanmar

Varat Sivayyapram[1], Chawakorn Kunsete[1], Xin Xu[2], Deborah R. Smith[3], Prapun Traiyasut[4], Sureerat Deowanish[1], Mu Mu Aung[5], Hirotsugu Ono[6], Daiqin Li[7], Natapot Warrit[1,8]

1 *Center of Excellence in Entomology and Department of Biology, Faculty of Science, Chulalongkorn University, Bangkok 10330, Thailand*
2 *College of Life Sciences, Hunan Normal University, Changsha, Hunan 410081, China*
3 *Department of Ecology & Evolutionary Biology, Haworth Hall, 1200 Sunnyside Avenue, University of Kansas, Lawrence, KS 66045, USA*
4 *Program in Biology, Faculty of Science, Ubon Ratchathani Rajabhat University, Ubon Ratchathani, Thailand*
5 *Forest Research Institute, Forest Department, Ministry of Natural Resources and Environmental Conservation, Yezin, Nay Pyi Taw, Myanmar*
6 *Department of Zoology, National Museum of Nature and Science, Tsukuba, Ibaraki 305–0005, Japan*
7 *School of Life Sciences, Hubei University, Wuhan, Hubei 430062, China*
8 *Department of Biomedical Science and Environmental Biology, Kaohsiung Medical University, Kaohsiung 80708, Taiwan*
Corresponding author: Natapot Warrit (Natapot.W@chula.ac.th)

Abstract

Seven new species of the primitive segmented spider genus *Liphistius* are described and assigned to species groups based on characters of the male palp and vulva plate. The *bristowei* group includes *L. dawei* Sivayyapram & Warrit, **sp. nov.** (♂♀) from southeastern Myanmar, *L. choosaki* Sivayyapram & Warrit, **sp. nov.** (♀) from northwestern Thailand, and *L. lansak* Sivayyapram & Warrit, **sp. nov.** (♀) from western Thailand; the *trang* group (Complex A) contains *L. kaengkhoi* Sivayyapram & Warrit, **sp. nov.** (♂♀), *L. hintung* Sivayyapram & Warrit, **sp. nov.** (♂♀), *L. buyphradi* Sivayyapram & Warrit, **sp. nov.** (♂♀), and *L. champakpheaw* Sivayyapram & Warrit, **sp. nov.** (♂♀) from central Thailand.

Key words: Morphology, Southeast Asia, taxonomy, trapdoor spiders

Academic editor: Alireza Zamani
Received: 16 November 2023
Accepted: 6 December 2023
Published: 24 January 2024

ZooBank: https://zoobank.org/7C2F288F-95EB-410A-BF6E-0C13990B472F

Citation: Sivayyapram V, Kunsete C, Xu X, Smith DR, Traiyasut P, Deowanish S, Aung MM, Ono H, Li D, Warrit N (2024) Seven new species of the segmented spider genus *Liphistius* (Mesothelae, Liphistiidae) in Thailand and Myanmar. ZooKeys 1189: 201–229. https://doi.org/10.3897/zookeys.1189.115850

Introduction

Liphistius is the sole genus of the family Liphistiidae (World Spider Catalog 2023), which, with its sister taxon Heptathelidae, comprises the suborder Mesothelae or segmented spiders, the most basal clade of living spiders (Platnick and Gertsch 1976). *Liphistius* retains several characters that are plesiomorphic among spiders, such as presence of abdominal tergites and placement of the spinnerets on the ventral median area of the abdomen (Selden 1996; Xu et al. 2015b; Selden and Ren 2017; Xu et al. 2021). All *Liphistius* species are endemic to Southeast Asia (Indonesia, Laos, Malaysia, Myanmar, Thailand) (World Spider Catalog 2023) except for *Liphistius nabang* Yu, F. Zhang & J. X. Zhang, 2021 which has been reported from Yunan, in southwestern China (Yu et al. 2021). Currently, 70 *Liphistius* species are recognized and can be classified into seven species groups based on male and female genitalia: the *batuensis* group, *birmanicus* group, *bristowei* group, *linang* group, *malayanus* group, *trang* group, and *tioman* group (Schwendinger 1990, 2017; World Spider Catalog 2023). Here, we describe seven new *Liphistius* species from specimens deposited at the Chulalongkorn University Natural History Museum (CUMZ), Bangkok, Thailand.

Materials and methods

A total of 138 *Liphistius* specimens (104 specimens of 29 previously described species and 34 specimens of new species described here) stored in the Museum were examined and dissected for their genitalia under a Zeiss Stemi DV4 stereomicroscope. The specimens were collected between 2017–2021. The male genitalia were examined from the left palp while the vulvae were dissected from the body and cleared by digesting soft tissue using 3M potassium hydroxide. The terminology of the genital characters follows (Schwendinger and Ono 2011; Schwendinger 2017; Schwendinger et al. 2019, 2022). All measurements are reported in millimeters. The spider's body lengths do not include the chelicerae or anal tubercle. Palp and legs measurements are given in the following format: total length (femur + patella + tibia + metatarsus + tarsus). The specimens were photographed using a Canon EOS 70D DSLR camera attached to a Stackshot Macro Rail (Cognisys Inc., USA). A Canon EF 100mm f/2.8L Macro IS USM lens was attached to the camera for shooting the spider dorsal and lateral habitus. A Laowa 25mm F 2.8 2.5X–5X Macro lens was attached to the camera for shooting the spider genitalia. The photos were recorded in raw file (.CR2) then convert into TIFF file (.tiff) using Canon Digital Professional 4. Multiple digital photos were combined by the focus stacking technique using Zerene Stacker v. 1.04 (Zerene Systems LLC, USA). The stacked photos were developed (combining and removing background) and labelled in Adobe Photoshop and Adobe Illustrator programs. For species identification, the spider morphologies and genitalia were compared with the original descriptions of previously described species. To protect *Liphistius* nesting sites from poaching, the species specific collecting sites and their GPS coordinates are not presented in this article. For more specific information, please contact VS or NW directly. Thai specimens are deposited at CUMZ and the Myanmar specimens will be deposited in the Biodiversity Research Centre of Myanmar which is under construction at the site of the Forest Department, Ministry of Natural Resources and Environmental Conservation at Yezin, Nay Pyi Taw.

Comparative material examined

***Liphistius albipes* Schwendinger, 1995** – Thailand • 1♂ 2♀; Phra Chaup Khirikhan, Thap Sakae District, along rural road to Chong Lom Water Reservoir; alt. 108 m; 26 November 2017; X. Xu, F. Liu, D. Li, V. Sivayyapram leg.; ARA-2020-051, ARA-2020-052, ARA-2020-053.

***Liphistius bicoloripes* Ono, 1988** – Thailand • 2♀; Ranong, Suk Samran District, Khlong Na Kha; alt. 52 m; 21 February 2021; V. Sivayyapram leg.; ARA-2021-057, ARA-2021-058.

***Liphistius bristowei* Platnick & Sedgwick, 1984** – Thailand • 1♀; Chiang Mai, Mueang Chiang Mai District, Suthep; alt. 1110 m; 18 November 2017; X. Xu, F. Liu, D. Li, V. Sivayyapram leg.; ARA-2020-026; • 8♀; Chiang Mai, Mae Chaem District, Tha Pha; alt. 1428 m; 17 June 2019; N. Warrit, V. Sivayyapram,

C. Kunsete, W. Nawanetiwong, P. Traiyasut leg.; ARA-2019-028, ARA-2019-032, ARA-2019-039, ARA-2019-040, ARA-2019-044, ARA-2019-046, ARA-2019-048, ARA-2019-050.

Liphistius castaneus **Schwendinger, 1995** – Thailand • 2♀; Ranong, Suk Samran District, Khlong Na Kha; alt. 52 m; 21 February 2021; V. Sivayyapram, leg.; ARA-2021-065, ARA-2021-066.

Liphistius dangrek **Schwendinger, 1996** – Thailand • 1♂ 1♀; Ubon Ratchathani, Na Chaluai District, Na Chaluai; alt. 354 m; 11 November 2018; P. Traiyasut leg.; ARA-2020-058, ARA-202-059.

Liphistius erawan **Schwendinger, 1996** – Thailand • 2♀; Kanchanaburi, Si Sawat District, Tha Kradan; alt. 272 m; 15 November 2017; X. Xu, F. Liu, D. Li, V. Sivayyapram leg.; ARA-2020-045, ARA-2020-046; • 1♂ 2♀; Kanchanaburi, Si Sawat District, Tha Kradan; alt. 229 m; 20 September 2018; V. Sivayyapram, C. Kunsete, W. Nawanetiwong leg.; ARA-2018-260, ARA-2018-261, ARA-2018-263; • 1♂ 2♀; Kanchanaburi, Sai Yok District, Tha Sao; alt. 380 m; 15 November 2018; V. Sivayyapram, C. Kunsete, W. Nawanetiwong leg.; ARA-2018-314, ARA-2018-315, ARA-2018-319; • 1♂ 2♀; Kanchanaburi, Sai Yok District, Tha Sao; alt. 158 m.; 27 January 2016; N. Warrit, V. Sivayyapram leg.; ARA-2017-118; ARA-2017-125; ARA-2017-127.

Liphistius fuscus **Schwendinger, 1995** – Thailand • 2♀; Krabi, Mueang Krabi District, Thab Prik; alt. 307 m; 20 February 2021; V. Sivayyapram leg.; ARA-2020-047, ARA-2020-048.

Liphistius hatyai **Zhan & Xu, 2022** – Thailand • 2♂ 1♀; Songkhla, Hat Yai District, Kho Hong; alt. 162 m; 13 November 2016; N. Warrit, V. Sivayyapram, N. Chatthanabun, P. Traiyasut leg.; ARA-2017-121, ARA-2017-122, ARA-2017-123.

Liphistius indra **Schwendinger, 2017** – Thailand • 5♀; Pattani, Khok Pho District, Sai Khao; alt. 83 m; 17 February 2021; V. Sivayyapram leg.; ARA-2021-001, ARA-2021-004, ARA-2021-006, ARA-2021-007, ARA-2021-010.

Liphistius isan **Schwendinger, 1998** – Thailand • 1♀; Sakon Nakhon, Mueang Sakon Nakhon District, Huai Yang; alt. 308 m; 24 May 2018; N. Warrit, V. Sivayyapram, C. Kunsete, W. Nawanetiwong, P. Traiyasut leg.; ARA-2018-194.

Liphistius jarujini **Ono, 1988** – Thailand • 1♀; Mueang Tak District, Mae Tho; alt. 881 m; 16 November 2017; X. Xu, F. Liu, D. Li, V. Sivayyapram leg.; ARA-2020-017.

Liphistius keeratikiati **Zhan & Xu, 2022** – Thailand • 3♀; Chumphon, Sawi District, Thung Raya; alt. 48 m; 4 May 2018; N. Warrit, V. Sivayyapram, C. Kunsete, W. Nawanetiwong, P. Traiyasut leg.; ARA-2018-027, ARA-2018-028, ARA-2018-033.

Liphistius lahu **Schwendinger, 1998** – Thailand • 1♀; Chiang Mai, Fang District, Ang Kang; alt. 1646 m; 21 November 2017; X. Xu, F. Liu, D. Li, V. Sivayyapram leg.; ARA-2020-028.

Liphistius maewongensis **Sivayyapram** et al., **2017** – Thailand • 1♂ 2♀; Kampang Phet, Klonglan District, Mae Wong National Park, 16.09°N, 99.12°E; alt. 946 m; 4 May 2018; N. Warrit, V. Sivayyapram, N. Chatthanabun leg.; ARA-2017-001, ARA-2017-002, ARA-2017-003.

Liphistius marginatus **Schwendinger, 1990** – Thailand • 1♂ 1♀; Tak, Mueang Tak District, Mae Tho; alt. 868 m; 20 September 2017; N. Chomphuphuang, C. Songsangchote leg.; ARA-2017-124, ARA-2017-125.

Liphistius nesioticus **Schwendinger, 1996** – Thailand • 2♀; Trat, Ko Chang District, Ko Chang, along rural road; alt. 84 m; 28 November 2017; X. Xu, F. Liu, D. Li, C. Kunsete leg.; ARA-2020-032, ARA-2020-043.

Liphistius niphanae **Ono, 1988** – Thailand • 4♀; Nakhon Si Thammarat, Lansaka District, Khao Kaeo; alt. 112 m; 23 January 2018; N. Warrit, V. Sivayyapram, C. Kunsete, W. Nawanetiwong, P. Traiyasut leg.; ARA-2018-038, ARA-2018-039, ARA-2018-040, ARA-2018-041; • 2♀; Nakhon Si Thammarat, Nopphitam District, Nopphitam; alt. 248 m; 15 February 2021; V. Sivayyapram leg.; ARA-2021-020, ARA-2021-021.

Liphistius onoi **Schwendinger, 1996** – Thailand • 3♀; Phitsanulok, Nakhon Thai District, Noen Phoem; alt. 1238 m; June 2017; N. Warrit, V. Sivayyapram, C. Kunsete, W. Nawanetiwong, P. Traiyasut leg.; ARA-2020-055, ARA-2020-056, ARA-2020-057.

Liphistius ornatus **Ono & Schwendinger, 1990** – Thailand • 7♀; Chanthaburi, Khao Khitchakut District, Pluang; alt. 79 m; 17 March 2018; N. Warrit, V. Sivayyapram, C. Kunsete, N. Chatthanabun, P. Traiyasut leg.; ARA-2018-106, ARA-2018-107, ARA-2018-108, ARA-2018-109, ARA-2018-110, ARA-2018-112, ARA-2018-114; • 1♂; Chanthaburi, Khao Khitchakut District, Pluang; alt. 79 m; 26 October 2021; N. Warrit, C. Kunsete, W. Nawanetiwong leg.; ARA-2021-078.

Liphistius phuketensis **Schwendinger, 1998** – Thailand • 3♀; Phuket, Thalang District, Thep Krasatti; alt. 89 m; 23 November 2017; X. Xu, F. Liu, D. Li, V. Sivayyapram leg.; ARA-2020-020, ARA-2020-021, ARA-2020-022.

Liphistius sayam **Schwendinger, 1998** – Thailand • 2♀; Chon Buri, Si Racha District, Bang Phra; alt. 326 m; 18 March 2018; N. Warrit, V. Sivayyapram, C. Kunsete, N. Chatthanabun, P. Traiyasut leg.; ARA-2018-204, ARA-2018-205.

Liphistius schwendingeri **Ono, 1988** – Thailand • 3♀; Ranong, Suk Samran District, Khlong Na Kha; alt. 52 m; 22 January 2018; N. Warrit, V. Sivayyapram, C. Kunsete, W. Nawanetiwong, P. Traiyasut leg.; ARA-2018-027, ARA-2018-028, ARA-2018-033.

Liphistius tenuis **Schwendinger, 1996** – Thailand • 3♀; Chanthaburi, Laem Sing District, Phliu; alt. 69 m; 6 February 2017; N. Warrit, V. Sivayyapram, P. Traiyasut leg.; ARA-2017-158, ARA-2017-159, ARA-2017-160.

Liphistius thaleri **Schwendinger, 2009** – Thailand • 5♀; Trang, Kantang District, Libong Island; alt. 37 m; 18 February 2021; V. Sivayyapram leg.; ARA-2021-022, ARA-2021-023, ARA-2021-024, ARA-2021-025, ARA-2021-028.

Liphistius tham **Sedgwick & Schwendinger, 1990** – Thailand • 2♀; Saraburi, Kaeng Khoi District, Thap Kwang, Kaeng; alt. 280 m; V. Sivayyapram leg.; ARA-2021-073, ARA-2021-074.

Liphistius thoranie **Schwendinger, 1996** – Thailand • 1♂; Nakhon Ratchasima, Mueang Nakhon Nayok, Hin Tung; alt. 1171 m; July 2017; C. Songsangchote leg.; ARA-2020-054; • 1♀; Nakhon Ratchasima, Mueang Nakhon Nayok, Hin Tung; alt. 754 m; 9 October 2016; N. Warrit, V. Sivayyapram, P. Traiyasut leg.; ARA-2020-041.

Liphistius trang **Platnick & Sedgwick, 1984** – Thailand • 4♀; Trang, Na Yong District, Chong; alt. 161 m; 23 January 2018; N. Warrit, V. Sivayyapram, C. Kunsete, W. Nawanetiwong, P. Traiyasut leg.; ARA-2018-050, ARA-2018-051, ARA-2018-052, ARA-2018-055.

Liphistius yamasakii **Ono, 1988** – Thailand • 5♀; Chiang Mai, Mae Chaem District, Tha Pha; alt. 1428 m; 13 June 2019; N. Warrit, V. Sivayyapram,

C. Kunsete, W. Nawanetiwong, P. Traiyasut leg.; ARA-2019-016, ARA-2019-017, ARA-2019-019, ARA-2019-021, ARA-2019-024 • 1♂1♀; Chiang Mai, Mae Chaem District, Tha Pha; alt. 1428 m; 28 October 2020; C. Kunsete, W. Nawanetiwong leg.; ARA-2021-076, ARA-2021-077.

***Liphistius yangae* Platnick & Sedgwick, 1984** – Thailand • 1♂; Satun, Khuan Don District, Wang Prachan; alt. 117 m; 25 January 2018; N. Warrit, V. Sivayyapram, C. Kunsete, W. Nawanetiwong leg.; ARA-2018-062; • 3♀; Songkhla, Hat Yai District, Hat Yai; alt. 37 m; 30 December 2018; C. Kunsete leg.; ARA-2018-370, ARA-2018-372, ARA-2018-377.

Systematics

Family Liphistiidae Thorell, 1869

Genus *Liphistius* Schiødte, 1849

Type species. *Liphistius desultor* Schiødte, 1849.

Diagnosis. *Liphistius* can be distinguished from the heptathelid genera by the male palp possessing a tibial apophysis; the vulva modified into a pore plate or plate-like spermatheca; and the nest structure equipped with signal lines, unique silk lines radiating from the burrow entrance (Platnick and Sedgwick 1984; Xu et al. 2015a).

Distribution. China (Yunnan Province), Indonesia (Sumatra), Laos, Peninsular Malaysia, Myanmar, and Thailand.

Liphistius dawei Sivayyapram & Warrit, sp. nov.

https://zoobank.org/9F369E2C-F3DB-4F63-ADE1-E4FD4C7F063B

Figs 1–3

Type material. ***Holotype*:** Myanmar • 1♂; Dawei, Pa Kar Ri; alt. 20 m; 4 May 2018; N. Warrit, V. Sivayyapram, C. Kunsete, N. Chatthanabun, P. Traiyasut leg.; ARA-2018-143. ***Allotype*:** Myanmar • 1♀; same data as for the holotype; ARA-2018-138. ***Paratypes*:** Myanmar • 1♂ 5♀; same data as for the holotype; ARA-2018-136, ARA-2018-137, ARA-2018-139, ARA-2018-140, ARA-2018-144, ARA-2018-147.

Other material. Myanmar • 3 juveniles; same data as for the holotype; ARA-2018-146, ARA-2018-148, ARA-2018-149.

Diagnosis. *Liphistius dawei* sp. nov. is similar to *L. inthanon* Zhan & Xu, 2022 and *L. yamasakii* Ono, 1988 in large body size with uniformly dark color. The male of *L. dawei* sp. nov. can be distinguished from those of *L. inthanon* and *L. yamasakii* by the palp: subtegulum with moderate apophysis, not enlarged at the tip; tegulum with finer dentate edge of proximal margin and more pronounced marginal apophysis (Fig. 3A–D; Ono 1988: fig. 8; Schwendinger 1990: fig. 18; Zhan et al. 2022: fig. 4A–G). The female of *L. dawei* sp. nov. can be distinguished from those of *L. inthanon* and *L. yamasakii* by the vulva: posterior stalk axe-blade shaped, constricted at the base; pore plate with less projecting posterior corners of the lateral lips (Fig. 3E, F; Ono 1988: figs 6, 7; Schwendinger 1990: fig. 19; Zhan et al. 2022: fig. 4H–M).

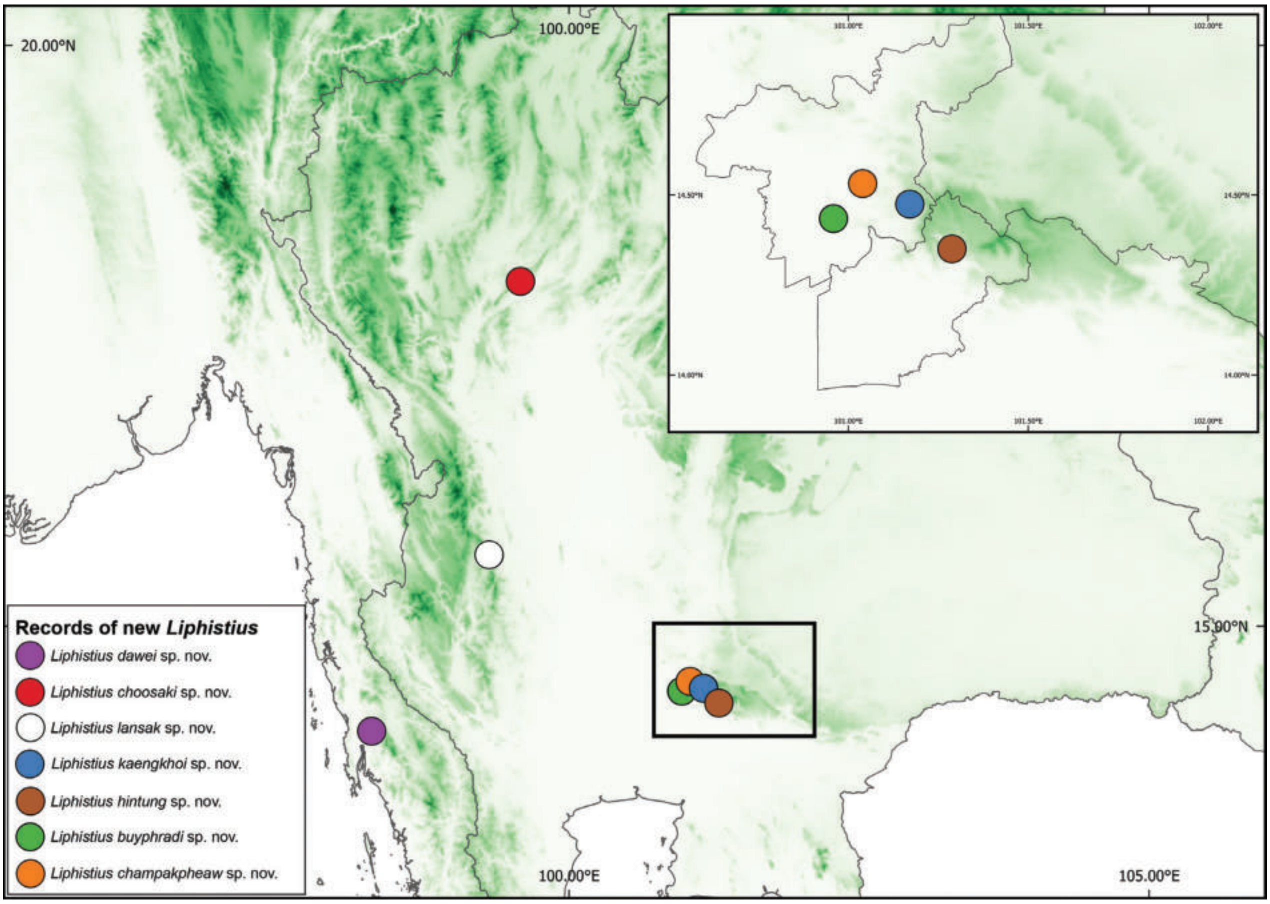

Figure 1. Map showing the localities of the new *Liphistius* species described.

Description. Male (Holotype: ARA-2018-143; Fig. 2A). ***Coloration (in alcohol)*:** carapace uniformly brown, with black stripe along the margins, bearing short black setae on cephalic region and coxal elevations; abdominal tergite brown, bearing short black setae, paler on the glabrous area; membranous part of the opisthosoma cream color with a smear of black pigment; chelicerae pale brown; palp and legs pale brown, without distinct annulations.

Palp (Fig. 3A–D): tibial apophysis short, truncate, carrying four black tapering megaspines; cumulus distinctly elevated, bearing long black bristles; paracymbium long, narrow, dark patch with spicules partially isolated by a pale band; subtegulum with moderated apophysis, not enlarged at the tip; contrategulum without apophysis, distal edge of contrategulum arched, leading to conical apex; tegulum kidney-shaped, wider than long, proximal margin convex with finely dentate edge, distal margin slightly concave with round and pronounced apophysis; pigmental bridge between contrategulum and tegulum indistinct; paraembolic plate indistinct, not projecting into a scale-like plate, sclerotized part of the embolus with two longitudinal ridges reaching to the tip.

***Measurements*:** Total length 20.15; carapace 9.75 long, 9.10 wide; opisthosoma 9.36 long, 7.28 wide; ocular tubercle 1.30 long, 1.56 wide; palpal coxa 3.12 long, 1.82 wide; labium 1.04 long, 1.82 wide; sternum 4.55 long, 2.73 wide (1.43 on ventral surface); palp 16.90 long (5.59 + 3.38 + 5.33 + – + 2.60); leg I 28.21 long (8.58 + 4.16 + 5.85 + 7.02 + 2.60); leg II 30.42 long (8.97 + 4.03 + 6.50 + 7.93 + 2.93); leg III 32.04 long (8.58 + 4.16 + 6.50 + 7.93 + 2.93); leg IV 39.91 long (10.7 + 4.29 + 8.19 + 12.48 + 4.68).

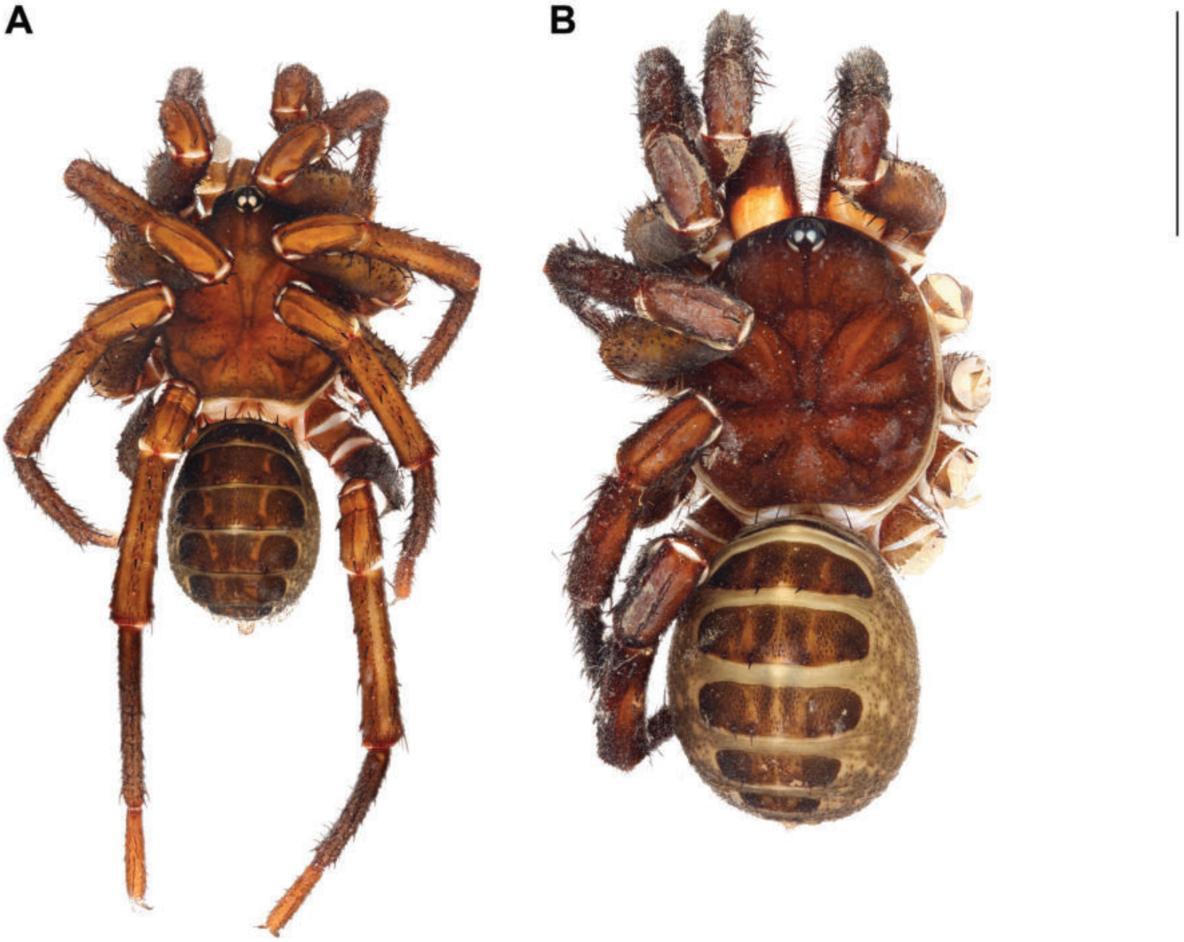

Figure 2. *Liphistius dawei* sp. nov. dorsal habitus **A** male, ARA-2018-143 (holotype) **B** female, ARA-2018-138 (allotype). Scale bar: 10 mm.

Female (Allotype: ARA-2018-138; Fig. 2B). ***Coloration (in alcohol)*:** carapace uniformly brown, bearing short black setae on the cephalic region and coxal elevations; abdominal tergites brown, darker in the area with short black setae; membranous part of the opisthosoma cream colored with thin layer of smear black marking; chelicerae bicolor, orange on proximal part and brown on distal part; palp and legs brown, without distinct annulations.

Vulva (Fig. 3E, F): vulva plate hexagonal, genital atrium with folded lateral margins, carrying lateral hairs; posterior stalk axe-blade shaped, constricted at the based, posterior margin convex; pore plate rectangular and wider than long, lateral margin thickened and projecting into a lips, more distinct on anterior portion, posterior corner slightly projecting, anterior margin thickened and projecting into a lip, slightly arched; receptacular cluster racemose, longer than wide; central dorsal opening wide longer than wide.

***Measurements*:** Total length 27.43; carapace 12.87 long, 12.09 wide; opisthosoma 14.04 long, 11.44 wide; ocular tubercle 1.69 long, 1.95 wide; palpal coxa 4.42 long, 2.47 wide; labium 1.82 long, 3.12 wide; sternum 6.24 long, 3.51 wide (2.08 on ventral surface); palp 22.23 long (8.06 + 4.16 + 5.07 + – + 4.94); leg **I** 28.47 long (9.75 + 4.94 + 5.98 + 5.46 + 2.34); leg **II** 29.51 long (9.62 + 5.07 + 5.98 + 5.72 + 3.12); leg **III** 30.42 long (8.97 + 5.33 + 5.85 + 7.28 + 2.99); leg **IV** 41.34 long (11.44 + 5.46 + 7.80 + 12.09 + 4.55).

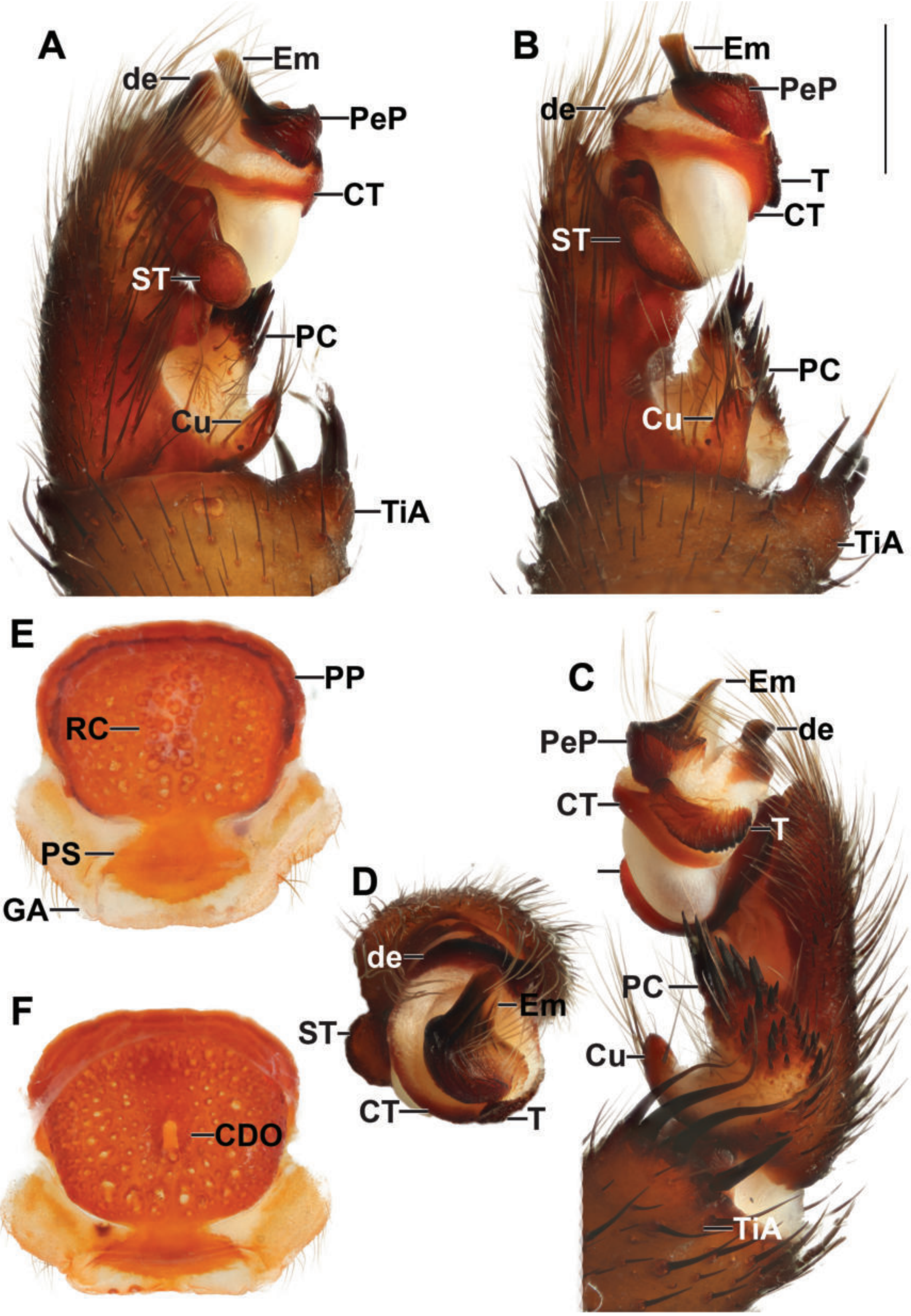

Figure 3. *Liphistius dawei* sp. nov. male palp and vulva plate **A–D** ARA-2018-143 (holotype) palp **A** prolateral view **B** ventral view **C** retrolateral view **D** distal view **E, F** ARA-2018-138 (allotype) vulva plate **E** ventral view **F** dorsal view. Abbreviations: CDO = central dorsal opening; CT = contrategulum; Cu = cumulus; de = distal edge of the contrategulum; Em = embolus; GA = genital atrium; mm = millimeter; PC = paracymbium; PeP = paraembolic plate; PP = poreplate; PS = posterior stalk; RC = receptacular cluster; ST = subtegulum; T = tegulum; TiA = tibial apophysis. Scale bar: 1 mm.

Etymology. The specific epithet *dawei* refers to the type locality of the new species in Dawei State, Myanmar.

Distribution. Known only from the type locality.

Comment. The new species was mentioned as *Liphistius* sp. DW in Sivayyapram et al. (2023).

Liphistius choosaki Sivayyapram & Warrit, sp. nov.

https://zoobank.org/B14F4BAB-5156-479D-93E0-5CDE9F8C2A50
Figs 1, 4

Type material. ***Holotype*:** THAILAND • 1♀; Phrae, Wang Chin District, Mae Koeng; alt. 265 m; 5 October 2019; N. Warrit, V. Sivayyapram, C. Kunsete, N. Chatthanabun, P. Traiyasut leg.; ARA-2019-057. ***Paratype*:** THAILAND • 1♀; same data as for the holotype; ARA-2019-056.

Other materials. THAILAND • 3 juveniles; same data as for the holotype; ARA-2019-059, ARA-2019-061, ARA-2019-062.

Diagnosis. *Liphistius choosaki* sp. nov. is similar to *L. dawei* sp. nov., *L. inthanon*, and *L. yamasakii* in its uniformly dark coloration. The female of *L. choosaki* sp. nov. can be distinguished from those of *L. dawei*, *L. inthanon*, and *L. yamasakii* by the characters of vulva: pore plate distinctly wider than long with almost straight anterior margin; and by its larger body size.

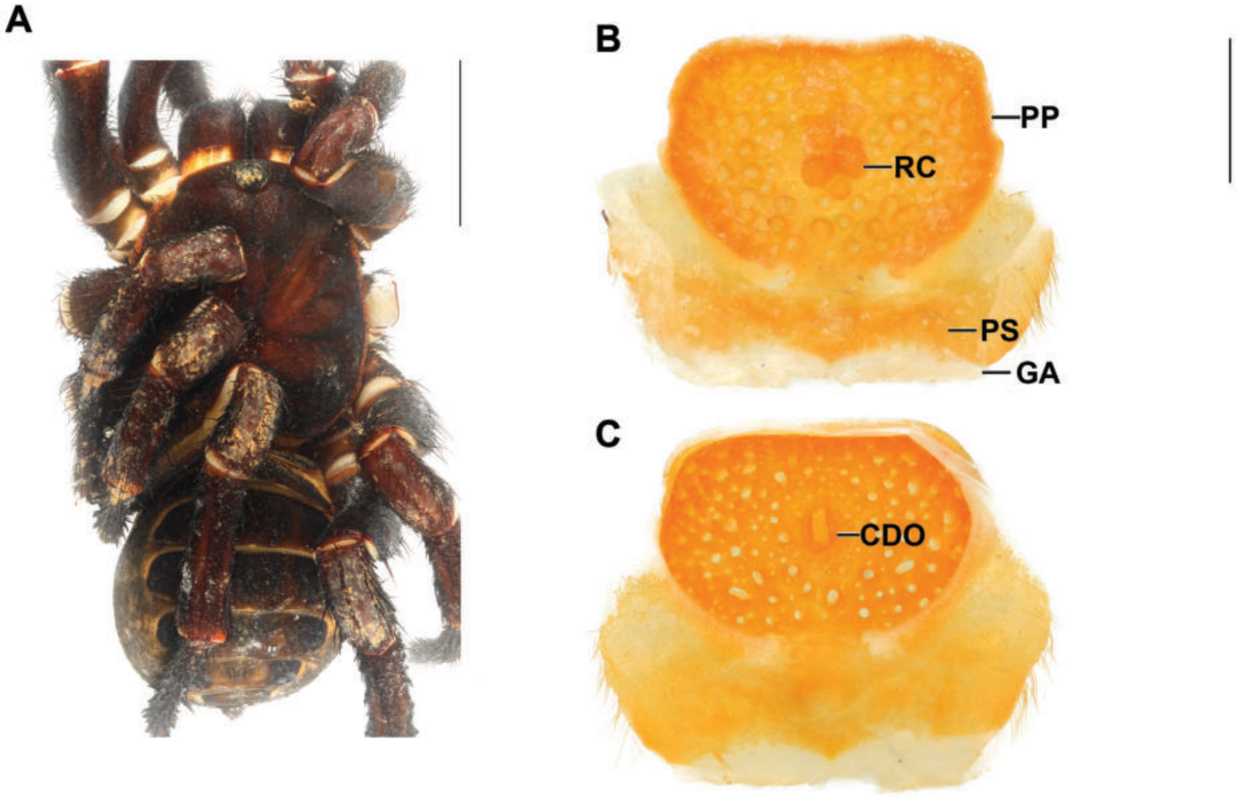

Figure 4. *Liphistius choosaki* sp. nov. female, ARA-2019-057 (holotype) **A** dorsal view **B, C** vulva plate **B** ventral view **C** dorsal view. Abbreviations: CDO = central dorsal opening; GA = genital atrium; mm = millimeter; PP = poreplate; PS = posterior stalk; RC = receptacular cluster. Scale bars: 10 mm (**A**); 1 mm (**B, C**).

Description. Male. Unknown.

Female (Holotype: ARA-2019-057; Fig. 4A). ***Coloration (in alcohol)*****:** carapace uniformly brown; abdominal tergites dark brown; membranous part of the opisthosoma cream color with thin mottled black marking; chelicerae bicolor, orange on proximal part and dark brown on distal part; palp and legs brown, without distinct annulations.

Vulva (Fig. 4B, C): vulva plate hexagonal, genital atrium with folded lateral margins, carrying lateral hairs; posterior stalk very wide, M-shaped posterior margin; pore plate rectangular, wider than long, lateral margin convex, anterior margin almost straight, all margins thickened and projected into a lip; receptacular cluster racemose, longer than wide; central dorsal opening wide longer than wide.

Measurements**:** Total length 36.40; carapace 18.33 long, 16.38 wide; opisthosoma 17.94 long, 15.34 wide; ocular tubercle 1.82 long, 1.95 wide; palpal coxa 5.46 long, 3.25 wide; labium 2.08 long, 4.29 wide; sternum 9.75 long, 3.90 wide (1.95 on ventral surface); palp 29.12 long (10.66 + 5.59 + 7.02 + – + 5.85); leg I 34.71 long (12.48 + 6.50 + 7.15 + 6.24 + 2.34); leg II 36.40 long (11.96 + 5.85 + 7.41 +7.54 +3.64); leg III 40.82 long (12.74 + 6.89 + 7.67 + 9.49 + 4.03); leg IV 53.69 long (15.21 + 7.41 + 10.79 + 14.95 + 5.33).

Etymology. The specific epithet *choosaki* honors the late Mr. Choosak Pungrusmee, father to Mr. Sarawut Pungrusmee and dedicated philanthropist to the study of biodiversity in our research laboratory.

Distribution. Known only from the type locality.

Comment. This new species name was mentioned as *Liphistius* sp. WKS in Sivayyapram et al. (2023).

Liphistius lansak **Sivayyapram & Warrit, sp. nov.**

http://zoobank.org/49787452-9ACB-4BB4-AD78-006CE5A02D25
Figs 1, 5

Type material. ***Holotype*****:** Thailand • 1♀; Uthai Thani, Lan Sak District, Rabam; alt. 200 m; 29 October 2020; V. Sivayyapram leg.; ARA-2021-067. ***Paratype*****:** Thailand • 1♀, same data as for the holotype; ARA-2021-068.

Diagnosis. *Liphistius lansak* sp. nov. is a small *Liphistius* species recognized by the unique vulva: pore plate with receptacular cluster flanked by a pair of large vesicles.

Description. Male. Unknown.

Female (Holotype: ARA-2021-067; Fig. 5A, B). ***Coloration (in alcohol)*****:** carapace pale brown with black marking on the cephalic region and the margin of the thoracic region; abdominal tergites pale brown, with black marking on the anterior and lateral margins of each plate; membranous part of the opisthosoma cream colored with thin mottled black marking; chelicerae dark brown, with black marking, except on the proximal part; palp and legs pale brown, with black annulations on the proximal and distal part of each joint (Fig. 5B).

Vulva (Fig. 5C, D): vulva plate hexagonal, wider than long, genital atrium without lateral hair; posterior stalk short but wide, posterior margin W-shaped; pore plate rectangular, wider than long, lateral margin not projected into a lip, anterior margin invaginated, thickened and projected into a lip; receptacular cluster

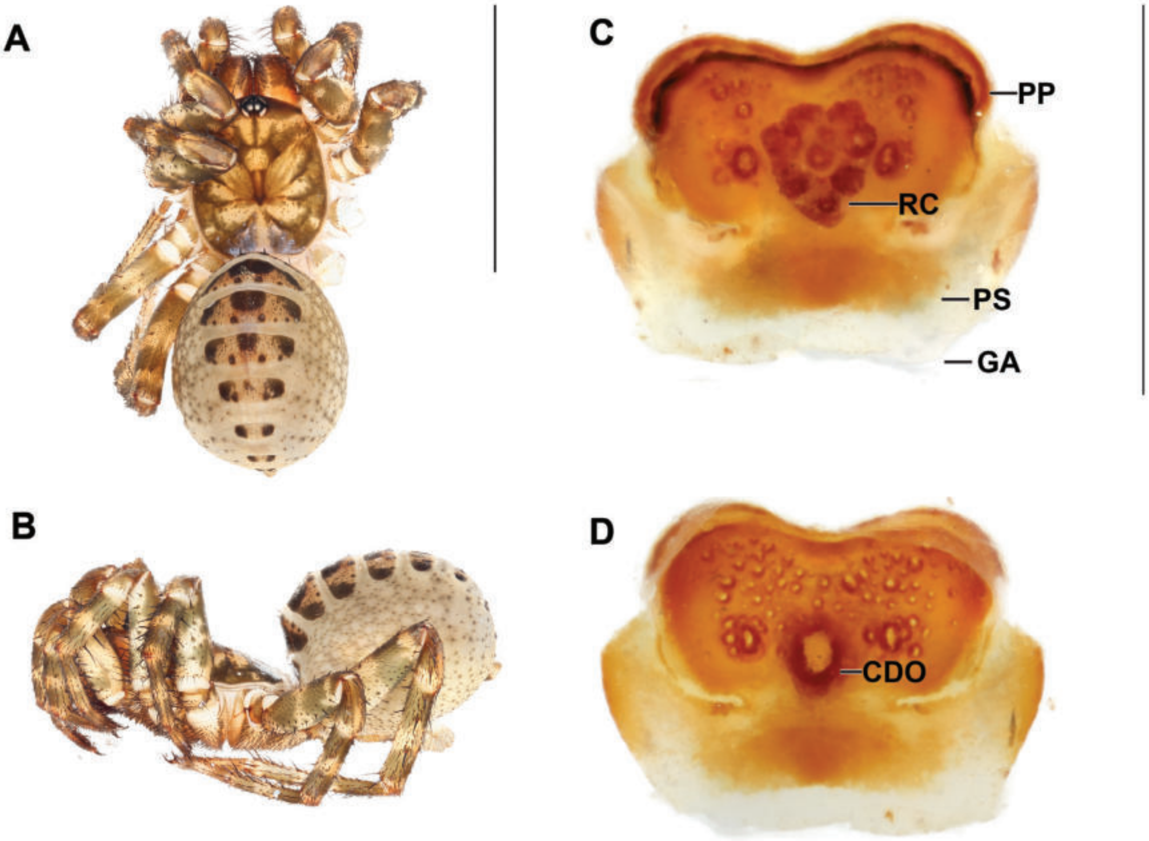

Figure 5. *Liphistius lansak* sp. nov. **A, B** female, ARA-2021-068 (holotype) **A** dorsal view **B** lateral view **C, D** vulva plate **C** ventral view **D** dorsal view. Abbreviations: CDO = central dorsal opening; GA = genital atrium; mm = millimeter; PP = poreplate; PS = posterior stalk; RC = receptacular cluster. Scale bars: 10 mm (**A, B**); 1 mm (**C, D**).

racemose, as long as wide, flanked by a pair of large vesicles; central dorsal opening round and wide.

***Measurements*:** Total length 14.17; carapace 5.98 long, 5.46 wide; opisthosoma 8.19 long, 6.89 wide; ocular tubercle 0.91 long, 1.04 wide; palpal coxa 2.21 long, 1.17 wide; labium 0.78 long, 1.82 wide; sternum 3.12 long, 1.95 wide (1.30 on ventral surface); palp 10.79 long (3.77 + 1.95 + 2.47 + – + 2.60); leg I 14.04 long (4.55 + 2.08 + 2.86 + 2.99 + 1.56); leg II 15.08 long (4.81 + 2.21 + 2.99 + 3.38 + 1.56); leg III 17.16 long (4.68 + 2.47 + 3.25 + 4.03 + 2.73); leg IV 20.94 long (5.33 + 2.47 + 4.03 + 5.98 + 3.13).

Etymology. The specific epithet *lansak* refers to Lan Sak District, the type locality of the new species in Uthai Thani, Thailand.

Distribution. Known only from the type locality.

Comment. This new species name was mentioned as *Liphistius* sp. HKK in Sivayyapram et al. (2023).

Liphistius kaengkhoi **Sivayyapram & Warrit, sp. nov.**

https://zoobank.org/BA62345B-B964-4845-B248-147400A0FAE6
Figs 1, 6, 7, 14

Type material. ***Holotype*:** THAILAND • 1♂; Saraburi, Kaeng Khoi District, Cha Om; alt. 127 m; 14 October 2018; N. Warrit, V. Sivayyapram, C. Kunsete,

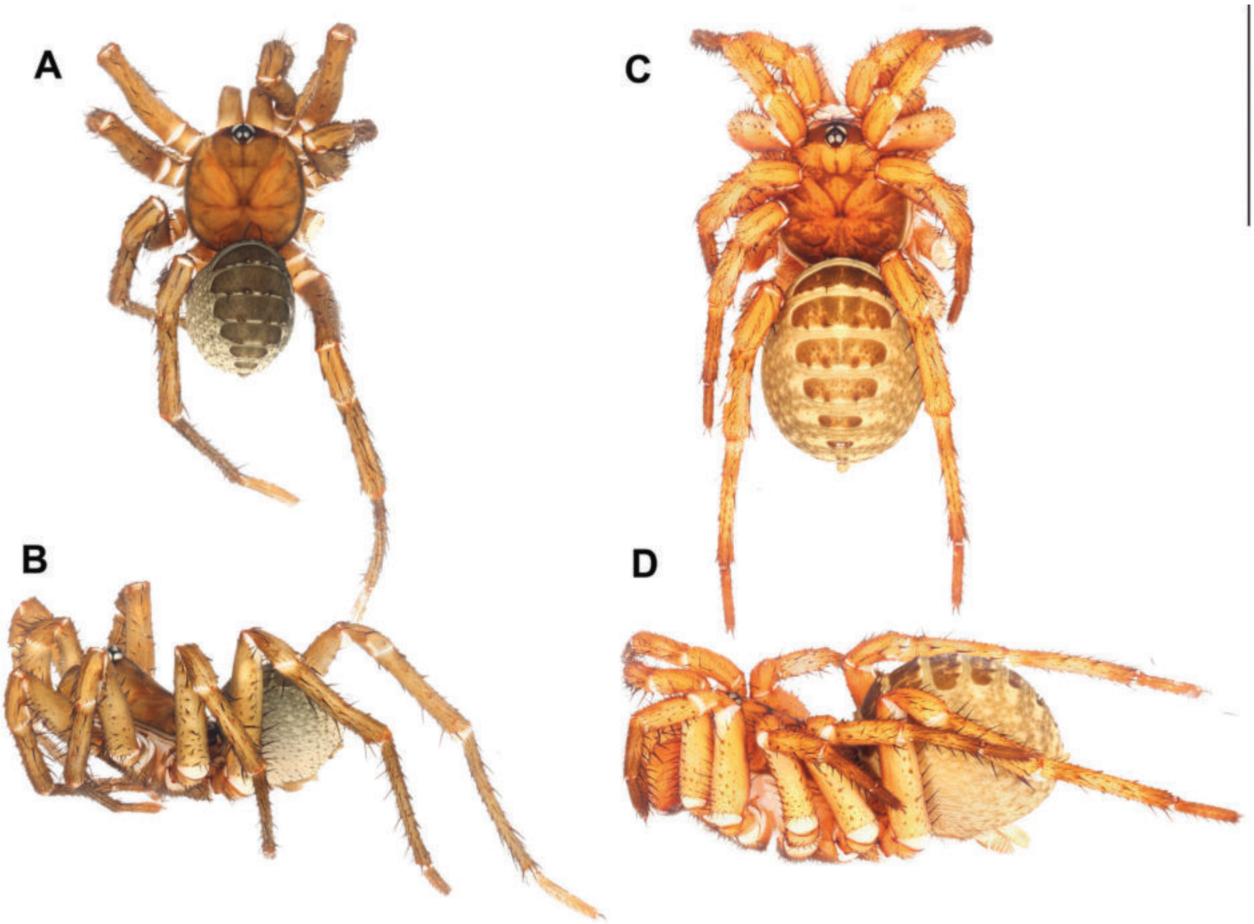

Figure 6. *Liphistius kaengkhoi* sp. nov. **A, B** male ARA-2018-284 (holotype) **C, D** female, ARA-2018-286 (allotype) **A, C** dorsal view **B, D** lateral view. Scale bar: 10 mm.

N. Chatthanabun, P. Traiyasut leg.; ARA-2018-284. ***Allotype*:** THAILAND • 1♀, same data as for the holotype; ARA-2018-286. ***Paratypes*:** THAILAND • 2♂ 4♀; same data as for the holotype; ARA-2018-281, ARA-2018-282, ARA-2018-283, ARA-2018-285, ARA-2018-289, ARA-2018-291.

Diagnosis. *Liphistius kaengkhoi* sp. nov. is similar to *L. buyphradi* sp. nov., *L. champakpheaw* sp. nov., *L. hintung* sp. nov., and *L. suwat* Schwendinger, 1996 in general appearance. The male of *L. kaengkhoi* sp. nov. can be distinguished from that of *L. suwat* by the paracymbium not bent outward; and the contrategulum without short blunt cone (Fig. 7; Schwendinger 1996: figs 43, 43A); from those of *L. buyphradi* sp. nov. and *L. champakpheaw* sp. nov. by the male palp with swollen paracymbium (flat in *L. buyphradi* sp. nov., *L. champakpheaw* sp. nov.; Figs 11, 13); *L. kaengkhoi* sp. nov. is very similar to *L. hintung* sp. nov. but can be distinguished by the shorter and finer dentate edge on the proximal margin of the tegulum and shorter paraembolic plate (Figs 7A–D, 9A–D). The female *L. kaengkhoi* sp. nov. is difficult to distinguish from those of the *L. buyphradi* sp. nov., *L. champakpheaw* sp. nov., *L. hintung* sp. nov., and *L. suwat* Schwendinger, 1996. Molecular phylogeny and species delimitation using *COI* and multi-locus data support monophyly and species status of all new species described here (Sivayyapram et al. 2023).

Description. Male (Holotype: ARA-2018-284; Fig. 6A, B). ***Coloration (in alcohol)*:** carapace brown with indistinct black mottling on cephalic region

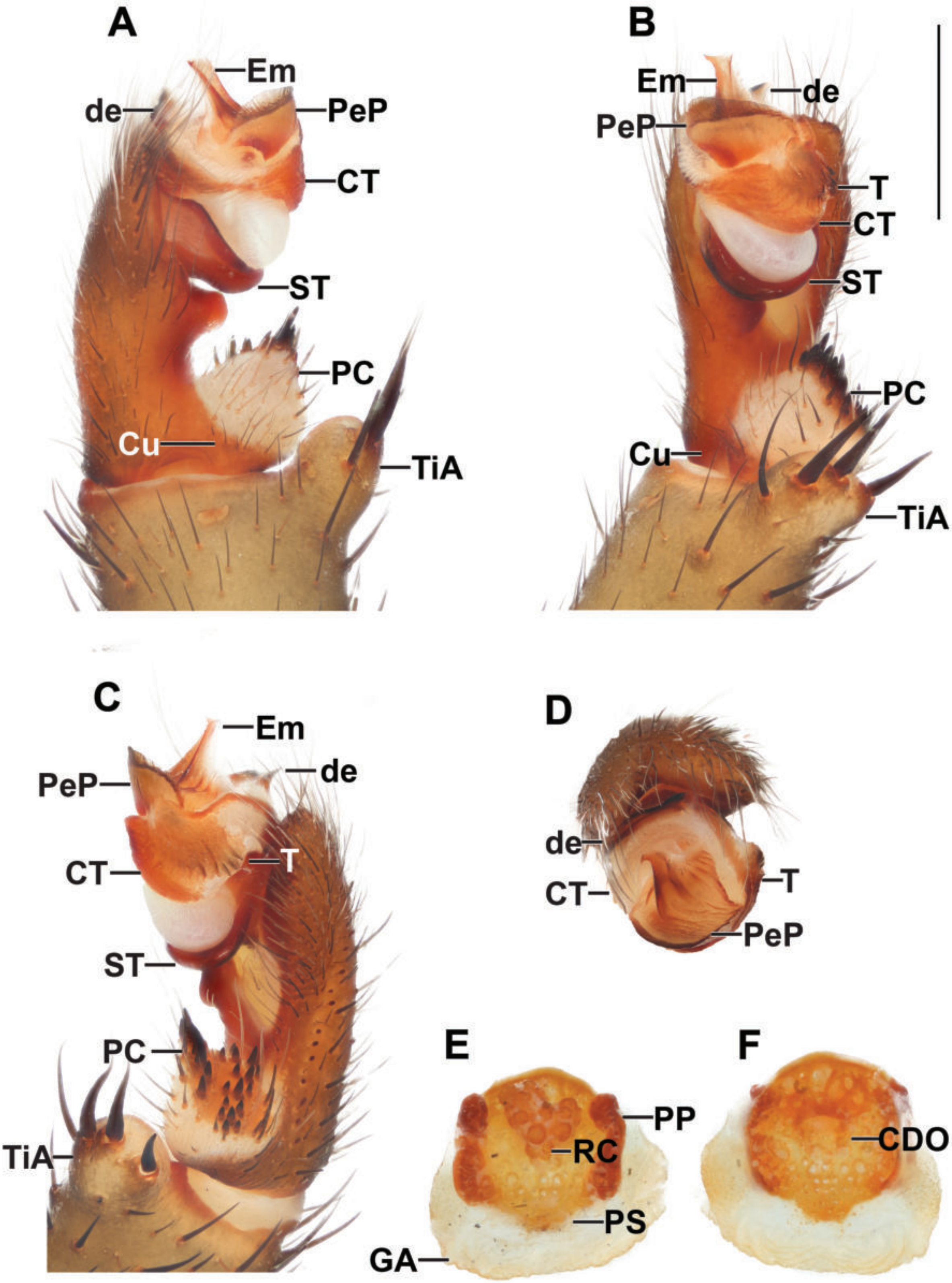

Figure 7. *Liphistius kaengkhoi* sp. nov. male palp and vulva plate **A–D** ARA-2018-284 (holotype) palp **A** prolateral view **B** ventral view **C** retrolateral view **D** distal view **E, F** ARA-2018-286 (allotype) vulva plate **E** ventral view **F** dorsal view. Abbreviations: CDO = central dorsal opening; CT = contrategulum; Cu = cumulus; de = distal edge of the contrategulum; Em = embolus; GA = genital atrium; mm = millimeter; PC = paracymbium; PeP = paraembolic plate; PP = poreplate; PS = posterior stalk; RC = receptacular cluster; ST = subtegulum; T = tegulum; TiA = tibial apophysis. Scale bar: 1 mm.

and coxal elevations; abdominal tergites black; membranous part of the opisthosoma cream colored with black mottling on antero-dorsal portion; chelicerae brown, paler on proximal portion; palp and legs brown without distinct annulation.

Palp (Fig. 7A–D): tibial apophysis large, carrying one long slender and three tapering megaspines; paracymbium short, almost round, dark patch with spicules isolated by a pale band; cumulus plain, bearing thin black bristles; subtegulum without apophysis; contrategulum without apophysis, distal edge of contrategulum long, slightly invaginate leading to the conical apex; tegulum large, axe-blade shaped, indistinctly separated from the contrategulum by corrugated surface, proximal margin with a short moderate dentate edge, distal margin almost straight, with round apophysis; pigmental bridge between tegulum and contrategulum sigmoid in shape; paraembolic plate projecting to a scale-liked plate, basally wide, leading into short triangular distal margin; embolus proper: sclerotized part with two longitudinal ridges reaching to the truncated apex.

***Measurements*:** Total length 11.44; carapace 5.85 long, 5.72 wide; opisthosoma 5.82 long, 5.07 wide; ocular tubercle 0.97 long, 1.17 wide; palpal coxa 2.21 long, 1.30 wide; labium 0.65 long, 1.3 wide; sternum 3.99 long, 1.95 wide (0.91 on ventral surface); palp 12.09 long (3.90 + 2.21 + 3.90 + – + 2.08); leg **I** 18.72 long (5.72 + 2.73 + 3.77 + 4.42 + 2.08); leg **II** 19.50 long (5.72 + 2.60 + 3.90 + 4.81 + 2.47); leg **III** 20.80 long (5.46 + 2.60 + 4.29 + 5.85 + 2.60); leg **IV** 26.25 long (6.89 + 2.99 + 5.20 + 7.67 + 3.51).

Female (Allotype: ARA-2018-286; Fig. 6C, D). ***Coloration (in alcohol)*:** carapace orange with thick black band on the anterior margin and black mottled marking in the posterior portion of the cephalic region and the thoracic region; abdominal tergites cream colored with large mottled black markings; membranous part of the opisthosoma cream with black mottled marking; chelicerae orange; palp and legs: femur to tibia orange, tarsi and metatarsi of legs **I**–**III** black, metatarsi of leg **IV** orange with black annulation on the proximal and distal area.

Vulva (Fig. 7E, F): vulva plate almost round, genital atrium without lateral hair; posterior stalk short, V-shaped; pore plate rectangular, lateral margins thickened and project into lips, anterior margin convex, less thicken, not project into a lip; receptacular clusters racemose, grape-like in shape; central dorsal opening wide.

***Measurements*:** Total length 16.2; carapace 6.89 long, 6.50 wide; opisthosoma 9.49 long, 9.67 wide; ocular tubercle 1.04 long, 1.04 wide; palpal coxa 2.60 long, 1.56 wide; labium 0.78 long, 1.95 wide; sternum 3.64 long, 2.21 wide (1.30 on ventral surface); palp 12.87 long (4.68 + 2.47 + 2.86 + – + 2.86); leg **I** 15.47 long (5.20+ 2.86 + 2.99 + 2.86 + 1.56); leg **II** 15.99 long (5.20 + 2.73 + 2.99 + 3.25 + 1.82); leg **III** 16.64 long (5.07 + 2.60 + 3.12 + 3.77 + 2.08); leg **IV** 23.81 long (7.02 + 3.38 + 4.18 + 6.24 + 2.99).

Etymology. The specific epithet *kaengkhoi* refers to Kaeng Khoi District, the type locality of the new species in Saraburi, Thailand.

Distribution. Known only from the type locality.

Comment. This new species name was mentioned as *Liphistius* sp. CK in Sivayyapram et al. (2023).

Liphistius hintung **Sivayyapram & Warrit, sp. nov.**

https://zoobank.org/05DD8E71-5B21-4756-ACB9-9A1C3B5E62F3

Figs 1, 8, 9, 14

Type material. ***Holotype*:** THAILAND • 1♂; Nakhon Nayok, Mueang Nakhon Nayok District, Hin Tung; alt. 90 m; 27 November 2018; D. Li, L. Yu V. Sivayyapram leg.; ARA-2018-299. ***Allotype*:** THAILAND • 1♀; same data as for the holotype; ARA-2018-296. ***Paratype*:** THAILAND • 1 juvenile; same data as for the holotype; ARA-2018-297.

Diagnosis. *Liphistius hintung* sp. nov. is similar to *L. kaengkhoi* sp. nov., *L. buyphradi* sp. nov., *L. champakpheaw* sp. nov., and *L. suwat* in its general appearance. *Liphistius hintung* sp. nov. is closely similar to *L. kaengkhoi* sp. nov. but can be distinguished by the male palp: tegulum with coarser proximal dental edge and longer paraembolic plate (Figs 7A–D, 9A–D). The female *L. hintung* sp. nov. is difficult to distinguish from those of the L. *kaengkhoi* sp. nov., *L. buyphradi* sp. nov., *L. champakpheaw* sp. nov., and *L. suwat* Schwendinger, 1996. Molecular phylogeny and species delimitation using *COI* and multi-locus data support monophyly and species status of all new species described here (Sivayyapram et al. 2023).

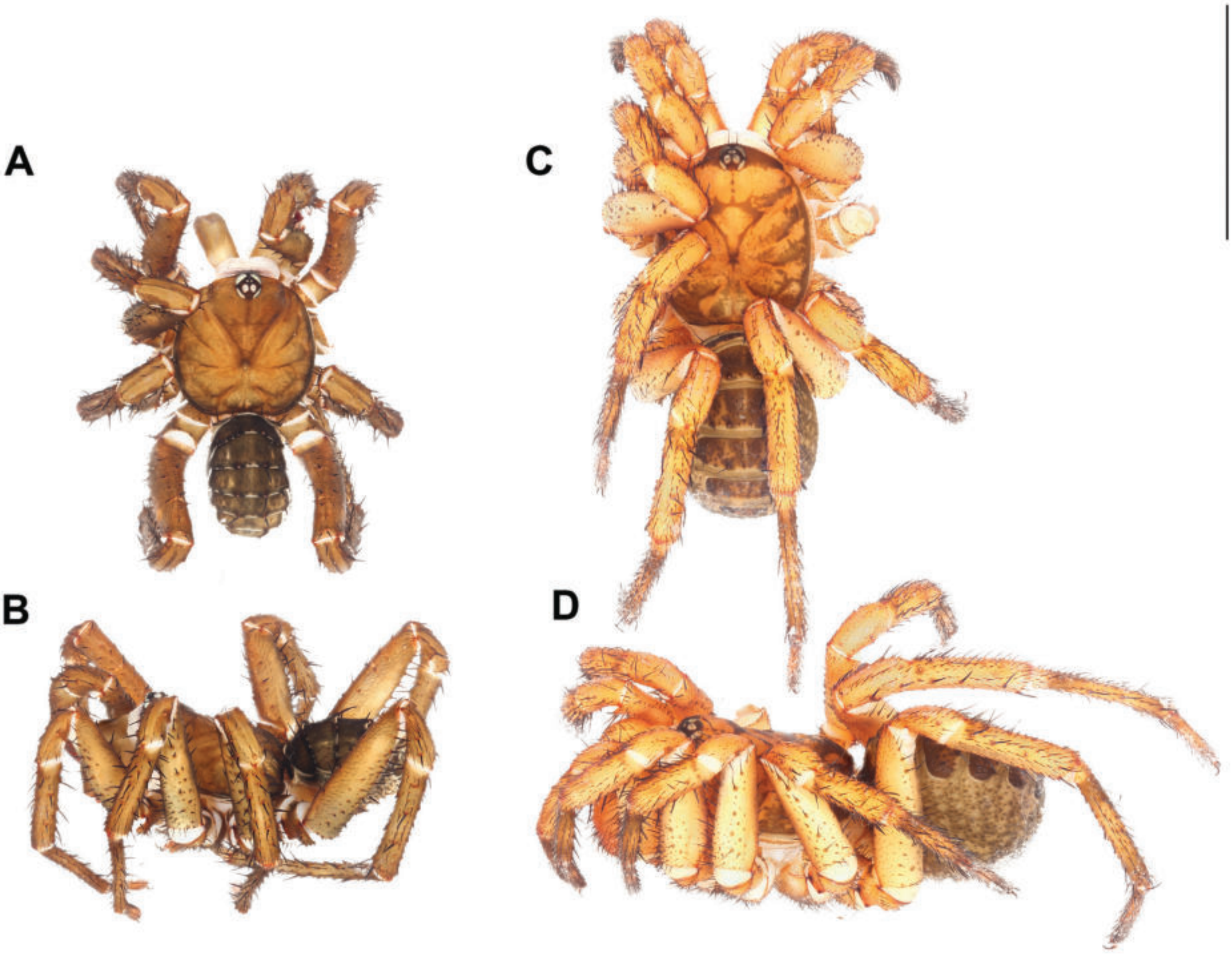

Figure 8. *Liphistius hintung* sp. nov. **A, B** male ARA-2018-299 (holotype) **C, D** female, ARA-2018-296 (allotype) **A, C** dorsal view **B, D** lateral view. Scale bar: 10 mm.

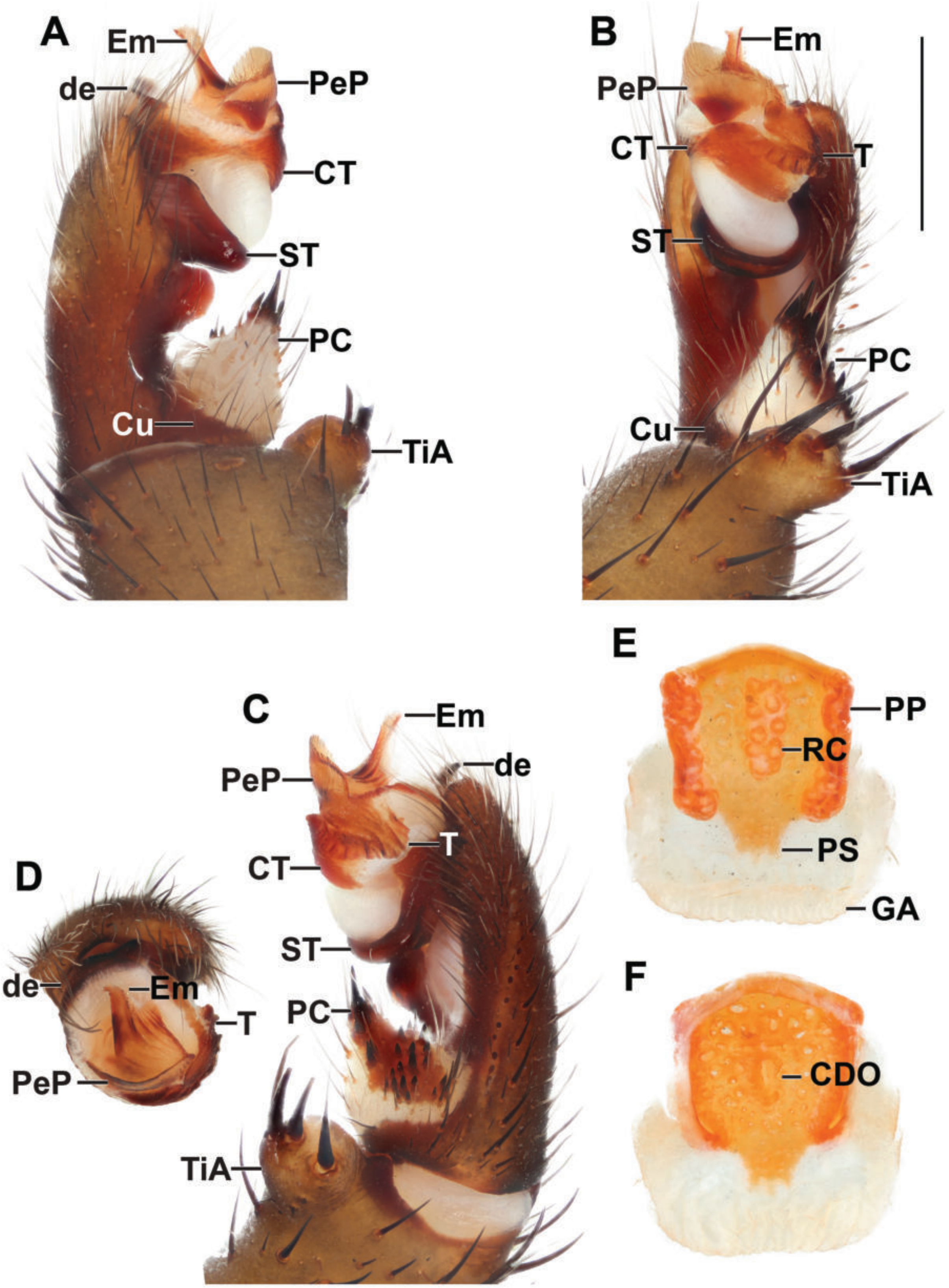

Figure 9. *Liphistius hintung* sp. nov. male palp and vulva plate **A–D** ARA-2018-299 (holotype) palp **A** prolateral view **B** ventral view **C** retrolateral view **D** distal view **E, F** ARA-2018-296 (allotype) vulva plate **E** ventral view **F** dorsal view. Abbreviations: CDO = central dorsal opening; CT = contrategulum; Cu = cumulus; de = distal edge of the contrategulum; Em = embolus; GA = genital atrium; mm = millimeter; PC = paracymbium; PeP = paraembolic plate; PP = poreplate; PS = posterior stalk; RC = receptacular cluster; ST = subtegulum; T = tegulum; TiA = tibial apophysis. Scale bar: 1 mm.

Description. Male (Holotype: ARA-2018-299; Fig. 8A, B). ***Coloration (in alcohol)*:** carapace pale brown, with black stripe along the lateral and posterior margins; abdominal tergites almost black, paler on the posterior ones; membranous part of the opisthosoma cream in color with black mottled spots; chelicerae olive green, paler at the proximal part; palp and legs uniformly brown.

Palp (Fig. 9A–D): tibial apophysis pronounce, carrying one long slender and three tapering megaspines; paracymbium conical, dark patch with spicules isolated by a pale band; cumulus plain, bearing some bristles; subtegulum without apophysis; contrategulum without apophysis, distal edge of contrategulum long and thick, slightly concave leading to the blunt apex; tegulum large, indistinctly separated from the contrategulum, axe-blade shaped, proximal margin with moderate long, coarsely dentate edge, distal margin oblique with large apophysis; pigmental bridge between the tegulum and contrategulum distinct; paraembolic plate projected into scale-like plate, basally wide with long and pointed distal edge; embolus proper: sclerotized part with two longitudinal ridges running to the truncate apex.

***Measurements*:** Total length 12.09; carapace 6.76 long, 6.37 wide; opisthosoma 5.33 long, 3.64 wide; ocular tubercle 1.17 long, 1.17 wide; palpal coxa 2.21 long, 1.56 wide; labium 0.78 long, 1.82 wide; sternum 3.64 long, 1.95 wide (1.04 on ventral surface); palp 12.35 long (3.90 + 2.34 + 4.03 + – + 2.08); leg I 19.37 long (5.85 + 2.99 + 3.90 + 4.42 + 2.21); leg II 19.89 long (5.72 + 2.73 + 4.03 + 5.20 + 2.21); leg III 22.88 long (6.11 +3.12 + 4.55 + 6.37 + 2.73); leg IV 27.81 long (7.14 + 3.25 + 5.72 + 8.45 + 3.25).

Female (Allotype: ARA-2018-296; Fig. 8C, D). ***Coloration (in alcohol)*:** carapace orange, with black marking behind the ocular tubercle running to the fovea and coxal elevations and black stripe along the carapace margins, thicker on the anterior margin; abdominal tergites pale brown with large black marking; membranous part of the opisthosoma cream colored with mottled black spots; palp and legs orange with black annulations on the metatarsus and tarsus.

Vulva (Fig. 9E, F): vulva plate hexagonal; genital atrium with a few hairs; posterior stalk trapezoidal, wider anteriorly; pore plate almost square, lateral margins thickened and projected into a lip, bearing indistinct anterolateral lobes; anterior margin convex, less thicken and not project into a lip; receptacular clusters racemose, longer than wide; central dorsal opening wide, longer than wide.

***Measurements*:** Total length 16.90; carapace 8.06 long, 7.02 wide; opisthosoma 8.32 long, 6.63 wide; ocular tubercle 1.17 long, 1.17 wide; palpal coxa 2.60 long, 1.43 wide; labium 1.04 long, 2.08 wide; sternum 3.77 long, 2.60 wide (1.56 on ventral surface); palp 13.91 long (4.94 + 2.47 + 3.38 + – + 3.12); leg I 16.90 long (5.59 + 3.12 + 3.38 + 3.12 + 1.69); leg II 17.81 long (5.72 + 2.99 + 3.77 + 3.51 + 1.82); leg III 18.72 long (5.59 + 3.12 + 3.77 + 4.16 + 2.08); leg IV 26.26 long (7.54 + 3.51 + 5.20 + 6.63 + 3.38).

Etymology. The specific epithet *hintung* refers to Hintung District, the type locality of the new species in Nakhon Nayok, Thailand.

Distribution. Known only from the type locality.

Comment. This new species name was mentioned as *Liphistius* sp. WTK in Sivayyapram et al. (2023)

Liphistius buyphradi Sivayyapram & Warrit, sp. nov.

https://zoobank.org/FFFB3423-C421-48AE-858F-6D1B8D169082
Figs 1, 10, 11, 14

Type material. ***Holotype*:** Thailand • 1♂; Saraburi, Mueang Saraburi District, Nong Pla Lai; alt. 90 m; 17 August 2017; N. Warrit, V. Sivayyapram, C. Kunsete, N. Chatthanabun, P. Traiyasut leg.; ARA-2017-139. ***Allotype*:** Thailand • 1♀; same data as for the holotype; ARA-2017-140. ***Paratype*:** Thailand • 1♀; same data as for the holotype; ARA-2017-138.

Diagnosis. *Liphistius buyphradi* sp. nov. is similar to *L. kaengkhoi* sp. nov., *L. champakpheaw* sp. nov., *L. hintung* sp. nov. and *L. suwat* in its general appearance. The male of *L. buyphradi* sp. nov. can be distinguished from those species, except for *L. champakpheaw* sp. nov., by the male palp with flat paracymbium (Fig. 14; Schwendinger 1996: fig. 43A); and from *L. champakpheaw* sp. nov. by the male palp with proximal edge of the tegulum moderately long, arched, and finely dentate (short, oblique in *L. champakpheaw* sp. nov.; Fig. 13C). The female *L. buyphradi* sp. nov. is difficult to distinguish from those of the *L. kaengkhoi* sp. nov., *L. champakpheaw* sp. nov., *L. hintung* sp. nov. and *L. suwat* Schwendinger, 1996. Molecular phylogeny and species delimitation using *COI* and multi-locus data support monophyly and species status of all new species described here (Sivayyapram et al. 2023).

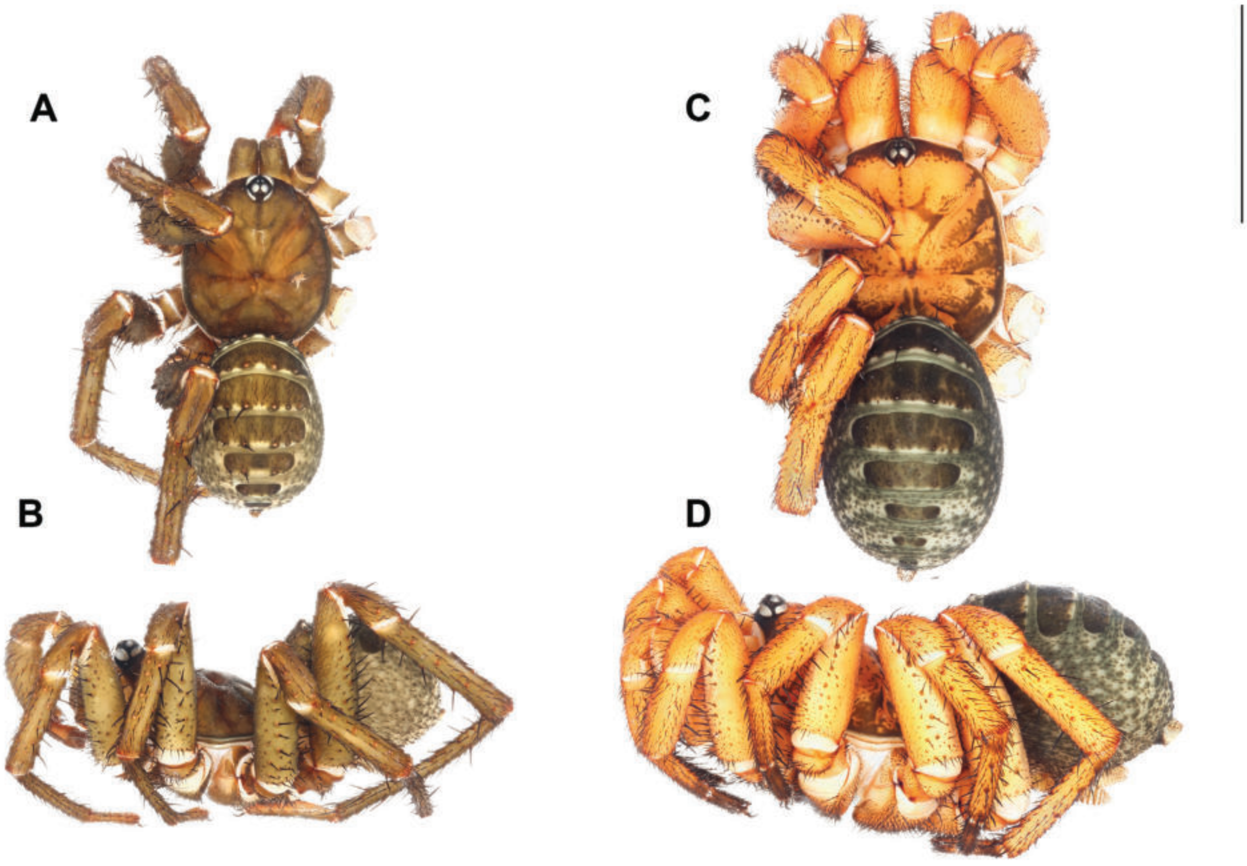

Figure 10. *Liphistius buyphradi* sp. nov. **A, B** male ARA-2017-139 (holotype) **C, D** female, ARA-2017-140 (allotype) **A, C** dorsal view **B, D** lateral view. Scale bar: 10 mm.

Description. Male (Holotype: ARA-2017-139; Fig. 10A, B). ***Coloration (in alcohol)*****:** carapace brown with black stripe along the margins; abdominal tergite olive green, except on the white posterior margins; membranous parts of the opisthosoma cream colored with black mottled spots; chelicerae olive green, paler on the proximal part; palp and legs olive green, without distinct annulation.

Palp (Fig. 11A–D): tibial apophysis round, carrying one long slender and three tapering megaspines; paracymbium round but flat, dark patch with spicules isolated by a pale band; cumulus plane, bearing long black bristles; subtegulum without apophysis; contrategulum without apophysis, distal edge of contrategulum narrow with a depression leading to the oblique conical dorsal apex; tegulum large, axe-blade shaped, possessing a long ridge on the surface, indistinctly separated from the contrategulum, proximal margin with arched, moderately dentate edge, distal margin oblique with moderately apophysis; pigmental bridge between tegulum and contrategulum distinct; paraembolic plate round, as long as wide, project into scale like-plate; embolus proper: sclerotized part with two longitudinal ridges reaching to the tip.

Measurements**:** Total length 15.60; carapace 7.80 long, 7.28 wide; opisthosoma 8.19 long, 7.02 wide; ocular tubercle 1.04 long, 1.04 wide; palpal coxa 2.10 long, 1.17 wide; labium 0.72 long, 1.44 wide; sternum 3.92 long, 2.16 wide (1.02 on ventral surface); palp 12.48 long (4.14 + 2.34 + 3.90 + – + 2.10); leg **I** 20.88 long (6.06 + 3.00 + 4.26 + 5.22 + 2.34); leg **II** 22.62 long (6.24 + 3.12 + 5.16 + 7.14 + 2.64); leg **III** 24.66 long (6.60 + 3.12 + 5.16 + 7.14 + 2.64); leg **IV** 31.44 long (8.22 + 3.30 + 6.54 + 9.66 + 3.72).

Female (Allotype: ARA-2017-140; Fig. 10C, D). ***Coloration (in alcohol)*****:** carapace orange with black marking behind the ocular tubercle and on the peripheral area of the thoracic region; abdominal tergites black, except on the white posterior margins; membranous part of the opisthosoma cream colored with black mottled spots; chelicerae orange, paler at the proximal part; palp and leg femora to metatarsi orange, distal part of metatarsi **I–III** with black mottled marking, tarsi **I–III** black, tarsi **IV** orange with black annulations on the proximal and distal parts.

Vulva (Fig. 12E, F): vulva plate almost round; genital atrium with lateral hairs; posterior stalk narrow, V-shaped; pore plate quadrangular slightly wider than long; lateral margins thickened, projected into a lip, bearing moderate anterolateral lobes; anterior margin arched, thickened, not projected into a lip; receptacular cluster racemose; central dorsal opening wide.

Measurements**:** Total length 24.70; carapace 10.66 long, 8.97 wide; opisthosoma 12.35 long, 8.84 wide; ocular tubercle 1.04 long, 1.04 wide; palpal coxa 3.24 long, 2.88 wide; labium 1.16 long, 2.48 wide; sternum 5.36 long, 2.80 wide (1.76 on ventral surface); palp 16.90 long (5.80 + 3.40 + 3.90 + – + 3.80); leg **I** 20.20 long (6.90 + 3.90 + 4.00 + 3.50 + 1.90); leg **II** 20.40 long (6.60 + 3.80 + 4.10 + 4.10 + 1.80); leg **III** 22.30 long (6.80 + 4.00 + 4.10 + 5.00 + 2.40); leg **IV** 30.80 long (8.40 + 4.20 + 6.10 + 8.20 + 3.90).

Etymology. The specific epithet *buyphradi* is dedicated to Mr. Phuri Buyphrad for providing information on the type locality of the new species.

Distribution. Known only from the type locality.

Comment. This new species name was mentioned as *Liphistius* sp. SL in Sivayyapram et al. (2023).

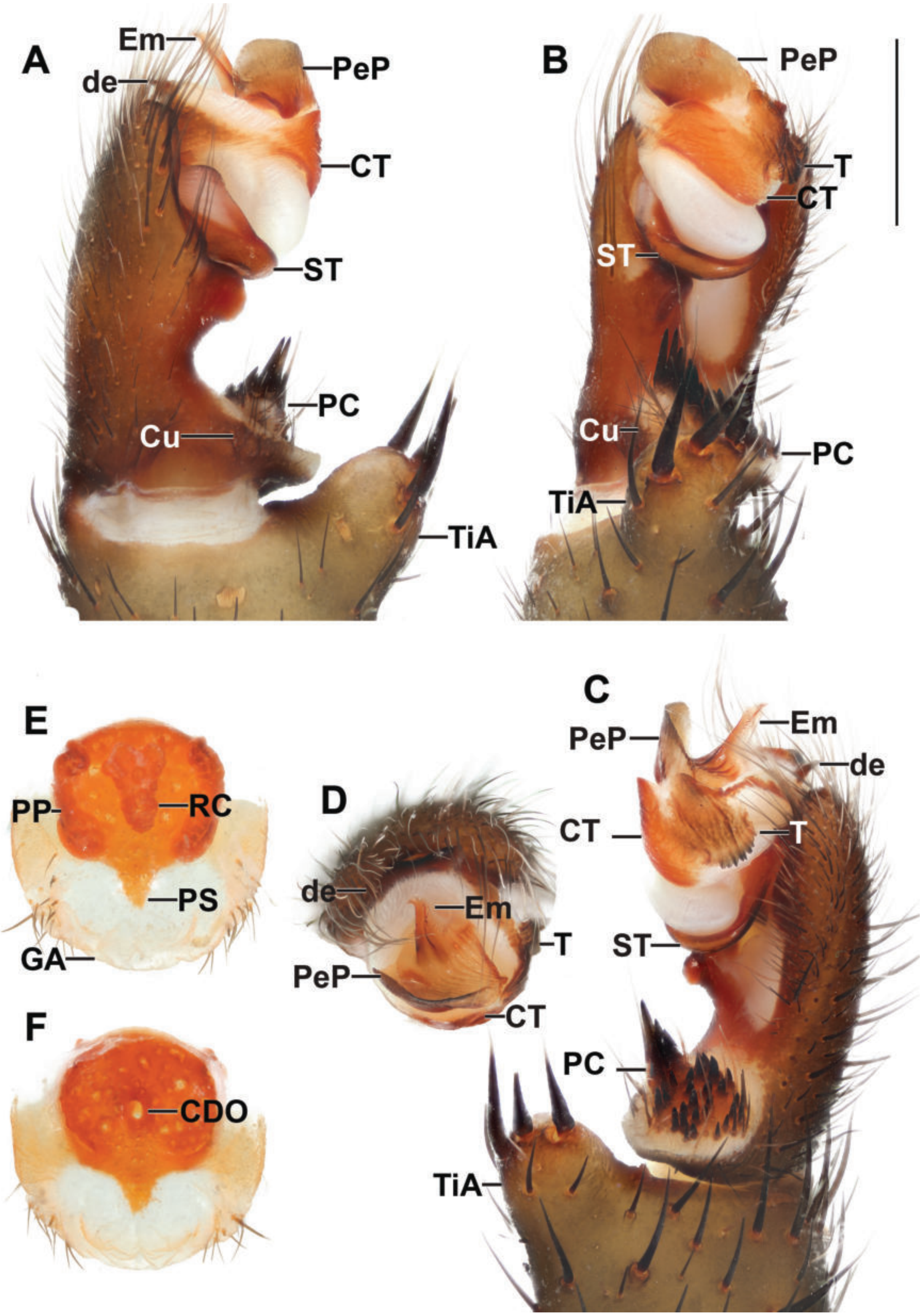

Figure 11. *Liphistius buyphradi* sp. nov. male palp and vulva plate **A–D** ARA-2017-139 (holotype) palp **A** prolateral view **B** ventral view **C** retrolateral view **D** distal view **E, F** ARA-2017-140 (allotype) vulva plate **E** ventral view **F** dorsal view. Abbreviations: CDO = central dorsal opening; CT = contrategulum; Cu = cumulus; de = distal edge of the contrategulum; Em = embolus; GA = genital atrium; mm = millimeter; PC = paracymbium; PeP = paraembolic plate; PP = poreplate; PS = posterior stalk; RC = receptacular cluster; ST = subtegulum; T = tegulum; TiA = tibial apophysis. Scale bar: 1 mm.

Liphistius champakpheaw **Sivayyapram & Warrit, sp. nov.**

https://zoobank.org/AB4110C0-8320-4090-BDAA-8C390A0584D4

Figs 1, 12–14

Type material. ***Holotype*:** THAILAND • 1♂; Saraburi, Kaeng Khoi District, Cham Phak Phaeo; alt. 82 m; 19 August 2017; N. Warrit, V. Sivayyapram, C. Kunsete, N. Chatthanabun, P. Traiyasut leg.; ARA-2017-146. ***Allotype*:** THAILAND • 1♀; same data as for the holotype; ARA-2017-146a.

Diagnosis. *Liphistius champakpheaw* sp. nov. is similar to *L. kaengkhoi* sp. nov., *L. hintung* sp. nov., *L. buyphradi* sp. nov., and *L. suwat* in its general appearance. *Liphistius champakpheaw* sp. nov. is closely similar to *L. buyphradi* sp. nov. but can be distinguished by the male palp with tegulum that is short, obliqued, with dentate proximal edge (moderately long, arched in *L. buyphradi* sp. nov., Fig. 11C). The female *L. champakpheaw* sp. nov. is difficult to distinguish from those of the *L. kaengkhoi* sp. nov., *L. hintung* sp. nov., *L. buyphradi* sp. nov., and *L. suwat* Schwendinger, 1996. Molecular phylogeny and species delimitation using *COI* and multi-locus data support monophyly and species status of all new species described here (Sivayyapram et al. 2023).

Description. Male (Holotype: ARA-2017-146; Fig. 12A, B). ***Coloration (in alcohol)*:** carapace brown, slightly paler in the central area, without any distinct markings;

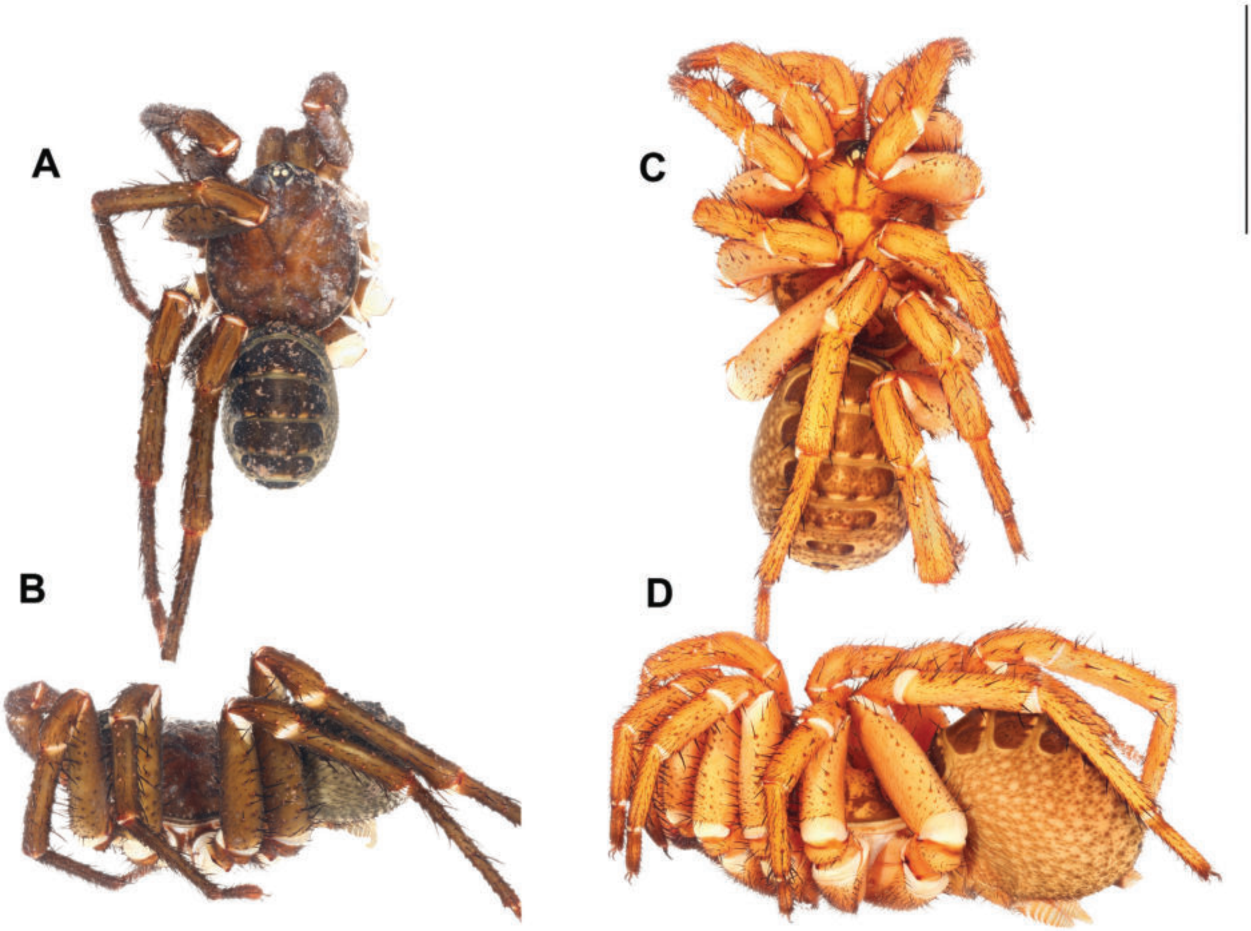

Figure 12. *Liphistius champakpheaw* sp. nov. **A, B** male ARA-2017-146 (holotype) **C, D** female, ARA-2017-146a (allotype) **A, C** dorsal view **B, D** lateral view. Scale bar: 10 mm.

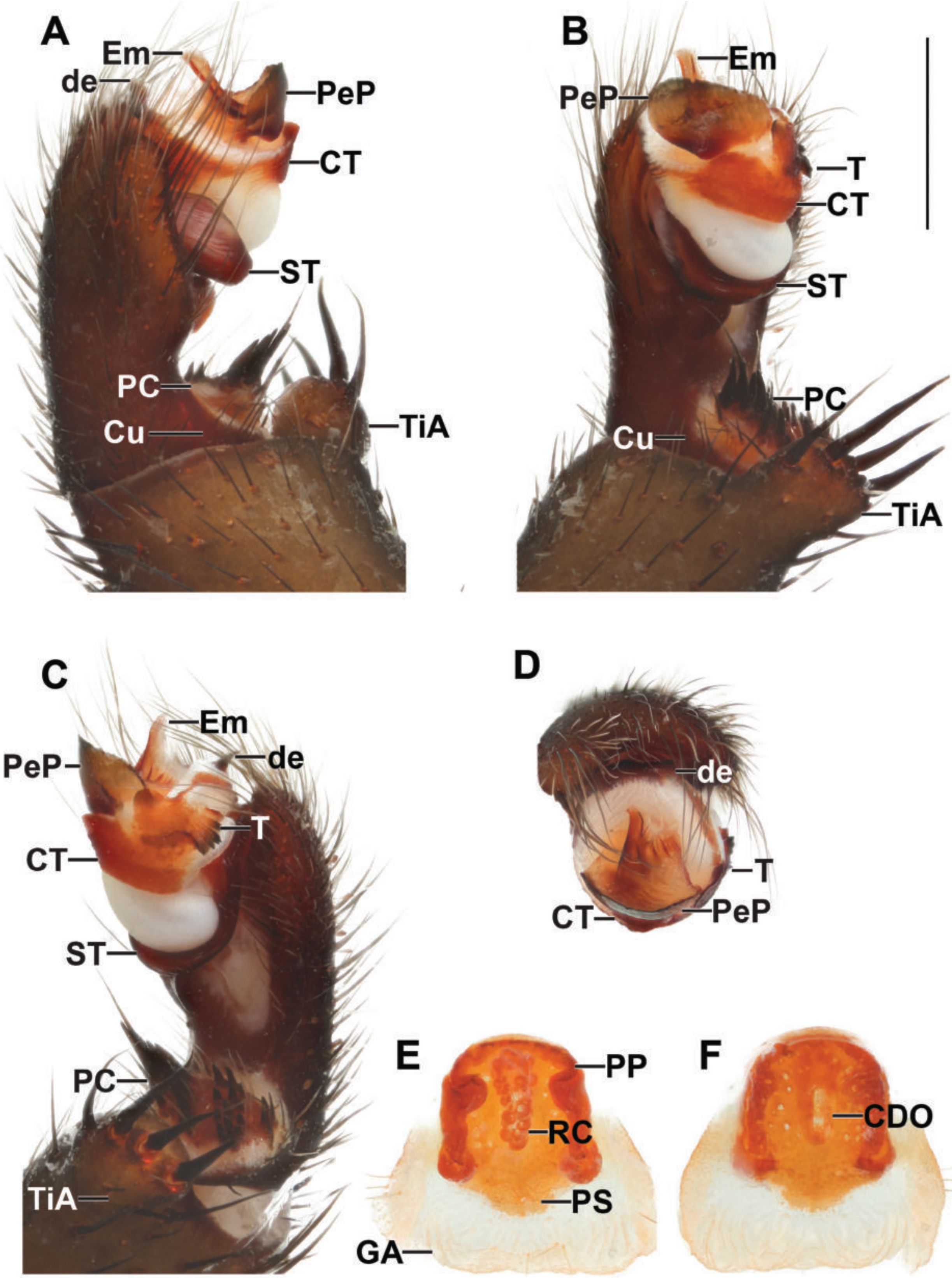

Figure 13. *Liphistius champakpheaw* sp. nov. male palp and vulva plate **A–D** ARA-2017-146 (holotype) palp **A** prolateral view **B** ventral view **C** retrolateral view **D** distal view **E, F** ARA-2018-146a (allotype) vulva plate **E** ventral view **F** dorsal view. Abbreviations: CDO = central dorsal opening; CT = contrategulum; Cu = cumulus; de = distal edge of the contrategulum; Em = embolus; GA = genital atrium; mm = millimeter; PC = paracymbium; PeP = paraembolic plate; PP = poreplate; PS = posterior stalk; RC = receptacular cluster; ST = subtegulum; T = tegulum; TiA = tibial apophysis. Scale bar: 1 mm.

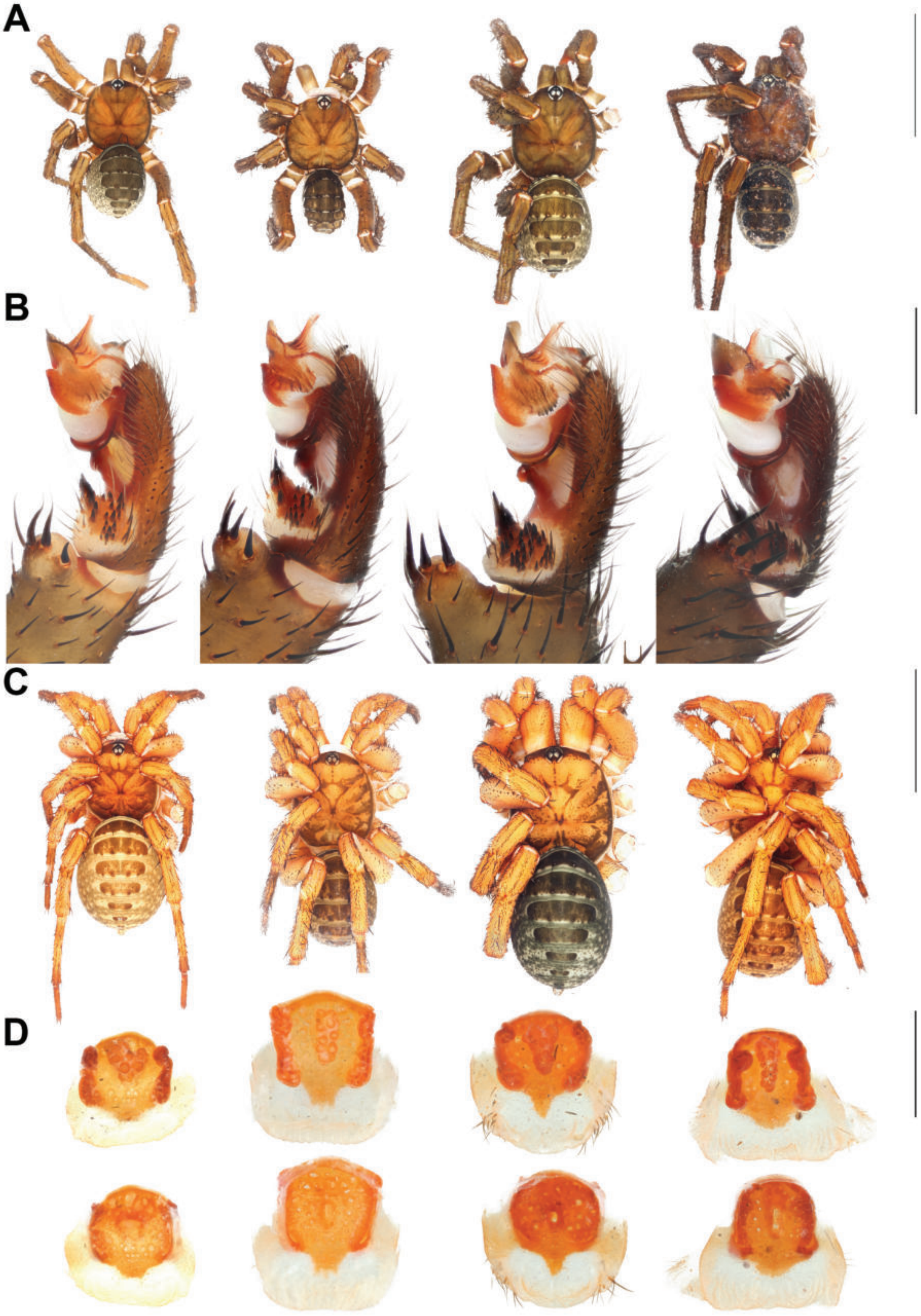

Figure 14. Left to right: *Liphistius kaengkhoi* sp. nov., *Liphistius hintung* sp. nov., *Liphistius buyphradi* sp. nov., and *Liphistius champakpheaw* sp. nov. **A** male dorsal view **B** male palp **C** female dorsal view **D** vulva plate. Scale bars: 10 mm (**A, C**); 1 mm (**B, D**).

abdominal tergites black, except for cream colored spots on the posterior margin; membranous part of the opisthosoma cream colored with black mottled spots; chelicerae olive green, paler at the proximal part; palp and legs uniformly brown.

Palp (Fig. 13A–D): tibial apophysis wide distally, carrying four tapering megaspines; paracymbium round but flat, dark patch with spicules isolated by a pale band; cumulus plain, bearing several long bristles; subtegulum without apophysis; contrategulum without apophysis, distal edge of the contrategulum long with slight concavity leading to the truncate apex; tegulum moderate, proximal margins with short, tooth-like coarsely dentate edge; distal margin oblique, with large apophysis; paraembolic plate projected into scale-like plate, large, basally wide, running to blunt distal margin; embolus proper: sclerotized part with two longitudinal ridges reaching to the tip.

Measurements**:** Total length 14.82; carapace 7.54 long, 7.02 wide; opisthosoma 7.41 long, 5.46 wide; ocular tubercle 1.17 long, 1.43 wide; palpal coxa 2.10 long, 1.17 wide; labium 0.78 long, 1.30 wide; sternum 3.90 long, 3.64 wide (1.17 on ventral surface); palp 12.22 long (4.03 + 1.56 + 4.42 + – + 2.21); leg **I** 23.53 long (6.89 + 2.86 + 5.07 + 6.24 + 2.47); leg **II** 24.83 long (7.02 + 2.99 + 5.07 + 6.76 + 2.99); leg **III** 28.34 long (7.28 + 3.38 + 5.72 + 8.32 + 3.64); leg **IV** 34.84 long (8.84 + 3.51 + 7.15 + 10.92 + 4.42).

Female (Allotype: ARA-2017-146a; Fig. 12C, D). ***Coloration (in alcohol)*****:** carapace orange with black markings on the coxal elevations and the carapace margins; abdominal tergites with black markings except for the cream color on the posterior margin; membranous part of the opisthosoma cream colored with mottled black spots; chelicerae orange; palp and legs orange with black annulation on the proximal and distal part of tarsi.

Vulva (Fig. 13E, F): vulva plate triangular, as long as wide; genital atrium with a few hairs and wrinkle posterior margin; posterior stalk U-shape, short but wide; pore plate quadrangular, slightly longer than wide; lateral margins thickened and projected into lips, bearing moderate anterolateral lobe; anterior margin arched, less thickened but not projected into a lip; receptacular cluster racemose longer than wide; central dorsal opening longer than wide.

Measurements**:** Total length 19.37; carapace 9.23 long, 7.41 wide; opisthosoma 9.88 long, 8.06 wide; ocular tubercle 1.17 long, 1.56 wide; palpal coxa 3.25 long, 2.08 wide; labium 1.17 long, 2.47 wide; sternum 5.07 long, 2.86 wide (1.69 on ventral surface); palp 15.73 long (5.59 + 3.12 + 3.77 + – + 3.25); leg **I** 18.72 long (6.24 + 3.51 + 3.77 + 3.38 + 1.82) leg **II** 18.59 long (5.72 + 3.38 + 3.77 + 3.90 + 1.82); leg **III** 20.15 long (6.11 + 3.38 + 3.90 + 4.42 + 2.34); leg **IV** 28.99 long (8.32 + 3.90 + 5.59 + 7.80 + 3.38).

Etymology. The specific epithet *champakpheaw* refers to Cham Pak Pheaw subdistrict, the type locality of the new species in Saraburi, Thailand.

Distribution. Known only from the type locality.

Comment. This new species name was mentioned as *Liphistius* sp. CPP in Sivayyapram et al. (2023).

Discussion

Here we described seven new *Liphistius* species can be assigned to two species groups, the *bristowei* group and the *trang* group, based on the characteristics of male and female genitalia.

The *bristowei* group

Liphistius dawei sp. nov. is assigned to the *bristowei* group by the male palp with an elevated cumulus, adjoining the embolus with the sclerotized part bearing two longitudinal ridges reaching to the tip, the paraembolic plate not projected into a scale-like plate, the subtegulum with an apophysis; and the vulva with projected corners of the pore plate. However, the vulva bears a unique posterior stalk constricted at the base which is more similar to the species belonging to the *birmanicus* group. *Liphistius choosaki* sp. nov. and *L. lansak* sp. nov. are also assigned to the *bristowei* group according to the vulva plate having a wide posterior stalk. The males of the two latter species are unknown.

The *trang* group

Liphistius kaengkhoi sp. nov., *L. hintung* sp. nov., *L. buyphradi* sp. nov., and *L. champakpheaw* sp. nov. are assigned to the *trang* group based on the characters of a detached embolus, a paraembolic plate projected to scale-like plate, the tegulum with a prominent distal margin, the subtegulum without an apophysis; and the vulva with small central dorsal opening and receptacular clusters. Specifically, all species are attributed to the complex A of the *trang* group according to the male palp with a plain cumulus, the contrategulum without an apophysis; and the female with an orange carapace and femora, the vulva with a square pore plate, a U-shape posterior stalk, and a racemose receptacular cluster.

Acknowledgements

We thank numerous people for their assistance, support, and advice during the field work: Chawatat Thanoosing, Chaowalit Songsangchote, Fengxiang Liu, Long Yu, Nontawat Chatthanabun, Pakorn Nalinrachatakan, Phanuwutt Senawong, Pratchaya Pramoj Na Ayutthaya, Puttita Pasukdee, Sirat Lertjintanakit, Teeradate Srimaneeyanon, Thitiya Tuntrakoon, Wasin Nawanetiwong.

We also thank Dr. Robert J Raven from University of Southern Queensland, Australia for his graceful kindness helping VS and CK to appreciate the world of spider morphology.

We thank the director of the Forest Research Institute, Forest Department, Ministry of Natural Resources and Environmental Conservation, Myanmar and Dr. Nobuyuki Tanaka, National Museum of Nature and Science, Japan for their support and permission for the biological inventory in Myanmar based on MOU between both countries.

We would like to thank the Plant Genetic Conservation Project under the Royal Initiative and the Department of National Park, Wildlife, and Plant Protection, Thailand for providing us access for specimen collecting in the last years.

Additional information

Conflict of interest

The authors have declared that no competing interests exist.

Ethical statement

No ethical statement was reported.

Funding

This research was supported by the 100th Anniversary Chulalongkorn University for Doctoral Scholarship and Overseas Research Experience Scholarship for Graduate Student fund to VS, the 90th Anniversary of Chulalongkorn University, Rachadapisek Sompote Fund (GCUGR1125641020D) to VS and NW and The National Science and Technology Development Agency (NSTDA) Fund, Thailand to NW.

Author contributions

Conceptualization: VS, NW, DRS. Data curation: CK, NW, XX, SD, PT, DL, VS. Formal analysis: NW, VS. Funding acquisition: NW. Investigation: DL, VS, CK, PT, SD, NW, DRS. Methodology: NW, XX, DL, VS, DRS, PT. Project administration: NW. Resources: SD, CK, PT, DL, XX, MMA, HO, NW. Supervision: DRS. Validation: NW, XX, VS, DL. Visualization: NW, VS, DRS. Writing – original draft: NW, VS, DRS. Writing – review and editing: DL, VS, DRS, XX, MMA, PT, NW, CK, HO, SD.

Author ORCIDs

Varat Sivayyapram https://orcid.org/0000-0002-8466-0270
Xin Xu https://orcid.org/0000-0001-5632-6622
Deborah R. Smith https://orcid.org/0000-0002-2581-5009
Hirotsugu Ono https://orcid.org/0000-0002-8568-4549
Daiqin Li https://orcid.org/0000-0001-8269-7734
Natapot Warrit https://orcid.org/0000-0002-6338-1782

Data availability

All of the data that support the findings of this study are available in the main text.

References

Ono H (1988) Liphistiid spiders (Araneae, Mesothelae) of northwest Thailand. Bulletin of the National Science Museum: Series A : Zoology 14(1): 35–41.

Platnick NI, Gertsch WJ (1976) The suborders of spiders: A cladistic analysis (Arachnida, Araneae). American Museum Novitates 2607: 1–15.

Platnick NI, Sedgwick WC (1984) A revision of the spider genus *Liphistius* (Araneae, Mesothelae). American Museum Novitates 2781: 1–31.

Schwendinger PJ (1990) On the spider genus *Liphistius* (Araneae: Mesothelae) in Thailand and Burma. Zoologica Scripta 19(3): 331–351. https://doi.org/10.1111/j.1463-6409.1990.tb00262.x

Schwendinger PJ (1996) New *Liphistius* species (Araneae, Mesothelae) from western and eastern Thailand. Zoologica Scripta 25(2): 123–141. https://doi.org/10.1111/j.1463-6409.1996.tb00155.x

Schwendinger PJ (2017) A revision of the trapdoor spider genus *Liphistius* (Mesothelae: Liphistiidae) in peninsular Malaysia; part 1. Revue Suisse de Zoologie 124: 391–445. https://doi.org/10.5281/zenodo.893555

Schwendinger PJ, Ono H (2011) On two *Heptathela* species from southern Vietnam, with a discussion of copulatory organs and systematics of the Liphistiidae (Araneae: Mesothelae). Revue Suisse de Zoologie 118: 599–637. https://doi.org/10.5962/bhl.part.117818

Schwendinger PJ, Syuhadah N, Lehmann-Graber C, Price L, Huber S, Hashim R, Bhassu S, Monod L (2019) A revision of the trapdoor spider genus *Liphistius* (Mesothelae: Liphistiidae) in Peninsular Malaysia; part 2. Revue Suisse de Zoologie 126: 321–353. https://doi.org/10.5281/zenodo.3463473

Schwendinger PJ, Huber S, Lehmann-Graber C, Ono H, Aung MM, Hongpadharakiree K (2022) A taxonomic revision of the *Liphistius birmanicus*-group (Araneae: Liphistiidae) with the description of five new species. Revue Suisse de Zoologie 129(2): 375–424. https://doi.org/10.35929/RSZ.0083

Selden PA (1996) First fossil mesothele spider, from the Carboniferous of France. Revue Suisse de Zoologie 2: 585–596.

Selden PA, Ren D (2017) A review of Burmese amber arachnids. The Journal of Arachnology 45(3): 324–343. https://doi.org/10.1636/JoA-S-17-029

Sivayyapram V, Kunsete C, Xu X, Smith DR, Traiyasut P, Deowanish S, Li D, Warrit N (2023) Molecular phylogeny, biogeography, and species delimitation of segmented spider genus *Liphistius* (Araneae: Liphistiidae) in Thailand. Zoological Journal of the Linnean Society, zlad149. https://doi.org/10.1093/zoolinnean/zlad149

World Spider Catalog (2023) World Spider Catalog. Version 23.0. Natural History Museum Bern.

Xu X, Liu F, Chen J, Ono H, Li D, Kuntner M (2015a) A genus-level taxonomic review of primitively segmented spiders (Mesothelae, Liphistiidae). ZooKeys 488: 121–151. https://doi.org/10.3897/zookeys.488.8726

Xu X, Liu F, Cheng R-C, Chen J, Xu X, Zhang Z, Ono H, Pham DS, Norma-Rashid Y, Arnedo MA, Kuntner M, Li D (2015b) Extant primitively segmented spiders have recently diversified from an ancient lineage. Proceedings of the Royal Society B: Biological Sciences 282(1808): 20142486. https://doi.org/10.1098/rspb.2014.2486

Xu X, Su Y-C, Ho SY, Kuntner M, Ono H, Liu F, Chang C-C, Warrit N, Sivayyapram V, Aung KPP, Pham DS, Norma-Rashid Y, Li D (2021) Phylogenomic analysis of ultraconserved elements resolves the evolutionary and biogeographic history of segmented trapdoor spiders. Systematic Biology 70(6): 1110–1122. https://doi.org/10.1093/sysbio/syaa098

Yu K, Zhang F, Zhang J-X (2021) First new species of the genus *Liphistius* Schiödte, 1849 from China (Araneae: Liphistiidae). Acta Arachnologica Sinica 30: 36–40. https://doi.org/10.3969/j.issn.1005-9628.2021.01.006

Zhan Y, Sivayyapram V, Liu F, Li D, Xu X (2022) Three new species of the spider genus *Liphistius* (Araneae, Mesothelae, Liphistiidae) from Thailand. ZooKeys 1104: 115–128. https://doi.org/10.3897/zookeys.1104.83264

ZooKeys 1189: 231–256 (2024)
DOI: 10.3897/zookeys.1189.111825

Research Article

New deep-sea species of *Aborjinia* (Nematoda, Leptosomatidae) from the North-Western Pacific: an integrative taxonomy and phylogeny

Julia K. Zograf[1], Alexander A. Semenchenko[2], Vladimir V. Mordukhovich[1,3]

1 *A.V. Zhirmunsky National Scientific Center of Marine Biology, FEB RAS, 690041, Vladivostok, Russia*
2 *Federal Scientific Center of the East Asia Terrestrial Biodiversity, FEB RAS, 690022, Vladivostok, Russia*
3 *Far Eastern Federal University, 690922, Vladivostok, Russia*
Corresponding author: Julia K. Zograf (zojulia@yandex.ru)

Abstract

Marimermithid nematodes parasitising invertebrates are mainly found in the deep-sea environments. Several adult and juvenile specimens marimermithids of the genus *Aborjinia* have been found in bottom sediments and inside Polychaeta during recent cruises to the Kuril-Kamchatka trench and the Kuril Basin (the Sea of Okhotsk). New species are described based on integrative study. *Aborjinia profunda* **sp. nov.** differs from *A. eulagiscae* by the location of the ventral gland cell bodies (posterior to the nerve ring vs posterior to the cardia), by the smaller body size (23–28 mm vs 103–132 mm) and shorter tail (193–263 μm vs 500–850 μm). BI and ML phylogenetic analyses based on 18S and 28S rDNA suggest that genus *Aborjinia* belongs to the family Leptosomatidae. Based on molecular and morphological characters the new genus *Paraborjinia* **gen. nov.** is proposed for *A. corallicola*. Within the family Leptosomatidae the new genus differs from all genera except *Aborjinia* by its endoparasitic lifestyle and hologonic ovaries. *Paraborjinia* **gen. nov.** differs from *Aborjinia* by the position of cephalic sensitive organs (outer labial and cephalic papillae in two separate circles vs outer labial and cephalic papillae in one circle) and by the parasitic adult (vs free-living in *Aborjinia*).

Key words: DNA barcoding, free-living nematodes, Kuril-Kamchatka Trench, Leptosomatidae, phylogenetic relationships, scanning electron microscopy

OPEN ACCESS

Academic editor: Alexei Tchesunov
Received: 29 August 2023
Accepted: 15 November 2023
Published: 17 January 2024

ZooBank: https://zoobank.org/FCBFC631-3C49-4B98-BD02-1C63654837FE

Citation: Zograf JK, Semenchenko AA, Mordukhovich VV (2024) New deep-sea species of *Aborjinia* (Nematoda, Leptosomatidae) from the North-Western Pacific: an integrative taxonomy and phylogeny. ZooKeys 1189: 231–256. https://doi.org/10.3897/zookeys.1189.111825

Introduction

In 1933 Ward described the very unusual nematodes *Thalassonema ophioctinis* Ward, 1933 from the brittle star *Ophiocten amitinum* Lyman, 1878 with an unclear taxonomical position. Forty years later Rubtzov and Platonova (1974) established a new family Marimermithidae which included two new genera *Trophomera* Rubtzov & Platonova, 1974 and *Marimermis* Rubtzov & Platonova, 1974. These nematodes resembled Mermithidae Braun, 1883 in lifestyle but differed in digestive system structure, anterior sensilla organization, and reproductive system. Later Rubtzov (1980) raised the family Marimermithidae to the rank of order. However, phylogenetic heterogeneity of the family was demonstrated in the following years. Simultaneously, the family Benthimermithidae Petter, 1980 also comprising internal parasites of marine invertebrates superficially similar to Mermithidae was described by Petter (1980). Later, Benthimermithidae was raised to the rank of order (Tchesunov 1995) and the genus *Trophomera* was transferred to the family Benthimermithidae, but the position of both orders (Marimermithida and Benthimermithida) in the nematode system remained uncertain. The rarity and peculiarities of the life cycle made studying these taxa difficult. Most species are known on the basis of only few, and often just a single, adult individual from sediments, so the host for most species remains unknown (Miljutin 2014a, b). Juveniles are found in the body cavities of a wide range of invertebrate hosts (e.g., Nematoda, Polychaeta, Priapulida, Bivalvia, Harpacticoida, Amphipoda, Isopoda); however, individuals without reproductive organs are usually unidentifiable (Miljutin 2014a, b). In addition, researchers often received samples fixed in formaldehyde, which limited the possibilities of investigation, particularly molecular studies.

Based on the morphological characters, Tchesunov (1997) suggested affinities between benthimermithids and Plectida and between marimermithids and Enoplia. Phylogenetic analyses based on a *Trophomera* SSU and LSU rDNA sequences provided support for a relationship between benthimermithids and plectids and resulted in the placement of all *Trophomera* sequences within the order Plectida (Tchesunov et al. 2009; Mardashova et al. 2011; Holovachov et al. 2013; Leduc and Zhao 2019). Leduc and Zhao (2019) proposed that the family Benthimermithidae be moved to the order Plectida.

The phylogenetic relationship of marimermithids remained unclear for many years. Marimermithid nematodes are parasites of invertebrates mainly found in deep-sea environments (Miljutin 2014a). Most marimermithids are large animals reaching several centimeters in length. Their morphology is quite simple and characterized by features usual for free-living nematodes, for example the presence of cephalic sense organs, a cylindrical pharynx, and a small cardium with a triradial internal lumen. On the other hand, their alimentary tract is often devoid of rectum and anus, caudal glands are absent or reduced in adults, hypodermal chords are hypertrophied, and the female genital system is adapted to facilitate the production of a large number of eggs. Such features are related to the parasitic way of life (Miljutin 2003).

The results from the phylogenetic analysis based on 18S rRNA of *Paraborjinia corallicola* (Westerman et al., 2021) suggest a relationship with the family Leptosomatidae Filipjev, 1916 (Westerman et al. 2021). The recent phylogenetic analyses based on the sequences of genes 18S and 28S RNA of *Marimermis maritima* Rubtzov & Platonova, 1974 and *Aborjinia* sp. showed placement of these species within the order Enoplida but in the different branches of the tree (Tchesunov et al. 2022). Thus, molecular analyses supported the relationship of marimermithids with the Enoplida and did not justify the order Marimermithida as a holophyletic taxon.

Although the first representatives of *Aborjinia* Özdikmen, 2010 were described 40 years ago, they are rarely found, little-known, and poorly studied; only one species is known. Several adult and juvenile specimens of *Aborjinia* were found in bottom sediments and inside Polychaeta during recent cruises to the Kuril-Kamchatka trench and the Kuril Basin (the Sea of Okhotsk). Here we provide an integrative taxonomic study and determine the phylogenetic position of *Aborjinia*.

Materials and methods

Study sites and sampling

Specimens of *Aborjinia* were collected in several locations during KuramBio I (July-August 2012), SokhoBio (July-August 2015), and KuramBio II (August-September 2016) expeditions to the Kuril–Kamchatka Trench and adjacent northwest Pacific at water depths of 3350–9290 m (Fig. 1, Table 1). Samples collected by Agassiz trawl (AGT), epibenthic-sledge (EBS), and giant-box corer (GKG). On deck, the sediment from the AGT was sieved through a 1000-μm mesh size, and the upper layer of sediment (0–20 cm) from the GKG was carefully sieved through 1000-, 500-, and 300-μm mesh sizes. Immediately after sieving, samples from AGT and GKG were sorted in seawater using stereomicroscopes, and nematodes were removed and fixed in 4% buffered formaldehyde for morphological studies and in DESS (solution of 0.25 M disodium EDTA and 20% dimethyl sulfoxide (DMSO), saturated with NaCl, pH 8.0) for DNA studies. On deck, the samples from EBS were immediately transferred into chilled (-20 °C) 96% ethanol and stored in a -20 °C freezer for at least 48 h for subsequent DNA studies. In the laboratories of the ship and home institutes, sorting of the fauna was done on ice in order to avoid DNA decomposition.

The NCBI database contains the *Leptosomatides* sequence HM564626, which has a very high level of similarity to the *Aborjinia* sequences. There is no unambiguous evidence in the literature of the incorrect identification of the indicated sequence, only an assumption (Tchesunov et al. 2022). Moreover, neither for the *Leptosomatides* TCR192 sample nor for *Aborjinia* sp. KKT is there any published morphological data. We were able to obtain two individuals (a female and a juvenile) of the genus *Leptosomatides* for morphological and molecular analysis and comparison with *Aborjinia*. Bottom sediments with specimens of *Leptosomatides* sp. were taken by scuba-divers in Ayan Bay (Sea of Okhotsk) in 2019 during a cruise onboard the R/V 'Academic Oparin' (Table 1). The sequences of these specimens are clustered within Leptosomatidae, and based on morphological analysis, specimens belong to genus *Leptosomatides* (Suppl. material 1). On deck, the sediment was sieved through 1000-, 500-, and 32-μm mesh sizes. Immediately after sieving, samples from 1000- and 500-μm mesh sizes were sorted in seawater using stereomicroscopes, and nematodes were removed and fixed in 10% formalin for morphological studies and in DESS for DNA studies. Half the samples from 32-μm mesh size were fixed with 4% buffered formaldehyde and half fixed with DESS.

Morphological analysis

The male specimens of *Aborjinia* were picked out from the formaldehyde-fixed samples under a stereoscopic microscope, transferred to glycerin using the Seinhorst's (1959) rapid method as modified by De Grisse (1969), and mounted on permanent slides. Drawings and DIC (differential interference contrast) photographs were made on an optical microscope Olympus BX 53 with the aid of a drawing tube and a digital camera, respectively.

The female specimen (DESS fixed, voucher M10) and a specimen of *Terebellides* sp. (Polychaeta: Terebellida: Trichobranchidae) with a parasitic juvenile of *Aborjinia* (ethanol fixed, voucher M11) in the body cavity were picked out from

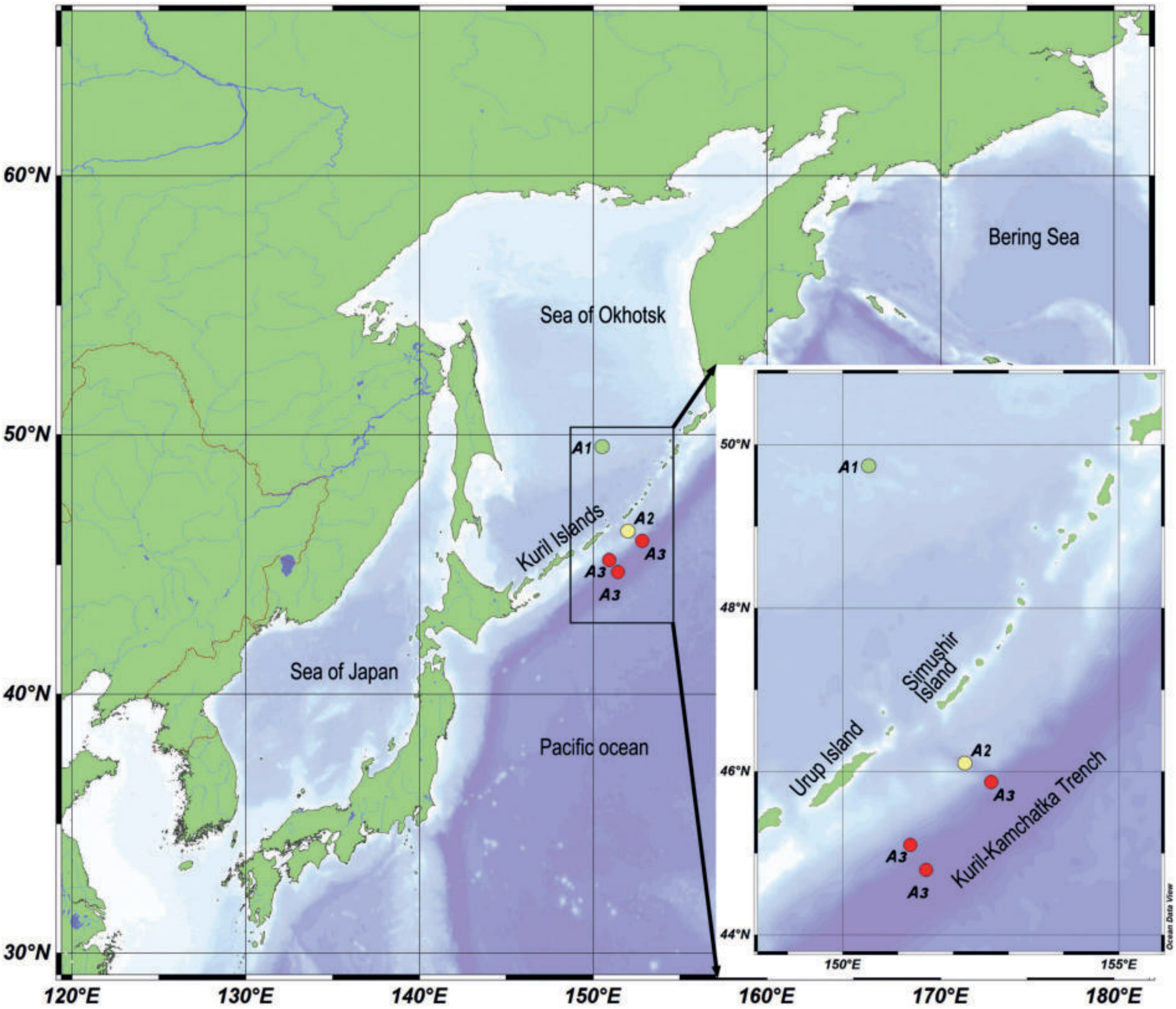

Figure 1. Map of the investigated area. Dots indicate sampled stations: A1 – *Aborjinia* sp. juvenile; A2 – *Aborjinia* sp. female; A3 – *Aborjinia profunda* sp. nov. male.

the fixative and placed in distilled water in a Petri dish. Photographs were made on an optical microscopes Nikon SMZ25 and Carl Zeiss Axio Observer 7 with the aid of a digital camera. After that, ~ 1 cm from the middle of the body of the nematode was cut off for genetic studies, and the remaining parts were placed back into the fixative.

Two male individuals fixed in formalin were cut to obtain pieces of the anterior end, middle part of pharynx, central part of body, and tail end. The specimens were then rinsed in the distilled water. After dehydration in graded ethanol series and ethanol-acetone mixture, the specimens were embedded in Spurr resin (Spur, Sigma). Semi-thin transverse sections (0.5 μm) were cut using a Leica Ultracat E Ultratome. The sections were first stained with methylene blue and azure II for 20 min at 60 °C and then with basic fuchsin for 4 min at room temperature (Humphrey and Pittman 1974), and mounted in Spurr resin on permanent glass slides. Photographs were made on an optical microscope Carl Zeiss AxioImager Z.2 with the aid of a digital camera. The acquired

Table 1. Localities, depth, and sampling data.

Species	Cruise	Gear	Area	GPS Coordinates	Depth [m]	Date [y/m/d]	Comments
Aborjinia sp. (specimen M11)	SokhoBio	Epibenthic sledge	6	48.0°N, 150.0°E	3347	2015/07/20	juvenile in body cavity of *Terebellides* sp.
Aborjinia sp. (specimen M10)	SokhoBio	Agassiz trawl	9	46.2°N, 152.1°E	3374	2015/07/25-27	female
Aborjinia profunda sp. nov.	KuramBio II	Agassiz trawl	A6	45.9°N, 152.8°E	6114	2016/08/25-27	male
Aborjinia profunda sp. nov.	KuramBio II	Box corer, Agassiz trawl	A9	44.7°N, 151.5°E	8235	2016/09/12-17	15 males
Aborjinia profunda sp. nov.	KuramBio II	Epibenthic sledge	A10	45.0°N, 151.1°E	5477	2016/09/16	male
Leptosomatides sp. (specimen L1, L2)	56 cruise of RV Akademic Oparin	Scuba-diver	49	56°25.405'N, 138°03.879'E	4-9	2019/08/02	female and juvenile

images were then adjusted for contrast and brightness using the ImageJ image processing software.

For the scanning electron microscopy, specimens were gradually dehydrated in a series of baths of increasing ethanol content, dried in a critical-point dryer, sputter-coated with gold, and observed and imaged with a Zeiss SIGMA 300VP scanning electron microscope (SEM).

The type material is deposited in the Senckenberg Museum, Frankfurt am Main, Germany (**SMF**) and in the Museum of the A.V. Zhirmunsky National Scientific Center of Marine Biology FEB RAS, Vladivostok, Russia (**MIMB**).

Abbreviations of the measured variables in the tables are as follows:

a	body length divided by maximum body diameter;
b	body length divided by pharyngeal length;
c	body length divided by tail length;
c’	tail length divided by corresponding body diameter at cloacal level;
L	body length (μm);
V	distance of the vulva from the anterior end (μm);
V (%)	distance of the vulva from the anterior end as percentage of body length (%).

DNA extraction, sequence processing, phylogenetic inference, and secondary structure predictions

Nematodes were picked out from the DESS or ethanol fixed samples under a stereoscopic microscope. Specimens < 3 cm were mounted on temporary slides with sterile distilled water and observed at different magnifications using a light microscope (Olympus BX 53) with differential interference contrast, and equipped with a digital camera. Specimens > 3 cm were observed at different magnifications using a stereoscopic microscope Nikon SMZ25 equipped with a digital camera. After the vouchering DNA from the middle part of the body (~ 1 cm) was extracted using the Qiagen DNeasy extraction kit according to the protocol. PCR mixture contained 5 μl Go Taq Green Master Mix (Promega Corp., Madison, WI, USA), 0.5 μM of each primer, 3 μl of nuclease-free water (Ambion) and 1 μl of genomic DNA. Fragments of the nuclear ribosomal DNA and internal transcribed spacers (18S rDNA, ITS1, 5.8S rDNA, ITS2 and D2-D3 region of 28S rDNA) were amplified. For 18S rDNA, we used the primer set

SSU_F_03 (f) and SSU_R_81 (r) (Blaxter et al. 1998) which amplifies a fragment of ~ 1800 bp. We used additional primers to sequence 18S rDNA amplicons: SSU_F_24_1 (f) (Meldal et al. 2007) and MN18R (r) (Floyd et al. 2005). The D2-D3 region of the 28S ribosomal DNA region was amplified using the primers D2a (f) and D3b (r) (Nunn 1992). The length of the obtained amplicon was ~ 700 bp. The internal transcribed spacer (ITS, includes ITS1, 5.8S rDNA and ITS2) region was amplified with the primers Vrain2F and Vrain2R (Vrain et al. 1992) which amplifies a fragment of ~ 1200 bp. The length of the obtained amplicon was 700 bp. PCR products were visualized on a 1.5%-TBE agarose gel GelDoc XR+ imaging systems (BioRad). Each PCR fragment was purified using Exonuclease I (ExoI) and Thermosensitive Alkaline Phosphatase (FastAP) (Thermo Fisher Scientific Inc., USA). PCR products were bidirectionally cycle sequenced using BigDye Terminator v. 3.1 Cycle Sequencing Kit (Applied Biosystems, Inc.), and bidirectionally sequenced on an ABI 3130XL automated sequencer using BigDye Terminator v. 3.1 Cycle Sequencing Kit (Applied Biosystems, Inc.). Sequences were manually assembled and edited using Finch TV and MEGA 7 (Kumar et al. 2016). Also, MEGA7 was used for calculated inter- and intraspecific p-distances.

The 18S and 28S rDNA sequences were checked and aligned at the nucleotide level using T-Coffee algorithm (Magis et al. 2014) on a MPI Bioinformatics Toolkit web service (Zimmermann et al. 2018). Bayesian phylogenetic analyses were conducted with MrBayes v. 3.2.7a (Ronquist et al. 2012). For tree reconstruction, we used the obtained sequences, as well as dataset from GenBank belonging to family Leptosomatidae, with lengths longer than 1000 bp for 18S and 650 bp for D2-D3 region 28S rDNA. PartitionFinder 2.1.1 (Lanfear et al. 2012) was used to select the best-fit partitioning scheme and models for each loci using the greedy algorithm with linked branch lengths for the corrected Bayesian Information Criterion as the optimality criterion for model selection. The best models for both ribosomal loci were SYM+I+G. Bayesian Inference was performed with two independent runs of Metropolis-coupled Markov chain Monte Carlo analyses, with each run comprising one cold chain and three heated chains at a default temperature setting of 0.1. The chains were run for 10 million generations and sampled every 100 generations. A burn-in of 2.5 million generations (or 25% of the sampled trees) was used. Moreover, trace files were visually inspected in Tracer 1.7 (Rambaut et al. 2018). We conducted Maximal likelihood (ML) analyses in IQ-Tree v. 2.2.0 (Minh et al. 2020) with 1 million ultra-fast bootstrap replications (Hoang et al. 2018) with model finding (Kalyaanamoorthy et al. 2017) algorithms. FigTree v. 1.4.4 was used to visualize phylogenetic trees after analysis.

ITS2 boundaries were identified by using hidden Markov models implemented in the ITS2 Ribosomal RNA Database (http://its2.bioapps.biozentrum.uni-wuerzburg.de/; Ankenbrand et al. 2015). The common folding pattern of ITS2 molecules for *Aborjinia* spp. was found by running the multilign and TurboFold algorithms on the RNAstructure webserver (http://rna.urmc.rochester.edu/RNAstructureWeb; Reuter and Mathews 2010) using the default parameters. We used 4SALE (Seibel et al. 2008) to generate the consensus secondary structure of our dataset after alignment sequence structures in ITS2 Ribosomal RNA Database. CBCAnalyzer (Wolf et al. 2005) was used to detect CBCs and hemi-CBCs (one-sided substitutions before CBCs) from aligned matrix.

Results

Taxonomic account

Family Leptosomatidae Filipjev, 1916

Diagnosis (Smol et al. 2014; emended). Large nematodes (up to 172 mm). Six inner labial sensilla mostly papilliform, six outer labial and four cephalic sensilla papilliform or setiform. Amphids pocket-shaped. Large number of metanemes with caudal filament usually present: dorsolateral and ventrolateral or only dorso-lateral orthometanemes and loxometanemes of type I. Many species with ocelli. Buccal cavity narrow, sometimes with tooth-like thickening. Pharynx inserts into the body cuticle in the region of buccal cavity, the cephalic capsule is variable in the form. Three pharyngeal glands open in the buccal cavity. Pharynx always smooth in outline. Secretory-excretory system, if present, usually restricted to the pharyngeal region, may consists of two cells. Female reproductive system didelphic-amphidelphic with antidromously reflexed ovaries. Males with two testes opposed. Gonad positions relative to intestine variable in species, with anterior and posterior gonad position reversed. Subventral or ventral precloacal papillae (never tubules) often present. Caudal glands mostly present, extending into the precaudal region. Marine and parasites of marine invertebrates.

Aborjinia Özdikmen, 2010

Diagnosis (emended after Tchesunov and Spiridonov 1985; Miljutin 2003, 2014a). Very large nematodes; at the larval stage parasitize marine invertebrates. Adult worms are free-living. Three lips. Pharynx cylindrical, muscular, with tri-radial internal lumen. Rectum and anus present. Outer labial and cephalic sensilla papilliform, situated in one circle. Amphideal fovea small, pore-like. Cervical setae absent. Excretory-secretory system consists of two cells. Female reproductive system didelphic, amphidelphic, ovaries hologonic. Male reproductive system didelphic, testes outstretched. Tail convex-conoid, broadly rounded.

Type species. *Aborjinia eulagiscae* (Tchesunov & Spiridonov, 1985): Özdikmen 2010, by original designation [= *Australonema eulagiscae* Tchesunov & Spiridonov, 1985].

Invalid species. *Aborjinia corallicola* Westerman, de Moura Neves, Ahmed & Holovachov, 2021.

= *Paraborjinia corallicola* (Westerman, de Moura Neves, Ahmed & Holovachov, 2021), comb. nov.

Aborjinia profunda sp. nov.

https://zoobank.org/FA1FD587-B2E2-49BB-996B-57F2D15AD74E
Figs 2–6

Diagnosis. Body 22.9–27.7 mm long in males. Six outer labial and cephalic sensilla papilliform, situated 19–21 μm from anterior end. Amphideal aperture located 37–40 μm from anterior end. Pharynx tubular without any valves or bulbs, tightly surrounded by the glandular tissue. Nerve ring situated ~ 40% of

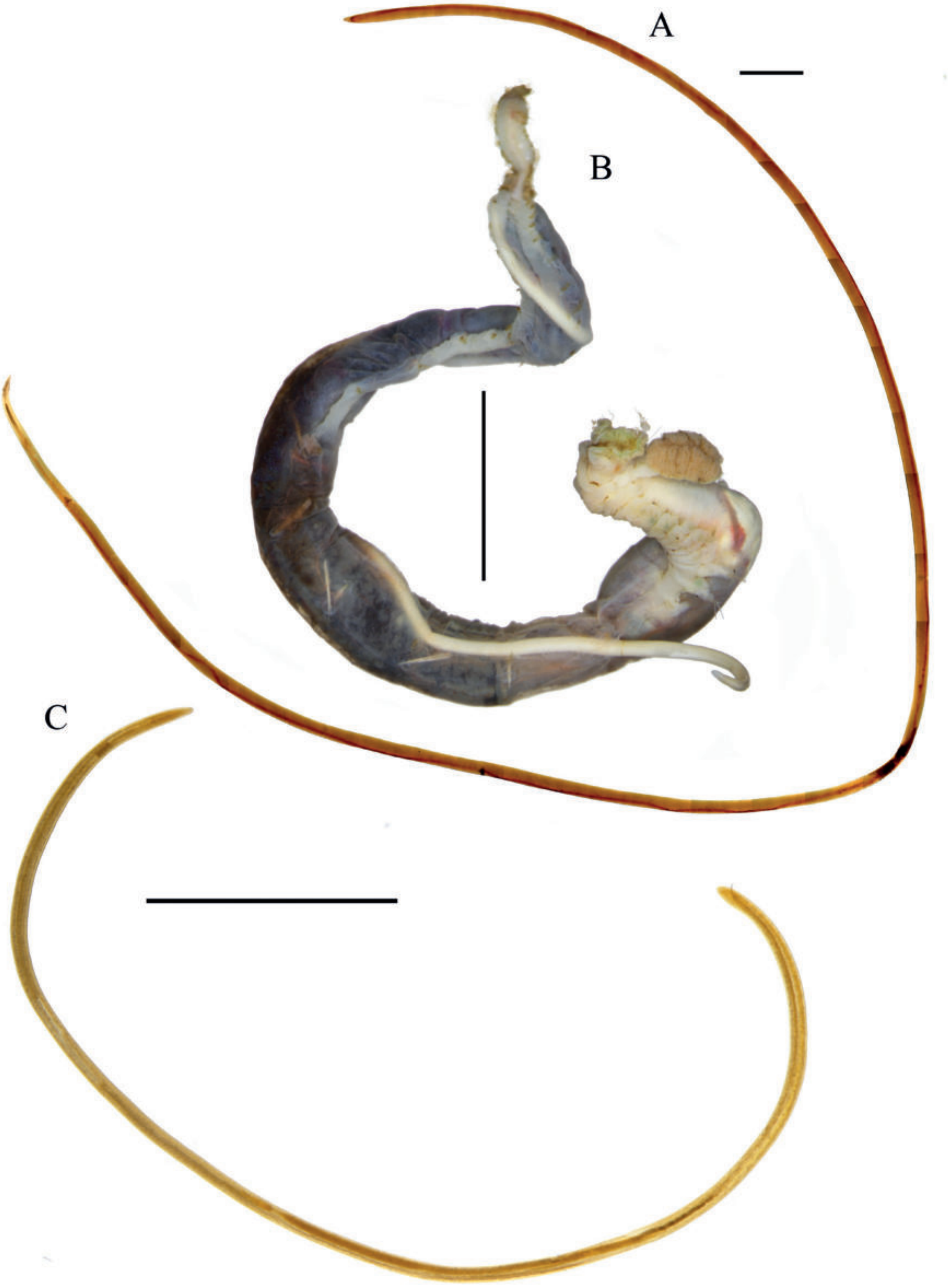

Figure 2. Examined species of *Aborjinia*, entire bodies, light microscopy **A** *Aborjinia* sp., female (assembled panorama) **B** *Terebelus* sp. with juvenile of *Aborjinia* sp. **C** *Aborjinia profunda* sp. nov., male. Scale bars: 5000 µm.

pharynx length from anterior end. Intestine well developed with wide lumen. Spicules slightly bent, 364–372 µm long. No pre- or postcloacal sensilla or supplements. Spinneret present.

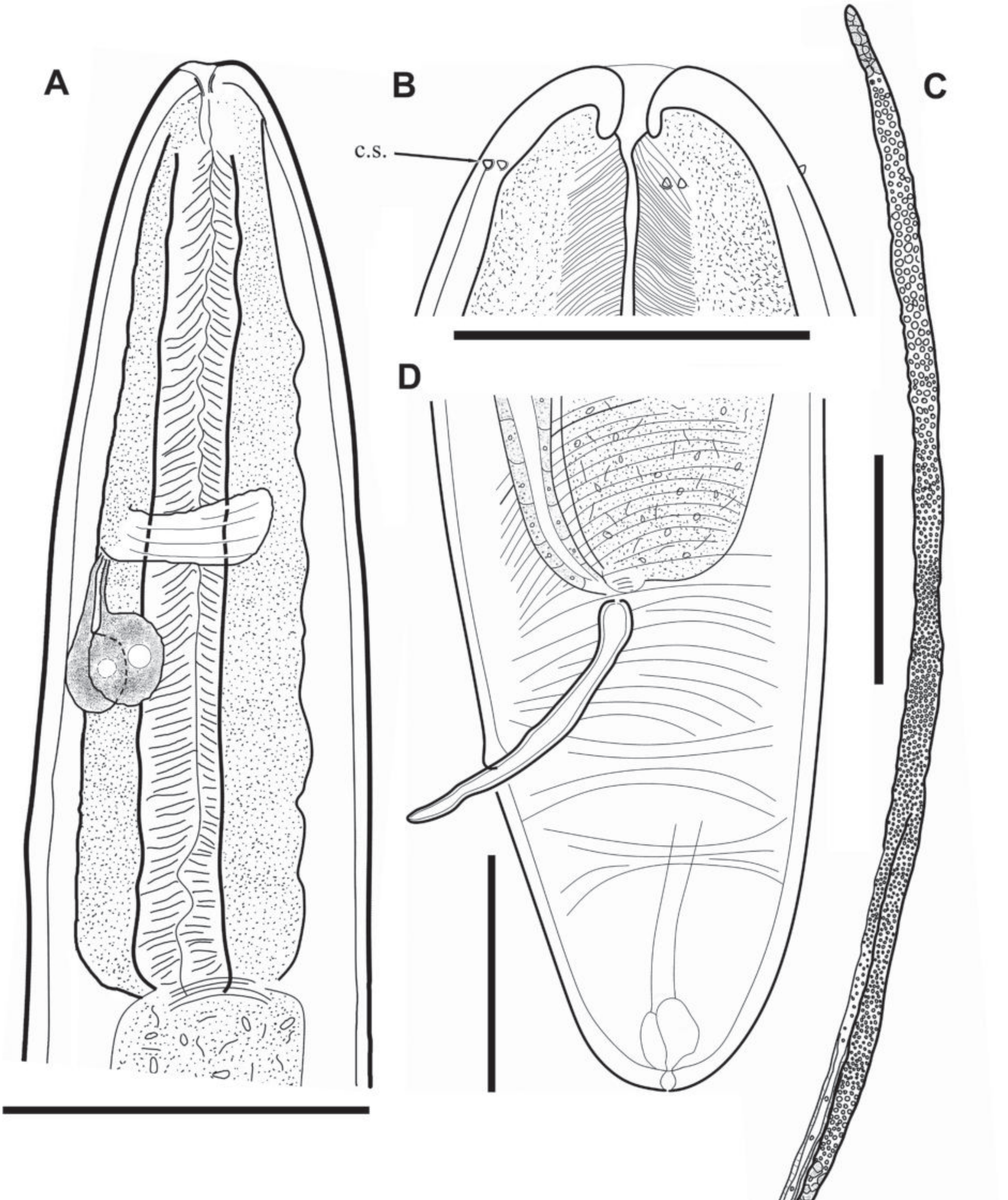

Figure 3. *Aborjinia profunda* sp. nov. **A** anterior end of male **B** head of male **C** male reproductive system **D** male tail. Abbreviation: c.s – cephalic sensilla. Scale bars: 100 μm (**B**); 200 μm (**D**); 500 μm (**A**); 2000 μm (**C**).

Type material examined. Three males (holotype and two paratypes). The holotype (SMF 14457) and paratype (SMF 14458) are deposited in the Senckenberg Museum, Frankfurt am Main, Germany. Paratype (MIMB 42307) is depos-

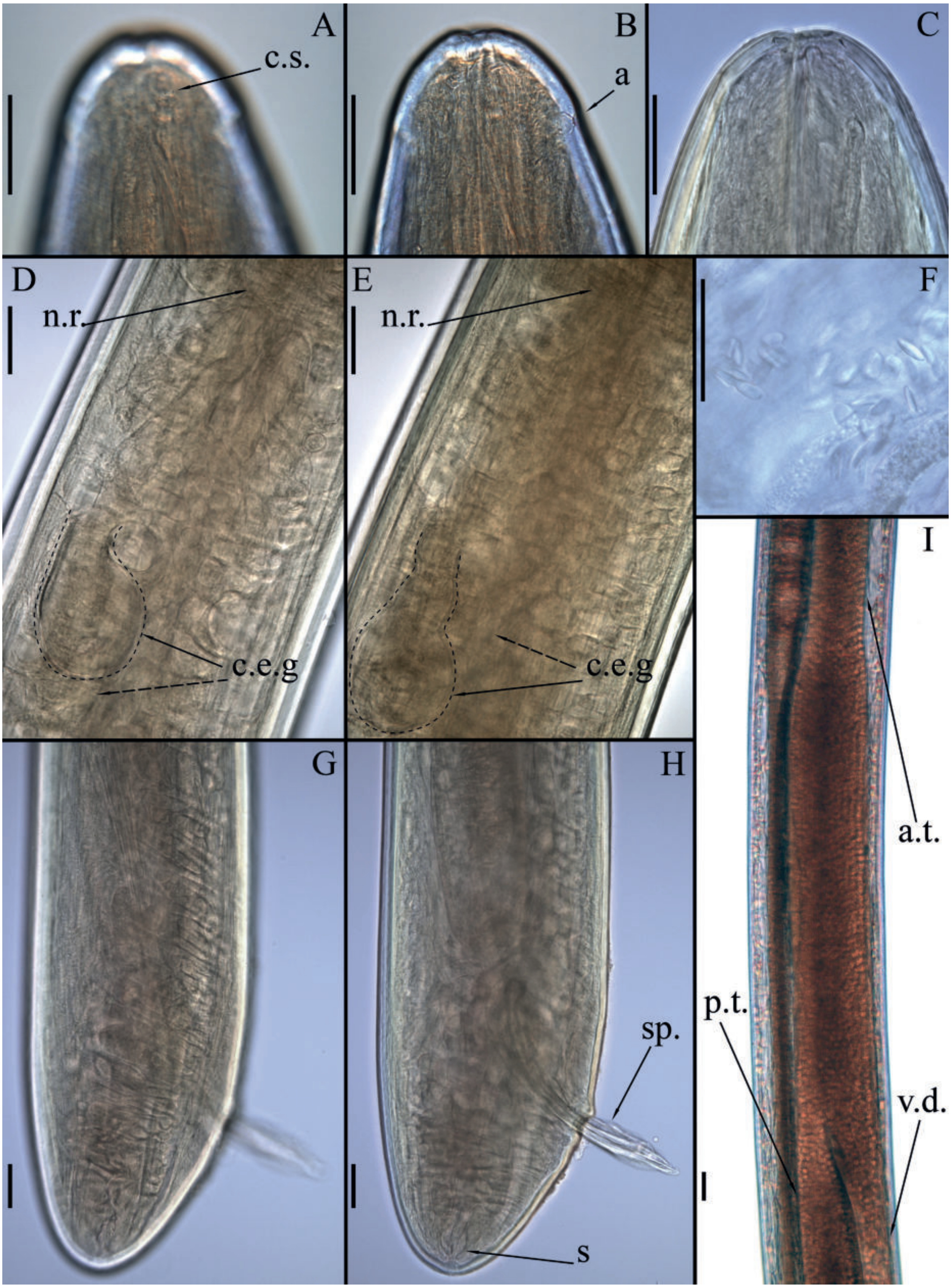

Figure 4. *Aborjinia profunda* sp. nov., male. Light microscopy, DIC **A–C** head **D, E** cellular bodies of the cervical excretory gland **F** crystalloid bodies **G, H** posterior end region **I** the vesicula seminalis region. Abbreviations: a – amphid, a.t. – anterior testis, c.s. – cephalic sensillum, c.e.g. – cervical excretory gland, n.r. – nerve ring, p.t. – posterior testis, s. – spinneret, sp. – spicules, vd – vas deferens. Scale bars: 50 μm.

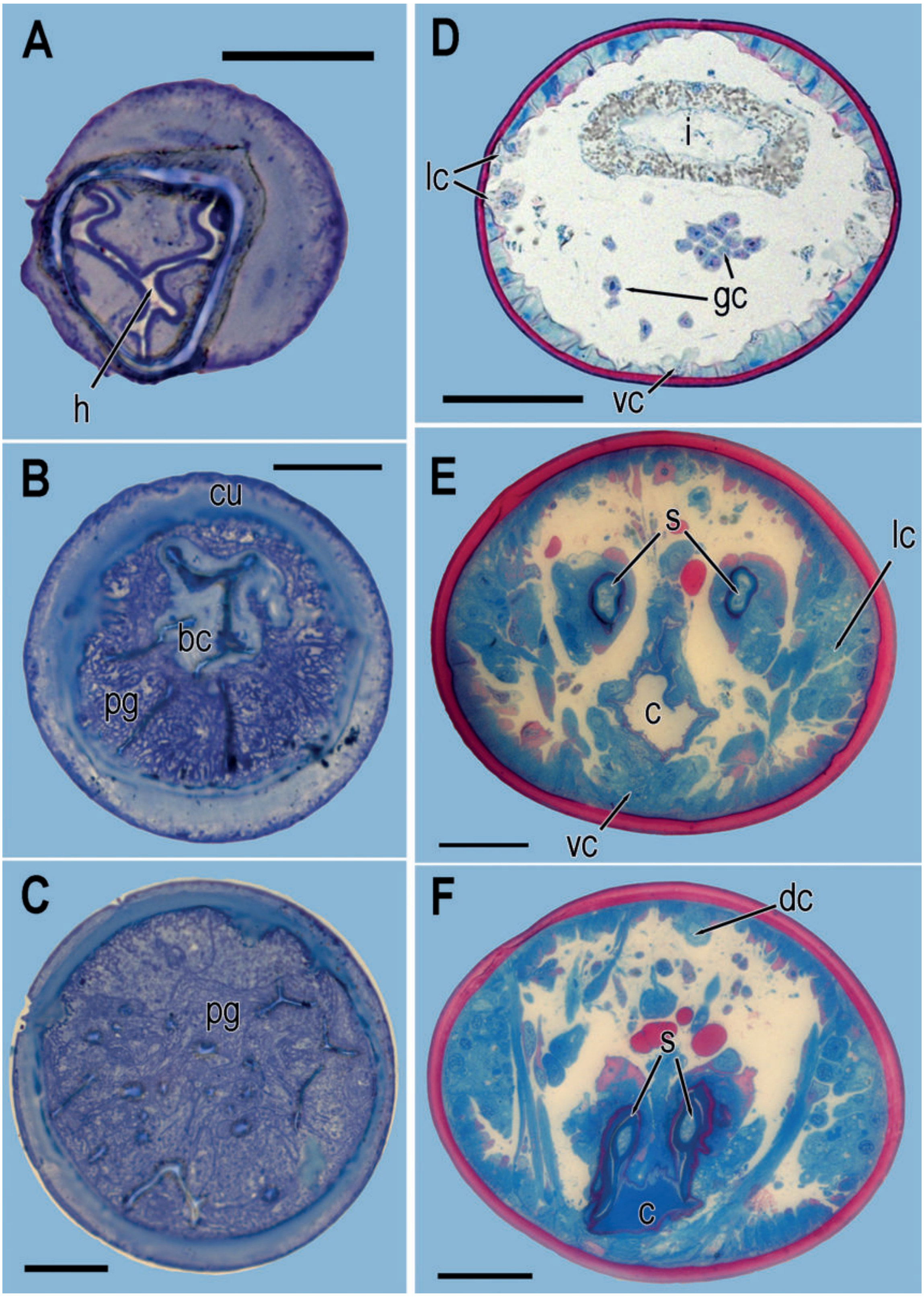

Figure 5. *Aborjinia profunda* sp. nov. Light microphotographs of transverse sections **A** buccal cavity at the upper level of the head (h) **B** buccal cavity surrounded with pharyngeal glands **C** pharyngeal region tightly filled with pharyngeal glands bodies **D** midbody with intestine and gonad **E** posterior region at the level of distal part of spicules **F** posterior region close to cloacal opening. Abbreviation: bc – buccal cavity, c – cloaca, cu – cuticle, gc – germinal cells, h – heilostoma, i – intestine, lc – lateral chords, pg – pharyngeal glands, s – spicules, vc – ventral chords. Scale bars: 20 µm (**A–C**); 50 µm (**E, F**); 100 µm (**D**).

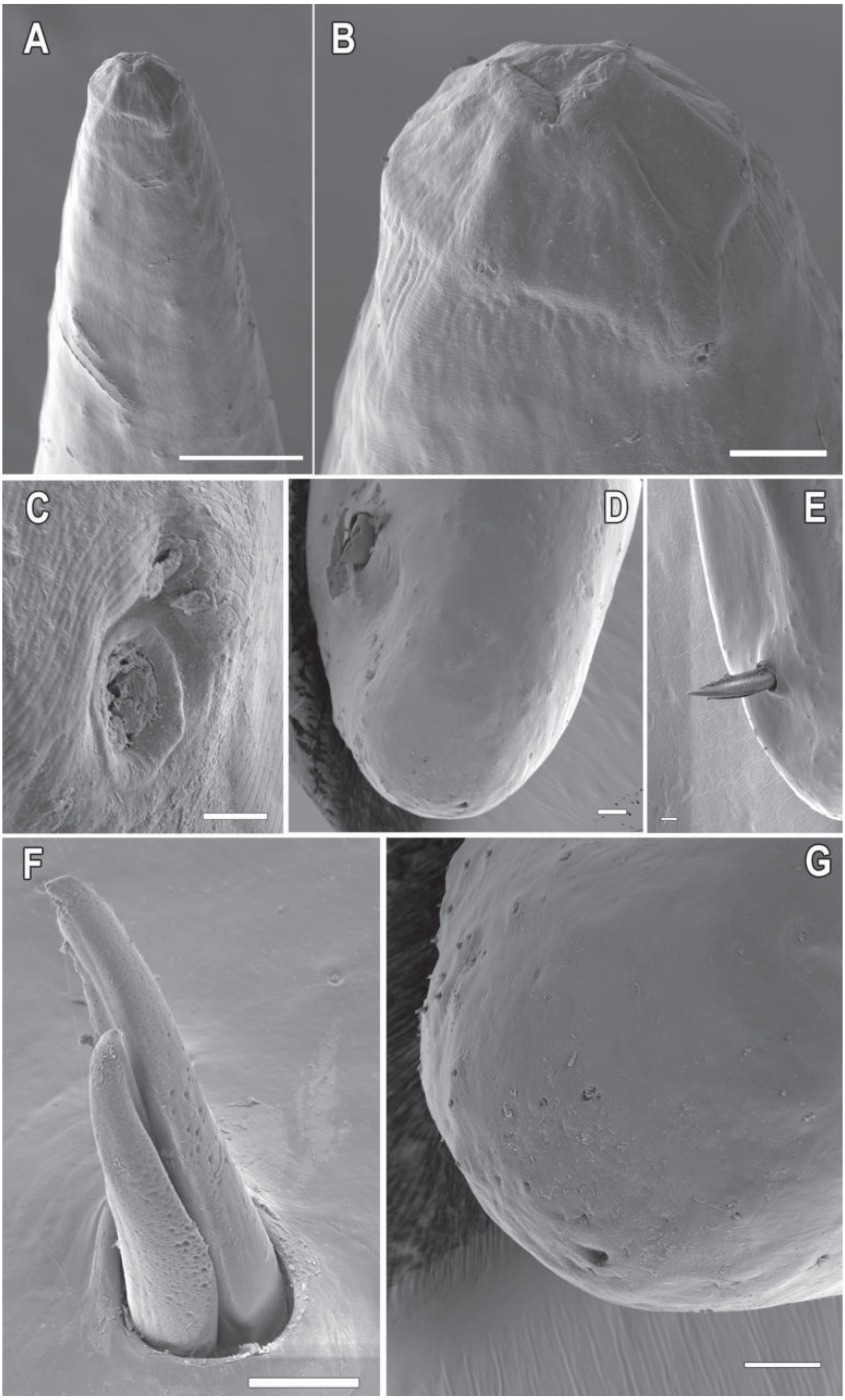

Figure 6. *Aborjinia profunda* sp. nov. SEM **A** anterior end of male **B** head of the male **C** amphideal fovea **D** posterior end of the male **E** spicules protruding from cloacal opening **F** spicules **G** tail tip with spinneret opening. Scale bars: 2 µm (**C**); 20 µm (**B, D, E, F, G**); 100 µm (**A**).

ited in the Zoological Museum of A.V. Zhirmunsky National Scientific Center of Marine Biology, Vladivostok, Russia.

Other material examined. One formalin-preserved specimen (male) and two DESS-preserved specimens (males). The Kuril-Kamchatka Trench, water depth 5477 m (45.0°N, 151.1°E), 6114 m depth (45.9°N, 152.8°E) Deposited in the Zoological Museum of A.V. Zhirmunsky National Scientific Center of Marine Biology, Vladivostok, Russia (MIMB 42308).

Type locality. The Kuril-Kamchatka Trench, water depth 8235 m (44.7°N, 151.5°E) (Fig. 1, Table 1).

Additional locality. The Kuril-Kamchatka Trench, water depth 5477 m (45.0°N, 151.1°E), 6114 m depth (45.9°N, 152.8°E) (Fig. 1, Table 1).

Etymology. Species name derived from the Latin *profundus* that means deepwater and refers to the deepwater habitat of described species.

Nucleotide sequences. GenBank accession numbers OP600452.1, OP600453.1 (small subunit ribosomal RNA gene, partial sequence; internal transcribed spacer 1, 5.8S ribosomal RNA gene, and internal transcribed spacer 2, complete sequence; and large subunit ribosomal RNA gene, partial sequence); OP407645.1, OP407646.1 (large subunit ribosomal RNA gene, partial sequence).

Description. Large nematodes, 22.9–27.7 mm long, with an average diameter 0.2–0.4 mm. Body cylindrical, tapering towards both extremities (Figs 2, 3). The cuticle finely striated under SEM, and thin (~ 5 μm; Fig. 6). Hypodermis and muscle layers are thin, cords are prominent (Fig. 5). Body pores distinct, irregularly arranged. Measurements tabulated in Table 2.

Head narrow, bluntly rounded with three lips. Inner labial sensilla papilliform, hardly visible under light microscope. Papilliform outer labial sensilla and cephalic sensilla in one circle, 1–2 μm long, situated 19–21 μm from anterior end (Fig. 6A, B). Amphideal opening pore-like, located 37–40 μm from anterior end. Pharynx tubular without any valves or bulbs, tightly surrounded by the

Table 2. Morphometrics (μm) of *Aborjinia profunda* sp. nov. and *Aborjinia* sp. (abbreviations of characters defined in the Materials and methods).

	***Aborjinia profunda* sp. nov.**			***Aborjinia* sp.**
	HT♂	♂	♂	**HT ♀**
L	27740	22900	25700	172000
Tail length	263	218	193	524
Nerve ring from anterior end	500	513	501	
Head diam. at level of cephalic setae	91	83	87	
Anal body diam.	289	217	230	467
Maximum body diam.	355	264	290	850
Pharyngeal length	1250	1199	1158	2148
Amphid from anterior end	33	37	43	
Spicule length	364	297	335	
Renetta cells from anterior end	792	742	725	5053
a	78.1	86.7	88.6	202.3
b	22.2	19.1	22.2	78.8
c	105.5	105	133.2	328.2
c’	0.91	1	0.83	1.1

glandular tissue (Figs 3A, 4). Nerve ring situated ~ 40% of pharynx length from anterior end. Intestine well developed with wide lumen. Ventral gland consists of two cells. Cell bodies ~ 80 µm long and 75 µm wide (~ 30% of corresponding body diam.), arranged in tandem and situated 725–792 µm from anterior end (Fig. 4D, E). Excretory pore not observed.

Male reproductive system didelphic, testes outstretched. Spicules paired, symmetrical, slightly bent, 364–372 µm long (Figs 3, 4). Gubernaculum not found. No pre- or postcloacal sensilla or supplements. Rectum and anal opening functional. Tail conical with terminal spinneret, caudal glands not observed.

Remarks. The new species differs from *A. eulagiscae* by the location of the ventral gland cell bodies (posterior to the nerve ring vs posterior to the cardia), by the smaller body size (23–28 mm vs 103–132 mm), and the shorter tail (193–263 µm vs 500–850 µm).

Aborjinia **sp.**

Figs 7, 8

Material examined. Anterior and posterior parts of the DESS fixed female. Eastern slope of the Kuril Islands, water depth 3374 m (Fig. 1, Table 1).

GenBank accession numbers. OP600454.1 (small subunit ribosomal RNA gene, partial sequence; internal transcribed spacer 1, 5.8S ribosomal RNA gene, and internal transcribed spacer 2, complete sequence; and large subunit ribosomal RNA gene, partial sequence); OP407647.1 (large subunit ribosomal RNA gene, partial sequence).

Description. Body opaque, cylindrical, slightly narrowing to both ends, 17.2 cm long (Figs 2, 7). Cuticle smooth under the light microscope. Inner labial sensilla papilliform, hardly visible under light microscope. Papilliform outer labial sensilla and cephalic sensilla in one circle (Fig. 8C). Amphideal opening pore-like. Buccal cavity small, narrow. Pharynx tubular without any valves or bulbs, cardia small. Intestinal lumen distinct only in its anterior most part. Secretory-excretory system consists of two big cells situated 5053 µm from anterior end (Fig. 8F). Excretory pore not observed. Reproductive system didelphic, amphidelphic with outstretched ovaries. Uteri large, tubular. Vulva located at midbody, a transverse slit. Tail conico-cylindrical. Anal opening present. Spinneret very vestigial (Fig. 8D), caudal glands not observed.

Molecular analysis. In total, six specimens were sequenced for the 18S rDNA, 28S rDNA (D2-D3 region), and ITS (including ITS1, 5.8S rDNA, and ITS2) genes. Of these, two specimens belong to *Leptosomatides* Filipjev, 1918, two specimens to *Aborjinia profunda* sp. nov., and one female and one juvenile belong to *Aborjinia* sp. The sequence length of 18S rDNA was 1694–1716 bp (14 variable sites, 11 parsimony-informative characters), 28S rDNA – 659–671 bp (66 variable sites, 59 parsimony-informative characters). The length of ITS for the genus *Aborjinia* was 1054–1094 bp (61 variable sites, 9 parsimony-informative characters) whereas for *Leptosomatides* sp. length was 1267 bp (3 variable sites).

To calculate genetic distances, as well as to reconstruct phylogenetic relationships, we used all available sequences of leptosomatids from GenBank (Suppl. materials 2, 3). The BI phylogeny using 18S rRNA reveal *Deontostoma* Filipjev, 1916 as the earliest branching lineage within Leptosomatidae.

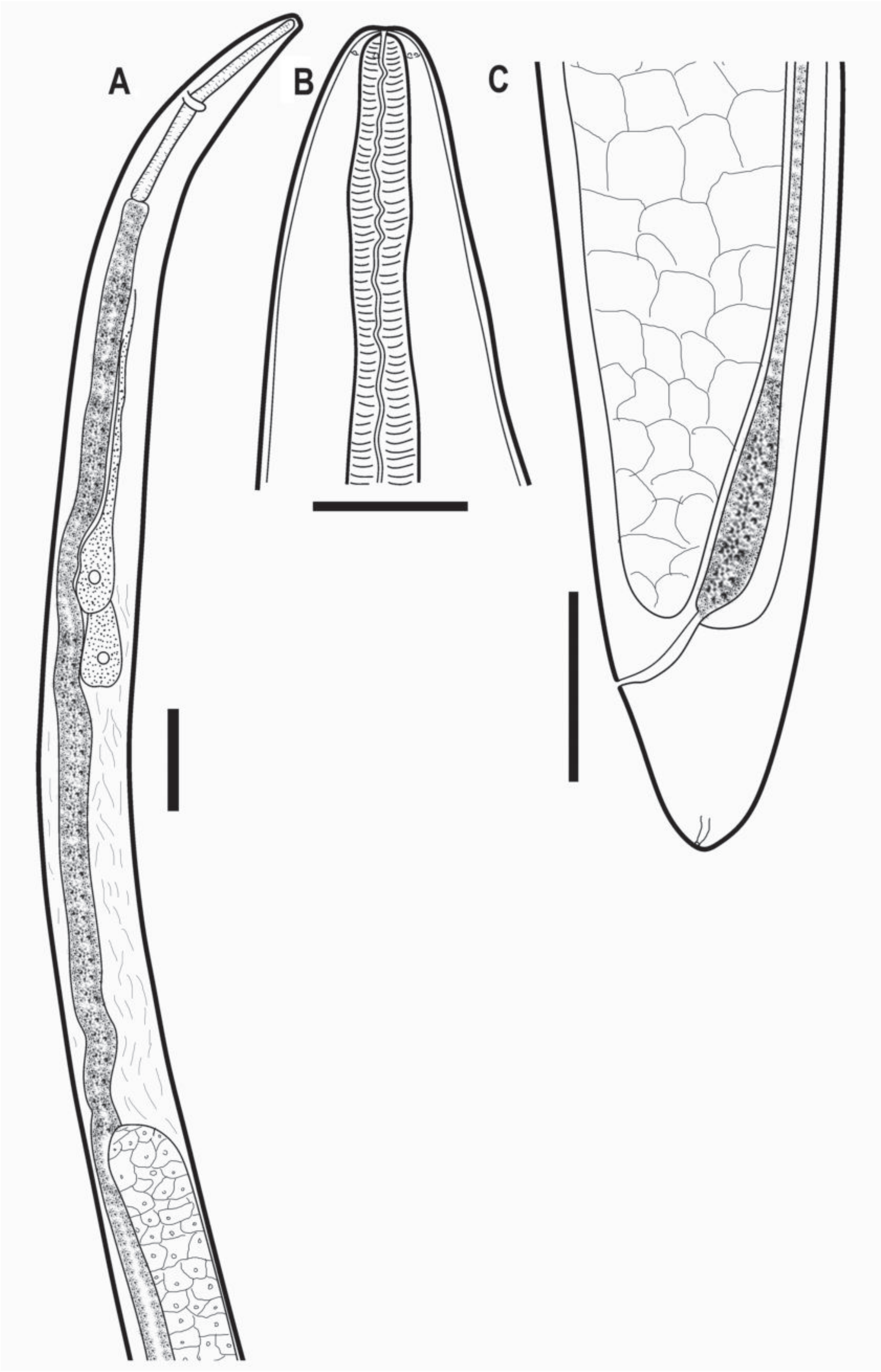

Figure 7. *Aborjinia* sp. **A** anterior end of female **B** head end of female **C** tail of female. Scale bars: 250 µm (**B**); 500 µm (**C**); 1000 µm (**A**).

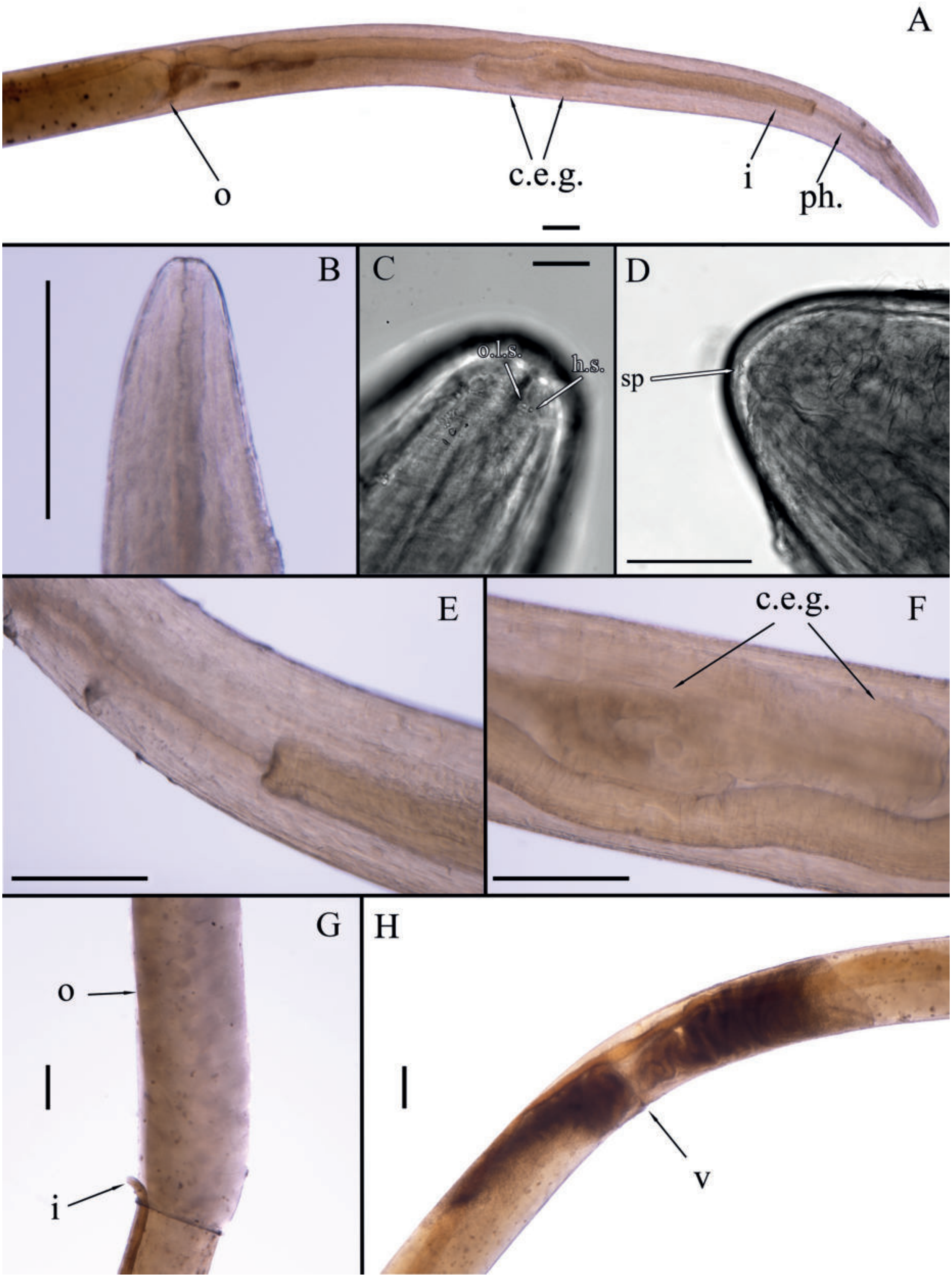

Figure 8. Light microscopy, DIC. *Aborjinia* sp., female **A** anterior end **B** head **C** anterior end with cephalic sensilla **D** tail end with spinneret **E** pharynx-intestine connection **F** cellular bodies of the cervical excretory gland **G** ovary **H** vulva region. Abbreviation: c.e.g. – cervical excretory gland, h.s. – cephalic sensilla; i – intestine, o – ovary, o.l.s. – outer labial sensilla, ph – pharynx, v – vulva. Scale bars: 50 µm (**C**); 100 µm (**D**); 500 µm (**A, B, E, F–H**).

However, this genus was shown to be polyphyletic which occupied two of the branches of the polytomous clade. A well supported clade (Bayesian PP, BPP = 1; ML bootstrap value percent, ML = 89) united the four samples of *Pseudocella* Filipjev, 1927. Another moderately supported clade uniting *Thoracostoma microlobatum* and two species of genus *Proplatycoma* Platonova, 1976 was uncovered (BPP = 0.78). Two species of *Platonova* Mordukhovich et al., 2019 and *Synonchus* Cobb, 1894 were placed as monophyletic clade with moderate support (BPP = 0.96; ML = 98), whereas the placement of *Cylicolaimus* de Man, 1889 was unsupported. *Thoracostoma trachygaster* Hope, 1967 was sister to obtained sequences and *Paraborjinia corallicola* (BPP = 0.99, ML = 86) and not monophyletic to *Thoracostoma microlobatum* and *Thoracostoma* sp., rendering that genus polyphyletic. A clade containing two samples of *Leptosomatides* (vouchers L1, L2) and a clade uniting samples of *Aborjinia* (excluding *Paraborjinia corallicola*) and *Leptosomatides* (HM564626) were high supported (BPP = 1; ML = 94 and BPP = 0.99; ML = 96, respectively). *Paraborjinia corallicola* was sister to previous clade with high Bayesian support (BPP = 0.99, ML = 72).

The phylogenetic relationships using 28S rRNA reveals opposite topology compared with 18S rRNA. *Paraborjinia corallicola*, the rest *Aborjinia* species and *Leptosomatides* (vouchers L1, L2) were the earliest branching lineages but supports of these clades were moderate or low. Genus *Thoracostoma* was also polyphyletic. *Deontostoma* was placed in one clade with *Thoracostoma microlobatum* (BPP = 0.99, ML = 83). *Pseudocella* and one out of three *Thoracostoma* were sister to *Platonova* (including *Synonchus*) (BPP = 0.95, ML = 88).

The average intergeneric p-distances within Leptosomatidae were 1.96% (0.57%–4.66%) and 13.30% (9.15%–17.12%) for 18S rDNA and 28S rDNA respectively if the two non-monophyletic species *Thoracostoma trachygaster* and *Thoracostoma microlobatum* Allgén, 1947 as well as *Paraborjinia corallicola* and the remaining *Aborjinia* belongs to different genera. Genus *Aborjinia* (including sequences HM564626 and HM564855, excluding *Paraborjinia corallicola*) differed from other genera of the family by 1.49% and 11.57% in average for 18S rDNA and 28S rDNA, respectively. Same values for genus *Leptosomatides* were 1.71% and 13.84% and for *Paraborjinia corallicola* were 3.78% and 16.15%, respectively.

The interspecific p-distance for 18S rDNA between *Aborjinia profunda* sp. nov. and *Aborjinia* sp. (voucher M10) was 0.24%, for 28S rDNA this value was 1.82%, and for ITS2 5.78% (Table 3). Using the programs RNA structure and 4SALE, homologous regions of *Aborjinia* ITS2 as well as *Aborjinia* sp. MZ504143 sequences were generally folded as comparable secondary structural motifs. Analyses revealed single secondary structure for all sequences contained four universal helices (Fig. 9). Comparison of sequences across taxa identified several hemi-compensatory base changes (hemi- CBCs, Table 4, Fig. 9) which in turn belonged to different types of changes (H1-H3). Various comparison pairs of *Aborjinia* species gave 3–7 hemi-CBCs while no double-sided changes (CBC) were found (Table 4).

Remarks. To date only three species (including the present material) were originally described in the genus *Aborjinia*: *Aborjinia corallicola*, *Aborjinia eulagiscae*, and *Aborjinia profunda* sp. nov. but *Aborjinia corallicola* is here transferred to *Paraborjinia* sp. nov. Both species (*A. eulagiscae* and *A. profunda* sp. nov.) are characterized by the outer labial and cephalic sensilla situated in one circle and the presence of two cells of secretory-excretory system. In the description

Table 3. Interspecific p-distances (%) between the obtained sequences. Distances for ITS and 28S are above and below the diagonal, respectively ("-" – data absent).

Taxon	1	2	3	4	5	6	7
1. *Aborjinia corallicola*		–	–	–	–	–	–
2. *Aborjinia* sp. (specimen M10)	15.85		5.78	4.62	4.34	–	24.11
3. *Aborjinia profunda* sp. nov.	16.46	1.82		3.47	4.34		23.21
4. *Aborjinia* sp. (specimen M11)	15.85	1.37	1.37		3.18		24.11
5. *Aborjinia* sp. (MZ504143)	16.02	1.22	1.83	1.22		–	24.11
6. *Leptosomatides* sp. (HM564855)	15.87	1.25	1.88	1.72	1.57		–
7. *Leptosomatides* sp. (specimen L1, L2)	16.07	9.02	8.72	8.72	9.04	9.15	

Table 4. Number of CBCs (above diagonal) and hemi-CBCs (under diagonal) in the ITS2 secondary structure.

Taxon	***Aborjinia* sp. (specimen M10)**	***Aborjinia profunda* sp. nov.**	***Aborjinia* sp. (specimen M11)**	***Aborjinia*_sp. (MZ504143.1)**
Aborjinia sp. (specimen M10)		0	0	0
Aborjinia profunda sp. nov.	6		0	0
Aborjinia sp. (specimen M11)	5	3		0
Aborjinia sp. (MZ504143)	5	7	4	

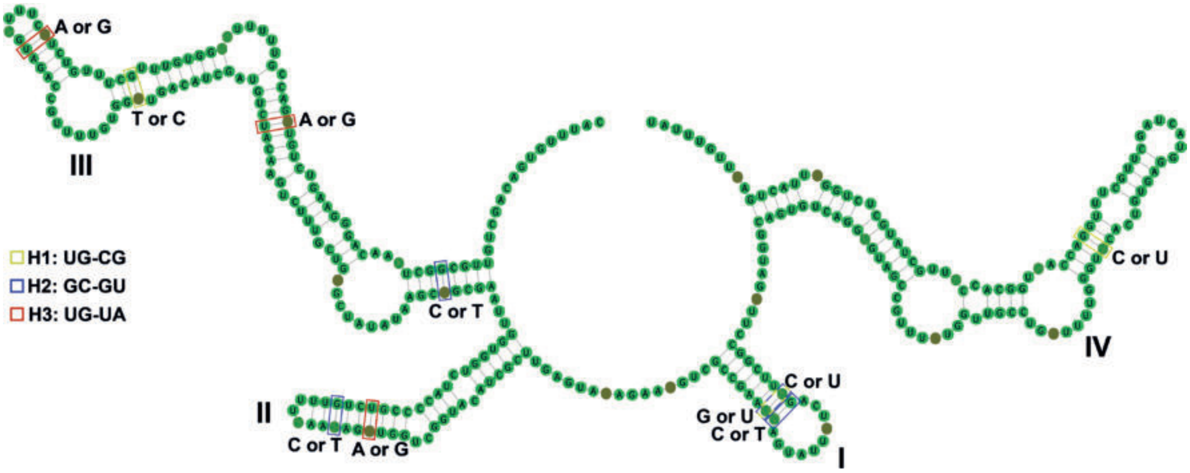

Figure 9. Consensus ITS2 secondary structure and the hemi compensatory base change (hemi-CBCs) derived from *Aborjinia* species. The four stems are labelled. Each type of base change (H1-H3) indicates by unique color. CU and GU change that relates to H1 or H2 depending on comparison pair.

of *P. corallicola* provided by Westerman et al. (2021) it is mentioned that outer labial sensillae and cephalic sensilla are situated in one circle. However, on the photograph provided in that paper these sensilla are situated in two separate circles. In addition, in *P. corallicola* the secretory-excretory system was not found, contrasting with the two giant and clearly visible cells in other *Aborjinia*. It should also be noted that, unlike other representatives of the genus, *P. corallicola* is parasitic as an adult. Based on above we assume that *P. corallicola* belongs to another genus. Our conclusion is also supported by the molecular phylogenetic tree (Fig. 10), values of intergeneric p-distances within Leptosomatidae, and interspecies p-distances within *Aborjinia* (Table 3). We propose the new genus *Paraborjinia* gen. nov. for *A. corallicola*.

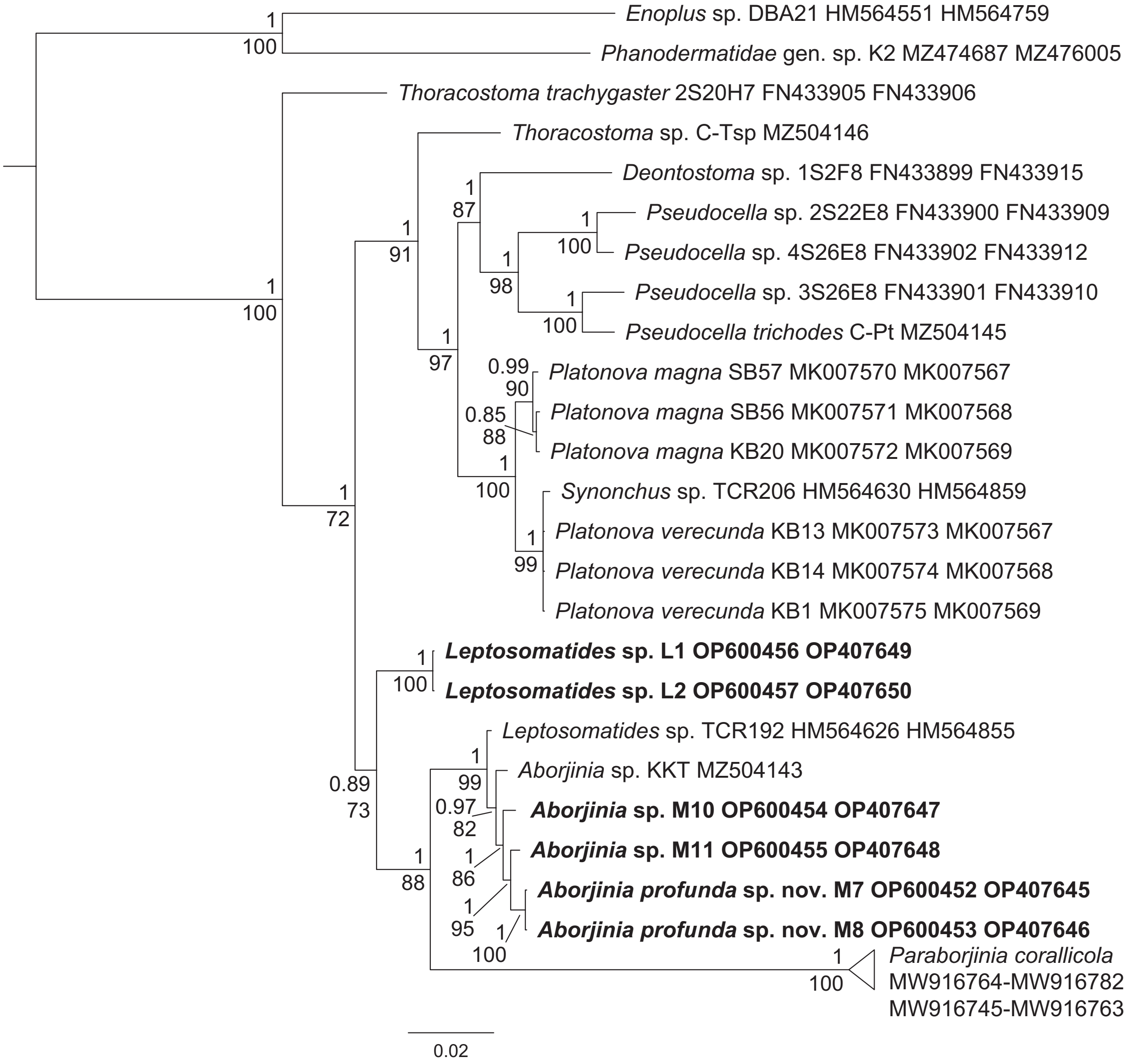

Figure 10. Bayesian phylogeny of the family Leptosomatidae, using concatenated 18S and 28S rDNA and SYM+ G model of nucleotide substitution. *Enoplus* sp. (Enoplidae) and Phanodermatidae gen. sp. were used as outgroup to root tree. Bayesian posterior probabilities (PP) are given above tree nodes and bootstrap support values found in the ML analysis are shown below nodes. Specimens obtained in this study are in bold.

***Paraborjinia* gen. nov.**

https://zoobank.org/5662ABEE-8888-4C29-ACF2-6EDDB2A63F0B

Type species. *Paraborjinia corallicola* (Westerman, de Moura Neves, Ahmed & Holovachov, 2021). Type locality: Atlantic Ocean, Labrador Shelf (60.6083°N, 61.7428°W), 426 m depth. Type host: *Acanella arbuscula*.

Diagnosis. Parasitic life style. Distinct body pores along the body. Outer labial and cephalic sensilla papilliform, situated in two circles. Amphideal aperture pore-like. Muscular and uniformly cylindrical pharynx. Intestine not modified into trophosome. Hologonic ovaries in females. Presence of caudal glands.

Differential diagnosis. Within the family Leptosomatidae the new genus differs from all genera except *Aborjinia* by having and endoparasitic lifestyle and hologonic ovaries. *Paraborjinia* gen. nov. differs from *Aborjinia* by the position of cephalic sensitive organs (outer labial and cephalic papilla in two separate circles in *Paraborjinia* vs outer labial and cephalic papilla in one circle in *Aborjinia*). *Paraborjinia* gen. nov. differs from *Aborjinia*, *Ananus*, and *Thalassonema* by the parasitic adult (vs free-living in *Aborjinia*, *Ananus*, and *Thalassonema*). *Paraborjinia* gen. nov. differs from *Ananus* by the presence of rectum and anus. In addition, in all described species of *Aborjinia* and *Ananus* the secretory-excretory system is well developed and consists of two prominent cells while in *Paraborjinia* the secretory-excretory system was not found.

Discussion

These results of the phylogenetic analyses are only preliminary due to the low number of sequences available. The different sets of species and genera for constructing the SSU and LSU phylogenetic trees, as well as the small number of sequences relative to the total number of species affect the different topologies. It is premature to make solid conclusions about the relationships of genera within Leptosomatidae based on the available data; however, concatenated 18S and 28S rDNA phylogenetic tree showed relatively high support values (Fig. 10). Recent studies have shown that the genus *Aborjinia* belongs to the family Leptosomatidae based on both molecular and morphological characters (Tchesunov et al. 2022) and our SSU and D2-D3 of LSU phylogenetic trees confirm the previous analyses.

The males of *Aborjinia profunda* sp. nov. and female *Aborjinia* sp. (specimen M10) have pronounced morphological differences and p-distances (28S and ITS). Moreover, for all known *Aborjinia* isolates, differences in the nucleotide sequences of LSU and ITS are observed (Table 4). The presence of sexual dimorphism is known for nematodes, including leptosomatids, and the values of p-distances are relatively small. In addition to the commonly used phylogenetic analysis and genetic distances, we used Compensatory Base Changes (CBCs) in Internal Transcriber Spacer 2 (ITS2) for species delimitation. ITS2 is useful locus for calculation of lower-level phylogenetic trees in many eukaryotic lineages (Young and Coleman 2004; Ahvenniemi et al. 2009) to predict the ability to interbreed successfully between putative biological species. Organisms that differ by even one CBC in the conserved ITS2 regions (helices 2 and 3) are unable to interbreed (Coleman 2009). At the same time, changes in single stranded region (hemi-CBC) do not contribute to the appearance of CBCs (Caisová et al. 2011) and lead to failure in sexual reproduction (Coleman 2009). Based on this evidence, when CBCs occur among species, Wolf et al. (2013) developed a generalized ‘CBC species concept’. Double-sided changes (CBC) were not found; therefore, there are no strict reasons for classifying the studied individuals as different species, but resolving the issue of the species status of some individuals requires further research.

Our results indicate a rather wide distribution of representatives of the genus *Aborjinia* in the deep-sea communities of the northwestern Pacific, including depths of more than 8000 m. Molecular and morphological (in particular, the two-celled renette, the presence of a spinerette, minute sensory sensilla, normal muscular pharynx) data support the assignment of *Aborjinia* to Leptosomatidae. Analysis of molecular data confirms the independence of the genera *Aborjinia* and *Paraborjinia* and demonstrates clearly supported differences from *Leptosomatides*. We agree with Tchesunov et al. (2022) that morphological uniformity can lead to misidentification of *Aborjinia* specimens, especially if fixed in ethanol. This may lead to an underestimation of the frequency of occurrence, abundance, and diversity of both representatives of the genus *Aborjinia* and parasitic leptosomatids in general.

Acknowledgements

The scanning electron microscopy investigations were done in the A.V. Zhirmunsky National Scientific Centre of Marine Biology FEB RAS. The authors are grateful to D.V. Fomin for assistance with the SEM facilities. The light microscopy investigations were done in the Laboratory of Ecology and Evolutionary Biology of Aquatic Organisms of the Far Eastern Federal University.

We are very grateful to Prof. Dr. A. Brandt (Senckenberg Research Institute and Natural History Museum, and Goethe University Frankfurt, Frankfurt) and to Dr. M.V. Malyutina (NSCMB FEB RAS) for invitation to join international projects and the deep-sea expeditions. We thank the crews of the RVs 'Sonne', 'Akademik M.A. Lavrentyev', 'Akademik Oparin' and the scientific teams of the expeditions for their assistance on board.

The authors are also grateful to Dr. Inna Alalykina (NSCMB FEB RAS) for help with taxonomic identifications of Polychaeta and Dr. Alexey Chernyshev, who found a sample of *Aborjinia* in the bottom sediments from the AGT.

Additional information

Conflict of interest

The authors have declared that no competing interests exist.

Ethical statement

No ethical statement was reported.

Funding

We thank the Ministry of Science and Higher Education of the Russian Federation for funding this study (grant 13.1902.21.0012, contract No. 075-15-2020-796).

Author contributions

All authors have contributed equally.

Data availability

All of the data that support the findings of this study are available in the main text or Supplementary Information.

References

Ahvenniemi P, Wolf M, Lehtonen MJ, Wilson P, German-Kinnari M, Valkonen JPT (2009) Evolutionary diversification indicated by compensatory base changes in ITS2 secondary structures in a complex fungal species *Rhizoctonia solani*. Journal of Molecular Evolution 69(2): 150–163. https://doi.org/10.1007/s00239-009-9260-3

Allgén CA (1947) West American Marine Nematodes (Papers from Dr. Th. Mortensen's Pacific Expedition 1914–16. LXXV). Videnskabelige Meddelelser fra Dansk naturhistorisk Forening i Kjøbenhavn 110: 65–219.

Ankenbrand MJ, Keller A, Wolf M, Schultz J, Förster F (2015) ITS2 database V: Twice as much. Molecular Biology and Evolution 32(11): 3030–3032. https://doi.org/10.1093/molbev/msv174

Blaxter ML, De Ley P, Garey JR, Liu LX, Scheldeman P, Vierstraete A, Vanfleteren JR, Mackey LY, Dorris M, Frisse LM, Vida JT, Thomas WK (1998) A molecular evolutionary framework for the phylum Nematoda. Nature 392(6671): 71–75. https://doi.org/10.1038/32160

Caisová L, Marin B, Melkonian M (2011) A close-up view on ITS2 evolution and speciation-a case study in the Ulvophyceae (Chlorophyta, Viridiplantae). BMC Evolutionary Biology 11(1): 1–24. https://doi.org/10.1186/1471-2148-11-262

Cobb NA (1894) *Tricoma* and other nematode genera. Proceedings of the Linnean Society of New South Wales 8: 389–421.

Coleman AW (2009) Is there a molecular key to the level of “biological species” in eukaryotes? A DNA guide. Molecular Phylogenetics and Evolution 50(1): 197–203. https://doi.org/10.1016/j.ympev.2008.10.008

De Grisse AT (1969) Redescription ou modifications de quelques techniques utilisées dans l’étude des nématodes phytoparasitaires. Mededelingen Rijksfakultiet Landbouwwetenschappen Gent 34: 352–369.

de Man JG (1889) Espèces et genres nouveaux de Nématodes libres de la mer du Nord et de la Manche. Mémoires de la Société Zoologique de France 2: 1–10. https://biostor.org/reference/61320

Filipjev IN (1916) Free-living nematodes in the collection of the Zoological Museum of the Imperial Academy of Sciences in Petrograd. Annuaire du Musée Zoologique de l’Académie Impériale des Sciences de Saint Pétersbourg 2: 159–116.

Filipjev IN (1918) Free-living marine nematodes of the Sevastopol area. Transactions of the Zoological Laboratory and the Sevastopol Biological Station of the Russian Academy of Sciences Series II. No 4 (Issue I/II).

Filipjev IN (1927) Les Nématodes libres des mers septentrionales appartenant a la famille des Enoplidae. Archiv für Naturgeschichte 91 A: 1–216.

Floyd RM, Rogers AD, Lambshead PJD, Smith CR (2005) Nematode-specific PCR primers for the 18S small subunit rRNA gene. Molecular Ecology Notes 5(3): 611–612. https://doi.org/10.1111/j.1471-8286.2005.01009.x

Hoang DT, Chernomor O, von Haeseler A, Minh BQ, Vinh LS (2018) UFBoot2: Improving the ultrafast bootstrap approximation. Molecular Biology and Evolution 35(2): 518–522. https://doi.org/10.1093/molbev/msx281

Holovachov O, Rodrigues CF, Zbinden M, Duperron S (2013) *Trophomera conchicola* sp. n.(Nematoda: Benthimermithidae) from chemosymbiotic bivalves *Idas modiolaeformis* and *Lucinoma kazani* (Mollusca: Mytilidae and Lucinidae) in Eastern Mediterranean. Russian Journal of Nematology 21: 1–12.

Hope WD (1967) Free-living marine nematodes of the genera *Pseudocella* Filipjev, 1927, *Thoracostoma* Marion, 1870, and *Deontostoma* Filipjev, 1916 (Nematoda: Leptosomatidae) from the West Coast of North America. Transactions of the American Microscopical Society 86(3): 307–334. https://doi.org/10.2307/3224598

Humphrey CD, Pittman FE (1974) A simple methylene blue-azure II-basic fuchsin stain for epoxy-embedded tissue sections. Stain Technology 49(1): 9–14. https://doi.org/10.3109/10520297409116929

Kalyaanamoorthy S, Minh BQ, Wong TKF, von Haeseler A, Jermiin LS (2017) ModelFinder: Fast model selection for accurate phylogenetic estimates. Nature Methods 14: 587–589. https://doi.org/10.1038/nmeth.4285

Kumar S, Stecher G, Tamura K (2016) MEGA7: Molecular evolutionary genetics analysis. Version 7.0 for bigger datasets. Molecular Biology and Evolution 33(7): 1870–1874. https://doi.org/10.1093/molbev/msw054

Lanfear R, Calcott B, Ho SY, Guindon S (2012) Partitionfinder: Combined selection of partitioning schemes and substitution models for phylogenetic analyses. Molecular Biology and Evolution 29(6): 1695–1701. https://doi.org/10.1093/molbev/mss020

Leduc D, Zhao ZQ (2019) Phylogenetic position of the parasitic nematode *Trophomera* (Nematoda, Benthimermithidae): A molecular analysis. Molecular Phylogenetic and Evolution 132: 177–182. https://doi.org/10.1016/j.ympev.2018.12.005

Magis C, Taly JF, Bussotti G, Chang JM, Di Tommaso P, Erb I, Espinosa-Carrasco J, Notredame C (2014) T-Coffee: Tree-based consistency objective function for alignment evaluation. Methods in Molecular Biology 1079: 117–129. https://doi.org/10.1007/978-1-62703-646-7_7

Mardashova MV, Aleoshin VV, Nikitin MA (2011) The origin of marine parasitic nematodes. Russian Journal of Nematology 19: e196.

Meldal BHM, Debenham NJ, De Ley P, De Ley IT, Vanfleteren JR, Vierstraete AR, Bert W, Borgonie G, Moens T, Tyler PA, Austen MC, Blaxter ML, Rogers AD, Lambshead PJD (2007) An improved molecular phylogeny of the Nematoda with special emphasis on marine taxa. Molecular Phylogenetics and Evolution 42(3): 622–636. https://doi.org/10.1016/j.ympev.2006.08.025

Miljutin D (2003) Histological studies on the anatomy of the parasitic stages of *Australonema* sp. (Nematoda: Marimermithida). Nematology 5(2): 275–291. https://doi.org/10.1163/156854103767139752

Miljutin DM (2014a) Order Marimermithida Rubtzov 1980, emend. Tchesunov 1995. In: Schmidt-Rhaesa A (Ed.) Handbook of Zoology. Gastrotricha, Cycloneuralia and Gnatifera (Vol. 2). Nematoda. De Gruyter, GmBH, Berlin/Boston, 345–350. https://doi.org/10.1515/9783110274257.345

Miljutin DM (2014b) Order Benthimermitida Tchesunov 1995. In: Schmidt-Rhaesa A (Ed.) Handbook of Zoology. Gastrotricha, Cycloneuralia and Gnatifera (Vol. 2). Nematoda. De Gruyter, GmBH, Berlin/Boston, 179–186.

Minh BQ, Schmidt HA, Chernomor O, Schrempf D, Woodhams MD, von Haeseler A, Lanfear R (2020) IQ-TREE 2: New models and efficient methods for phylogenetic inference in the genomic era. Molecular Biology and Evolution 37(5): 1530–1534. https://doi.org/10.1093/molbev/msaa015

Mordukhovich VV, Semenchenko AA, Fadeeva NP, Zograf JK (2019) One new genus and two new free-living deep-sea nematode species with discussion of phylogeny of the family Leptosomatidae Filipjev, 1916. Progress in Oceanography 178: e102160. https://doi.org/10.1016/j.pocean.2019.102160

Nunn G (1992) Nematode molecular evolution: an investigation of evolutionary patterns among nematodes based upon DNA sequences. Ph.D. thesis, University of Nottingham, Nottingham, 187 pp.

Özdikmen H (2010) Substitute names for some Nematoda. Munis Entomology & Zoology 5: 780–784.

Petter A-J (1980) Une novella famille de Nématodes parasites d'Invertébrés marins, les Benthimermithidae. Annales de Parasitologie Humaine et Comparee 55(2): 209–224. https://doi.org/10.1051/parasite/1980552209

Platonova TA (1976) Lower Enoplida (free-living marine nematodes) of the seas of the USSR (in Russian). Issledovaniya Fauny Morei (Nematody i ikh rol' v meiobentose) 15: 3–164.

Rambaut A, Drummond AJ, Xie D, Baele G, Suchard MA (2018) Posterior summarization in Bayesian phylogenetics using Tracer 1.7. Systematic Biology 67(5): 901–904. https://doi.org/10.1051/parasite/1980552209

Reuter JS, Mathews DH (2010) RNAstructure: Software for RNA secondary structure prediction and analysis. BMC Bioinformatics 11(1): e129. https://doi.org/10.1186/1471-2105-11-129

Ronquist FM, Teslenko M, van der Mark P, Ayres DL, Darling A, Höhna S, Larget B, Liu L, Suchard MA, Huelsenbeck JP (2012) MRBAYES 3.2: Efficient Bayesian phylogenetic inference and model selection across a large model space. Systematic Biology 61(3): 539–542. https://doi.org/10.1093/sysbio/sys029

Rubtzov IA (1980) The new marine parasitic nematode, *Abos bathycola*, from priapulids and a taxonomic position of the family Marimermithidae in the class Nematoda. Parazitologia 14: 177–181. [In Russian]

Rubtzov IA, Platonova TA (1974) A new family of marine parasitic nematodes. Zoologicheskij Zhurnal 53: 1445–1458. [In Russian]

Seibel PN, Müller T, Dandekar T, Wolf M (2008) Synchronous visual analysis and editing of RNA sequence and secondary structure alignments using 4SALE. BMC Research Notes 1(1): e91. https://doi.org/10.1186/1756-0500-1-91

Seinhorst JW (1959) A rapid method for the transfer of nematodes from fixative to anhydrous glycerin. Nematologica 4(1): 67–69. https://doi.org/10.1163/187529259X00381

Smol N, Muthumbi A, Sharma J (2014) Order Enoplida. In: Schmidt-Rhaesa A (Ed.) Handbook of Zoology. Gastrotricha, Cycloneuralia and Gnatifera (Vol. 2). Nematoda. De Gruyter, GmBH, Berlin/Boston, 193–249. https://doi.org/10.1515/9783110274257.193

Tchesunov AV (1995) New data of the anatomy of marimemithid nematode *Marimermis maritima*, and a review of the system of Marimermithida. Nematologica 41: e347.

Tchesunov AV (1997) On the histological anatomy of *Marimermis maritima* Rubtzov et Platonova, 1974 (Nematoda: Enoplia: Marimermithida), parasite of a sea urchin. Fundamental and Applied Nematology 20: 349–356.

Tchesunov AV, Spiridonov SE (1985) *Australonema eulagiscae* gen. et sp. n. (Nematoda, Marimermithida) – a parasite of a Polychaete from Antarctics. Vestnik Zoologii 2: 16–21.

Tchesunov AV, Kuzmin AA, Aleshin VV (2009) Position of Benthimermithidae (parasites of marine invertebrates) as derived from morphological and molecular data. Russian Journal of Nematology 17: e162.

Tchesunov AV, Nikolaeva OV, Rusin LY, Sanamyan NP, Panina EG, Miljutin DM, Gorelysheva DI, Pegova AN, Khromova MR, Mardashove MV, Mirhailov KV, Yushin VV, Petrov NB, Lyubetsky VA, Nikitin MA, Aleoshin VV (2022) Paraphyly of Marimermithida refines primary routes of transition to parasitism in roundworms. Zoological Journal of the Linnean Society 20: 1–15. https://doi.org/10.1093/zoolinnean/zlac070

Vrain TC, Wakarchuk DA, Levesque AC, Hamilton RI (1992) Intraspecific rDNA restriction fragment length polymorphism in the *Xiphinema americanum* group. Fundamental and Applied Nematology 15: 563–573.

Ward HB (1933) On *Thalassonema ophioctinis*, a nematode parasitic in the brittle star *Ophiocten amitinum*. Parasitology 19(4): 262–268. https://doi.org/10.2307/3271583

Westerman R, de Moura Neves B, Ahmed M, Holovachov O (2021) *Aborjinia corallicola* sp. n., a new nematode species (Nematoda: Marimermithidae) associated with the bamboo coral *Acanella arbuscula* (Johnson). Systematic Parasitology 98(5–6): 559–579. https://doi.org/10.1007/s11230-021-09996-y

Wolf M, Friedrich J, Dandekar T, Müller T (2005) CBCAnalyzer: Inferring phylogenies based on compensatory base changes in RNA secondary structures. In Silico Biology 5(3): 291–294.

Wolf M, Chen S, Song J, Ankenbrand M, Müller T (2013) Compensatory base changes in ITS2 secondary structures correlate with the biological species concept despite intragenomic variability in ITS2 sequences – a proof of concept. PLOS ONE 8(6): e66726. https://doi.org/10.1371/journal.pone.0066726

Young I, Coleman AW (2004) The advantages of the ITS2 region of the nuclear rDNA cistron for analysis of phylogenetic relationships of insects: A *Drosophila* example. Molecular Phylogenetics and Evolution 30(1): 236–242. https://doi.org/10.1016/S1055-7903(03)00178-7

Zimmermann L, Stephens A, Nam SZ, Rau D, Kübler J, Lozajic M, Gabler F, Söding J, Lupas AN, Alva V (2018) A completely reimplemented MPI bioinformatics toolkit with a new HHpred server at its core. Journal of Molecular Biology 430(15): 2237–2243. https://doi.org/10.1016/j.jmb.2017.12.007

Supplementary material 1

Light microscopy, DIC. *Leptosomatides* sp., female

Authors: Julia K. Zograf, Alexander A. Semenchenko, Vladimir V. Mordukhovich

Data type: jpg

Explanation note: Light microscopy, DIC. *Leptosomatides* sp., female. **A** – anterior end. **B** – posterior end. **C–E** – head. **F** – vulva region. **G** – tail. Scale bars: 100 μm.

Link: https://doi.org/10.3897/zookeys.1189.111825.suppl1

Supplementary material 2

Bayesian 18S rDNA phylogeny of the family Leptosomatidae, using the SYM+I+G model of nucleotide substitution

Authors: Julia K. Zograf, Alexander A. Semenchenko, Vladimir V. Mordukhovich

Data type: pdf

Explanation note: *Enoplus taipingensis* (Enoplidae) and *Phanoderma* sp. (Phanodermatidae) were used as outgroups to root the tree. Bayesian posterior probabilities (PP) are given above tree nodes and bootstrap support values found in the ML analysis are shown below nodes.

Link: https://doi.org/10.3897/zookeys.1189.111825.suppl2

Supplementary material 3

Bayesian 28S rDNA phylogeny of the family Leptosomatidae, using the SYM+I+G model of nucleotide substitution

Authors: Julia K. Zograf, Alexander A. Semenchenko, Vladimir V. Mordukhovich

Data type: pdf

Explanation note: *Enoplus* sp. (Enoplidae) and *Phanoderma* sp. (Phanodermatidae) were used as outgroups to root the tree. Specimens obtained in this study are indicated in bold.

Link: https://doi.org/10.3897/zookeys.1189.111825.suppl3

ZooKeys 1189: 257–273 (2024)
DOI: 10.3897/zookeys.1189.112784

Research Article

A new species of the genus *Achalinus* (Squamata, Xenodermatidae) from southwest Hunan Province, China

Hui Li[1], Le-Qiang Zhu[1], Bei Xiao[1], Jie Huang[2], Shao-Wu Wu[3], Li-Xun Yang[3], Zhi-Qiang Zhang[4], Xiao-Yang Mo[1]

1 *Vertebrate Zoology Laboratory, College of Life Science, Hunan Normal University, Changsha 410081, China*
2 *College of Biology Resources and Environmental Sciences, Jishou University, Jishou 416000, China*
3 *Forestry Bureau of Tongdao Dong Autonomous County, Huaihua 418500, China*
4 *Institute of Wildlife Conservation, Central South University of Forestry and Technology, Changsha 410004, China*
Corresponding authors: Zhi-Qiang Zhang (csfuzzq@126.com); Xiao-Yang Mo (moxiaoyang@hunnu.edu.cn)

Abstract

A new species of xenodermid snake, *Achalinus nanshanensis* H. Li, L.-Q. Zhu, Z.-Q. Zhang & X.-Y. Mo, **sp. nov.**, is described based on three specimens collected from Nanshan National Park and Tongdao County of southwest Hunan Province. This new species is genetically distinct amongst its congeners with the mitochondrial COI uncorrected *p*-distance ranging from 4.4% (in *A. yangdatongi*) to 17.7% (in *A. meiguensis*). In addition, this new species can be distinguished from its congeners by a combination of the following morphological characters: (1) dorsal scales with 23 or 25 rows throughout and strongly keeled; (2) tail relatively longer so that TaL/ToL = 0.215–0.248; (3) length of suture between internasals significantly longer than that between prefrontals, LSBI/LSBP = 1.66–1.84; (4) single loreal scale present; (5) SPL 6 in number, with the fourth and fifth contacting eye; (6) IFL 6 in number, with the first three touching the first pair of chin shields; (7) TMP is 2-2-4/2-2(3)-4, with the anterior pair elongated and in contact with the eye; (8) ventrals 2 + 147–158; (9) subcaudals 64–77, unpaired; (10) dorsal body brownish black, with a bright yellow neck collar extending to the head and abdomen in the occipital region. The recognition of the new species increases the number of described *Achalinus* species to 28, of which 21 are found in China.

Key words: *Achalinus nanshanensis* sp. nov., molecular analyses, morphology, taxonomy

Academic editor: Robert Jadin
Received: 15 September 2023
Accepted: 25 December 2023
Published: 17 January 2024

ZooBank: https://zoobank.org/102C8154-87DF-4B55-8994-F625B8F3E46A

Citation: Li H, Zhu L-Q, Xiao B, Huang J, Wu S-W, Yang L-X, Zhang Z-Q, Mo X-Y (2024) A new species of the genus *Achalinus* (Squamata, Xenodermatidae) from southwest Hunan Province, China. ZooKeys 1189: 257–273. https://doi.org/10.3897/zookeys.1189.112784

Introduction

Xenodermidae is composed of six known genera (*Xenodermus* Reinhardt, 1836, *Achalinus* Peters, 1869, *Stoliczkia* Jerdon, 1870, *Fimbrios* Smith, 1921, *Parafimbrios* Teynié, David, Lottier, Le, Vidal & Nguyen, 2015, and *Paraxenodermus* Deepak, Lalronunga, Lalhmingliani, Das, Narayanan, Das & Gower, 2021). The genus *Achalinus* is the most diverse genus of the family Xenodermidae (Uetz et al. 2022). It contains 27 recognized species and is widely distributed in eastern and southeastern Asia, where it ranges from northern Vietnam to southwestern China and partly into Japan. In the past five years, 18 species have been described in this genus (Wang et al. 2019; Ziegler et al. 2019; Li et al. 2020, 2021; Luu et al. 2020; Miller et al. 2020; Hou et al. 2021; Huang et al. 2021; Ha et al. 2022; Yang et al. 2022, 2023; Zhang et al. 2023; Ma et al. 2023a, 2023b). However, because of unresolved taxonomic problems and the poorly known distribution patterns of many species, the diversity of this genus remains underestimated.

During recent herpetological surveys in southwest Hunan, China, three *Achalinus* snake specimens were collected in Tongdao County and Nanshan National Park. The specimens exhibit the morphological characteristics of the genus *Achalinus*, which include a small, elongated, cylindrical body; strongly keeled, lanceolate scales with a metallic luster; and the lack of preocular and postocular scales, featuring a single loreal scale and temporals that are in direct contact with the eyes (Peters, 1869; Zhao et al. 1998; Zhao, 2006), but they could not be assigned to any known species. Extensive morphological examinations and further molecular analyses revealed that these specimens represent a separately evolving lineage within the genus *Achalinus* and can be distinguished from recognized congeners. We herein describe this overlooked *Achalinus* population as a new species, based on an iterative taxonomic approach.

Materials and methods

Sampling

Three odd-scaled snake specimens were collected in Hunan Province, China: two specimens (HNNU230902, HNNU230903) were collected in Nanshan National Park, and one specimen (HNNU230901) was collected in Tongdao County (Fig. 1). The three specimens were collected in the field, fixed in 75% ethanol, and deposited in the Vertebrate Zoology Laboratory, College of Life Science, Hunan Normal University. For molecular analyses, 33 sequences were used, among which 30 (sequences 4–33 in Table 1) were obtained from GenBank which include 27 sequences of 23 *Achalinus* species. Additionally, sequences of *Fimbrios klossi*, Smith, 1921, *Parafimbrios lao*, Teynié, David, Lottier, Le, Vidal & Nguyen, 2015 and *Xenodermus javanicus*, Reinhardt, 1836 were used as outgroups. Details are shown in Table 1.

Morphological examination

Morphological descriptions follow Zhao (2006). Abbreviations in this study are as follows: snout–vent length (**SVL**, length from tip of snout to anterior margin of the cloaca); tail length (**TaL**, length from posterior margin of cloaca to tip of tail); total length (**ToL**, length from snout tip to tail end; head length (**HL**, length from the tip of snout to the posterior margin of mandible; head width (**HW**, width from the widest part of the head in dorsal view); eye diameter (**ED**, diameter from the most anterior corner of the eye to the most posterior corner); loreal height (**LorH**, height from the highest part to the lowest part of the loreal in lateral view); loreal length (**LorL**, length from the most anterior loreal to the most posterior loreal in lateral view); length of the suture between internasals (**LSBI**); length of the suture between prefrontals (**LSBP**). Three characters were measured with a ruler to the nearest 1 mm: **SVL**, **TaL**, and **ToL**; other measurements were measured used digital calipers to the nearest 0.1 mm.

Table 1. Localities, voucher information, COI GenBank accession numbers, and references for all samples used in this study.

No.	Species	Voucher	Locality	GenBank	References
1	*A. nanshanensis* sp. nov.	HNNU230901	Tongao, Huaihua, Hunan, China	OR523368	This study
2	*A. nanshanensis* sp. nov.	HNNU230902	Nanshan National Park, Hunan, China	OR523369	This study
3	*A. nanshanensis* sp. nov.	HNNU230903	Nanshan National Park, Hunan, China	OR523370	This study
4	*A. ater*	SYSr00852	Huaping Nature Reserve, Guangxi, China	MN380334	Wang et al. 2019
5	*A. dabieshanensis*	AHU2018EE0710	Fuziling Provincial Reserve, Anhui, China	MW316598	Zhang et al. 2023
6	*A. damingensis*	ANU20220009	Shanglin, Nanning, Guangxi, China	OP644487	Ynang et al. 2023
7	*A. dehuaensis*	YBU13013	Dehua, Fujian, China	MZ442642	Li et al. 2021
8	*A. emilyae*	IEBR4465	HoanhBo, Quang Ninh, Vietnam	MK330857	Ziegler et al. 2019
9	*A. formosanus*	RN2002	Taiwan, China	KU529452	Unpublished
10	*A. huangjietangi*	HSR18030	Huangshan, Anhui, China	MT380191	Huang et al. 2021
11	*A. hunanensis*	CIB119039	Huaihua, Hunan, China	OQ848425	Ma et al. 2023
12	*A. hunanensis*	CIB119040	Ningxiang, Hunan, China	OQ848426	Ma et al. 2023
13	*A. juliani*	IEBRA.2018.8	HaLang, Cao Bang, Vietnam	MK330854	Ziegler et al. 2019
14	*A. meiguensis*	GP835	Mianyang, Sichuan, China	MZ442641	Li et al. 2021
15	*A. niger*	RN0667	Taiwan, China	KU529433	Unpublished
16	*A. ningshanensis*	ANU20220006	Ningshan, Shaanxi, China	ON548422	Yang et al. 2022
17	*A. ningshanensis*	ANU20220007	Ningshan, Shaanxi, China	ON548423	Yang et al. 2022
18	*A. panzhihuaensis*	KIZ040189	Yanbian, Sichuan, China	MW664862	Hou et al. 2021
19	*A. pingbianensis*	YBU18273	Honghe, Yunnan, China	MT365521	Li et al. 2020
20	*A. quangi*	sp4	northern Vietnam	OQ197471	Anh et al. 2023
21	*A. rufescens*	SYSr001866	Hongkong, China	MN380339	Wang et al. 2019
22	*A. spinalis*	SYSr001327	Badagong Mountains, Hunan, China	MN380340	Wang et al. 2019
23	*A. timi*	IEBRA.2018.10	ThuanChau, Son La, Vietnam	MK330856	Ziegler et al. 2019
24	*A. tranganensis*	VNUFR.2018.21	NinhBinh, Vietnam	MW023086	Luu et al. 2020
25	*A. vanhoensis*	VNUFR.2019.13	VanHo, Son La, Vietnam	ON677935	Ha et al. 2022
26	*A. yangdatongi*	KIZ034327	Wenshan Nature Reserve, Yunnan, China	MW664865	Hou et al. 2021
27	*A. yangdatongi*	YPX51447	Xichou county, Yunnan, China	MW664864	Xu et al, 2023
28	*A. yangdatongi*	YPX51446	Xichou county, Yunnan, China	MW664863	Xu et al, 2023
29	*A. yunkaiensis*	SYSr001443	Dawuling Forestry Station, Guangdong, China	MN380329	Wang et al. 2019
30	*A. zugorum*	IEBR4698	Bac Me, Ha Giang, Vietnam	MT502775	Miller et al. 2020
31	*Fimbrios klossi*	IEBR3275	Quang Ngai, Vietnam	KP410744	Teynié et al. 2015
32	*Parafimbrios lao*	MNHN2013.1002	Louangphabang, Laos	KP410746	Teynié et al. 2015
33	*Xenodermus javanicus*	–	Sumatera Barat, Indonesia	KP410747	Teynié et al. 2015

The scale features and their abbreviations are as follows: loreals (**Lor**); supralabials (**SPL**); infralabials (**IFL**); number of chin shield pairs (**Chins**); infralabials touching the first pair of chin shields (**IFL-1st Chin**); postoculars (**PtO**); temporals (**TMP**); supraoculars (**SPO**); temporals (**TEM**), number of anterior temporals that touch the eye (**aTEM-Eye**) (head bilateral scale counts are given as left/right), pre-ventral scales (**PrV**), ventral scales (**VEN**), subcaudal (**SC**), entire or divided state of the anal scales (**Anal**), dorsal scale rows (**DSR**) (counted at one-head-length behind the head, at midbody, and at one-head-length before the anal); the number of maxillary teeth (**MT**). We also make comparisons with other species of the genus *Achalinus* based on available literature (Peters 1869; Boulenger 1888, 1908; Van 1912; Pope 1935; Bourret 1937; Hu and Zhao 1966; Hu et al. 1975; Zong and Ma 1983; Ota and Toyama

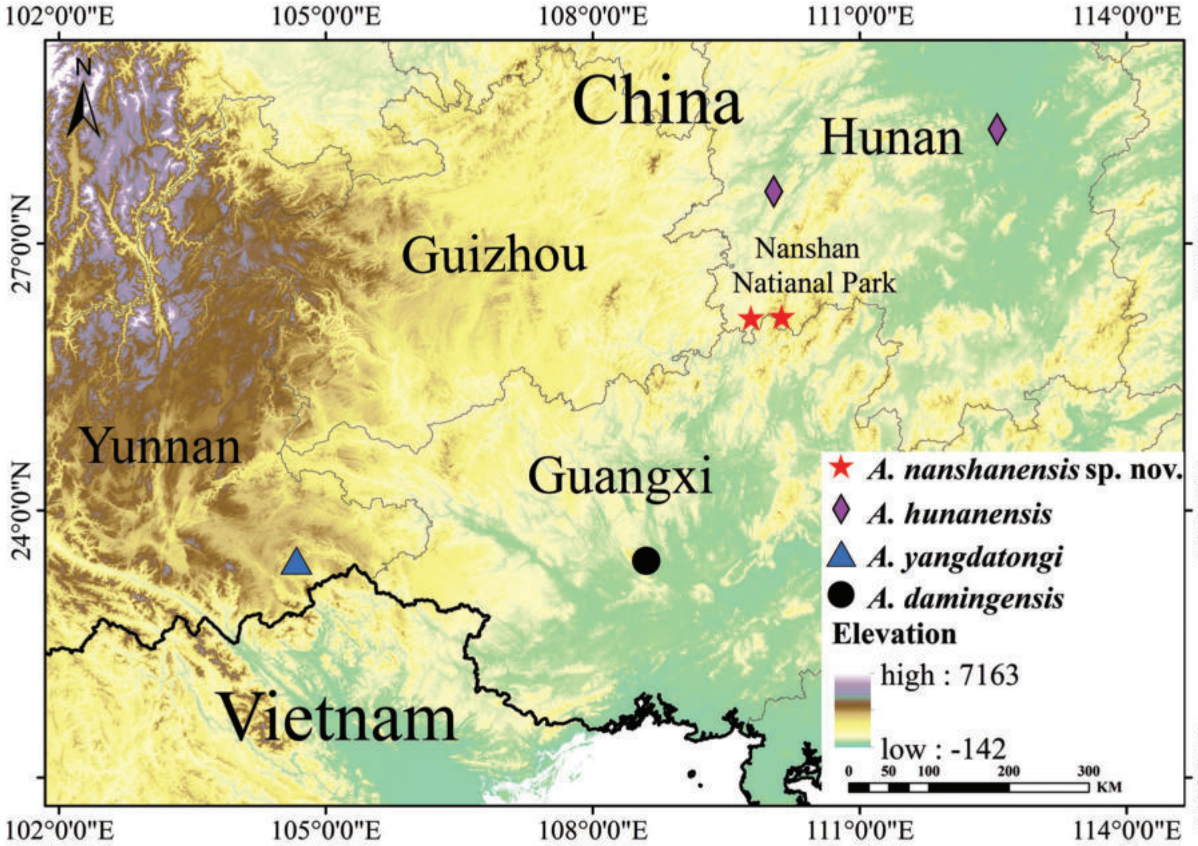

Figure 1. Distribution of some species of the genus *Achalinus*, Red star: the type locality of *A. nanshanensis* sp. nov. (HNNU230902, HNNU230903): Nanshan Nation Park, Shaoyang City, Hunan Province, China; *A. nanshanensis* sp. nov. (HNNU230901): Tongdao County, Huaihua City, Hunan Province, China. Blue triangle: the type locality of *A. yangdatongi* in Xichou County, Yunnan Province; Black circle: the type locality of *A. damingensis* in Shanglin County, Guangxi Province. Purple diamond: the type locality of *A. hunanensis* in Hecheng District and Ningxiang County, Hunan Province.

1989; Zhao et al. 1998; Zhao 2006; Wang et al. 2019; Ziegler et al. 2019; Li et al. 2020; Luu et al. 2020; Miller et al. 2020; Hou et al. 2021; Huang et al. 2021; Ha et al. 2022; Yang et al. 2022, 2023; Ma et al. 2023a, 2023b; Xu et al. 2023; Zhang et al. 2023). The sex was determined by the presence/absence of everted hemipenes.

Phylogenetic analyses

Genomic DNA was extracted from preserved liver tissue using the TIANamp Genomic DNA Kit. The fragment of the mitochondrial DNA gene encoding cytochrome c oxidase subunit I (COI) was amplified using the primer pairs Chfm4 and Chrm4 (Che et al. 2012). The polymerase chain reaction (PCR) was performed in 20 μL of reactant with the following cycling conditions: 95 °C for 4 min, 35 cycles of denaturing at 94 °C for 40 s, annealing at 53 °C for 40 s, and extending at 72 °C for 1 min, and a final extending step of 72 °C for 10 min. The PCR products were sequenced at Shanghai Map Biotech Co., Ltd.

The COI sequences (629 bp) were assembled using SeqMan in the DNASTAR software package (Burland 2000), and compared and aligned using MEGA 7 software (Kumar et al. 2018). The uncorrected pairwise distances (*p*-distance) were calculated in MEGA 7. MrBayes 3.2.4 (Ronquist et al. 2012) was used to conduct the Bayesian inference analysis under the best-fitting model GTR + I + G4, which was selected by ModelFinder identified via AICc (Darriba et al. 2012). A maximum-likelihood analysis (Nguyen et al. 2015) was executed using IQ-TREE 2 under the best-fit model TIM3 + F + I + G4 selected by Modelfinder according to AICc.

Results

Molecular analyses

The maximum-likelihood (ML) and Bayesian-inference (BI) analyses resulted in essentially identical topologies, which are integrated in Fig. 2 with the distances given in Table 2. The new species is nested within the genus *Achalinus*, and its affinity to *A. yangdatongi*, *A. damingensis*, *A. ningshanensis*, and *A. hunanensis* considerably strong supported (BI, PP = 0.85; ML, BS = 93%). In addition, the *p*-distance among all species within the genus ranges from 4.4–17.7% (Table 2), the minimum genetic distance between the new species and its congers is greater than the lowest one (3.2–3.4% between *A. ningshanensis* and *A. hunanensis*). Given that the *Achalinus* populations from Tongdao County and Nanshan National Park possess significant morphological differences from all known congeners, we describe it as a new species below.

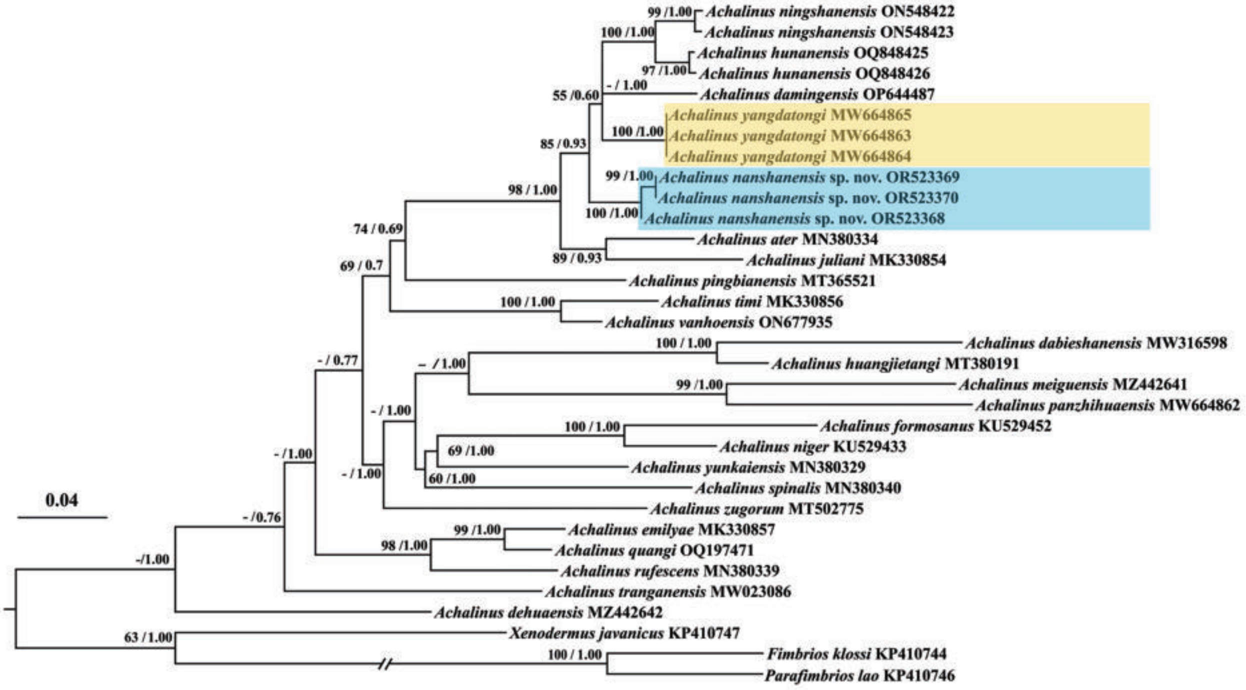

Figure 2. Phylogenetic tree of the genus *Achalinus* inferred from CO1 gene fragments (629 bp) by maximum-likelihood analysis. The numbers above the branches represent the supporting values: SH-like approximate likelihood ratio test and Bayesian posterior probabilities (the ones lower than 50 are displayed as "-"). *Achalinus nanshanensis* sp. nov. is highlighted in blue and *A. yangdatongi* in yellow.

Table 2. Uncorrected *p*-distances (%) among *Achalinus* species inferred from mitochndrial COI gene.

	1–3	4	5	6	7	8	9	10	11–12	13	14	15	16–17	18	19	20	21	22	23	24	25	26–28	29
1–3 *A. nanshanensis* sp. nov.	0–0.5																						
4 *A. ater*	6.7–6.9																						
5 *A. dabieshanensis*	16.0	14.7																					
6 *A. damingensis*	5.3–5.8	8.2	15.8																				
7 *A. dehuaensis*	14.3–14.6	16.5	18.4	16.0																			
8 *A. emilyae*	12.8–13.0	11.7	17.7	13.0	15.5																		
9 *A. formosanus*	14.4–14.9	14.1	19.0	14.9	15.9	13.9																	
10 *A. huangjietangi*	16.6	15.0	8.9	16.3	16.5	14.5	15.6																
11–12 *A. hunanensis*	4.7–5.6	7.1–7.3	16.9–17.1	6.1–6.3	14.9–15.3	13.0–13.2	13.7–14.0	16.8	0.5														
13 *A. juliani*	7.7–7.9	7.1	15.8	8.5	14.9	12.3	12.5	14.6	8.7–8.8														
14 *A. meiguensis*	17.7	15.4	17.7	16.8	18.1	15.4	15.6	15.2	16.4	16.8													
15 *A. niger*	12.8–13.3	13.5	15.8	14.3	15.9	12.2	9.1	13.9	13.2–13.3	12.3	13.9												
16–17 *A. ningshanensis*	5.1–5.6	7.6–7.7	17.1–17.2	7.2–7.8	16.3–16.5	13.5–14.1	14.8–15.1	17.2	**3.2–3.4**	9.1–9.6	17.0	14.6	0.7										
18 *A. panzhihuaensis*	15.1–15.5	16.2	16.6	15.5	15.3	16.6	16.0	15.2	16.2	15.5	11.6	14.4	17.1–17.4										
19 *A. pingbianensis*	11.6–11.8	11.8	15.3	11.3	14.9	12.9	14.6	13.0	11.1	12.1	16.8	11.8	11.7–12.4	14.9									
20 *A. quangi*	12.8–13.1	11.7	18.1	13.1	15.4	**3.5**	13.9	15.0	13.2	12.7	15.2	13.4	12.8–13.4	16.9	13.9								
21 *A. rufescens*	11.9–12.0	12.7	16.9	13.8	14.3	8.0	14.1	14.3	12.1	12.3	17.3	12.3	12.3–12.7	16.0	12.9	7.9							
22 *A. spinalis*	13.9–14.1	15.2	16.6	15.1	14.3	13.9	13.9	13.4	13.9	13.9	16.0	15.6	15.1–15.6	15.8	13.3	13.9	13.0						
23 *A. timi*	13.6–13.8	13.3	16.4	13.5	16.0	13.1	13.8	14.8	12.0	14.1	15.8	13.6	13.6	15.5	12.3	13.6	13.9	14.3					
24 *A. tranganensis*	13.0–13.1	12.7	15.3	13.9	13.9	11.5	16.8	13.4	14.0	13.3	16.4	15.2	14.3–15.2	16.4	13.3	12.2	11.5	14.6	13.8				
25 *A. vanhoensis*	12.4–12.8	13.1	15.5	12.6	16.0	12.2	14.0	14.6	11.5	13.6	15.6	12.1	12.1–12.4	15.5	10.8	12.4	13.8	12.9	5.2	13.3			
26–28 *A. yangdatongi*	**4.4**	6.2	16.6	5.6	14.0	12.8	14.4	14.6	5.1	7.3	17.1	5.9	5.8–5.9	15.5	11.3	12.6	11.5	14.2	13.1	12.8	11.3		
29 *A. yunkaiensis*	12.5–12.8	12.8	14.9	12.5	14.7	13.1	12.3	12.5	12.0	12.5	15.8	13.7	13.0–13.7	15.7	11.6	13.6	13.3	12.0	14.1	13.5	13.6	12.0	
30 *A. zugorum*	12.8–13.0	13.1	15.3	12.8	14.3	12.3	13.1	14.3	11.8	13.1	15.0	12.8	12.8	15.3	11.0	12.7	13.5	13.3	13.6	11.9	11.9	12.2	10.9

Taxonomic account

Achalinus nanshanensis H. Li, L.-Q. Zhu, Z.-Q. Zhang & X.-Y. Mo, sp. nov.

https://zoobank.org/353AD101-0B8D-4C85-88FE-0E0C63120051
Fig. 3, Table 3

Type materials. ***Holotype:*** China • adult ♂; Hunan Province, Shaoyang City, Chengbu County, Nanshan National Park; 26°11'46.34"N, 110°07'56.38"E, alt. 1665 m; 1 Sept. 2023; Hui Li & Leqiang Zhu leg.; HNNU230903. ***Paratypes:*** China • 1 adult ♂; Hunan Province, Huaihua City, Tongdao County; 25°54'42.37"N, 109°44'31.39"E; alt. 300 m; 14 Oct. 2022; Shaowu Wu & Lixun Yang leg.; HNNU230901 • 1 adult ♂; same locality and date as holotype; HNNU230902.

Etymology. The new species is named for on its type locality. We suggest the Chinese common name 南山脊蛇 (pin yin: Nán Shān Jĭ Shé) and the English common name Nanshan odd-scaled snake.

Diagnosis. The new species can be distinguished from other members of *Achalinus* by the following characteristics: (1) dorsal scales with 23 or 25 rows throughout and strongly keeled; (2) tail relatively longer so that TaL/ToL = 0.215–0.248; (3) length of suture between internasals significantly longer than that between prefrontals, LSBI/LSBP = 1.66–1.84; (4) single loreal scale present; (5) SPL 6 in number, with the fourth and fifth contacting eye; (6) IFL 6 in number, with the first three touching the first pair of chin shields; (7) TMP is

Table 3. Main morphological characters of *Achalinus nanshanensis* sp. nov.

	Voucher		
	HNNU230903	**HNNU230901**	**HNNU230902**
	Holotype	**Paratype**	**Paratype**
Sex	Adult male	Adult male	Adult male
SVL	362	302	300
TaL	99	99	99
TL	461	401	399
TaL/TL	0.215	0.247	0.248
HL	10.95	10.07	10.18
HW	7.25	5.96	6.37
ED	1.11	1.10	1.09
SPL	6/6	6/6	6/6
SPL-Eye	4th–5th	4th–5th	4th–5th
IFL	6	6	6
Chin	2	2	2
IFL-1stChin	1st–3rd	1st–3rd	1st–3rd
SPO	1	1	1
LorH	0.83	0.77	0.72
LorL	1.86	1.45	1.46
LorH / LorL	0.47	0.53	0.49
LSBI	1.78	1.52	1.49
LSBP	1.07	0.86	0.81
LSBI / LSBP	1.66	1.76	1.84
TEM	2+2+4	2+2+4	2+2(rarely 3)+4
aTEM-Eye	2	2	2
DSR	23-23-23	23-23-23	25-25-25
VEN	155	158	147
SC	64	77	72
Anal	1	1	1

Figure 3. General view of *Achalinus nanshanensis* sp. nov. (HNNU230902) in life. Photo by Le-Qiang Zhu.

2-2-4/2-2(3)-4, with the anterior pair elongated and in contact with the eye; (8) ventrals 2 + 147–158; (9) subcaudals 64–77, unpaired; (10) dorsal body brownish black with a bright-yellow neck collar extending to the head and abdomen in the occipital region.

Description of holotype. Adult male with a total length of 461 mm (SVL 362 mm and TaL 99 mm), tail relatively long, TaL/ToL 0.215, body slender and cylindrical. Head distinct from neck, rostral small, triangular, only upper tip visible from above. Head length 10.95 mm, head width 7.25 mm. Length of suture between internasals much longer than that between prefrontals (LSBI 1.78 mm, LSBP 1.07 mm, LSBI/LSBP 1.66). Frontal pentagonal pointed backwards, much shorter than parietals; each parietal bordered with an elongated nuchal, with no preoculars and postoculars. Nostril at anterior part of nasal scale, posterior margin of nostril with a distinct nostril cleft. A single loreal scale present, extending from nasal scale to eye, distinctly wider than high. Eyes small, ED 1.11 mm. Two aTMP and four pTMP present; aTMPs elongated, upper one much smaller than the lower one; upper one in contact with eye, lower one also in contact with parietal scale. SPL 6 in number, the fourth and fifth in contact with the eye, the sixth longest. Two pairs of shields present, the first three in contact with first chin shield. One mental scale present, the first IFL in contact with each other after the mental scale, followed by another 5 IFL in contact with each other. Dorsal scales 23-23-23, strongly keeled; dorsum with no longitudinal vertebral stripe. VEN 155 in number. SC 64 in number, uniserial, anal entire.

Coloration of holotype in life. Scales possess a subtle iridescent quality. The dorsum's distinguishing characteristic is its reflective, brownish-black appearance,

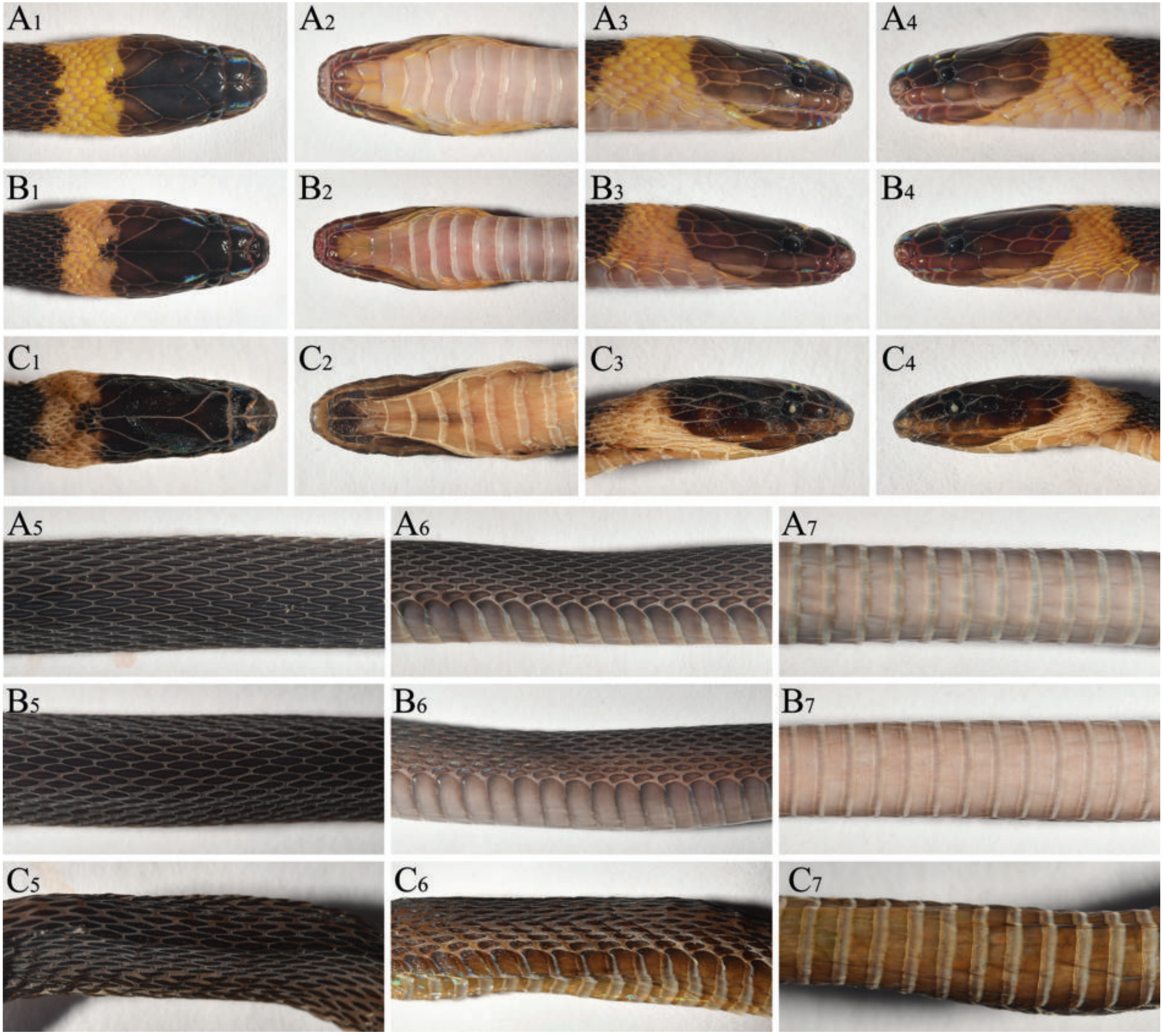

Figure 4. The view of *Achalinus nanshanensis* sp. nov. **A** HNNU230903 (holotype) **B** HNNU230902 (paratype) **C** HNNU230901 (paratype), remaining photos by Le-Qiang Zhu.

with a notable bright-yellow patch that extends to the head and abdomen in the occipital region. The first pair of chin shields displays black coloration at the front, while the second pair is entirely white. The eyes are uniformly black. The ventral side is prevalently grayish white, with the edges of the ventral scales gradually transitioning from grayish white to black. The ventral coloration of the tail mirrors that of the dorsum, featuring a brownish-black hue.

Coloration in preservative. (Figs 4, 5) All scales retain a subtle iridescence. The coloration darkens as it transitions from the dorsum to the venter, with the dorsal surface of the body primarily appearing brownish black. Notably, the collar of the neck is a paler grayish white.

Distribution and habits. (Fig. 6) *Achalinus nanshanensis* sp. nov. is currently known from Hunan Province, China, and specifically from Nashan National Park, Shaoyang City, and Tongdao County in Huaihua City. It has a known elevational range of 300–1665 m above sea level. All three specimens were found during the night, with the holotype and one paratype found near a mountain

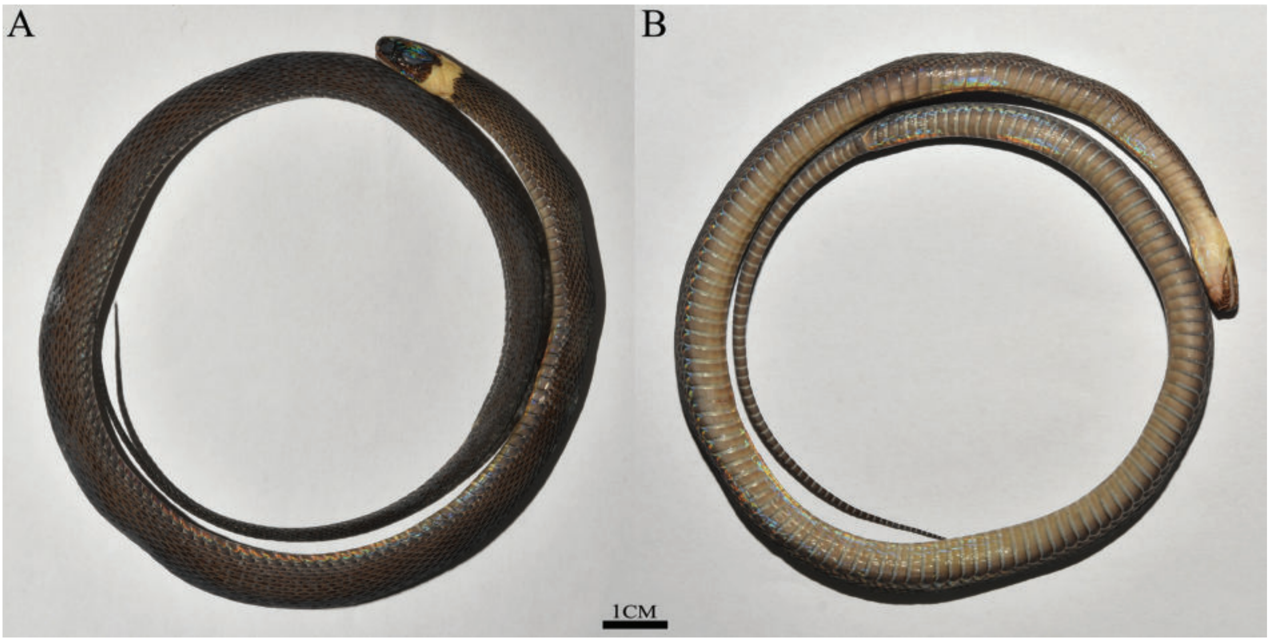

Figure 5. Holotype of *Achalinus nanshanensis* sp. nov. (HNNU230903) in preservative **A** dorsal view **B** ventral view. Photos by Hui Li.

Figure 6. Habitat of *Achalinus nanshanensis* sp. nov. (HNNU230902, HNNU230903), Nanshan National Park, Chengbu County, Shaoyang City, Hunan Province, China. Photo by Le-Qiang Zhu.

stream where the air temperature was 18 °C and the relative humidity was 80%. These individuals were close to shrubs in a subtropical broadleaved evergreen forest. They were found making their way from leaf litter to the stream. The other specimen was found in a bamboo forest near a steam.

Comparison. A summary of morphological characteristics is listed in Table 4. Phylogenetically, *A. nanshanensis* sp. nov. is closest to *A. yangdatongi* Hou, Wang, Guo, Chen, Yuan & Che, 2021 and *A. damingensis* Xu, Yang, Wu, Gong, Huang & Huang, 2023. However, *A. nanshanensis* sp. nov. differs from *A. yangdatongi* in having fewer ventral scales (147–158 vs 155–177), maxillary teeth (18 vs 24–26) and more temporals (2+2/3+4 vs 2+2/3+2/3), shorter loreal (0.47–0.53 vs 0.57) (Table 5). The new species differs from *A. damingensis* in having more temporals (2-2/3-4 vs 2-2-3) and fewer ventral scales (147–158 vs 165).

Table 4. A morphological comparison of male species of the genus *Achalinus*. Morphological data of examined congeners were taken from the literature. "–" & "?" = unavailable, "*" = female species (sevral species of genus *Achalinus* recorded only female samples).

Species	TaL/ToL	MT	LorH/LorL	LSBI vs. LSBP	DSR	Lor	PtO	SPL	SPL-Eye	IFL	IFL-1st Chin	TEM	aTEM-Eye	VEN	SC
A. nanshanensis sp. nov.	0.215–0.248	18	0.47–0.53	>1	(23–25)-(23–25)-(23–25)	1	0	6	4–5	6	1–3	2+2+4/2+2(3)+4	2	147–158	64–77
A. ater	0.190 ~ 0.220	–	0.40	> 1	(21–23)-(21–25)-(21–25)	1	0	6	4–5	5–6	1–3	2+2+3	2	146–164	50–66
A. dabieshanensis	0.177 ~ 0.223	–	0.73 ~ 0.81	< 1	23-23-23	1	0	6	4–5	5	1–3	2+2+4	2	141–151	46–55
A. damingensis	427	–	–	>1	23-23-23	1	0	6	4–5	6	1–3	2+2+3	2	165	74
A. dehuaensis	0.262 ~ 0.286	31–33	–	> 1	23-23-23	1	0	6	4–5	5	1–3	2+2(3)+3(4)	1–2	142–143	74–81
*A. emilyae**	0.183 ~ 0.203	27–28	–	> 1	23-23-23	1	0	6	4–5	5	1–3	2+2+3	1	157–161	56–63
A. formosanus	0.159	17	–	= 1	29(27)-27-25	0	0	6	4–5	6–7	–	2+2	1	158–184	61–83
*A. hainanus**	0.258 ~ 0.266	–	–	= 1	23-23-23	1	0	6	4–5	5	1–3	1+2+3(4)	1	165–168	67–69
A. huangjietangi	0.211 ~ 0.232	–	0.70 ~ 0.74	< 1	23-23-23	1	0	6	4–5	5–6	1–3(4)	2+2+3(4)	2	157–160	59–67
A. hunanensis	0.221 ~ 0.225	23	0.62 ~ 0.70	> 1	23-23-23	1	0	6	4–5	5–6	1–3(4)	2+2+4	2	163–165	69–72
A. jinggangensis	0.174 ~ 0.217	–	–	> 1	23-23-23	0	0	6	4–5	6	1–4	2(1)+2+3(4)	2	156–164	51–64
A. juliani	0.264 ~ 0.265	28	–	> 1	25-23-23	1	0	6	4–5	6	1–3(4)	2+2+4	2	163–169	81–91
A. meiguensis	0.142 ~ 0.238	17	–	–	(21–23)-(19–21)-(19–21)	1	1	6	4–5	6	1–3	2(3)+2(3)	1	146–173	39–60
A. niger	0.151 ~ 0.179	–	0.67	< 1	25-25-23	1	0	6	4–5	6	1–3(4)	2+2(3)	2	169–185	52–72
*A. ningshanensis**	0.121 ~ 0.161	–	0.45 ~ 0.58	= 1	23-23-23(21)	1	0	6	4–5	5	1–2(3)	2+2(3)+3(4)	1–2	159–174	41–46
A. panzhihuaensis	0.246	28	0.67	–	23-23-19	1	1	6	4–5	6	1–3	2+2+3	1	160	73
A. pingbianensis	0.243	–	–	= 1	23-23-23	0	0	7	5–6	6	1–3	2+2+3	1	164	56
A. rufescens	0.191 ~ 0.221	23	0.90	> 1	23-(23–25)-23	1	0	6	4–5	5	1–3	2(1)+2+3(4)	1–2	148–156	58–69
A. spinalis	0.150 ~ 0.250	16–20	–	< 1	(23–25)-(23–25)-(23–25)	1	0	6	4–5	5–6	1–3	2+2(3)	1–2	138–175	48–67
A. timi	0.213	27	–	> 1	25-25-23	0	0	6	4–5	6	1–3	2+2+3	1	170	72
A. tranganensis	0.254(+)	29	–	> 1	25-23-23	1	0	6	4–5	6	1–3	2+2+3	2	171	73(+)
A. vanhoensis	0.264	32	–	> 1	25-23-23	0	0	6/7	4–5/5–6	6	1–4	2+3+3	2	176	84
A. werneri	0.250 ~ 0.300	–	–	= 1	?-(21–23)-?	1	0	6	4–5	6	–	2+3(4)	–	157–191	67–98
A. yangdatongi	0.261 ~ 0.262	26	0.57	> 1	23-23-23	1	0	6	4–5	5–6	1–3	2+2+2/3	2	155-161	76-82
A. yunkaiensis	0.185 ~ 0.203	20–24	0.49 ~ 0.64	= 1	23-23-23	1	0	6	4–5	6	1–3(4)	2+2+3(4)	2	150–162	49–56
A. zugorum	0.229	28	–	> 1	25-23-23	0	0	6	4–5	7	1–3	2+2+3	2	173	70

Table 5. Comparisons of main morphological characters of *Achalinus nanshanensis* sp. nov., *A.yangdatongi*, and *Achalinus damingensis*.

	***A. nanshanensis* sp. nov.**	***A. yangdatongi***		***A. damingensis***
Sex	**Males**	**Males**	**Females**	**Males**
SVL	300–392	241–293	292–424	322
TaL	99	85–104	73–93	105
TL	399–461	–	–	427
TaL/TL	**0.215–0.248**	**0.261–0.262**	0.180–0.200	**0.25**
HL	10.07–10.95	8.5–11.60	9.52–11.45	–
HW	5.96–7.25	–	–	–
MT	**18**	**26**	**24**	–
ED	1.09–1.11	–	–	–
SPL	6/6	6/6	6/6(rarely 5/5)	6/6
SPL-Eye	4th–5th	4th–5th	4th–5th	4th–5th
IFL	6	5/6	6	6/6
Chin	2	2	2	2
IFL-1stChin	1st–3rd	1st–3rd	1st–3rd	1st–3rd
SPO	1	1	1	1
LorH / LorL	0.47–0.53	0.57	0.49	–
LSBI vs LSBP	>1	>1	>1	>1
TEM	**2+2(rarely 3)+4**	**2+2+2/3**	**2+2/3+2/3**	**2+2+3**
aTEM-Eye	2	2	2	2
DSR	23(25)-23(25)-23(25)	23-23-23	23-23-23	23-23-23
VEN	**147–158**	**155**	**170–171**	**165**
SC	64–77	76	59–64	74
Anal	1	1	1	1

The new species differs from *A. hunanensis* Ma, Shi, Xiang, Shu & Jiang, 2023 in having fewer ventral scales (147–158 vs 163–165), maxillary teeth (18 vs 23), and a bright-yellow collar around the neck.

The new species differs from *A. ningshanensis* Yang, Huang, Jiang, Burbrink, Gong, Yu, Zhang, Huang & Huang, 2022 in having more infralabials (6 vs 5), two pairs of chin shields (vs 3 pairs), LSBI significantly longer than LSBP (vs suture between internasals is similar in length when compared to the suture between prefrontals).

The new species differs from *A. ater* in having more temporals (2+2/3+4 vs 2+2+3), fewer ventral scales (147–158 vs 160–170), more SC (64–77 vs 47–70) and a bright-yellow collar around the neck.

The new species differs from *A. juliani* Ziegler, Nguyen, Pham, Nguyen, Pham, van Schingen, Nguyen & Le, 2019 in having fewer ventral scales (147–158 vs 173–179), fewer subcaudals (64–77 vs 77–91), and a bright-yellow collar around the neck.

The new species differs from *A. pingbianensis* Li, Yu, Wu, Liao, Tang, Liu & Guo, 2020 in having a separated loreal (vs loreal fused with prefrontal), more subcaudals (64–77 vs 56), LSBI significantly longer than LSBP (vs length of suture between internasals subequal to that between prefrontals), two anterior temporals in contact with the eye (vs only the upper anterior temporal in contact with the eye), fewer supralabials (6 vs 7), and a bright-yellow collar around the neck.

The new species differs from *A. timi* Ziegler, Nguyen, Pham, Nguyen, Pham, Van Schingen, Nguyen & Le, 2019 in having one loreal (vs no loreals), more infralabials (6 vs 5), temporals (2+2/3+4 vs 2+2+3), fewer ventral scales (147–158 vs 170), and fewer tooth (18 vs 27).

The new species differs from *A. vanhoensis* Ha, Ziegler, Sy, Le, Nguyen & Luu, 2022 in having fewer ventral scales (147–158 vs 176), fewer subcaudals (64–77 vs 84) and more temporals (2+2/3+4 vs 2+3+3).

The new species differs from *A. dabieshanensis* Zhang, Liu, Huang & Zhang, 2023, *A. huangjietangi* Huang, Peng & Huang, 2021, *A. niger* Maki, 1931 and *A. spinalis* Peters, 1869 by LSBI significantly longer than LSBP (vs suture between internasals). Furthermore, the new species differs from *A. dabieshanensis* in having more infralabials (6 vs 5). It differs from *A. huangjietangi* and *A. spinalis* in having more subcaudals in males (64–77 vs 59–67 and 64–77 vs 48–67, respectively). It differs from *A. niger* in having comparatively longer tail (0.215–0.248 vs 0.151–0.179).

The new species differs from *A. formosanus* Boulenger, 1908, *A. jinggangensis* Zong & Ma, 1983 and *A. zugorum* Miller, Davis, Luong, Do, Pham, Ziegler, Lee, De Queiroz, Reynolds & Nguyen, 2020 in having a separated loreal (vs no loreal). Furthermore, the new species differs from *A. formosanus* in having fewer dorsal scale rows (23–25)-(23–25)-(23–25) vs (29)27-27-25). It differs from *A. jinggangensis* in having more subcaudals (64–77 vs 51–64) and from *A.* zugorum in having fewer infralabials (6 vs7) and more temporals (2+2/3+4 vs 2+2+3).

The new species differs from *A. meiguensis* Hu & Zhao, 1966 in having more dorsal scale rows (23-23-23 vs (21–23)-(19–21)-(19–21), more subcaudals (64–77 vs 50–60), and having two pairs of chin shields (vs three pairs of chin shields).

The new species differs from *A. panzhihuaensis* Hou, Wang, Guo, Chen, Yuan & Che, 2021 in having more temporals (2+2/3+4 vs 2+3+3) and fewer ventral scales (147–158 vs 160).

The new species differs from *A. dehuaensis* Li, Wu, Xu, Zhu, Ren, Guo & Dong, 2021 in having more infralabials (6 vs 5) and fewer maxillary teeth (18 vs 31–33), and a bright-yellow collar around the neck.

The new species differs from *A. emilyae* Ziegler, Nguyen, Pham, Nguyen, Pham, van Schingen, Nguyen & Le, 2019 in having more infralabials (6 vs 5), temporals (2+2/3+4 vs 2+2+3), and a bright-yellow collar around the neck, and the new species differs from *A. emilyae* in the color of its dorsum (brownish-black vs pale yellowish brown).

The new species differs from *A. hainanus* Huang, 1975 in having more infralabials (6 vs 5), temporals (2+2/3+4 vs 1+2+3(4) and LSBI significantly longer than LSBP (vs suture between internasals similar size when compared to the suture between prefrontals).

The new species differs from *A. rufescens* Boulenger, 1888 in having more infralabials (6 vs 5) and two pairs of chin shields (vs three pairs of chin shields).

The new species differs from *A. tranganensis* Luu, Ziegler, Ha, Lo, Hoang, Ngo, Le, Tran & Nguyen, 2020 in having more temporals (2+2/3+4 vs 2+2+3) and fewer ventral scales (147–158 vs 171).

The new species differs from *A. werneri* Van Denburgh, 1912 in having a shorter tail (0.215–0.248 vs 0.250–0.300), fewer ventrals (147–158 vs 157–191) and LSBI significantly longer than LSBP (vs suture between internasals similar size when compared to the suture between prefrontals).

The new species differs from *A. yunkaiensis* Wang, Li & Wang, 2019 in having a comparatively longer tail in males (0.215–0.248 vs 0.185–0.203), more subcaudals (64–77 vs 49–56) and LSBI significantly longer than LSBP (vs suture between internasals similar size when compared to the suture between prefrontals).

Discussion

With the discovery of *Achalinus nanshanensis* sp. nov., the number of *Achalinus* species now stands at 28, with 21 occurring in China: *A. ater* (Bourret, 1937), *A. dabieshanensis* (Zhang et al., 2023), *A. damingensis* (Yang et al., 2023), *A. dehuaensis* (Hou et al., 2021), *A. emilyae* (Ziegler et al., 2019), *A. formosanus* (Boulenger, 1908), *A. hainanus* (Huang, 1975), *A. huangjietangi* (Huang et al., 2021), *A. hunanensis* (Ma et al., 2023), *A. jinggangensis* (Zong & Ma, 1983), *A. meiguensis* (Hu & Zhao, 1966), *A. niger* (Maki, 1931), *A. ningshanensis* (Yang et al., 2022), *A. panzhihuaensis* (Hou et al., 2021), *A. pingbianensis* (Li et al., 2020), *A. rufescens* (Boulenger, 1888), *A. sheni* (Ma et al., 2023) *A. spinalis* (Peters, 1869), *A. nanshanensis* sp. nov. (this study), *A. yangdatongi* (Hou et al., 2021), and *A. yunkaiensis* (Wang et al., 2019). The genus *Achalinus* is known for its remarkable cryptic diversity, which has attracted extensive research. Nevertheless, some fundamental questions remain unanswered. Notably, a molecular comparison between populations of *A. ater* in Guangxi, China, and at its type locality at Tam Dao in northern Vietnam. Similarly, limited research has been made comparing *A. spinalis* found in China and at the type locality. This situation prompts us to reconsider the distribution of *A. ater* and *A. spinalis* in China.

Recent research has continued to underscore the remarkably high diversity within the genus *Achalinus*, which has lead to the discovery of an increasing number of species. However, several factors contribute to the difficulty in accurately identifying snakes of this genus based solely on morphology. *Achalinus* species display a conservative morphology; sexual dimorphism has been identified (particularly larger TaL/TL in males, more VEN in females, and more SC in males) (Ziegler et al. 2019; Hou et al. 2021; Huang et al. 2021; Li et al. 2021; Zhang et al. 2023); additionally, the possible existence of juvenile dimorphism has been suggested (Zhang et al. 2023). Furthermore, due to their secretive life history and morphological similarities, many cryptic species may well be hidden in plain sight within known widely distributed species (Ziegler et al. 2019; Li et al. 2020; Luu et al. 2020; Miller et al. 2020; Hou et al. 2021; Yang et al. 2022; Ma et al. 2023a; Yang et al. 2023). This poses a considerable challenge to future efforts aimed at comparing and identifying new species.

Molecular methods have played a pivotal role in the rapid discovery of *Achalinus* species (Yang et al. 2023). In addition, there are *A. yunkaiensis* and *A. sheni* distributed in the same region of *A. nanshanensis* sp. nov., which indicates that further study is necessary to conduct by using different geographic populations and molecular methods to revise their evolutionary history.

Acknowledgements

We thank Sheng-Chao Shi and Shun Ma (Chengdu Institute of Biology, Chinese Academy of Sciences) for their help in formal analysis.

Additional information

Conflict of interest

The authors have declared that no competing interests exist.

Ethical statement

No ethical statement was reported.

Funding

County biodiversity resources survey project in Miao Autonomous County of Chengbu, Hunan Province (no. 2021-326-430529); County Biodiversity Resources Survey Project in Dong Autonomous County of Tongdao, Hunan Province (no. 2021-326-430529); Central Financial Subsidy Project of Jintongshan National Nature Reserve in Hunan Province in 2022 (no. 2022-34).

Author contributions

Hui Li: methodology, formal analysis, validation, writing-original draft, writing-review and editing; Le-Qiang Zhu: methodology, investigation, formal analysis; Bei Xiao: methodology, formal analysis; Jie Huang: methodology, formal analysis; Shao-Wu Wu: methodology, investigation; Li-Xun Yang: methodology, investigation; Zhi-Qiang Zhang: conceptualization, data curation, project administration, resources, supervision, writing-review and editing; Xiao-Yang Mo: conceptualization, data curation, project administration, resources, supervision, writing-review and editing.

Author ORCIDs

Hui Li https://orcid.org/0009-0009-6318-3223
Le-Qiang Zhu https://orcid.org/0009-0006-3820-529X
Bei Xiao https://orcid.org/0009-0006-0740-5360
Jie Huang https://orcid.org/0009-0005-2565-3109
Shao-Wu Wu https://orcid.org/0009-0001-1769-2088
Li-Xun Yang https://orcid.org/0009-0008-3664-5333
Zhi-Qiang Zhang https://orcid.org/0009-0004-8658-9625
Xiao-Yang Mo https://orcid.org/0009-0003-2352-8975

Data availability

All of the data that support the findings of this study are available in the main text.

References

Boulenger GA (1888) Description of two new snakes from Hongkong, and note on the dentition of *Hydrophis viperina*. Annals & Magazine of Natural History 7(2): 43–44. https://doi.org/10.1080/00222938809460874

Boulenger GA (1908) Description of a new frog and a new snake from Formosa. Annals & Magazine of Natural History 2(8): 221–222. https://doi.org/10.1080/00222930808692472

Bourret RL (1937) Notes herpétologiques sur l'Indochine française. XV. Lézards et serpents reçus au Laboratoire des Sciences Naturelles de l'Université au cours de l'année 1937. Descriptions de deux espèces et de deux variétés nouvelles. Bulletin général de l'Instruction Publique, Hanoi, 17e Année (1937–1938), (4 Décembre 1937), Annexe: 57–80.

Burland TG (2000) DNASTAR's Lasergene sequence analysis software. Methods in Molecular Biology (Clifton, N.J.) 132: 71–91. https://doi.org/10.1385/1-59259-192-2:71

Che J, Chen HM, Yang JX, Jin JQ, Jiang K, Yuan ZY, Murphy RW, Zhang YP (2012) Universal COI primers for DNA barcoding amphibians. Molecular Ecology Resources 12(2): 247–258. https://doi.org/10.1111/j.1755-0998.2011.03090.x

Darriba D, Taboada GL, Doallo R, Posada D (2012) jModelTest 2: More models, new heuristics and parallel computing. Nature Methods 9(8): 772. https://doi.org/10.1038/nmeth.2109

Ha NV, Ziegler T, Sy TD, Le MD, Nguyen TQ, Luu VQ (2022) A new species of the genus *Achalinus* (Squamata: Xenodermidae) from Son La Province, Vietnam. Zootaxa 5168(3): 375–387. https://doi.org/10.11646/zootaxa.5168.3.8

Hou SB, Wang K, Guo P, Chen JM, Yuan ZY, Che J (2021) Two new species and a new country record of the genus *Achalinus* (Reptilia: Squamata: Xenodermidae) from China. Zootaxa 4950(3): 528–546. https://doi.org/10.11646/zootaxa.4950.3.6

Hu SQ, Zhao EM (1966) Three new species of reptiles from Szechwan. Acta Zoologica Sinica 3(2): 158–164. [In Chinese with English abstract]

Hu SQ, Zhao EM, Huang ZJ (1975) Three new species of reptiles from Hainan Island, Guangdong Province. Acta Zoologica Sinica 21(4): 379–385. [In Chinese with English abstract]

Huang RY, Peng LF, Yu L, Huang TQ, Jiang K, Ding L, Chang JK, Yang DC, Xu YH, Huang S (2021) A new species of the genus *Achalinus* from Huangshan, Anhui, China (Squamata: Xenodermidae). Asian Herpetological Research 12(2): 178–187. https://doi.org/10.16373/j.cnki.ahr.200075

Kumar S, Stecher G, Li M, Knyaz C, Tamura K (2018) MEGA X: Molecular Evolutionary Genetics Analysis across computing platforms. Molecular Biology and Evolution 35(6): 1547–1549. https://doi.org/10.1093/molbev/msy096

Li K, Yu M, Wu YY, Liao LH, Tang K, Liu Q, Guo P (2020) A new species of the genus *Achalinus* (Squamata: Xenodermatidae) from southeastern Yunnan Province, China. Zootaxa 4860(1): 116–128. https://doi.org/10.11646/zootaxa.4860.1.6

Li K, Wu YY, Xu RY, Zhu F, Ren JL, Guo P, Dong BJ (2021) A new species of the *Achalinus rufescens* complex (Xenodermidae: *Achalinus*) from Fujian Province, China. Zootaxa 5026(2): 239–254. https://doi.org/10.11646/zootaxa.5026.2.5

Luu VQ, Ziegler T, Ha NV, Lo OV, Hoang TT, Ngo HT, Le MD, Tran DH, Nguyen TQ (2020) A new species of *Achalinus* (Squamata: Xenodermidae) from Trang An Landscape Complex, Ninh Binh Province, Vietnam. Zootaxa 4877(1): 174–184. https://doi.org/10.11646/zootaxa.4877.1.8

Ma S, Shi SC, Xiang SJ, Shu F, Jiang JP (2023a) A new species of *Achalinus* Peters, 1869 (Squamata, Xenodermidae) from Hunan Province, China. ZooKeys 1166: 315–331. https://doi.org/10.3897/zookeys.1166.103055

Ma S, Xu YH, Qi S, Wang YY, Tang SS, Huang S, Jiang JP (2023b) Discovery of a new cryptic *Achalinus* Peters, 1869 (Serpentes, Xenodermidae) species from Hunan Province, China. ZooKeys 1181: 9–21. https://doi.org/10.3897/zookeys.1181.109462

Miller AH, Davis HR, Luong AM, Do QH, Pham CT, Ziegler T, Lee JL, Queiroz KD, Reynolds RG, Nguyen TQ (2020) Discovery of a new species of enigmatic odd-scaled snake (Serpentes: Xenodermidae: *Achalinus*) from Ha Giang Province, Vietnam. Copeia 108(4): 796–808. https://doi.org/10.1643/CH2020060

Nguyen LT, Schmidt HA, Haeseler AV, Minh BQ (2015) IQ-TREE: A fast and effective stochastic algorithm for estimating maximum likelihood phylogenies. Molecular Biology and Evolution 32(1): 268–274. https://doi.org/10.1093/molbev/msu300

Ota H, Toyama M (1989) Taxonomic redefinition of *Achalinus* formosanus Boulenger (Xenoderminae: Colubridae: Ophidia), with description of a new subspecies. Copeia 1989(3): 597–602. https://doi.org/10.2307/1445485

Peters WCH (1869) Über neue Gattungen und neue oder weniger bekannte Arten von Amphibien (*Eremias*, *Dicrodon*, *Euprepes*, *Lygosoma*, *Typhlops*, *Eryx*, *Rhynchonyx*, *Elapomorphus*, *Achalinus*, *Coronella*, *Dromicus*, *Xenopholis*, *Anoplodipsas*, *Spilotes*, *Tropidonotus*). Monatsberichte der königlichen Akademie der Wissenschaften zu Berlin, 1869: 432–447.

Pope CH (1935) The Reptiles of China. Turtles, crocodilians, snakes, lizards. Natural History of central Asia. Vol. X. American Museum of Natural History, New York, 604 pp. https://doi.org/10.5962/bhl.title.12104

Ronquist F, Teslenko M, Van DMP, Ayres DL, Darling A, Hohna S (2012) MrBayes 3.2: Efficient Bayesian phylogenetic inference and model choice across a large model space. Systematic Biology 61(3): 539–542. https://doi.org/10.1093/sysbio/sys029

Uetz P, Freed P, Hošek J (2022) The Reptile Database. http://www.reptile-database.org [Accessed 3 September 2022]

Van DJ (1912) Concerning certain species of reptiles and amphibians from China, Japan, the Loo Choo Islands, and Formosa. Proceedings of the California Academy of Sciences 3(4): 187–258.

Wang J, Li Y, Zeng ZC, Lyu ZT, Sung YH, Li YY, Lin CY, Wang YY (2019) A new species of the genus *Achalinus* from southwestern Guangdong Province, China (Squamata: Xenodermatidae). Zootaxa 4674(4): 471–481. https://doi.org/10.11646/zootaxa.4674.4.6

Xu RY, Li K, Zhang H, He H, Zhu F, Wu YY, Guo P (2023) Expanded description of *Achalinus yangdatongi* (Serpentes: Xenodermidae). Current Herpetology 42(1): 1–8. https://doi.org/10.5358/hsj.42.1

Yang DC, Huang RY, Jiang K, Burbrink FT, Gong YA, Yu J, Zhang Y, Huang TQ, Huang S (2022) A new species of the genus *Achalinus* (Squamata: Xenodermidae) from Ningshan County, Shaanxi Province, China. Zootaxa 5190(1): 127–140. https://doi.org/10.11646/zootaxa.5190.1.5

Yang DC, Xu YH, Wu JX, Gong YA, Huang RY, Xiang J, Feng ZL, Huang TQ HUANG S (2023) A new species of the genus *Achalinus* (Squamata: Xenodermidae) from Nanning, Guangxi, China. Zootaxa 5319 (3): 389–402. https://doi.org/10.11646/zootaxa.5319.3.5

Zhang TR, Gong YA, Yang DC, Huang RY, Huang S (2023) A New Snake Record of *Achalinus huangjietangi* in Fujian Province, China. Journal of Wildlife, 1–4. [2023-08-30] [In Chinese]

Zhao EM (2006) Snakes of China. Anhui Science and Technology Publishing House, Hefei, 152–158. [In Chinese]

Zhao EM, Huang MH, Zong Y (1998) Fauna Sinica: Reptilia. Vol. 3. Squamata, Serpentes. Science Press, Beijing, 522 pp. [In Chinese]

Ziegler T, Nguyen TQ, Pham CT, Nguyen TT, Pham AV, Schingen MV, Nguyen TT, Le MD (2019) Three new species of the snake genus *Achalinus* from Vietnam (Squamata: Xenodermatidae). Zootaxa 4590(2): 249–269. https://doi.org/10.11646/zootaxa.4590.2.3

Zong Y, Ma J (1983) A new species of the genus *Achalinopsis* from Jiangxi and the restoration of this genus. Acta Herpetologica Sinica 2(2): 61–63. [In Chinese]

ZooKeys 1189: 275–286 (2024)
DOI: 10.3897/zookeys.1189.114478

Research Article

DNA Barcoding of Central European Gasteruptiidae and the rarely-collected families Evaniidae, Stephanidae, Trigonalidae, and Aulacidae (Hymenoptera, Apocrita)

Christian Schmid-Egger[1], Stefan Schmidt[2], Petr Bogusch[3]

1 Fischerstr. 1, 10317 Berlin, Germany
2 SNSB-Zoologische Staatssammlung München, Munich, Germany
3 University of Hradec Králové, Faculty of Science, Department of Biology, Hradec Králové, Czech Republic
Corresponding author: Stefan Schmidt (schmidt.s@snsb.de)

Abstract

The study presents DNA barcoding results of five families of Hymenoptera in Germany. DNA barcodes are provided for 24 of the 25 species of *Gasteruption* occurring in Central Europe, including 18 of the 19 species recorded from Germany. The genetic diversity was higher than expected, with five species exhibiting two or more Barcode Index Number (BINs), whereas BIN sharing occurred in four species. *Gasteruption foveiceps* Semenov, 1892, **stat. nov.** is removed from synonymy with *G. nigrescens* Schletterer, 1885 and treated as a distinct species.

Key words: Central Europe, COI, DNA barcoding, insects, morphology, taxonomy

Academic editor: Kees van Achterberg
Received: 26 October 2023
Accepted: 15 December 2023
Published: 17 January 2024

ZooBank: https://zoobank.org/723A1672-9C71-4BA5-9692-6DD9BA7F5E54

Citation: Schmid-Egger C, Schmidt S, Bogusch P (2024) DNA Barcoding of Central European Gasteruptiidae and the rarely-collected families Evaniidae, Stephanidae, Trigonalidae, and Aulacidae (Hymenoptera, Apocrita). ZooKeys 1189: 275–286. https://doi.org/10.3897/zookeys.1189.114478

Introduction

The present study provides the first attempt to compile a comprehensive DNA barcode library for Gasteruptiidae species recorded from Central Europe. We also included the barcodes of four species from the families Evaniidae, Stephanidae, Trigonalidae and Aulacidae. For practical reasons and because records from other countries of Central Europe are not available, we concentrate on the German species. The families Aulacidae, Evaniidae, Stephanidae and Trigonalidae are represented by a single or a few species in each family in Germany (Saure 2001).

The family Gasteruptiidae is represented in Europe by the single genus *Gasteruption*. The genus is represented in Central Europe with 25 species (Bogusch 2021). The majority of Central European species are predator-inquilines of various stem- and wood-nesting bee species (Apiformes), in particular of the genus *Hylaeus* (Colletidae). Several species attack nests of other bee species (families Megachilidae and Apidae) or, rarely, representatives of families Crabronidae and Vespidae (Wall 1994; Bogusch et al. 2018; Parslow et al. 2020; Bogusch 2021). Several species also parasitise soil-nesting bee species of the family Halictidae, such as *Gasteruption hastator*, or nests of bees and wasps in vertical sand or loess walls (Parslow et al. 2020). The current taxonomy of this group was studied by van Achterberg and Talebi (2014) and Bogusch (2021), with the biology and host associations by Parslow et al. (2020).

The initial phase of the DNA barcoding projects focussed on species occurring in southern Germany, as part of the ‘Barcoding Fauna Bavarica’ project of the SNSB-Zoologische Staatssammlung München, Germany (ZSM). The project started in 2009 and aimed at assembling DNA barcodes for all Bavarian animal species (Hendrich et al. 2010; Hausmann et al. 2013). Since 2012, the ‘German Barcode of Life’ (GBOL) project added additional sequences. Previous barcode releases of Aculeata (Hymenoptera) dealt with the Anthophila or bees (Schmidt et al. 2015), the Spheciformes or digger wasps (Schmid-Egger et al. 2019), the genus *Polistes* or paper wasps (Vespidae) (Schmid-Egger et al. 2017), and the remaining Vespoidea (Schmid-Egger and Schmidt 2021).

The present study focuses on Central European species of Gasteruptiidae, including 24 of the 25 species recorded from Central Europe, and three additional species from southern Europe. In addition, four species of the families Evaniidae, Stephanidae, Trigonalidae and Aulacidae are included. For detailed species numbers, see Table 1. Identification and taxonomy of species from Central Europe follow Bogusch (2021).

The barcoding projects were conducted in close cooperation with the Biodiversity Institute of Ontario, University of Guelph, within the framework of the International Barcode of Life initiative. All sequences and the associated project data are available through the Barcode of Life Data Systems (BOLD). The dataset includes mainly Central European specimens but covers additional specimens from the Mediterranean area.

Materials and methods

Sampling

The present study covers the family Gasteruptiidae from Germany and adjacent areas, with a single genus *Gasteruption*. The main source of material includes specimens from Central Europe deposited in the collections of the SNSB-Zoologische Staatssammlung München, Germany (**ZSM**), Biologiezentrum Linz, Austria (**OLL**) and the private collections of Christian Schmid-Egger (**CSE**) and Petr Bogusch (**PB**). Some specimens of Central European species were collected in countries other than Germany, mainly in northern Italy, because these species are rare or even close to extinction in Central Europe and, therefore, virtually impossible to obtain from this region. Specimens from the remaining families are deposited in the ZSM or the private collection of CSE.

Specimens were identified to species level using van Achterberg and Talebi (2014) and Bogusch (2021). A complete list of voucher specimens that were treated in the present study is given in Suppl. material 1.

DNA sequencing

For DNA extraction, a single leg was removed from each specimen and sent to the Canadian Centre for DNA Barcoding (CCDB) in Guelph, Canada, for DNA extraction and barcode sequencing. DNA extraction, PCR amplification, and sequencing were conducted using standardised high-throughput protocols (Ivanova et al. 2006). The 658bp target region, starting from the 5' end of the mitochondrial cytochrome *c* oxidase I (COI) gene, includes the DNA barcode region of the animal kingdom (Hebert et al. 2003). Specimens that were successfully sequenced are listed in Suppl. material 1, with sequence lengths and the number of unresolved bases. All specimen data are accessible in BOLD as a single citable dataset (dx.doi.org/10.5883/DS-GBGAST). The data include collecting locality, geographic coordinates, elevation, collector, one or more digital images, identifier, and voucher depository. Sequence data can be obtained through BOLD and include a detailed Laboratory Information Management System (LIMS) report, primer information, and access to trace files.

Data analysis

We only analyse *Gasteruption* sequences here. Sequences of remaining Hymenoptera families are not shown here, but data are available in the BOLD system. Sequence divergence statistics were calculated using the Kimura two-parameter model of sequence evolution (Kimura 1980). Barcode Index Numbers (BINs) were assigned by the BOLD system, representing globally unique identifiers for clusters of sequences that correspond closely to biological species (Ratnasingham and Hebert 2013). For BIN assignment, a minimum sequence length of 500 bp is required, and sequences between 300 and 500 bp can join an existing BIN but will not create or split BINs. BINs provide an interim taxonomic system and a way to signify Molecular Taxonomic Units (MOTUs) prior to detailed taxonomic studies including morphology. Sequences were aligned using the BOLD Aligner (amino acid-based hidden Markov models). The analyses are based on sequences with a minimum length of 500 bp and <1% ambiguous bases. Genetic distances and summary statistics were calculated using analytical tools in BOLD and are given as mean and maximum pairwise distances for intraspecific variation and as minimum pairwise distances for interspecific variations.

Species studied

All *Gasteruption* species known from Central Europe were studied (Table 1), based on information in Bogusch (2021), except *G. lugubre*, a very rare species known from the European Alps and some countries in southeast Europe to Turkey. Also, we added three species occurring in southern Europe (*G. dolichoderum*, *G. foveiceps* and *G. schlettereri*) for better comparison with similar species, and to assist in their identification. For other Hymenoptera families, see below.

Results

For the present study, 152 sequences of 24 species of *Gasteruption* were analysed, with a length of at least 500 bp and less than 1% ambiguous bases. The dataset thus includes DNA barcodes of 24 of the 25 *Gasteruption* species known to occur in Central Europe (Table 1), including 18 of the 19 species recorded from Germany.

Table 1. *Gasteruption* species included in the present study showing their presence (+) in Central European countries (D = Germany, CZ = Czech Republic, SLO = Slovakia, A = Austria, H = Hungary, CH = Switzerland). All species known from Central Europe are considered in the table; some additional species from southern Europe are also analysed and mentioned here.

Species from Central Europe	D	CZ	SLO	A	H	CH	Notes
Gasteruption assectator (Linnaeus, 1758)	+	+	+	+	+	+	See Fig. 1
Gasteruption boreale (Thomson, 1883)	+	+	+	+	+		
Gasteruption caucasicum (Guérin-Méneville, 1844)	+	+	+	+	+	+	
Gasteruption diversipes (Abeille de Perrin, 1879)	+	+	+	+	+	+	
Gasteruption *dolichoderum* Schletterer, 1889							Not known from Central Europe
Gasteruption erythrostomum (Dahlbom, 1831)	+	+	+	+	+	+	
Gasteruption forticorne Semenov, 1892			+	+	+		
Gasteruption foveiceps Semenov, 1892							Not known from Central Europe
Gasteruption freyi (Tournier, 1877)	+	+	+	+	+	+	
Gasteruption goberti (Tournier, 1877)					+	+	
Gasteruption hastator (Fabricius, 1804)	+	+	+	+	+	+	See Fig. 2
Gasteruption hungaricum Szépligeti, 1895	+	+	+	+	+		
Gasteruption insidiosum Semenov, 1892			+		+		
Gasteruption jaculator (Linnaeus, 1758)	+	+	+	+	+	+	
Gasteruption laticeps (Tournier, 1877)	+	+	+	+	+	+	
Gasteruption lugubre Schletterer, 1889	+			+		+	Not available for study
Gasteruption merceti Kieffer, 1904	+	+	+	+	+	+	
Gasteruption minutum (Tournier, 1877)	+	+	+	+		+	See Fig. 3
Gasteruption nigrescens Schletterer, 1885	+	+	+	+	+	+	
Gasteruption nigritarse (Thomson, 1883)	+	+	+	+	+		
Gasteruption opacum (Tournier, 1877)	+	+	+	+	+	+	
Gasteruption paternum Schletterer, 1889		+	+	+	+	+	
Gasteruption phragmiticola Saure, 2006	+	+	+		+		
Gasteruption schlettereri Magretti, 1890							Not known from Central Europe
Gasteruption subtile Thomson, 1883	+	+	+	+	+	+	
Gasteruption tournieri Schletterer, 1885	+	+	+	+	+	+	
Gasteruption undulatum (Abeille de Perrin, 1879)	+	+	+	+	+	+	
Gasteruption variolosum (Abeille de Perrin, 1879)				+		+	
Total	**19**	**20**	**21**	**22**	**20**	**19**	

Taxonomic treatment

DNA barcoding allows the identification of *Gasteruption* to the species level or, in a few cases, to the species group level because of BIN sharing. The species that exhibited BIN sharing or BIN divergence, or that are otherwise taxonomically challenging, are discussed below.

Gasteruption jaculator (Linnaeus, 1758)

Gasteruption jaculator is widespread and common in Central Europe. The species exhibited BIN divergence, with a maximum intraspecific distance of 3.28% and separation into two different BINs. There are no morphological differences and no hint for species separation. The second BIN was also found in a single specimen from Slovakia, but generally, only a few specimens were examined. Further research is needed.

Gasteruption erythrostomum **(Dahlbom, 1831)**

Gasteruption erythrostomum is widespread and common in Central Europe. The species exhibited BIN divergence, with a maximum intraspecific distance of 3.39% and separation into two different BINs. There are no morphological differences and no indication of the presence of separate species. One BIN was only found in two specimens from Bavaria (Germany), whereas the other BIN is widespread in the study area.

Gasteruption foveiceps **Semenov, 1892, stat. nov.**

The present specimens of *Gasteruption foveiceps* originated from northern Italy (Aosta, Lombardy) and were formerly identified as *G. nigrescens* by CSE. However, a detailed examination by PB, considering the marked BIN difference in the species group, led to the discovery of different character states. Taking into account the morphological characters and synonyms of *G. nigriceps*, and the shape of the head and the shiny area between the antesternal and praepectal carinas (van Achterberg and Talebi 2014), the two specimens from Italy fit well with *G. foveiceps*. Thus, *G. foveiceps* is not a synonym of *G. nigrescens* but should be regarded as a valid species that occurs in southern Europe.

Gasteruption schlettereri **Magretti, 1890, *G. diversipes* (Abeille de Perrin, 1879) and *G. forticorne* Semenov, 1892**

Our original dataset includes altogether 14 specimens of this species complex, forming five clusters each with a BIN, but without a clear morphological distinction between *G. schletterei*, *G. forticorne* and *G. diversipes*. We cannot solve the taxonomic problems in this group with the few specimens at hand.

A single specimen of *G. diversipes* from Slovakia forms a cluster with specimens of *Gasteruption schlettereri* from northern Italy and Croatia. They most probably belong to the same species, apart from the fact that the morphological characters of both taxa are different (identified by Cornelis van Achterberg and PB).

The other cluster comprises specimens from Hungary, Slovakia and Croatia, and agrees with *G. forticorne* by morphology. So, *G. forticorne* and "*G. diversipes*" can be identified in Central Europe with the key of Bogusch (2021) but the second taxon still has to be checked for the correct name. The situation in southern Europe is more complicated and needs final revision. The diagnostic characters for *G. forticorne*, like length of malar space, or colour of genitalia in *G. schlettereri* males, seem to be highly variable. Currently, European specimens identified as *G. schlettereri* probably belong to *G. diversipes* and *G. forticorne* and the real *G. schlettereri* occurs in the Middle East. Our present treatment is, therefore, provisional.

Gasteruption laticeps **(Tournier, 1877)**

Gasteruption laticeps is widespread in Central Europe. The species exhibited BIN divergence, with a maximum intraspecific distance of 2.58% and separation into two different BINs. One BIN was recently found in eastern Central

Europe and Greece (no records from Germany are available), and the other was found in southern France and the Aosta Valley in northern Italy. Probably it is a species separation in an eastern and southwestern distribution centre, as described in *Myrmosa atra* Panzer, 1801 or in the sibling species *Smicromyrme rufipes* (Fabricius, 1878) and *S. frankburgeri* Schmid-Egger, 2022 (Schmid-Egger and Schmidt 2021, 2022). The species group is in need of further investigation.

Gasteruption paternum **Schletterer, 1889**

Gasteruption paternum is a rare species occurring in Central Europe, especially in the Pannonian lowlands, recorded from the following countries: Austria, Croatia, Czech Republic, France, mainland of Greece and Crete, Hungary, Italy, Slovakia and Switzerland. In all these countries, only a few specimens were recorded in the whole history of studies on this group (Bogusch 2021). The species exhibited BIN divergence, with a maximum intraspecific distance of 5.11% and separation into two different BINs. One BIN with one specimen originating from Tyrol in Austria, the other from the Italian Alps (Piedmont). The species complex needs further research.

Gasteruption assectator **(Linnaeus, 1758) aggregate**

Fig. 1

Johansson and van Achterberg (2016) revised the *Gasteruption assectator* aggregate and resurrected two species, *G. boreale* and G. *nigritarse*, from synonymy. However, all three species remain difficult to identify by the morphology and the main morphological identification characters are continuous. Our results of the genetic barcoding showed no BIN divergence between the three taxa but some weak clustering into different clades of most (not all) examined species. This was also found in a study by Parslow et al. (2021), which also consistently recovered these species as one clade.

Additionally, specimens from higher altitudes with differently sculptured mesonotum form a separate sister group to other barcoded specimens. This situation seems to indicate the presence of a new species, as discussed by van Achterberg and Talebi (2014). Further research is needed to assess if the *G. assectator* aggr. includes only one highly variable species or three or more valid and different species. The use of a nuclear gene may lead to more precise results, as shown by Praz et al. (2019) in bees of the *Andrena bicolor* species group.

Gasteruption hastator **(Fabricius, 1804)**

Fig. 2

Gasteruption hastator is a widespread species of southern Central Europe and very common in southern Europe. The species exhibited BIN divergence, with a maximum intraspecific distance of 2.63% and separation into two different BINs. One BIN with one specimen origin from Aosta Valley in northwest Italy, the other from various locations. The species needs further research and may consist of a species complex, also seen under the impression of a very long list of synonyms (van Achterberg and Talebi 2014).

Figure 1. Male of *Gasteruption assectator* from Saxony (Germany). (Photo W.H. Liebig).

Gasteruption insidiosum Semenov, 1892

Gasteruption insidiosum is a rare species of the Middle East, reaching East Europe with its north-western part of the distribution. The specimen from Turkey forms a sister group to the group of *G. erythrostomum*, *G. nigrescens*, *G. foveiceps* and *G. phragmiticola*, while the specimen from Slovakia is also part of this group, next to *G. erythrostomum*. Because the specimen from Slovakia differs in several characters from true *G. insidiosum* from Turkey, Greece and Bulgaria, it could be a separate species or belong to some of the synonyms of this species. However, the species descriptions are incomplete and short and some of the types are unavailable, so further research is needed to decide on the identification of the specimen from Slovakia.

Figure 2. Female of *Gasteruption hastator* from Saxony (Germany). It is the only largely red-coloured *Gasteruption* species in Central Europe. (Photo W.H. Liebig).

Figure 3. Female of *Gasteruption minutum* from Saxony (Germany) (Photo W.H. Liebig).

Discussion

DNA barcoding of German species

For the present study, 18 of the 19 of the *Gasteruption* species that are known to occur in Germany were analysed by DNA barcoding. In two recent DNA barcoding studies dealing with German Apiformes (bees) (Schmidt et al. 2015) and German Spheciformes (Schmid-Egger et al. 2019, 88% of the German species were covered, although the number of German species is, with 584 species in bees and 273 species in Spheciformes, much larger compared to *Gasteruption*. For Europe, 25 of the 26 species recorded from Central Europe (Bogusch 2021) were available for study.

BIN diversity

The most surprising result in this study is the unexpectedly high BIN diversity, suggesting a higher-than-expected species diversity. Five species exhibited two or more BINs. BIN sharing (i.e., two or more species that share the same BIN and are not separable by DNA barcoding) occurred in four species.

We refer to the discussion in Schmid-Egger and Schmidt (2021) on how to deal with and interpret the BIN diversity and problems with a lack of clear morphological characters. The present study confirms findings from previous studies that there are more genetically (BIN) based entities than morphological taxa in any examined Hymenoptera family. Although the BIN can change as more sequences are added, we suggest, whenever possible, to include the Barcode Index Number (BIN) in any further treatment of the species with BIN diversity, including a link to the BIN or the specimens in BOLD, in case the BINs represent distinct species.

Other Hymenoptera families

The present study provided the opportunity to deal with some rare and poorly known Hymenoptera families with a reference to the German fauna. The families treated here include six species, five of which were DNA barcoded (Table 2). *Brachygaster minutus* (Evaniidae) is a parasitoid of cockroach ootheca (Blattoidea), and *Stephanus serrator* (Stephanidae) parasitises larva of longhorn beetles (Cerambycidae). *Pseudogonalos hahnii* (Trigonalidae) is a hyperparasitoid larva of Ichneumonoidea and can develop only when its egg is ingested by a parasitised caterpillar of an owlet moth (Erebidae and Noctuidae). Aulacidae

Table 2. Species of Hymenoptera families with a single, or very few, species from Germany that are included in the present study. For checklists of German species see Saure (2001); for *Pristaulacus*, also Turrisi (2011). All mentioned genera include only one species in Germany, apart from *Pristaulacus* with five German species (Turrisi 2011).

Family	Species
Evaniidae	*Brachygaster minutus* (Olivier, 1792)
Stephanidae	*Stephanus serrator* (Fabricius, 1798)
Trigonalidae	*Pseudogonalos hahnii* (Spinola, 1840)
Aulacidae	*Aulacus striatus* Jurine, 1807
Aulacidae	*Pristaulacus compressus* (Spinola, 1808)

are koinobiont endoparasitoids of wood-boring larvae of Xiphydriidae (Hymenoptera), Cerambycidae and Buprestidae (Coleoptera). The genus *Pristaulacus* was revised by Turrisi (2011). Distribution of the species is insufficiently known, but it can be assumed that most or all species are widespread. The species are rarely collected, with few specimens present in museum collections.

Acknowledgments

The collection and processing of specimens were funded by the Bayerisches Staatsministerium für Wissenschaft und Kunst (project ‘Barcoding Fauna Bavarica’) and by the German Federal Ministry of Education and Research (Bundesministerium für Bildung und Forschung, Berlin, Germany, project German Barcode of Life). The sequence analyses for this study were supported, in part, by Genome Canada through the Ontario Genomics Institute, while informatics support was provided through a grant from the Ontario Ministry of Research and Innovation. The authors are indebted to Olga Schmidt for her technical assistance. We also thank Wolf-Harald Liebig for providing photos.

Additional information

Conflict of interest

The authors have declared that no competing interests exist.

Ethical statement

No ethical statement was reported.

Funding

PB was supported by a Specific Research Grant from University of Hradec Králové, Nr. 2102/2023.

Author contributions

All three authors conducted the DNA barcoding, SS was responsible for the barcode analysis, CS and PB wrote the taxonomic part, all three authors wrote the manuscript

Author ORCIDs

Stefan Schmidt https://orcid.org/0000-0001-5751-8706
Petr Bogusch https://orcid.org/0000-0002-4554-6141

Data availability

All of the data that support the findings of this study are available in the main text or Supplementary Information.

References

Bogusch P (2021) The genus *Gasteruption* Latreille, 1796 (Hymenoptera: Gasteruptiidae) in the Czech Republic and Slovakia: distribution, checklist, ecology, and conservation status. Zootaxa 4935(1): 1–63. https://doi.org/10.11646/zootaxa.4935.1.1

Bogusch P, Van Achterberg C, Šilhán K, Astapenková A, Heneberg P (2018) Description of mature larvae and ecological notes on *Gasteruption* Latreille (Hymenoptera, Evanioidea, Gasteruptiidae) parasitizing hymenopterans nesting in reed galls. Journal of Hymenoptera Research 65: 1–21. https://doi.org/10.3897/jhr.65.26645

Hausmann A, Hendrich L, Balke M, Morinière J, Schmidt S, Segerer A, Hebert PDN (2013) A major contribution of the ZSM to the genetic library of life: 35,000 insect species barcoded in 7 years. In: Kroh A, Berning B, Haring E, Harzhauser M, Sattmann H, Walochnik J, Zimmermann D, Zuschin F (Eds) Abstract Volume NOBIS. Vienna, Austria, 86 pp.

Hebert PDN, Cywinska A, Ball SL, deWaard JR (2003) Biological identifications through DNA barcodes. Proceedings. Biological Sciences 270(1512): 313–321. https://doi.org/10.1098/rspb.2002.2218

Hendrich L, Balke M, Haszprunar G, Hausmann A, Hebert P, Schmidt S (2010) Barcoding Fauna Bavarica – Capturing Central European Animal Diversity. In: Nimis P, Vignes Lebbe R (Eds) Proceedings of the International Congress. Tools for Identifying Biodiversity: Progress and Problems. Trieste, EUT Edizioni Universitá di Trieste, 347 pp.

Ivanova NV, Dewaard JR, Hebert PDN (2006) An inexpensive, automation-friendly protocol for recovering high-quality DNA: technical note. Molecular Ecology Notes 6: 998–1002. https://doi.org/10.1111/j.1471-8286.2006.01428.x

Johansson N, Van Achterberg C (2016) Revision of the Palaearctic Gasteruption assectator aggregate, with special reference to Sweden (Hymenoptera, Gasteruptiidae). ZooKeys 615: 73–94. https://doi.org/10.3897/zookeys.615.8857

Kimura M (1980) A simple method for estimating evolutionary rates of base substitutions through comparative studies of nucleotide sequences. Journal of Molecular Evolution 16: 111–120. https://doi.org/10.1007/BF01731581

Parslow BA, Schwarz MP, Stevens MI (2020) Review of the biology and host associations of the wasp genus *Gasteruption* (Evanioidea: Gasteruptiidae). Zoological Journal of the Linnean Society 189(4): 1105–1122. https://doi.org/10.1093/zoolinnean/zlaa005

Parslow BA, Schwarz MP, Stevens MI (2021) Molecular diversity and species delimitation in the family Gasteruptiidae (Hymenoptera: Evanioidea). Genome 64(3): 253–264. https://doi.org/10.1139/gen-2019-0186

Praz C, Müller A, Genoud D (2019) Hidden diversity in European bees: *Andrena amieti* sp. n., a new Alpine bee species related to *Andrena bicolor* (Fabricius, 1775) (Hymenoptera, Apoidea, Andrenidae). Alpine Entomology 3: 11–38. https://doi.org/10.3897/alpento.3.29675

Ratnasingham S, Hebert PDN (2013) A DNA-based registry for all animal species: The Barcode Index Number (BIN) system. PLOS ONE 8(8): e66213. https://doi.org/10.1371/journal.pone.0066213

Saure C (2001) Aulacidae. Dathe HH, Taeger A, Blank SM (Eds) Entomologische Nachrichten und Berichte Beiheft 7: 29.

Schmid-Egger C, Schmidt S (2021) Unexpected diversity in Central European Vespoidea (Hymenoptera, Mutillidae, Myrmosidae, Sapygidae, Scoliidae, Tiphiidae, Thynnidae, Vespidae), with description of two species of Smicromyrme Thomson, 1870. ZooKeys 1062: 49–72. https://doi.org/10.3897/zookeys.1062.70763

Schmid-Egger C, Schmidt S (2022) *Smicromyrme frankburgeri* Schmid-Egger (Hymenoptera, Mutillidae), a replacement name for *S. burgeri* Schmid-Egger, 2021, preoccupied by *S. burgeri* Lelej, 2020. ZooKeys 1097: 133–134. https://doi.org/10.3897/zookeys.1097.83215

Schmid-Egger C, Van Achterberg K, Neumeyer R, Morinière J, Schmidt S (2017) Revision of the West Palaearctic Polistes Latreille, with the descriptions of two species – an integrative approach using morphology and DNA barcodes (Hymenoptera, Vespidae). ZooKeys 713: 53–112. https://doi.org/10.3897/zookeys.713.11335

Schmid-Egger C, Straka J, Ljubomirov T, Blagoev GA, Morinière J, Schmidt S (2019) DNA barcodes identify 99 per cent of apoid wasp species (Hymenoptera: Ampulicidae, Crabronidae, Sphecidae) from the Western Palearctic. Molecular Ecology Resources 19(2): 476–484. https://doi.org/10.1111/1755-0998.12963

Schmidt S, Schmid-Egger C, Morinière J, Haszprunar G, Hebert PDN (2015) DNA barcoding largely supports 250 years of classical taxonomy: Identifications for Central European bees (Hymenoptera, Apoidea partim). Molecular Ecology Resources 15(4): 985–1000. https://doi.org/10.1111/1755-0998.12363

Turrisi GF (2011) Systematic revision of the sibling species belonging to the *Pristaulacus compressus* group (Hymenoptera: Aulacidae). Insect Systematics & Evolution 42(1): 1–27. https://doi.org/10.1163/187631211X545132

Van Achterberg C, Talebi A (2014) Review of Gasteruption Latreille (Hymenoptera, Gasteruptiidae) from Iran and Turkey, with the description of 15 new species. ZooKeys 458: 1–187. https://doi.org/10.3897/zookeys.458.8531

Wall I (1994) Seltene Hymenopteren aus Mittel-, West- und Südeuropa (Hymenoptera Apocrita: Stephanoidea, Evanioidea, Trigonalyoidea. Entomofauna 15: 137–184.

Supplementary material 1

List of voucher specimens

Authors: Christian Schmid-Egger, Stefan Schmidt, Petr Bogusch

Data type: pdf

Explanation note: List of voucher specimens with specimen ID, country of origin, collection date, specimen depository, Barcode Index Number (BIN) and sequencing success (COI-fragment length in bp, in square brackets number of unresolved bases).

Link: https://doi.org/10.3897/zookeys.1189.114478.suppl1

Supplementary material 2

Barcoding statistics

Authors: Christian Schmid-Egger, Stefan Schmidt, Petr Bogusch

Data type: pdf

Explanation note: Barcoding statistics with mean intraspecific distance, maximum intraspecific distance, nearest neighbour species, distance to nearest neighbour species, Barcode Index Number (BIN), country, and number of specimens. Asterisks indicate species with BIN sharing.

Link: https://doi.org/10.3897/zookeys.1189.114478.suppl2

ZooKeys 1189: 287–325 (2024)
DOI: 10.3897/zookeys.1189.111041

Research Article

Midget cave spiders (Araneae, Leptonetidae) from Jiangxi and Fujian Province, China

Bin-Lu Liu[1]*, Yan-bin Yao[1,2]*, Zi-Min Jiang[1], Yong-hong Xiao[1], Ke-Ke Liu[1]

1 *College of Life Science, Jinggangshan University, Ji'an 343009, Jiangxi, China*
2 *Jinshan College of Fujian Agriculture and Forestry University, Fuzhou 350007, Fujian, China*
Corresponding author: Ke-Ke Liu (kekeliu@jgsu.edu.cn)

Abstract

Eleven leptonetid species belonging to four genera collected in Jiangxi and Fujian Provinces, China are presented. Ten new species of midget cave spiders from southern China are diagnosed, described, and illustrated: *Leptonetela dawu* Yao & Liu, **sp. nov.**, *L. yuanhaoi* Yao & Liu, **sp. nov.** and *L. zuojiashanensis* Yao & Liu, **sp. nov.** from Jiangxi; *Longileptoneta guadunensis* Yao & Liu, **sp. nov.**, *L. huboliao* Yao & Liu, **sp. nov.**, *L. jiaxiani* Yao & Liu, **sp. nov.**, *L. letuensis* Yao & Liu, **sp. nov.**, *L. renzhouensis* Yao & Liu, **sp. nov.**, *L. tianmenensis* Yao & Liu, **sp. nov.,** and *Pararana mingxuani* Yao & Liu, **sp. nov.** from Fujian. Furthermore, *Falcileptoneta monodactyla* (Yin, Wang & Wang, 1984) is recorded from Jiangxi province for the first time. Distributions records are given for all investigated species.

Key words: Asia, biodiversity, distribution, leptonetid spiders, new species, taxonom

Academic editor: Peter Michalik
Received: 11 August 2023
Accepted: 31 December 2023
Published: 18 January 2024

ZooBank: https://zoobank.org/C921C517-275E-4B3E-8CCC-9C2E214FEB1E

Citation: Liu B-L, Yao Y-b, Jiang Z-M, Xiao Y-h, Liu K-K (2024) Midget cave spiders (Araneae, Leptonetidae) from Jiangxi and Fujian Province, China. ZooKeys 1189: 287–325. https://doi.org/10.3897/zookeys.1189.111041

Introduction

The midget cave spider family Leptonetidae Simon, 1890 is one of the smallest taxa in haplogyne spider families, with 374 species belonging to 22 genera (WSC 2023). At present, eight genera and 135 species are known from China. Among these genera, species of *Leptonetela* Kratochvíl, 1978 have been reported as being the most diverse in China.

Most records and descriptions of this family from China were contributed by the Chinese arachnologist Shu-Qiang Li and his team, such as of the genera *Jingneta* Wang & Li, 2020, *Leptonetela*, *Longileptoneta* Seo, 2015, *Pararana* Lin & Li, 2022 and *Rhyssoleptoneta* Tong & Li, 2007 (Wang and Li 2011; Wang et al. 2017, 2020; Lan et al. 2021; Zhu and Li 2021; Lin et al. 2022). In addition, many more genera have been recorded or described from China by other authors with eight species from northern provinces (Tong and Li 2008; Wang et al. 2020; Zhu and Li 2021; Liu and Zhang 2022), and the remaining species from the southern provinces of China. Despite advances in the taxonomic knowledge of the family, there are still many more genera and species to discover from southern China that have unusual morphological characteristics.

---

* These authors contributed equally to this work.

While working on the leptonetid fauna of the Jiangxi and Fujian provinces, southern China, we discovered and examined in detail eleven species including one known and ten new leptonetids. The goal of this paper is to formally describe the new species and to report the first species of *Falcileptoneta* Komatsu, 1970 from Jiangxi Province.

Materials and methods

Specimens were examined using a Zeiss Stereo Discovery V12 stereomicroscope with a Zoom Microscope System. Both male palps and female genitalia were detached and examined in 80% ethanol, using a Zeiss Axio Scope A1 compound microscope with a KUY NICE CCD. The female genitalia were cleared in trypsin enzyme solution to dissolve soft tissues. For SEM photographs, specimens were dried under natural conditions, coated with gold using a small ion-sputtering apparatus ETD-2000, or without coating, and examined with a ZEISS EVO LS15 scanning electron microscope. Specimens including detached male palps and female genitalia were stored in 75% ethanol after examination. All the specimens are deposited in Animal Specimen Museum, Life Science of College, Jinggangshan University (**ASM-JGSU**).

To maintain uniformity of genitalia terminology within these genera, including *Falcileptoneta*, *Leptonetela*, *Longileptoneta*, and *Pararana*, the terms that are used are primarily from the Spider Anatomy Ontology on BioPortal (Ramírez and Michalik 2019). In the past, different terms have been used to refer to the same structure, and terms have been used incorrectly. Although some of these terms have synonyms in both males and females, the ones used here will hopefully become a standard for future studies of these genera, if applicable. Measurements were taken with the Axio Vision software (SE64 Rel. 4.8.3) and are given in millimeters. Leg measurements are given as total length (femur, patella, tibia, metatarsus, tarsus).

Taxonomic account

Family Leptonetidae Simon, 1890
Genus *Falcileptoneta* Komatsu, 1970

Falcileptoneta monodactyla (Yin, Wang & Wang, 1984)
Figs 1, 2

Leptoneta monodactyla Yin, Wang & Wang, 1984: 366, fig. 2a–d (holotype male, not examined; Hunan, Yanling); Song 1987: 104, fig. 67 (♂); Song et al. 1999: 51, fig. 21H–I (♂); Yin et al. 2012: 156, fig. 26a–d (♂); Liu et al. 2020: 3, figs 1A–E, 2A, B, 3A–C (♂).

Falcileptoneta monodactyla Wang, Li & Zhu, 2020: 689 (transferred from *Leptoneta*).

Material examined. 1 ♂, 26°30'41.64"N, 115°59'19.02"E, 346 m, Jinjing Cave, Cuiweifeng Forest Park, Ningdu County, Ganzhou City, Jiangxi Province, China, 23 January 2021, K. Liu, D. Zhao & Z. Meng leg. (Lep-3).

Diagnosis and description. See Liu et al. (2020) for both sexes.

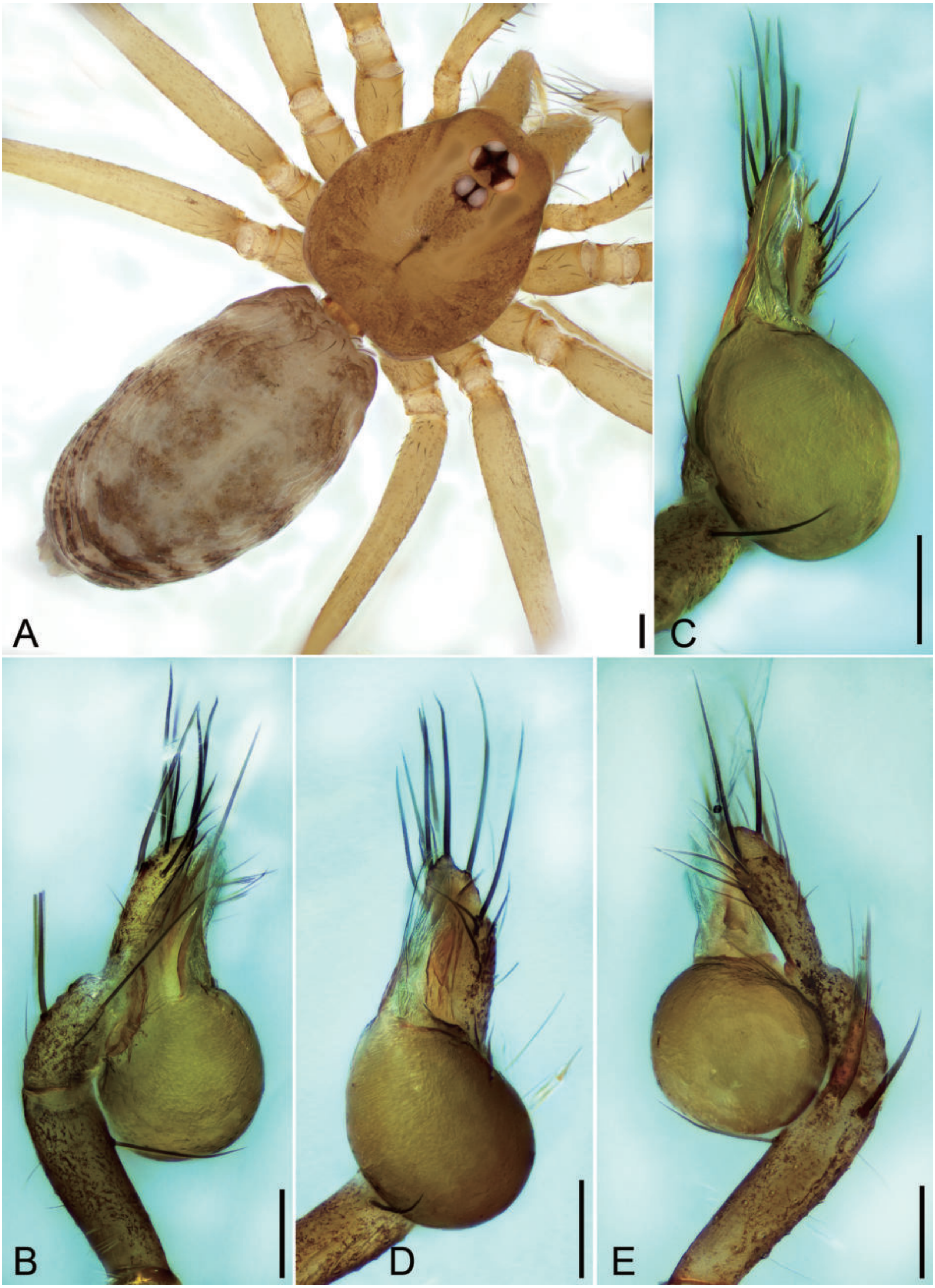

Figure 1. *Falcileptoneta monodactyla* (Yin, Wang & Wang, 1984), male **A** habitus, dorsal view **B** palp, prolateral view **C** same, ventral view **D** same, ventro-retrolateral view **E** same, retrolateral view. Scale bars: 0.1 mm.

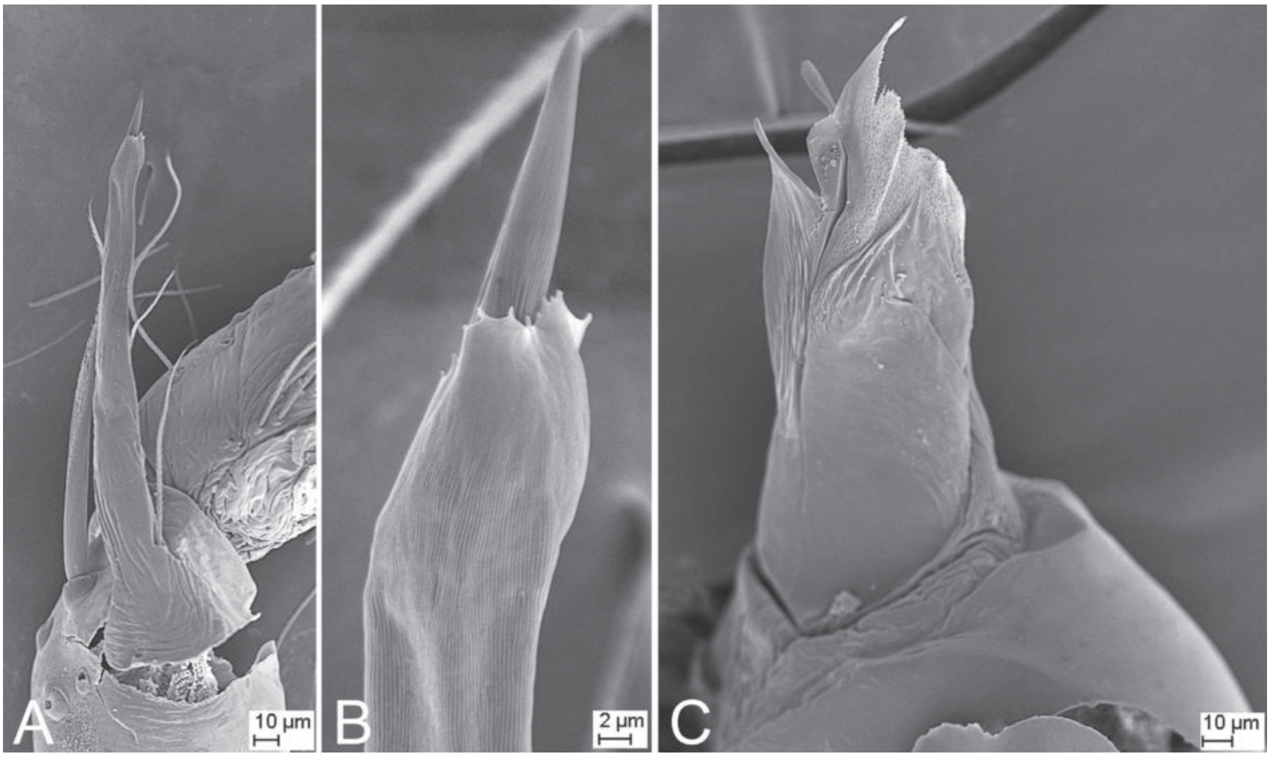

Figure 2. SEM micrographs of *Falcileptoneta monodactyla* (Yin, Wang & Wang, 1984), male right palp **A** tibial apophysis, retrolateral view **B** same, detail tip of tibial apophysis and spine, retrolateral view **C** tegular apophysis, ventral view.

Distribution. Known from Jiangxi (new record) and Hunan (Liu et al. 2020), China (Fig. 29).

Genus *Leptonetela* Kratochvíl, 1978

Leptonetela dawu Yao & Liu, sp. nov.

https://zoobank.org/106D7200-E479-4F1C-A997-B1D976CC70E4
Figs 3, 4, 8A–D
Vernacular name: 大乌小弱蛛

Material examined. ***Holotype*:** ♂, **China:** Jiangxi Province, Ji'an City, Qingyuan District, Donggu Town, Dawu Mountain, 26°40'48.69"N, 115°25'07.79"E, 1031 m, 25.X.2020, K. Liu, Y. Ying & S. Yuan leg. (Lep-8). ***Paratype*:** 7 ♂, 2 ♀, the same data as the holotype (Lep-8).

Diagnosis. The male of this species is similar to *Leptonetela sexdentata* Wang & Li, 2011 (see Wang and Li 2011: 15, figs 53A–D) in having a tongue-shaped prolateral lobe, but can be distinguished from it by dorsal habitus with obvious black-brown stripes (vs pale in *L. sexdentata*) and the foot-shaped median apophysis (vs square-shaped) (Figs 3, 8A–D). Females resemble that of *Leptonetela rudong* Wang & Li, 2017 (see Wang et al. 2017: 362, fig. 31C) in having a sub-rectangular atrium, but can be separated from it by the spermathecal stalk with seven spirals (vs six) and the slightly curved spermathecae (vs straight) (Fig. 4C).

Description. Male (holotype). Habitus as in Fig. 3A. Total length 1.75. Carapace 0.82 long, 0.76 wide. Eye sizes and interdistances: ALE 0.09, PME 0.08,

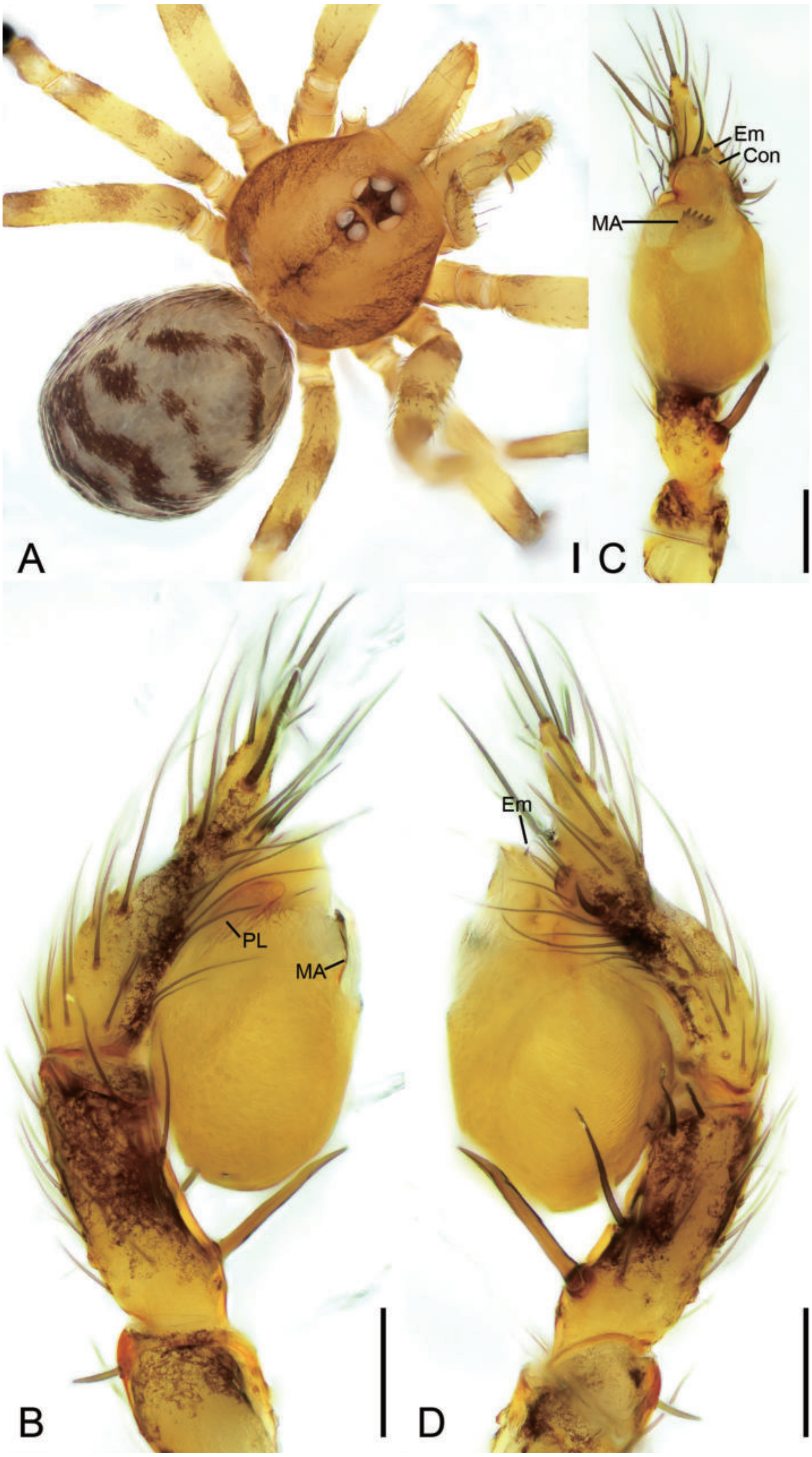

Figure 3. *Leptonetela dawu* sp. nov., male holotype **A** habitus, dorsal view **B** palp, prolateral view **C** same, ventral view **D** same, retrolateral view. Abbreviations: Con – conductor, Em – embolus, MA – medial apophysis, PL – prolateral lobe. Scale bars: 0.2 mm (**A**); 0.1 mm (**B–D**).

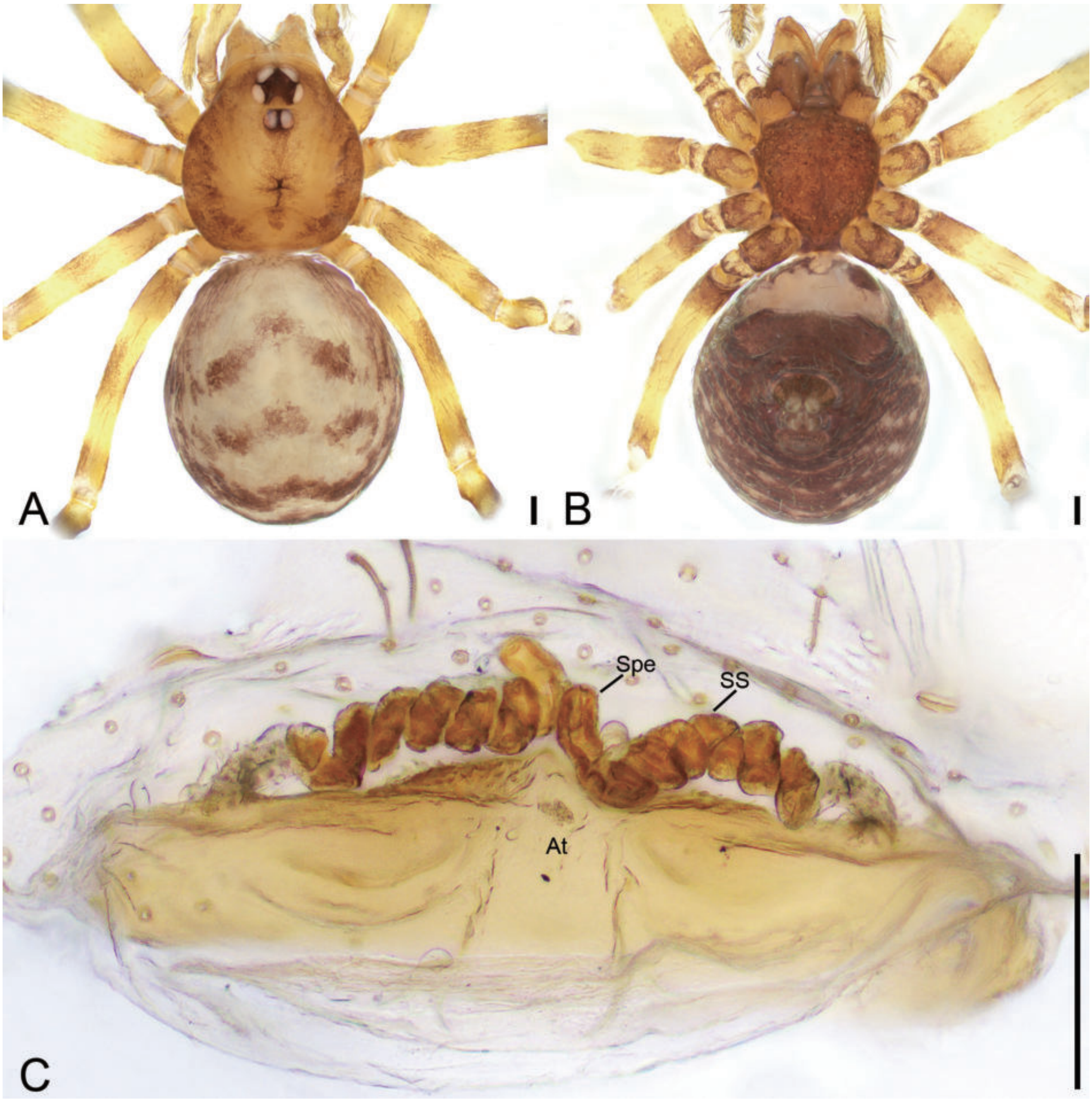

Figure 4. *Leptonetela dawu* sp. nov., female paratype **A** habitus, dorsal view **B** same, ventral view **C** vulva, dorsal view. Abbreviations: At – atrium, Spe – spermathecae, SS – spermathecae stalk. Scale bars: 0.1 mm.

PLE 0.09; ALE–PME 0.12, PLE–PLE 0.11, PLE–PME 0.03; AER 0.17, PER 0.22. Clypeus 0.12 high. Chelicerae (Fig. 3A) with ten promarginal and five retromarginal teeth. Sternum shield-shaped, longer than wide, posterior end arch-shaped, smooth. Leg measurements: **I** 4.30 (1.13, 0.25, 1.21, 0.98, 0.73); **II** 3.32 (1.01, 0.19, 0.80, 0.74, 0.58); **III** 3.07 (1.00, 0.18, 0.68, 0.74, 0.47); **IV** 3.74 (0.97, 0.21, 1.06, 0.94, 0.56). Pedicel 0.12. Abdomen 0.98 long, 0.77 wide.

Coloration (Fig. 3A). Carapace yellow to dark brown, with radial, dark brown, mottled markings on lateral margin and mottled stripes medially. Chelicerae, endites, labium, and sternum yellow-brown. Legs yellow, with distinct annulations. Abdomen pale to dark brown, with five dark chevron-shaped stripes.

Palp (Figs 3B–D, 8A–D). Tibia with four long setae retrolaterally, the basal one thick, two short spines distally; cymbium with one thick, conspicuous spine prolaterally, one short, thick spine retrolaterally, and one long spine distally. Tip of bulb: prolateral lobe finger-like; median apophysis relatively long, foot-shaped, distal margin with ten teeth, the retrolateral one very large with blunt tip; conductor long, membranous, apically curved; embolus spine-like, very short, under the conductor.

Female (paratype). Total length 1.85. Carapace 0.89 long, 0.73 wide. Eye sizes and interdistances (Fig. 4A): ALE 0.09, PME 0.08, PLE 0.08; ALE–PME 0.10, PLE–PLE 0.11, PLE–PME 0.03; AER 0.16, PER 0.21. Clypeus 0.11 high. Chelicerae (Fig. 4B) with nine promarginal and five retromarginal teeth. Leg measurements: I (1.21, 0.28, other segments broken); II 3.19 (0.93, 0.21, 0.82, 0.79, 0.44); III (0.87, 0.24, other segments broken); IV (1.17, 0.18, other segments broken). Pedicel 0.05. Abdomen 1.22 long, 0.95 wide.

Vulva (Fig. 4C). Internal genitalia with sub-rectangular atrium, finger-like spermathecae, and convoluted spermathecal stalk including six coils.

Distribution. Known only from the type locality in Jiangxi Province, China (Fig. 29).

Etymology. The name is taken from the type locality; noun in apposition.

Leptonetela yuanhaoi Yao & Liu, sp. nov.

https://zoobank.org/74BE5C72-CB07-4A26-B274-BA45EA120254
Figs 5, 6, 8E–L
Vernacular name: 渊浩小弱蛛

Material examined. ***Holotype*:** ♂, **China:** Jiangxi Province, Ji'an City, Taihe County, Zhonglong Town, Zhonglong Village, Ziyao Mountain, 26°43'23.15"N, 115°13'31.70"E, 388 m, 28.X.2020, K. Liu, Y. Ying, K. Huang & S. Yuan leg. (Lep-7). ***Paratype*:** 4 ♀, the same data as the holotype (Lep-7); 1 ♂, 26°42'58.10"N, 115°13'39.00"E, 206 m, other data as same as holotype (Lep-5); 1 ♂, 26°43'15.05"N, 115°13'37.85"E, 332 m other data same as holotype (Lep-6); 1 ♀, 26°43'05.30"N, 115°13'36.28"E, 228 m, other data same as holotype (Lep-1).

Diagnosis. The male of this species is similar to that of *Leptonetela sexdentata* Wang & Li, 2011 (Wang and Li 2011: 15, fig. 53B–D) in having the tibia with a row of spines retrolaterally including one thick strong spine proximally and three thin spines, but can be separated from it by the tongue-shaped prolateral lobe (vs finger-like) and the median apophysis with narrow base (vs broad) and five teeth distally (under microscope) (vs six) (Figs 5B–D, 8E–L). The males also resemble that of *L. dawu* sp. nov. in having the conductor with curved apex and the spine-like embolus, but can be separated from it by the leaf-shaped median apophysis (vs foot-shaped) (Figs 5B–D, 8E–L). The female can be easily distinguished from *L. sexdentata* (Wang and Li 2011: 15, fig. 54C) by the transversely extended spermathecal stalk (vs directed anteromedially) with four regular spirals (vs irregular) (Fig. 6C).

Description. Male (holotype). Habitus as in Fig. 5A. Total length 2.06. Carapace 0.91 long, 0.75 wide. Eye sizes and interdistances: ALE 0.09, PME 0.08, PLE 0.09; ALE–PME 0.13, PLE–PLE 0.10, PLE–PME 0.05; AER 0.18, PER 0.22.

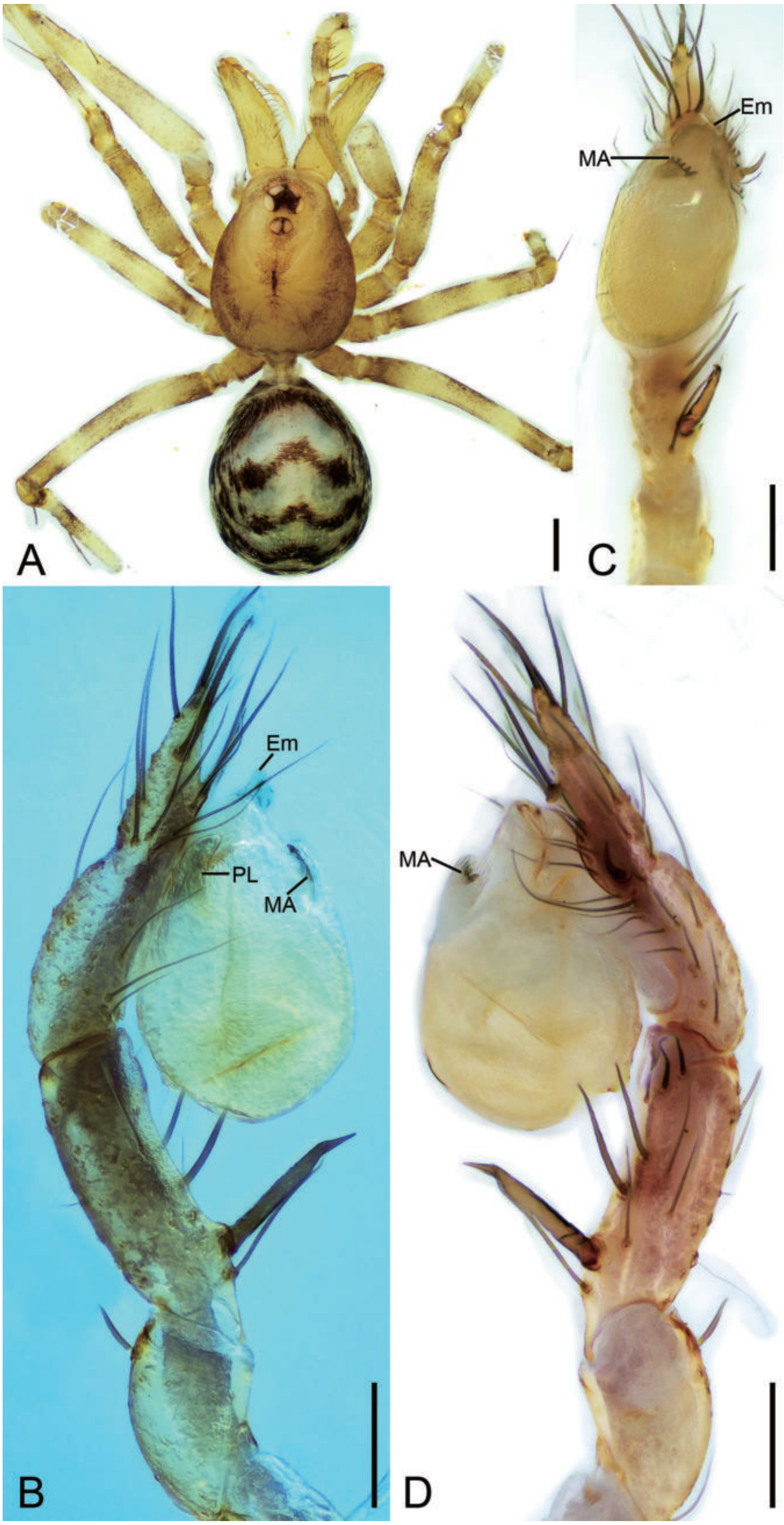

Figure 5. *Leptonetela yuanhaoi* sp. nov., male holotype **A** habitus, dorsal view **B** palp, prolateral view **C** same, ventral view **D** same, retrolateral view. Abbreviations: Em – embolus, MA – medial apophysis, PL – prolateral lobe. Scale bars: 0.1 mm.

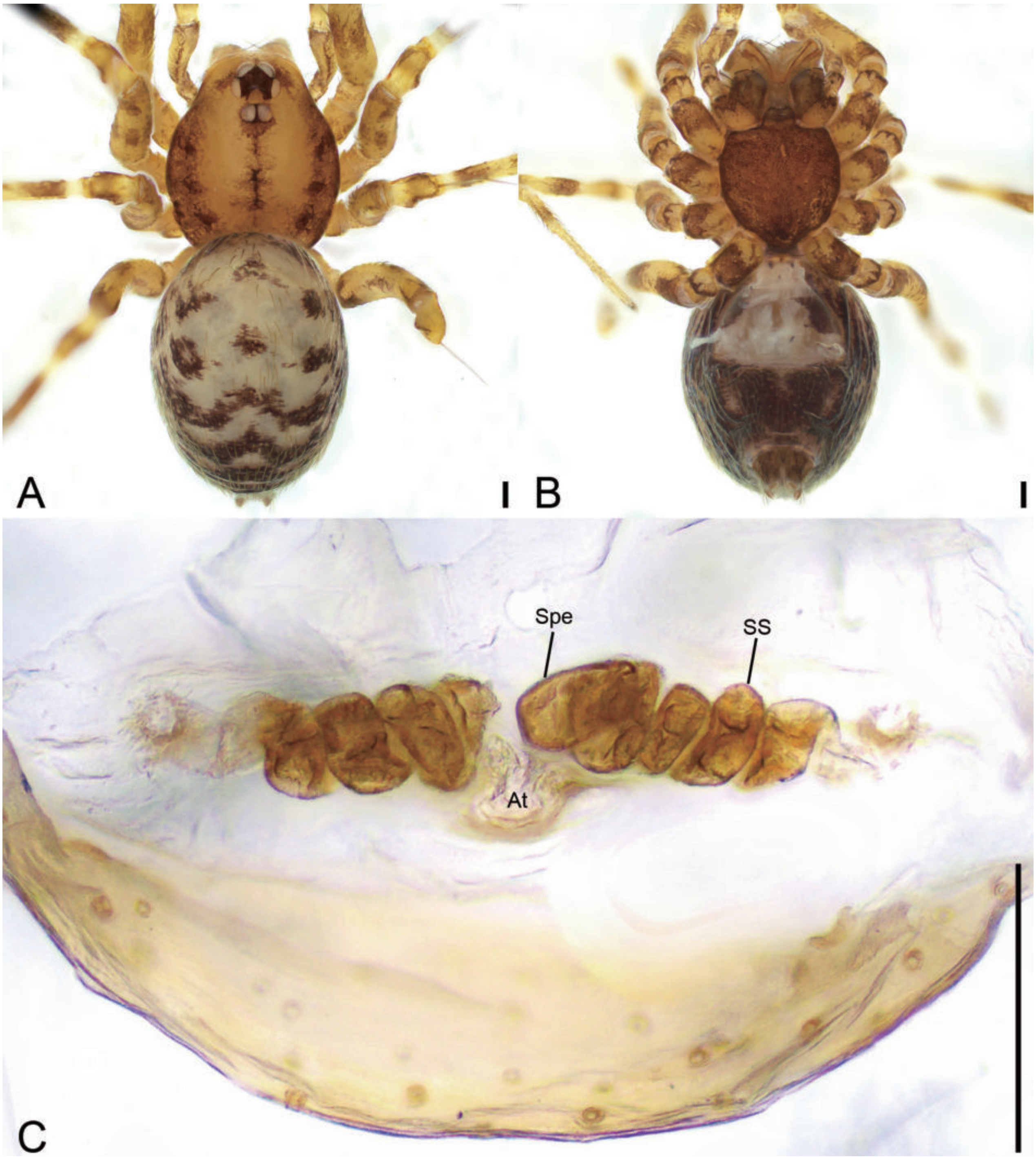

Figure 6. *Leptonetela yuanhaoi* sp. nov., female paratype **A** habitus, dorsal view **B** same, ventral view **C** vulva, dorsal view. Abbreviations: At – atrium, Spe – spermathecae, SS – spermathecae stalk. Scale bars: 0.1 mm.

Clypeus 0.13 high. Chelicerae (Fig. 5A) with eight promarginal and six retromarginal teeth. Endites with several long spines anterolaterally. Sternum shield-shaped, nearly as long as wide, with dense scale-like surface, posterior end blunt. Leg measurements: **I** 4.60 (1.13, 0.32, 1.28, 1.04, 0.83); **II** 3.28 (0.75, 0.21, 0.96, 0.72, 0.64); **III** 2.94 (0.77, 0.21, 0.75, 0.81, 0.40); **IV** 3.82 (1.09, 0.15, 0.94, 0.98, 0.66); formula: **I**, **IV**, **II**, **III**. Pedicel 0.12. Abdomen 1.02 long, 0.89 wide.

Coloration (Fig. 5A). Carapace yellow to dark brown, with dark radial stripes and mottled markings on lateral margin, and an oval dark brown band medially.

Chelicerae yellow. Endites yellow to dark brown, mottled. Labium yellow to dark brown. Legs with dark annulations on each segment except tarsi. Abdomen with four dark chevron-shaped stripes.

Palp (Figs 5B–D, 8E–L). Tibia with five long setae retrolaterally, the proximal one very thick, long, strong, spine-like; cymbium with one long conspicuous seta prolaterally, one short, strong, thick spine retrolaterally and one long spine distally. Tip of bulb: prolateral lobe tongue-like, relatively short; median apophysis leaf-shaped, distal margin with four to ten teeth, prolateral one very small, retrolateral one very large with triangular tip; conductor membranous, relatively broad, near the base of median apophysis, longer than median apophysis; embolus short, transparent, broad, slightly bending retrolaterally.

Female (paratype). Habitus as in Fig. 6A, B. Total length 1.70. Carapace 0.84 long, 0.71 wide. Eye sizes and interdistances: ALE 0.08, PME 0.08, PLE 0.08; ALE–PME 0.11, PLE–PLE 0.12, PLE–PME 0.04; AER 0.15, PER 0.20. Clypeus 0.10 high. Chelicerae (Fig. 6B) with nine promarginal and five retromarginal teeth. Endites with several long spines anterolaterally. Sternum (Fig. 6B) shield-shaped, nearly as long as wide, with dense scale-like surface, lateral margin thickened, posterior end blunt. Leg measurements: **I** 3.53 (1.00, 0.19, 1.05, 0.77, 0.52); **II** 2.80 (0.78, 0.20, 0.65, 0.59, 0.58); **III** 2.36 (0.71, 0.16, 0.56, 0.57, 0.36); **IV** 3.48 (0.97, 0.23, 0.89, 0.84, 0.55). Pedicel 0.06. Abdomen 1.06 long, 0.78 wide.

Coloration (Fig. 6A, B). Darker than male.

Vulva (Fig. 6C). Internal genitalia with sub-trapezoidal atrium, slightly swollen spermathecae. and convoluted spermathecal stalk including three coils.

Distribution. Known only from the type locality in Jiangxi Province, China (Fig. 29).

Etymology. The species is named after Mr Yuanhao Ying, who collected the type specimens.

Comments. We compared the palps of the new species with that of the very similar species *L. dawu* sp. nov. several times. This similarity is probably because the males of these two species have very similar characters: tibial spines, cymbial spine, and embolus. The distance between Dawu Mountain and Ziyao Mountain is approximately 25 km (linear distances), which is very close. Despite the close distance, we consider them as different species based on the morphological differences listed. This hypothesis will be confirmed or rejected in the future when molecular data and analysis can be provided.

Leptonetela zuojiashanensis **Yao & Liu, sp. nov.**

https://zoobank.org/1530D5D5-57E8-4792-83A2-7A3E4FC85771
Figs 7, 8M–P
Vernacular name: 左家山小弱蛛

Material examined. ***Holotype***: ♂, **China:** Jiangxi Province, Yichun City, Wanzai County, Luocheng Town, Jiulongshan Forest Park, Zuojiashan Village, 28°21'07.52"N, 114°30'27.58"E, 164 m, 6.II.2021, K. Liu, D. Zhao, Z. Meng, Z. He & W. Li leg. (Lep-4).

Diagnosis. The male of this species is similar to that of *Leptonetela gubin* Wang & Li, 2017 (in Wang et al. 2017: 386, fig. 48B–D) in having the curved cymbium forming an angle of ca 100° with tibial axis and the horn-like

Figure 7. *Leptonetela zuojiashan* sp. nov., male holotype **A** habitus, dorsal view **B** palp, prolateral view **C** same, ventral view **D** same, retrolateral view. Abbreviations: Em – embolus, PL – prolateral lobe, PS – prolateral sclerite. Scale bars: 0.1 mm.

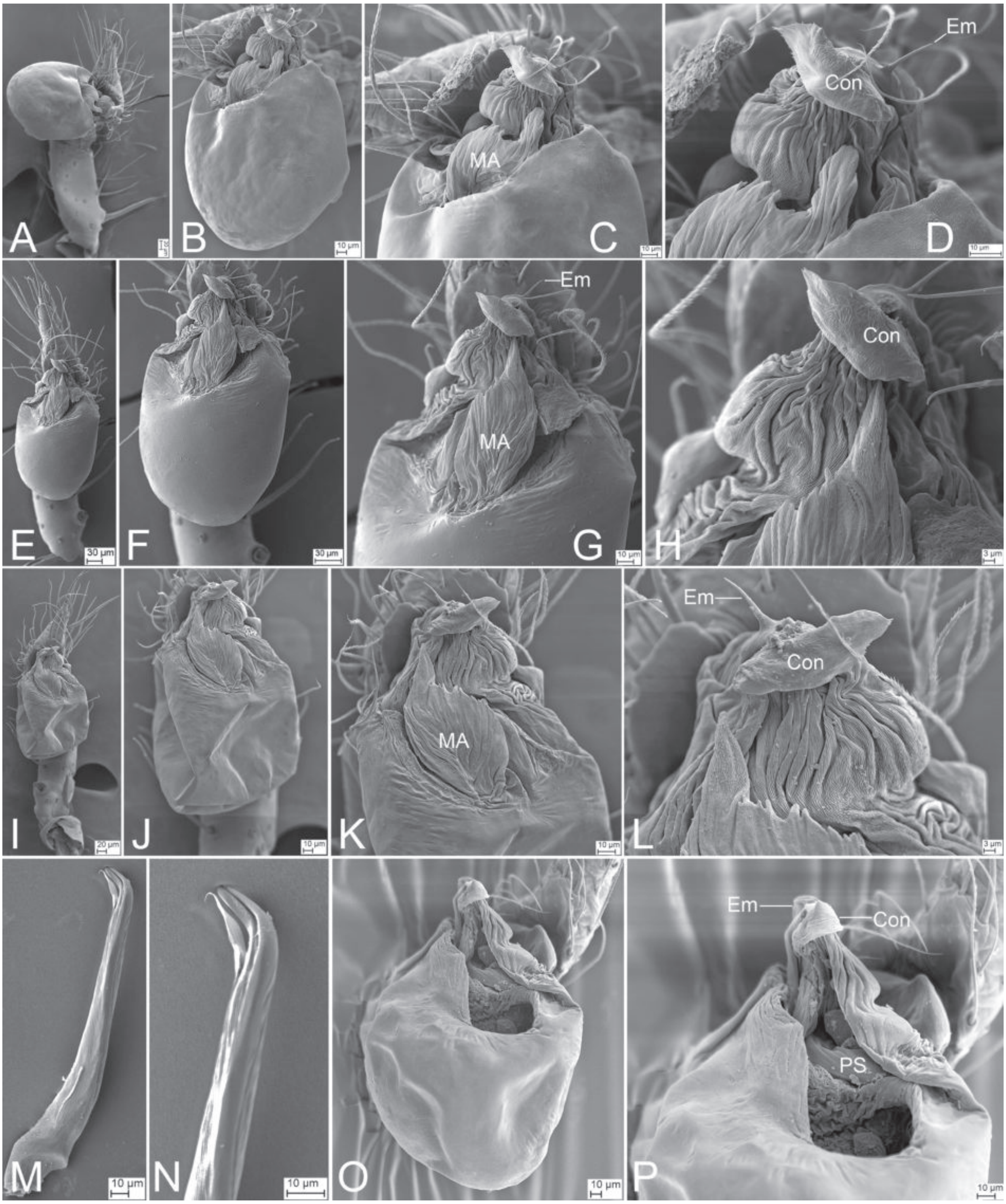

Figure 8. SEM micrographs of male palps, *Leptonetela* spp. **A** *Leptonetela dawu* sp. nov., left palp, ventral view **B** same, ventral view **C** same, detail of tegular apophysis, ventral view **D** same, detail of conductor and embolus, ventral view **E** *L. yuanhaoi* sp. nov., left palp, ventral view **F** same, ventral view **G** same, detail of tegular apophysis, ventral view **H** same, detail of conductor and embolus, ventral view **I** *L. yuanhaoi* sp. nov., right palp, ventral view **J** same, ventral view **K** same, detail of tegular apophysis, ventral view **L** same, detail of conductor, ventral view **M** *L. zuojiashanensis* sp. nov., right palp, tibial spine, prolateral view **N** same, detail of the tip, prolateral view **O** same, bulb, ventral view **P** same, detail of tegular apophysis, ventral view. Abbreviations: Con – conductor, Em – embolus, MA – medial apophysis, PS – prolateral sclerite.

prolateral sclerite, but can be separated from it by the tibia having two spines including one very thick and strong spine proximally (vs a row of spines and lacking a thick and strong spine) (Figs 7B–D, 8M–P). It also resembles that of *L. mengzongensis* Wang & Li, 2011 (Wang and Li 2011: 10, fig. 24B–D) in having the horn-like prolateral sclerite, but can be easily distinguished from it by the tibia with a thick and strong proximal spine (vs slender) (Figs 7B–D, 8M, N).

Description. Male (holotype). Habitus as in Fig. 7A. Total length 2.08. Carapace 0.92 long, 0.89 wide. Eye sizes and interdistances: ALE 0.10, PME 0.09, PLE 0.11; ALE–PME 0.14, PLE–PLE 0.11, PLE–PME 0.05; AER 0.20, PER 0.24. Clypeus 0.13 high. Chelicerae (Fig. 7A) with seven promarginal and five retromarginal teeth. Sternum (Fig. 7A) hexagonal, longer than wide, posterior end blunt. Leg measurements: **I** 6.17 (1.71, 0.35, 1.66, 1.45, 1.00); **II** 4.93 (1.32, 0.32, 1.39, 1.11, 0.79); **III** 3.90 (0.96, 0.39, 1.01, 0.97, 0.57); **IV** (1.55, 0.29, other segments broken). Pedicel 0.10. Abdomen 1.06 long, 0.82 wide.

Coloration (Fig. 7A). Carapace yellow to dark brown, with dark radial stripes and mottled markings on lateral margin. Chelicerae yellow. Endites yellow, with mottled dark spots. Labium, anterior part dark brown, posterior part yellow. Sternum dark brown, medially with a yellow stripe. Legs yellow to dark brown. Abdomen with three pairs of dark brown spots and three dark chevron-shaped stripes.

Palp (Figs 7B–D, 8M–P). Tibia with two long spines retrolaterally, the basal one very thick and strong, with the trifurcate tip; cymbium lacking spine. Tip of bulb: prolateral lobe finger-like; prolateral sclerite relatively long, buffalo-horn-shaped; conductor membranous, narrowed, with curved tip; embolus short, indistinct, strongly bending dorsally.

Female. Unknown.

Distribution. Known only from the type locality in Jiangxi Province, China (Fig. 29).

Etymology. The name is taken from the type locality.

Genus *Longileptoneta* Seo, 2015

Longileptoneta guadunensis Yao & Liu, sp. nov.

https://zoobank.org/CFBD8259-59E8-41C9-8DF4-5FF173E53CCA
Figs 9, 10, 28A
Vernacular name: 挂墩长弱蛛

Material examined. ***Holotype*:** ♂, **China:** Fujian Province, Nanping City, Wuyishan County Level City, Xingcun Town, Guadun Village, 27°43'56.88"N, 117°39'30.29"E, 3.X.2023, Y. Yao, J. Gong & M. Wu leg. (Lep-13). ***Paratype*:** 1 ♂, same data as the holotype (Lep-13).

Diagnosis. This species is similar to that of *Longileptoneta shenxian* Wang & Li, 2020 (in Wang et al. 2020: 698, fig. 12A–D) and *L. yamasakii* Ballarin & Eguchi, 2022 (Ballarin and Eguchi 2022: 373, figs 1C, 3A–C) in having the banded median apophysis with transparent tip, but can be distinguished from it by the carapace with six eyes (vs absent in *L. shenxian*), the tibia with one canine tooth-like apophysis armed with a short straight spine (vs one columnar apophysis, armed with one long, curved spine in *L. shenxian* and *L. yamasakii*) and the

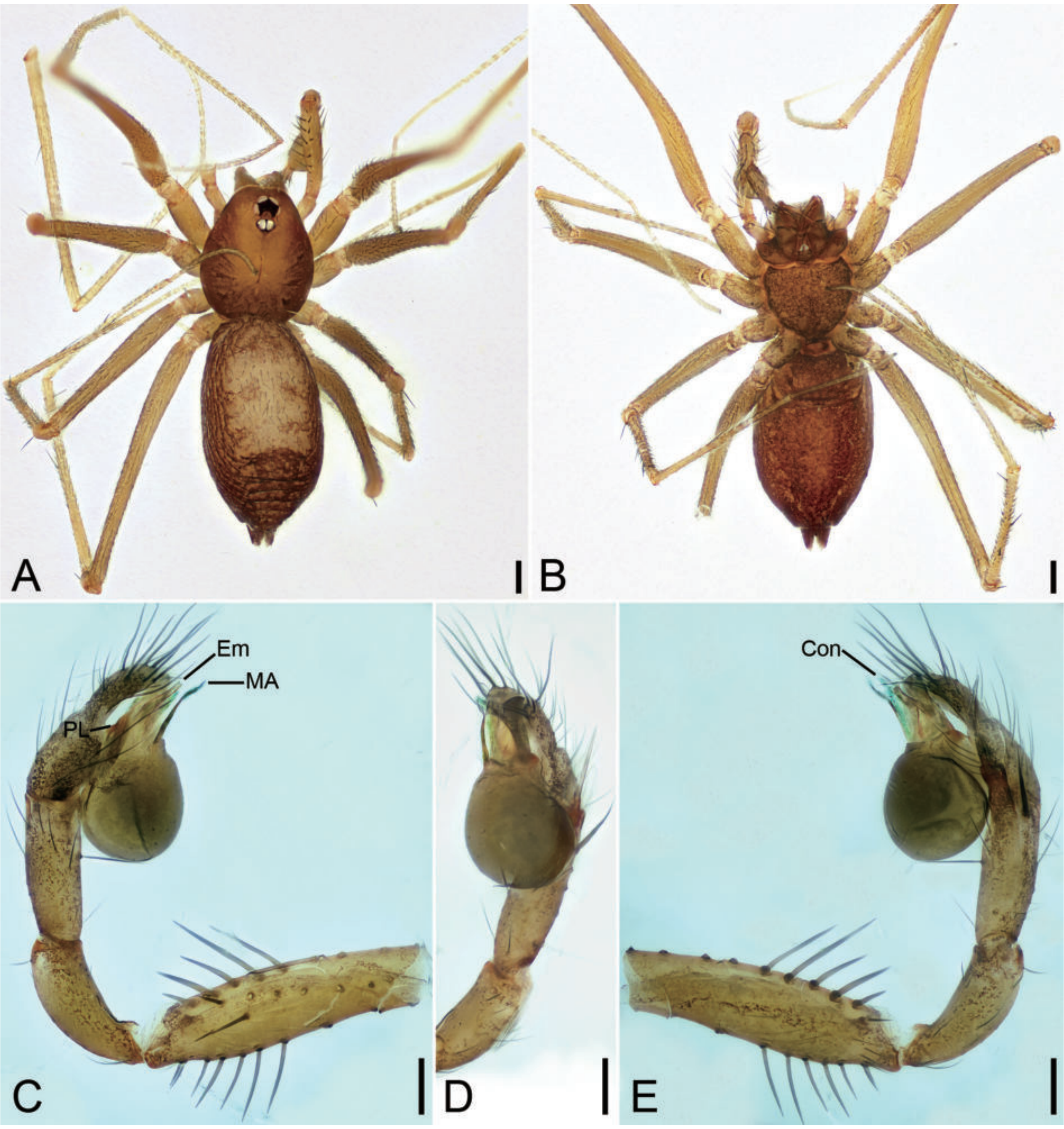

Figure 9. *Longileptoneta guadunensis* sp. nov., male holotype **A** habitus, dorsal view **B** same, ventral view **C** palp, prolateral view **D** same, ventral view, slightly retrolateral **E** same, retrolateral view. Abbreviations: Con – conductor, Em – embolus, MA – medial apophysis, PL – prolateral lobe. Scale bars: 0.2 mm (**A, B**); 0.1 mm (**C–E**).

wedge-shaped prolateral lobe (vs mastoid in *L. shenxian* and sub-triangular in *L. yamasakii*) (Figs 9C–E, 10D, E).

Description. Male (holotype). Habitus as in Fig. 9A, B. Total length 2.32. Carapace 0.86 long, 0.75 wide. Eye sizes and interdistances: ALE 0.08, PME 0.08, PLE 0.08; ALE–PME 0.11, PLE–PLE 0.12, PLE–PME 0.04; AER 0.14, PER 0.18. Clypeus 0.13 high. Chelicerae (Fig. 9B) with eight promarginal and six retromarginal teeth. Endites with several long spines laterally. Labium sub-rectangular, with several long setae. Sternum (Fig. 9B) shield-shaped, wider than long, posterior end blunt. Leg measurements: **I** 8.03 (2.08, 0.28, 2.63, 1.84, 1.20); **II** 4.73

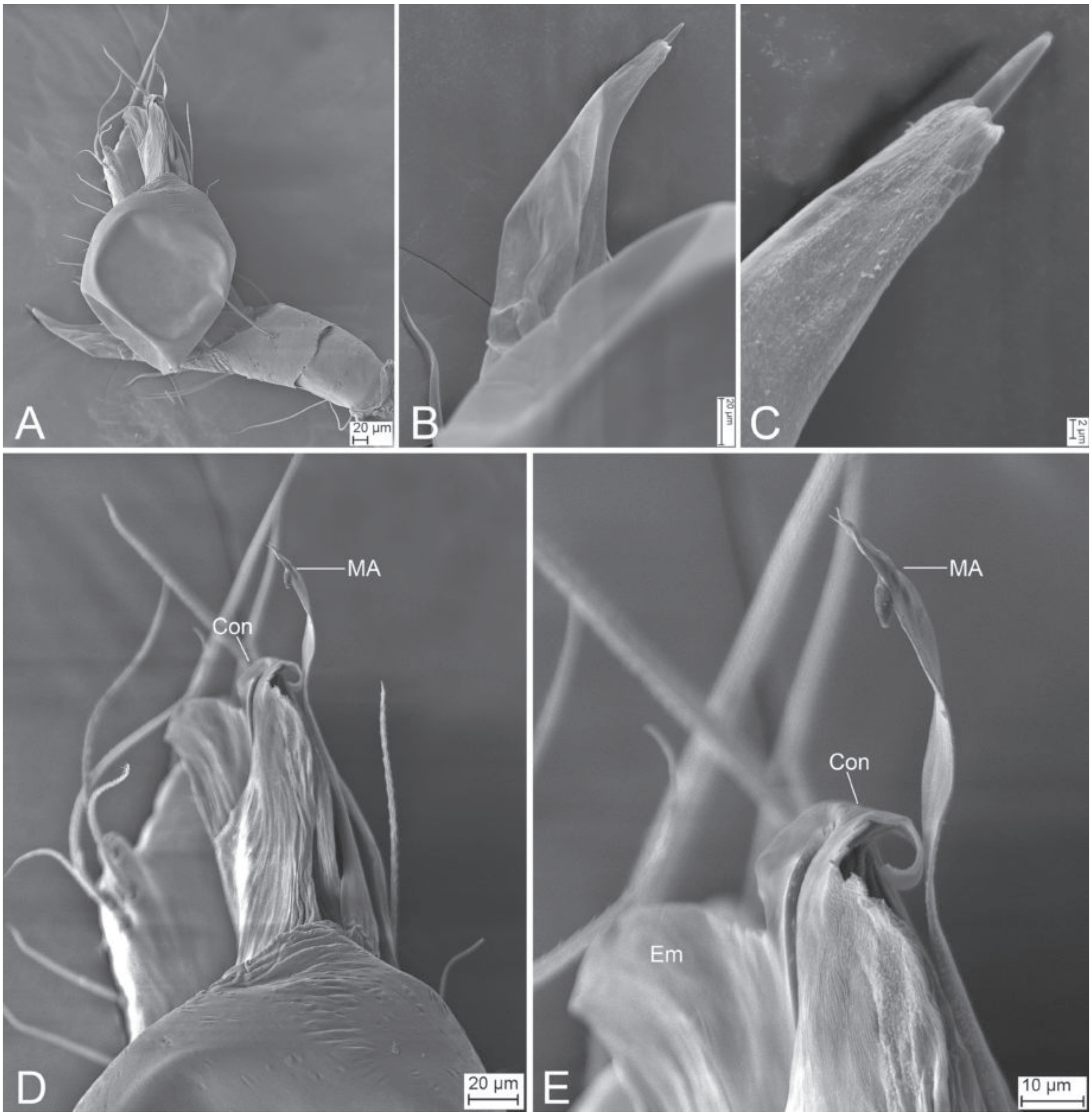

Figure 10. SEM micrographs of *Longileptoneta guadunensis* sp. nov., right palp, male holotype **A** ventral view **B** tibial apophysis, ventral view **C** detail of the tip of tibial apophysis, ventral view **D** detail of tegular apophysis, ventral view **E** same, ventral view. Abbreviations: Con – conductor, Em – embolus, MA – medial apophysis.

(1.52, 0.23, 1.28, 0.97, 0.73); III 4.45 (1.17, 0.19, 1.29, 1.08, 0.72); IV 6.08 (1.51, 0.25, 1.98, 1.57, 0.77). Pedicel 0.05. Abdomen 1.42 long, 0.83 wide.

Coloration (Fig. 9A, B). Carapace yellow to black-brown, with radial dark stripes near submargin. Chelicerae, endites and labium brown. Sternum yellow to dark brown, mottled. Legs yellow, with sparse mottling. Abdomen dorsally yellowish, mottled in lateral and posterior parts; venter brown, mottled.

Palp (Figs 9C–E, 10). Femur with three rows of long strong spines ventrally, dorsally, and prolaterally; patella without spine; tibia with two spines: one canine tooth-like apophysis, armed with a short straight spine subapically, and a thick and long spine near the base of anterior one. Cymbium with a constriction subapically. Tip of bulb: one long banded median apophysis, distally furcate; prolateral lobe wedge-shaped, large; conductor membranous, anteriorly curved. Embolus indistinct, with broad base.

Female. Unknown.

Distribution. Known only from the type locality in Fujian Province, China (Fig. 29).

Etymology. The name is taken from the type locality.

Longileptoneta huboliao **Yao & Liu, sp. nov.**

https://zoobank.org/28EAA35E-4067-43E3-B40F-10B70FF5A93B
Figs 11–13, 28B
Vernacular name: 虎伯寮长弱蛛

Material examined. ***Holotype*****:** ♂, **China:** Fujian Province, Zhangzhou City, Nanjing County, Huboliao Nature Reserve, Huboliao area, 24°31'2.88"N, 117°14'53.47"E, 08.XI.2023, Y. Yao, J. Gong, R. Zhao & M. Wu leg. (Lep-15). ***Paratype*****:** 1 ♀, the same data as the holotype (Lep-15); 1 ♂, 24°31'20.98"N, 117°17'32.01"E, 09.XI.2023, Y. Yao, J. Gong, R. Zhao & M. Wu leg. (Lep-15).

Diagnosis. The male of this species is similar to that of *Longileptoneta shenxian* Wang & Li, 2020 (in Wang et al. 2020: 698, fig. 12A–D) in having the bulb with an extruded coniform anterior part and three rows of spines, but can be distinguished from it by the carapace with six eyes (vs absent), the tibia with one long columnar apophysis armed with a long spine (vs one short columnar apophysis, armed with one long, curved spine) and the long needle-like prolateral sclerite (vs thick) (Figs 11, 12). The female can be easily separated from *L. shenxian* (Wang et al. 2020: 698, fig. 13C) by the bell-shaped atrium, but can be separated by the carapace with six eyes (vs absent) and the distal spermathecal stalk lacking a coil (vs present) (Fig. 13).

Description. Male (holotype). Habitus as in Fig. 11A, B. Total length 2.11. Carapace 0.96 long, 0.82 wide. Eye sizes and interdistances: ALE 0.08, PME 0.07, PLE 0.07; ALE–PME 0.12, PLE–PLE 0.11, PLE–PME 0.05; AER 0.15, PER 0.19. Clypeus 0.18 high. Chelicerae (Fig. 11B) with nine promarginal and eight retromarginal teeth. Endites with several long setae laterally. Labium sub-rectangular, anteriorly with more than two pairs of strong setae. Sternum (Fig. 11B) shield-shaped, slightly longer than wide, with several long setae on the surface, posterior end blunt. Leg measurements: I 8.04 (1.93, 0.31, 2.55, 2.18, 1.07); II 5.58 (1.54, 0.28, 1.62, 1.34, 0.80); III 4.20 (1.00, 0.27, 1.29, 1.09, 0.55); IV 6.23 (1.76, 0.29, 2.05, 1.57, 0.56). Pedicel 0.11. Abdomen 1.03 long, 0.67 wide.

Coloration (Fig. 11A, B). Carapace reddish to black-brown, with radial dark brown stripes along submargin. Chelicerae and endites reddish to dark brown. Labium brown. Sternum brown, mottled. Legs reddish to black-brown, mottled. Abdomen medial part reddish, other parts dark brown, mottled; venter dark brown, mottled.

Palp (Figs 11C–E, 12). Femur with three rows of short strong spines ventrally, dorsally, and prolaterally; patella lacking spine; tibia with one long columnar apophysis, armed with a long straight spine. Tip of bulb: prolateral lobe willow leaf-shaped; prolateral sclerite long, needle-like; conductor membranous, with serrate tip. Embolus with blunt tip, shorter than prolateral sclerite.

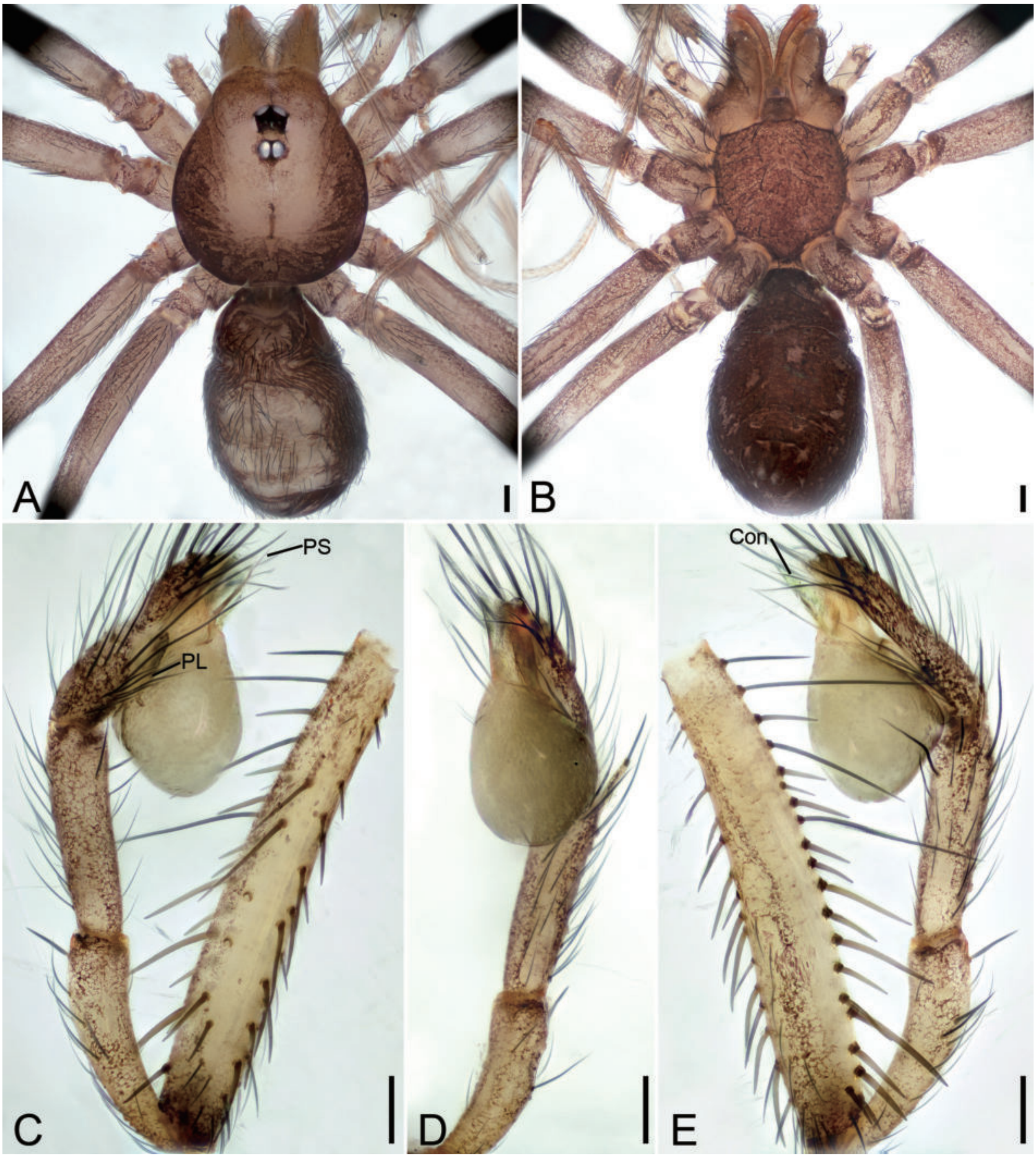

Figure 11. *Longileptoneta huboliao* sp. nov., male holotype **A** habitus, dorsal view **B** same, ventral view **C** palp, prolateral view **D** same, ventro-retrolateral view **E** same, retrolateral view. Abbreviations: Con – conductor, PL – prolateral lobe, PS – prolateral sclerite. Scale bars: 0.1 mm.

Female (paratype). Habitus as in Fig. 13A, B. Total length 1.77. Carapace 0.89 long, 0.76 wide. Eye sizes and interdistances: ALE 0.08, PME 0.07, PLE 0.07; ALE–PME 0.12, PLE–PLE 0.1, PLE–PME 0.05; AER 0.15, PER 0.18. Clypeus 0.14 high. Chelicerae (Fig. 13B) with nine promarginal and eight retromarginal teeth. Endites with several long spines anterolaterally. Sternum (Fig. 13B) shield-shaped, nearly as long as wide, with dense scale-like surface, lateral

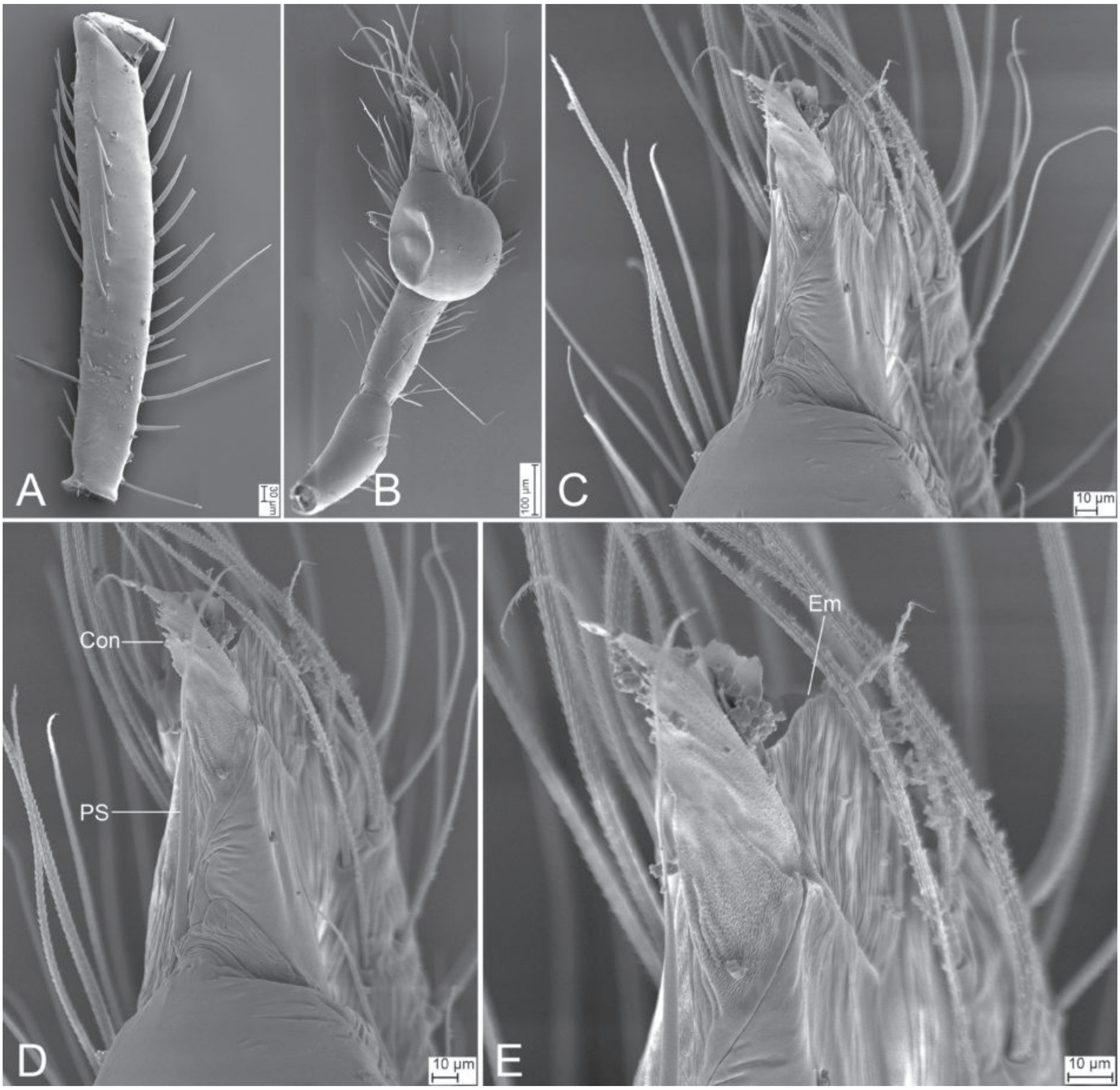

Figure 12. SEM micrographs of *Longileptoneta huboliao* sp. nov., male palp **A** femur, prolateral view **B** palp, ventral view **C** detail of tegular apophysis, ventral view **D** same, ventral view **E** detail of embolus, ventral view. Abbreviations: Con – conductor, Em – embolus, PS – prolateral sclerite.

margin thickened, posterior end blunt. Leg measurements: I 6.25 (1.90, 0.23, 1.97, 1.53, 0.62); II 5.19 (1.44, 0.26, 1.52, 1.22, 0.75); III 4.18 (1.13, 0.28, 1.24, 0.89, 0.64); IV 6.38 (1.66, 0.28, 2.07, 1.58, 0.79). Pedicel 0.04. Abdomen 0.84 long, 0.59 wide.

Vulva (Fig. 13C). Internal genitalia with semicircle atrium, oval spermathecae, and convoluted spermathecal stalk including three coils.

Note. The right spermathecal stalk and spermathecae were extruded deformation after covering cover slip when we took a photo under microscope.

Distribution. Known only from the type locality in Fujian Province, China (Fig. 29).

Etymology. The name is taken from the type locality, noun in apposition.

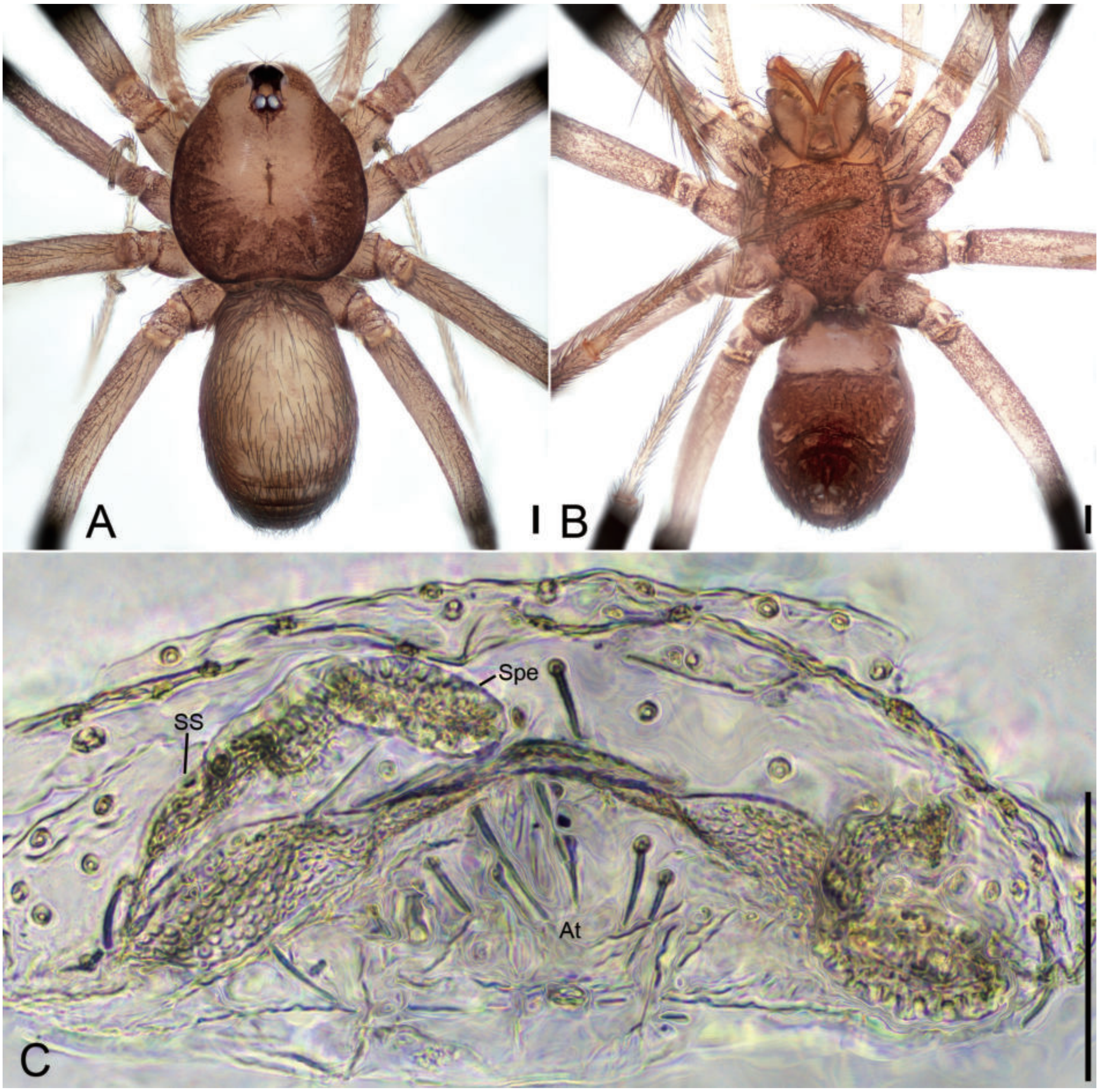

Figure 13. *Longileptoneta huboliao* sp. nov., female paratype **A** habitus, dorsal view **B** same, ventral view **C** vulva, dorsal view. Abbreviations: At – atrium, Spe – spermathecae, SS – spermathecae stalk. Scale bars: 0.1 mm.

Longileptoneta jiaxiani **Yao & Liu, sp. nov.**
https://zoobank.org/1D1C5F43-5FFE-4C15-9987-E304121393C9
Figs 14–16, 28C
Vernacular name: 嘉贤长弱蛛

Material examined. ***Holotype*****:** ♂, **China:** Fujian Province, Fuzhou City, Cangshan District, Jinshan campus in Fujian Agriculture and Forestry University, 26°2'21.12"N, 119°19'56.66"E, 29.IV.2023, Y. Yao, J. Gong & M. Wu leg. (Lep-10). ***Paratype*****:** 1 ♀, the same data as the holotype (Lep-10).

Diagnosis. The male of this species is similar to that of *L. shenxian* Wang & Li, 2020 (in Wang et al. 2020: 698, fig. 12A–D) in having the bulb with an

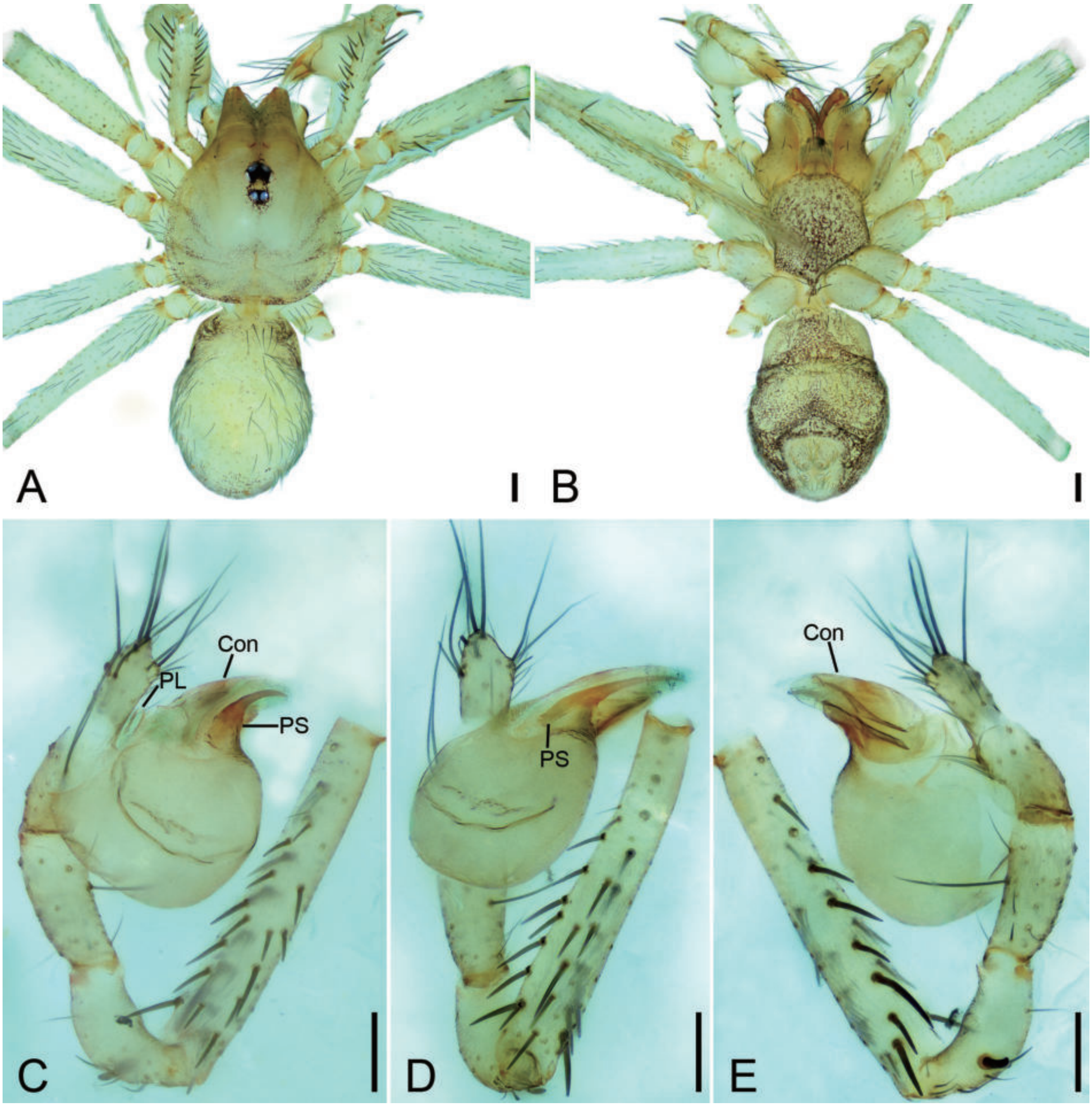

Figure 14. *Longileptoneta jiaxiani* sp. nov., male palp, holotype **A** habitus, dorsal view **B** same, ventral view **C** palp, prolateral view **D** same, ventral view, slightly prolateral **E** same, retrolateral view. Abbreviations: Con – conductor, PL – prolateral lobe, PS – prolateral sclerite. Scale bars: 0.1 mm.

extruded coniform anterior part and the spine-like prolateral sclerite, but can be distinguished from it by the carapace with six eyes (vs absent) and the patella with a very strong and thick spine (vs absent), and the hook-shaped embolus (vs the narrowed lamellar embolus) (Figs 14C–E, 15). The female resembles *L. shenxian* (Wang et al. 2020: 698, fig. 13A–C) in having a bell-shaped atrium, but can be separated by the carapace with eyes (vs lacking) and the C-shaped spermathecal stalk (vs S-shaped) (Fig. 16).

Description. Male (holotype). Habitus as in Fig. 14A, B. Total length 1.46. Carapace 0.68 long, 0.65 wide. Eye sizes and interdistances: ALE 0.05, PME 0.04, PLE 0.05; ALE–PME 0.07, PLE–PLE 0.07, PLE–PME 0.03; AER 0.10, PER

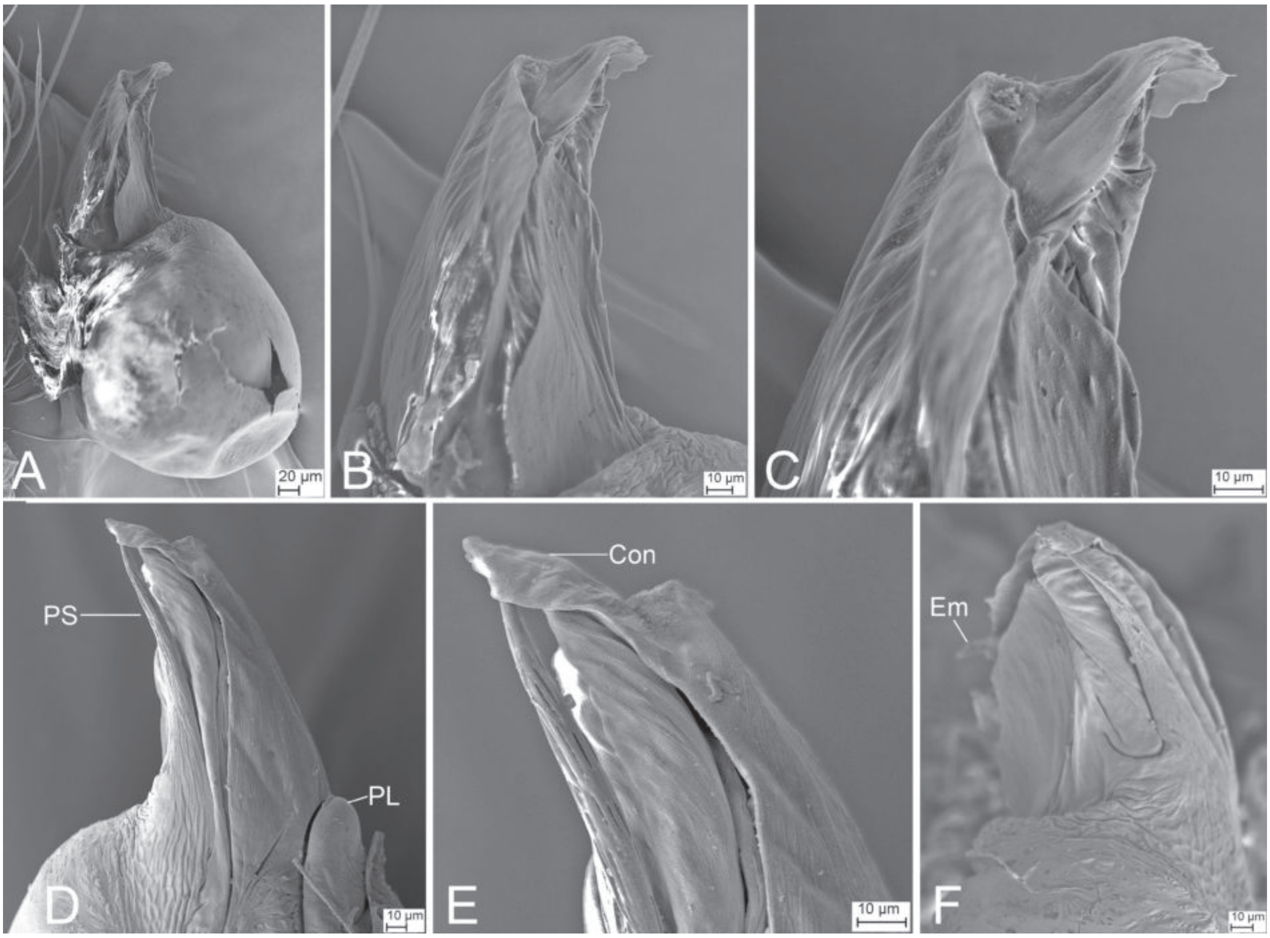

Figure 15. SEM micrographs of *Longileptoneta jiaxiani* sp. nov., right male palp, holotype **A** right palp, retrolateral view **B** same, detail of tegular apophysis, retrolateral view **C** same, retrolateral view **D** same, detail of tegular apophysis, prolateral view, **E** same, detail of conductor, prolateral view **F** same, detail of embolus, ventral view. Abbreviations: Con – conductor, Em – embolus, PL – prolateral lobe, PS – prolateral sclerite.

0.12. Clypeus 0.13 high. Chelicerae (Fig. 14B) with eight promarginal and five retromarginal teeth. Endites with several long spines laterally and seven leaf-shaped setae. Labium sub-rectangular, anterolaterally with two pairs of strong setae and anteriorly with eight setae. Sternum (Fig. 14B) shield-shaped, longer than wide, with dense setae laterally, posterior end blunt. Leg measurements: **I** 5.23 (1.34, 0.19, 1.61, 1.29, 0.80); **II** (1.42, 0.28, other segments broken); **III** 4.52 (1.19, 0.29, 1.15, 1.08, 0.81); **IV** (1.68, 0.24, other segments broken). Pedicel 0.06. Abdomen 0.73 long, 0.53 wide.

Coloration (Fig. 14A, B). Carapace yellowish to black, with radial dark stripes submedially and mottled markings on lateral margin. Chelicerae yellow to dark brown. Endites yellow. Labium yellow. Sternum yellow to black, mottled. Legs yellow. Abdomen, dorsally yellow, mottled in anterior and posterior parts; venter mottled.

Palp (Figs 14C–E, 15). Femur with four rows of short strong spines ventrally, dorsally, and prolaterally; patella with one thick, strong spine proximally; tibia lacking spine and apophysis. Cymbium with a distinct constriction medially. Tip of bulb: one spine-like prolateral sclerite; prolateral lobe lamellar; conductor membranous, with banded tip, slightly shorter than prolateral sclerite. Embolus indistinct, wrapping with conductor, hook-shaped.

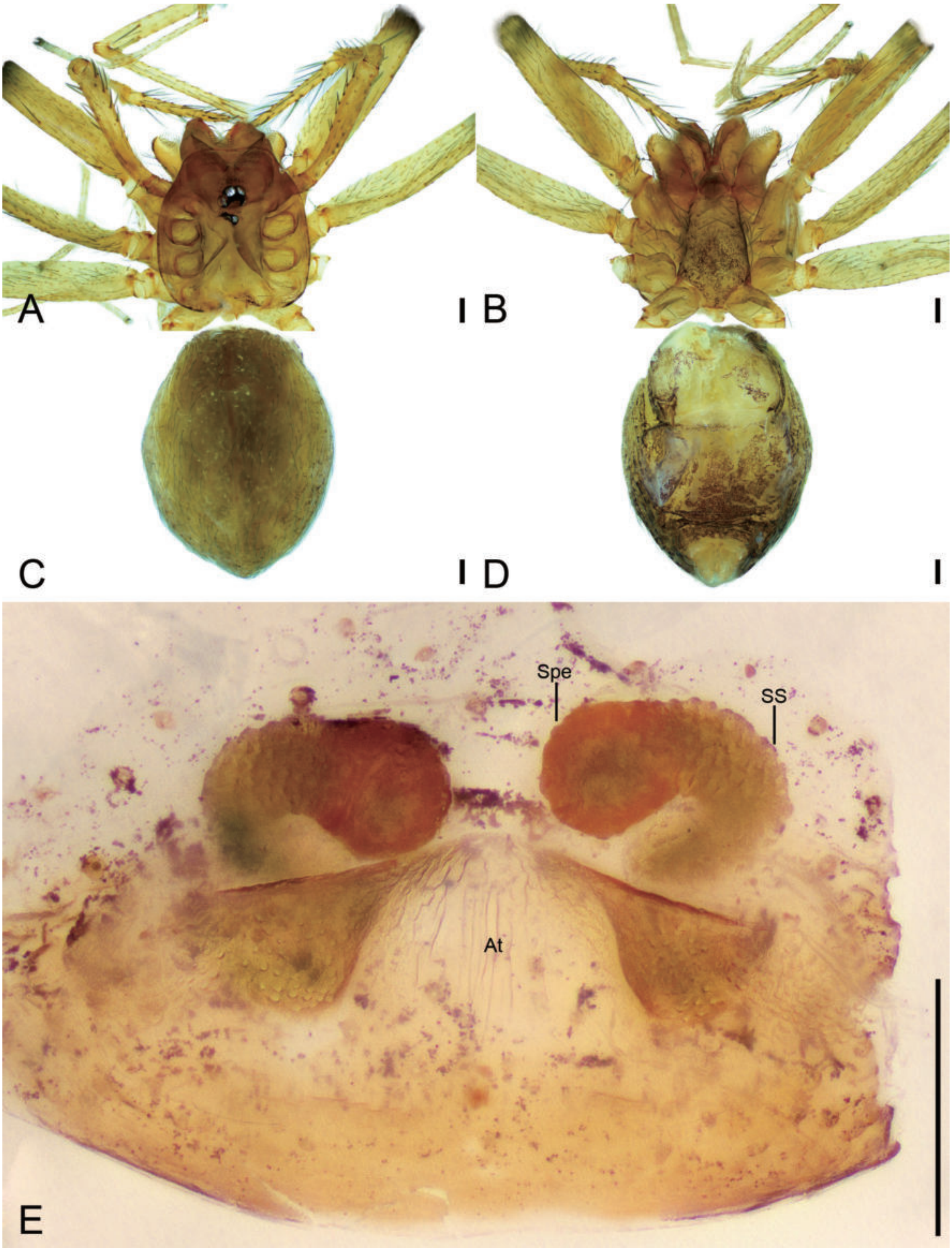

Figure 16. *Longileptoneta jiaxiani* sp. nov., female paratype **A** carapace, dorsal view **B** same ventral view **C** abdomen, dorsal view **D** same, ventral view **E** vulva, dorsal view. Abbreviations: At – atrium, Spe – spermathecae, SS – spermathecae stalk. Scale bars: 0.1 mm.

Female (paratype). Habitus as in Fig. 16A–D. Total length 1.92. Carapace 0.78 long, 0.67 wide. Eye sizes and interdistances: ALE 0.05, PME 0.04, PLE 0.05; ALE–PME 0.09, PLE–PLE 0.09, PLE–PME 0.05; AER 0.10, PER 0.15.

Clypeus 0.15 high. Chelicerae (Fig. 16B) with eight promarginal and seven retromarginal teeth. Endites with several long spines anterolaterally. Sternum (Fig. 16B) shield-shaped, nearly as long as wide, with dense scale-like surface, lateral margin thickened, posterior end blunt. Leg measurements: I (1.40, 0.29, 1.69, other segments broken); II 4.33 (1.21, 0.29, 1.23, 0.99, 0.61); III 3.41 (0.98, 0.13, 0.93, 0.81, 0.56); IV (1.34, 0.21, 1.48, 1.16, other segments broken). Abdomen 1.14 long, 0.80 wide.

Vulva (Fig. 16E). Internal genitalia with sub-trapezoidal atrium, slightly swollen spermathecae, and convoluted spermathecal stalk including three coils.

Distribution. Known only from the type locality in Fujian Province, China (Fig. 29).

Etymology. The species is named after Mr Jiaxian Gong, who collected the type specimens.

Longileptoneta letuensis **Yao & Liu, sp. nov.**

https://zoobank.org/AAB005C2-29DD-462B-94F6-DB83706C1911

Figs 17, 18, 28D

Vernacular name: 乐土长弱蛛

Material examined. ***Holotype***: ♂, **CHINA:** Fujian Province, Zhangzhou City, Nanjing County, Huboliao Nature Reserve, Letu Rainforest area, 24°54'11.82"N, 117°13'15.3"E, 11.XI.2023, Y. Yao, J. Gong, R. Zhao & M. Wu leg. (Lep-16).

Diagnosis. The male of this species can be easily distinguished from other members of this genus by the very large curved tibial apophysis armed with a short spine-like tip (Fig. 17E).

Description. Male (holotype). Habitus as in Fig. 17A, B. Total length 1.78. Carapace 1.04 long, 0.64 wide. Eye sizes and interdistances: ALE 0.04, PME 0.04, PLE 0.04; ALE–PME 0.07, PLE–PLE 0.07, PLE–PME 0.03; AER 0.09, PER 0.12. Clypeus 0.06 high. Chelicerae (Fig. 17B) with eight promarginal and six retromarginal teeth. Endites with several long spines laterally. Sternum (Fig. 17B) shield-shaped, nearly as long as wide, with abundant long setae on surface, posterior end blunt. Leg measurements: I 4.75 (1.34, 0.24, 1.46, 1.14, 0.57); II 3.60 (0.95, 0.24, 1.10, 0.86, 0.45); III 2.80 (0.85, 0.22, 0.79, 0.58, 0.36); IV 4.3 (1.19, 0.24, 1.28, 1.02, 0.57). Pedicel 0.08. Abdomen 0.67 long, 0.66 wide.

Coloration (Fig. 17A, B). Carapace yellowish, with radial yellow stripes submarginally. Chelicerae, endites and labium yellow. Sternum yellowish, mottled. Legs yellowish. Abdomen dorsally yellowish, with three pairs of indistinct reddish spots; venter mottled.

Palp (Figs 17C–E, 18). Femur with two rows of short strong spines ventrally and prolaterally; patella without spine; tibia with a very long curved apophysis, distally armed with a short straight spine, longer than tibia. Cymbium with a distinct constriction medially. Tip of bulb: one long flagelliform prolateral sclerite; prolateral lobe oval; conductor membranous, medially with a groove. Embolus indistinct.

Female. Unknown.

Distribution. Known only from the type locality in Fujian Province, China (Fig. 29).

Etymology. The name is taken from the type locality.

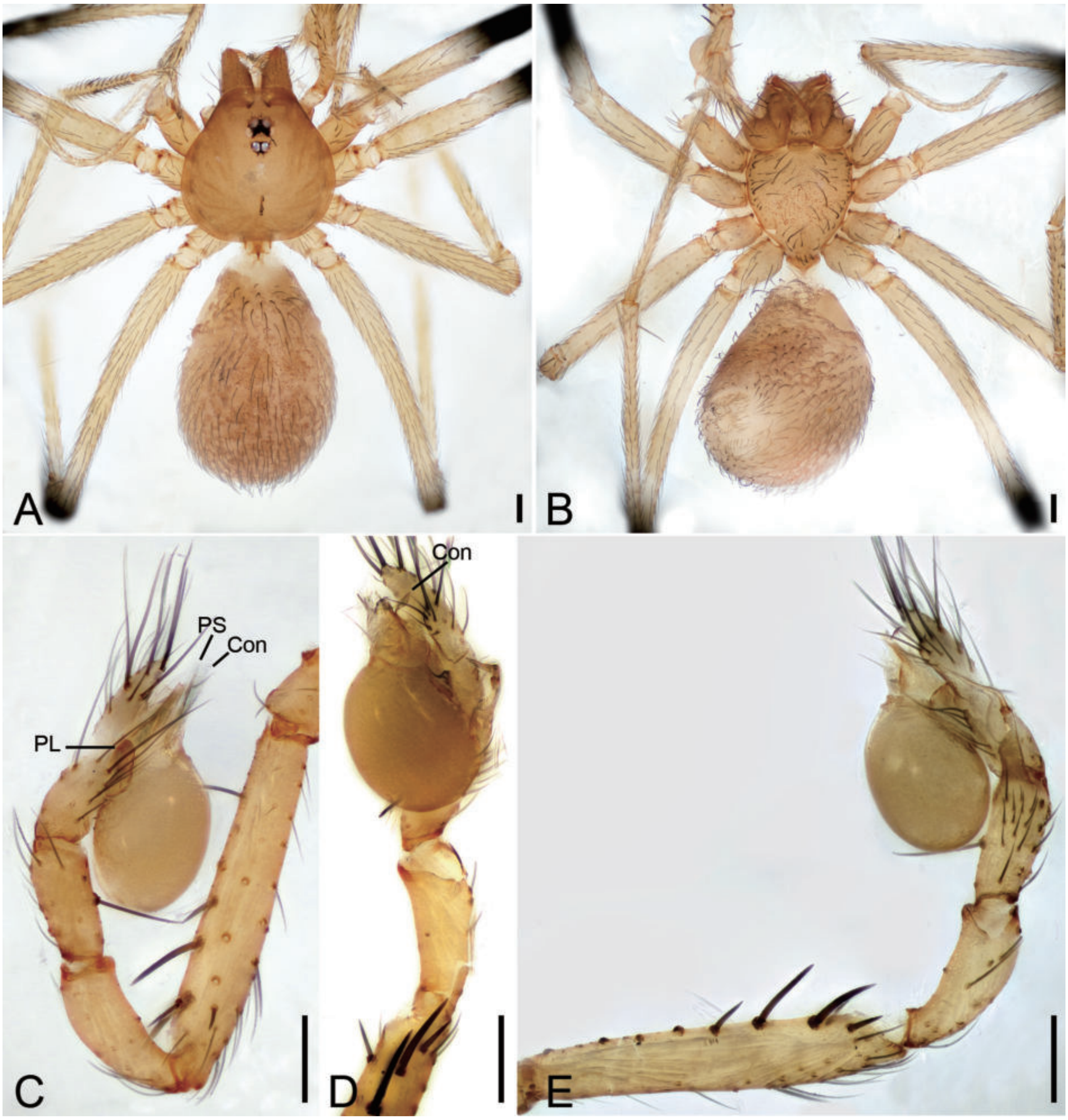

Figure 17. *Longileptoneta letuensis* sp. nov., male holotype **A** habitus, dorsal view **B** same, ventral view **C** palp, prolateral view **D** same, ventral view, slightly retrolateral **E** same, retrolateral view. Abbreviations: Con – conductor, PL – prolateral lobe, PS – prolateral sclerite. Scale bars: 0.1 mm.

Longileptoneta renzhouensis Yao & Liu, sp. nov.

https://zoobank.org/EA2C7512-B01E-4021-934F-8E40EE47555F
Figs 19–21, 28E
Vernacular name: 仁洲长弱蛛

Material examined. ***Holotype*:** ♂, **China:** Fujian Province, Fuzhou City, Minhou County, Jingxi Town, Renzhou Village, Sandiejing Forest Park, 26°16'3.31"N, 119°09'5.08"E, 24.X.2023, Y. Yao, J. Gong, R. Zhao & M. Wu leg. (Lep-14).

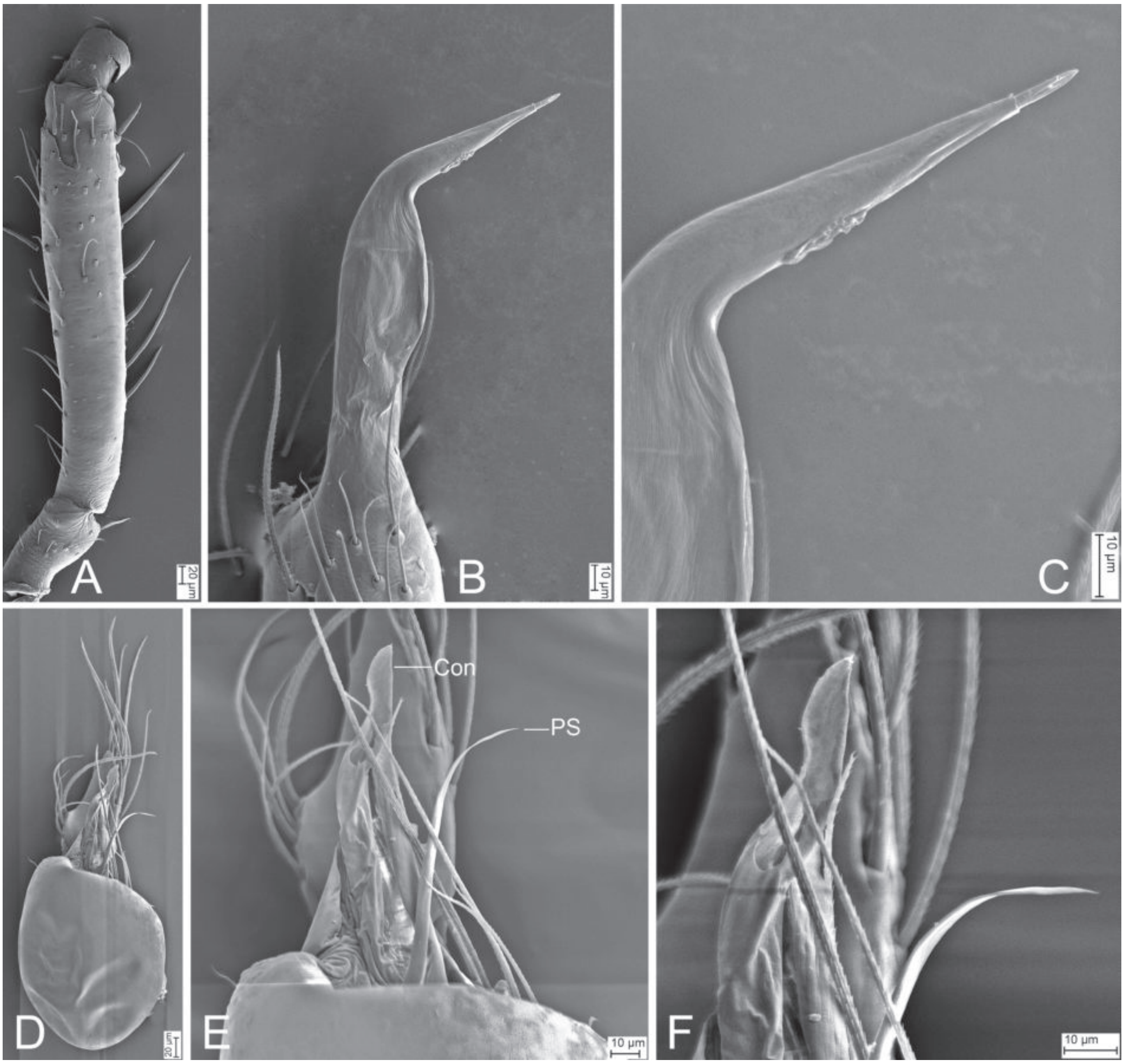

Figure 18. SEM micrographs of *Longileptoneta letuensis* sp. nov., male right palp **A** femur, retrolateral view **B** tibial apophysis, retrolateral view **C** detail of the tip of tibial apophysis, retrolateral view **D** bulb, ventral view **E** same, detail of tegular apophysis, ventral view **F** same, detail of conductor, ventral view. Abbreviations: Con – conductor, PS – prolateral sclerite.

***Paratype*:** 2 ♂, 2 ♀, the same data as the holotype (Lep-14); 1 ♂, 29.X.2023, other data as same as the holotype (Lep-14).

Diagnosis. The male of this species can be easily distinguished from other members of this genus by the very long curved spine-like prolateral sclerite with a feathery tip (Figs 19C–E, 20). The female resembles *L. zhuxian* Wang & Li, 2020 (Wang et al. 2020: 700, fig. 16C) in having spheroid spermathecae and the subtrapezoid atrium, but can be separated by the slightly curved spermathecal stalk (vs waved) (Fig. 21C).

Description. Male (holotype). Habitus as in Fig. 19A, B. Total length 2.73. Carapace 1 long, 0.9 wide. Eye sizes and interdistances: ALE 0.08, PME 0.08, PLE 0.08; ALE–PME 0.13, PLE–PLE 0.12, PLE–PME 0.04; AER 0.16, PER 0.20.

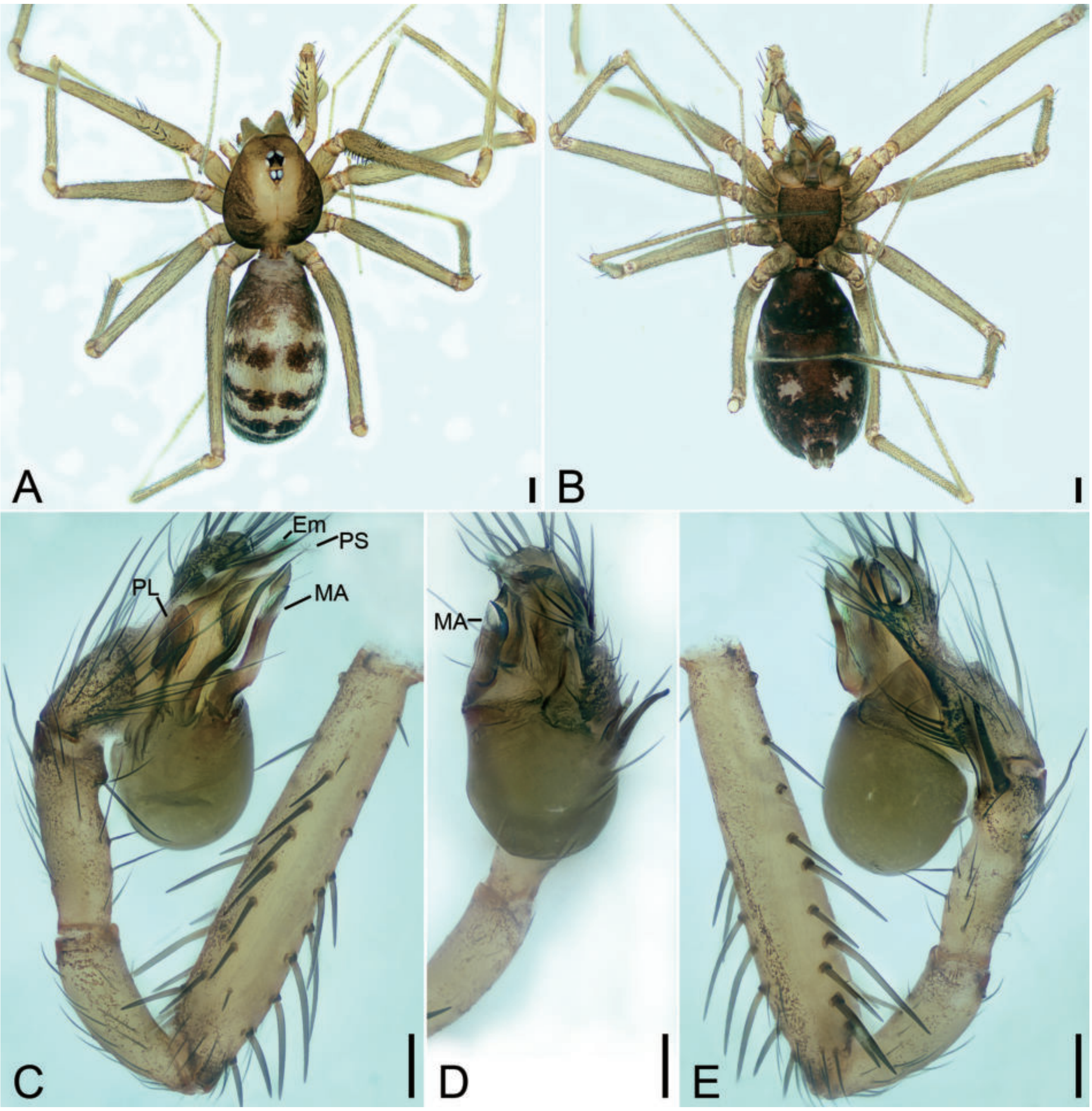

Figure 19. *Longileptoneta renzhouensis* sp. nov., male holotype **A** habitus, dorsal view **B** B habitus, ventral view **C** palp, prolateral view **D** same, ventral view **E** same, retrolateral view. Abbreviations: Em – embolus, MA – medial apophysis, PL – prolateral lobe, PS – prolateral sclerite. Scale bars: 0.2 mm (**A, B**); 0.1 mm (**C–E**).

Clypeus 0.22 high. Chelicerae (Fig. 19B) with nine promarginal and ten retromarginal teeth. Endites with several long setae laterally. Labium sub-rectangular, anteriorly with more than three pairs of strong setae. Sternum (Fig. 19B) shield-shaped, slightly longer than wide, with sparse setae on surface, posterior end blunt. Leg measurements: **I** 8.38 (2.21, 0.33, 2.62, 2.19 1.03); **II** 5.62 (1.57, 0.31, 1.86, 1.26, 0.62); **III** 5.21 (1.37, 0.34, 1.40, 1.26, 0.84); **IV** 6.95 (1.76, 0.33, 2.22, 1.68, 0.96). Pedicel 0.11. Abdomen 1.60 long, 1.01 wide.

Coloration (Fig. 19A, B). Carapace yellow, with radial yellow stripes submarginally, clypeus mottled. Chelicerae and endites yellow to dark brown, mottled. Labium brown, mottled. Sternum dark brown, mottled. Legs yellow to dark

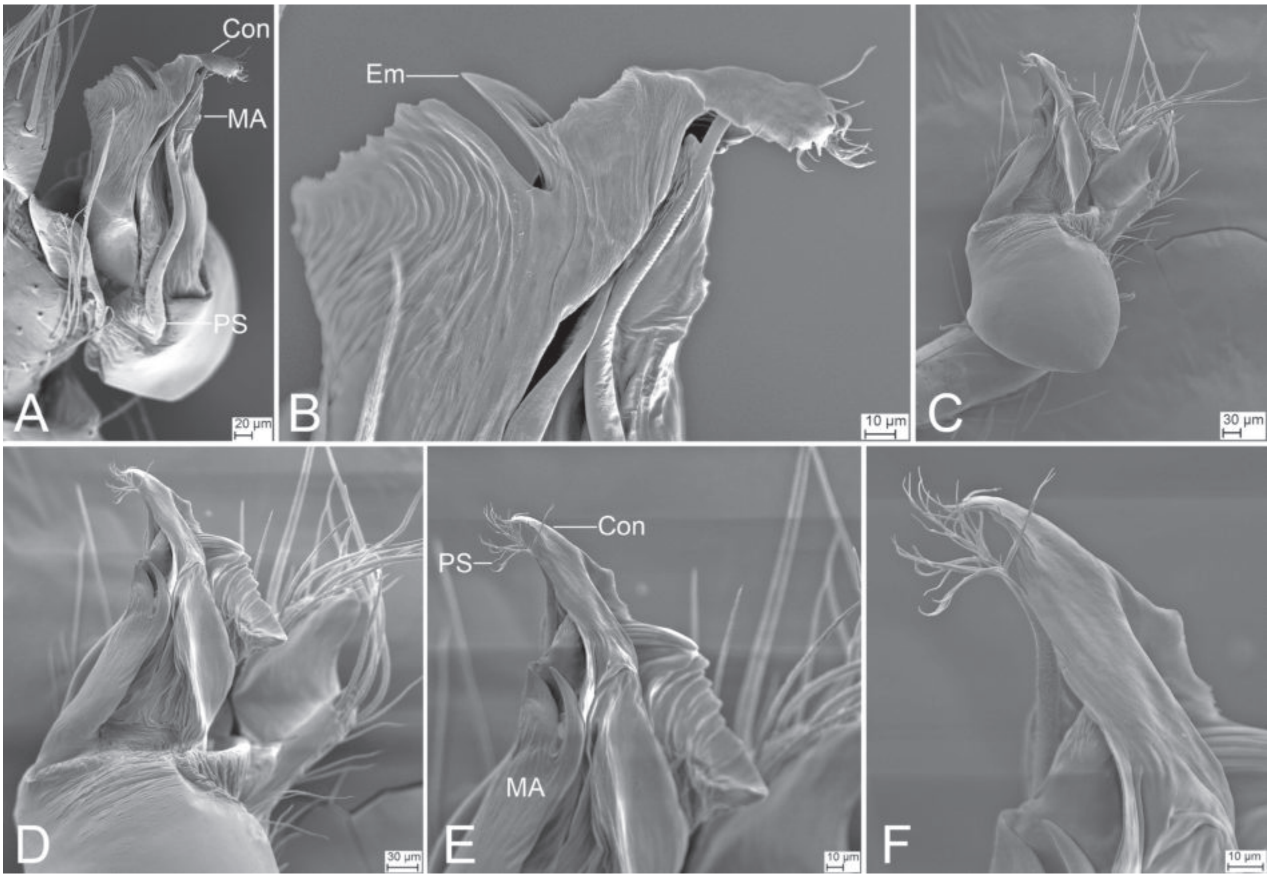

Figure 20. SEM micrographs of *Longileptoneta renzhouensis* sp. nov., male palp **A** palp, prolateral view **B** detail of tegular apophysis, prolateral view **C** palp, ventral view **D** same, detail of tegular apophysis, ventral view **E** same, ventral view **F** same, detail of conductor and prolateral sclerite, ventral view. Abbreviations: Con – conductor, Em – embolus, MA – medial apophysis, PS – prolateral sclerite.

brown, mottled. Abdomen dorsally yellowish, with three pairs of black spots, anterior part mottled; venter black, mottled.

Palp (Figs 19C–E, 20). Femur with three rows of short strong spines ventrally, dorsally, and prolaterally; patella lacking spine; tibia with one columnar apophysis, armed with one straight spine, and one long and very thick spine, slightly shorter than the apophysis. Cymbium with a distinct constriction medially. Tip of bulb: one broad median apophysis, with a furcate tip, including one long membranous and one hook-shaped; prolateral lobe finger-like; conductor membranous, touching with prolateral sclerite; prolateral sclerite waved, needle-like, with a feathery tip. Embolus short hook-shaped, with a broad base.

Female (paratype). Habitus as in Fig. 21A, B. Total length 2.23. Carapace 0.94 long, 0.86 wide. Eye sizes and interdistances: ALE 0.09, PME 0.08, PLE 0.08; ALE–PME 0.11, PLE–PLE 0.11, PLE–PME 0.04; AER 0.17, PER 0.18. Clypeus 0.19 high. Chelicerae (Fig. 21B) with nine promarginal and ten retromarginal teeth. Endites with several long spines anterolaterally. Sternum (Fig. 21B) shield-shaped, nearly as long as wide, with dense scale-like surface, lateral margin thickened, posterior end blunt. Leg measurements: **I** 7.40 (1.98, 0.31, 2.42, 1.57, 1.12); **II** 5.56 (1.51, 0.33, 1.63, 1.23, 0.86); **III** 4.59 (1.33, 0.31, 1.21, 1.03, 0.71); **IV** 6.70 (1.98, 0.33, 1.96, 1.47, 0.96). Pedicel 0.04. Abdomen 1.41 long, 0.84 wide.

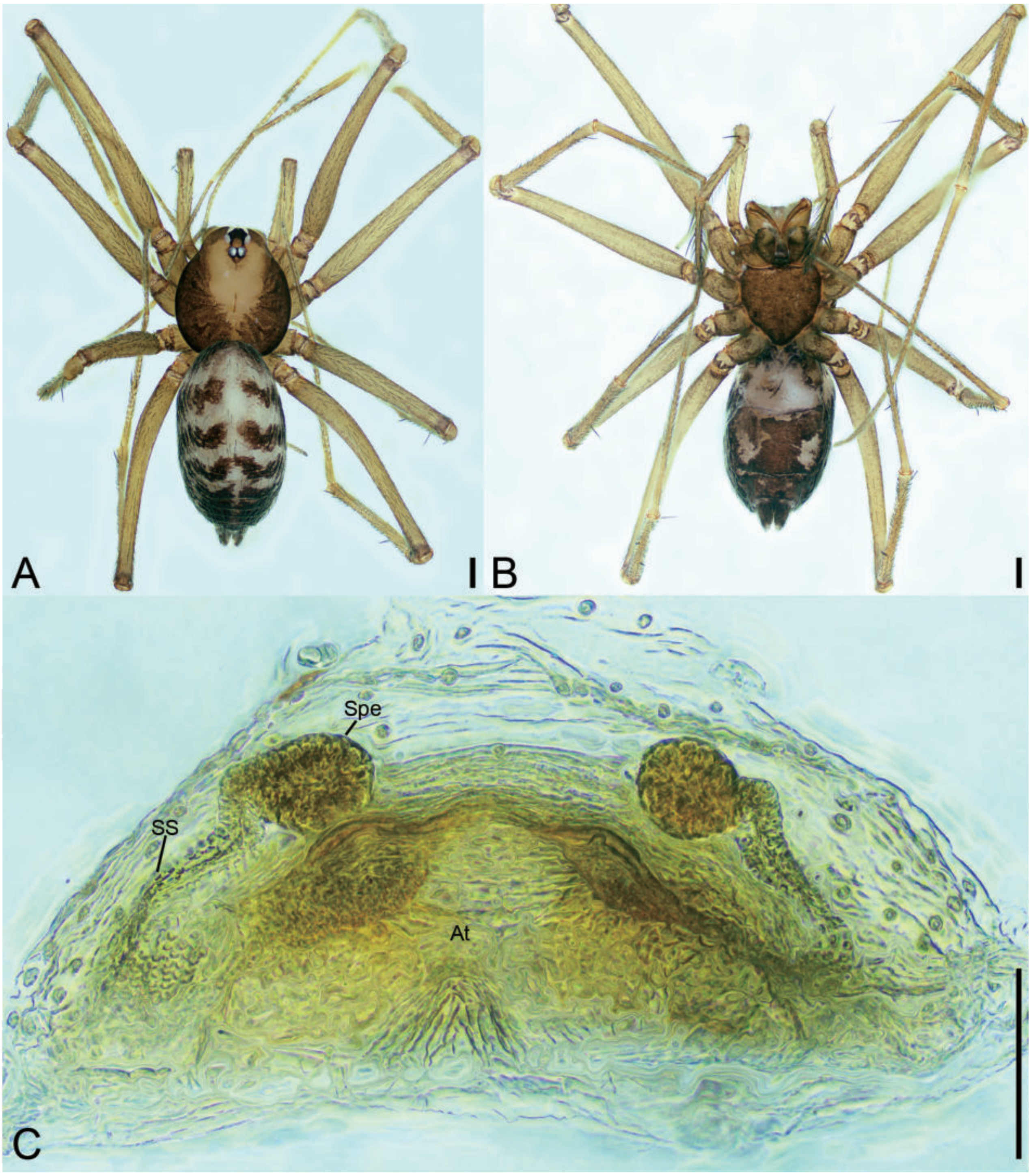

Figure 21. *Longileptoneta renzhouensis* sp. nov., female paratype **A** habitus, dorsal view **B** same, ventral view **C** vulva, dorsal view. Abbreviations: At – atrium, Spe – spermathecae, SS – spermathecae stalk. Scale bars: 0.2 mm (**A, B**); 0.1 mm (**C**).

Vulva (Fig. 21C). Internal genitalia with sub-trapezoidal atrium, spherical spermathecae, and slightly curved spermathecal stalk.

Distribution. Known only from the type locality in Fujian Province, China (Fig. 29).

Etymology. The name is taken from the type locality.

Longileptoneta tianmenensis Yao & Liu, sp. nov.

https://zoobank.org/DC584FE1-B618-452A-96C1-97625ED931B0
Figs 22–24, 28F
Vernacular name: 天门山长弱蛛

Material examined. ***Holotype*:** ♂, **China:** Fujian Province, Fuzhou City, Yongtai County, Geling Town, Yangxi Village, Tianmen Mountain, 25°49'5.34"N, 119°00'40.79"E, 10.IV.2023, J. Gong, R. Zhao & M. Wu leg. (Lep-11). ***Paratype*:** 2 ♀, 14.X.2023, Y. Yao & M. Wu leg, other data as same as the holotype (Lep-11).

Diagnosis. The male of this species is similar to that of *L. huboliao* sp. nov. in having the femur with three rows of strong spines, one columnar tibial apophysis, armed with a short spine-like tip on palp and a needle-like prolateral sclerite, but can be easily distinguished from it by the rod-like median apophysis (vs lacking) the membranous conductor lacking a serrulate tip (vs present) (Figs 22C–G, 23). The female resembles *L. huboliao* sp. nov. in having a bell-like atrium and the spermathecal stalk lacking a spiral twist, but can be separated by the oval spermathecae (vs tube-shaped) (Fig. 24C).

Description. Male (holotype). Habitus as in Fig. 22A, B. Total length 2.14. Carapace 0.94 long, 0.82 wide. Eye sizes and interdistances: ALE 0.10, PME 0.08, PLE 0.07; ALE–PME 0.10, PLE–PLE 0.13, PLE–PME 0.03; AER 0.17, PER 0.18. Clypeus 0.18 high. Chelicerae (Fig. 22B) with nine promarginal and eight retromarginal teeth. Endites with several long setae laterally. Labium sub-rectangular, anteriorly with more than two pairs of strong setae. Sternum (Fig. 22B) shield-shaped, slightly longer than wide, with sparse setae on surface, posterior end blunt. Leg measurements: I 8.41 (2.63, 0.23, 2.94, 2.06, 0.55); II 6.62 (1.88, 0.24, 1.99, 1.44, 1.07); III 5.34 (1.50, 0.24, 1.50, 1.27, 0.83); IV 7.05 (1.90, 0.29, 2.12, 1.93, 0.81). Pedicel 0.06. Abdomen 1.11 long, 0.70 wide.

Coloration (Fig. 22A, B). Carapace yellowish to black-brown, with dark radial stripes on lateral margin. Chelicerae yellow to brown, mottled. Labium dark brown. Sternum yellow to black, mottled. Legs yellow, mottled. Abdomen, dorsally yellowish, with two pairs of spots; venter dark.

Palp (Figs 22C–G, 23). Femur with three rows of short strong spines ventrally, dorsally, and prolaterally; patella lacking strong spine; tibia with a columnar apophysis, armed with one short straight spine. Cymbium with a distinct constriction medially. Tip of bulb: one rod-like median apophysis, thick; prolateral lobe oval, lamellar; conductor membranous, shorter than median apophysis. Embolus hook-shaped, beneath conductor.

Female (paratype). Habitus as in Fig. 24A, B. Total length 2.22. Carapace 1.01 long, 0.88 wide. Eye sizes and interdistances: ALE 0.09, PME 0.07, PLE 0.06; ALE–PME 0.12, PLE–PLE 0.12, PLE–PME 0.06; AER 0.17, PER 0.19. Clypeus 0.11 high. Chelicerae (Fig. 24B) with nine promarginal and twelve retromarginal teeth. Endites with several long spines anterolaterally. Sternum (Fig. 24B) shield-shaped, nearly as long as wide, with dense scale-like surface, lateral margin thickened, posterior end blunt. Leg measurements: I 9.06 (2.42, 0.32, 2.86, 2.21, 1.25); II 6.69 (1.73, 0.33, 2.07, 1.65, 0.91); III 5.20 (1.46, 0.31, 1.39, 1.20, 0.84); IV 6.65 (2.02, 0.27, 1.96, 1.48, 0.92). Abdomen 1.2 long, 0.88 wide.

Vulva (Fig. 24C). Internal genitalia with sub-trapezoidal atrium, slightly swollen spermathecae, and convoluted spermathecal stalk including three coils.

Figure 22. *Longileptoneta tianmenensis* sp. nov., male holotype **A** habitus, dorsal view **B** same, ventral view **C** femur, retrolateral view **D** same, prolateral view **E** palp, prolateral view **F** same, ventral view **G** same, retrolateral view. Abbreviations: Con – conductor, Em – embolus, MA – medial apophysis, PL – prolateral lobe, PS – prolateral sclerite. Scale bars: 0.2 mm (**A, B**); 0.1 mm (**C–G**).

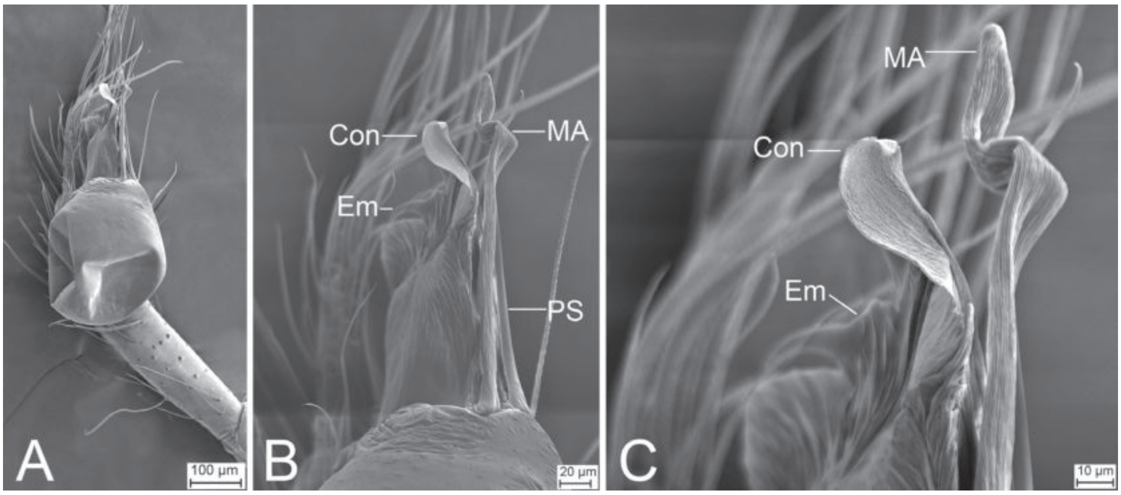

Figure 23. SEM micrographs of *Longileptoneta tianmenensis* sp. nov., male right palp, holotype **A** ventral view **B** detail of tegular apophysis, ventral view **C** same, ventral view. Abbreviations: Con – conductor, Em – embolus, MA – medial apophysis, PS – prolateral sclerite.

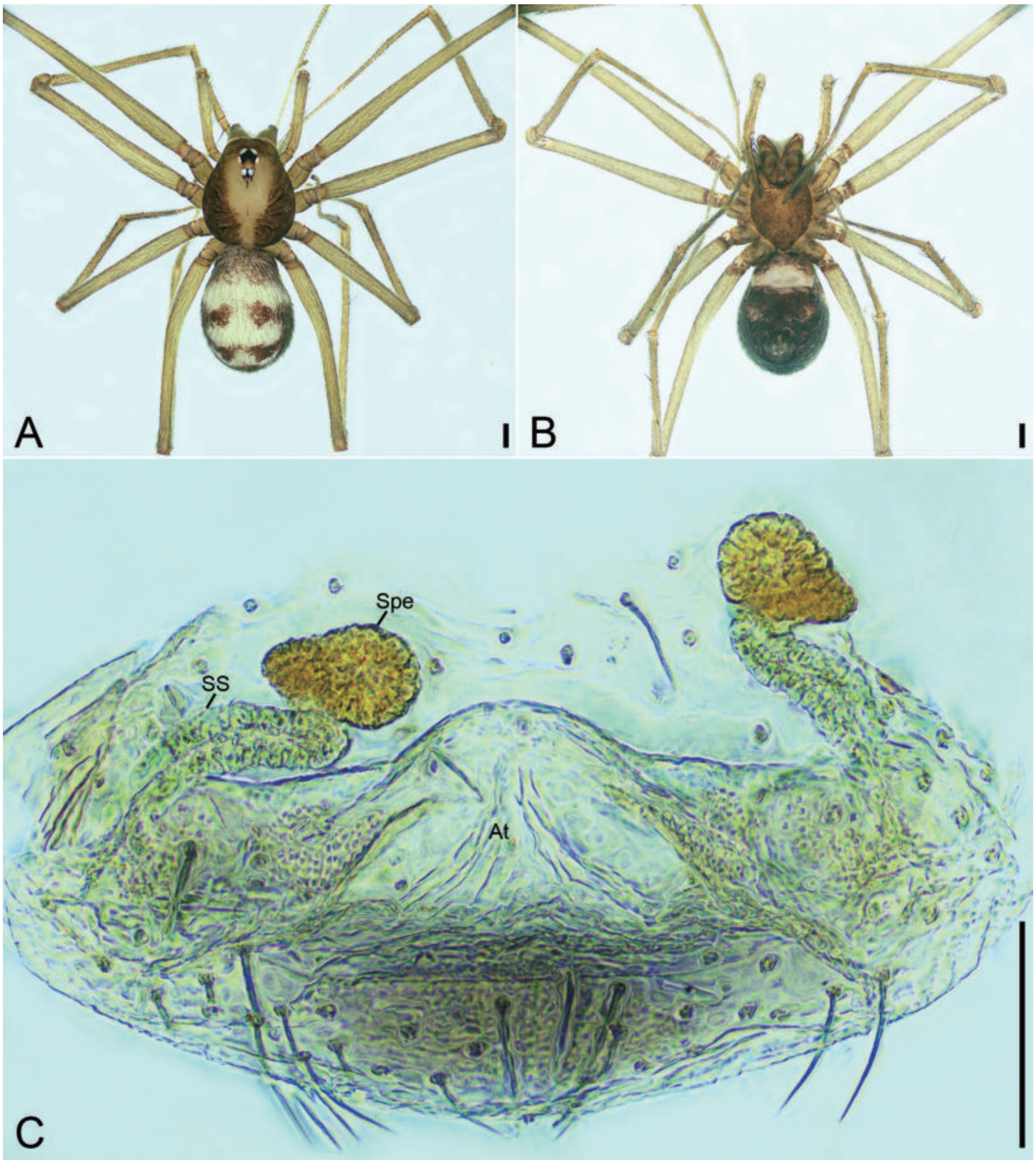

Figure 24. *Longileptoneta tianmenensis* sp. nov., female paratype **A** habitus, dorsal view **B** same, ventral view **C** vulva, dorsal view. Abbreviations: At – atrium, Spe – spermathecae, SS – spermathecae stalk. Scale bars: 0.2 mm (**A, B**); 0.1 mm (**C**).

Distribution. Known only from the type locality in Fujian Province, China (Fig. 29).

Etymology. The name is taken from the type locality.

Genus *Pararana* Lin & Li, 2022

Pararana mingxuani Yao & Liu, sp. nov.

https://zoobank.org/CDB6306E-1FF8-49B4-B68C-F2ECEA5FD3D5
Figs 25–27, 28G, H
Vernacular name: 明轩拟正弱蛛

Material examined. ***Holotype***: ♂, Fujian Province, Fuzhou City, Yongtai County, Geling Town, Xiyang Village, Tianmen Mountain, 25°49'7.6"N, 119°1'5.07"E, 10.IV.2023, R. Zhao, J. Gong & M. Wu leg. (Lep-9). ***Paratype*****:** 1 ♂, 1 ♀, Fujian Province, Fuzhou City, Minhou County, Nanyu Town, 25°58'24.05"N, 119°13'15.87"E, 5.VI.2023, Y. Yao, W. Zhang, M. Wu & R. Zhao leg. (Lep-9).

Diagnosis. The male of this species is similar to that of *Pararana gaofani* Lin & Li, 2022 (Lin et al. 2022: 217, figs 17A–C, 18A, B) in having the cymbium with a notch and the swollen patella, but can be easily separated by the patella with seven short tooth-like spines (vs four long relatively thick spines), the tibia with a thick spine (vs absent), the long lamellar median apophysis (vs the relatively short horn-like median apophysis) and the slightly curved rod-like embolus (vs horn-like) (Figs 25B–D, 26). The female can be easily distinguished by the oval atrium and the short S-shaped spermathecal stalk (Fig. 27C).

Description. Male (holotype). Habitus as in Fig. 25A. Total length 2.32. Carapace 0.97 long, 0.81 wide. Eye sizes and interdistances: ALE 0.05, PME 0.04, PLE 0.05; ALE–PME 0.10, PLE–PLE 0.06, PLE–PME 0.05; AER 0.11, PER 0.13. Clypeus 0.23 high. Chelicerae (Fig. 25A) with 13 promarginal and five retromarginal teeth. Endites with several long setae laterally and seven leaf-shaped setae anteriorly. Labium sub-rectangular, anterolaterally with two pairs of strong setae and anteriorly with eight setae. Sternum shield-shaped, longer than wide, with sparse setae on surface, posterior end very blunt. Leg measurements: **I** (2.00, 0.33, other segments broken); **II** 5.86 (1.54, 0.32, 1.78, 1.42, 0.80); **III** 4.78 (1.35, 0.29, 1.15, 1.19, 0.80); IV (1.77, 0.28, other segments broken). Pedicel 0.08. Abdomen 1.36 long, 0.76 wide.

Coloration (Fig. 25A). Carapace yellow, with dark radial stripes. Chelicerae yellow to brown. Endites yellow to dark brown. Labium yellow brown. Legs with dark annulations on each segment except tarsi. Abdomen yellow.

Palp (Figs 25B–D, 26). Femur with four rows of short strong spines ventrally, dorsally, and prolaterally; patella expanded, with seven stout spines; tibia with a very thick spine retrolaterally. Cymbium with a notch subapically. Bulb: prolateral lobe banded, long; embolus rod-like, slightly curved, with a broad base and a net-shaped surface; median apophysis lamellar, shorter than conductor; conductor membranous, with serrulate margin; retrolateral lobe blunt, tongue-shaped, touching base of conductor.

Female (paratype). Habitus as in Fig. 27A, B. Total length 1.83. Carapace 0.86 long, 0.76 wide. Eye sizes and interdistances: ALE 0.06, PME 0.04, PLE 0.05; ALE-PME 0.07, PLE-PLE 0.07, PLE-PME 0.05, AER 0.09, PER 0.14, Clypeus 0.20 high. Chelicerae (Fig. 27B) with 12 promarginal and four retromarginal teeth. Endites with several long spines anterolaterally. Sternum (Fig. 27B) shield-shaped, nearly as long as wide, with dense scale-like surface, lateral margin thickened, posterior end blunt. Leg measurements: **I** 4.68 (1.20, 0.24, 1.40, 1.13, 0.71); **II** 4.74 (1.18, 0.20, 1.49, 1.17, 0.70); **III** 3.03 (0.82, 0.20, 0.79, 0.74, 0.48); IV (1.03, 0.21, other segments broken). Pedicel 0.04. Abdomen 1.17 long, 0.84 wide.

Coloration (Fig. 27A, B). Darker than male.

Vulva (Fig. 27C). Internal genitalia with bell-shaped atrium, the spheroidal spermathecae and the S-shaped spermathecal stalk including two turns.

Distribution. Known only from the type locality in Fujian Province, China (Fig. 29).

Etymology. The species is named after Mr Mingxuan Wu, who collected the type specimens.

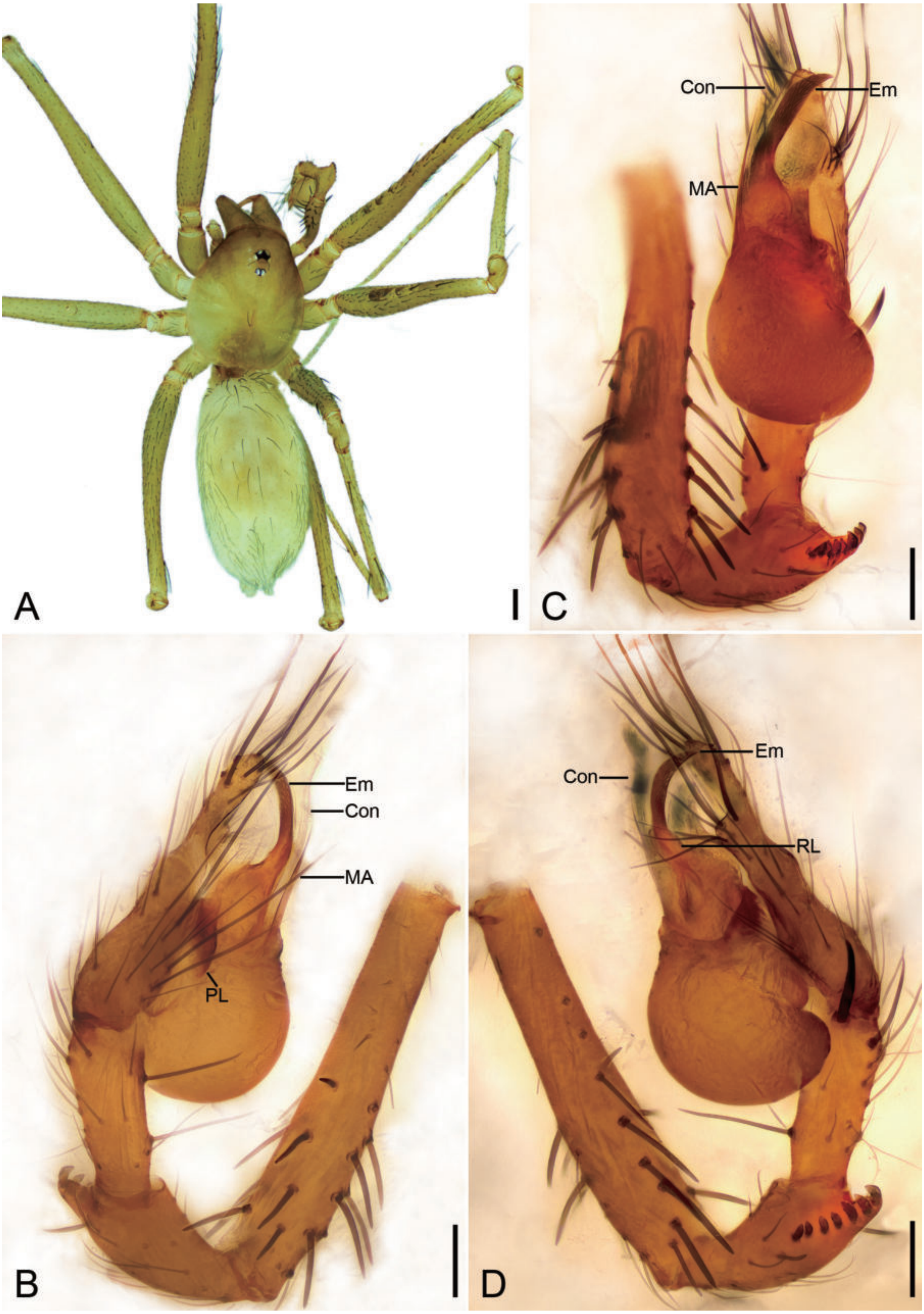

Figure 25. *Pararana mingxuani* sp. nov., male holotype **A** habitus, dorsal view **B** palp, prolateral view **C** same, ventral view **D** same, retrolateral view. Abbreviations: Con – conductor, Em – embolus, MA – medial apophysis, PL – prolateral lobe, RL – retrolateral lobe. Scale bars: 0.2 mm (**A**); 0.1 mm (**B–D**).

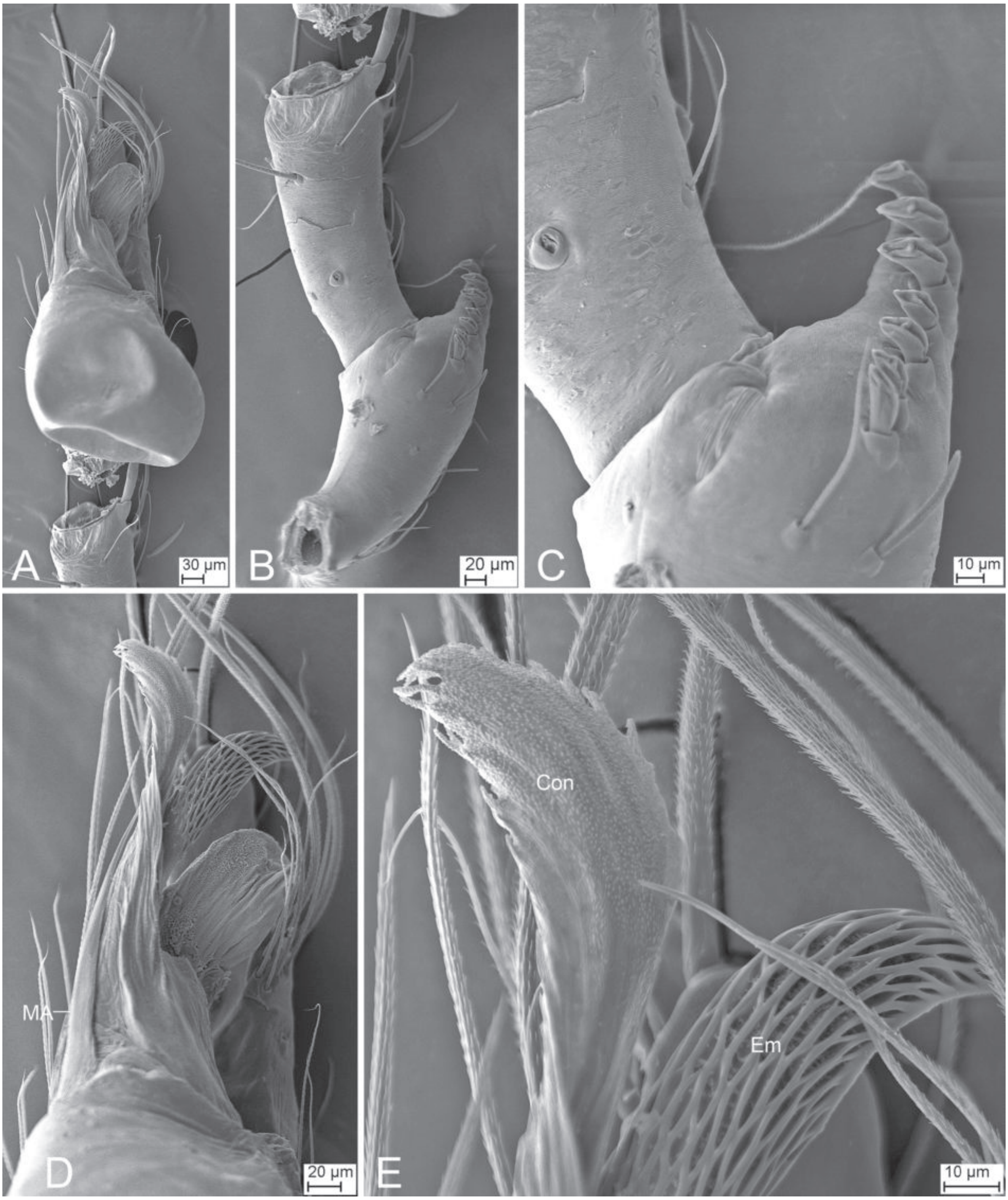

Figure 26. SEM micrographs of *Pararana mingxuani* sp. nov., male palp **A** ventral view **B** patella, retrolateral view **C** detail of patellar spines, retrolateral view **D** detail of tegular apophysis, ventral view **E** detail of conductor and embolus, ventral view. Abbreviations: Con – conductor, Em – embolus, MA – medial apophysis.

Discussion

At present, China is the most diverse region for Leptonetidae (144 species), followed by the USA (60 species), Korea (58 species), Japan (53 species), France

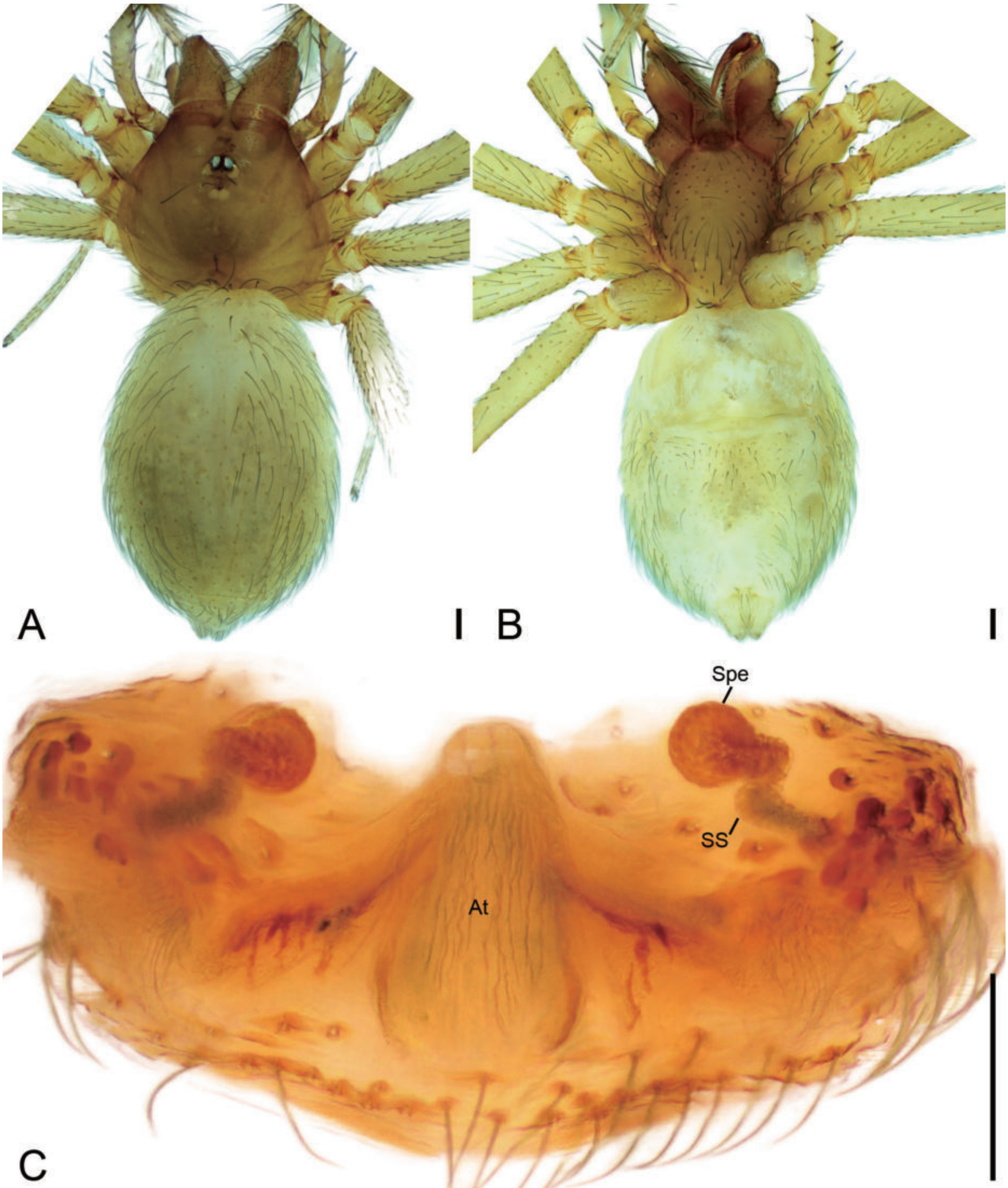

Figure 27. *Pararana mingxuani* sp. nov., female paratype **A** habitus, dorsal view **B** same, ventral view **C** vulva, dorsal view. Abbreviations: At – atrium, Spe – spermathecae, SS – spermathecae stalk. Scale bars: 0.1 mm.

(26), and Greece (16), with few species found in the remaining regions (29 species; WSC 2023). Within 15 years (2008 to 2022) the total number of leptonetid species recorded from China increased six times (WSC 2023), mostly after the profusely illustrated revisions of the Chinese representatives by Wang et al. (2017) and the Japanese species by Ballarin and Eguchi (2022). These two studies have revealed remarkable sexually dimorphic traits and relevant

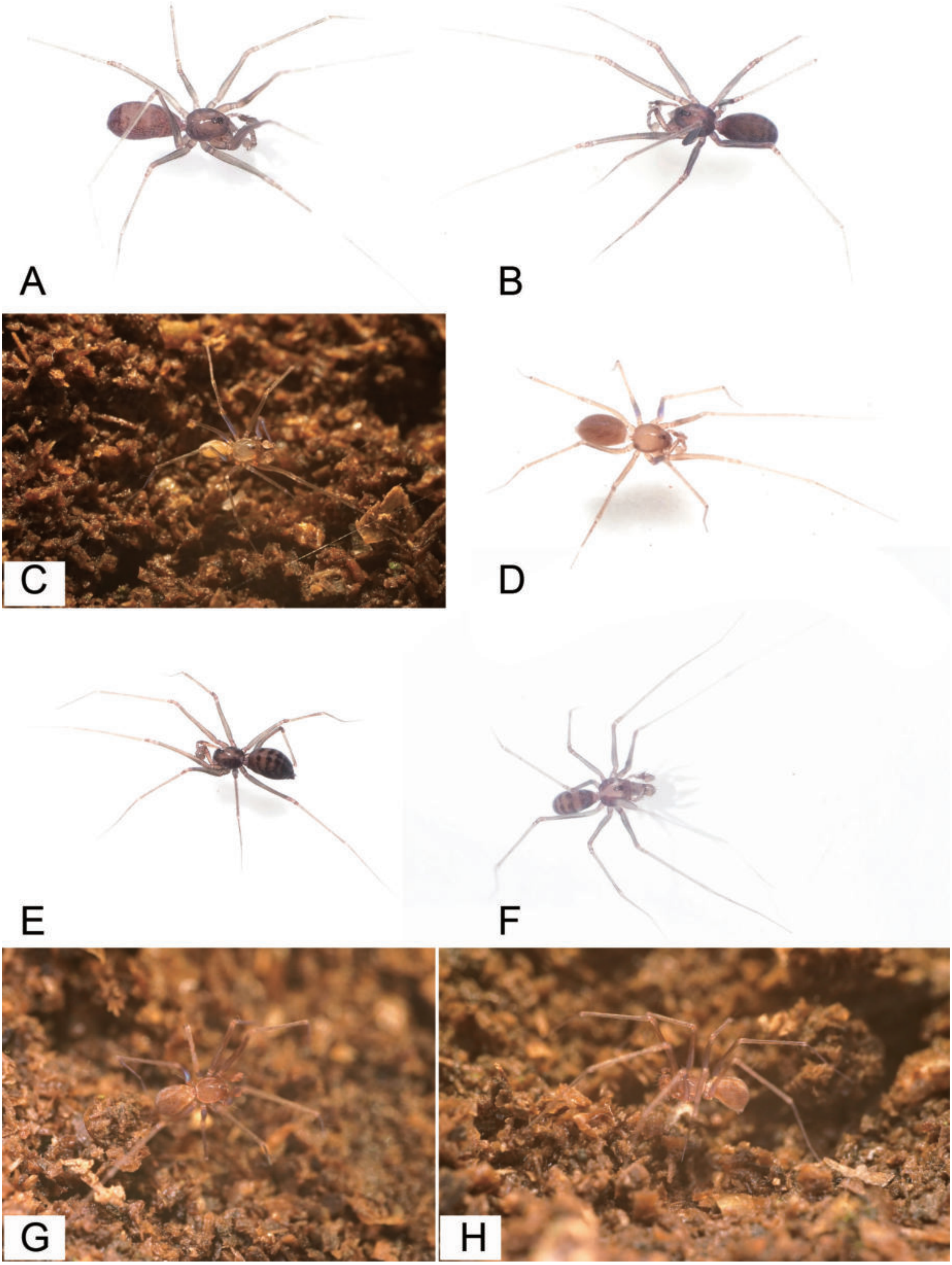

Figure 28. Photographs of living specimens from China. **A** *Longileptoneta guadunensis* sp. nov., **B** *L. huboliao* sp. nov. **C** *L. jiaxiani* sp. nov. **D** *L. letuensis* sp. nov. **E** *L. renzhouensis* sp. nov. **F** *L. tianmenensis* sp. nov. **G, H** *Pararana mingxuani* sp. nov.

Figure 29. Records of *Falcileptoneta monodactyla* (Yin, Wang & Wang, 1984), *Leptonetela dawu* sp. nov., *L. yuanhaoi* sp. nov. and *L. zuojiashan* sp. nov. from Jiangxi; *Longileptoneta guadunensis* sp. nov., *L. huboliao* sp. nov., *L. jiaxiani* sp. nov., *L. letuensis* sp. nov., *L. renzhouensis* sp. nov., *L. tianmenensis* sp. nov., and *Pararana mingxuani* sp. nov. from Fujian, China.

morphological features that have provided useful information for the present taxonomic work.

It is interesting to note that the species *Falcileptoneta monodactyla* has no also been found from Jiangxi Province. Considering the locality of the holotype, Yanling county in Hunan province, it is likely that this species is more widely distributed in the Hunan and Jiangxi provinces.

The *Longileptoneta* species are very difficult to differentiate as their embolus is hidden in the tegular apophyses. Although the genera *Falcileptoneta* and *Longileptoneta* are clearly distinguished from all other leptonetid genera, ambiguity can occur in cave species lacking eyes, such as *Falcileptoneta taizhensis* (Chen & Zhang, 1993), *Longileptoneta gutan* Wang & Li, 2020, and *L. shenxian* (Wang et al. 2020). A very obvious feature reveals that they are living in caves and become vestigial. Each of these two genera seems to be monophyletic, which need to be confirmed by future phylogenetic studies.

The genus *Pararana* Lin & Li, 2022 was monotypic before this work and described based on a single male specimen (Lin et al. 2022). The diagnostic characters of the genus are inadequate as no females are known for the type species *Pararana gaofani* Lin & Li, 2022 (Lin et al. 2022). Based on the female of *P. mingxuani* sp. nov., this genus can be characterized by a long atrium and very short spermathecal stalks. Since more *Pararana* species from China can be expected to be discovered, this genus will be more easily understood in future research.

Acknowledgements

We thank Jia-xian Gong, Wei Zhang, Ming-xuan Wu, and Rui Zhao (from Fujian Agriculture and Forestry University), and Yuan-hao Ying, Si-liang Yuan, Ke-qiang Huang, Dan-chen Zhao, Ze-yuan Meng, Zi-xi He, Zi-yi Zhao, and Wen-hui Li (from Jinggangshan University) for their assistance during the field work. We also thank Dr Nathalie Yonow for improving the English of the manuscript and the two reviewers Dr Ivan L. F. Magalhaes and Tamas Szuts, as well as the subject editor Dr Peter Michalik and the copy editor Dr Zdravka Zorkova, for providing detailed corrections and suggestions.

Additional information

Conflict of interest

The authors have declared that no competing interests exist.

Ethical statement

No ethical statement was reported.

Funding

This study was supported by the Natural Science Foundation of China (32000301/32160243) and the Science and Technology Innovation Project for College Students.

Author contributions

Bin-Lu Liu and Yan-bin Yao collected the images and data. Yong-hong Xiao, Zi-Min Jiang designed the study. Keke Liu drafted the MS.

Author ORCIDs

Bin-Lu Liu https://orcid.org/0009-0009-3080-8987
Yan-bin Yao https://orcid.org/0000-0002-2560-9299
Zi-Min Jiang https://orcid.org/0000-0001-9044-3312
Yong-hong Xiao https://orcid.org/0000-0002-8074-9366
Ke-Ke Liu https://orcid.org/0000-0001-7822-3667

Data availability

All of the data that support the findings of this study are available in the main text.

References

Ballarin F, Eguchi K (2022) Taxonomic notes on leptonetid spiders from the Ryukyu Archipelago with the description of two new species and the first record of the genus *Longileptoneta* from Japan (Araneae: Leptonetidae). Zootaxa 5213(4): 371–387. https://doi.org/10.11646/zootaxa.5213.4.3

Lan TQ, Zhao Z, Kim ST, Yoo JS, Lee SY, Li SQ (2021) Five new species of the genera *Falcileptoneta* and *Longileptoneta* (Araneae, Leptonetidae) from South Korea. ZooKeys 1010: 97–116. https://doi.org/10.3897/zookeys.1010.59915

Lin YJ, Zhao HF, Koh JKH, Li SQ (2022) Taxonomy notes on twenty-eight spider species (Arachnida: Araneae) from Asia. Zoological Systematics 47(3): 198–270. https://doi.org/10.11865/zs.2022303

Liu B, Zhang F (2022) A new eyeless Leptonetid spider from Beijing, China (Araneae, Leptonetidae). Acta Arachnologica Sinica 31(1): 44–48. https://doi.org/10.3969/j.issn.1005-9628.2022.01.007

Liu JX, Huang ZG, Xu X, Yin HQ (2020) Redescription of types of three species of Leptonetidae Simon, 1890 from China (Arachnida, Araneae). ZooKeys 1000: 1–17. https://doi.org/10.3897/zookeys.1000.57660

Ramírez MJ, Michalik P (2019) The Spider Anatomy Ontology (SPD)—A Versatile Tool to Link Anatomy with Cross-Disciplinary Data. Diversity 11(10): e202. https://doi.org/10.3390/d11100202

Tong YF, Li SQ (2008) Six new cave-dwelling species of Leptoneta (Arachnida, Araneae, Leptonetidae) from Beijing and adjacent regions, China. Zoosystema 30: 371–386.

Wang CX, Li SQ (2011) A further study on the species of the spider genus *Leptonetela* (Araneae: Leptonetidae). Zootaxa 2841(1): 1–90. https://doi.org/10.11646/zootaxa.2841.1.1

Wang CX, Xu X, Li SQ (2017) Integrative taxonomy of *Leptonetela* spiders (Araneae, Leptonetidae), with descriptions of 46 new species. Zoological Research 38(6): 321–448. https://doi.org/10.24272/j.issn.2095-8137.2017.076

Wang CX, Li SQ, Zhu WH (2020) Taxonomic notes on Leptonetidae (Arachnida, Araneae) from China, with descriptions of one new genus and eight new species. Zoological Research 41(6): 684–704. https://doi.org/10.24272/j.issn.2095-8137.2020.214

WSC (2023) World Spider Catalog. Natural History Museum Bern. Version 24.0. https://wsc.nmbe.ch/ [Accessed 25 May 2023]

Zhu WH, Li SQ (2021) Five new leptonetid spiders from China (Araneae: Leptonetidae). Zootaxa 4984(1): 281–299. https://doi.org/10.11646/zootaxa.4984.1.21

ZooKeys 1189: 327–336 (2024)
DOI: 10.3897/zookeys.1189.113678

Research Article

Argyrotaenia socoromaensis sp. nov. (Lepidoptera, Tortricidae), a sexually dimorphic micromoth with polyphagous larvae from the arid Andes of northern Chile

Héctor A. Vargas[1]

1 *Departamento de Recursos Ambientales, Facultad de Ciencias Agronómicas, Universidad de Tarapacá, Arica, Chile*
Corresponding author: Héctor A. Vargas (havargas@academicos.uta.cl; lepvargas@gmail.com)

Abstract

Argyrotaenia socoromaensis **sp. nov.** (Lepidoptera, Tortricidae, Tortricinae, Archipini) from the arid Andes of northern Chile is described and illustrated. Adults are sexually dimorphic, with differences in wing size, shape and pattern. The larvae feed on *Stevia philippiana* Hieron. (Asteraceae) and *Lupinus oreophilus* Phil. (Fabaceae). Genetic distance between DNA barcodes of male and female adults reared from larvae collected on the two hosts was 0–0.2% (K2P). The discovery of *A. socoromaensis* **sp. nov.** represents the first record of the genus *Argyrotaenia* Stephens, 1852 and the tribe Archipini for the Chilean fauna of Tortricidae.

Key words: Andes, arid environments, DNA barcoding, larval polyphagy, new record, new species, sexual dimorphism, taxonomy

Academic editor: Christian Schmidt
Received: 4 October 2023
Accepted: 21 December 2023
Published: 18 January 2024

ZooBank: https://zoobank.org/B090FFEB-73B5-4B0A-8136-1FB2DB2F36B5

Citation: Vargas HA(2024) *Argyrotaenia socoromaensis* sp. nov. (Lepidoptera, Tortricidae), a sexually dimorphic micromoth with polyphagous larvae from the arid Andes of northern Chile. ZooKeys 1189: 327–336. https://doi.org/10.3897/zookeys.1189.113678

Introduction

The updated, online world catalogue of the family Tortricidae (Gilligan et al. 2018) includes 116 species in the genus *Argyrotaenia* Stephens, 1852 (Tortricinae, Archipini). The widespread Palearctic *A. ljungiana* (Thunberg, 1797), senior synonym of the type species *Tortrix politana* Haworth, 1811, is the only Old World representative of the genus, while all the others occur from Canada to Argentina in the New World (Razowski 1997; Brown and Cramer 1999; Gilligan et al. 2018). As part of recent taxonomic studies of the Caribbean fauna of the tribe Archipini, some species included in *Argyrotaenia* by Gilligan et al. (2018) were either transferred to other genera or synonymized, and new ones were described (Austin et al. 2019; Austin and Dombroskie 2020a, b), bringing the current total to 114. Several members of the genus, such as *A. ljungiana* and *A. sphaleropa* (Meyrick, 1909), are pests of cultivated plants (Trematerra and Brown 2004; Gilligan and Epstein 2012; Gonsebatt et al. 2018; Ruiz-Galván et al. 2023).

Forty-three species of *Argyrotaenia* have their type locality in South America (Gilligan et al. 2018). Although some of them were described from Argentina, Bolivia and Peru (e.g., Razowski 1988; Razowski and Becker 2000, 2010; Trematerra and Brown 2004; Razowski and Wojtusiak 2010), the genus remained unknown in neighboring Chile (Razowski and Pelz 2010). However, recent surveys on the arid western slope of the central Andes yielded the first individuals of *Argyrotaenia* in this country. Subsequent morphological examination revealed that they belong to an undescribed species resembling the little-known *A. oriphanes* (Meyrick, 1930), described from Agualani, Puno, Peru. However, the two species can be separated based on differences in wing pattern and genitalia morphology of the male. As the Chilean specimens were reared from larvae collected on plants belonging to two distantly related families and showed differences in size, shape and pattern of male and female forewings, their conspecificity was assessed with mitochondrial DNA sequences of the barcode region (Hebert et al. 2003).

The aim of this contribution is to describe a sexually dimorphic, polyphagous new species of *Argyrotaenia* from the arid western slope of the central Andes, a discovery that represents the first record of this genus and the tribe Archipini from Chile.

Material and methods

The adult specimens examined in this study were reared from larvae collected on inflorescences of *Stevia philippiana* Hieron. (Asteraceae) and *Lupinus oreophilus* Phil. (Fabaceae) in April, 2021 and May, 2023 in the surroundings of Socoroma Village (18°17'22"S, 69°35'12"W) at about 3400 m elevation on the western slope of the Andes in the Parinacota Province of northern Chile. The abdomen of each adult was removed and placed in hot KOH 10% for a few minutes for dissection of the genitalia, which were stained with Eosin Y and Chlorazol Black and mounted on slides with Euparal. The holotype, paratypes and their genitalia slides are deposited in the “Colección Entomológica de la Universidad de Tarapacá” (IDEA), Arica, Chile.

Genomic DNA was extracted from legs of the micromoths using the the QIAamp Fast DNA Tissue Kit (Qiagen). PCR amplification of the barcode region (Hebert et al. 2003) was performed with the primers LCO1490 and HCO2198 (Folmer et al. 1994) using a protocol of 5 min at 94 °C, 35 cycles of 30 s at 94 °C, 30 s at 47 °C, 1 min at 72 °C and a final elongation step of 10 min at 72 °C. DNA purification and sequencing were performed at Macrogen Inc. (Santiago, Chile). The sequences obtained were deposited in the BOLD database of the Barcode of Life Data System (Ratnasingham and Hebert 2007). The software MEGA11 (Tamura et al. 2021) was used to perform sequence alignment with the ClustalW method and to assess the genetic divergence between sequences with the Kimura 2-Parameter (K2P) method.

Results

DNA barcoding

Three DNA barcode sequences were obtained from the holotype male (BOLD Process ID NCMIC001-23) reared from *S. philippiana*, and the two paratype females (BOLD Process IDs NCMIC002-23, NCMIC003-23) reared from *S. philippiana* and *L. oreophilus*. Genetic divergence between them was 0–0.2% (K2P), confirming that the three specimens belong to a single species with sexually dimorphic adults and polyphagous larvae. The three sequences were clustered under a single Barcode Index Number (BIN) in BOLD (BOLD:AFL1620) with 4.5% p-distance to nearest neighbor.

Taxonomy

Argyrotaenia socoromaensis **sp. nov.**
https://zoobank.org/DFA712C0-A92E-427E-8E62-CFB43466FD79
Figs 1–3

Type locality. CHILE, Parinacota Province, Socoroma (18°17'22"S, 69°35'12"W), 3400 m elevation on the western slope of the Andes.

Type material. ***Holotype*****:** CHILE • ♂; Parinacota, Socoroma; June, 2023; H.A. Vargas leg.; ex-larva inflorescence; *Stevia philippiana*; May, 2023; "HOLOTYPE *Argyrotaenia socoromaensis* Vargas" [red handwritten label]; IDEA-LEPI-2023-01; HAV-1661 [genitalia slide]; NCMIC001-23 [BOLD Process ID] (IDEA). ***Paratypes*****:** CHILE • 1 ♀; same data as for the holotype; IDEA-LEPI-2023-02; HAV-1678 [genitalia slide]; NCMIC002-23 [BOLD Process ID] • 1 ♀; same locality and collector as previous; May, 2021; ex-larva inflorescence; *Lupinus oreophilus*; April, 2021; IDEA-LEPI-2023-03; HAV-1470 [genitalia slide]; NCMIC003-23 [BOLD Process ID] (IDEA).

Diagnosis. Adults of *A. socoromaensis* sp. nov. are sexually dimorphic. The forewing of the holotype male is 10.3 mm long, distal third of the costal margin is almost straight, there are few yellowish-brown scales on the basal fascia, and median fascia is continuous with tornal blotch. In contrast, females have a forewing length of 6.5–8.2 mm, the distal third of the costal margin slightly concave, there are abundant yellowish-brown scales on the basal fascia, and median fascia is conspicuously separated from tornal blotch by the postmedian interfascia. The wing pattern and genitalia of the male of *A. socoromaensis* sp. nov. resemble those of the Peruvian *A. oriphanes* (Clarke 1958, plate 124, figs 4–4b). However, the forewing of *A. socoromaensis* sp. nov. lacks white blotches on the costal half of the basal fascia, and has the median fascia with internal margin strongly sinuous in the middle and external margin slightly sinuous, while the forewing of *A. oriphanes* has broad white blotches on the costal half of the basal fascia, and the medial fascia with internal margin straight in the middle and external margin abruptly indented near the costa. In the male genitalia, the uncus is slightly apically broadened, the sacculus is broadly convex before middle and the phallus is mostly straight in *A. socoromaensis* sp. nov., in contrast with the uncus strongly apically broadened, sacculus with ventral margin straight before middle, and phallus strongly curved of *A. oriphanes*. The female of *A. oriphanes* remains unknown, impeding comparisons.

Description. Male (*N* = 1; Fig. 1A). ***Head*****.** Vertex mostly whitish gray, dark gray near anterior margin; frons mostly dark gray with a whitish gray transverse stripe near ventral margin. Antenna with scape whitish gray on external surface, dark gray on medial surface, pedicel and flagellum dark gray, flagellum ciliated ventrally. Labial palpus dark gray on external surface, whitish gray on medial surface. ***Thorax*** (forewing length 10.3 mm). Mostly whitish gray and dark gray dorsally with scattered yellowish-brown scales; whitish gray laterally. Foreleg dark gray on external surface, whitish gray on medial surface, tibial epiphysis dark gray; midleg similar to foreleg but whitish gray tibial spurs; hindleg whitish gray with scattered dark gray scales, tibial spurs concolorous. Forewing with distal third of costa almost straight; fasciae and blotches mostly dark gray with scattered whitish gray and yellowish-brown scales; interfasciae mostly whitish

Figure 1. Habitus of *Argyrotaenia socoromaensis* sp. nov. **A** holotype male, dorsal view **B** paratype female, dorsal view. Scale bar: 5 mm.

gray with scattered yellowish-brown and dark gray scales; fringe gray; basal fascia triangular with external margin trilobed, yellowish-brown scales mostly concentrated near costa; antemedian interfascia with dark gray scales mostly on costal half and yellowish-brown scales mostly on posterior half; median fascia broadening from costa to posterior margin, continuous with tornal blotch, darker near costa, lighter near tornus, internal margin strongly sinuous in the middle, external margin slightly sinuous; postmedian interfascia with narrow, short posterior expansion in the middle not reaching the tornus; subapical blotch semicircular. Hind wing and fringe gray. ***Abdomen.*** Mostly dark gray with scattered whitish gray scales. Male genitalia (Fig. 2A–C). Uncus elongated, anterior third somewhat conical, posterior two-thirds flattened, mostly parallel-sided, slightly broadened apically, apex rounded. Tegumen V-shaped in dorsal view, length in the middle about half of uncus. Gnathos arms as long as uncus, posteriorly curved, distally fused, apex rounded. Vinculum U-shaped. Transtilla a transverse stripe. Juxta diamond-shaped with small V-shaped dorsal excavation with a group of setae near each tip. Valva rectangular, slightly straightening apically, mostly membranous with rounded apical corners; scattered setae, more dense at apex; dorsal margin straight, costa undifferentiated;

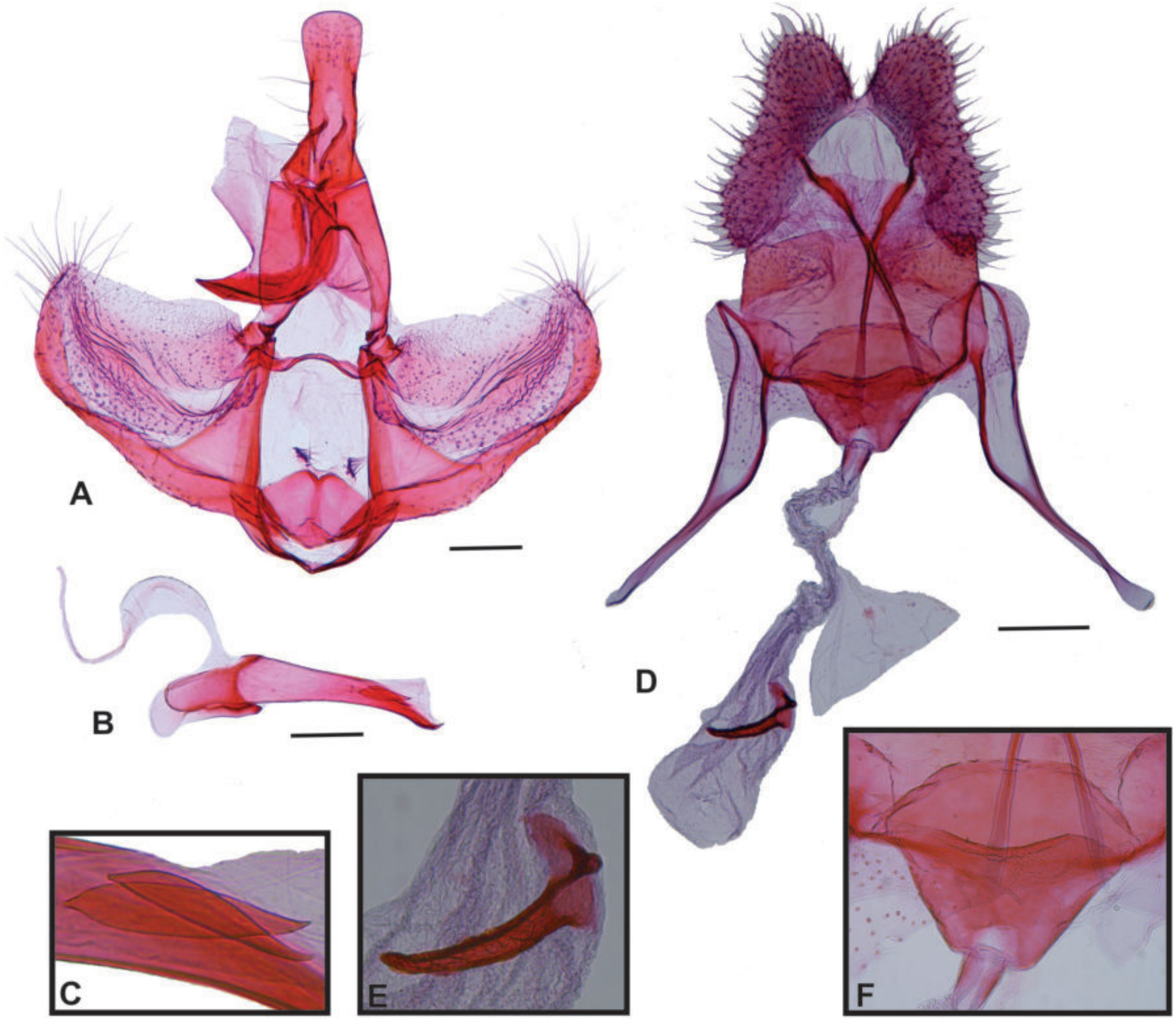

Figure 2. Genitalia of *Argyrotaenia socoromaensis* sp. nov. **A** male genitalia, ventral view, phallus removed **B** phallus, lateral view **C** cornuti **D** female genitalia, ventral view **E** signum **F** antrum. Scale bars: 0.2 mm.

longitudinal fold lobe-like near transtilla, broadened, slightly sclerotized distally; presaccular gap broad near vinculum, not well-defined toward apex of valva; sacculus narrow, broadly convex before middle, distal third curved to apex of valva. Phallus mostly straight, length similar to valva, progressively narrowing apically, apex slightly curved; caulis small; coecum about a sixth of phallus length, with a keel-shaped antero-ventral projection; vesica with two cornuti.

Female (*N* = 2; Fig. 1B). ***Head.*** Vertex and frons yellowish gray. Antenna with scape whitish gray on external surface, dark gray on medial surface, pedicel and flagellum dark gray, flagellum ciliated ventrally. Labial palpus whitish gray on basal half and dark gray with scattered yellowish gray scales on distal half of external surface, whitish gray on medial surface. ***Thorax*** (forewing length 6.5–8.2 mm). Mostly whitish gray dorsally, yellowish gray tegulae; whitish gray laterally. Foreleg mostly dark gray on external surface with scattered yellowish gray scales, whitish gray on medial surface, tibial epiphysis dark gray; midleg mostly whitish gray with scattered dark gray scales, whitish gray tibial spurs; hindleg whitish gray with scattered dark gray scales, tibial spurs whitish gray. Forewing with distal third of costa slightly concave; maculation mainly similar to male, but basal fascia with

Figure 3. Habitat and host plants of *Argyrotaenia socoromaensis* sp. nov. **A** habitat at the type locality, near Socoroma Village, at 3400 m elevation on the arid western slope of the Andes of northern Chile **B** *Stevia philippiana* Hieron. (Asteraceae) **C** *Lupinus oreophilus* Phil. (Fabaceae).

abundant yellowish-brown scales mostly near tegula; antemedian interfascia with yellowish-brown scales mostly between posterior lobe of the basal fascia and posterior margin of the wing; median fascia with almost uniform width from costa to discal cell, broadened from discal cell to posterior margin of the wing; postmedian interfascia with broad posterior expansion reaching tornus, clearly separating medial fascia from tornal blotch; subapical blotch somewhat triangular. Hind wing similar to male, but termen slightly concave near apex. ***Abdomen.*** Mostly dark gray with scattered whitish gray scales. Female genitalia (Fig. 2D–F). Papillae anales elongate, flattened, narrow, slightly broadened posteriorly, roughened, with setae. Apophyses posteriores about 1.2 times length of papillae anales; apophyses anteriores about 1.4 times length of papillae anales. Sterigma a narrow stripe between the antrum and apophyses anteriores, angled near antrum; antrum somewhat cup-shaped, truncate anteriorly, ventral wall about half the length of dorsal wall, posterior margin of ventral wall slightly convex, posterior margin of dorsal wall rounded; ductus bursae membranous, narrow, about half the length of apophyses anteriores, colliculum about half the length of ventral wall of antrum; ductus seminalis arising near the middle of ductus bursae; corpus bursae membranous, elongated, about 1.5 times the length of ductus bursae, signum spine-like, slightly curved, capitulum small, rounded.

Etymology. The specific epithet is derived from the type locality.

Distribution (Fig. 3A). *Argyrotaenia socoromaensis* sp. nov. is known only from the type locality in the surroundings of Socoroma Village, at about 3400 m elevation on the western slope of the Andes in the Parinacota Province, northern Chile.

Host plants (Fig. 3B, C). The adult specimens of *A. socoromaensis* sp. nov. examined in this study were reared from larvae collected on inflorescences of *Stevia philippiana* Hieron. (Asteraceae) and fruits of *Lupinus oreophilus* Phil. (Fabaceae).

Discussion

The uniqueness of the fauna of Tortricidae of Chile has been widely recognized (Obraztsov 1964; Razowski 1988; Brown 1999; Razowski and Pelz 2010). More than 80% of the species recorded in this country are endemic (Urra 2020). South-central Chile also harbors some endemic genera, among them *Accuminulia* Brown, 1999, *Parvulia* Urra, 2016 and *Natria* Urra, 2020 (Brown 1999; Urra 2016, 2020), while some other genera inhabiting this area have relatively narrow geographic ranges in South America with additional records restricted to neighboring countries, as in the case of *Chileulia* Powell, 1986, *Proeulia* Obraztsov, 1964 and *Ptychocroca* Brown & Razowski, 2003 (Brown and Razowski 2003; Razowski and Pelz 2010; Cepeda and González 2015). In contrast, species recorded in northern Chile belong to more widespread genera, such as *Cryptophlebia* Walsingham, 1900 and *Strepsicrates* Meyrick, 1888 (Clarke 1987; Vargas-Ortiz and Vargas 2018). The discovery of *A. socoromaensis* sp. nov. reinforces this pattern by adding the record of another widespread genus to the arid environments of northern Chile.

Host plant records of the Palearctic *A. ljungiana* and many Nearctic *Argyrotaenia* suggest that polyphagy is very common in this genus, while a few species have narrower host ranges, feeding on plants belonging to a single family (Brown et al. 2008). Such variation in host ranges can occur even among members of the same species group (Landry et al. 1999). Host plants have been recorded for only a few Neotropical species (Brown et al. 2008). Among the South American fauna, published host records mainly involve *A. loxonephes* (Meyrick, 1937) and *A. sphaleropa* (Meyrick, 1909), two remarkably polyphagous pest species whose larvae feed on plants belonging to 16 and 21 families, respectively (Trematerra and Brown 2004). The polyphagy of *A. socoromaensis* sp. nov. fits the more common host range currently recognized for the genus.

Sexual dimorphism, mostly related to wing pattern, has been documented for several members of *Argyrotaenia* (Obraztsov 1961; Powell 1965; Austin and Dombroskie 2020a). Correct association of males and females can be particularly difficult in species with marked sexual dimorphism, as in the case of *A. montezumae* (Walsingham, 1914), whose female was originally described under another specific name currently recognized as a synonym (Obraztsov 1961; Gilligan et al. 2018). The remarkable sexual dimorphism of *A. socoromaensis* sp. nov. involves differences in wing size, shape, and pattern.

DNA barcodes have been used successfully to explore host plant ranges and to associate females and males of sexually dimorphic species of Tortricidae (Hulcr et al. 2007; Corley and Ferreira 2017; Austin and Dombroskie 2020a). Although the description provided here for *A. socoromaensis* sp. nov. is based on only three specimens, the analysis of their DNA barcodes accurately supports the recognition of the male holotype and the two female paratypes as members of a single species with sexually dimorphic adults and polyphagous larvae. The discovery of *A. socoromaensis* sp. nov. raises to 105 the species and 38 the genera recorded for the Chilean fauna of Tortricidae (Razowski and Pelz 2010; Cepeda and Curkovic 2020; Urra 2020), and highlights the need to explore further the overlooked diversity of micromoths of the natural environments of the arid western slopes of the central Andes.

Acknowledgements

I thank John W. Brown for important comments and suggestions on a previous version, Wilson Huanca-Mamani for the use of facilities for DNA extraction and Lafayette Eaton for checking the English.

Additional information

Conflict of interest

The author has declared that no competing interests exist.

Ethical statement

No ethical statement was reported.

Funding

This study was supported by project UTA-MAYOR 9731–22.

Author contributions

The author solely contributed to this work.

Author ORCIDs

Héctor A. Vargas https://orcid.org/0000-0002-5355-3157

Data availability

All of the data that support the findings of this study are available in the main text.

References

Austin KA, Dombroskie JJ (2020a) A taxonomic revision of the Archipini of the Caribbean (Lepidoptera, Tortricidae, Tortricinae). ZooKeys 982: 33–147. https://doi.org/10.3897/zookeys.982.52363

Austin KA, Dombroskie JJ (2020b) New combinations in Neotropical Archipini and Atteriini (Lepidoptera: Tortricidae: Tortricinae), with the description of a new genus. Proceedings of the Entomological Society of Washington 122(1): 1–11. https://doi.org/10.4289/0013-8797.122.1.1

Austin KA, Dombroskie JJ, Matthews DL, Miller JY (2019) A review of the Archipini of The Bahamas with the description of a new species of *Argyrotaenia* Stephens (Tortricidae). Journal of the Lepidopterists Society 73(1): 5–17. https://doi.org/10.18473/lepi.73i1.a2

Brown JW (1999) A new genus of tortricid moths (Tortricidae: Euliini) injurious to grapes and stone fruits in Chile. Journal of the Lepidopterists Society 53: 60–64.

Brown JW, Cramer A (1999) Five new species of Argyrotaenia (Tortricidae: Archipini) from Mexico and the southwestern United States. Journal of the Lepidnpterists'. Society 53: 114–125.

Brown JW, Razowski J (2003) Description of *Ptychocroca*, a new genus from Chile and Argentina, with comments on the *Bonagota* Razowski group of genera (Lepidoptera: Tortricidae: Euliini). Zootaxa 303(1): 1–31. https://doi.org/10.11646/zootaxa.303.1.1

Brown JW, Robinson G, Powell JA (2008) Food plant database of the leafrollers of the world (Lepidoptera: Tortricidae) (Version 1.0). http://www.tortricid.net/foodplants.asp

Cepeda DE, Curkovic T (2020) A new species of *Proeulia* Clarke (Lepidoptera: Tortricidae) from Central Chile. Revista Chilena de Entomologia 46(3): 493–499. https://doi.org/10.35249/rche.46.3.20.15

Cepeda DE, González RH (2015) Nueva especie del género *Proeulia* Clarke, con registros adicionales de distribución geográfica para cinco especies (Lepidoptera: Tortricidae). Revista Chilena de Entomologia 40: 1–8.

Clarke JFG (1958) Catalogue of the type specimens of microlepidoptera in the British Museum (Natural History) described by Edward Meyrick (Vol. 3), Tortricidae, Olethreutidae, Noctuidae. Trustees of the British Museum, London, 600 pp.

Clarke JFG (1987) Two new species of *Cryptophlebia* Walsingham from Chile (Lepidoptera: Olethreutidae). Acta Entomológica Chilena 14: 7–12.

Corley MFV, Ferreira S (2017) DNA Barcoding reveals sexual dimorphism in *Isotrias penedana* Trematerra, 2013 (Lepidoptera: Tortricidae, Chlidanotinae). Zootaxa 4221(5): 594–600. https://doi.org/10.11646/zootaxa.4221.5.7

Folmer O, Black M, Hoeh W, Lutz R, Vrijenhoek R (1994) DNA primers for amplification of mitochondrial cytochrome c oxidase subunit I from diverse metazoan invertebrates. Molecular Marine Biology and Biotechnology 3: 294–299.

Gilligan TM, Epstein ME (2012) TortAI, Tortricids of Agricultural Importance to the United States (Lepidoptera: Tortricidae). Identification Technology Program (ITP), USDA/APHIS/PPQ/CPHST, Fort Collins, CO. https://idtools.org/id/leps/tortai/

Gilligan TM, Baixeras J, Brown JW (2018) T@RTS: Online World Catalogue of the Tortricidae (Ver. 4.0). http://www.tortricid.net/catalogue.asp

Gonsebatt GF, Chalup AE, Ruberti D, Seta S, Leone A, Coniglio R, Moyano MI (2018) Primer registro de *Argyrotaenia tucumana* (Lepidoptera: Tortricidae) en montes de duraznero, *Prunus persicae* (L.) Batsch, del sur de la provincia de Santa Fe. Revista de la Sociedad Entomológica Argentina 77(2): 28–31. https://doi.org/10.25085/rsea.770203

Hebert PDN, Cywinska A, Ball SL, deWaard JR (2003) Biological identification through DNA barcode. Proceedings of the Royal Society B, Biological Sciences 270(1512): 313–321. https://doi.org/10.1098/rspb.2002.2218

Hulcr J, Miller SE, Setliff GP, Darrow K, Mueller ND, Hebert PDN, Weiblen GD (2007) DNA barcoding confirms polyphagy in a generalist moth, *Homona mermerodes* (Lepidoptera: Tortricidae). Molecular Ecology Notes 7(4): 549–557. https://doi.org/10.1111/j.1471-8286.2007.01786.x

Landry B, Powell JA, Sperling FAH (1999) Systematics of the *Argyrotaenia franciscana* (Lepidoptera: Tortricidae) species group: evidence from mitochondrial DNA. Annals of the Entomological Society of America 92(1): 40–46. https://doi.org/10.1093/aesa/92.1.40

Obraztsov NS (1961) Descriptions of and notes on North and Central American species of *Argyrotaenia*, with description of a new genus (Lepidoptera, Tortricidae). American Museum Novitates 2048: 1–42.

Obraztsov NS (1964) Neotropical Microlepidoptera, V: Synopsis of the species of the genus *Proeulia* from central Chile (Lepidoptera: Tortricidae). Proceedings of the United States National Museum 116(3501): 183–195. https://doi.org/10.5479/si.00963801.116-3501.183

Powell JA (1965) Supplementary notes on North American and Mexican species of *Decodes* and *Argyroteania*, with descriptions of new species (Lepidoptera: Tortricidae). Proceedings of the Biological Society of Washington 78: 65–80.

Ratnasingham S, Hebert PDN (2007) BOLD: The Barcode of Life Data System (http://www.barcodinglife.org). Molecular Ecology Notes 7(3): 355–364. https://doi.org/10.1111/j.1471-8286.2007.01678.x

Razowski J (1988) New Genera and Species of the Neotropical Archipini (Lepidoptera, Tortricidae). Acta Zoologica Cracoviensia 31: 387–422.

Razowski J (1997) Generic composition of the New World Archipini (Lepidoptera, Tortricidae) with description of two new genera and two new species. Miscellània Zoològica 20: 125–130.

Razowski J, Becker VO (2000) Revision of the Neotropical *Argyrotaenia* Stephens, with notes on *Diedra* Rubinoff & Powell (Lepidoptera: Tortricidae). Acta Zoologica Cracoviensia 43: 307–332.

Razowski J, Becker VO (2010) Systematic and distributional data on Neotropical Archipini (Lepidoptera: Tortricidae). Acta Zoologica Cracoviensia 53B(1): 9–38. https://doi.org/10.3409/azc.53b_1-2.09-38

Razowski J, Pelz V (2010) Tortricidae from Chile (Lepidoptera: Tortricidae). SHILAP Revista de Lepidopterologia 38: 5–55.

Razowski J, Wojtusiak J (2010) Tortricidae (Lepidoptera) from Peru. Acta Zoologica Cracoviensia 53B(1): 73–159. https://doi.org/10.3409/azc.53b_1-2.73-159

Ruiz-Galván I, Bautista-Martínez N, Soto-Rojas L, Pineda-Guillermo S, Romero-Nápoles J (2023) Identification and distribution of leafrollers (Lepidoptera, Tortricidae) associated with berries (Rosaceae) cultivated in Mexico. ZooKeys 1146: 185–196. https://doi.org/10.3897/zookeys.1146.81734

Tamura K, Stecher G, Kumar S (2021) MEGA11: Molecular evolutionary genetics analysis version 11. Molecular Biology and Evolution 38(7): 3022–3027. https://doi.org/10.1093/molbev/msab120

Trematerra P, Brown JW (2004) Argentine *Argyrotaenia* (Lepidoptera: Tortricidae): Synopsis and descriptions of two new species. Zootaxa 574(1): 1–12. https://doi.org/10.11646/zootaxa.574.1.1

Urra F (2016) *Parvulia*, nuevo género de Tortricidae (Lepidoptera) de la zona central de Chile. Boletín del Museo Nacional de Historia Natural 65: 161–167. https://doi.org/10.54830/bmnhn.v65.2016.91

Urra F (2020) *Natria mauritius*, nuevo género y nueva especie de tortrícido (Lepidoptera: Tortricidae) de la cordillera de Nahuelbuta, Chile. Revista Chilena de Entomologia 46(3): 357–364. https://doi.org/10.35249/rche.46.3.20.01

Vargas-Ortiz M, Vargas HA (2018) A new species of *Strepsicrates* Meyrick (Lepidoptera: Tortricidae) from the Atacama Desert of northern Chile previously misidentified as *S. smithiana* Walsingham. Zootaxa 4370(5): 569–579. https://doi.org/10.11646/zootaxa.4370.5.8

ZooKeys

ZooKeys 1189: 337–347 (2024)
DOI: 10.3897/zookeys.1189.115996

Research Article

Hotwheels gen. nov., a new ground spider genus (Araneae, Gnaphosidae) from southwest China

Bo Liu[1], Feng Zhang[1]

1 *The Key Laboratory of Zoological Systematics and Application, Hebei Basic Science Center for Biotic Interaction, College of Life Sciences, Hebei University, Baoding, Hebei 071002, China*
Corresponding author: Feng Zhang (dudu06042001@163.com)

Abstract

A new monotypic ground spider genus, *Hotwheels* **gen. nov.**, is described, with the type species *H. sisyphus* **sp. nov.** (♂♀) from southwest China. This new genus is not assigned to any of the known subfamilies of Gnaphosidae, belonging only to the *Echemus* group of genera. It resembles *Synaphosus* Platnick & Shadab, but it can be differentiated by the presence of a median apophysis. Descriptions, illustrations and a records map are provided.

Key words: Description, morphology, new species, taxonomy

Academic editor: Sarah Crews
Received: 20 November 2023
Accepted: 27 December 2023
Published: 18 January 2024

ZooBank: https://zoobank.org/E7B9E7E0-7D64-469A-9B6C-96EBAE1944F9

Citation: Liu B, Zhang F (2024) *Hotwheels* gen. nov., a new ground spider genus (Araneae, Gnaphosidae) from southwest China. ZooKeys 1189: 337–347. https://doi.org/10.3897/zookeys.1189.115996

Introduction

Gnaphosidae is a highly diverse spider family, containing 2466 extant species in 151 genera (WSC 2023). Southwest China mostly lies within the Oriental Realm and has the highest diversity of spiders in China (Holt et al. 2013; Yao and Li 2021), including 87 species of 25 genera of gnaphosid spiders (WSC 2023). Three new ground spider genera (*Meizhelan* Lin & Li, 2023, *Platnickus* Liu & Zhang, 2023, *Yuqilin* Lin & Li, 2023) have been reported from southwest China in just 2023 (Lin and Li 2023; Liu and Zhang 2023). However, ground spider research in southwest China and neighbouring countries is severely limited, with a lack of regional revisions (WSC 2023). Our knowledge of the diversity of gnaphosids in southwest China is far from adequate, and many new taxa remain to be discovered.

While examining the ground spider collections from southwest China, we found several specimens of an unknown species resembling *Synaphosus* Platnick & Shadab, 1980 in somatic characters and genitalic structures, but it can be differentiated by the presence of a median apophysis, which indicates a new genus should be established.

Material and methods

All specimens were preserved in 75% ethanol and examined and measured under a Leica M205A stereomicroscope. Photographs were taken using an Olympus BX51 microscope equipped with a Kuy Nice CCD camera and were imported into Helicon Focus v.7 for stacking. Final figures were retouched using Adobe Photoshop 2020. A map was generated in QGIS v.3.24.2. All measurements are given in millimeters. Leg measurements are shown as: total length (femur, patella, tibia, metatarsus, tarsus). Epigynes were removed and cleared in a pancreatin solution (Álvarez-Padilla and Hormiga 2007). All specimens studied are deposited in the Museum of Hebei University (**MHBU**), Baoding, China.

Morphological terminology follows Azevedo et al. (2017). Abbreviations used in this study are: ALE, anterior lateral eye; AME, anterior median eye; BH, basal haematodocha; C, conductor; CA, apophysis of conductor; CD, copulatory duct; CO, copulatory opening; DSS, duct of secondary spermatheca; DTM, distal tubular membrane; E, embolus; ED, ejaculatory duct; EP, embolar process; FD, fertilization duct; H, hood; MA, median apophysis; MaAm, major ampullate gland spigots; MH, median haematodocha; Pi, piriform gland spigots; PLE, posterior lateral eye; PME, posterior median eye; PS, primary spermatheca; R, embolar radix; RTA, retrolateral tibial apophysis; SD, sperm duct; SS, secondary spermathecae; ST, subtegulum; T, tegulum; TM, terminal membrane of embolus.

Taxonomy

Family Gnaphosidae Banks, 1892

Genus *Hotwheels* gen. nov.

https://zoobank.org/1E5BA5C9-E641-4F3D-B4DC-ED0525F6416E
火轮蛛属

Type species. *Hotwheels sisyphus* sp. nov.

Etymology. The generic name refers to Hot Wheels, a collectible die-cast toy car made by Mattel, as the long, coiled embolus of this new genus resembles a Hot Wheels track; neuter in gender.

Diagnosis. The new genus resembles *Synaphosus* Platnick & Shadab, 1980 by metatarsi III and IV having a preening brush, the male palp has a long embolus and large conductor, and the epigyne has a hood and long copulatory ducts (Figs 2–4C, D, 5). It can be distinguished from *Synaphosus* by: 1) the presence of a median apophysis (Figs 2, 3A–D) vs. median apophysis absent (Fig. 3F, G; Ovtsharenko et al. 1994: figs 12–14); 2) the basal half of the embolus which rotates counterclockwise (Fig. 2A) vs. basal half of the embolus rotates clockwise (Ovtsharenko et al. 1994: figs 12–14; Marusik and Omelko 2018: figs 8–11, 20–24, 26–36); 3) a weakly sclerotized conductor without an apophysis or outgrowth (Figs 2A, 3A–D) vs. a partially sclerotized conductor with an apophysis or outgrowth (Fig. 3F, G; Marusik and Omelko 2018: figs 8–11, 20–24, 26–36); and 4) the copulatory duct is circular, wide anteriorly, and almost twice the width of the primary spermathecae (Fig. 5) vs. copulatory duct twisted, narrow anteriorly, and narrower than the primary spermathecae (Ovtsharenko et al. 1994: figs 15, 16; Marusik and Omelko 2018: figs 5–7, 12, 13, 17–19, 39–41).

Description. Small-sized (total length: males = 4.86–5.44; females = 5.45–5.98). In dorsal view, carapace elongate-ovoid, anterior eye row slightly recurved, posterior eye row straight; PME oblique, flat (Figs 1A, 4A). Cheliceral promargin with 4 or 5 teeth, retromargin with 3 or 4 teeth (Fig. 1C, D). Leg formula: 4123.

Trochanters not notched. Metatarsi III and IV with preening brushes. Sternum elongate oval, with straight anterior edge, pointed posteriorly (Figs 1B, 4B). Anterior lateral spinnerets with 6 enlarged piriform gland spigots, separated by almost 1.2 times their diameter (Fig. 1E, F). Color in alcohol (Figs 1A, B, 4A, B): carapace yellow-brown; cephalic groove and radial furrow black; fovea distinct, longitudinal. Legs yellow-brown. Abdomen grey, males with anterior dorsal scutum, almost half of abdominal length and more than half of width.

Male palp and epigyne. Same as for the species.

Comments. Murphy (2007) made a formal grouping of gnaphosids without subfamilies, Azevedo et al. (2017) based subfamilies on the results of a morphological phylogenetic analysis, and Lin and Li (2020) erected a monotypic subfamily, Solitudinae. *Hotwheels* sp. nov. cannot be placed in any known Gnaphosidae subfamily because the cheliceral promargin has 4 or 5 teeth, and the retromargin has 3 or 4 teeth (Fig. 1C, D) vs. cheliceral promargin with keel in Herpyllinae (Azevedo et al. 2017: fig. 20e, g) and cheliceral retromargin with a serrated keel or a rounded lamina in Gnaphosinae (Azevedo et al. 2017: fig. 20b, d, f); metatarsi III and IV with preening brush (Fig. 4C, D) vs. metatarsi III and IV with preening comb in Zelotinae (Azevedo et al. 2017: fig. 22h); fertilization ducts directed laterally (Fig. 5B, D) vs. fertilization ducts directed posteriorly in Leptodrassinae (Ott 2012: fig. 40); trochanters not notched (Fig. 1B) vs. trochanters notched in Drassodinae (Azevedo et al. 2017: fig. 24); leg IV tarsus straight (Fig. 4C, D) vs. leg IV tarsus curved in Solitudinae (Lin and Li 2020: fig. 1E, F). It can be placed in the *Echemus* group of genera by the abdomens plain-coloured dorsally and males having an anterior dorsal scutum (Figs 1A, B, 4A, B) (Murphy 2007).

Composition. Only the type species.

Hotwheels sisyphus **sp. nov.**

https://zoobank.org/0437E3C2-DC00-4BA4-865A-E6E6DDDB55A0
Figs 1–5
西西弗斯火轮蛛

Type material. ***Holotype*** ♂, China: Guizhou Prov., Bijie City, Hezhang Co., Yemachuan Town, Dayan Cave, 27.132997°N, 104.818279°E, 1392 m elev., 2.X. 2019, leg. Z. Feng & L. Zhao. ***Paratype*****:** 1♀1♂, same data as holotype; 1♂1♀, China: Guizhou Prov., Qianxinan Buyei and Miao Autonomous Pref., Xingren City, Xinlongchang Town, Lianzhuang Vil., Daxiao Cave, 25.438033°N, 105.116197°E, 1473 m elev., 5.VIII.2022, leg. Y. Hou & L. Zhang; 1♂, China: Sichuan Prov., Leshan City, Emei Mt, Jiulinggang, 29.558433°N, 103.347167°E, 1811 m elev., 13.IV.2018, leg. Z. Zhang & L. Wang; 1♂1♀, China: Yunnan Prov., Honghe Autonomous Pref., Mile Co., Hongxi Town, Bailong Cave, 1.IV.2018, leg. H. Wang.

Etymology. The specific name is derived from Sisyphus, a king in Greek mythology who offended Zeus and whose punishment was to repeatedly roll a huge stone up a hill only to have it roll back down, because the circular copulatory ducts are like Sisyphus's cyclic mission; noun in apposition.

Description. Male. ***Holotype*** (Fig. 1A, B): total length 5.08; carapace 2.56 long, 1.95 wide; abdomen 2.52 long, 1.70 wide. ***Eye sizes and interdistances*****:** AME 0.15, ALE 0.16, PME 0.10, PLE 0.13; AME–AME 0.04, AME–ALE 0.01,

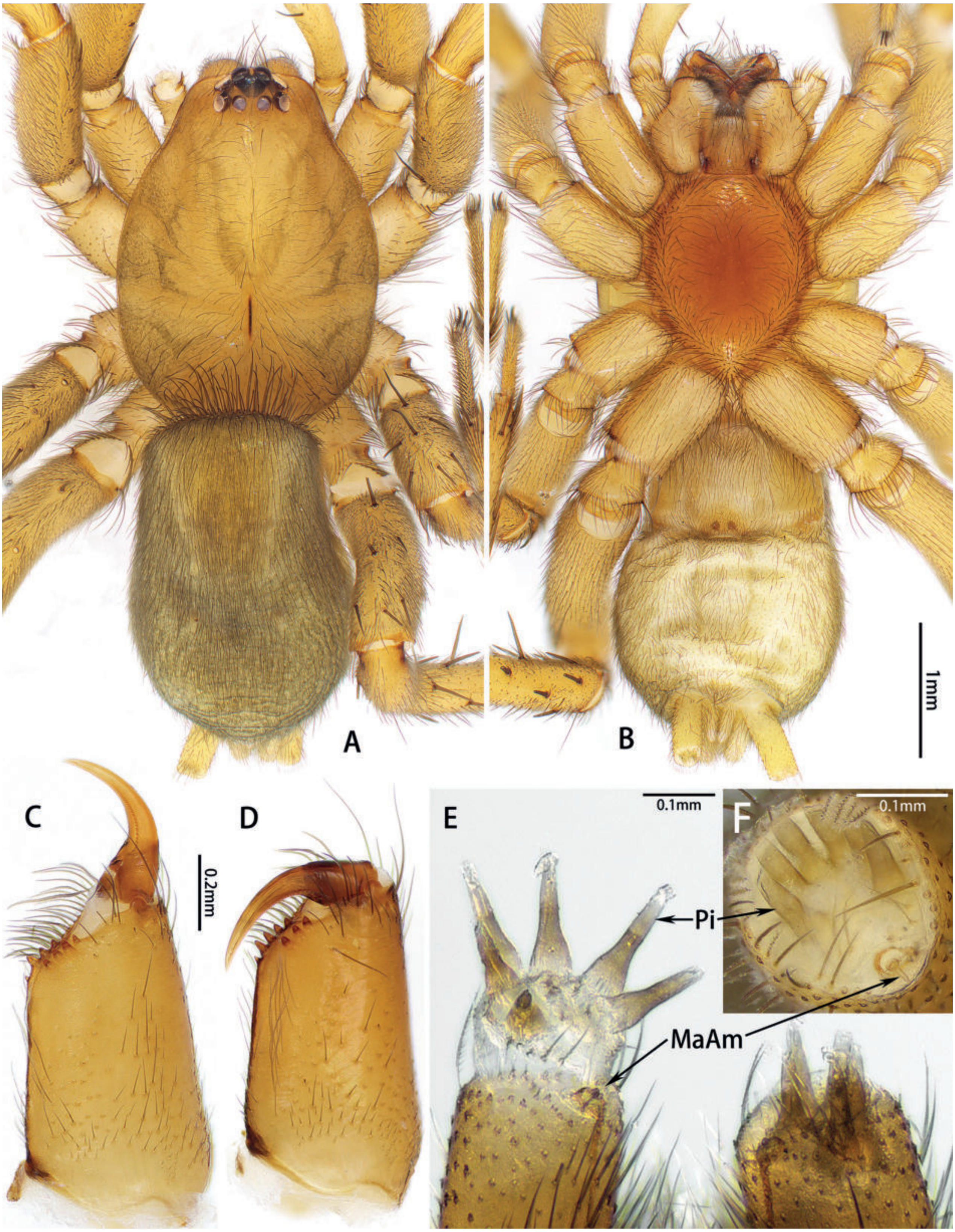

Figure 1. *Hotwheels sisyphus* sp. nov., male (**A–C, F**) and female (**D, E**) **A, B** habitus, dorsal and ventral view **C, D** left chelicera, retrolateral view **E, F** spigots on anterior lateral spinneret. Abbreviations: MaAm = major ampullate gland spigot, Pi = piriform gland spigot.

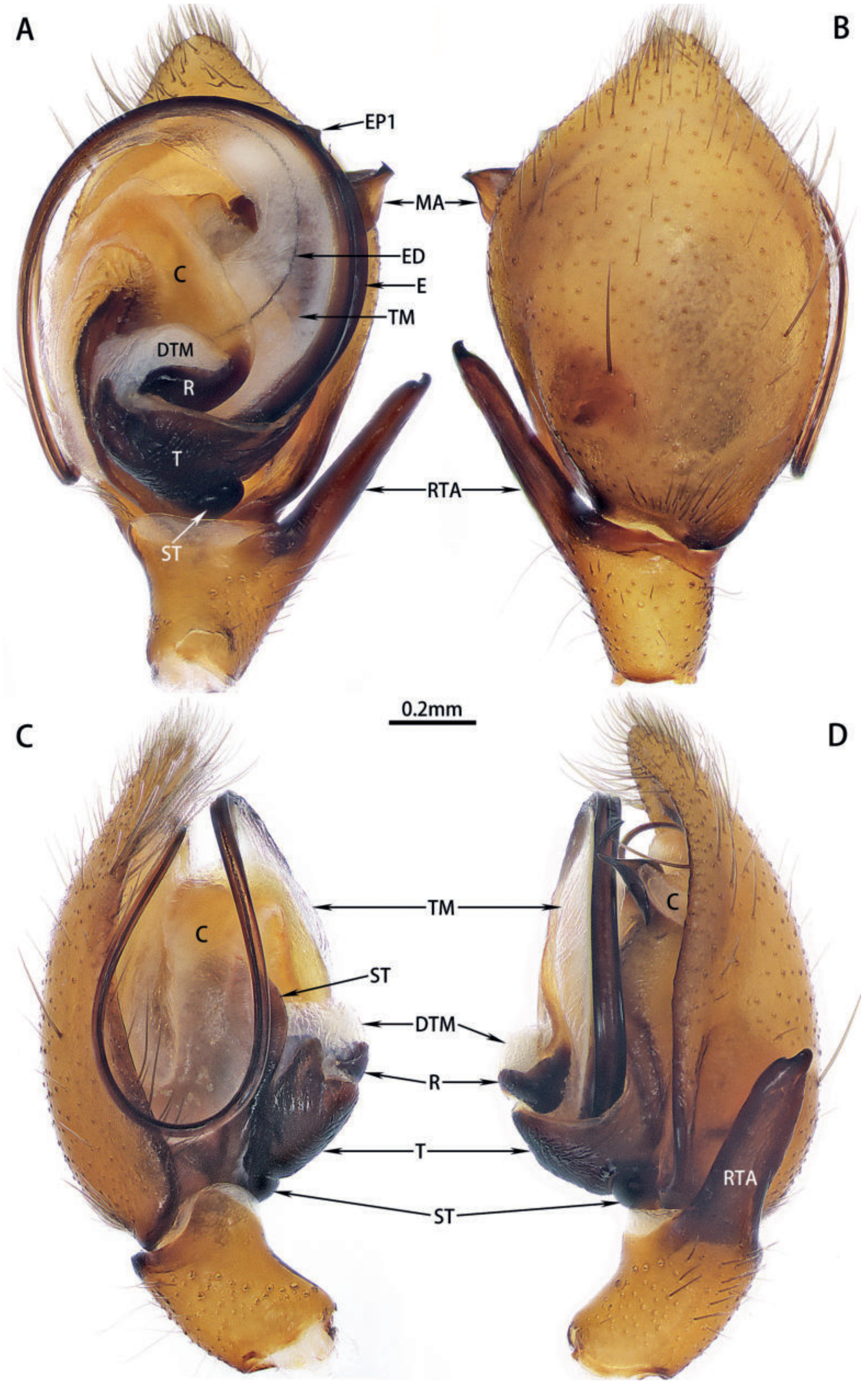

Figure 2. Male left palp of *Hotwheels sisyphus* sp. nov. **A** ventral view **B** dorsal view **C** prolateral view **D** retrolateral view. Abbreviations: C = conductor, DTM = distal tubular membrane, E = embolus, ED = ejaculatory duct, EP1 = embolar process, MA = median apophysis, R = embolar radix, RTA= retrolateral tibial apophysis, ST = subtegulum, T = tegulum, TM = terminal membrane.

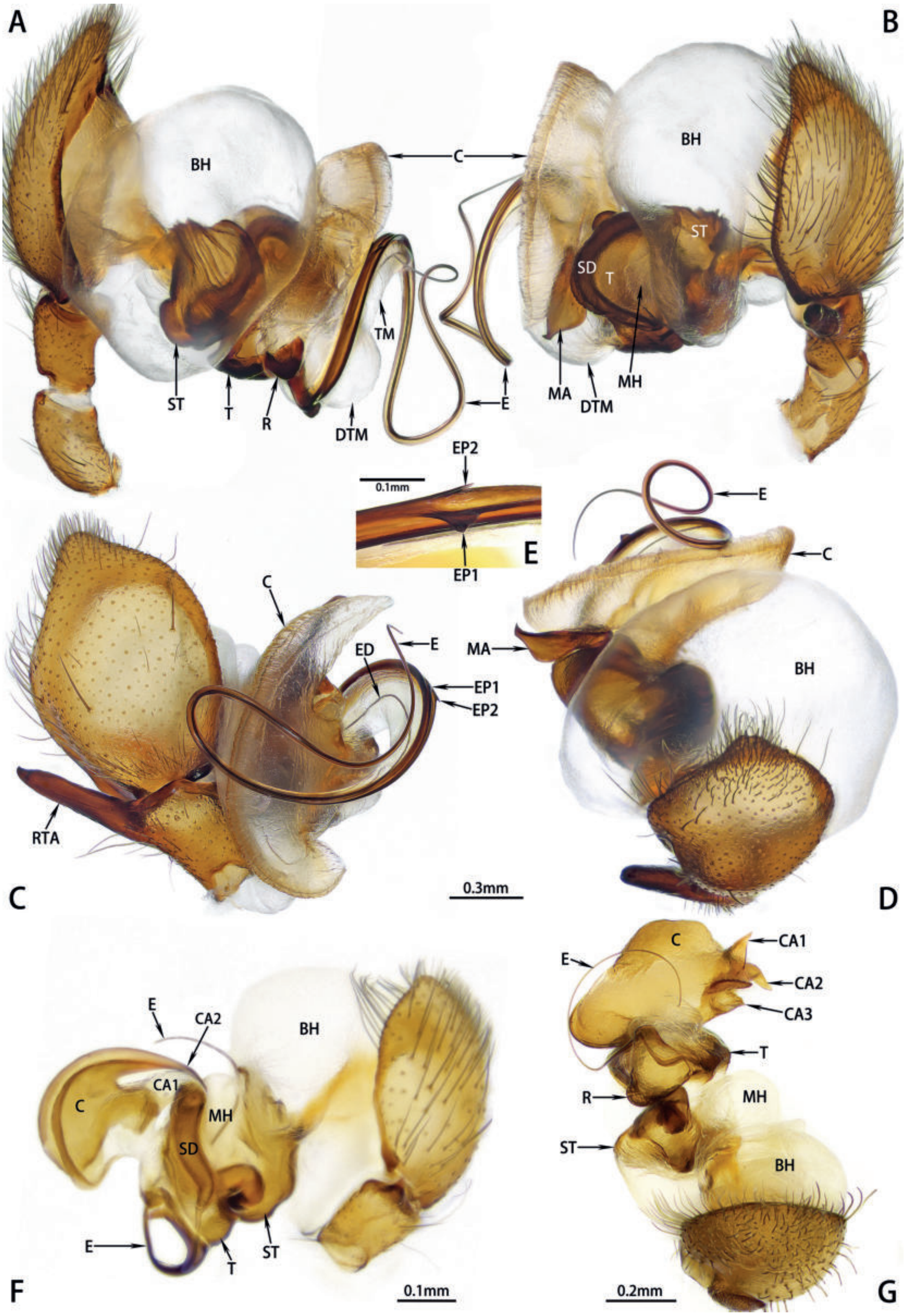

Figure 3. Expanded male left palp of *Hotwheels sisyphus* sp. nov. (**A–E**), *Synaphosus palearcticus* Ovtsharenko, Levy & Platnick, 1994 (**F**) and *S. cangshanus* Yang, Yang & Zhang, 2013 (**G**). **A** prolateral view **B** retrolateral view **C** dorsal view **D** frontal view **E** embolar processes **F** retrolateral view **G** anterior view. Abbreviations: C = conductor, CA1–3 = apophysis of conductor, BH = basal haematodocha, DTM = distal tubular membrane, E = embolus, ED = ejaculatory duct, EP1–2 = embolar process, MA = median apophysis, MH = median haematodocha, R = embolar radix, RTA= retrolateral tibial apophysis, SD = sperm duct, ST = subtegulum, T = tegulum, TM = terminal membrane.

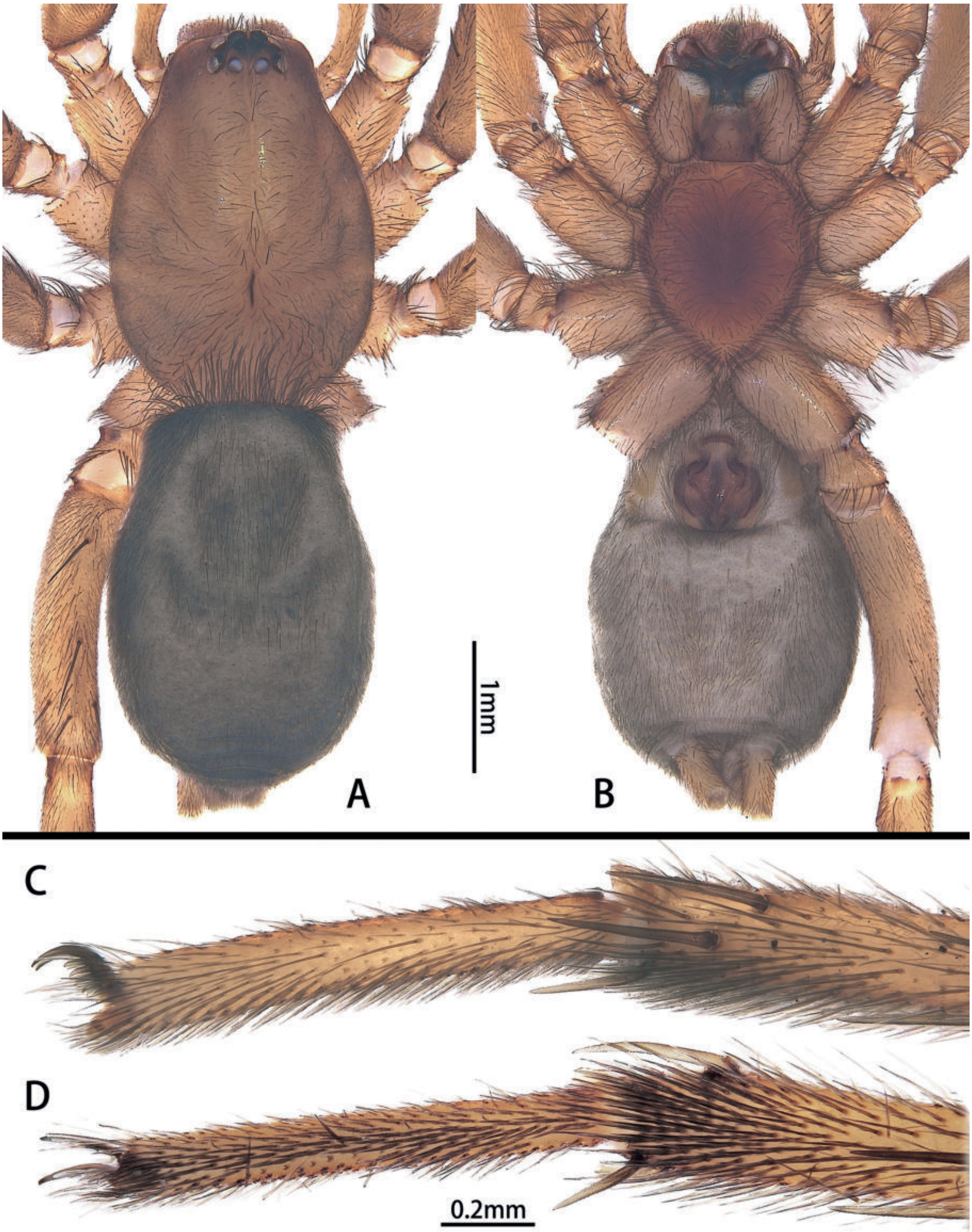

Figure 4. *Hotwheels sisyphus* sp. nov., female **A, B** habitus, dorsal and ventral view **C, D** right tarsus and metatarsus IV, preening brush, in prolateral (**C**) and ventral view (**D**).

PME–PME 0.08, PME–PLE 0.02, ALE–PLE 0.03. ***Leg measurements*:** I 7.28 (2.11, 0.92, 1.76, 1.39, 1.10), II 6.18 (1.83, 0.80, 1.48, 1.13, 0.94), III 5.62 (1.62, 0.65, 1.18, 1.26, 0.91), IV 7.89 (1.97, 0.81, 1.91, 2.06, 1.14). Cheliceral promargin and retromargin with 4 teeth (Fig. 1C).

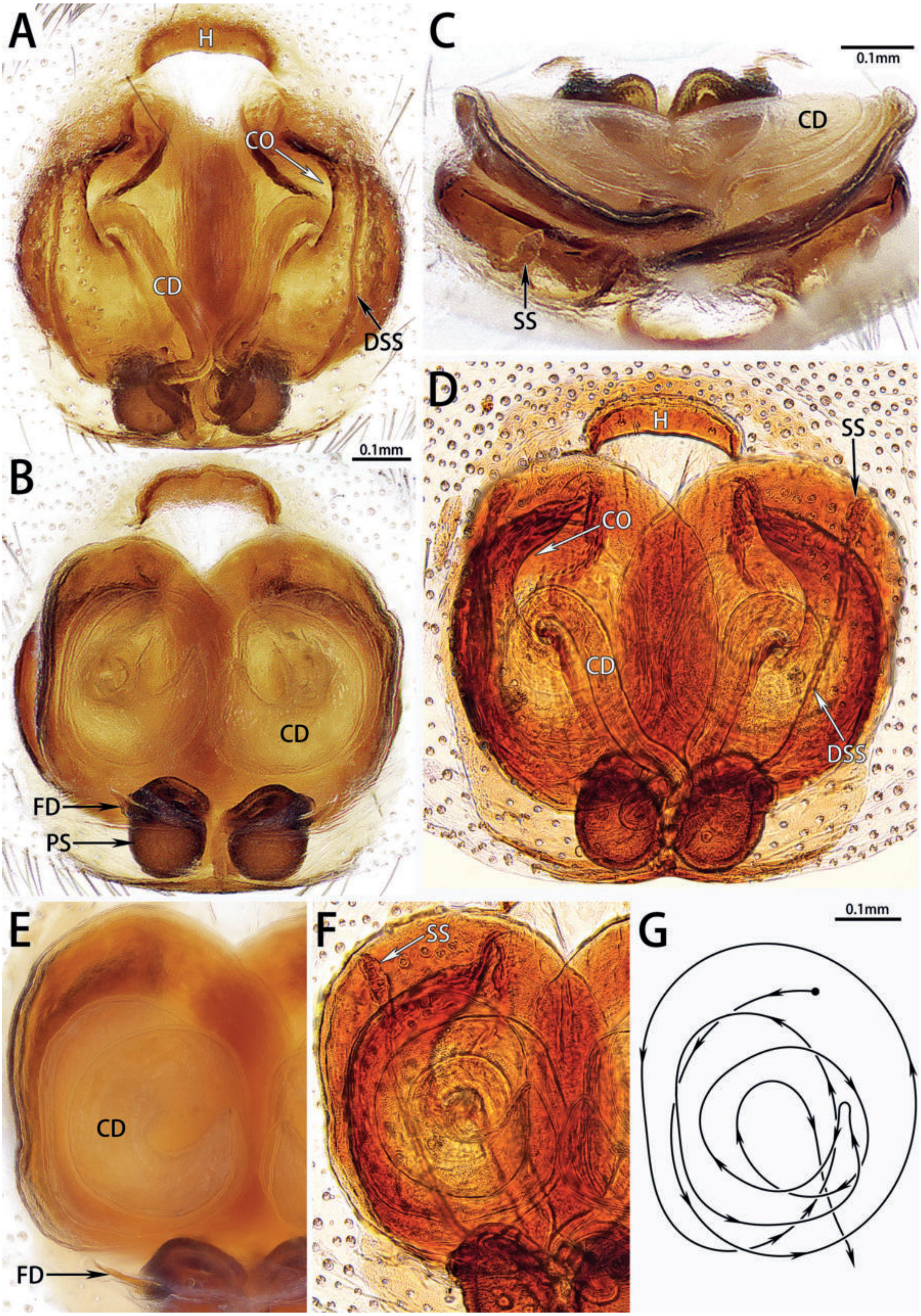

Figure 5. Epigyne of *Hotwheels sisyphus* sp. nov., intact (**A–C, E, G**) or macerated in clove oil (**D, F**), in ventral (**A, D**), frontal (**C**) and dorsal (**B, E, F**) view **G** CD path. Abbreviations: CD = copulatory duct, CO = copulatory opening, DSS = duct of secondary spermatheca, FD = fertilization duct, H = hood, PS = primary spermatheca, SS = secondary spermatheca.

Palp in regular state (Fig. 2). Femur and patella unmodified. Tibia with long retrolateral apophysis, nearly 2× longer than tibia, with prolateral curved tip. Cymbium pear shaped, without apical spines. Median apophysis on retrolateral apex of tegulum, nearly 2× wider than tegulum, pointed, curved. Conductor weakly sclerotized, folded and covered on tegulum and subtegulum, posterior part hidden behind median apophysis. Distal tubular membrane connects radix to tegulum. Embolus long, originates at about 7–8 o'clock, basal half rotated anticlockwise, with terminal membrane and two embolar processes (EP1, EP2), posterior half usually hidden behind conductor. Ejaculatory duct distinct.

Expanded palp (Fig. 3A–E). Basal haematodocha large, well developed. Subtegulum smaller than tegulum. Median haematodocha small. Conductor originates at tegulum prolaterally, expanded, crescent shaped with thickened border. Distal tubular membrane expanded, spherical. Terminal membrane inflated.

Female. *Paratype* (Fig. 4): total length 5.77; carapace 2.83 long, 2.02 wide; abdomen 2.94 long, 2.05 wide. ***Eye sizes and interdistances*:** AME 0.16, ALE 0.15, PME 0.11, PLE 0.13; AME–AME 0.03, AME–ALE 0.01, PME–PME 0.09, PME–PLE 0.06, ALE–PLE 0.04. ***Leg measurements*:** I 7.15 (2.16, 0.98, 1.68, 1.22, 1.11), II 6.17 (1.84, 0.90, 1.39, 1.12, 0.92), III 5.98 (1.62, 0.67, 1.24, 1.38, 1.07), IV 8.34 (2.37, 0.80, 1.80, 2.25, 1.12). Cheliceral promargin with 5 teeth, retromargin with 3 teeth (Fig. 1D).

Epigyne (Fig. 5). Epigynal plate elongated oval. Anterior folds form hood. Copulatory openings large, distinct, located mediolaterally. Copulatory ducts long, wide anteriorly, almost twice as wide as primary spermathecae, circular anteriorly and medially, membranous medially. Primary spermathecae small and globular. Secondary spermathecae small, with long ducts. Fertilization ducts extend laterally.

Distribution. China (Guizhou, Sichuan, Yunnan) (Fig. 6).

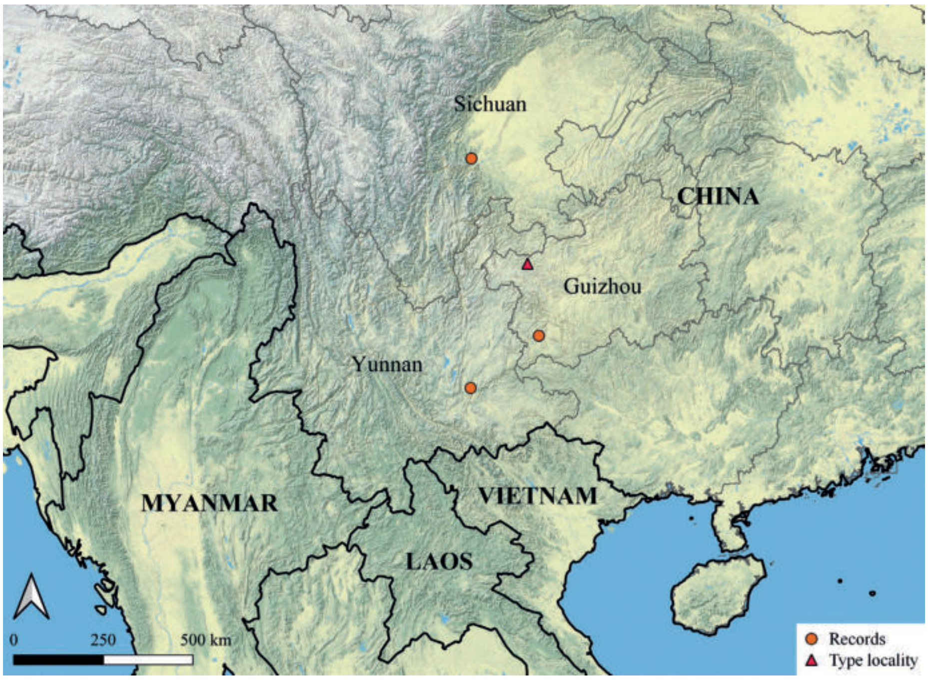

Figure 6. Map showing type locality and other records of *Hotwheels sisyphus* sp. nov.

Acknowledgements

Thanks to Zhisheng Zhang and Luyu Wang (School of Life Sciences, Southwest University, Chongqing, China), Zegang Feng, Lingchen Zhao, Yanmeng Hou and Lu Zhang (College of Life Sciences, Hebei University, Baoding, China) for field work. We are grateful to Yuri Marusik (Institute for Biological Problems of the North RAS, Magadan, Russia), Chi Jin (School of Landscape and Ecological Engineering, Hebei University of Engineering, Handan, China) and an anonymous reviewer for their valuable comments on the manuscript, Sarah Crews (California Academy of Sciences, San Francisco, USA) for her editorial efforts.

Additional information

Conflict of interest

The authors have declared that no competing interests exist.

Ethical statement

No ethical statement was reported.

Funding

This study was supported by the National Natural Science Foundation of China (No. 32170468), and by the Science & Technology Fundamental Resources Investigation Program (Grant No. 2022FY202100).

Author contributions

Investigation: BL. Writing – original draft: BL. Writing – review and editing: FZ.

Author ORCIDs

Bo Liu https://orcid.org/0000-0003-3740-7173
Feng Zhang https://orcid.org/0000-0002-3347-1031

Data availability

All of the data that support the findings of this study are available in the main text.

References

Álvarez-Padilla F, Hormiga G (2007) A protocol for digesting internal soft tissues and mounting spiders for scanning electron microscopy. The Journal of Arachnology 35(3): 538–542. https://doi.org/10.1636/Sh06-55.1

Azevedo GHF, Griswold CE, Santos AJ (2017) Systematics and evolution of ground spiders revisited (Araneae, Dionycha, Gnaphosidae). Cladistics 34(6): 579–626. https://doi.org/10.1111/cla.12226

Holt BG, Lessard JP, Borregaard MK, Fritz SA, Araújo MB, Dimitrov D, Fabre PH, Graham CH, Graves GR, Jønsson KA, Nogués-Bravo D, Wang Z, Whittaker RJ, Fjeldså J, Rahbek C (2013) An update of Wallace's zoogeographic regions of the world. Science 339(6115): 74–78. https://doi.org/10.1126/science.1228282

Lin YJ, Li SQ (2020) Description on *Solitudes dushengi* gen. nov et sp. nov. from Xinjiang, China (Araneae: Gnaphosidae). Zoological Systematics 45: 312–315. https://doi.org/10.11865/zs.202036

Lin YJ, Li SQ (2023) On nine ground spiders from Xishuangbanna, China (Araneae, Gnaphosidae), including two new genera and seven new species. ZooKeys 1174: 141–174. https://doi.org/10.3897/zookeys.1174.106340

Liu B, Zhang F (2023) Revision of the genus *Scopoides* Platnick, 1989 from China, with description of a new genus (Araneae, Gnaphosidae). ZooKeys 1172: 203–215. https://doi.org/10.3897/zookeys.1172.105034

Marusik YM, Omelko MM (2018) New data on *Synaphosus* (Araneae: Gnaphosidae) from Southeast Asia. Zootaxa 4374(2): 235–248. https://doi.org/10.11646/zootaxa.4374.2.4

Murphy J (2007) Gnaphosid Genera of the World. British Arachnological Society, Cambridgeshire, 46–47.

Ott R (2012) *Neodrassex*, a new genus of the *Leptodrassex* group (Araneae, Gnaphosidae) from South America. Iheringia. Série Zoologia 102(3): 343–350. https://doi.org/10.1590/S0073-47212012000300015

Ovtsharenko VI, Levy G, Platnick NI (1994) A review of the ground spider genus *Synaphosus* (Araneae, Gnaphosidae). American Museum Novitates 3095: 1–27.

WSC (2023) World Spider Catalog. Version 24. Natural History Museum Bern. https://doi.org/https://doi.org/10.24436/2 [Accessed on 1 December 2023]

Yao ZY, Li SQ (2021) Annual report of Chinese spider taxonomy in 2020. Shengwu Duoyangxing 29(8): 1058–1063. https://doi.org/10.17520/biods.2021140

ZooKeys 1189: 349–363 (2024)
DOI: 10.3897/zookeys.1189.113982

Research Article

A taxonomic study of four rare pteromalid genera: *Amblyharma* Huang & Tong, *Fusta* Xiao & Ye, *Nazgulia* Hedqvist and *Platecrizotes* Ferrière from the Eastern Palaearctic (Chalcidoidea, Pteromalidae, Pachyneurinae)

Ekaterina V. Tselikh[1], Jaehyeon Lee[2], Deok-Seo Ku[3]

1 *Zoological Institute, Russian Academy of Sciences, St. Petersburg 199034, Russia*
2 *Department of Plant Medicine, Gyeongsang National University, Jinju 52828, Republic of Korea*
3 *The Science Museum of Natural Enemies, Geochang 50147, Republic of Korea*
Corresponding author: Ekaterina V. Tselikh (tselikhk@gmail.com)

Abstract

The four morphologically similar genera *Amblyharma* Huang & Tong, 1993, *Fusta* Xiao & Ye, 2015, *Nazgulia* Hedqvist, 1973 and *Platecrizotes* Ferrière, 1934 from the Eastern Palaearctic are reviewed. Redescriptions of genera and all available types of Eastern Palaearctic species are provided. An identification key to genera is given. A new species from South Korea, *Platecrizotes jedii* **sp. nov.** is described and illustrated.

Key words: Description, key, new record, new species, Pachyneurinae, parasitoid, redescription, taxonomy

Academic editor: Andreas Köhler
Received: 10 October 2023
Accepted: 27 December 2023
Published: 19 January 2024

ZooBank: https://zoobank.org/169BC6E5-615C-4AAF-B6D6-E355DE5F1B44

Citation: Tselikh EV, Lee J, Ku D-S (2024) A taxonomic study of four rare pteromalid genera: *Amblyharma* Huang & Tong, *Fusta* Xiao & Ye, *Nazgulia* Hedqvist and *Platecrizotes* Ferrière from the Eastern Palaearctic (Chalcidoidea, Pteromalidae, Pachyneurinae). ZooKeys 1189: 349–363. https://doi.org/10.3897/zookeys.1189.113982

Introduction

Pteromalidae is one of the largest families of parasitic Hymenoptera, whose members are distributed in all zoogeographical regions of the world. It currently contains eight subfamilies and 415 genera (Burks et al. 2022). As a result of their large taxonomic and biological diversity, pteromalid wasps play a significant role as natural regulators of a number of phytophagous insects in natural and anthropogenic ecosystems and are potentially useful as biological control agents. Despite such high taxonomic diversity, abundance and significance, pteromalid wasps have not been sufficiently studied, in both taxonomic and faunistic investigations, and many species remain to be described.

This work is dedicated to four morphologically similar pteromalid genera that are poorly studied in the Eastern Palaearctic region: *Amblyharma* Huang & Tong, 1993, *Fusta* Xiao & Ye, 2015, *Nazgulia* Hedqvist, 1973 and *Platecrizotes* Ferrière, 1934, all belonging to the subfamily Pachyneurinae.

The monotypic genera *Amblyharma* Huang & Tong (type species *Amblyharma anfracta* Huang & Tong, 1993) and *Fusta* Xiao & Ye (type species *Fusta wuhuica* Xiao & Ye, 2015) are distributed only in the Eastern Palaearctic. The genus *Nazgulia* Hedqvist (type species *Nazgulia petiolata* Hedqvist, 1973) is recorded in both the Eastern and Western Palaearctic. *Platecrizotes* Ferrière (type species *Platecrizotes sudanensis* Ferrière, 1934) contains four species distributed in the Palaearctic (*P. europaeus* Bouček, 1964 and *P. sudanensis* Ferrière, 1934), Oriental (*P. keralensis* Sureshan, Raseena Farsana & Nikhil, 2015), Afrotropical (*P. sudanensis* Ferrière) and Neotropical (*P. argentinensis* De Santis, 1988) regions (Noyes 2019).

Unfortunately, the biology of most species in these genera is unknown, but available records suggest that they are mostly primary parasitoids of dipterans in the families Drosophilidae – *Drosophila* sp. (*P. europaeus* and *P. keralensis*), Anthomyiidae – *Atherigona soccata* Rondani, 1871 and Chloropidae – *Scoliophthalmus micantipennis* Duda, 1935 (*P. sudanensis*), lepidopterans in the families Lasiocampidae – *Dendrolimus* sp. (*A. anfracta*) and Noctuidae – *Sesamia cretica* Lederer, 1857 (*P. sudanensis*), and coleopterans in the family Curculionidae – *Cryptobathys setarius* Hustache, 1936 (*P. sudanensis*) (Noyes 2019).

The present paper is intended as a taxonomic study of the genera *Amblyharma* Huang & Tong, *Fusta* Xiao & Ye, *Nazgulia* Hedqvist and *Platecrizotes* Ferrière from the Eastern Palaearctic. These are small, rarely represented genera with only single specimens in collections. The original descriptions of the genera and species are incomplete and often contain significant errors; high-quality illustrations have not been published. The lack of contemporary keys for the identification of these pteromalids genera remains a major problem.

Therefore, the aim of this work is a comprehensive taxonomic study with redescriptions of genera and all available types of Eastern Palaearctic species and a description of a new species of *Platecrizotes* from South Korea. An identification key for these four genera is given.

Materials and methods

The specimens examined in this study are deposited in the collections of the Institute of Zoology of the Chinese Academy of Sciences (Beijing, China; **IZAS**), the National Museum in Prague (Prague, Czech Republic; **NMPC**), the National Institute of Biological Resources (Incheon, Republic of Korea; **NIBR**), the Naturhistoriska Riksmuseet (Stockholm, Sweden; **NHRS**), and the Zoological Institute of the Russian Academy of Sciences (St Petersburg, Russia; **ZISP**).

Morphological terminology, including sculpture and wing venation, follows Bouček and Rasplus (1991), Gibson (1997), and Burks et al. (2022). The flagellum consists of two or three anelli, five or six funicular segments, and the four-segmented clava. The antennal formula includes the number of segments: scapus, pedicellus, anelli, funicular segments, claval segments. The following abbreviations are used: **POL** – posterior ocellar line, the minimum distance between the posterior ocelli; **OOL** – ocello-ocular line, the minimum distance between a posterior ocellus and compound eye; **C1–C4** – claval segments; **M** – marginal vein; **S** – stigmal vein; **PM** – postmarginal vein; **F1–F6** – funicular segments; **Mt2–Mt8** – metasomal tergites (Mt1 – petiole). The scape is measured without the radicle; the pedicel is measured in lateral view. The distance between the clypeal lower margin and the toruli is measured from the lower margins of the toruli. Eye height is measured as the maximum diameter, eye length as the minimum diameter. The mesosoma and metasoma are measured in lateral view, the latter including the ovipositor sheaths.

Specimens were examined using Olympus SZX12 and Nikon SMZ745T microscopes. Photographs were taken with a Canon EOS 70D digital camera mounted on an Olympus SZX10 microscope (ZISP specimens), and a Nikon DS-Ri1 digital camera mounted on a Nikon AZ100M microscope (IZAS specimens). The acquired images were then processed with Helicon Focus.

Taxonomy

Class Hexapoda Blainville, 1816
Order Hymenoptera Linnaeus, 1758
Family Pteromalidae Dalman, 1820

Subfamily Pachyneurinae Ashmead, 1904

The four genera *Amblyharma* Huang & Tong, *Fusta* Xiao & Ye, *Nazgulia* Hedqvist and *Platecrizotes* Ferrière are morphologically similar in having moderately depressed mesosoma with complete and shallow notauli (Figs 2, 7, 8, 10, 14, 16, 20), reticulate metapleuron (Figs 9, 14, 24), distinct petiole (Figs 1, 10, 16, 27), M of fore wing widened proximally (Figs 4, 12, 15, 19, 26). The differences between these genera are given in the key.

Key to genera *Amblyharma* Huang & Tong, *Fusta* Xiao & Ye, *Nazgulia* Hedqvist and *Platecrizotes* Ferrière

1 Antennal formula 11264 (Figs 6, 17) **2**
– Antennal formula 11354 (Figs 11, 25) **3**
2 Pronotum with carina (Fig. 5). Lower margin of clypeus protruding (Fig. 3). F1 as long as F2 (Fig. 6). Propodeum with strong plicae (Fig. 1). Mesosoma (with propodeum) 1.50 times as long as wide (Fig. 2)...................... .... ***Amblyharma* Huang & Tong, 1993**
– Pronotum without carina (Fig. 16). Lower margin of clypeus not protruding (Fig. 17). F1 shorter than F2 (Fig. 17). Propodeum with weak plicae (Fig. 16). Mesosoma (with propodeum) 1.90 –2.00 times as long as wide (Fig. 16) ....***Nazgulia* Hedqvist, 1973**
3 Clypeal margin emarginate (Fig. 11). Antennal toruli above ocular line (Fig. 11). Pronotum with carina. Right mandible with 3 teeth, left with 4 teeth. M of fore wing long and not strongly widened, 9.80 times as long as wide (Fig. 12). Hind tibia with one spur ....***Fusta* Xiao & Ye, 2015**
– Clypeal margin rounded (Fig. 22). Antennal toruli below ocular line (Fig. 22). Pronotum without carina (Fig. 21). Right and left mandibles with 4 teeth. M of fore wing short and strongly widened, less than 6.00 times as long as wide (Figs 19, 26). Hind tibia with two spurs .... ***Platecrizotes* Ferrière, 1934**

Genus *Amblyharma* Huang & Tong, 1993

Amblyharma Huang & Tong, 1993: 395–397, 399–400. Type species *Amblyharma anfracta* Huang & Tong, 1993, by original designation and monotypy.

Redescription. Head without occipital carina. Gena without hollow at mouth corner; gena lamina absent. Lower margin of clypeus protruding and emarginate in the middle; tentorial pits indistinct (Fig. 3). Antennal formula 11264;

anelli small, F1-F6 transverse, antennal clava not large, micropilosity area small and occupies the lower part of 2 last claval segments (Figs 3, 6). Antennal toruli situated above level of lower edges of eyes; antennal protuberance absent; scrobes shallow. Mandibles not visible.

Mesosoma moderately depressed (Fig. 7). Pronotum little narrower than mesoscutum, with collar margin carinate. Notauli complete and shallow (Fig. 2). Scutellum moderately depressed, without conspicuous sublateral grooves, with distinct reticulate frenal area, but without frenal groove (Fig. 1). Metapleuron entirely reticulate. Propodeum with strong plicae; without costula and median carina, but middle part convex; nucha short and convex; propodeal spiracles near to front margin of sclerite (Fig. 1). Prepectus distinct, triangular, longer than tegula. Fore wing hyaline with distinct speculum; M widened proximally and tapering in distal part; M longer than S (Fig. 4). Hind coxa dorsally bare; hind tibia with one spur.

Metasoma on distinct reticulate, elongate petiole (Fig. 1). Metasoma ovate, flattened dorsally, shorter than combined length of mesosoma and head; Mt2 large with hind margin weak produced in middle (Figs 2, 7). Cerci with setae subequal in length. Hypopygium situated at one-third the length of metasoma. Ovipositor not much protruding.

Distribution. Eastern Palaearctic.

Amblyharma anfracta Huang & Tong, 1993

Figs 1–7

Amblyharma anfracta Huang & Tong, 1993: 397. Holotype female (IZAS, examined).

Type material. ***Holotype*:** female, “Hebei Province (Shijiazhuang), 1987.VIII.11”, “ex. *Carcelia rasella* Baranoff (Li Wegao)”, “*Amblyharma anfracta* ♀ Huang”, “HOLOTYPE”, “IOZ(E) 932939” (IZAS).

Description. Female. Body length 2.30 mm; fore wing length 1.70 mm.

***Coloration*.** Head in dorsal view black, in frontal view dark green with metallic diffuse coppery lustre. Antenna with scape and pedicel yellowish-brown, flagellum brown. Mesosoma and all coxae black; propodeum dorsally dark green with metallic diffuse coppery lustre. All femora brown; tibiae and tarsi yellowish-brown. Fore wing hyaline, venation yellowish-brown. Metasoma dark brown; ovipositor sheaths yellowish-brown.

***Sculpture*.** Head reticulate; clypeus radially striate. Mesosoma and propodeum reticulate, nucha of propodeum alutaceous. Metasoma weakly alutaceous and shiny.

***Head*.** Head in dorsal view 2.20 times as broad as long and 1.15 times as broad as mesoscutum; in frontal view 1.28 times as broad as high. POL 1.25 times as long as OOL. Eye height 1.30 times eye length and 1.75 times as long as malar space. Distance between antennal toruli and lower margin of clypeus 0.95 times distance between antennal toruli and median ocellus. Antenna with scape 0.86 times as long as eye height and 1.13 times as long as eye length; pedicel 1.80 times as long as broad and 1.70 times as long as F1; combined length of pedicel and flagellum 0.74 times breadth of head; F1–F6 transverse with 1 row of sensilla; clava 2.10–2.20 times as long as broad, with small micropilosity area on C3 and C4.

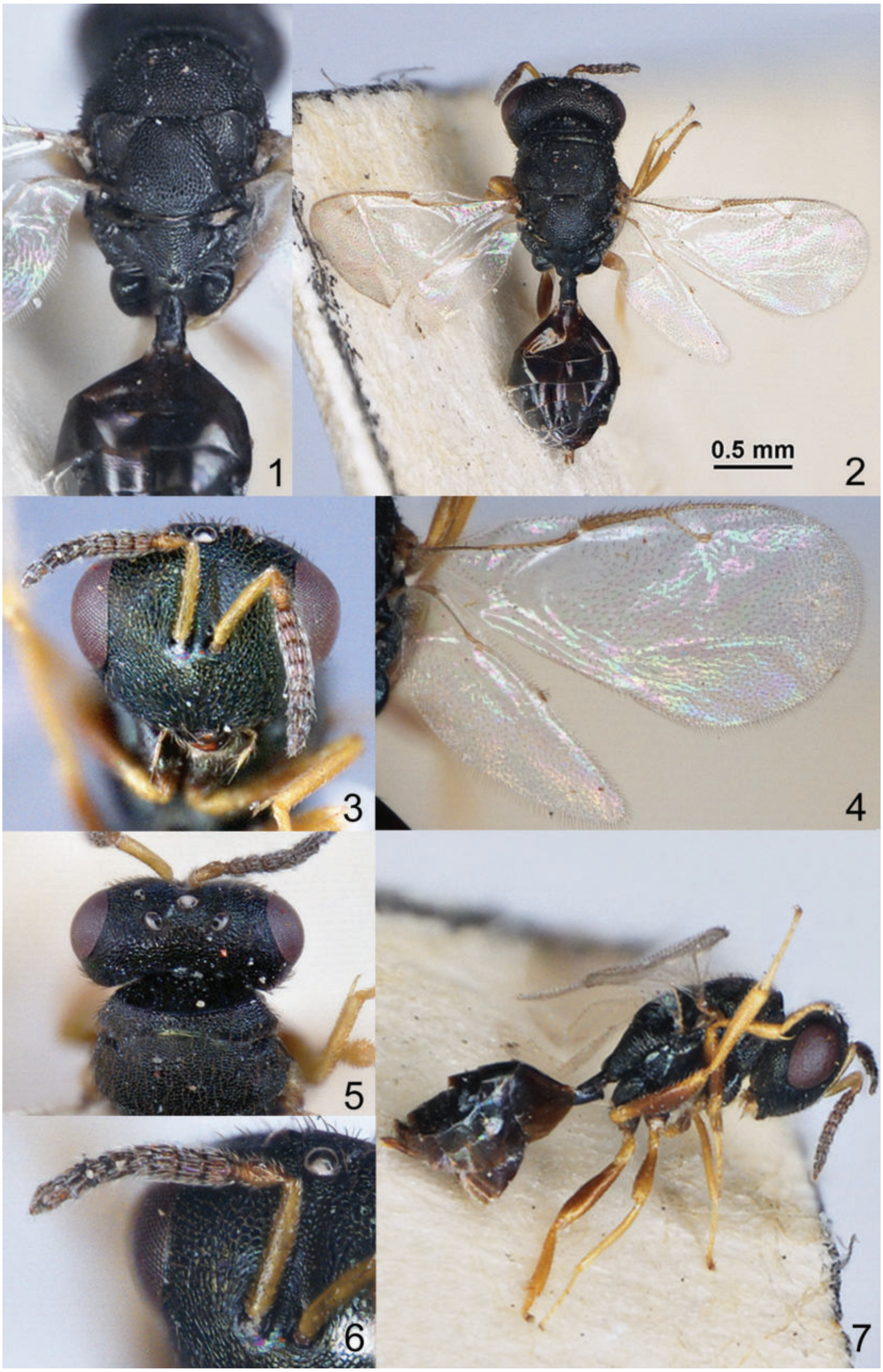

Figures 1–7. 1, 3 *Amblyharma anfracta* Huang & Tong, 1993, female, holotype **1** mesosoma and part metasoma, dorsal view **2** habitus, dorsal view **3** head, frontal view **4** wings **5** head, pronotum and mesoscutum, dorsal view **6** antenna **7** habitus, lateral view.

***Mesosoma*.** Mesosoma 1.57 times as long as broad. Pronotum 0.40 times as long as mesoscutum. Scutellum 0.90 times as long as broad. Propodeum medially 0.68 times as long as scutellum; nucha 0.30 times length of propodeum. Fore wing 2.10–2.12 times as long as its maximum width; basal cell, cubital vein and basal vein pilose; speculum closed below; M 0.96–1.00 times as long as PM and 1.62–1.65 times as long as S.

***Metasoma*.** Metasoma 1.46 times as long as broad, 0.95 times as long as mesosoma and 0.74 times as long as mesosoma and head. Petiole 1.66 times as long as broad. Mt2 0.35 times median length of metasoma; Mt8 0.30 times longer than maximum width. Ovipositor sheath projecting slightly beyond apex of metasoma.

Male. The only one known male of this species is the one referred to in Huang & Tong, 1993. Unfortunately, it was not possible to study this specimen in the IZAS collection.

Distribution. Peoples' Republic of China (Hebei).

Genus *Fusta* Xiao & Ye, 2015

Fusta Xiao, Ye, 2015: 151–153. Type species *Fusta wuhuica* Xiao & Ye, 2015, by original designation and monotypy.

Redescription. Head without occipital carina. Gena without hollow at mouth corner; gena lamina absent. Lower margin of clypeus protruding and emarginate in the middle; tentorial pits indistinct (Fig. 11). Antennal formula 11354; anelli small, F1–F6 transverse, antennal clava not large, micropilosity area small and occupies the lower part of 2 last claval segments (Fig. 11). Antennal toruli situated above level of lower edges of eyes., Right mandible with 3 teeth, left with 4 teeth.

Mesosoma moderately depressed (Fig. 8). Pronotum little narrower than mesoscutum, with collar margin carinate. Notauli complete and shallow (Fig. 10). Scutellum depressed, without conspicuous sublateral grooves, with distinct reticulate frenal area, but without frenal groove. Metapleuron entirely reticulate (Fig. 8). Propodeum without plicae, costula and median carina; nucha subglobose and reticulate; propodeal spiracles near to front margin of sclerite (Fig. 10). Prepectus distinct, triangular, shorter than tegula. Fore wing hyaline, without speculum; M widened proximally and tapering in distal part; M much longer than S (Fig. 12). Hind coxa dorsally bare; hind tibia with one spur.

Metasoma on distinct transverse petiole. Metasoma short ovate, flattened laterally, shorter than combined length of mesosoma and head (Fig. 8); Mt2 and Mt3 large, hind margin Mt2 arched in middle (Fig. 10). Cerci with setae subequal in length. Hypopygium situated at 0.6 length of metasoma. Ovipositor not much protruding.

Remarks. The original description of the genus (Ye et al. 2015) indicated that both mandibles were with 3 teeth, but after studying the holotype it was concluded that the right mandible was with 3 teeth, the left with 4 teeth.

Distribution. Eastern Palaearctic.

Fusta wuhuica **Xiao & Ye, 2015**

Figs 8–12

Fusta wuhuica Xiao & Ye, 2015: 153–154. Holotype female (IZAS, examined).

Type material. ***Holotype***: female, "China: Anhui: Wuhu, viii.2011, rice fields", "Coll. HU Hao-Yuan", "*Fusta wuhuica* Xiao et Ye, 2014", "HOLOTYPE", "IOZ(E) 1812583" (IZAS).

Description. Female. Body length 1.30 mm; fore wing length 1.20 mm.

***Coloration*.** Head in frontal view dark green with metallic diffuse coppery lustre, in dorsal view dark blue-green with metallic diffuse coppery lustre; antenna with scape, pedicel, anelli and F1-F5 yellowish-brown, clava brown. Mesosoma, propodeum and all coxae dark blue-green with metallic diffuse coppery lustre; all femora, tibiae and tarsi yellow. Fore wing hyaline, venation yellowish-brown. Metasoma in dorsal view dark blue-green, in ventral view brown; ovipositor sheaths black.

***Sculpture*.** Head reticulate; clypeus radially striate. Mesosoma, propodeum with nucha reticulate; petiole weakly reticulate. Metasoma weakly alutaceous and shiny.

***Head*.** Head in dorsal view 1.90 times as broad as long and 1.33 times as broad as mesoscutum; in frontal view 1.25 times as broad as high. POL 0.92 times as long as OOL. Eye height 1.50 times eye length and 2.60 times as long as malar space. Distance between antennal toruli and lower margin of clypeus 0.60 times distance between antennal toruli and median ocellus. Antenna with scape 0.70 times as long as eye height and 1.07 times as long as eye length; pedicel 1.88 times as long as broad and 3.44 times as long as F1; combined length of pedicel and flagellum 0.78 times breadth of head; F1–F5 transverse with 1 row of sensilla; clava 2.00 times as long as broad, with small micropilosity area on C3 and C4.

***Mesosoma*.** Mesosoma 1.58 times as long as broad. Pronotum 0.80 times as long as mesoscutum. Scutellum 1.10 times as long as broad. Propodeum medially 0.90 times as long as scutellum; nucha 0.45 times length of propodeum. Fore wing 2.82 times as long as maximum width; basal cell, cubital vein, basal vein pilose; speculum absent; M 1.66 times as long as PM and 2.35 times as long as S.

***Metasoma*.** Metasoma 1.40 times as long as broad, 0.80 times as long as mesosoma and 0.60 times as long as mesosoma and head. Petiole 0.60 times as long as broad. Mt2 0.25 times median length of metasoma; Mt8 1.15 times longer than maximum width. Ovipositor sheath projecting slightly beyond apex of metasoma.

Male. Unknown.

Remarks. The description of the species *F. wuhuica* by Xiao and Ye (2015) provides measurements that do not coincide with our measurements made during the study of the type material: body length 1.70 mm (redescription – 1.30 mm); head in dorsal view 3.17 times as broad as long (1.90); eye height 3.30 times eye length (1.50); fore wing 2.57 times as long as maximum width (2.82); M 1.33 times as long as P (1.66).

Distribution. Peoples' Republic of China (Anhui).

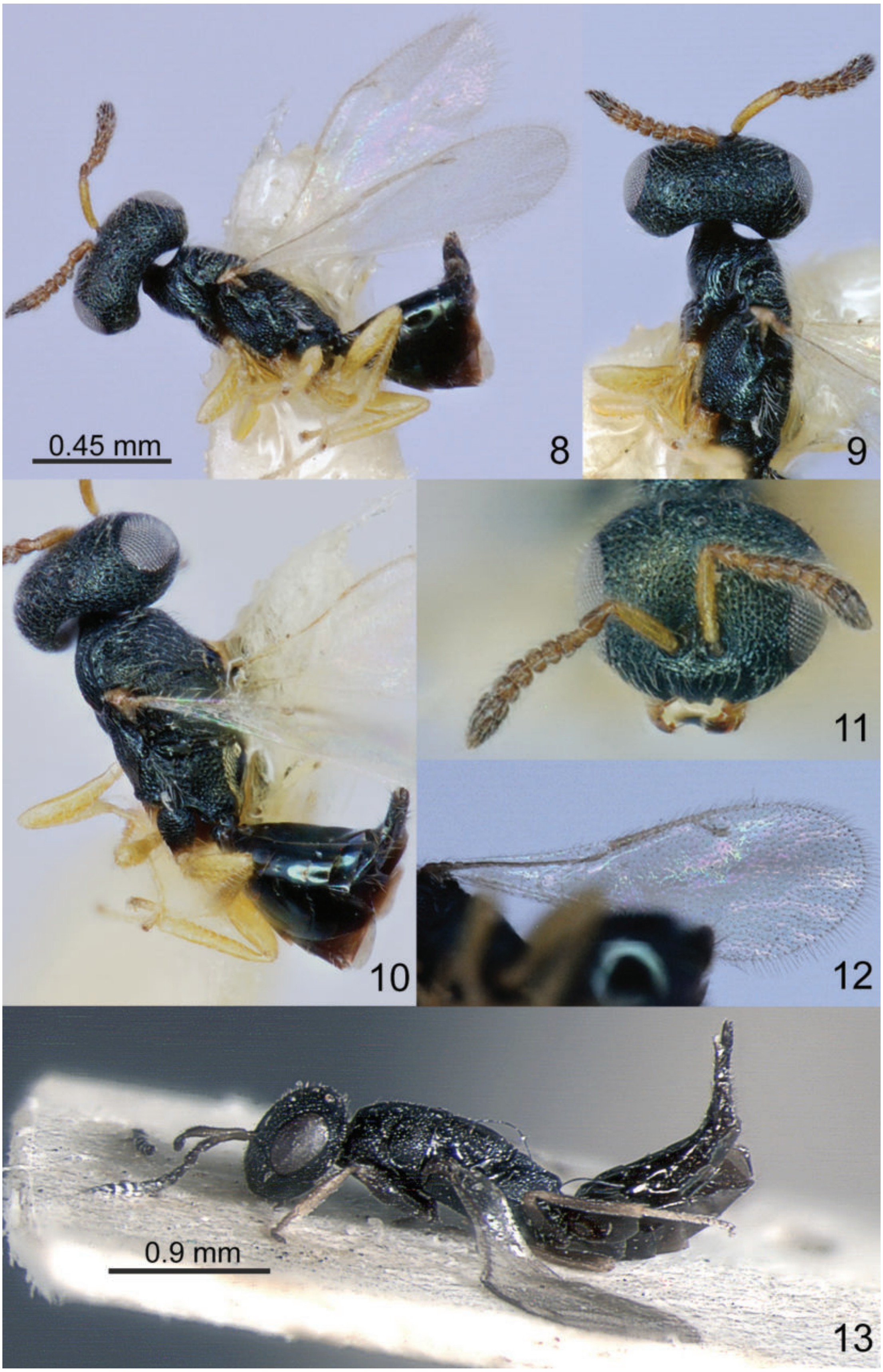

Figures 8–13. 8–12 *Fusta wuhuica* Xiao & Ye, 2015, female, holotype **8** head, dorsal view, mesosoma and metasoma, lateral view **9** head, dorsal view and mesosoma, lateral view **10** habitus, dorso-lateral view **11** head, frontal view **12** fore wing **13** *Nazgulia petiolata* Hedqvist, 1973, female, holotype, habitus, lateral view.

Genus *Nazgulia* Hedqvist, 1973

Nazgulia Hedqvist, 1973: 239–240. Type species *Nazgulia petiolata* Hedqvist, 1973, by original designation and monotypy.

Redescription. Head without occipital carina. Gena without hollow at mouth corner; gena lamina absent. Lower margin of clypeus not protruding, emarginate in the middle; tentorial pits indistinct (Fig. 17). Antennal formula 11264; anelli small, F1 transverse and shorter than F2, F2 longer than broad, F3-F6 subquadrate, antennal clava not large, micropilosity area small and occupies the lower part of 2 last claval segments (Fig. 17). Antennal toruli situated on level of lower edges of eyes; antennal protuberance absent; scrobes shallow. Both mandibles with 4 teeth (Fig. 17).

Mesosoma moderately depressed (Figs 13, 14). Pronotum narrower than mesoscutum; collar margin not carinate. Notauli complete (Fig. 16). Scutellum depressed, without conspicuous sublateral grooves, with distinct reticulate frenal area and shallow frenal groove (Fig. 16). Metapleuron entirely reticulate (Fig. 14). Propodeum with weak plicae; costula and median carina absent; nucha subglobose and reticulate; propodeal spiracles near to front margin of sclerite (Fig. 16). Prepectus distinct triangular, longer than tegula. Fore wing hyaline, with speculum; M widened proximally and tapering in distal part; M slightly longer than S (Fig. 15). Hind coxa dorsally bare; hind tibia with one spur.

Metasoma on distinct petiole, longer than broad. Metasoma lanceolate, as long as combined length of mesosoma and head (Figs 13, 14); Mt2 large with hind margin arched in middle. Cerci with setae subequal in length. Hypopygium situated at one-half length of metasoma. Ovipositor not much protruding.

Remarks. The original description of the genus by Hedqvist (1973) indicated that the notauli were incomplete, but after studying the holotype and additional non-type material it was concluded that the notauli are complete.

Distribution. Palaearctic.

Nazgulia petiolata Hedqvist, 1973

Figs 13–17

Nazgulia petiolata Hedqvist, 1973: 240. Holotype female (NMP, examined).

Type material. ***Holotype*:** female, “Nrk. Asbro 25/5 1950 K: J. Hedqvist”, “HOLOTYPUS Nazgulia gen.n. petiolata sp.n. ♀ K-J Hedqvist det. 1973”, “NHRS-HEVA 000002235” (NHRS).

Additional material examined. Russia: 1 female, “Sakhalin Prov., Sokol Vill., 7–9.VII.2011, E. Tselikh and D. Rachin” (ZISP).

Description. Female. Body length 2.70–3.5 mm; fore wing length 1.90–2.10 mm.

***Coloration*.** Head, mesosoma and propodeum dark blue-green or black with metallic diffuse coppery lustre. Antenna with scape, pedicel and flagellum brown. All coxae dark blue-green or black with metallic diffuse coppery lustre; all femora dark brown with metallic blue-violet lustre; all tibiae and tarsi yellowish-brown. Fore wing hyaline, venation yellowish-brown. Metasoma dark brown partially with metallic blue-violet lustre; ovipositor sheaths black.

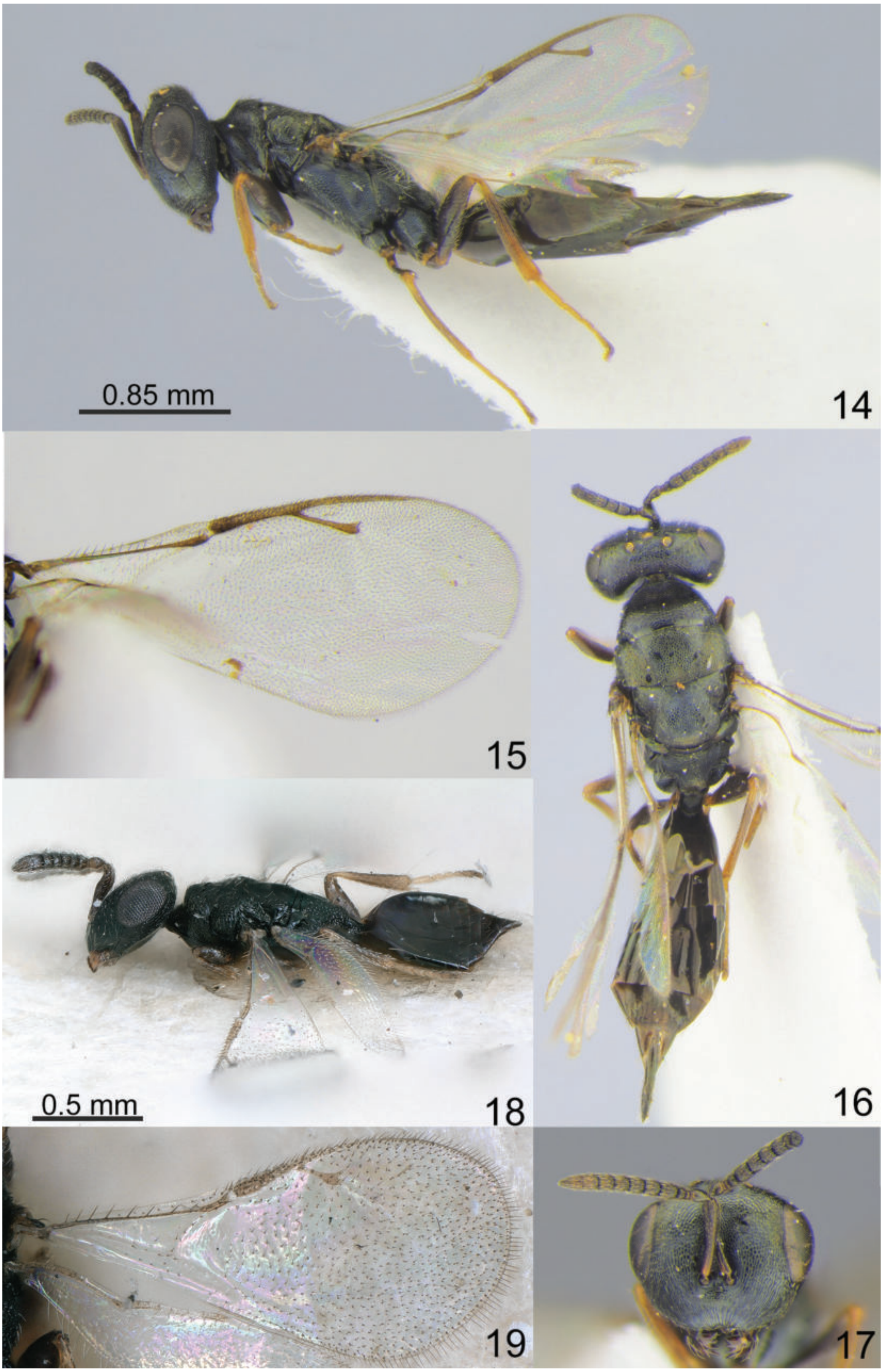

Figures 14–19. 14–17 *Nazgulia petiolata* Hedqvist, 1973, female, non-type **14** habitus, lateral view **15** fore wing **16** habitus, dorsal view **17** head, frontal view **18, 19** *Platecrizotes europaeus* Bouček, 1964, female, holotype **18** habitus, lateral view **19** fore wing.

***Sculpture*.** Head reticulate; clypeus and malar space radially striate. Mesosoma, propodeum with nucha and petiole reticulate. Metasoma weakly alutaceous and shiny.

***Head*.** Head in dorsal view 2.17–2.19 times as broad as long and 1.19–1.20 times as broad as mesoscutum; in frontal view 1.20–1.22 times as broad as high. POL 1.00–1.09 times as long as OOL. Eye height 1.50 times eye length and 1.40–1.60 times as long as malar space. Distance between antennal toruli and lower margin of clypeus 0.60–0.64 times distance between antennal toruli and median ocellus. Antenna with scape 0.87–0.90 times as long as eye height and 1.30–1.40 times as long as eye length; pedicel 1.60–1.42 times as long as broad and 1.70–2.70 times as long as F1; combined length of pedicel and flagellum 0.85–0.90 times breadth of head; F1 transverse, F2 1.14–1.25 times as long as broad, F3-F6 subquadrate, all with 1 row of sensilla; clava 2.00–2.30 times as long as broad, with small micropilosity area on C3 and C4.

***Mesosoma*.** Mesosoma 1.84–1.89 times as long as broad. Pronotum 0.65–0.80 times as long as mesoscutum. Scutellum 0.85–0.90 times as long as broad. Propodeum medially 0.60–0.73 times as long as scutellum; nucha 0.40 times length of propodeum. Fore wing 2.32 times as long as its maximum width; basal cell partly or wholly pilose, cubital vein and basal vein pilose; speculum closed below; M 0.84–0.90 times as long as PM and 1.33–1.35 times as long as S.

***Metasoma*.** Metasoma 2.60–2.90 times as long as broad, 1.28–0.96 times as long as mesosoma and 0.76–1.00 times as long as mesosoma and head (metasoma is deformed in the specimens studied so the measurements are approximate). Petiole 1.75–2.00 times as long as broad. Mt2 0.20 times median length of metasoma; Mt8 1.15–1.20 times longer than maximum width. Ovipositor sheath projecting beyond apex of metasoma.

Male. Not studied.

Remarks. One characteristic of this species is that the antenna has two anelli, but there is a tendency towards reduction in the size of F1 in some Palaearctic specimens (see Bouček and Rasplus 1991 and Fig. 17).

Distribution. Netherlands, Sweden, Russia (Far East).

Genus *Platecrizotes* Ferrière, 1934

Platecrizotes Ferrière, 1934: 90. Type species *Platecrizotes sudanensis* Ferrière, 1934, by original designation and monotypy.

Redescription. Head without occipital carina. Gena without hollow at mouth corner; gena lamina absent. Lower margin of clypeus protruding and rounded; tentorial pits indistinct (Fig. 22). Antennal formula 11354; anelli small, F1–F5 transverse, antennal clava not large, micropilosity area small and occupies the lower part of 2 last claval segments. Antennal toruli situated above level of lower edges of eyes; antennal protuberance absent; scrobes shallow. (Fig. 25) Both mandibles with 4 teeth.

Mesosoma depressed (Fig. 20). Pronotum narrower than mesoscutum; collar margin not carinate (Fig. 21). Notauli complete and shallow; metapleuron reticulate (Fig. 24). Scutellum depressed, without conspicuous sublateral grooves, frenal area and frenal groove. Metapleuron entirely reticulate. Propodeum with weak plicae indicated anteriorly; costula and median carina absent; nucha short and convex; propodeal spiracles near to front margin of sclerite (Fig. 27). Prepectus distinct, triangular, longer than tegula. Fore wing hyaline, with speculum; M widened proximally and tapering in distal part; M longer than S (Figs 19, 26). Hind coxa dorsally bare; hind tibia with two spurs.

Metasoma on distinct reticulate petiole, longer or shorter than broad (Fig. 27). Metasoma ovate, flattened dorsally, shorter than combined length of mesosoma and head; Mt2 and Mt3 large, hind margin Mt2 produced in middle (Figs 18, 20). Cerci with setae subequal in length. Hypopygium situated at one-quarter the length of metasoma. Ovipositor not much protruding.

Distribution. Palaearctic, Oriental, Afrotropical and Neotropical regions.

Platecrizotes jedii **sp. nov.**

https://zoobank.org/C8A41CAA-913C-41D0-AE62-A26A242B8F15
Figs 20–27

Type material. ***Holotype*****:** female, South Korea: “Gyeonggi-do, Pocheon-si, Soheul-eup, 37°45'29.2"N, 127°10'0.4"E, 15.VI.2015, Park, Choi, Nam, Shin, Kim” (NIBR). ***Paratype*****:** female, “Jeollabuk-do, Gunsan-si, Okdo-myeon, Sinsido-ri, malaise trap, 04–18.VIII.2017, H.G. Lee” (ZISP).

Description. Female. Body length 1.10–1.30 mm; fore wing length 0.80–1.05 mm.

Coloration**.** Head and mesosoma black. Antenna with scape black, pedicel and flagellum brown. All coxae black, all femora and tibiae brown, tarsi yellowish-brown. Fore wing hyaline, venation yellowish-brown. Metasoma dark brown partially with metallic coppery-violet lustre; ovipositor sheaths brown.

Sculpture**.** Head reticulate; clypeus alutaceous. Mesosoma with pronotum and mesoscutum reticulate; axillae weakly reticulate; scutellum alutaceous or weakly alutaceous and shiny; propodeum reticulate, nucha alutaceous; petiole weakly reticulate. Metasoma weakly alutaceous and shiny.

Head**.** Head in dorsal view 2.20–2.29 times as broad as long and 1.22–1.24 times as broad as mesoscutum; in frontal view 1.16–1.20 times as broad as high. POL 1.13–1.21 times as long as OOL. Eye height 1.52–1.54 times eye length and 1.80–2.00 times as long as malar space. Distance between antennal toruli and lower margin of clypeus 0.35–0.41 times distance between antennal toruli and median ocellus. Antenna with scape 1.00–1.05 times as long as eye height and 1.52–1.61 times as long as eye length; pedicel 1.14–1.21 times as long as broad and 1.30–1.40 times as long as F1; combined length of pedicel and flagellum 0.77–0.81 times breadth of head; F1-F5 transverse, all with 1 row of sensilla; clava 1.89–2.05 times as long as broad, with small micropilosity area on C3 and C4.

Mesosoma**.** Mesosoma 1.76–1.80 times as long as broad. Pronotum 0.75–0.85 times as long as mesoscutum. Scutellum 0.85–0.90 times as long as broad. Propodeum medially as long as scutellum; nucha 0.20–0.25 times length of propodeum. Fore wing 2.20–2.23 times as long as maximum width; basal cell, cubital vein and basal vein pilose; speculum closed below; M 2.00–2.16 times as long as PM and 1.78–1.93 times as long as S.

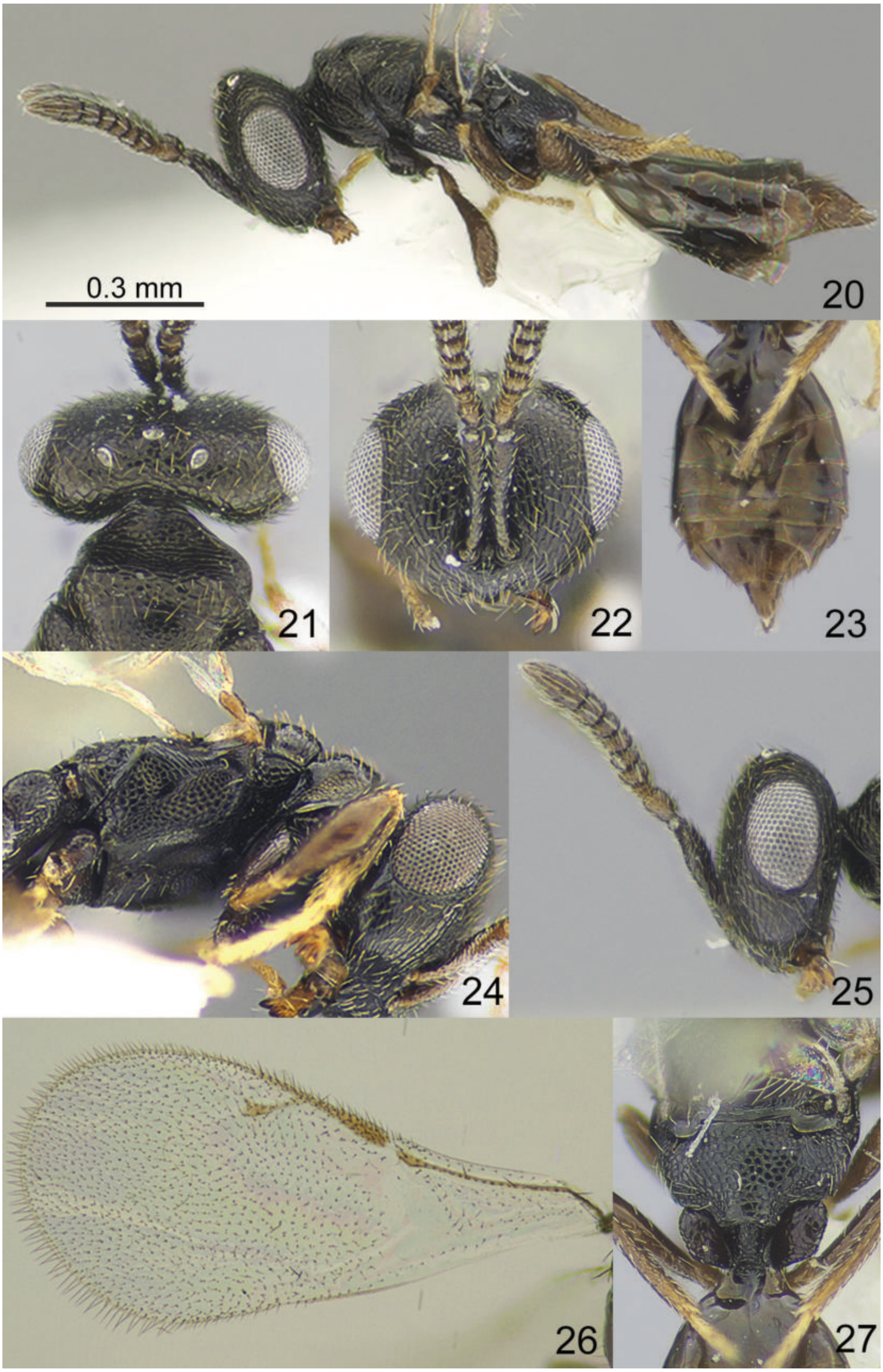

Figures 20–27. 20–27 *Platecrizotes jedii* sp. nov., female, holotype **20** habitus, lateral view **21** head and pronotum, dorsal view **22** head, frontal view **23** metasoma, dorsal view **24** head and mesosoma, lateral view **25** head, lateral view and antenna **26** fore wing **27** propodeum and petiole, dorsal view.

***Metasoma*.** Metasoma 1.77–1.84 times as long as broad, 0.90–1.05 times as long as mesosoma and 0.78–0.86 times as long as mesosoma and head. Petiole 1.70–1.80 times as long as broad. Mt2 0.40–0.43 times median length of metasoma; Mt8 1.10–1.20 times longer than maximum width. Ovipositor sheath projecting slightly beyond apex of metasoma.

Male. Unknown.

Etymology. The species is named in honour of the "Star Wars" character – "Jedi" of George Lucas.

Distribution. Korean Peninsula.

Remarks. This species is similar to *P. europaeus* Bouček, 1964 (Figs 18, 19) in having black coloration of the head and mesosoma; S of the fore wing with a relatively small stigma; lower margin of the clypeus strongly protruding. However, *Platecrizotes jedii* sp. nov. has the fore wing with PM shorter than S (vs PM longer than S), M 5.65–6.06 times as long as broad and the proximally widened part occupying 0.50 of the vein length (vs M 3.80–4.90 times as long as broad and proximally widened part occupying 0.80 of vein length), speculum closed below (vs open); petiole 1.70–1.90 times as long as broad (vs 0.50–0.60); and all tibiae brown (vs yellowish-brown).

Acknowledgements

The authors are very thankful to Tomáš Hovorka (NMPC) for providing the photo of the type of *P. europaeus* Bouček.

Additional information

Conflict of interest

The authors have declared that no competing interests exist.

Ethical statement

No ethical statement was reported.

Funding

This work was supported by a grant from the National Institute of Biological Resources (NIBR), funded by the Ministry of Environment (MOE) of the Republic of Korea (NIBR202304203, NIBR201801201). And it was partially funded by Russian State Research (project No. 122031100272-3).

Author contributions

All authors have contributed equally.

Author ORCIDs

Ekaterina V. Tselikh https://orcid.org/0000-0002-9184-043X
Jaehyeon Lee https://orcid.org/0000-0002-3666-6029
Deok-Seo Ku https://orcid.org/0000-0002-6274-6479

Data availability

All of the data that support the findings of this study are available in the main text.

References

Bouček Z (1964) On three little known genera of Pteromalidae with descriptions of three new European species (Hymenoptera). Casopis Ceskoslovenské Spolecnosti Entomologické 61: 254–264.

Bouček Z, Rasplus J-Y (1991) Illustrated key to West-Palaearctic genera of Pteromalidae (Hymenoptera: Chalcidoidea). Institut National de la Recherche Agronomique, Paris, 140 pp.

Burks R, Mitroiu M-D, Fusu L, Heraty JM, Janšta P, Heydon S, Dale-Skey Papilloud N, Peters RS, Tselikh EV, Woolley JB, Noort S, Baur H, Cruaud A (2022) From hell's heart I stab at thee! A determined approach towards a monophyletic Pteromalidae and reclassification of Chalcidoidea (Hymenoptera). Journal of Hymenoptera Research 94: 13–88. https://doi.org/10.3897/jhr.94.94263

Ferrière C (1934) Notes sur les Pireninae, avec descriptions de deux nouvelles espèces. Mitteilungen der Schweizerische Entomologische Gesellschaft 16: 83–93.

Gibson G (1997) Morphology and Terminology. In: Gibson GAP, Huber JT, Woolley JB (Eds) Annotated Keys to the Genera of Nearctic Chalcidoidea (Hymenoptera). NRC Research Press, Ottawa, 16–44.

Hedqvist KJ (1973) Two new genera and species of the family Pteromalidae from Sweden. Entomologica Scandinavica 4(3): 237–240. https://doi.org/10.1163/1876312X74X00100

Huang DW, Tong XW (1993) Two new genera and two new species of Pteromalidae (Hymenoptera: Chalcidoidea). Sinozoologica 10(5): 395–400.

Noyes JS (2019) Universal Chalcidoidea Database – World Wide Web Electronic Publication. https://www.nhm.ac.uk/our-science/data/chalcidoids/database/ [Accessed on 12.10.2022]

Ye HZ, Hu HY, Xiao H (2015) A new genus and species of Pteromalidae (Hymenoptera) from China. Oriental Insects 48(3–4): 151–154. https://doi.org/10.1080/00305316.2014.959785